DANMARKS OG GRØNLANDS GEOLOGISKE UNDERSØGELSE RAPPORT 2016/1

Paleoproterozoic hydrothermal graphite-sulfide ± gold mineralization from the Tasiilaq area, South-East Greenland

Katrine Baden

GEOLOGICAL SURVEY OF DENMARK AND GREENLAND
DANISH MINISTRY OF ENERGY, UTILITIES AND CLIMATE

G E U S

DANMARKS OG GRØNLANDS GEOLOGISKE UNDERSØGELSE RAPPORT 2016/01

Paleoproterozoic hydrothermal graphite-sulfide ± gold mineralization from the Tasiilaq area, South-East Greenland

Katrine Baden
Preface by Jochen Kolb

Master of Science in Geology
Submitted: 18.06.2013
University of Copenhagen

GEOLOGICAL SURVEY OF DENMARK AND GREENLAND
DANISH MINISTRY OF ENERGY,UTILITIES AND CLIMATE

GEUS

Introduction

In 2010, the Geological Survey of Denmark and Greenland and the Bureau of Minerals and Petroleum, now the Greenlandic Ministry of Mineral Resources, organized a joint field expedition to the Tasiilaq area in South-East Greenland as part of the South-East Greenland Mineral Endowment Task (SEGMENT). This field expedition had the main focus on collecting stream sediment and fresh water samples for regional geochemical mapping, but also was joined by geologists doing reconnaissance mapping. Several areas with abundant quartz veins and sulphide mineralization were detected and sampled, but gold anomalies are restriced to tens of ppb in the collected samples. In 2011 however, one sample discovered by a local prospector won the Ujarrasiorit competition, the local Greenlandic mineral hunt, containing 18.2 vol.% iron sulphides and 11.1 ppm gold. This sample was collected on the north side of the Johan Petersen Fjord, where it leads into the Sermilik Fjord. This find made it necessary to reinvestigate the samples from 2010 and study the potential gold mineral system.

This volume contains the Masters of Science in Geology thesis by Katrine Baden, who will start a PhD project at GEUS from 2016. Katrine used petrographic observations in order to establish a paragenetic sequence of metamorphic and hydrothermal minerals. Selected analyses by the electron microprobe at Copnehagen University were the basis for geothermobarometric calculations. Furthermore, she used LA-ICP-MS analysis of hydrothermal monazite and xenotime, yielding an absolute age frame for the mineralization. The hydrothermal gold mineralization and the hydrothermal alteration associated with the quartz veins have distinctly different mineral assemblages, but both formed in the hypozonal regime after the metamorphic peak during regional exhumation at 1850-1750 Ma in the late stages of the Nagssugtoqidian Orogen. Katrine speculates that orogenic gold mineral systems have been active and that the grade of gold mineralization depends on the effectivity of the structural control.

Table of Contents

Abstrakt

Guldforekomster i afsidesliggende områder er blevet interessante for mineindustrien, grundet de seneste års stigende guldpriser. Denne afhandling undersøger petrologien, mineralogien, geokemien og geokronologien af syv udvalgte stenprøver fra Tasiilaq-regionen i det sydøstlige Grønland. Seks af prøverne blev taget ved Helheim Fjord synformen (figur 3). Disse har et guldindhold på <3 ppb. Den syvende prøve kommer fra en lokalitet nær Johan Petersen Fjord (figur 3). Prøven har et indhold på 11,1 g/t guld og 18,2% jernsulfider.

Fra en paragnejs prøve taget i synformen er en temperatur på ~640℃ og et tryk på ~5,3 kbar blevet udregnet. Forholdene tolkes til at afspejle den orogene begivenhed, der forårsagede sammenfoldningen af urelaterede litologier i Tasiilaq-regionen fra ca. 1870-1820 Ma. Prøverne er alle hydrothermal omdannede, typisk med dissemineret grafit og jernsulfider til følge. Hydrothermalt rekrystalliserede monazit-korn fra paragneiss har givet U/Pb aldre fra 1961± 47 Ma til 1752±22 Ma, med en hovedpart af aldre omkring 1850-1750 Ma. Denne hovedvægt af aldre fra 1850-1750 Ma tolkes til at repræsentere alderen for den hydothermale omdannelse. At grafit er meget almindeligt i prøverne fra synformen tyder på at den hydrothermale omdannelse og de hydrothermale fluider var ufokuserede og dækkede et stort areal. Guldmineraliseringen var ligeledes udbredt og ufokuseret, hvilket resulterede i lave guldværdier.

Den guldførende prøve er en garnetit med hydrotermal omdannelse karakteriseret af grafit og jernsulfider. Temperature på ~500-660℃ er udregnet for prøven, hvilket overlapper med temperaturforholdene fra synformen. Prøven blev taget i nærheden af en regional forkastning, og kunne udgøre en strukturelt fokuseret mineralisering på en anden eller tredjeordens forkastning.

Det fremgår således, at Helheim Fjord synformen kan have haft gunstige forhold for guldmineralisering, men mislykkedes på grund af manglen på en fokalzone/fælde.

***Keywords*:** Guld, grafit, hydrothermal omdannelse, Tasiilaq-regionen, det østlige Nagsugtoqidianske Orogen

Abstract

Due to the rising gold prices in recent years also gold deposits in remote locations have become of interest to the mining industry. This thesis investigates the petrology, mineralogy, geochemistry and geochronology of seven selected rock samples from the Tasiilaq region in South-East Greenland. Six of the samples were taken at the Helheim Fjord synform (figure 3). These have gold grades of <3 ppb. The seventh sample is from a locality near Johan Petersen Fjord (figure 3). The sample holds 11.1 g/t gold, and 18.2% iron sulfides.

A temperature of ~640℃ and a pressure of ~5.3 kbar has been calculated for a paragneiss sample from the synform-location. The conditions are interpreted to reflect the orogenic event which caused the interleaving of unrelated lithologies in the Tasiilaq at 1870-1820 Ma. The samples are hydrothermally altered, with a late stage overprint of graphite and commonly also iron sulfides. Hydrothermally recrystallized monazite grains from the paragneiss have yielded U/Pb ages of 1961±47 Ma to 1752±22 Ma, with a clustering of ages around 1850-1750 Ma. The clustering is interpreted to represent an age estimate of the hydrothermal event. That graphite is omnipresent in the samples from the synform suggests that the hydrothermal event was unfocussed and widespread. Thus the gold mineralization was also widespread and unfocussed, which resulted in low gold grades.

The temperatures obtained for the gold-bearing garnetite-sample overlaps with that of the synform-location, at ~500-660℃. The rock is a garnetite with a late-stage hydrothermal overprint of graphite and iron sulfides. The sample was taken in the proximity of a regional fault, and could represent a structurally-controlled mineralization on a second or third order fault structure.

Thus, it appears that the Helheim Fjord synform may have had favorable conditions for gold mineralizarion, but failed due to the lack of a focal zone/trap.

***Keywords*:** Gold, graphite, hydrothermal alteration, the Tasiilaq-region, the eastern Nagsugtoqidian Orogen

1. Introduction

World-class gold ores generally occur in greenschist facies while smaller deposits occur in amphibolite and granulite facies, in terrains associated with subduction accretion settings (McCuaig & Kerrich, 1998). These large gold deposits are invariably located proximal to regional-scale structures, but occur on second or third order splays, where low stress makes a high fluid flux possible (McCuaig & Kerrich, 1998). The hydrothermal fluid of large ore deposits are rich in Au-transporting sulfur complexes, high in pH-buffering CO_2, above 200℃ hot and have a relatively low salinity (Phillips, Evans, 2004). The hydrothermal alteration commonly causes carbonation and sulfidication of the wall rock. The mineralization is often enriched in Au, and rare earth elements (REE) but have low concentrations of other semi-precious metals (McCuaig & Kerrich, 1998).

This thesis investigates seven selected rock samples from the Tasiilaq region in South-East Greenland. One sample won the Ujarrasiorit competition in 2011, on the basis of holding 18.2% ironsulfides and 11.1g/t gold. The sample was taken on the north side of the Johan Petersen Fjord, where the fjord intersects with the Sermilik Fjord (figure 3). The other six rock samples were collected in the summer of 2010 from a 10 m long section, on the south side of the Helheim Fjord (figure 3, location A). The outcrop was sampled as it appeared to be a gossan, related to a possible gold mineralization (Kolb, 2010).

The samples represent a pyroxene garnetite (BMP vjar. 2011-0092, the sample which won the Ujarrasiorit, hereafter known as the 'Ujarrasiorit'-sample), an ultramafic rock (sample 525133), an amphibolite (sample 525134) an orthopyroxenit (sample 525135) and three garnet-graphite paragneisses (sample 525137, 525138 and 525139). Samples 525137, 525138 and 525139 are gathered in a paragneisses group as mineralogy and trace mineral content are similar (Table 1, page 28). Graphite is the only mineral which is present in all rock samples. The sample series from the Helheim Fjord synform represent the general hydrothermal alteration observed in the area (personal correspondence with Jochen Kolb). The two mineralizations are compared in regard to temperature, pressure and hydrothermal alteration, to evaluate their gold-mineralization-potential.

This thesis will

- Describe the regional geology of the Tasiilaq area, based on current literature.
- Describe rock samples and polished thin sections and establish mineralogy, structural and textural relations.
- Establish the paragenetic sequence on the basis of textural relations.
- Establish the semi-quantitative composition of single mineral phases from selected thin sections (ultra mafic rock, amphibolite, paragneiss-group) by the use of Secondary Electron Microscopy (SEM) and Energy Dispersive Spectroscopy (EDS).
- Establish pressure and/or temperature of the latest metamorphic event, using selected samples (sample 525138, Ujarassiorit) based on Wavelength Dispersive Spectroscopy (WDS) analyses by single-mineral analyses of plagioclase, biotite and garnet and geothermobarometric models.
- Establish single-mineral U-Pb ages in suitable samples (paragneiss-group) by Laser Ablation Inductively Coupled Plasma Mass Spectroscopy (LA-ICP-MS).
- Develop a genetic model for metamorphism and hydrothermal alteration at the Helheim Fjord syncline.

2. Orogenic gold

Orogenic gold deposits have formed episodically during the middle Archean and younger Precambrian, and continuously throughout the Phanerozoic. A global episode of gold-vein formation took place from 2.1 to 1.8 Ga, where supracrustal sedimentary rocks became significant as host rocks for gold ores (Goldfarb et al., 2000). This episode correlates with growth of new continental crust and major mantle overturning in the hot early earth, with associated plumes causing extreme heat at the base of the crust (Goldfarb et al., 2000). The massive melting and extensive granitoid emplacement lead to an extensive buoyant continental crust, and a depleted lower crust. The resulting land masses were large, equidirectional and stable continental masses. Such continental blocks are thermally and geometrically ideal for long term preservation of auriferous crustal material (Goldfarb et al., 2000).

Consistent characteristics of orogenic gold-only deposits include deformed and variably metamorphosed host rocks, an association to major compressional and transpressional structures and spacio-temporal association with granitoids of variable compositions (Phillips and Evans, 2004, Goldfarb et al., 2000). Significant gold deposits cluster where blocks of Archean and Paleoproterozoic rock is well-exposed in near-surface, regardless of the immediate host rock lithology (Goldfarb et al., 2000). The mineralized lodes form over a broad range of upper- to mid-crustal temperatures, at ~200 to 650℃ and 1 to 5 kbar (Groves, 1993). Large-scale fluid migration along major deep-seated structures takes place in most orogens, as moderate to high temperatures are reached (~500℃, Goldfarb et al., 2000). Gold-bearing aqueous fluids from the world's major gold-only deposits are remarkably similar; they show temperatures of above 200 ℃, are rich in CO_2 (20 to 30 mol%), sulphur bearing and have relatively low salinity (Phillips and Evans, 2004). Sulfur will be partially released into the hydrothermal fluids as an effect of prograde desulfidication during heating, if syngenetic sulfide-minerals are present in the wall rock (Goldfarb et al., 2000). Additionally, sulfide-bearing fluids can carry significant amounts of leachable gold. After migrating through fracture networks, the gold is eventually deposited in secondary and tertiary faults systems, adjacent main faults. If the temperature exceeds 700℃ in or below the fluid source area, the fluid and melt will migrate up simultaneously; hence the the deposition of gold at shallower crustal levels. The spacial and temporal association of granitoid rocks and gold in orogenic belts, is also related to this temperature dependency (Goldfarb et al., 2000). Where the high temperature events occur, but deep-seated faults are missing, gold ores are commonly minor (Goldfarb et al., 2008).

Recently, it has been suggested that aqueous fluids rich in CO_2 are essential in gold-only deposits, due to their ability to buffer fluid pH by complexation with reduced sulphur, at a level that can maintain elevated concentrations of gold and cause gold deposition in favorable host rocks (Phillips and Evans, 2004).

Reduction of CO_2 rich fluids during a hydrothermal event can cause deposition of graphite (Křibek et al., 2008). Yet graphite can also have an organic origin, either as in-situ metamorphosed detrital organic matter, or as C mobilized by metamorphic-hydrothermal fluids and redeposited as graphite (Henne & Craw, 2012). Organic matter has long been known to be of importance for the enrichment of metals in sedimentary rocks, and is also an important agent in the formation of other types of ore deposits in higher temperature environments (Bierlein et al., 2001). Hydrocarbons can physically prevent low-grade minerals from sealing the porosity of the host lithology, and the interaction of hydrothermal fluids and carbonaceous units can locally cause redox-controlled precipitation of native gold (Bierlein et al., 2001).

Gold and graphite are closely associated in many gold deposits around the world. Such a relation is e.g. found in the Otago Schist belt, where the largest active gold mine in New Zealand is located along with several other deposits (Craw, 2002). Hence, rocks rich in graphite are potential targets for gold exploration.

3. Geology of the Tasiilaq area

The eastern part of the Nagssugtoqidian Orogen is a 200 km east-west trending area called Tasiilaq (Nutman et al., 2008). The Tasiilaq area is described in two parts; a southern and northern area. The boundary between the two areas is placed west of Kitaq, running southeast following the fjord west of the settlement Isertoq (Figure 1). The Tasiilaq area was previously known as the Ammassalik area, thus older references use that term (Chadwick et al., 1989, Kalsbeek et al., 1993, Nutman et al., 2008).

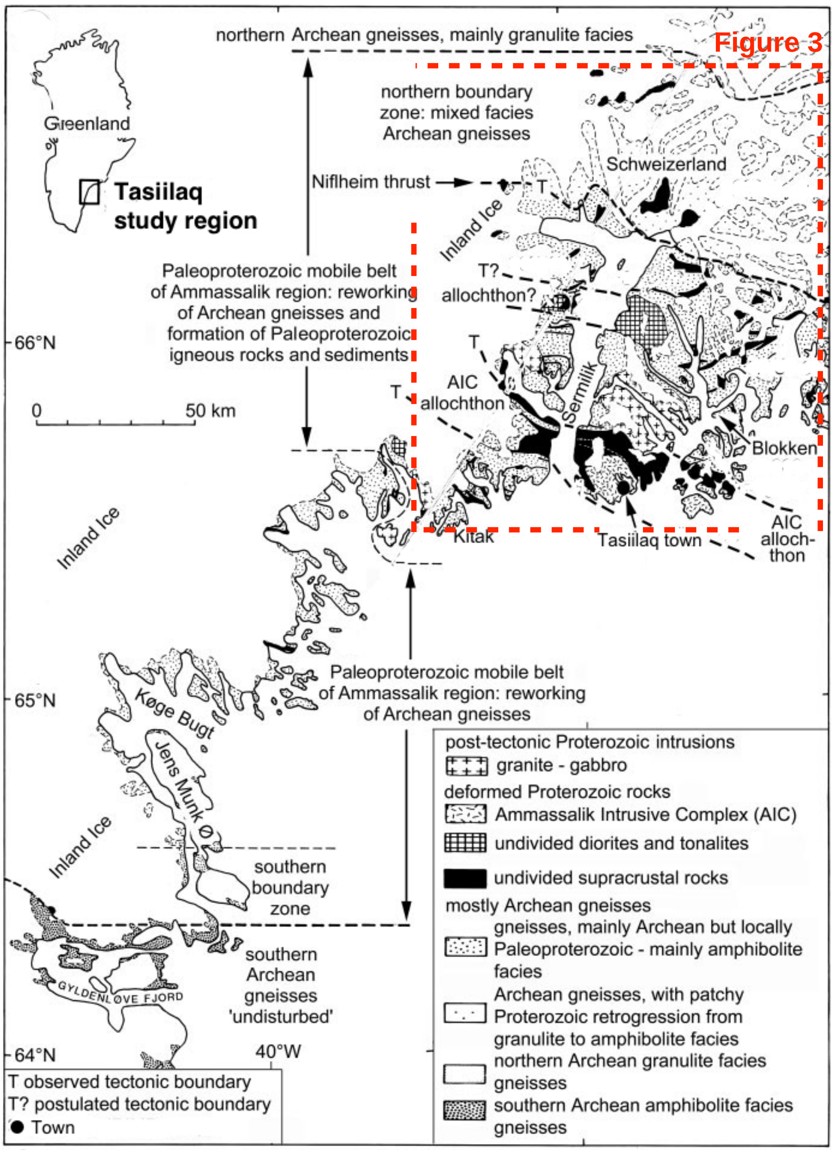

Figure 1. Sketch geological map of the Tasiilaq area, with main lithological divisions. The outlined area is presented in figure 3 (modified after Nutman et al., 2008).

Archean trondhjemite-tonalite-granodiorite gneiss (TTG) is the dominant lithology in the southern part of the Tasiilaq area (figure 1). The northern part of the area has a complex layer-cake structure, where the TTG gneisses have been interleaved with Paleoproterozoic supracrustal rocks during a 1870 Ma to 1840 Ma collisional event (Nutman et al., 2008). Magmatic suites are present in the mid-northern end of the region, the most studied being the Ammassalik Intrusive Complex (AIC, Friend & Nutman., 1989). The AIC belongs to a regional magmatic arc, which were emplaced at the edge of the southern Archean crust during the Paleoproterozoic (Nutman et al., 2008).

3.1. Lithology

In the northern part of the Tasiilaq area, sheets of metasedimentary rocks, amphibolites and ultramafic rocks constitute an association of lithologies, which has been interleaved with TTG gneiss (figure 3, Chadwick et al., 1989). The northern area is characterized by at least four intrusive plutonic events, which consists of; gabbro, diorite-tonalite, granite-granodiorite-diorite and norite-gabbro-diorite-granodiorite (figure 3, Chadwick et al., 1989).

(1) The mixed lithological package which includes amphibolites, ultramafic rocks, marbles, schists and paragneisses is a supracrustal association (Chadwick et al., 1989). In the northern area, the paragneisses are volumetrically the largest lithology of the association (Hall et al., 1989). The thickness of the paragneiss layers vary from a few meters and up to 1 km (Chadwick et al., 1989). The mineral assemblage of the paragneiss is dominated by biotite, muscovite, quartz and feldspar. Garnet, kyanite, sillimanite and graphite are also common (Nutman et al., 2008). Garnet-rich paragneisses with 11% MnO are locallly occur (Hall et al., 1989). The paragneiss is also locally rich in sulfides such as pyrite, pyrrhotite and chalcopyrite. Some sulfide-rich quartz seams have disseminated flakes of graphite, but graphite also occurs throughout the paragneisses. Compositional layering of the paragneissses is common, and primary sedimentary structures have also been observed. The mineralogy supports high pressure metamorphism, as the paragneiss is garnet- and kyanite bearing (Chadwick et al., 1989). Locally granulite facies assemblages are also present (Chadwick et al., 1989).

Amphibolites are secondary to the paragneisses in volume, and commonly interlayered with the paragneisses. The amphibolitic layers range in thickness from approximately 30 cm to 1 m (Hall et al., 1989). The layers are typically compositionally banded and often rich in garnet. Disseminated sulfides are locally present, and veneers of malachite have been found locally. Graphite is commonly present in the amphibolites (Chadwick et al. 1989).

Volumetrically, the ultramafic rocks are minor. They form lenticular bodies or pods of up to 200 m in width and 1 km in length (Hall et al., 1989). The rocks are dominated by olivine and tremolite, which form coarse prisms and nodular intergrowths. Green amphibole, anthopyllite, pale mica, talc and chlorite are minor constituents (Chadwick et al. 1989). Orthopyroxene can also be found mainly as porphyroblasts (Hall et al., 1989).

The least abundant lithology in the supracrustal association is marble. Marble occurs in thin layers of 1-2 m thickness, typically interlayered with diopside-rich paragneisses. They are grey, rich in graphite and can have coarse aggregates of diopside (Hall et al., 1989).

(2) TTG gneisses are a major lithology on either side of the Sermilik Fjord. The thickness of the layers is hard to estimate due to deformation, but generally range in size from 10 m to 1 km (figure 3, Chadwick et al. 1989). In the southern area, the TTG gneiss relatively underformed, and dominates an area of about 130 km in length (figure 1). It has a similar composition across the area, and is a quartzo-feldspathic gneiss, with variable content of biotite and hornblende due to compositional boudins. Pegmatite layers are also common as concordant seams or lenses. The banding is at the scale of 1-30 cm, for both compositional layers and pegmatites (Chadwick et al. 1989). Accessory garnet is locally present (Nutman et al., 2008).

Older litterature refers to the TTG gneisses as orthogneisses (Chadwick et al., 1989, Kalsbeek et al., 1993, Nutman et al., 2008)

(3) In the extreme north (figure 1) brown orthogneisses are the dominant lithology. They are compositionally similar to the TTG gneiss, but of a different metamorphic facies (Chadwick et al. 1989). No geothermobarometric data has been obtained for the orthogneisses, but they commonly bear orthopyroxene and infrequently garnet, which suggest low- to medium pressure metamorphism with high temperatures which is distinctive of granulite facies metamorphism (Karlsbeek et al., 1993).

(4) The Ammassalik Intrusive Complex occurs in the central part of the region (figure 3). The complex is a norite-gabbro-dioritie-granodiorite body with medium- to coarse-grained rocks. Diorite is the most dominant lithology. The color varies and darker, more mafic (circa 50% mafic minerals) types are dominant. The diorite consists of variable portions of andesine, hypersthene, augite, hornblende and biotite (Chadwick et al. 1989). Some samples hold quartz and accessory apatite, opaque minerals and zircon. A few samples with rutile and carbonate have been observed (Hansen & Kalsbeek, 1989).

As the AIC intruded into the TTG gneiss it caused widespread anatexis. The resulting anatectic halo is rich in garnet, hypersthene and contains sillimanite rather than kyanite (Nutman et al., 2008). Major element analyses of AIC diorites show compositional affinities with arc andesites (Nutman et al., 2008 reference to Friend, unpublished whole rock analyses).

Moderate pressure (hypersthene-granulite to amphibolite facies) have been suggested based on the mineral assemblage and the relatively undeformed nature of the intrusion (Karlsbeek et al., 1993). The associated anatectic, silimanite- and orthopyroxene-bearing dioritic rocks yielded temperatures of 830-850℃ for clinopyroxene-orthopyroxene thermometry and 7.5 kbar for clinopyroxene-plagioclase barometry (Nutman & Friend, 1989).

(5) Other igneous suites are present in the northern area, on either side of the Sermilik Fjord. Suites of granites, diorites and locally also gabbros have sharp intrusive contacts and narrow contact aureoles. The mineralogy of the dolerite-tonalite complex is dominated by coarse-grained biotite hornblende-feldspar quartz diorites or tonalites with accessory garnet. Mafic xenoliths are locally abundant. Veining of dark dioritic rocks by granite is common in in the granite-diorite-gabbro complex, and xenoliths of dioritic rocks can be found in granitic rocks (Chadwick et al. 1989). The mineralogy of the complex indicates emplacement at low to moderate pressure (Kalsbeek et al., 1993).

(6) The southern part of the Tasiilaq area has two major lithologies; TTG-gneiss and metadolerites. The metadolerites occur as dykes. Several generations of dykes are found in the Tasiilaq region (Hall et al. 1989). In the southern area, they occur throughout most of the TTG gneiss, but are much less frequent than in the northern area (Chadwick et al. 1989). The dykes appear as amphibolites in terrains of higher metamorphic facies (Nutman et al., 2008). The mineralogy of the dykes is dominated by hornblende, diopside and feldspar (primarily microcline) with accessory apatite and sphene. In places, the amphibolite dykes have garnetiferous microgabbroic cores (Chadwick et al., 1989). The dykes locally contain eclogite relicts and high pressure granulite assemblages, suggestive of eclogite facies metamorphism with up to 11 kbar, at circa 750℃ (Nutman & Friend, 1989). The amphibolites of the supracrustral association are distinguished from the amphibolite dykes by the presence of graphite as an accessory mineral (Chadwick et al. 1989). The dykes are up to 60 m wide and and up to several kilometers long. They have epidote-rich marginal retrogression zones of <30 m width.

Zircons from a dyke north of the AIC show depressed HREE abundance, and no significant negative Eu anomalies. This indicates that the zircons grew in a garnet-rich and plagioclase-free environment (Nutman et al., 2008). Inclusions of quartz, clinopyroxene and Ca-rich garnet were found in the zircons; no plagioclase inclusions were found. The feldspar-absent inclusionary mineralogy of the zircons, supports the high-pressure conditions, as growth during subsequent isothermal recrystallization would have involved lower pressure, and thus the presence of plagioclase (Nutman et al., 2008).

3.2. Structure

The northern area of the Tasiilaq region is characterized by the interleaved layers of the supracrustal association and TTG gneisses, which causes the previously mentioned coarse layer-cake structure

(Chadwick et al., 1989). The supracrustal rocks and TTG gneiss are overprinted by at least three episodes of folding, the latest with NW-trending axial surfaces (Chadwick & Vasudev, 1989). Faulting is common in the northern part of the area, and is typically normal and dipping NE (Chadwick & Vasudev, 1989).
The structural setting of the southern area is relatively simple compared to that of the north. It is dominated by nappes and NE-dipping shear zones (Chadwick & Vasudev, 1989). Shear zones are common, and tend to dip NE, with principal displacement from NE to SW indicated by fabrics in mylonites (Chadwick et al., 1989).

Several regional structural boundaries have been interpreted for the northern part of the Tasiilaq area (figure 1, and figure 3). The Niflheim thrust was defined by Chadwick & Vasudev (1989) at the boundary of the brown orthogneiss and the TTG gneiss (figure 1). A more complex array of faulting has been suggested by Kolb, 2010, for the Nifelheim thrust (figure 3).
Two thrust faults are located on either side of the AIC (figure 1 and 3). A similar setting may be present at either side of the diorite-tonalite complex, though field indications are weak (Nutman et al., 2008). The additions of Kolb, 2010 (figure 3) supports the interpretation of a thrust fault in on the south side of the complex.

3.3. Geochronology

Relative ages of the Síportôq supracrustral association and the surrounding TTG gneiss have been debated but not agreed on in the literature (Chadwick et al. 1989, Kalsbeek, 1993). The absence of reliable field criteria has complicated the interpretations.
Based on field relations it has been suggested that the TTG gneisses are relatively younger than the Síportôq supracrustral association (Chadwick et al., 1989). But geochronological studies do not agree (Kalsbeek et al., 1993, Nutman et al., 2008).

(1) The paragneisses of the Síportôq supracrustral association have been dated by Kalbeek et al. (1993), using wholerock Sm/Nd and Rb/Sr analyses to yield conflicting ages. The Sm-Nd model T_{DM} age yielded 2.88 Ga to 2.75 Ga, which is an age related to the protolith (Nutman et al., 2008). The Rb/Sr analyses yielded an errorchron with a slope providing an age of 1870±50 Ma (Kalsbeek et al., 1993). The Rb-Sr analyses reflect the age of Paleoproterozoic deposition rater than the age of the protolith (Nutman et al., 2008).
Single mineral U/Pb dating on zircons from the metasediments have also been conducted (Nutman et al., 2008). Twenty two zircons yielded $^{207}Pb/^{206}Pb$ ages from 2800 to 2600 Ma (Nutman et al., 2008). These authors suggest that the ages represents the maximum depositional age of the sediment. Eight of the analyses provided discordant Paleproterozoic ages. The discordance is interpreted to reflect loss of Pb from Archean zircons during the Proterozoic. The paragneiss-zircons also display rims of overgrowth and recrystallization with near-concordant Paleoproterozoic ages. The rims display a spread in $^{207}Pb/^{206}Pb$ ages above what is expected from zircons of the same population. A model of unmixing was applied to the rim data, and ages of 1740±40 Ma, 1835±19 Ma and 1874 ±23 Ma were extracted (Nutman et al., 2008). Though the ages are model data, it is likely that the zircons underwent complex recrystallization and regrowth in the Paleoproterozoic (Nutman et al., 2008).

(2) Nutman et al. (2008) also conducted single mineral U/Pb dating on zircons from the TTG gneiss from the northern part of the Tasiilaq area. Rims of zircons from the location ‘Blokken’ (figure 1 and 3) have been dated at ~2720 Ma (Nutman et al., 2008). The eight oldest zircon cores yielded a weighted mean $^{207}Pb/^{206}Pb$ age of 3035 ± 14 Ma, which is suggested to be close to the age of the igneous protolith (Nutman et al., 2008). The zircon cores and whole zircon grain analyses yielded a

spread of $^{207}Pb/^{206}Pb$ ages, which is likely to have been caused by a partial loss of radiogenic Pb in a Neoarchean high-grade metamorphic event (Nutman et al., 2008).

(3) Samples of the brown orthogneiss from the northern part of the Tasiilaq area yielded abundant, oscillatory zoned zircons. These have cathodoluminescence-bright (CL-bright), low Th/U rims which yielded a weighted mean $^{207}Pb/^{206}Pb$ age of 2720±6 Ma, which is similar to the 2723±49 Ma obtained in zircon-rims from the TTG gneiss (Nutman et al., 2008). This suggest granulite facies metamorphism at 2720 Ma in the northernpart of the Tasiilaq area (Nutman et al., 2008).
The protolith of the orthogneiss is much younger than that of the Blokken gneiss, with a weighted mean zircon age at $^{207}Pb/^{206}Pb$ 2863±11 Ma (Nutman et al., 2008). The range in age of the igneous protolith from rocks occurring side by side suggest that the gneisses are polyphase in nature (Nutman et al., 2008).

(4) Nutman et al. (2008) dated the AIC based on oscillatory-zoned zircons at 1881±10 Ma, which is interpreted as the age of igneous crystallization (Nutman et al., 2008).

(5) It is likely that the tonalite-diorite complex is related to the AIC and of similar geological origin (Nutman et al., 2008). A weighted mean model $^{207}Pb/^{206}Pb$ age of 1901± 9 Ma was obtained for a diorite sample (Nutman et al., 2008). Analyses of zircon rims yielded a weighted mean $^{207}Pb/^{206}Pb$ age of 1840±56 Ma, which is interpreted to be recrystallization in a tectonic event shorty after formation (Nutman et al., 2008). Thus, both the age of crystallization and metamorphism is similar to that of the AIC.
The granite-granodiorite-diorite igneous complex and the associated gabbro have been dated at ~1680 Ma using zircon (U/Pb, Kalbeek et al., 1993). These represent the youngest igneous events in the area.

(6) A sample from a metaddolerite dyke yielded zircons with CL-bright rims. The CL-dull core yielded $^{207}Pb/^{206}Pb$ ages from 2015 Ma to 1800 Ma (Nutman et al., 2008). The oldest samples of 2015±15 Ma are interpreted to reflect the approximate time of intrusion of the dyke (Nutman et al., 2008). Though there is a general spread of ages, it is thought that the zircons are of one generation that experienced variable ancient loss of radiogenic Pb. The CL-bright rims yielded $^{207}Pb/^{206}Pb$ ages of 1836±58 Ma, which reflect a time of recrystallization during metamorphism (Nutman et al., 2008).
A $^{207}Pb/^{206}Pb$ age of 1867±28 Ma was obtained from a single zircon from a dyke of eclogite facies, located north of the AIC (Nutman et al., 2008). The age reflects a high pressure metamorphic event.

3.4. Tectonometamorphic and geodynamic evolution

The oldest metamorphic event in the area is represented by Archean rocks in the northern part of the Tasiilaq area. They experience by loss of Pb at a circa 2720 Ma granulite facies metamorphic event (Nutman et al., 2008). These rocks and the northern most area was not disturbed in the later Paleoproterozoic event(s) (Nutman et al., 2008). The AIC and diorite-tonalite complex indicate local high temperature, low pressure metamorphism at 1900 to 1880 Ma coeval with the igneous emplacement (figure 2, Nutman et al., 2008). North of the AIC, a metadiabse dyke suggest eclogite facies conditions at ~1870 Ma (figure 2, Nutman et al., 2008). Regrowth of zircons in many lithologies at 1870 to 1820 Ma reflects both high pressure eclogite facies metamorphism recorded in the paragneiss of the supracrustal assiciation, as well as the regional amphibolite facies metamorphism (figure 2, Nutman et al., 2008).

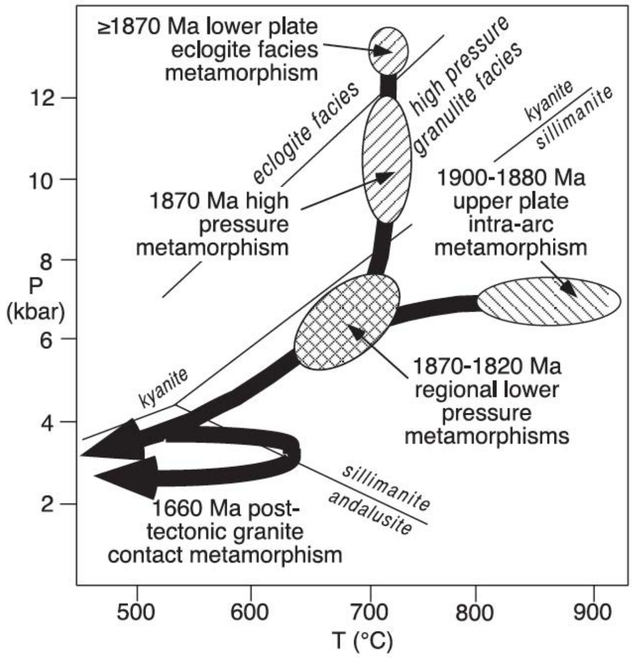

Figure 2. Pressure-temperature-time evolution of the Tasiilaq area during the Paleoproterozoic (Nutman et al., 2008).

Nutman et al., 2008 suggest that the AIC is related to a regional magmatic arc, which was active during the Paleoproterozoic. Along with the supracrustal rocks, the magmatic arc was emplaced over a southern terrane of Archean continental crust and its cover series, causing the previously described southern tectonic transport as well as at least a doubling of the continental crust (Nutman et al., 2008). High pressure metamorphic assemblages are indicative of collisional orogeny and crustal thickening. A doubling of the continental crust could cause the 1867±28 Ma eclogite facies metamorphic conditions observed in the northern metadolerite dykes (figure 2, Nutman et al., 2008). The collisional orogeny marks the end of arc magmatism and would have caused subsequent folding.

The coarse layer cake structure of the Tasiilaq area is a result of Paleoproterozoic collisional orogeny, that caused Archean basement gneisses to be interleaved with the cover sequence (supracrustal association). Geochronology and field relations indicate that the supracrustal association represents a Paleoproterozoic cover sequence to the Archean TTG gneiss (Nutman et al., 2008). Due to the common history of folding, the package has a regional overprint of amphibolite facies metamorphism at 1870-1820 Ma (Nutman et al., 2008). The recrystallization and obtained ages are thus likely to reflect the age of high-grade metamorphism in unrelated lithologies as they were folded together in the collisional stage of the orogeny (figure 2, Nutman et al., 2008). Simultaneous or subsequent deformation could have caused both local thickening and thinning of supracrustal sheets (Kalsbeek et al., 1993). The geographical extend of the metamorphism is reflected in the absence of recrystallization in zircons from the Archean TTG gneisses, in the northern part of the Tasiilaq area. Metamorphic rims in zircons from the Blokken-area (figure 2 and 3) yielded ages of ~2720 Ma, indicating that the described Paleoproterozoic disturbance of zircons is limited to some loss of radiogenic Pb rather than new zircon growth (Nutman et al., 2008).
As the Tasiilaq area represents a collisional orogen, a suture should be present. If a primary suture can be found it will have a cryptic structure, since it has experienced at least two episodes of folding and at least one episode of shearing (Nutman et al., 2008).

Geological evolution of the Tasiilaq area	
~1680 Ma:	Post-tectonic intrusions - contact metamorphism (Kalsbeek et al., 1993)
1870-1820 Ma:	Collisional stage of orogeny and crustal thickening Folding and thrusting - Interleaving of unrelated lithologies Local granulite facies metamorphism Regional amphibolite facies metamorphism (Nutman et al., 2008)
1867 ± 28 Ma:	Highest observed pressure (11 kbar), high T low P metamorphism (Nutman et al., 2008)
1881 ± 10 Ma:	Intrusion of the AIC coeval high T low P metamorphism (intra-arc metamorphism) (Nutman et al., 2008)
1901 ± 9 Ma:	Intrusion of the diorite-tonalite complex coeval high T low P metamorphism (intra-arc metamorphism) (Nutman et al., 2008)
2015 ± 15 Ma:	Intrusion of metadolerite dykes (Nutman et al., 2008)
2200 - 1900 Ma:	Deposition of the cover sequence (paragneiss protolith) (Nutman et al., 2008)
~2720 Ma:	High grade metamorphic event Disturbance of the northern gneisses U/Pb-ratio (Nutman et al., 2008)
3035 - 2734 Ma:	Intrusion of the TTG gneiss protolith (Nutman et al., 2008)

Table 1. Chronological list of major events in the Tasiilaq area.

In the extreme north, the pods and layers have been disrupted, as the brown orthogneiss becomes the dominant lithology (Chadwick et al. 1989). The brown orthogneisses in the northern area are thought to represent a different terrain at a higher crustal level, which was juxtaposed against the eclogite facies TTG gneiss and the mixed package of supracrustal rocks during the collisional event (Nutman et al., 2008). An overview of the tectonometamorphic and geodynamic evolution can be found in table 1.

3.5. Relation to the Nagssugtoqidian Orogen

There is a close parallelism in ages of rock units and metamorphic events in the Tasiilaq area and the Nagssugtoqidian Orogen of West Greenland, as well as geophysical indications of a common orogenic affiliation, thus the Tasiilaq area is considered the eastern part of the Nagssugtoqidian Orogen (Nutman et al., 2008).

The collisional stage of the orogeny has been dated at 1870 to 1840 Ma in the Tasiilaq area (Numan et al., 2008). Overlapping ages of 1850 to 1840 Ma for regional peak metamorphism was obtained in the western part (Karlsbeek & Nutman, 1996). The ages of the arc suites in Tasiilaq, 1881±10 Ma for the AIC and 1901±9 Ma for the diorite-tonalite complex, overlap with the 1920 to 1870 Ma that have been obtained from zircons of arc suites located in the western Nagssugtoqidian (Karlsbeek &

Nutman, 1996). Metadolerite dykes of Tasiilaq have a minimum age of 2015±15 Ma (U/Pb, zircon), similar to 2036±5 Ma and 2046±8 Ma (U/Pb, zircon) obtained for the Kangâmiut dykes in the Nagssugtoqidian of west Greenland (Nutman et al., 1999). By a combination of previous studies and obtained data, Nutman et al., 2008, suggest that the Nagssugtoqidian orogen belongs to an array of fragmented continental arcs which are assembled by plate tectonic processes during the Paleoproterozoic, to form the continental crust of Greenland.

3.6. Geology of the study area - the Helheim Fjord Synform

Six samples from area A were collected from a 10 m long gossan, set in a synclinal structure (sample 525133, 525134, 525135, 525137, 525138 and 525139 - area A, figure 3). The syncline of the supracrustral association is folded into TTG gneiss. The TTG gneiss which is exposed south of the syncline is finely banded and has a mylonitic texture. The contact zone between the syncline and the TTG gneiss is marked by a sinistral oblique-slip shear zone (foliation: 136/84 (dip direction/dip), stretching lineation: 226/25, Kolb, 2010).

The syncline itself is characterized by paragneisses interleaved with amphibolite and marble. Near the contact zone, a unit of heterogeneous marble, with boudinaged bands of marble containing muscovite, biotite, calcite and orthopyroxenite lenses is found. Sample 525135 is from a orthopyroxenite lens, with quartz veins and pyrrhotite alteration (Kolb, 2010). Lenses of ultramafic rocks are also present in the contact zone (sample 525133, Kolb, 2010). The marble horizon is overlain by a 5-10 m thick amphibolite with quartz-pyrrhotite-biotite alteration and quartz veins. The gossan itself is described as a 10 m wide garnet-muscovite-plagioclase-quartz gneiss with magnetite, garnet and leucosome veins (sample 525137, Kolb, 2010). Garnet-rich parts form lenses, within a circa 6 m long succession of biotite-gneiss (sample 525138, Kolb 2010). Quartz veins and alteration halos surrounding these are common. Sample 525139 is from an approximately 4 meter wide alteration zone of pyrrhotite and garnet surrounds a quartz vein. Amphibolite lenses are also a component in the gossan, and host quartz veins with alteration halos of pyrrhotite and biotite (sample 525134, Kolb, 2010).

The seventh sample was collected in area B, and was submitted for the Ujarassiorit competition in 2011 in which it won (Sample Ujarassiorit). Area B contains rocks of the Síportôq supracrustral association interleaved with TTG gneiss, and thus it appears lithologically resemblant of area A, based on the geological map (figure 3).

4. Methods

The following eight thin sections have been examined with a petrographic microscope and SEM: 525133, 525134a, 525134b, 525135, 525137, 525138, 525139 and ‘Ujarassiorit’. Petrographic microscopy was carried out to establish mineralogy and textural relations. The thin sections 525137, 525138, 525139 and ‘Ujarassiorit’ were selected for microprobe analyses and geothermobarometry, to obtain temperature and pressure conditions by garnet-biotie (GB) geothermometry and garnet-biotite-plagioclase-quartz (GBPQ) geobarometry. Single mineral U/Pb analyses were carried out on thin section 525137, 525138 and 525139 by LA-ICP-MS, to establish geochronology.

4.1. Petrographic microscopy

Petrographic microscopy was carried out on a Zeiss Axioscope 40 in the petrographic laboratory at the Geological Survey of Denmark and Greenland (GEUS). The microscope is fitted with a MRc5 Axiovision digitalcamera, that runs on AxioVision 4.6 software. All photomicrographs were taken using this setup (figure A1 to A16 in appendix A). Mineral abbreviations follow Siivola & Schmid (2007).

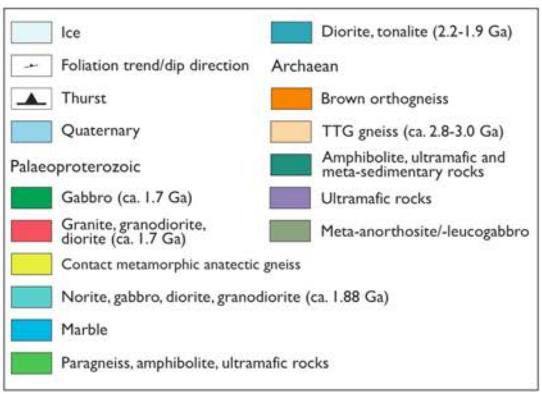

Figure 3. Grønlands Geologiske Undersøgelse (GGU) map 'Skjoldungen' with modification of Kolb, 2010. Geological map of the northern part of the Tasiilaq area, southeast Greenland. Sample location A and B are outlined in circles.

4.2. Secondary Electron Microscopy

Back-Scatter Electron (BSE) imaging and semi-quantitative Energy-Dispersive X-ray Spectroscopy (EDS) analyses were carried out on the Phillips XL 40 SEM at the venues of GEUS. In semi-quantitative EDS the collected spectral data is compared to a internal standard within the computer software system, provided by the manufactures of the EDS system. For further discussion of the method see appendix A, the section on “Secondary Electron Microscopy & Electron Microprobe”.

The following parameters were applied for semi-quantitative EDS analyses:

- 15 sec counting time
- 17 keV accelerating voltage
- 5.5 μm probe diameter (spot size)
- 1.50×10^{-8} A beam current

4.3 Electron Microprobe

Single-mineral quantitative major element analyses were carried out on the JEOL JXA-8200 Superprobe EMP at the Institute of Geography and Geology, the University of Copenhagen. In-house iron- and silicate standards were applied for the Wavelength Dispersive X-ray Spectrometer (WDS) analyses. BSE imaging was carried out on the EMP, and an element map of garnet was obtained, with a processing time of 7 hours and 50 minutes. The garnet was analysed for Mn, Mg, Fe, and Ca. For further discussion of the method see appendix A, the section on “Secondary Electron Microscope & Electron Microprobe”.

The following parameters were applied for WDS analyses:

- 30 sec counting time
- 15 keV accelerating voltage
- 5 μm probe diameter (spot size)
- 1.50×10^{-8} A beam current

The EMP provided wt% oxide data, which is recalculated to cation data for use in the thermo- and barometric models. Cations per formula unit were calculated after Deer et al., 1966, with recalculations of H_2O/Al in biotite after Tindle and Web (1990) and recaclulations of Fe^{2+}/Fe^{3+} in garnet after Droop, 1987 (appendix D). For the recalculation to cations per formula unit I have assumed:

- All Fe is Fe^{3+} substituting for Al in plagioclase
- Fe is the only element present with variable valency in plagioclase
- Oxygen is the only anion in plagioclase and garnet
- The cation sites are full in all applied minerals

The geobarometer of Wu et al. (2001) has been applied to thin section 525138. Thermobarometers of Thompson (1976), Holdaway & Lee (1977), Ferry & Spear (1978), Perchuk & Lee (1983), Dasgupta et al. (1991), Bhattacharya et al. (1992), Holdaway (2000), have been applied to both thin section 525138 and the Ujarassiorit thin section.

4.4 Laser Ablation Sector Field Inductively Coupled Plasma Mass Spectrometry

All U/Pb measurements were carried out in the laboratory at GEUS by Element2 Sector Field Inductively Coupled Plasma Mass Spectrometry (SF-ICP-MS) running a New Wave UP 213 Laser Ablation (LA) system, following the procedures of Frei & Gerdes (2009). The GJ-1 zircon standard was applied as the external standard, and the Pleŝovice zircon was used as reference standard. Zircon standards were used for all analysed mineral species. Data reduction was done using the GEUS in-house software Iolite, which is Igor Pro 6.22A-based. For further discussion of the method see appendix A, the section on “Laser Ablation Inductively Coupled Plasma Mass Spectrometry”.

The following parameters were applied:

- 25 μm laser beam diameter (E ~ 10 J/cm^2)
- 5 Hz repetition rate
- 30 sec. counting time
- 30 sec. laser beam warmup
- 20 sec. washout time (pre-ablation)

The the calculated ages are based on selected proportions of the isotope signal (figure A24 in appendix A). Out of the twenty two successful analyses seven were corrected for common Pb. Common Pb is corrected for by the use of the ^{202}Hg, where the constant of $^{202}Hg/^{204}Hg$ is used to determine the proportion of ^{204}Pb in isotope mass 204. The isotopic composition of all lead is then corrected accordingly. Corrections of common Pb is also based on a visual interpretation, as an average of the often erratic signal is used (figure A24 in appendix A).

5. Results

The metamorphic rocks are described and named after the recommendations by the IUGS subcommission on the systematics of metamorphic rocks (Schmidt et al., 2007).

The samples constitute a pyroxene garnetite (‘Ujarrasiorit’-sample), an ultramafic rock (sample 525133), an amphibolite (sample 525134) an orthopyroxenit (sample 525135) and three garnet-graphite paragneisses (sample 525137, 525138 and 525139). All samples are surface-samples and appear weathered. The Ujarassiorit sample is from location B and all other samples are from location A (figure 3). Further descriptions of thin sections can be found in appendix B.

5.1 Description of rock samples

Pyroxene-garnetite - the ‘Ujarassiorit’-sample

Sample name: BMP vjar. 2011-0092

The pyroxene-garnetite is a a dark grey, holocrystalline, fine-grained (0.5mm-2mm), equigranular rock. It appears slightly foliated as brown biotite forms noncontinuous foliation of 0.3 to 0.5 mm across. Biotite makes up 5-7 vol%, as platey subhedral grains of up to 2 mm across. Biotite which has been found as inclusions in garnet is both greenish-brown and brown, whereas biotite found throughout the sample is only brown.

Garnet is the most abundant mineral and makes up approximately 60-65 vol%. It appears reddish-brown and both as a ground mass as well as in vein-like structures (veins are 0.6 mm across). Black subhedral prismatic pyroxenes constitute 20-25 vol% as grains of 1-2 mm. Pyrrhotite cannot be recognized in the hand sample, due to secondary alteration. It constitutes <3 vol% and is present as anhedral crystals of 0.2-1 mm across. K-feldspar appears similar to quartz but is more abundant and displays polysynthetic twinning (<1vol%, grains <0.5 mm).

Graphite is present throughout the sample as fibrous grains of up to 2 mm across and makes up 2-4 vol%. It seems to be slightly more frequent near the biotite-rich floiation. Accessory phases include muscovite (<0.2 mm) and subhedral quartz grains (<0.4 mm). Hematite is found in micro cracks and veins (≦0.3 mm across) throughout the sample.

Ultramafic rock of the supracrustral association

Sample name: 525133

The ultramafic rock is a dark greenish grey, holocrystalline, aphanitic and very fine-grained rock. It is relatively dense and it is magnetic. At the fresh cut surface it is possible to see black, branch-like veins (1-1.5 mm across) which are cut by silvery veins (<1mm across). The veins are subparalel and oriented perpendicular to a weathered rusty surface. The veins consists of chlorite, but chlorite is also present as anhedral grains (figure A2 and A3 in appendix A). Chlorite makes up 5-10% of the entire sample. Tiny grains (up to 0.03 mm) of pyrrhotite and pyrite are found in the center of the veins, and these chlorite grains have bands of pyrrhotite (figure A4 in appendix A). Pyrrhotite and pyrite is also disseminated throughout the sample (both <0.4 mm). Subhedral olivine grains of less than 0.5 mm across constitute 70-80 vol% of the sample. Amphibole is present as 0.3-0.6 mm long euhedral grains and makes up 10-15% of the mode. Plagioclase with polysynthetic twinning is anhedral, up to 0.3 mm across and makes up 2-3 vol%. Spinel is present as euhedral crystals of <0.7 mm across and makes up 3-5vol%. of the sample Pyrrhotite is common at the rim of spinel grains. Graphite occurs as an accessory mineral, yet fibrous crystals of up to 0.5 mm has occationally been observed.

Amphibolite of the supracrustral association

Sample name: 525134, thin section 525134a and 525134b

The amphibolite is a dark green holocrystalline rock, with two distinct parts. The rock has an upper brown vuggy part (2.5 cm) which is separated from the lower green, holocrystaline part (1.5 cm) by a thin discontinuous white band (3 mm across). The brown section where vugs of 0.5-2 mm across are found, does not hold any sulfides as these have been leached by supergene alteration. The holocrystalline green part generally has 1-2% disseminated pyrrhotite and pyrite (1-4 mm in size), yet locally pyrite grains of up to 1 cm are present (thin section 525134b). The grain size in the brown part of the sample is finer than in the green part (1-3 mm), though the mineralogy of the two parts are otherwise the same. The sample is dominated by a euhedral elongated green hornblende crystals which are 1-4 mm long and constitute 50-60 vol%. Elongated and euhedral clinopyroxenes appear similar to the amphibolites in size, but constitute only about 2-3 vol%. The elongated hornblende and clinopyroxene are orientated parallel to the foliation. Plagioclase with polysynthetic twinning forms subhedral crystals of <3 mm across and makes up 20-30% of the mode. Alkali feldspar is also present as subhedral crystals, but constitutes only a few vol%. Veins of goethite are common in thin section 525134a, and associated with euhedral magnetite grains of 0.5-2 mm across (figure A4 in appendix A). The largest vein is approximately 1 mm across and appears in the lower green part of the sample where goethite and magnetite make up 2-3 vol% of the sample. Magnetite is also found as a mineral separate to the veins, but often appear altered (figure A5 in appendix A). Ilmenite, chalcopyrite and apatite are present as accessory phases, and found in the local mineralization represented by thin section 525134a, along with the largest pyrite crystals.

Orthopyroxenite of the supracrustral association

Sample name: 525135

The orthopyroxenite is a dark greyish-green holocrystalline, medium grained (1-5 mm) rock. Rusty veins and vugs are found at the cut surface. The vugs are 1-2 mm across, but frequent, vein-like vugs are 4-7 mm long and <1mm wide. In the proximity of the vugs the grain size is fine (<0.5mm to 1mm), whereas is fine to medium grained (1mm-5mm) in massive parts. Green euhedral pyroxenes of 2-5 mm in length constitute 95-97 vol% of the rock. Amphibole constitutes only a few percent of the mode, and generally has a smaller grain size (1-3 mm). The amphiboles and pyroxenes are both parallel to the foliation. Sub- to anhedral grains of plagioclase grains (<1-3 mm) make up 3-5 vol% of the rock. Hematite and graphite are present but as accessory phases (figure A6 in appendix A).

Paragneisses of the supracrustral association

Sample name: 525137, 525138 and 525139

The garnet-graphite gneiss is rusty grey, holocrystaline, fine- to medium grained (1-4 mm) and foliated. The foliation varies in color from dark brown to rusty beige, and varies in size from a few mm to approximately 2 cm. The foliation is slightly wavy and often pinches out. The foliation planes are highlighted by brown euhedral biotite grains of 2-4 mm in length, which constitute 15-30 vol% of rock. The lighter foliation planes are dominated by quartz and feldspars.

Quarts constitutes 20-40% of the mode, forms sub- to anhedral grains of 0.5-4 mm across and locally displays undulatory extinction. Plagioclase makes up 15-25 % of the sample and is commonly of a larger grain size than quartz (1 to 4 mm). It commonly displays polysynthetic twinning (figure A16 in appendix A). Myrmekite can be found in thin section 525137 (figure A7 in appendix A). Alkali feldspar is resemblant to plagioclase in size, but appears in three different ways; with no twinning, with cross-hatch twinning and with karlsbad twinning. It makes up 5-10 vol%.

Sulfide minerals are associated with biotite, thus these are locally more abundant. Both pyrrhotite and pyrite are present, but pyrite constitutes less than 1 vol% whereas pyrrhotite makes up 1-3 vol %. Pyrrhotite often appears in structures where subhedral grains are surrounded by smaller grains of pyrrhotite (<2 mm, figure A12 and A13 in appendix A). Chloritization of biotite is extensive and most biotites are to some degree affected (figure A14 in appendix A). Rutile exolution-needles are common in biotite where chlorite-alteration is pronounced. The rutile needles are at µm-scale and is an accessory phase. Chlorite makes up 3-10% of the modus. Muscovite is associated with both chlorite and quartz veins, where they form euhedral grains of 0,2-1 mm. They are often found in ‘sandwich’-structures, where chlorite-biotite-muscovite and graphite are interlayered (figure A16 in appendix A). Muscovite constitutes only a few percent of the total modus. Graphite is present as euhedral fibrous grains of 0.5-2 mm throughout the gneiss. It is more abundant in the proximity of biotite, though it make up only about a percent of the modus. Dark red subhedral grains of garnet is found in hand sample 525138 (figure A8 and A9 in appendix). It is unevenly distributed, 0.5-2 mm across and in thin sections it appears highly fractured. Inclusions of pyrrhotite, graphite and olivine have been observed in garnet. Most garnets are only weakly zoned (figure 4 and 5, see section ‘Element Maps’). Garnets make up 1-2 vol% in thin section 525138. The accessory mineral monazite is more abundant than accessory zircon, and has anhedral grains of up to 0.3 mm. It commonly has a halo of euhedral pyrite crystals (figure 16, and figure A18 and A20 in appendix A). Xenotime, titanite and apatite are also present as accessory phases.

All the observed minerals are listed in table X, according to thin section number. BSE images with pointers at analysed sites, EDS spectra and semi-qualitative data for all analysed samples can be found in appendix D.

Group	Mineral	**Uja.**	**525133**	**525134a**	**525134b**	**525135**	**525137**	**525138**	**525139**
Silicates	Qz	x		x	x		x	x	x
	Pl	o	o	x	x	o	x	x	x
	Afs	o		x	o		o	x	x
	Bt	x		x	x		x	x	x
	Ms						o	x	o
	Chl		x				o	x	o
	Ol		x					(x)	
	Grt	x			x*			x	
	Hbl		x	x	x	o			
	Opx	x	x			o			
	Cpx	x		x	o				
	Ttn							x*	
	Zrn	o			o		x	x	x
Phosphates	Xtm							x	
	Mnz						x	x	x
	Ap	x		x				x	
Sulfides	Py	x	x	x			x	x	x
	Po	x		x	x		x		x
	Ccp			x					
Oxides	Spl		x						
	Rt							x	
	Ilm			x					
	Fe-ox	o	x	x	x	o	o		
	Al-ox	x*							
Native elements	Gr	o	o		o	o	o	o	o

Table 1. Mineral content of the thin sections. x = mineral observed in thin section and/or in WDS/EDS. When the x is in brackets, it has only been observed as an inclusion in garnet using SEM/EDS (Appendix C). When an x is marked with an * it has only been found using EDS on the electron micrprobe, and is not represented in appendix C. o = mineral observed by petrographic microscope only (appendix B).

5.2 Mineral chemistry

The garnets of the paragneiss are almandines, commonly high in Mn (~10wt%, appendix D). An element map was obtained of one of the largest grains in thin section 525138. The garnet was analysed for Mn, Mg, Fe, and Ca (in order; figure 4, 5, 6 and 7). The EMP/WDS map displays zoning in Mn/Mg (figure 4 and 5).

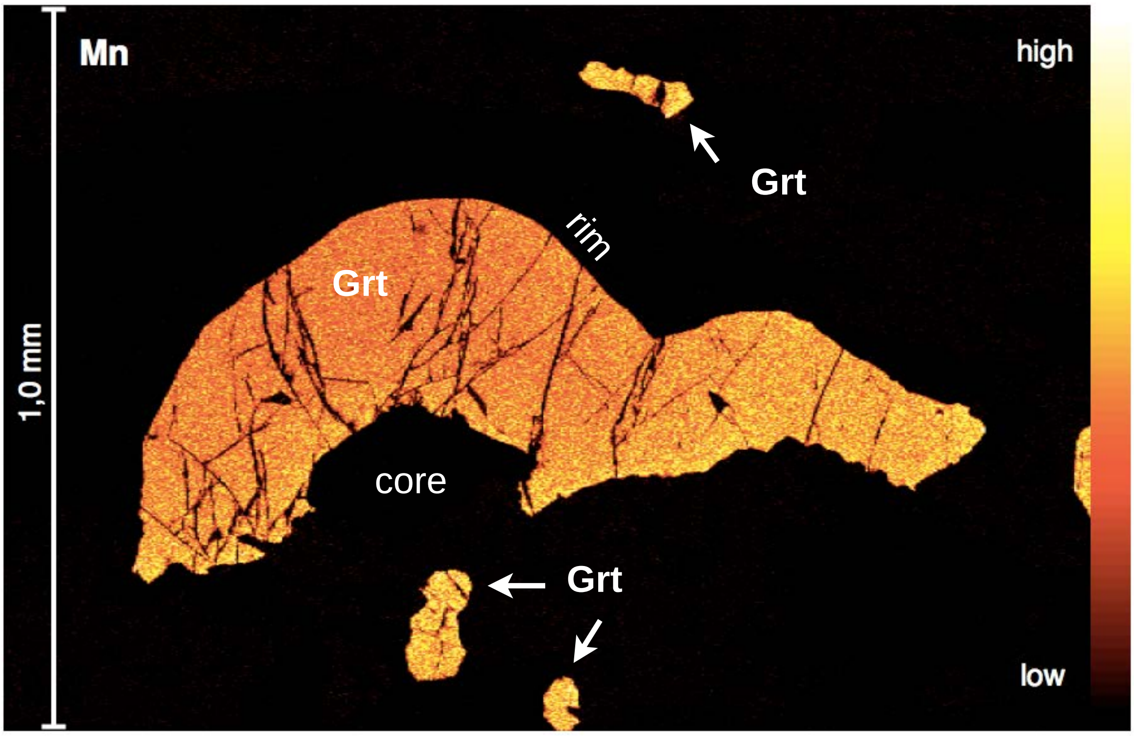

Figure 4. EMP element map for Mn in a garnet from thin section 525138. A core and a rim section of the grain has been interpreted on the basis of the grains morphology.

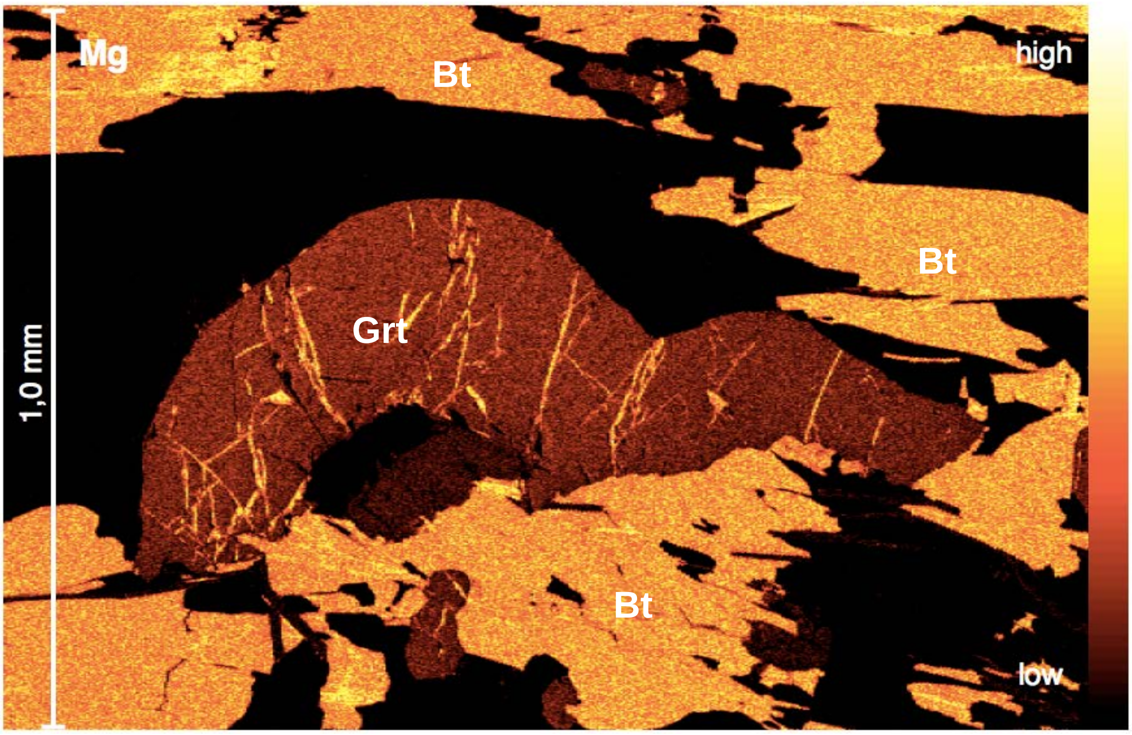

Figure 5. EMP element map for Mg in a garnet from thin, thin section 525138.

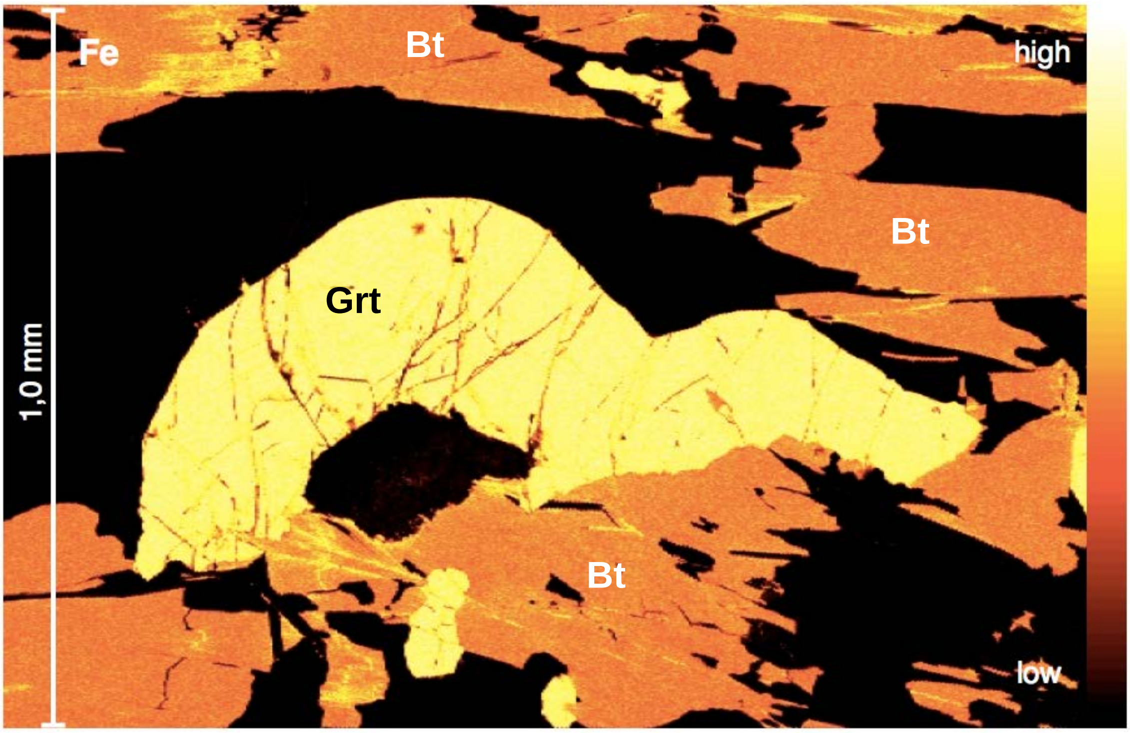

Figure 6. EMP element map of Fe in a garnet from thin, thin section 525138.

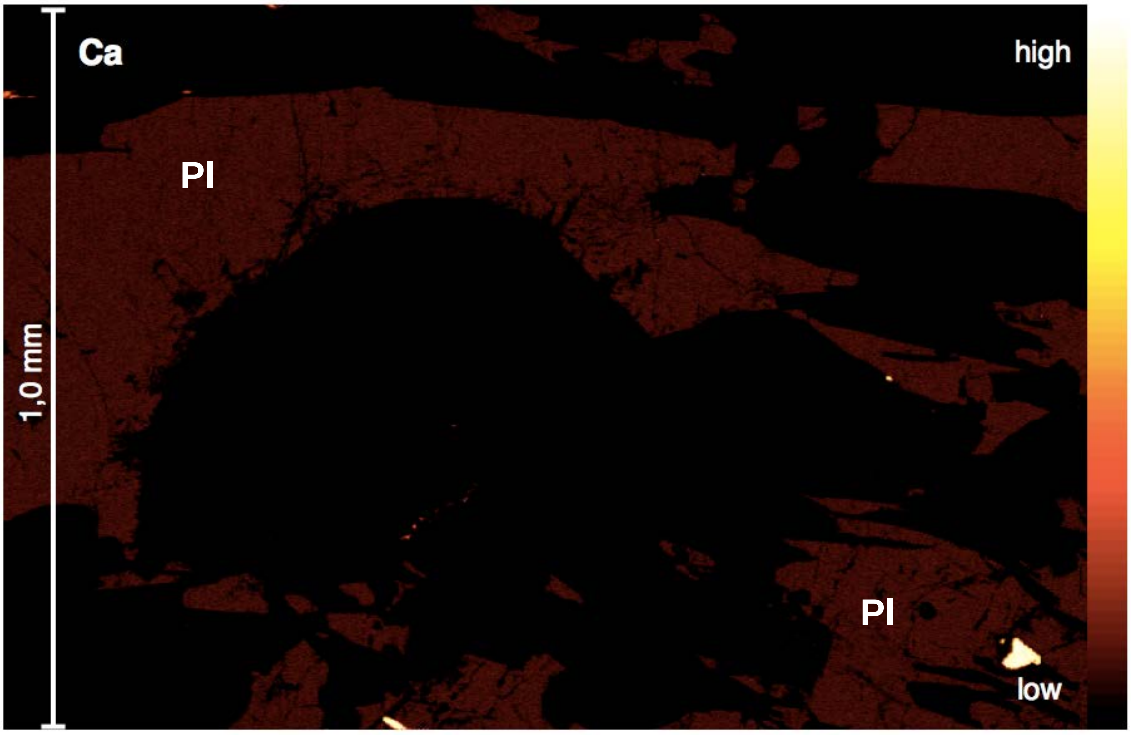

Figure 7. EMP element map of Ca in a garnet from thin, thin section 525138.

End-member calulcations for the garnets of the paragneiss show variations from 63,1 to 65,3 in almandine, 14.7 to 20.8 in spessartine, 11.06 to 15.9 in pyrope and 4.4 to 4.8 in grossular.

Garnet is omnipresent in the garnetite-sample. The garnet-analyses from the Ujarassiorit thin section have been divided into two groups on the basis of chemistry. The Mn-rich garnet group shows variations from 55.1 to 58.9 in almandine, 21.1 to 24.3 in spessartine, 6.3 to 7.9 in pyrope and 11.6 to 16.0 in grossular. The Mn-poor garnet group show variations from from 64.6 to 65.2 i almandine, 15.7 to 16.4 in spessartine, 8.8 to 9.0 in pyrope and 10.0 to 10.2 in grossular. The garnets from the garnetite are generally Mn-rich (~10wt%) like the garnets from the paragneiss, but they are generally higher in Ca (~5 wt%, approximately 3wt% more). All analyses and endmember calculations can be found in appendix D.

Biotite occurs as a mineral in the hydrothermal stage, as well as in both of the metamorphic stages, in the pyroxene-garnetite and paragneiss-group (figure 12). Thus a groups of various composition was expected. In the paragneiss group the composition of biotites are fairly consistant within the seperate samples, but in general they have a spread in endmember-composition from ~35-50 in annite to ~50-65 in phlogopite (appendix D). The biotite in the garnetite-sample also show a fairly constant composition at ~56-70 in annite and ~30-44 in phlogopite (appendix D). No groupings are present within the composition of biotite, in any sample.

Plagioclases were also analysed. End-member calculation yielded low variation with the group of paragneiss thin sections (thin section 525137, 525138 and 525139). The albite end-member yields the highest values at 62,9 to 73,0 for all three thin sections, the anorthite comes in second at 25,8 to 35,7 and only 0,8 to 2,1 are ascribed to the orthoclase end member (appendix D).

Fe was the only metal present in the pyrrhotite mineral lattice in pyrrhotite-bearing thin sections, at the scale of the resolution which the EDS/SEM provided (appendix C). Variation in the chemistry of pyrrhotite could be viewed in BSE-images (figure A17 in appendix A), but has not been reflected in EDS-analyses (appendix C). All single-mineral WDS-analyses, recalulations and end-member calculations can be found in appendix D.

5.3 Paragenetic sequence diagrams

The paragenetic sequence has been established on the basis of textural relations observed in microscope and in SEM (figure 8-12, appendix A, appenidix B).

The first stage metamorphic assemblage of the garnetite constitutes amphibole, orthopyroxene, clinopyroxene and biotite (Figure 8). The pyroxene is substituted by amphibolite. Garnet becomes omnipresent in the second metamorphic stage (M2), with amphibole and biotite as minor phases. The hydrothermal stage is characterized by biotite and the presence of iron sulfides, as well as graphite and minor amounts of apatite and quartz. Pyrrhotite is substituted by graphite, occasionally extensively so (figure A1 in appendix A). Both brown and green biotite is present as inclusions in garnet. The green biotite is fairly uncommon. Brown biotite is present throughout the thin section. Graphite is more abundant in the garnetite sample, than in any other sample. Three stages have been established for the garnetite sample; a metamorphic stage 1 (M1), a metamorphic stage 2 (M2), and a hydrothermal stage (figure 8).

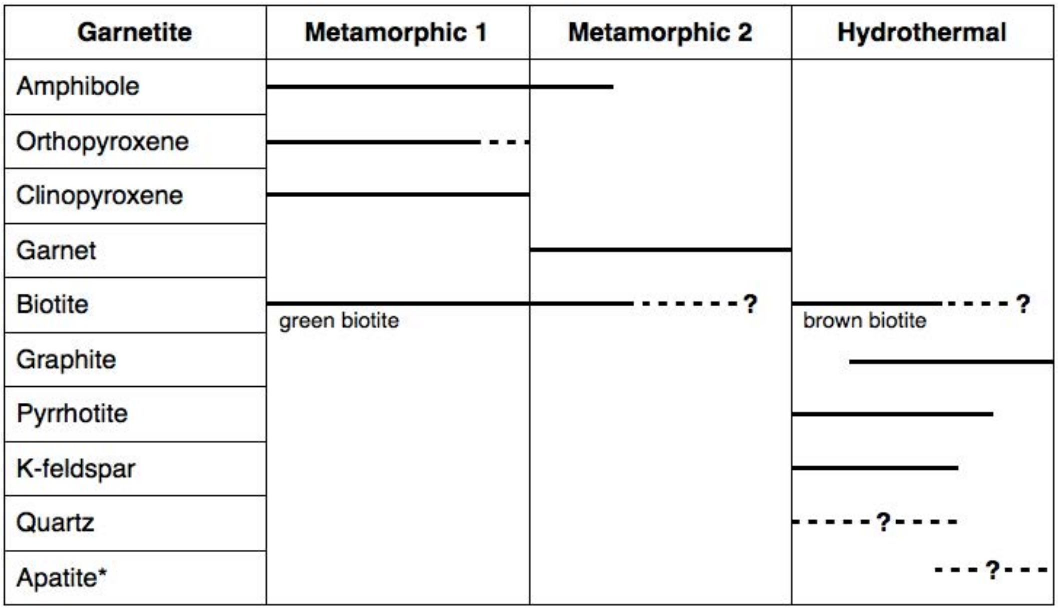

Figure 8. Paragenetic sequence diagram for the garnetite. The samples marked with an asterisk minerals which have only been observed in SEM/EDS. Dashed lines mark uncertainties within the paragenetic sequence.

The ultramafic rock has a metamorphic stage 1 assemblage of olivin, amphibole and orthopyroxene (M1). Amphibole and orthopyroxene substitutes for olivine. Green grains of spinel substitutes the M1 assemblage generally, and often has rims of pyrite as it is in turn substituted by the hydrothermal mineral assemblage. The hydrothermal alteration is characterized by extensive chloritization (figure A2 in appendix A). Pyrrhotite and Fe-oxides are also present during the hydrothermal stage. Graphite is present throughout the hydrothermal stage. The ultra mafic rock has three paragenetic stages; a metamorphic stage 1, a metamorphic stage 2 and a hydrothermal stage (figure 9).

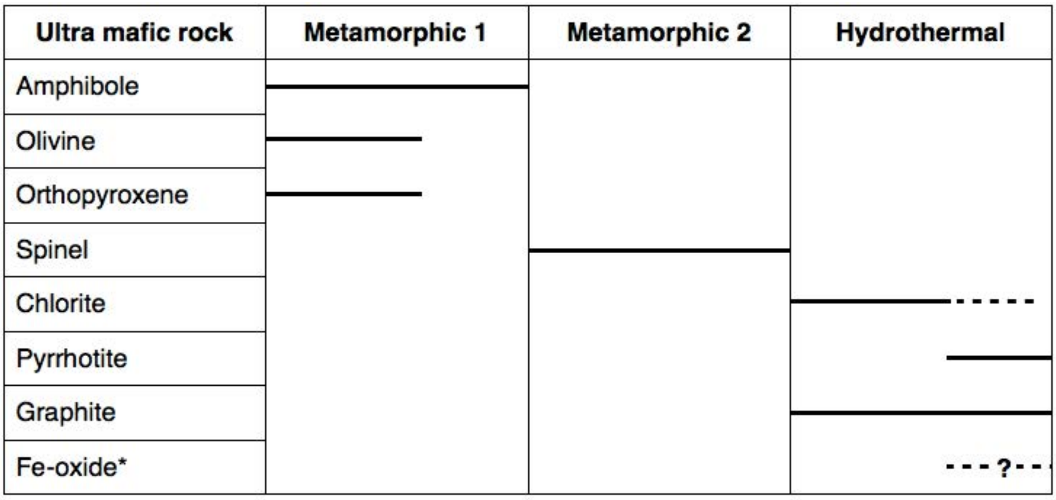

Figure 9. Paragenetic sequence diagram for the ultra mafic rock. The Fe-oxide is marked with an asteriks, as it has only been observed in SEM/EDS. Dashed lines mark uncertainties within the paragenetic sequence.

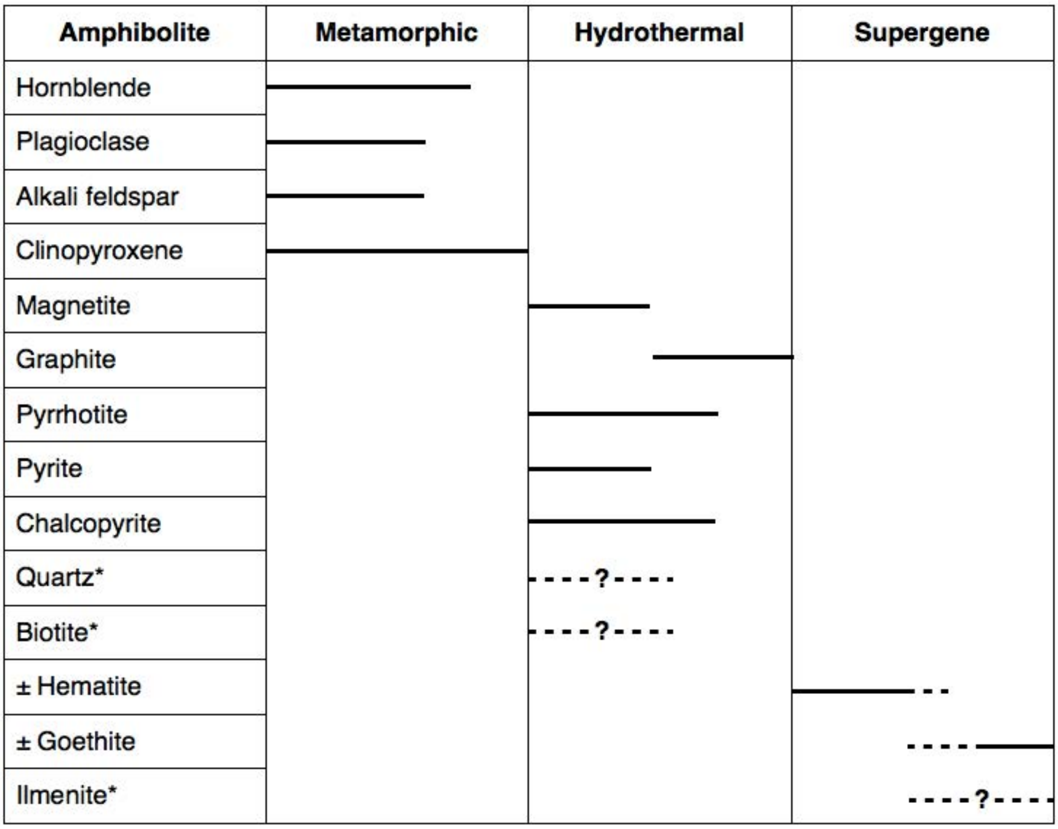

Figure 10. Paragenetic sequence diagram for the amphibolite. The asterisk marks minerals which have only been observed in SEM/EDS. Dashed lines mark uncertainties within the paragenetic sequence. A mineral is marked ± if it has only been observed in on of the thin sections.

The metamorphic assemblage of the amphibolite constitutes clinopyroxene, hornblende, plagioclase and alkali-feldspar. The feldspars share mineral boundaries, and no crossing-relations have been observed. Both are substituted by hornblende and clinopyroxene. Clinopyroxene and hornblende also formed at the same time, since they share mineral boundaries, yet clinopyroxene substitutes hornblende occationally. The hydrothermal alteration is characterized by extensive pyrrhotite and pyrite alteration (figure A4 and A5 in appendix A). Magnetite is a minor Fe-bearing mineral present during the hydrothermal stage, and often appears to be altered to pyrite (figure A5 in appendix). Quartz and biotite have only been found with SEM/EDS, and are only present as trace minerals. Hematite, and goethite are present in the supergene stage. These often form veins, where hematite is at the side of a goethite rim (figure A4 in appendix A). Ilmenite was found using EDS, and appeared to be related to the supergene alteration (table 2). The amphibolite has three paragenetic stages; a metamorphic stage, a hydrothermal stage and a supergene stage (figure 10).

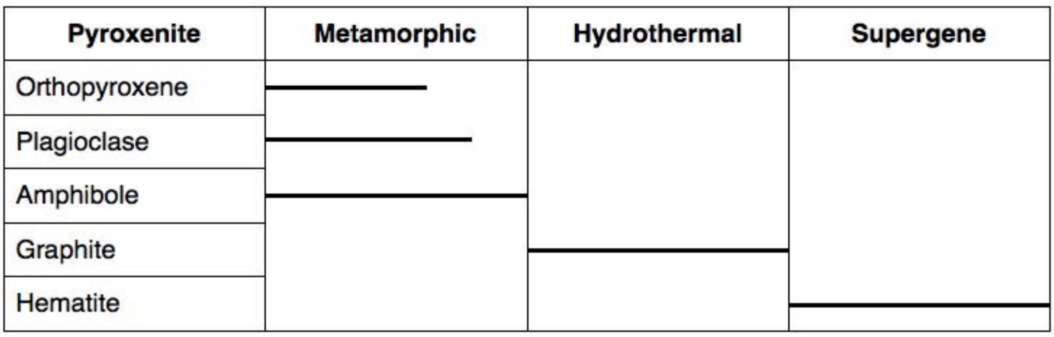

Figure 11. Paragenetic sequence diagram for the pyroxenite.

The pyroxenite sample is the least altered of all the samples. Orthopyroxene is the ‘canvas of the sample’, as it is by far the most abundant and replaced by all other minerals in the assemblage. Plagioclase and amphibolite are sparse and rarely in proximity, yet plagioclase substitutes plagioclase locally. Hematite has been ascribed to a supergene stage following the finds in sample 525134, but it is possible that it belongs to the hydrothermal stage (figure A6 in appendix A). The pyroxenite has three paragenetic stages; a metamorphic stage, an hydrothermal stage and a supergene stage (figure 11).

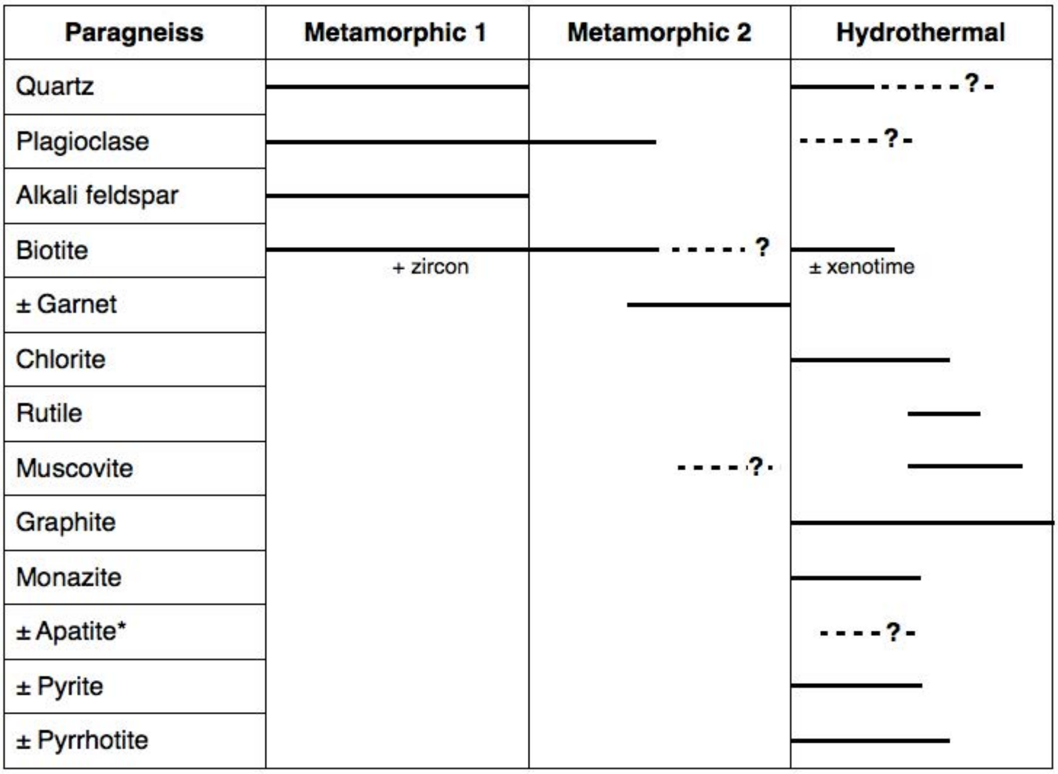

Figure 12. Paragenetic sequence diagram for the paragneiss-group; thin section 525137, 525138, 525139. The asterisk marks minerals which have only been observed in SEM/EDS. Dashed lines marks uncertainties within the paragenetic sequence. A mineral is marked ± if it not observed in all thin sections of the series.

A common paragenetic sequence is suggested for the paragneisses (figure 12). The metamorphic assemblage is characterized by quartz, alkali-feldspar, plagioclase and biotite (M1). Quartz and alkali feldspars have only been observed as boundary-sharing minerals. Both minerals also share boundaries with plagioclase and feldspar, but are also replaced thereby. Plagioclase and biotite have both been found as inclusions in garnet and biotite occasionally shares a mineral boundary with garnet (M2). The garnets are commonly poikiloblastic. The grain size of the inclusions can make it hard to determine the mineralogy, yet muscovite may be present as an inclusion mineral in garnet.
The hydrothermal stage is characterized by extensive chloritization of biotite, and secondary exolution of rutile-needles (figure A14 in appendix A). ‘Sandwich-structures’ where muscovite, graphite and biotite have been interlayered are common (figure A16 in appendix A), but all are also present as independent minerals. Biotite is present in two stages. Zircon is common as an inclusion in early biotite of the magmatic stage. Xenotime has been identified (SEM/EDS), within a biotite of the hydrothermal stage (a biotite associated with muscovite). Monazite is present within plagioclase and on occasion also in biotite of the hydrothermal stage. It commonly has haloes of pyrite (figure 14). Graphite is omnipresent within the rock, at the hydrothermal stage. It seems to have a slight association with hydrothermal muscovite (figure A10 and A11 in appendix A). Three paragenetic

stages have been identified for the paragneiss; a metamorphic stage 1, a metamorphic stage 2 and a hydrothermal stage (figure 12).

5.4 Geothermobarometry

Thin section 525138 is the only garnet-bearing thin section in the paragness-group. Grt-Bt-Pl data from the paragneiss was used to estimate temperature and pressure (appendix D); a pressures of ~5279 bar (Wu et al., 2004, table A1 in appendix A) and a temperatures of ~460-640℃ (table A1 in appendix A) was obtained. The temperature for the pyroxene-garnetite was calculated using the pressure from the paragneiss, as the composition of the garnets in the two samples are similar and as they appear to be from (appendix D). Temperatures of ~500-660℃ was obtained. Changing the pressure by ±1 kbar yields a ~4°C deviation in temperature. Garnet analyses from the Ujarassiorit sample have been seperated into two groups; Mn-poor and Mn-rich. Due to the complex morphology of the garnets it was not possible to establish whether the analyses was done on cores or rims of grains.

Eight geothermometers have been applied for reference purposes, to both samples (figure 13). Both samples display a variations in model temperatures of ~170℃ (table 1, appenix A).

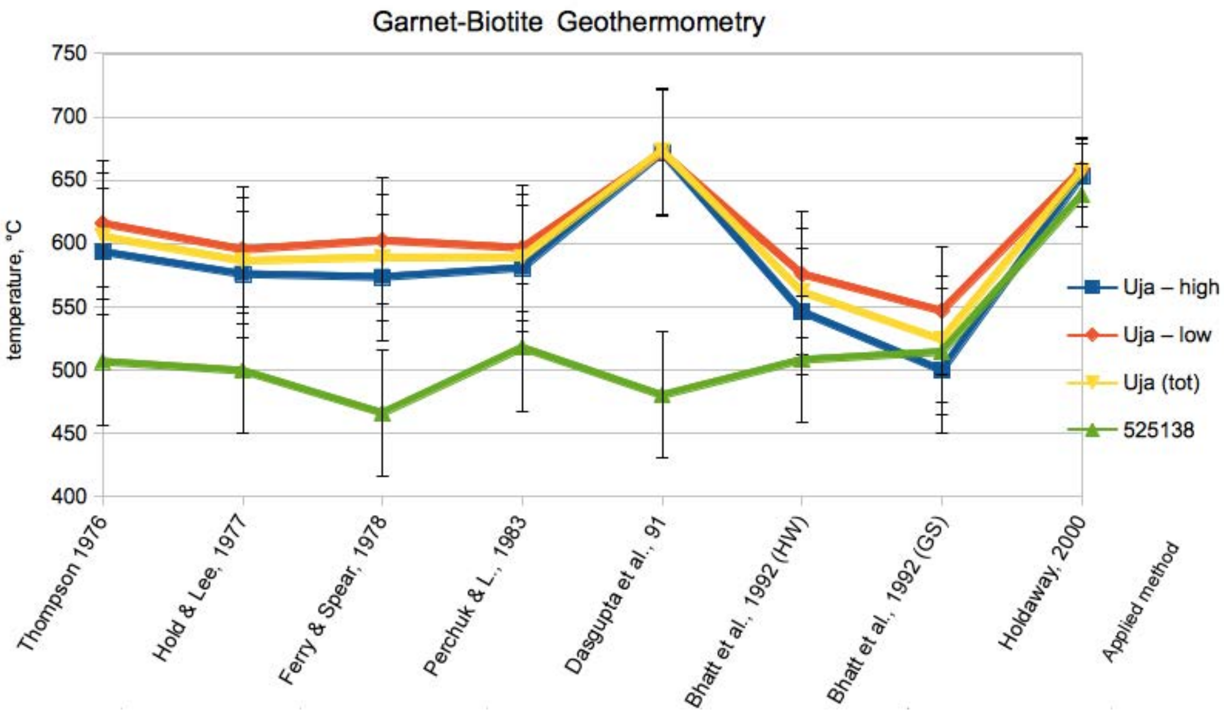

Figure 13. Comparison of the calculated GB temperatures for the Ujarassiorit thin section and thin section 525138 (paragneiss). Uja = Ujarrasiorit thin section, 'high' is the Mn-rich group, 'low' is the Mn-poor group. Uja (tot) is an average of all obtained analyses of garnet in the Ujarassiorit thin section. Temperatures were calculated after: Thompson, 1976, Holdaway & Lee, 1977, Ferry & Spear, 1978, Perchuk & Lee, 1983, Dasgupta et al., 1991, Bhattacharya et al., 1992, Holdaway, 2000. The model error has been added as error-bars to the graph; for Holdaway, 2000, an error bar of ±25℃ has been added, for all other thermometers an error bar of ±50℃ has been added. The temperatures can be found in a table A1, in appendix A.

5.5. Geochronology

BSE-bright accessory minerals of more than 25μm were targeted for EDS-analyses on the EMP, as it was discovered that the paragneisses were rich in accessory monazite. Out of 29 analysed minerals 27 turned out to be monazite, a single zircon and a single xenotime (analyses carried out on EMP after MS). Many of these have grain sizes of more than 25μm and grains of up to 0.3 mm are common (figure 14). Monazites are frequently found in plagioclase and occasionally found in biotite (figure 14, biotite: figure A22 in appendix A). Many of the monazites have rims of euhedral pyrite (figure 16). These can be seen as 'fuzzy' BSE-bright haloes of all the monazites in figure 14. The monazites are commonly zoned, though at various extends (figure 15 and figure A18 and A21 in appendix A).

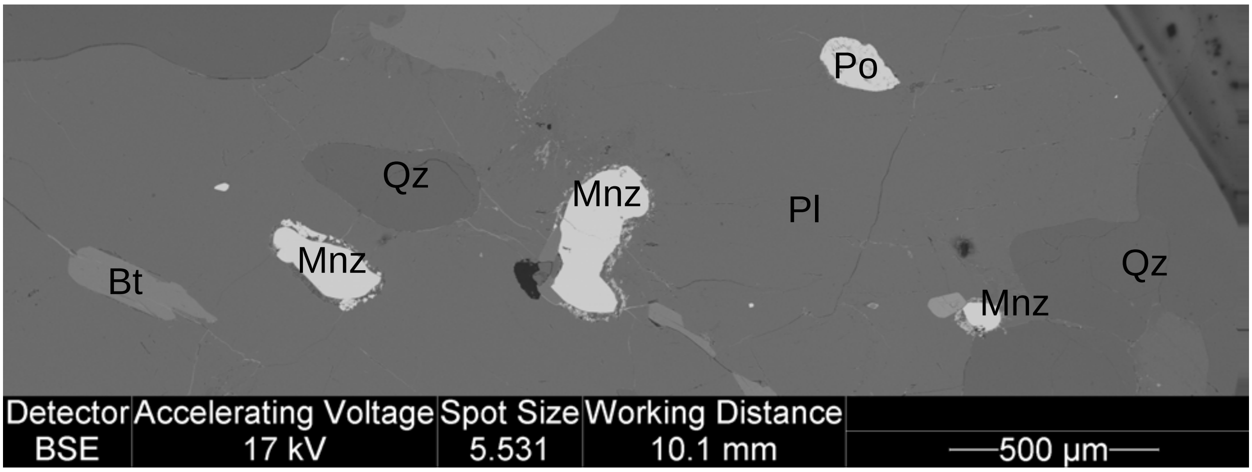

Figure 14. Example of monazite grains with pyrite rims in plagioclase, thin section 525137 (paragneiss).

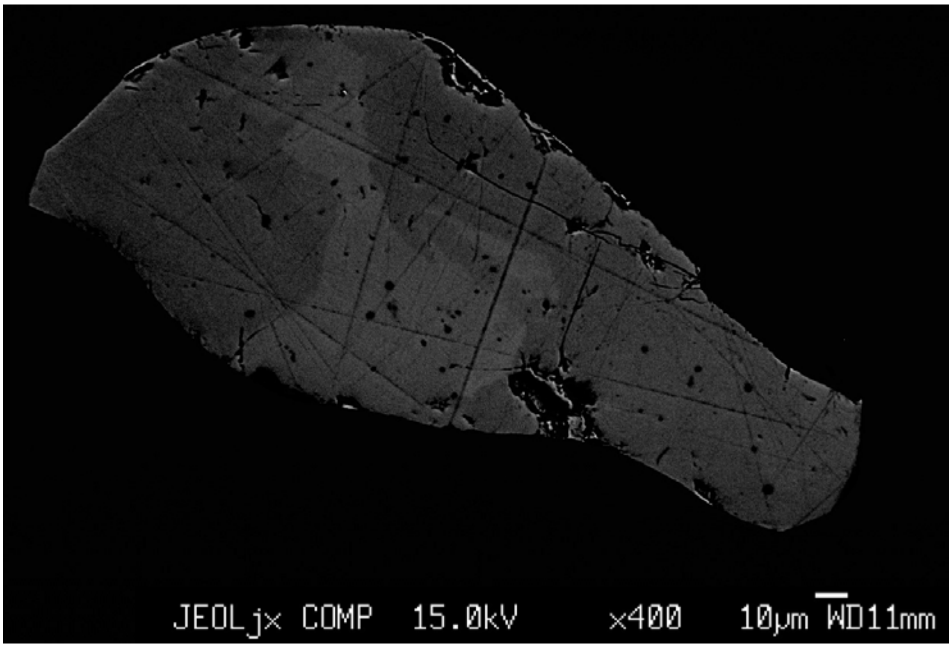

Figure 15. Example of zoning (heterogenity) of monazite, thin section 525137 (paragneiss).

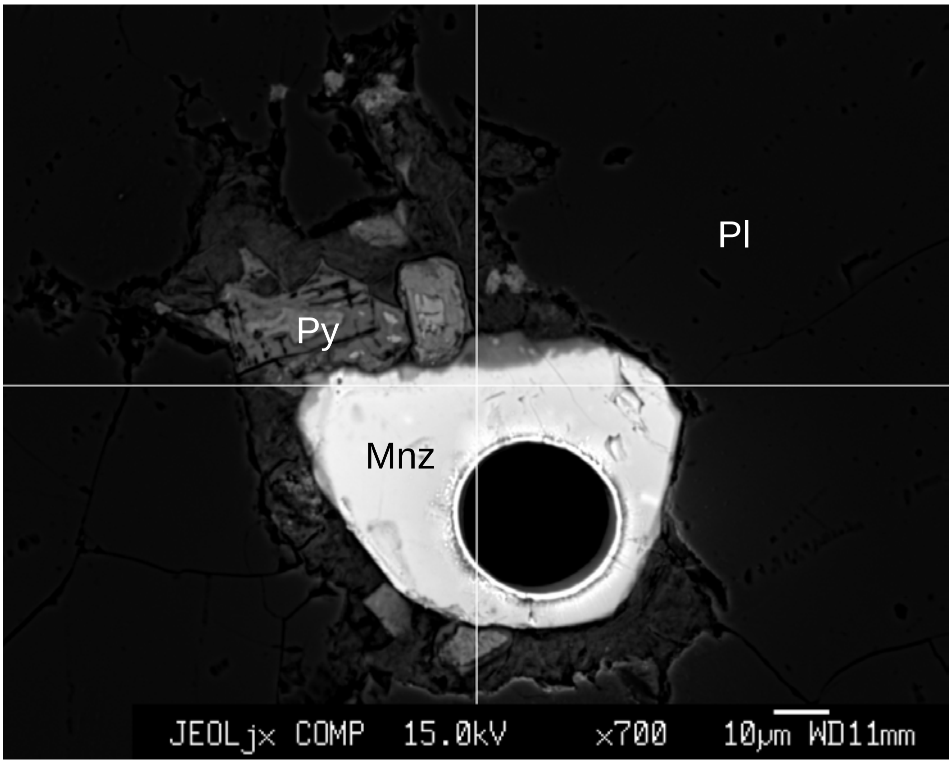

Figure 16. Example of a pyrite halo of a monazite in thin section 525138 (paragneiss). The hole in the middle of the monazite is from LA-ICP-MS.

Monazite, xenotime and zircon was used in U/Pb dating by LA-ICP-MS. Monazite was the only mineral species to be analysed in thin sections 525137 and 525139, where as a single zircon and a single xenotime was also analysed in thin section 525138 (appendix E).
The analysed zircon provided an $^{207}Pb/^{206}Pb$ age of 1803±23 Ma (appendix E). The youngest obtained age is from a xenotime in sample 525139, at 1723±60 Ma (appendix E). The monazites provided a span in ages from 1752±22 Ma to 1961±47 Ma (figure 17, appendix E), with the majority of the ages occurring between 1850 Ma and 1750 Ma (17 out of 22 U/Pb monazite ages). Monazites from sample 525138 did in general provide a greater span of ages (~136 Ma, versus ~30 Ma in 525137 and ~40 Ma in 525139) than the other two rocks. A data table of all obtained LA-ICP-MS U/Pb analyses can be found in appendix E. Not all analyses were corrected for common Pb, but those that are have ages similar to uncorrected ages, and the correction is thus considered valid (appendix E)
The obtained LA-ICP-MS analyses have been plotted in Terra-Wasserburg diagrams, to display the level of concordance (figure A24, A25 and A26 in appendix A). The highest level of discordance is found in specimens from thin section 525138 (figure 17), yet most analyses are concordant within the 2SE uncertainty (appendix E). As displayed in figure A24, A25 and A26 in appendix A, all ages have a discordance of less than 10%.

Seven samples have been corrected for common Pb. The analyses have 2-3% common lead (figure A24 in appendix A, and appendix E). Pb-correction of monazites generally yield older ages, but in 3 out of 7 analyses the correction are within the original error (appendix E).

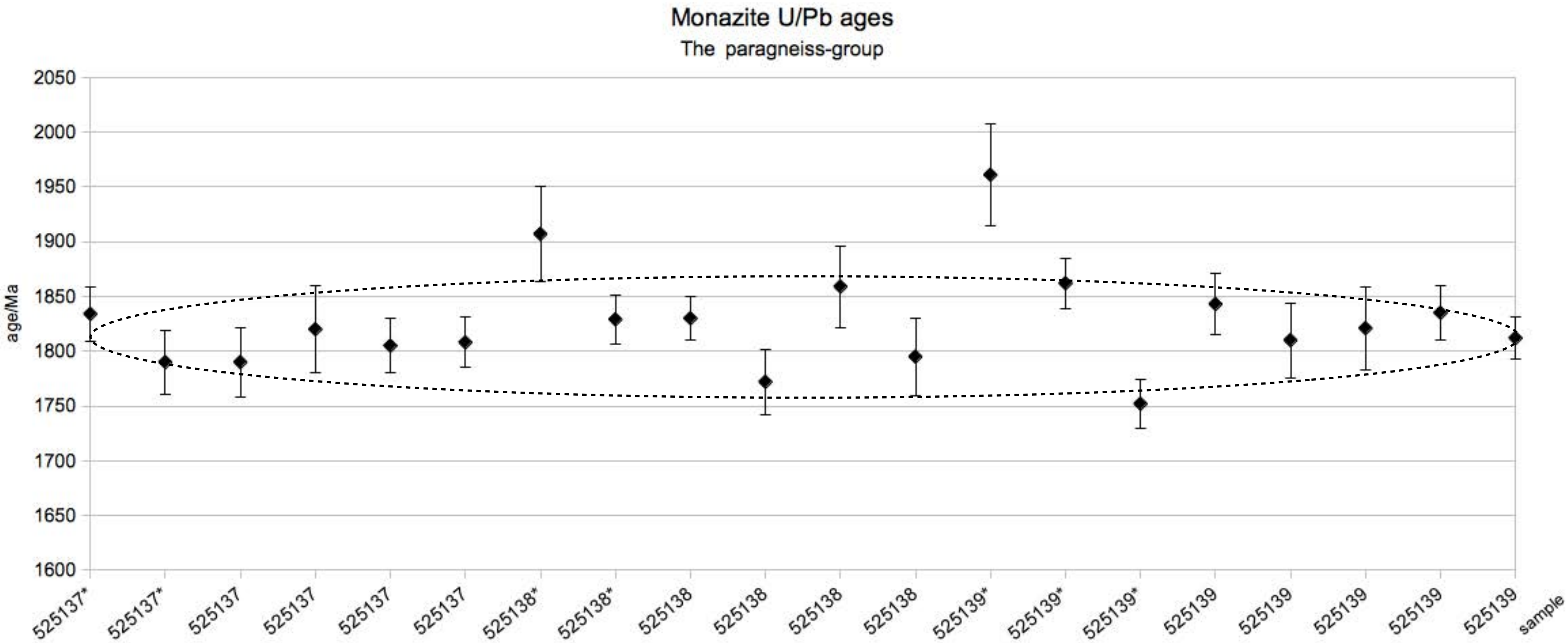

Figure 17. Plot of corrected and uncorrected LA-ICP-MS $^{207}Pb/^{206}Pb$ monazite ages. Analyses/samples marked with an asterisk have been common Pb-corrected. The ellipsoid represents a visual interpretation of the monazite ages, where uncorrected ages have been given higher significance.

6. Discussion

6.1. Wall rock

The composition and age-relation of wall rock(s) is important to the gold deposit potential. The wall rock at the Helheim Fjord synform is underlaid by Archean TTG gneiss which has been interleaved with a Paleoproterozoic supercrustal association (ultramafic rocks, pyroxenites, amphibolites, paragneisses and marble) following the collisional stage of the Nagsugtoqidian Orogey (Nutman et al., 2008).

Archean TTG gneisses generally represent early continental crust formed by partial melting of hydrous mafic crust (Goldfarb et al., 2000). In the Tasiilaq area these are polyphase Archean gneisses. During the Paleoproterozoic the gneiss was intruded by metadolerite dykes (2015±15 Ma, Nutman et al., 2008). The TTG gneiss and dykes formed the basement on which the supracrustal rocks were deposited. The origin, interrelation and age of the supracrustal association is however not certain (Nutman et al., 2008). Paragneisses with structures similar to a coarse trough cross-bedding have been observed, which suggest a marine-sedimentary origin of, at least parts, of the paragneiss (Chadwick et al. 1989). The marine origin is supported by the presence of marble in the synform.

Ultramafic rocks are also present in the western part of the Nagssugtoqidian Orogen, where they have been suggested to represent mantle fragments, and reflect the crustal scale tectonic activity (Kalsbeek and Manatschal, 1999). Thus, the ultramafic rocks may not be part of the superacrustal association, until the succession is interleaved and metamorphosed in relation to the orogeny.

6.2. Metamorphic evolution

Both pressure and temperature conditions are make-or-break parameters of gold deposits. The paragneiss is at amphibolite facies at the obtained pressure of ~5.3 kbar and temperature of 460-640℃ (Winter, 2001). This is consistent with the regional low pressure metamorphism of Nutman et al. (2008), presented in figure 2. It is also consistent with the presence of leucosome veins at the Helheim Fjord synform, as the conditions is in the transition zone where melting of wet granitic rock is possible (Winter, 2001). Both kyanite and silimanite have previously been observed in the paragneiss of the supracrustal association (Chadwick et al., 1989), yet have not been observed in the paragneiss samples studied here. Al-silicates are not present due to the relatively low Al-content of the paragneisses (appendix F).

The temperature and pressure obtained from the paragneiss are likely to reflect the metamorphic conditions at the Helheim Fjord synform as the paragneiss samples are representative of the conditions in the area.

The obtained temperature for the garnetite overlap with that of the paragneiss at 500℃-650℃. The temperatures were calculated using the pressure obtained from the paragneisses, though the garnetite sample was taken from a location near the high temperature, low pressure AIC (figure 3). As a ±1 kbar change yielded ±4℃, it is likely that the calculated temperature does however reflect the actual temperature condition within the ±25℃ error margin (Holdaway, 2000).

In general the GB thermometers do not provide consistent temperatures, though the amphibolite-facies conditions should be ideal for use in GB thermometry (Holdaway, 2004). The GB thermometer is based on biotite and garnet Margules activity models, of which there are numerous varieties (Holdaway, 2004). The models are build on different methods, and are to some extend based on different data, but the similarities should outweigh the differences (Holdaway, 2004). The GB thermometers do however provide a variation in temperatures for both samples, as well as generally lower temperatures for the paragneiss sample than for the garnetite. It is possible that temperatures were higher at the garnetite location, as an effect of the previously mentioned proximity to the AIC.

The thermometer of Holdaway (2000) is based on the combination of three activity models, and currently provides the best estimates and the most precise estimations at ±25℃ (Holdaway, 2004).

All the applied geothermobarometric models require chemical equilibrium within the minerals used. As that may be an approximation in regard to both the paragneiss and the garnetite sample the obtained pressure and temperatures reflect minimum conditions (Holdaway, 2004).
The assumption of equlibrium requires the minerals to be of the same paragnetic origin. Though an attempt is made to avoid areas of extensive hydrothermal alteration, when analyzing biotite for use in the GB geothermometer and GBPQ geobarometer, it is possible that biotite of the hydrothermal stage was included. Yet there appears to be a limited range of compositions of the biotite (appendix D). This suggests that metamorphism and hydrothermal alteration occurred as a continuous event.

Mineral zoning is an issue to the assumption of equilibrium. Zonation in garnet is common (Deer et al., 1966). The omnipresent garnet of the garnetite is of a morphology which renders it difficult to separate grain boundaries from internal fractures, and cores from rims. Two garnet-groups were established on the basis of Fe-Mn variations (appendix D). The temperature variation of the two groups are however well within the ±25℃ error margin at the calculated variation of ±4℃ (table 1A, appendix A). Though a higher degree of major element variation is present within the garnet of the garnetite, the composition resembles the garnets of the paragneiss group. The almandine end member is high within both rocks, and both are also enriched in Mn (appendix D). Almandines are typically found in garnetiferous schists in regional metamorphism of argillaceous sediments (Deer et al., 1966).

In the obtained element map of a garnet from the paragneiss, a weak zonation is present; the core of the garnet is slightly enriched in Mn and depleted in Mg (figure 4 and 5). FeO+MgO generally substitutes for CaO+MnO with increasing metamorphic grade (Deer et al., 1966). If we assume that Mn can reflect the CaO+MnO, and Mg can reflect FeO+MgO, the grain represents a shift towards higher metamorphic grade - if we also assume the morphological core/rim-interpretation in figure 4.

The obtained temperature and pressure coincides with the 1870-1820 regional lower pressure metamorphic conditions suggested by Nutman et al., 2008, for both locations. The temperature and pressure are however not ideal gold forming conditions (McCuaig & Kerrich, 1998). Yet one sample has abundant gold, the other very little; thus the temperature was not the critical difference of the two mineralizations.

6.3 Hydrothermal alteration

An ideal gold-bearing solution has a temperature of ≥200℃, is rich in CO_2 (20-30 mol%), sulfur-bearing, with sulfide complexes predominantly in the reduced stage (Phillips & Evans, 2004). The presence of sulfide minerals and graphite suggest that sulfide complexes and CO_2 would have been present in the hydrothermal event at both the Helheim Fjord synform and the garnetite-location. Yet the garnetite sample is the only sample which show gold grades of economic interest.
The graphite overprint is more pronounced in the Ujarrasiorit sample than in any other examined sample. The sample is from location B, just north of the AIC and close to a first order fault (figure 3). As previously mentioned, orogenic gold deposits are often related to secondary and tertiary fault systems, adjacent main faults. It is possible that the close-by regional fault creates a second or third order fault at the location, which acts as a focal zone and/or trap for the precipitation of gold. Such a setting could account for the high gold grades of the sample and the intensive graphite overprint. This support the suggestion of a structurally-controlled mineralization.
A structural trap is probably missing at the Helheim Fjord synform. The presence of graphite in all the examined samples from the synform suggest that the hydrothermal fluids were unfocussed and

widespread. The low gold grades of the samples, reflects the unfocussed nature of the hydrothermal fluids. As previously mentioned, the samples represent the general hydrothermal alteration in the synform-area.

Graphite in orogenic gold deposits is typically related to organic material, derived from metapelites (Goldfarb et al., 2000). It is likely that the sedimentary rocks of the supracrustal association supplied the organic material. At the temperatures suggested for the metamorphic event (>460℃), the hydrothermal fluids could have have dissolved organic matter. The late stage overprint suggest that that no graphite is in its primary site of deposition, but is present only as a hydrothermal mineral. Graphite can be precepitated by reduction of a CO_2-rich fluid (Křibek et al., 2008). The presence of sulfide minerals in the hydrothermal stage supports the indications of a reducing hydrothermal fluid. The source of sulfide minerals are likewise typically metapelites, and the sulfide minerals can likewise be redeposited during a hydrothermal event (Goldfarb et al., 2000).

Pyrite rims can be found at most monazite grains. Sulfidic rims are the result of favorable conditions for precipitation of pyrite by irradiation from radioactive elements included in the mineral lattice of monazite (Procháka et al., 2011). The rims concentrate relatively large amounts of water in the very small volume close to the monazite grains. Therefore the monazite is vulnerable to hydrothermal alteration, and metamorphic recrystallization even at relatively low temperatures (<700℃, Procháka et al., 2011).
U/Pb ages of 1752±22 Ma to 1961±47 Ma have been obtained for monazites from paragneiss. The hydrothermal alteration is not coeval with the metamorphic event (e.g. figure 12) at 1870-1820 Ma. The ages of more than ~1870 Ma is likely to be a 'mixed age', reflecting a combination of older, unaltered isotope compositions and younger hydrothermally altered rim-sites. The monazites display chemical variation (figure 15 and figure A18 and A21 in appendix A). The variation could reflect that the grains did not recrystallize completely during the hydrothermal event, but monazites recrystallize easily and at relatively low temperatures (Procháka et al., 2011). A zircon, which is not readily altered, was also analyzed an yielded an age of 1803±23 Ma, suggesting that the ages are 'mixed' (appendix E). Monazite ages of 1850-1750 Ma are nevertheless predominant (17 out of 22 monazite ages), and it is likely that the hydrothermal alteration took place during this time, presumably after the regional metamorphic event or shortly following. The garnetite sample has zircon as an accessory phase, but an attempt was not made to date these as they were rendered unsuited for LA-ICP-MS analyses due to complex zoning and internal damage (figure A23 in appendix A).
CL-imaging should be taken on in further studies, to investigate the extend of variation within the analyzed grains. Such imaging could form the basis of further investigation by rare earth elements and/or selective dating of sites.

The compositional variation within the dated monazites may be reflected by inclusion of common Pb. If a common Pb-signal can be distinguished from the background (figure A24 in appendix A) it commonly shows an erratic increase and decrease, rather than a uniform elevation, which could be caused by variations in the mineral at a very small scale (25μm broad, max. 30μm deep pitt).
The unevenness of the ^{204}Pb-signal (common Pb-indicator) is a source of error, as an average of the signal is used in correction. Selecting too small a proportion of the Pb-signal for use in the analyses, or having limited useable signal also affects the final age (figure A24 in appendix A). The effect of common Pb is generally considered less pronounced in the applied ^{207}Pb/^{206}Pb ages, than in ages utilizing U-isotopes, as common Pb will affect ^{207}Pb/^{206}Pb equally. Not all samples were correct for common Pb, as the common Pb signal was either not present or could not be distinguished from the background signal (figure A24 in appendix A).

The age-results may also be affected by the application of a zircon as standard. Monazite has a different mineral matrix than zircon, though both zircon and monazite should in theory exclude common Pb. The quality of such a setup is difficult to estimate, as it depends on the comparability of the matrix of the two minerals (personal correspondence with Tonny Bernt Thomsen, GEUS). Thus the obtained ages should be considered estimates. The procedure has not previously been used at the laboratory of GEUS. Yet the low discordance suggest that the obtained ages are reasonable, and errors are also within what could be expected (personal correspondence with Tonny Bernt Thomsen, GEUS).

6.4. Evolution of the Helheim Fjord synform

The Archean TTG gneiss and metadolerite dykes constitutes a basement association, to the paragneiss-protolith-cover. Following the collisional stage of orogeny the TTG gneiss, metadolerite dykes and paragneiss-protolith was interleaved and metamorphosed (circa 1870 to 1820 Ma, Nutman et al., 2008). The metamorphic event took place at ~640℃ and ~5.3 kbar, at the Helheim Fjord synform, which is equal to amphibolite facies conditions (Winter, 2000). A hydrothermal event took place from ~1850-1750 (figure 17). The hydrothermal event was widespread, and commonly represented by graphite and iron sulfides.

Though slate belts are known for the association of gold and graphite, it is unlikely that the mineralization in the Tasiilaq area represents such a setting. Slate belts are typically of greenschist facies, and their mineralization is characterized by hydothermal alteration of pyrite and arsenopyrrite (Craw, 2002). Pyrrhotite is the dominant iron sulfide in the studied samples, and amphibolite facies assemblages and conditions have been infered.

7. Conclusions

- The orogenic event which caused the interleaving of unrelated lithologies in the Tasiilaq area is represented by temperatures of ~640℃ and a pressure of ~5.3 kbar, at the Helheim Fjord synform. This is equal to amphibolite-facies conditions.
- Monazite grains from the Paleoproterozoic paragneiss have yielded U/Pb ages of 1961±47 Ma to 1752±22 Ma, with a clustering of ages around 1850-1750 Ma. The clustering is interpreted to represent an approximate age of the hydrothermal event.
- The hydrothermal fluid had gold potential; the presence of hydrothermal graphite and iron sulfides suggest that the fluid was CO_2-rich and had hydrosulfur complexes. Hydrosulfide complexing with gold is consistent with low salinites, and the presence of hydrosulphur consistent with a reducing fluid. As the hydrothermal event was coeval with the metamorphic event, temperatures would also have been well above the <200℃ suggested for an ideal gold-bearing fluid (Phillips & Evans, 2004).
- That graphite is omnipresent in the samples from the synform-location suggest that the hydrothermal event was unfocussed and widespread. Thus the percipitation of Au was also widespread and unfocussed, which resulted in low gold grades.
- The temperatures obtained for the gold-bearing garnetite-samples overlaps with that of the synform-location, at ~500-660℃, and the single-mineral major element chemistry of garnet and biotite is resemblant of that found in the paragneiss group. The sample likewise show a hydrothermal overprint of graphite and iron sulfides.
- It is possible that the close-by regional fault is followed by a second or third order fault, which acts as a focal zone and/or trap for the precipitation of gold. Thus, the Ujarrasiorit sample represents a structurally controlled gold mineralization.

I suggest that further field studies should concentrate on the structural relations in the area, if the aim is to locate possible gold deposits. No such investigations have been published since 1989 (Chadwick & Vasudev, 1989).

8. Acknowledgements

I thank Jochen Kolb from GEUS for taking on the role of external supervisor, and guiding me through both the the writing process and hours spent at the microscope. I also thank Tod Waight from the University of Copenhagen for supervising in general and especially for helping with EMP analyses. Matthijs Smidt from the University of Copenhagen, also provided help at the EMP for which I am thankful. This study was made possible by GEUS. I have several people at GEUS to thank; Nynke Keulen and Jørgen Kystol for assisting me in SEM analyses, and coating of samples, and Tonny Bernt Thomsen for assisting me in LA-ICP-MS analyses as well data treatment and later discussion of results.

9. List of appendices

Electronic appendices can be found on the enclosed CD. Appendix A is exclusively included in print.

The appendices applied in this thesis constitute:

- **Appendix A.** Applied analytical methods and additional figures
- **Appendix B.** Thin Section Descriptions: ‘Appendix_B_ThinSection’
- **Appendix C.** Secondary Electron Microscopy - EDS analyses: ‘Appendix_C_SEM’
- **Appendix D.** Electronmicroprobe Formula Unit Calculations: ‘Appendix_D_EMP’
- **Appendix E.** Single mineral U/Pb LA-ICP-MS data: ‘Appendix_E_LAICPMS’
- **Appendix F.** Whole rock analyses: ‘Appendix_E_WR’

10. References

Bhattacharya, A., Mohanty, L., Maji, A., Sen, S.K., Raith, M., 1992, Non-ideal mixing in the phlogopite-annite binary: constrains from experimental data on Mg-Fe partitioning and a reformulation of the biotite-garnet geothermometer, v. 111, p. 87-93

Bierlein, F.P., Cartwright, I., 2001, The role of carbonaceous "indicator" slates in the genesis of lode gold mineralization in the western Lachlan Orogen, Victoria, southeastern Australia, Bulletin of the Society of Economic Geologists, v. 96, no. 3, p. 431-451

Chadwick, B., Dawes, P.R., Escher, J. C., Friend, C. R. L., Hall, R.P., Kalsbeek, F., 1989, The Proterozoic mobile belt in the Ammassalik region, South-East Greenland (Ammassalik mobile belt): An introduction and reappraisal, Grønlands Geologiske Undersøgelse, Rapport 146, p. 5-12

Craw, D., 2002, Geochemistry of late metamorphic hydrothermal alteration and graphitisation of host rock, Macraes gold mine, Otago Schist, New Zealand, v. 191, p. 257-275

Dasgupta, S., Sengupta, P., Guha, D., Fukuoka, M., 1991, A refined garnet-biotite Fe-Mg exhange geothermometer and its application in amphibolites and granulites, Contributions to Mineralogy and Petrology, v. 109, p. 130-137

Deer, W.A., Howie, R.A., Zussman, J., 1966, An Introduction to the Rock Forming Minerals, 1 ed., Longman Scientific & Technical, Harlow, 517 p.

Droop, G.T.R., 1987, A general equation for estimating Fe^{3+} concentrations in ferromagnesian silicates and oxides from microprobe analyses, using stoichiometric criteria, Min. Mag. 51, p. 431-435.

Ferry, J.M. and Spear, F.S., 1978, Experimental calibration of the partitioning of Fe and Mg between biotite and garnet. Contributions to Mineralogy and Petrology, v. 66, p. 113–117

Frei, D., Gerdes, A., 2009, Precise and accurate in situ U–Pb dating of zircon with high sample throughput by automated LA-SF-ICP-MS, Chemical Geology, v. 261, p. 261-270

Friend, C.L.R., Nutman, A.P., 1989, Reconnaissance P, T studies of Proterozoic crustal evolution of the Ammassalik area, South-East Greenland, Grønlands Geologiske Undersøgelse, Rapport 146, p. 41-45

Goldfarb, R.J., Groves, D.I. Gardoll, S., 1993, Orogenic gold and geologic time: a global synthesis, Ore Geology Reviews, v. 18, p. 1–75

Groves, D.I., 1993. The crustal continuum model for late-Archaean lode-gold deposits of the Yilgarn Block, Western Australia. Mineral Deposita, v. 28, p. 366–374

Hall, R.P., Chadwick, B., Escher, C.J., Vasudev, V.N., 1989, Supracrustal rocks in the Ammassalik region, South-East Greenland, Grønlands Geologiske Undersøgelse, Rapport 146, p. 17-22

Hall, R.P., Hughes, D.J., Joyner, L., 1989, Basic dykes of the southern Ammassalik region, South-East Greenland: preliminary mineralogical and geochemical results, Grønlands Geologiske Undersøgelse, Rapport 146, p. 79-82

Holdaway., M.J., 2000, Application of new experimental and garnet Margules data to the garnet-biotite geothermometer, American Mineralogist, v. 85, p. 881-892

Holdaway, M.J. and Lee, S. M., 1977, Fe-Mg cordierite stability in high-grade pelitic rocks based on experimental, theoretical, and natural observations. Contributions to Mineralogy and Petrology, v. 63, p. 175–198

Kalsbeek, F., Austrheim, H., Bridgewater, D., Hansen, B.T., Pedersen, S., Taylor, P.N., 1993, Geochronology of Archaean and Proterozoic events in the Ammassalik area, South-East Greenland,

and comparisons with the Lewisian of Schotland and the Nagssugtoqidian of West Greenland, Precambrian Research, v. 62, p. 239-270

Kalsbeek, F., Manatschal, G., 1999 Geochemestry and tectonic significance of peridotitic and meta-komatiitic rocks from the Ussuit area, Nagssugtoqidian orogen, West Greenland, Precambrian Reasearch, v. 94, p. 101-120

Kalsbeek, F., and Nutman, A. P., 1996, Anatomy of the early Proterozoic Nagssugtoqidian orogen, West Greenland, explored by reconnaissance SHRIMP U/Pb zircon dating, Geology, v. 24, p. 515-518

Kalsbeek, F., Taylor, P.N., 1989, Program of geochronology and isotope geochemestry in the Ammassalik region, South-East Greenland: outline and preliminary results, Grønlands Geologiske Undersøgelse, Rapport 146, p. 13-16

Kolb, J., 2010, personal field notes in the archives of the Geological Survey of Denmark and Greenland

Křibek, B., Sýkorvá, I., Machovič, V., Laufek, F., 2008, Graphitization of organic matter and fluid-deposited graphite in Palaeoproterozoic (Birimian) black shales of the Kaya-Goren greenstone belt (Burkina Faso, West Africa), Journal of Metamorphic Geology, v. 26, p. 937-958

McCuaig,T.C., Kerrich, R., 1998, P-T-t-deformation-fluid characteristics of lode gold deposits: evidence from alteration systematics, Ore Geology Reviews, v. 12, s. 381-453

Nutman, A.P., Kalsbeek., F., Friend, C.R.L., 2008, The Nagssugtoqidian Orogen in South-East Greenland: Evidence for Paleoproterozoic Collision and Plate Assembly, American Journal of Science, Vol. 308, p. 529-572

Nutman, P.N., Kalsbeek, F., Marker, M., van Gool., J.A.M., Bridgewater, D., 1999, U/Pb zircon ages of Kangâmiut dykes and detrital zircons in metasediments in the Paleoproterozoic Nagssugtoqidian Orogen (West Greenland): Clues to the pre-collisional history of the orogen, Precambrian Research, v. 93, p. 87-104

Perchuk, L.L. and Lavrent'eva, 1983, Experimental investigation of exchange equilibria in the system cordierite-garnet-biotite, in Saxena, S.K., Ed., Kinetics and Equilibrium in Mineral Reactions, Advances in Physical Geochemistry, v. 3, p. 199–239

Phillips, G.N., Evans, K.A., 2004, Role of CO_2 in the formation of gold deposits, Nature, v. 429, p. 860-863

Procházka, V.C., Seydoux-Guillaume, A., Trojek, T., Goliás, V., Korbelova, Z., Matéjka, D., Novotná, 2011, Alteration halos around radioactive minerals in plutonic and metamorphic rocks of the northern Moldanubian area, Bohemian massif, European Journal of Mineralogy, v. 23, p. 551-556

Siivola, J, and Schmid, R. A, 2007, Systematic nomenclature for metamorphic rocks: 12. List of mineral abbreviations. Recommendations by the IUGS Subcommission on the Systematics of Metamorphic Rocks, *Recommendations*, web version of 01.02.2007, 14 p.

Thompson, A.B., 1976, Mineral reactions in pelitic rocks: II. Calculation of some *P-T-X* (Fe-Mg) phase relations. American Journal of Science, v. 276, p. 401–454

Tindle, A.G., Webb, P.C., 1990, Estimation of lithium contents in trioctahedral micas using microprobe dataapplication to micas from granitic rocks European Journal of Mineralogy, v. 2, p. 595–610

Winter, J.D., 2001, An introduction to Igneous and Metamorphic Petrology, 1. ed., Prentice-Hall Inc., 695 p.

Wu, C.M., Zhang, J., Ren, L.D., 2004, Emperical Garnet-Biotite-Plagioclase-Quartz (GBPQ) Geobarometry in Medium- to High-Grade Metapelites, Journal of Petrology, v. 45, n. 9, p. 1907-1921

10.1. References cited in appendix A only

Frei, D., Gerdes, A., 2009, Precise and accurate in situ U–Pb dating of zircon with high sample throughput by automated LA-SF-ICP-MS, Chemical Geology, v. 261, p. 261-270

Reed, S.J.B., 2005, Electron Microprobe Analyses and Scanning Electron Microscopy in Geology Cambridge University Press, New York, 232 p.

Applied analytical methods

Secondary Electron Microscopy & Electron Microprobe

Secondary Electron Microscope (SEM) and Electron Microprobe (EMP) are both electron microbeam instruments, which can provide images and analyses of specimens with the use of a focussed beam of electrons and an array of detectors (Reed, 2005). As electrons will react with anything they encounter, the electron microbeam instruments are vacuum-based systems. A specimen which goes into a SEM or EMP must be solid and dry to avoid any degassing during vacuuming and subsequent contamination of the instrument (Reed, 2005). Furthermore the samples must be conductive; this is commonly accomplished by coating the sample with carbon. The coating prevents electrostatic buildup, provided that the sample is sufficiently electrically grounded, thus it is typically taped to the specimen holder with a conductive tape.

A SEM is typically build for imaging. The Phillips XL 40 SEM is fitted with a secondary electron (SE) detector, a backscattered electron (BSE) detector, cathodoluminescence (CL) detector and two detectors for energy-dispersive X-ray spectroscopy (EDS).

SE emission is produced when the electrons eject a loosely bound outer electron from a given element in the sample, and thus it reflects the surface and its structure. BSE emission is produced by elastic scattering of of the primary electrons (Reed, 2005). BSE is considered a surface signal, but BSE images also reflect density as elements of higher atom numbers will more efficiently backscatter electrons, and thus appear relatively brighter (Reed, 2005).

The Phillips XL 40 SEM can conduct semi-quantitative analyses of major element chemistry with the use of EDS. EDS is based on identification of characteristic X-ray energies. Characteristic X-rays are produced when an electron in an inner orbit is ejected by a primary electron, which leaves the electron in an ionized state. As an electron transitions between bound orbitals, it releases surplus energy as characteristic X-ray photons. The energy is recorded and represents a characteristic X-ray peak, which is named after the shell in which the initial vacancy occurred and from where the vacancy is filled. The intensity of the characteristic X-ray peak is proportional to the mass concentration of the respective element (Reed, 2005). The EDS performs standard-free analyses, where calculated element intensities are derived from internal standards, rather than measured standards. The accuracy of such a system is difficult to evaluate, but it is not as good as that of a system using measured standards (Reed, 2005).

The JEOL JXA-8200 Superprobe is optimized for chemical analyses, as it applies measured standards in addition to the wavelength dispersive X-ray spectrometer (WDS). It is fitted with the same types of detectors as the SEM, except for a cathodoluminescence-detector. In addition it has WDS and a videocamera mounted coaxially with the electron beam.

The WDS detector is based on dispersion of the characteristic X-rays in a crystal according to their wavelength, by the means of Braggs reflection (Reed, 2005). X-rays of a certain wavelength will be reflected from a crystal with the interplanar spacing (d), at a certain angle of incidence (θ, Braggs angle). Thus the WDS has multiple crystals with varying d-spacing. To obtain a constant Bragg angle, the electron source, reflective crystal and electron detector must all be on the circumference of an imaginary circle; this circle is called the Rowland circle (Reed, 2005). The EMP is fitted with a videocamera, and the specimen must always be in focussed to keep the sample on the Rowland circle, which is part of keeping a constant Bragg angle (Reed, 2005).

Laser Ablation Inductively Coupled Plasma Mass Spectrometry

Laser Ablation Inductively Coupled Plasma Mass Spectrometry (LA-ICP-MS) is a mass spectrometry analytical tool. Analyses can be carried out directly on solid samples, by the use of a focussed, pulsing laser beam. The laser beam generates an aerosol from the specimen. The aerosol is transported into inductively coupled plasma (ICP) by an carrier gas (He). In the plasma, the aerosol is vaporized, atomized and ionized. The generated ions are then transported from an interface of atmospheric pressure through a skimmer cone, and into the high pressure of the mass analyzer.
Although it is possible to use a variety of mass spectrometers in connection with ICP, the applied MS uses a sector field analyzer (Frei & Gerdes, 2009). Here, ions are separated on the basis of mass-to-charge ratios, deflecting the more charged and faster-moving, lighter ions more by the use of a magnetic and electric field. After separation of the ions in the mass analyzer, the ions are counted. The applied Element2 LA-ICP-MS has a single electron multiplier for electron detection. The dynamic range of the electron multiplier allows for both high and low intensity isotopes to be measures simultaneously, thus multiple element can be accounted for in one analyses (Frei & Gerdes, 2009).
In theory, the LA-ICP-MS is capable of detecting concentrations as low as 1 ppb, without any sample preparation (Frei & Gerdes, 2009). Unlike SEM or EMP, the method does not require the sample to be coated - coating would be a source of contamination in LA-ICP-MS.

For the measured ^{207}Pb and ^{206}Pb the age (t) can be interpolated from the equation:

$$\left(\frac{^{207}Pb}{^{206}Pb}\right)^{*} = \frac{1}{137.88} \times \left[\frac{(e^{\lambda_2 t} - 1)}{(e^{\lambda_1 t} - 1)}\right]$$

Where $(^{207}Pb/^{206}Pb)^{*}$ is the radiogenic lead component, 1/137.88 is the $^{235}U/^{238}U$ constant, and λ the decay constant for the respective parent to daughter decay (^{235}U to ^{207}Pb and ^{238}U to ^{206}Pb). The equations assumes no initial lead.

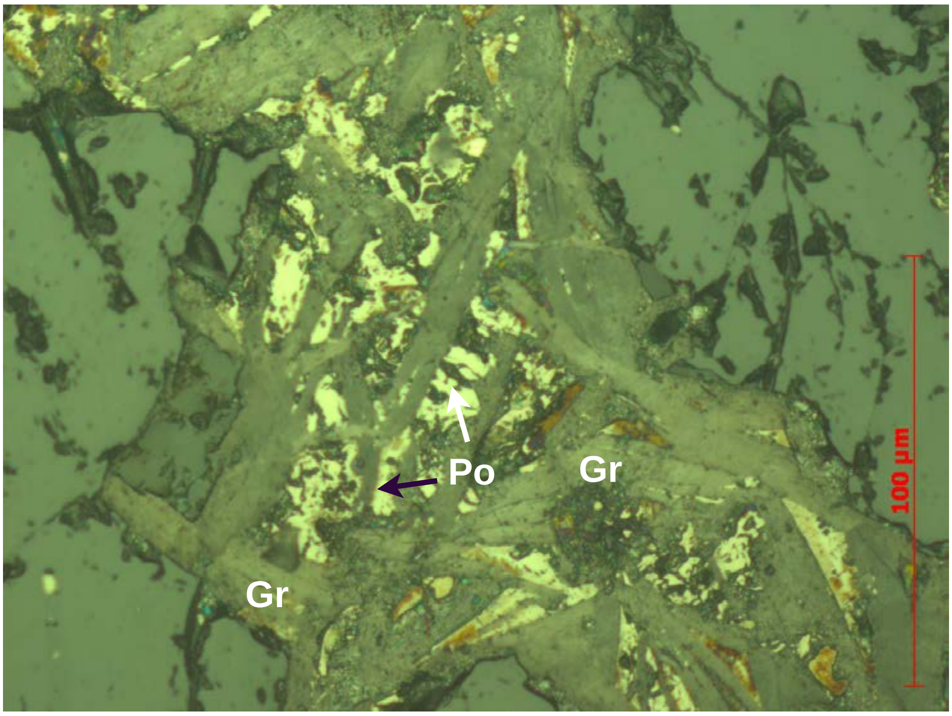

Figure A1. Photomicrograph of the Ujarrasiorit thin section, in reflected light. Example of extensive graphitization of a pyrrhotite grain.

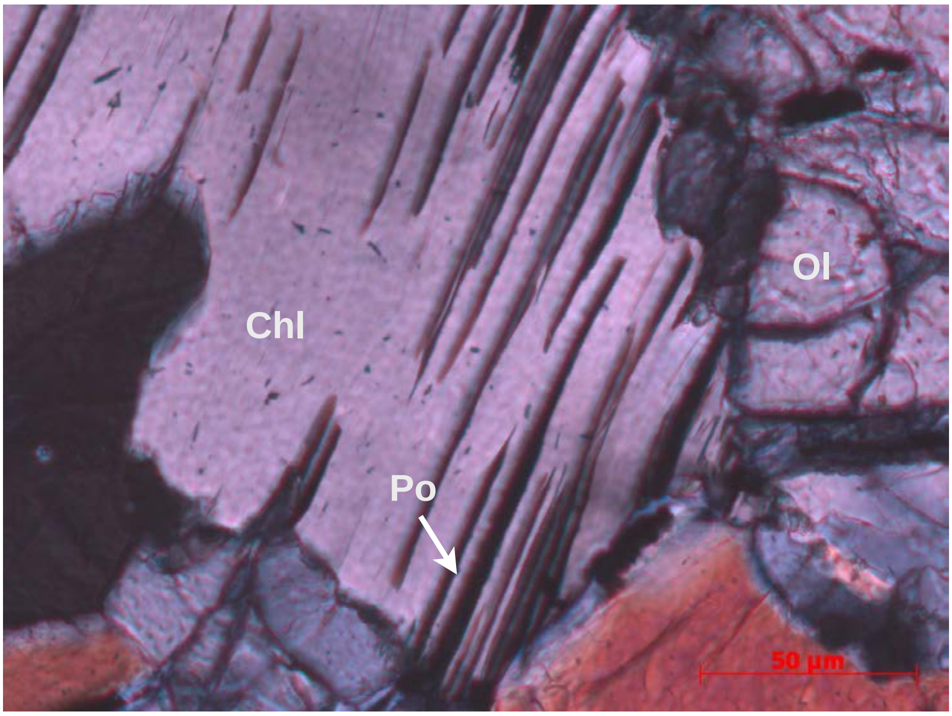

Figure 2A. Photomicrograph of thin section 525133, in transmitted light and with crossed polarizers. Example of massive chlorite with pyrrhotite ‘veins‘. A closeup of the pyrrhotite can be found in figure 3A.

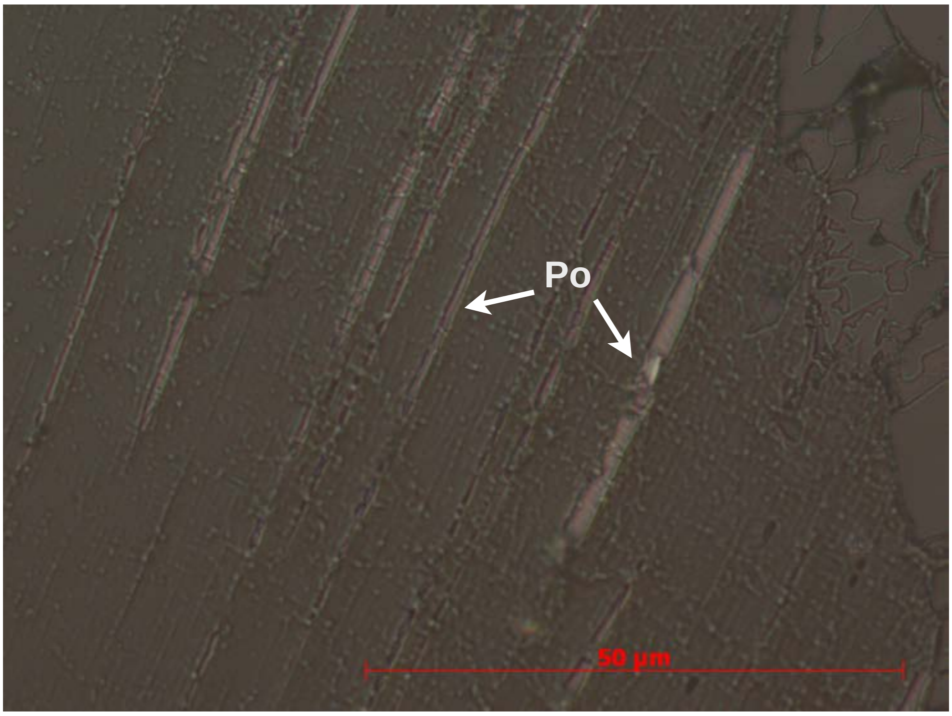

Figure A3. Photomicrograph of thin section 525133, in reflected light. Close-up of the pyrrhotite vein in chlorite. A correspondent overview can be found in figure 2A.

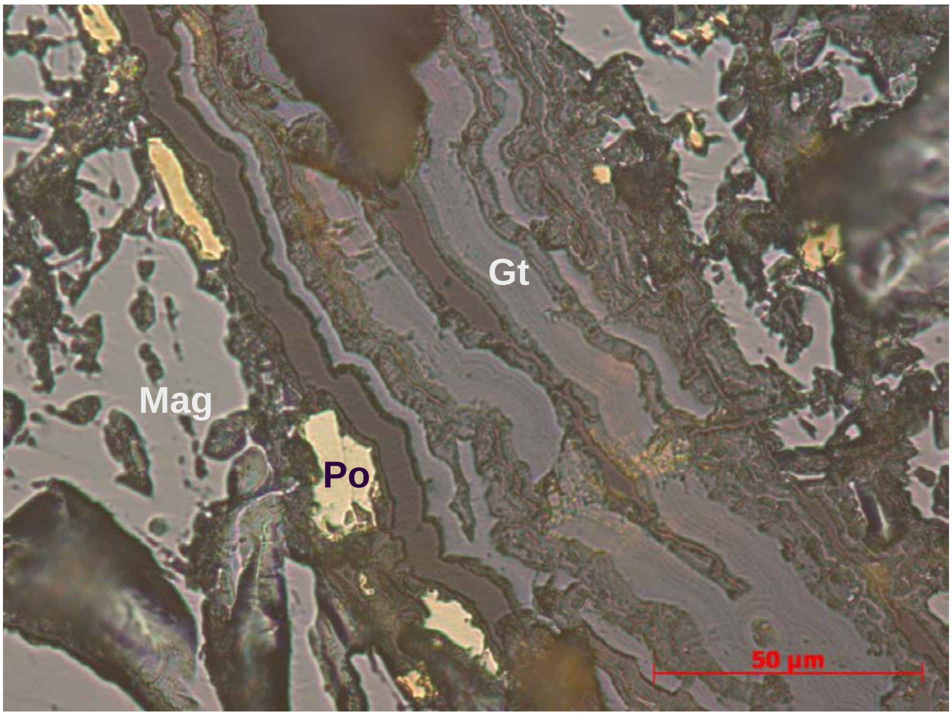

Figure A4. Photomicrograph of thin section 525134a, in reflected light. Example of a goethite-pyrrhotite-vein, through a magnetite-bearing section.

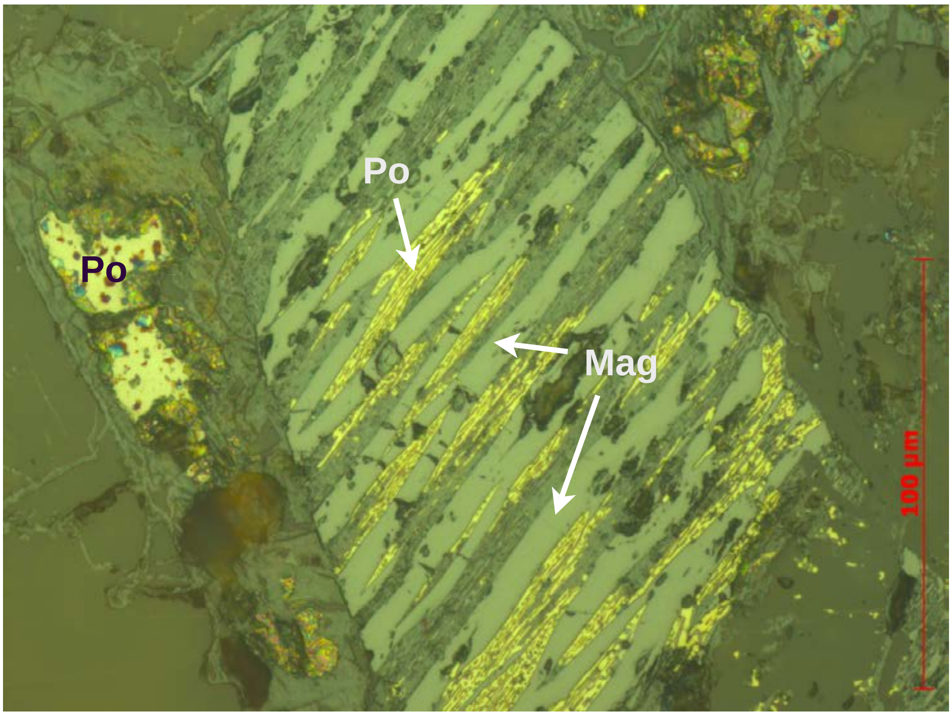

Figure A5. Photomicrograph of thin section 525134a, in reflected light. Example of magnetite alteration in thin section 525134a.

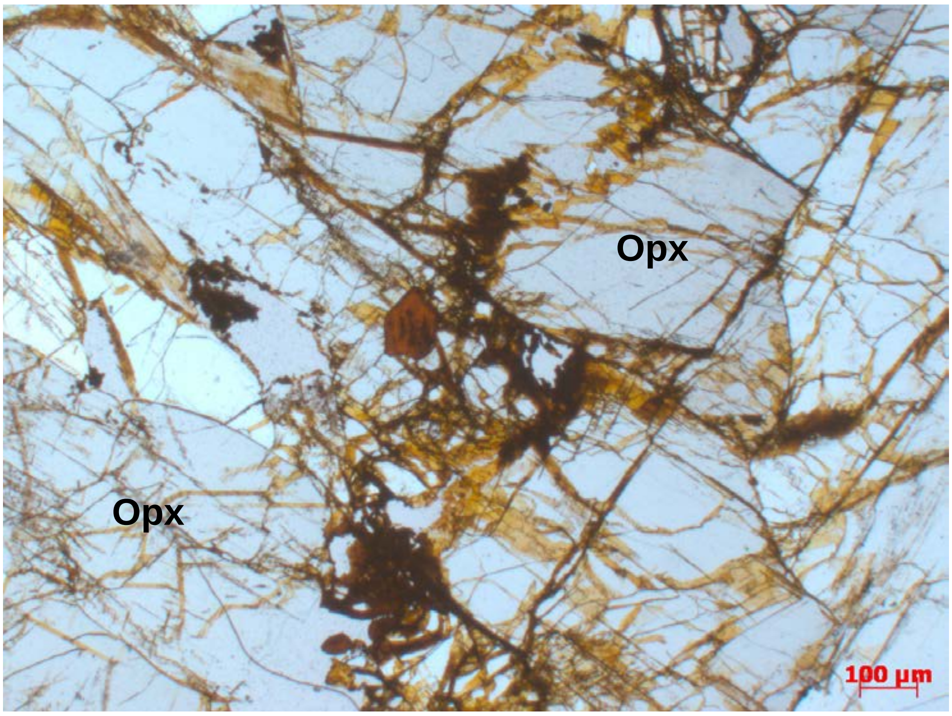

Figure A6. Photomicrograph of thin section 525135, in transmitted light. Example of supergene hematite alteration.

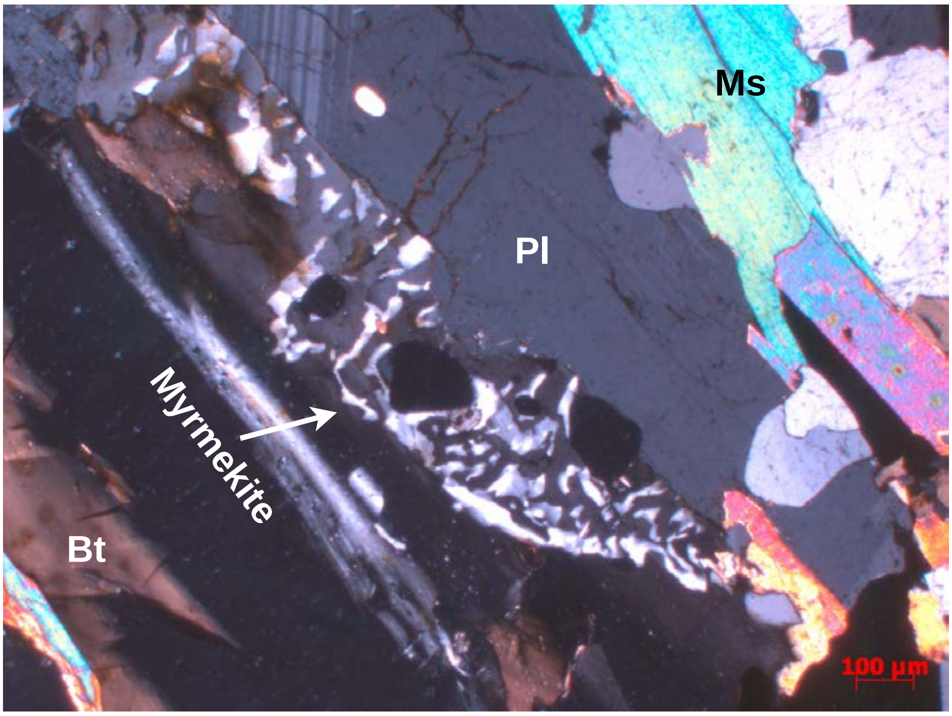

Figure A7. Photomicrograph of thin section 525137, in transmitted light and with crossed polarizers. Example of myrmekite.

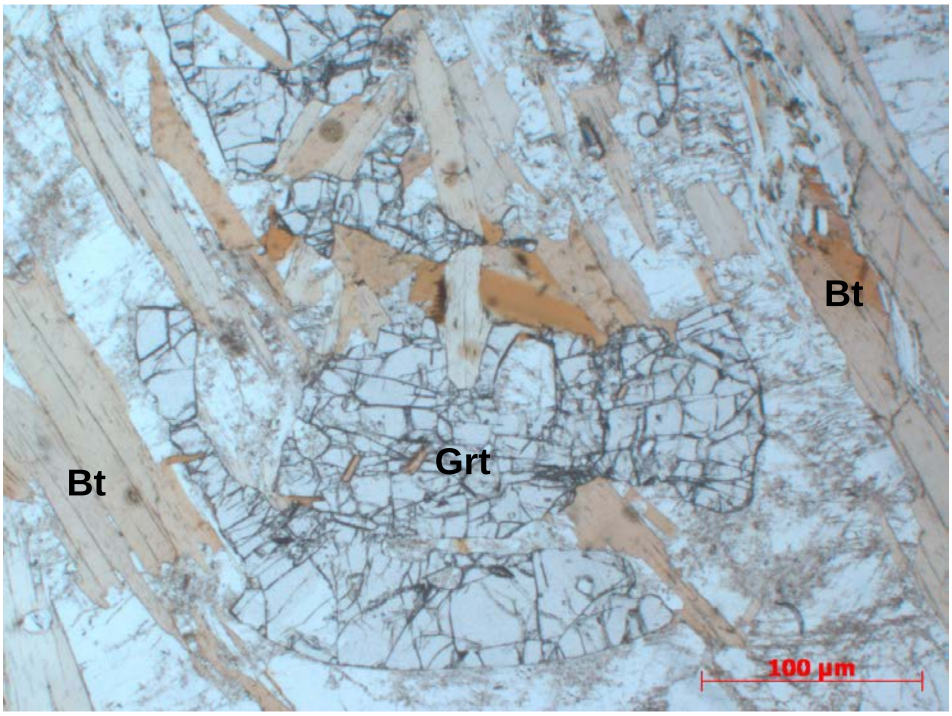

Figure A8. Photomicrograph of thin section 525138, in transmitted light. Example of extensive fracturing, relation to biotite and inclusionary mineralogy.

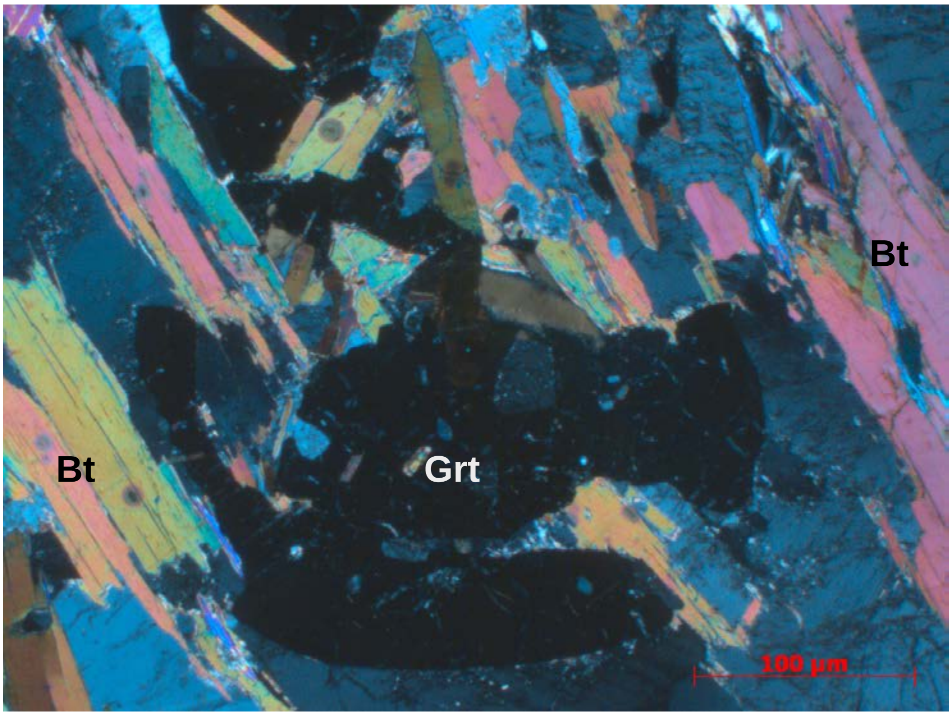

Figure A9. Photomicrograph of thin section 525138, in transmitted light and with crossed polarizers. Example of the surrounding micas, and stage of alteration.

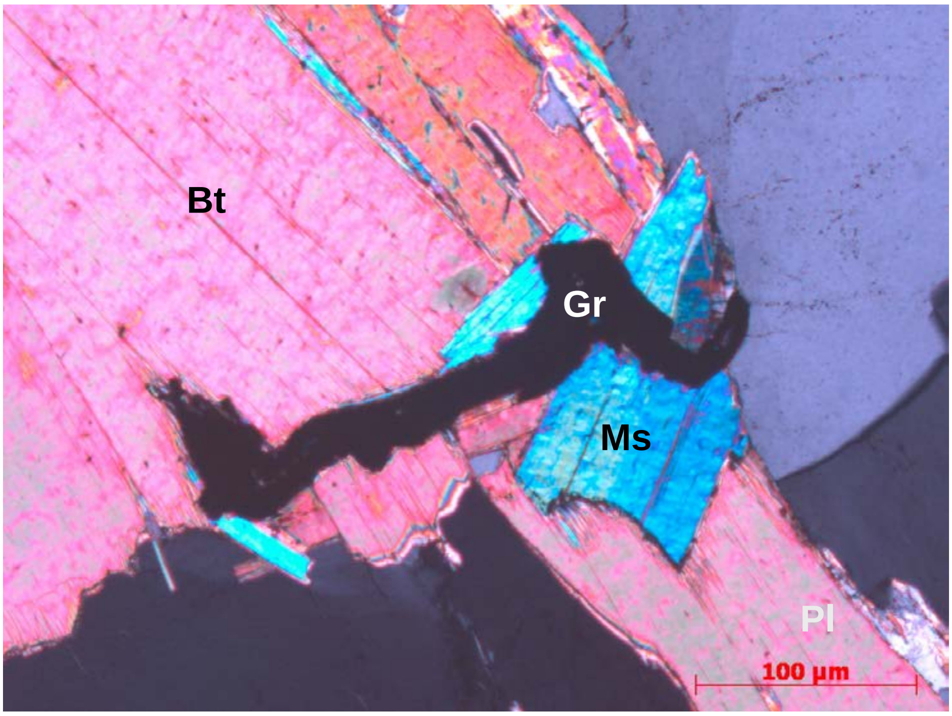

Figure A10. Photomicrograph of thin section 525138, in transmitted light and with crossed polarizers. Example of the relation between biotite, muscovite and graphite. A reflected light photomicrograph of the same area can be found in figure X.

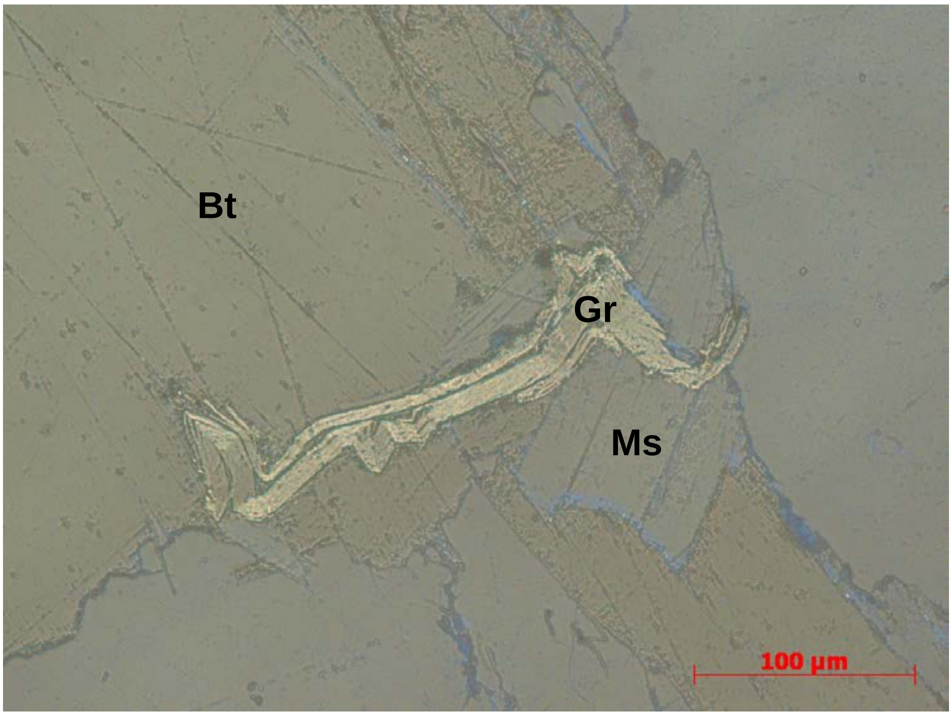

Figure A11. Photomicrograph of thin section 525138, in reflected light. Example of the relation between biotite, muscovite and graphite.

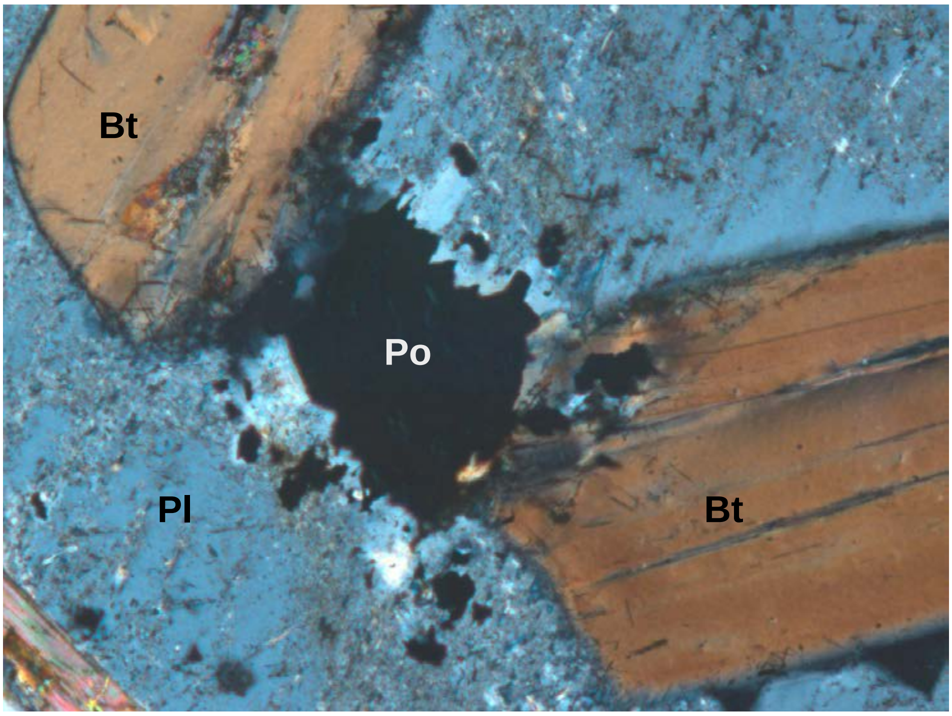

Figure A12. Photomicrograph of thin section 525139, in transmitted light and with crossed polarizers. Example of the morphology of pyrrhotite and its relation to biotite. The image was taken at 10x and is ~0,5 mm across.

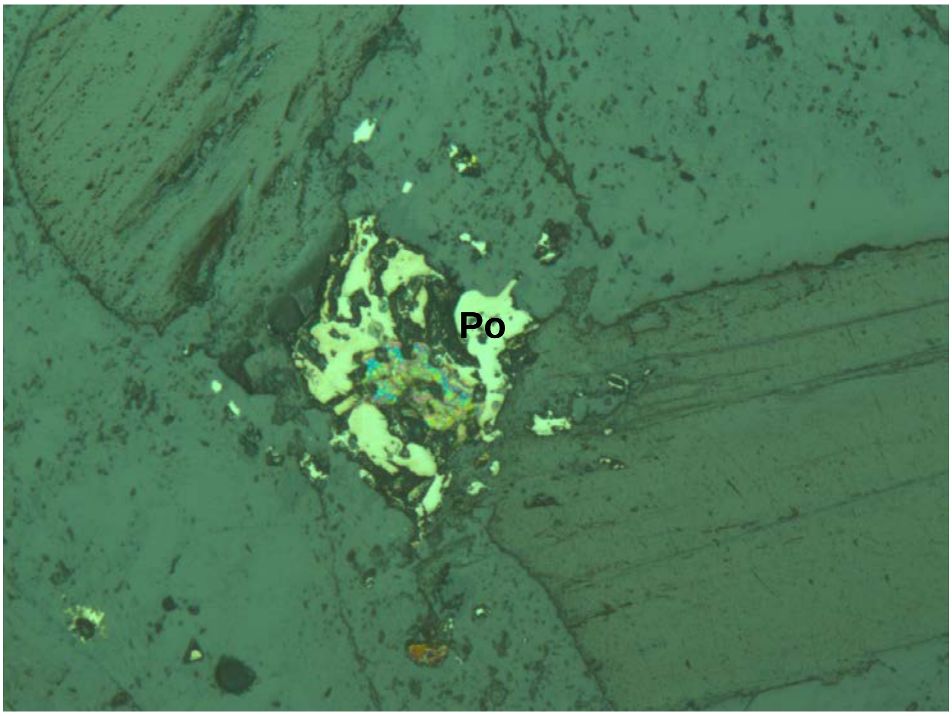

Figure A13. Photomicrograph of thin section 525139, in transmitted light and with crossed polarizers. Example of the morphology of pyrrhotite and its relation to biotite. The image was taken at 10x and is ~0,5 mm across.

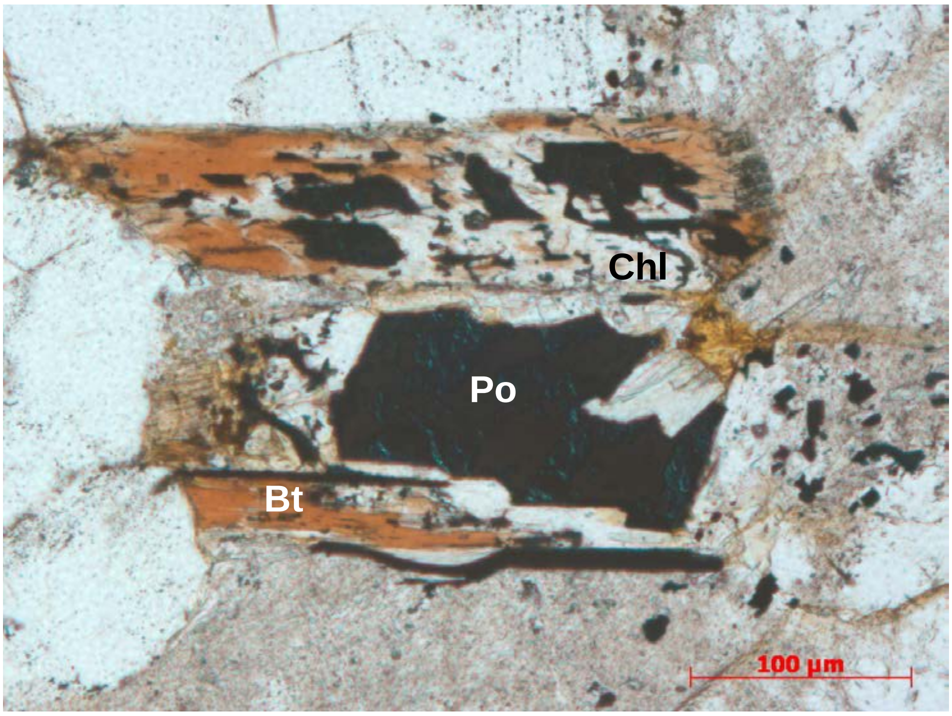

Figure A14. Photomicrograph of thin section 525139, in transmitted light. Example of chloritization of biotite, and its relation to muscovite, pyrrhotite and graphite. See figure A15 for image in crossed polarizers.

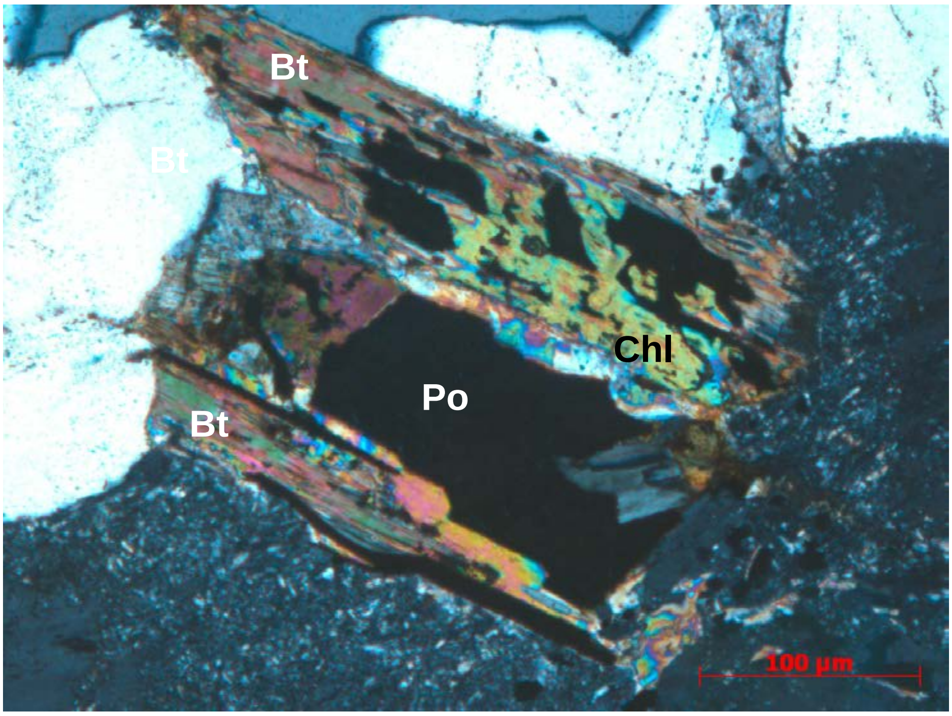

Figure A15. Photomicrograph of thin section 525139, in transmitted light with crossed polarizers. Example of chloritization of biotite, and its relation to muscovite, pyrrhotite and graphite. Figure A14 is in transmitted light.

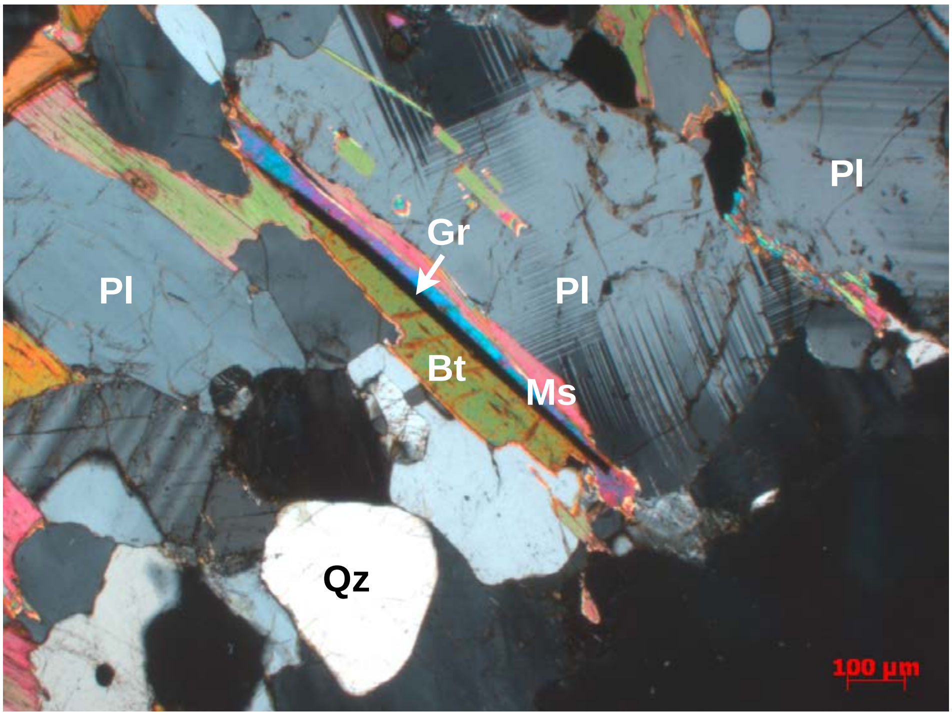

Figure A16. Photomicrograph of thin section 525139, in transmitted light and with crossed polarizers. Example of twinning in plagioclase and the 'sandwich'-structure of the paragneiss-group.

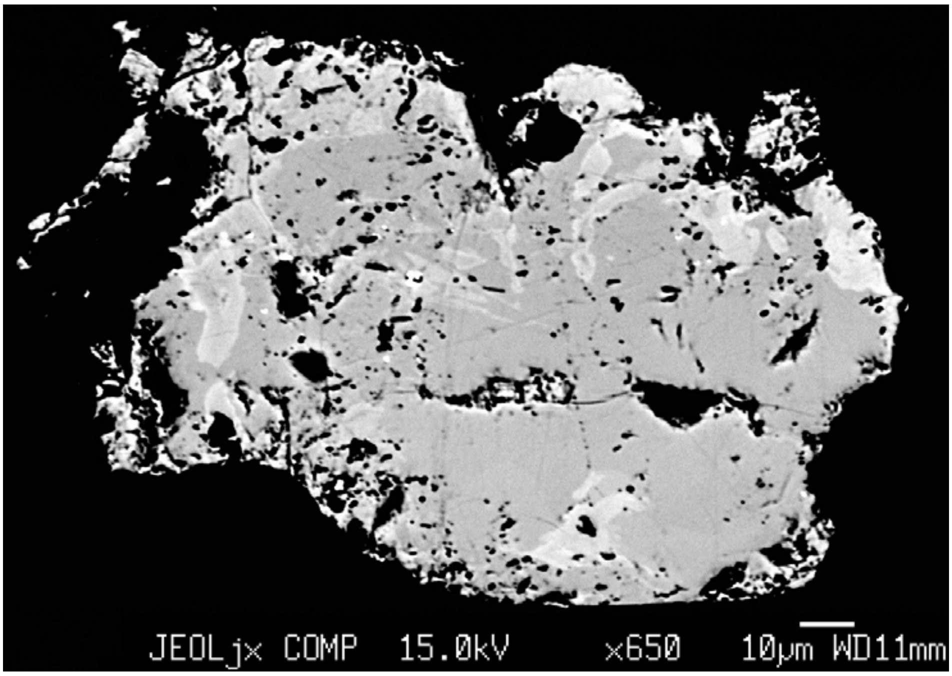

Figure A17. BSE-image of pyrite grain in thin section 525139. The rim appears bright and heterogen.

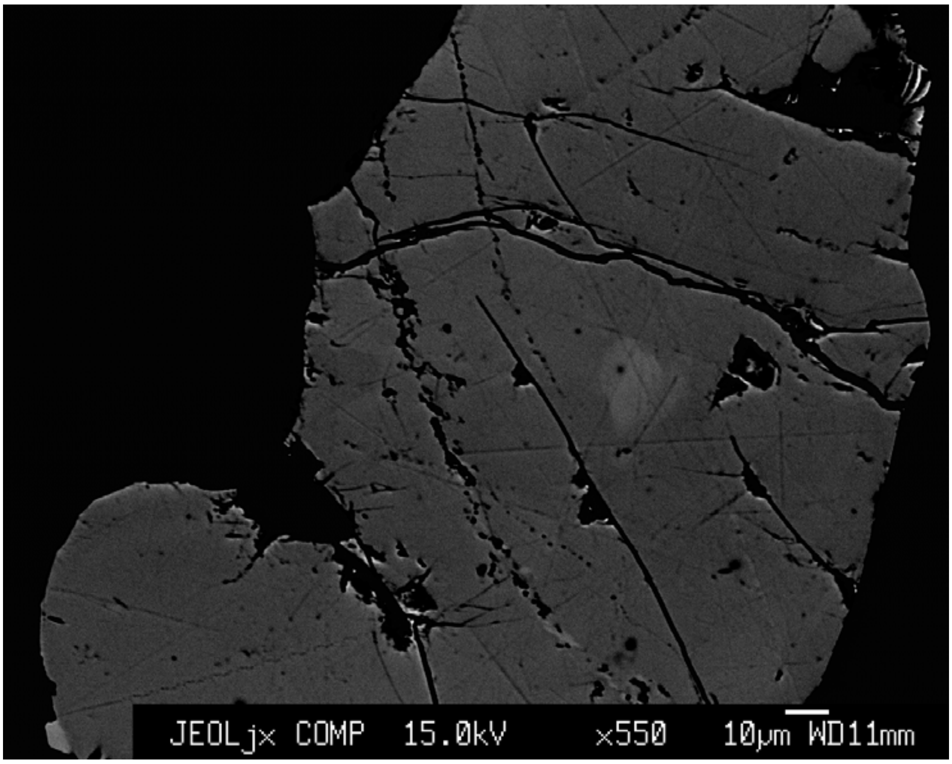

Figure A18. Example of zoning in monazite, thin section 525137. The largest monazite in the middle of figure A19 is this grain.

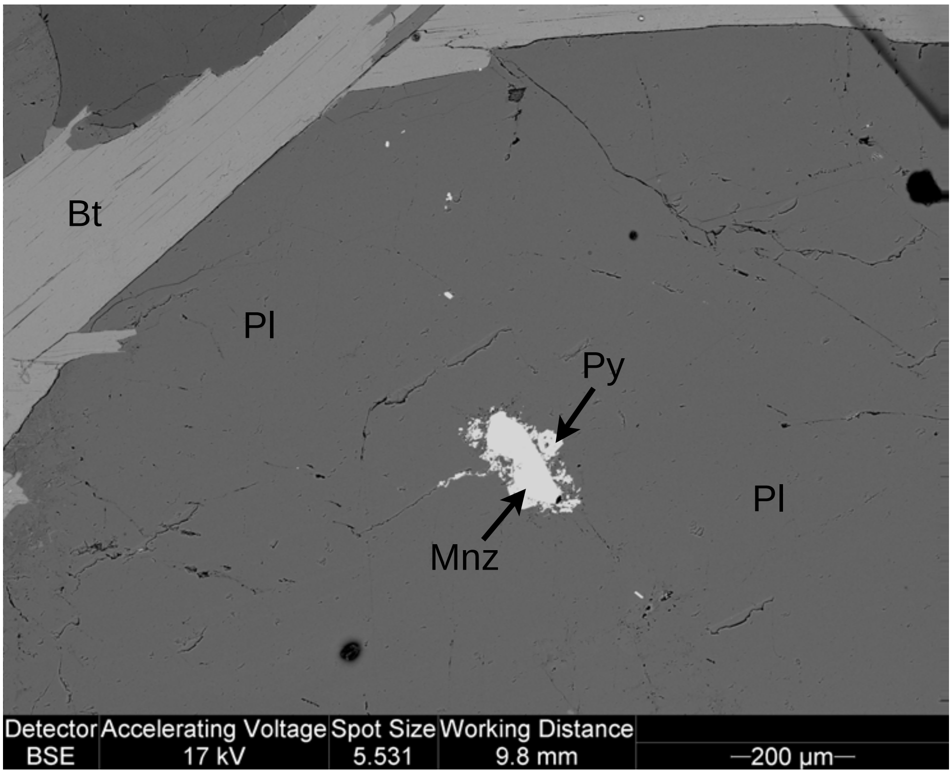

Figure A19. Example of monazite with a pyrite rim in plagioclase, thin section 525139 (mineral abbreviations after Siivola & Schmid, 2007). Pyrite is also present along cracks in the plagioclase.

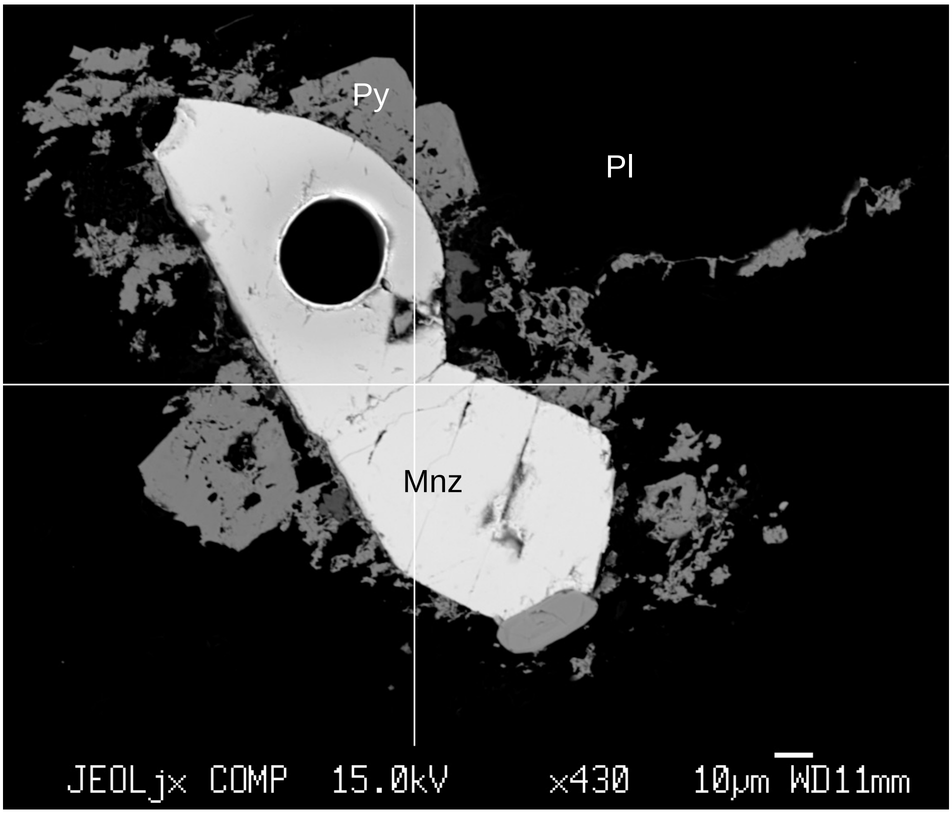

Figure A20. Example of monazite with a pyrite rim in plagioclase, thin section 525139 (mineral abbreviations after Siivola & Schmid, 2007). The same mineral as in figure A19 and A21. The round black hole in the monazite is from LA-ICP-MS analyses.

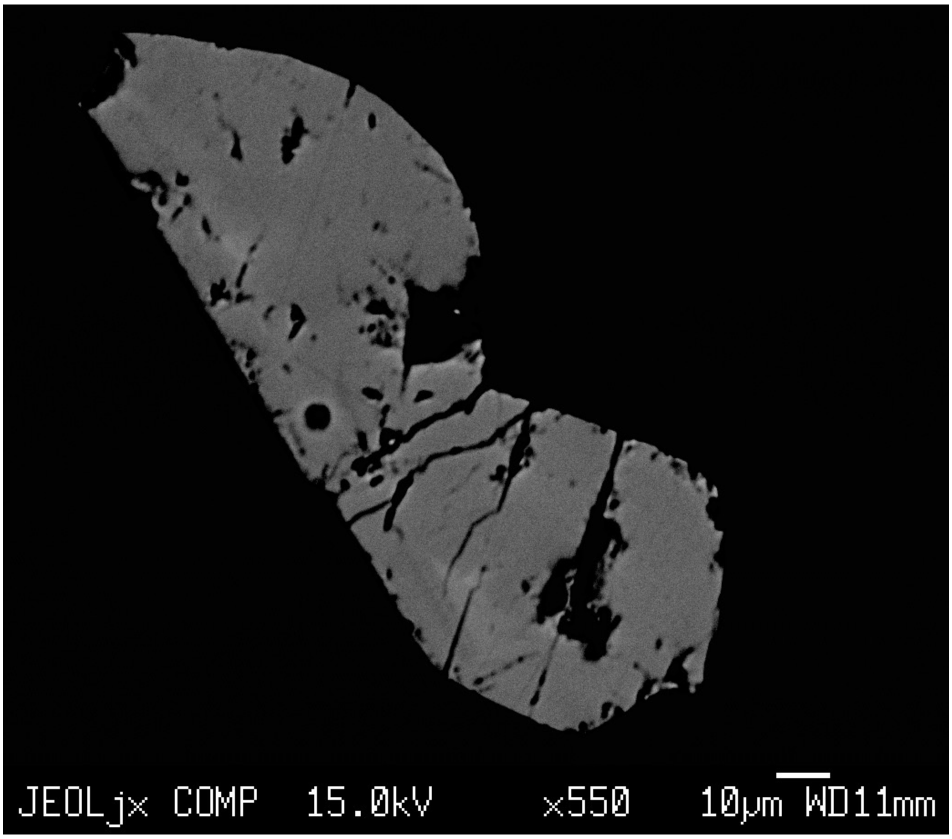

Figure A21. Example of zoning of monazite, thin section 525139. It is the same grain as in figure A19 and A20.

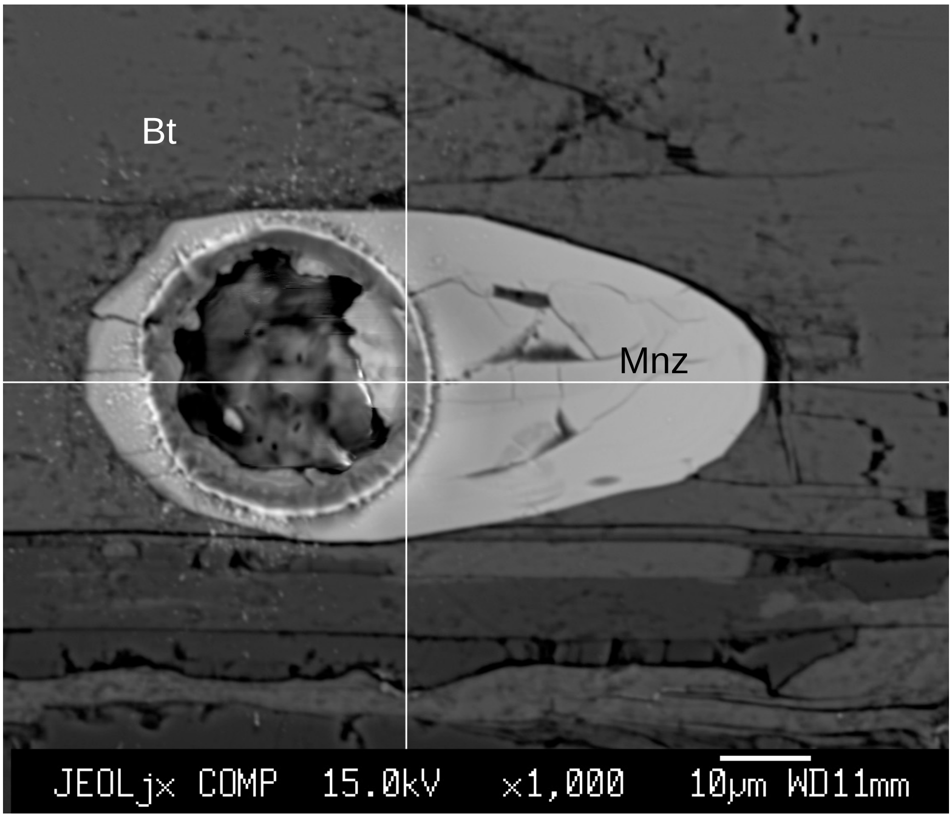

Figure A22. Monazite in biotite, thin section 525138 (mineral abbreviations after Siivola & Schmid, 2007). The round hole in the monazite is from LA-ICP-MS analyses.

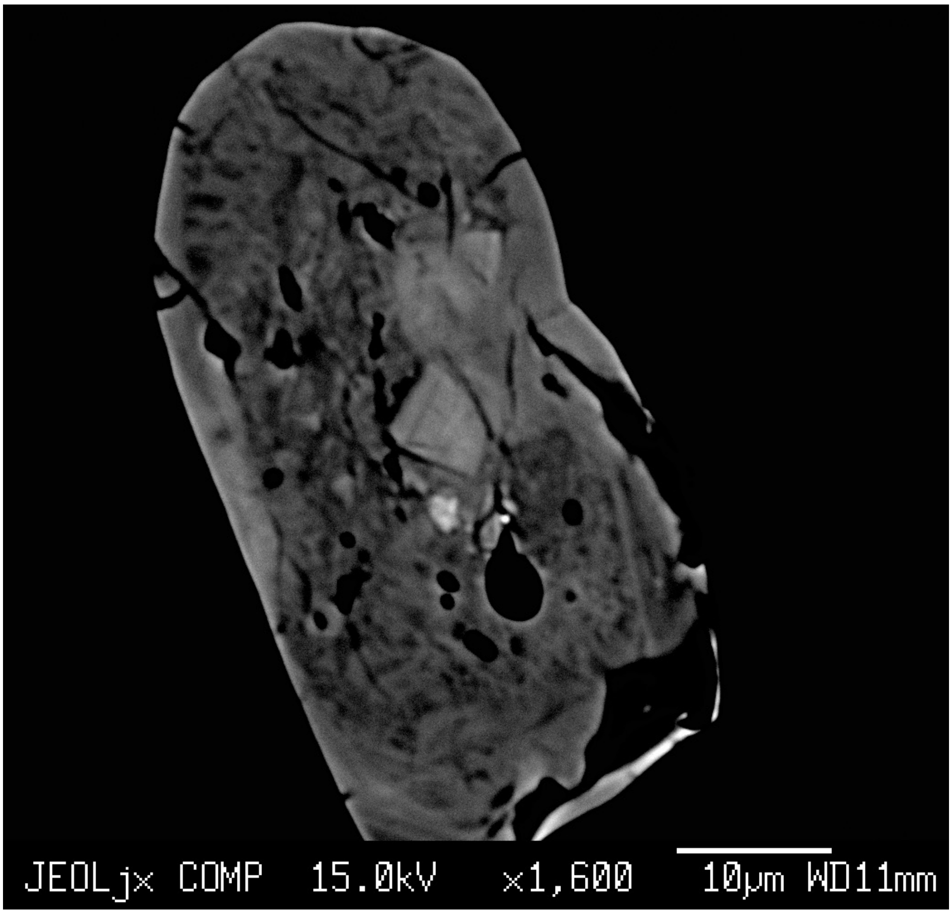

Figure A23: Example of zircon grain from the Ujarrasiorit thin section.

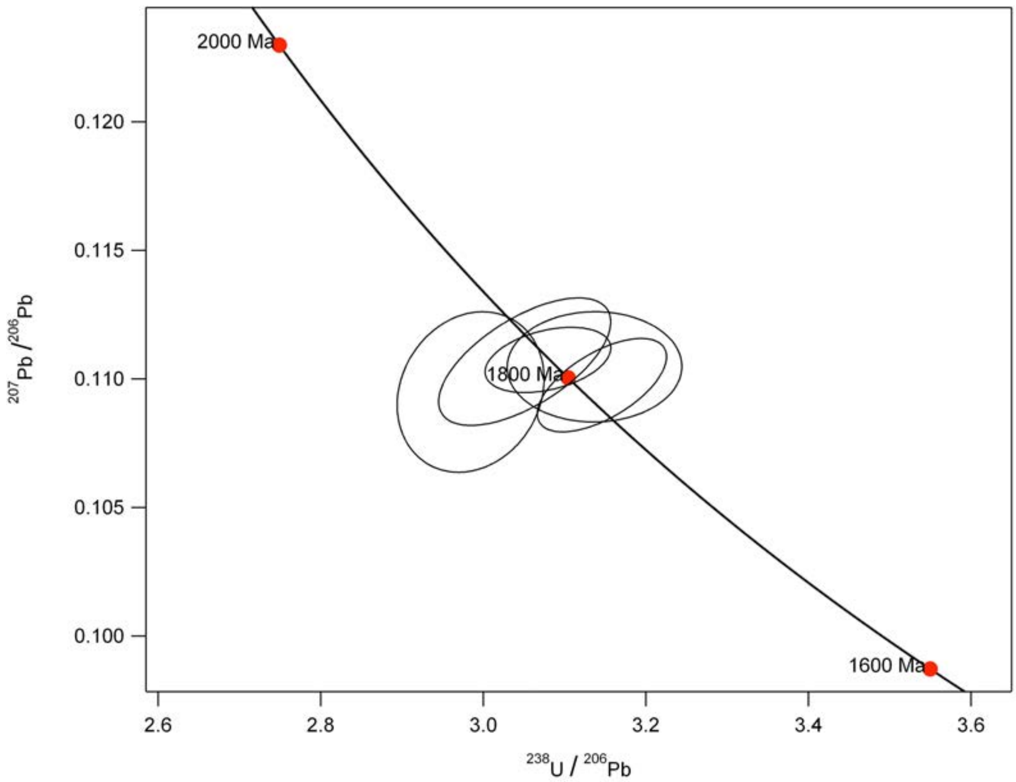

Figure A25. Terra-Wasserburg diagrams of LA-ICP-MS U/Pb monazite analyses from thin section 525137. Analytical errors are depicted at 2σ.

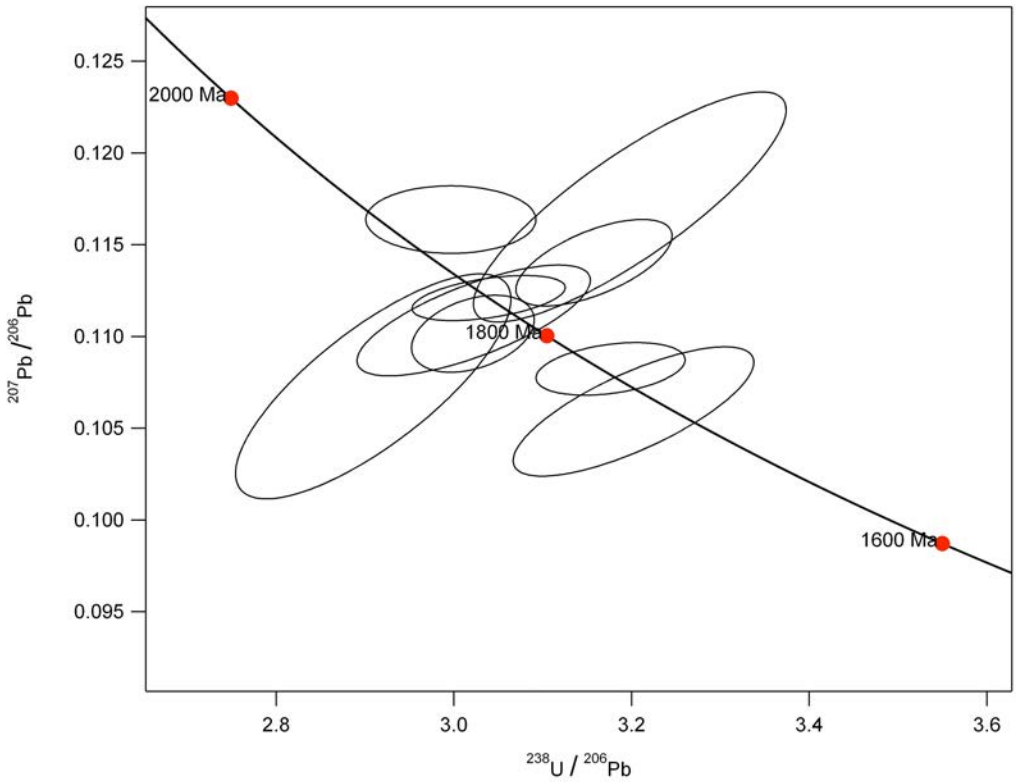

Figure A26. Terra-Wasserburg diagrams of LA-ICP-MS U/Pb monazite, xenotime and zircon data from thin section 525138. Analytical errors are depicted at 2σ.

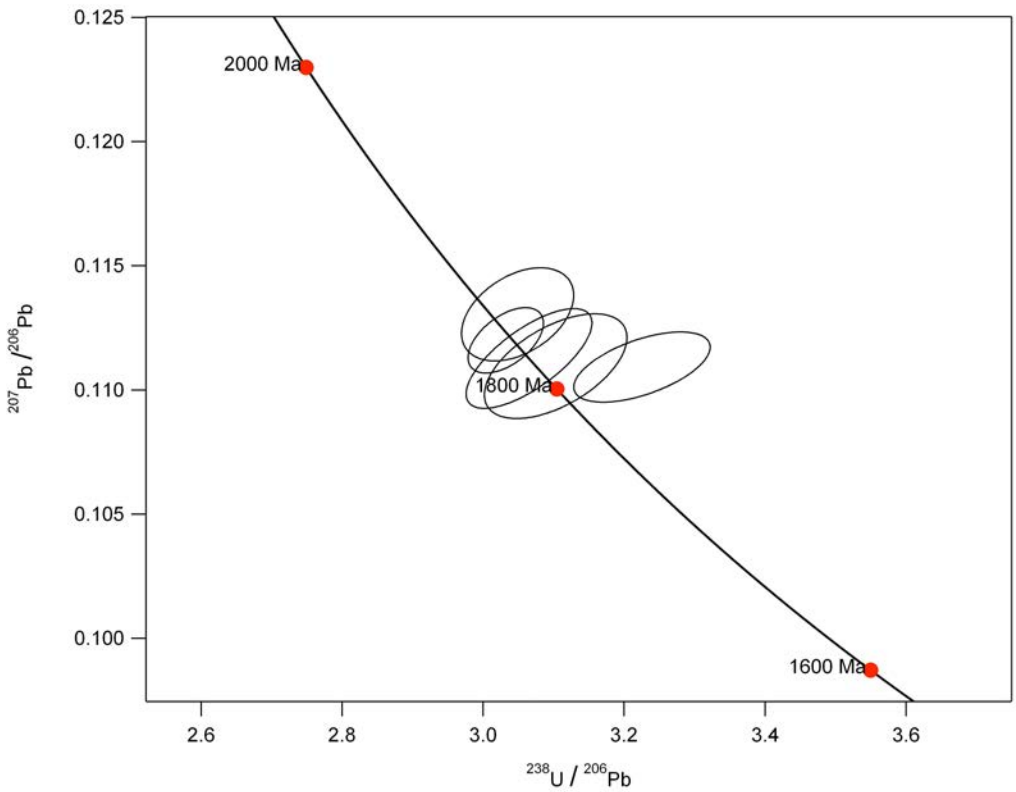

Figure A27. Terra-Wasserburg diagrams of LA-ICP-MS U/Pb monazite data from thin section 525139. Analytical errors are depicted at 2σ.

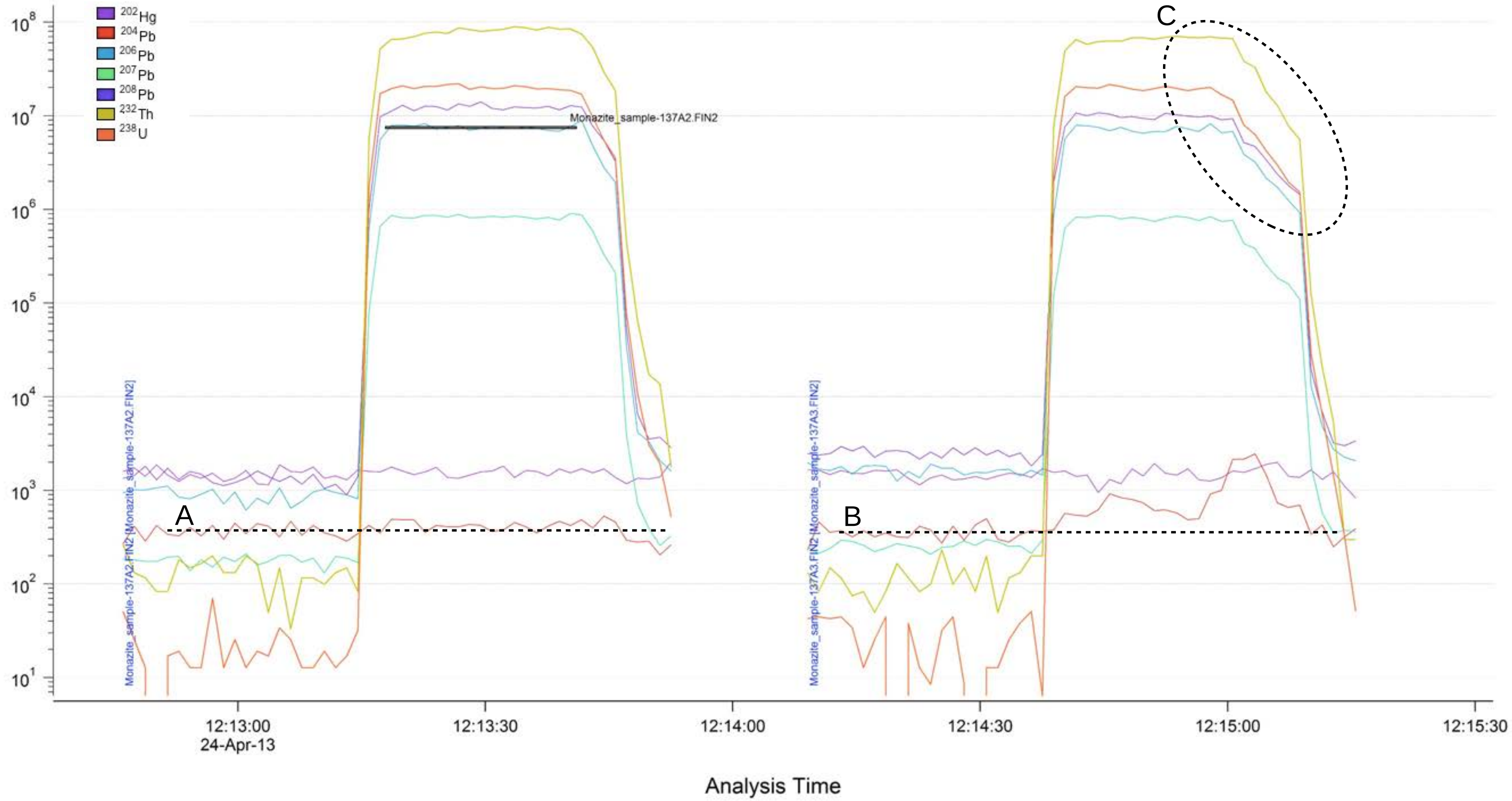

Figure A24. Raw LA-ICP-MS signal, in a time versus counts per second diagram. A: The stippled line depicts an estimated average of the background 204Pb. A minor elevation of 204Pb may be present, as the 204Pb signal seems slightly elevated above the average line. No correction for common Pb was done. B: The stippled line depicts an estimated average of the background 204Pb. As the 204Pb signal is elevated above the average line common Pb is present, and a correction was therefore done. C: The counts per second drops at the end of the signal, as an effect of the laser burning through the thin section. The box marked 'monazite_sample137A2.FIN2' outlines the extend of the signal selected for use in calculation of the U/Pb age.

Model Sample	1976	1977	1978	1983	1991	1992 (HW)	1992 (GS)	2000
Uja - high	593	576	573	581	672	546	500	652
Uja - low	616	595	602	596	672	576	547	657
Uja (tot)	605	586	589	589	673	561	524	655
525138	506	499	466	517	480	508	514	638

Table A1. Garnet-biotite geothermometry - temperatures in °C. Temperatures calculated after: 1976 = Thompson, 1976, 1977 = Holdaway & Lee, 1977, 1978 = Ferry & Spear, 1978, 1983 = Perchuk & Lee, 1983, 1991 = Dasgupta et al., 1991, 1992 = Bhattacharya et al., 1992, 2000 = Holdaway, 2000.

Description of the Ujarrasiorit thin section

The thin section has a brownish green color, and many opaque minerals (~ 10%). A faint brown vein runs at the middle of the section, along the long axis (4-6mm thick). It appears monomineralic and is made up of a faint beige mineral. A mineral with a golden metallic luster boarders the vein at single sections, but is also is disseminated throughout the sample. Another opaque mineral is also disseminated throughout section.

A tabulated description of minerals in the thin section can be found in table B1.

Thin section Ujarassiorit	**PPL color (pleochroism)**	**Relief**	**Anisotropic/ Isotropic**	**Crystal habit**	**Birefringe** δ	**Twinning, structures etc.**	**Other**
Garnet 50-60%	fainth brown, pink tint	high (+)	iso	massive, anhedral, matrix	-	occurs in a vein-like structure - 1/3 of the width of the section thick (0,6 mm)	by far the largest crystals in the section - even outside the 'vein' Has brown biotite as an inclusion mineral, along with plagioclase, K-feldspar and quartz
Pyroxene 25-30%	yellowish orange (moderate)	mod. high (+)	an	sub- to euhedral 1-2 mm	1. order orange	60°/120° fractures	inclined extinction
Biotite 5-7%	green (strong)	mod. high (+)	an	tabular, eu- to anhedral <2 mm	1. order green		
Feldspar Plagioclase 1-2%	colorless	mod. high (+)	an	anhedral blocky <0.6 mm	grey	polysynthetic twinning	

Thin section Ujarassiorit	**PPL color (pleochroism)**	**Relief**	**Anisotropic/ Isotropic**	**Crystal habit**	**Birefringe δ**	**Twinning, structures etc.**	**Other**
Feldspar K-feldspar <1%	colorless	low	an	equant, anhedral <0.4 mm	grey	no twinning - recognized by being biaxial (-)	
RFL *Pyrrhotite* *1-3%*	pale yellow	-	an	massive (blotchy apperance) 0.2-1mm	grey-dusty blue	bleb-like holes	no apparent mineral association, found throughout the section
RFL *Graphite* *2-4%*	off-white	-	an	fibrous, euhedral	grey-beige	kink-bands	appear to be associated with biotite
Quartz <1%	colorless/weak grey	low (+)	an	massive, anhedral <0.4 mm	grey $\delta \sim <0.01$	Uniaxial (+)	not very common - appears slightly yellow in bottom of section
Hematite (?) Supergene <1%	Greyish white	-	iso	In cracks, and as veins	-	only found in veins	veins have rusty brown color in ppl - possibly internal reflections (red?) -

Table B1. Minerals observed in thin section 525139

Description of thin section 525133

The overall color of the thin section is dark green. A dark green mineral dominates the section, and is evenly distributed in the thin section (olivine, table B2). The thin section does not display any apparent foliation or other textures when viewed by the naked eye. However, veins are common at the microscopic level, and all orientated in the same direction (chlorite, table B2). The veins are associated with the dark green isotropic mineral (spinel, table B2).

A tabulated description of minerals in the thin section can be found in table B2.

Thin section 525133	PPL color (pleochroism)	Relief	Anisotropic / Isotropic	Crystal habit	Birefringe	Twinning, structures etc.	Other
Olivine 70-80%	pale green	high (+)	an	equant, subhedral <0.5 mm	2. order green δ ~ 0,050	highly fractured	
Amphibole 10-15%	light blue/ green (weak)	mod. high (+)	an	prismatic, rhombes, sub- to euhedral	1. order blue δ ~ 0,020 0.3-0.6 mm	Inclined extinction	120°/60° fractures
Pyroxene 2-%%	colorless	mod. (+)	an	prismatic, rhombes, sub- to euhedral	1. order orange		90° fractures
Chlorite 5-10%	colorless	mod. (+)	an	massive, anhedreal & in veins	colorless - grey δ ~ 0,010	lamellae of yellow reflective mineral	uniaxial (+) pyrrhotite is often found in the center of veins minerals seem to be perpendicular to the vein making the vein appear plumose

Thin section 525133	PPL color (pleochroism)	Relief	Anisotropic / Isotropic	Crystal habit	Birefringe	Twinning, structures etc.	Other
Spinel 3-5%	dark green	extreme (+)	iso	spherical, euhedral ~ 0.7 mm	-	pyrrhotite common at the rim of spinel	
Plagioclase 2-3%	light beige	mod. (+)	an	massive, anhedral	white δ ~ 0,010	polysynthetic twinning	more common in the lower part of the thin section
RFL *Pyrrhotite* *<1%*	yellow (moderate)	-	an	? in veins - commonly as tiny grains	grey-dusty blue	found both inside chlorite veins and as a separate mineral grain (~ 0.03 mm)	often in the proximity of spinel
RFL *Pyrite* *<<1%*	pale yellow	-	iso	found both as massive and cubic, sub- to anhedral <0.4 mm	-		associated with veins - *tiny* grain size (-0,003mm)
RFL *Graphite* *<<1%*	off-white (extreme)	-	an	fibrous, euhedral up to 5 mm	off-white-beige		uncommon in this thin section

Table B2. Minerals observed in thin section 525133 during microscopy.

Description of thin section 525134a

Thin section 525134a represents a local mineralization of iron oxides and sulfides. This mineralization is no longer available in the hand sample. The overall color of the section is rusty brown, but the upper right corner and lower left corner are monomineralic, and dominated by equant grains of a mineral with a golden metallic lustre (pyrite, table 2). There are three larger grains of the golden mineral, the largest being ~1 cm in diameter, the others slightly smaller. A mineral with golden metallic lustre is also found disseminated throughout the section. The golden mineral makes up ~1/3 of the entire volume of the thin section. The rest of the thin section appears a beige-brown and fairly translucent. The translucent part of the section is characterized by having many fractures and veins, to an extend where it appears brecciated.

A tabulated description of minerals in the thin section can be found in table B3.

Thick section 525134a	PPL color (pleochroism)	Relief	Anisotropic/ Isotropic	Crystal habit	Birefringe	Twinning, structures etc.	Other
RFL *Pyrite* *40-45%*	pale yellow	-	iso	found both as massive and cubic, sub- to anhedral up to 1 cm	-	pyrite also appears in cracks and veins as well as disseminated	seems to be related to magnetite in some circumstances
RFL *Magnetite* 5-10%	grey	-	iso	massive, and also in veins 0,5-2 mm (4 mm - see 'other')	-	blebs or lines of yellow ore mineral as inclusions in magnetite common	yellow ore = pyrite - alteration - cubic to cubic? (larger grains - 4 mm)
RFL *Goethite* *1-2%*	grey (weak)	-	an	marmillary, in veins 0,5 - 5 mm dia.	slightly darker grey (weak)	Internal reflections common (yellow, orange)	associated with magnetite - only found in veins
RFL *Pyrrhotite* *<<1%*	yellow (moderate)	-	an	massive <5 mm	grey-dusty blue		associated with pyrite
gangue (thick section) 40-50%	-	-	-	-	-	-	brecciated

Table B3. Minerals observed in thin section 525134a during optical microscopy.

Description of thin section 525134b

The thin section has two areas of different color; an upper rusty brown part (furthest away from the sample number, grain size <0,5mm) and a lower part, which is distinctly green and more corse grained (0.5mm-2mm) (Hornblende, table B4). The thin section has a low percentage of a mineral with a golden metallic luster (1-2%), which is restricted to the lower green part of the thin section (Pyrrhotite, table B4). The thins section also displays veins. These are translucent but the bordered by brown minerals and minerals with golden metallic luster, and can thus be viewed even with the naked eye (biotite, table B4). The largest vein is about 0.5mm in dia., and there are two other smaller veins in the section which can be viewed without a microscope. Under a microscopic it is possible to see that the upper, brown part of the section has a lot of vugs (8-12% of the volume). With a microscope and a low magnification it is also possible to observe that elongated minerals highlights a general orientation of minerals in this thin section.

A tabulated description of minerals in the thin section can be found in table B4.

Thin section 525134b	PPL color (pleochroism)	Relief	Anisotropic/ Isotropic	Crystal habit	Birefringe	Twinning, structures etc.	Other
Amphibole, Hornblende 60-70%	light blue/ green (weak)	mod. high (+)	an	prismatic, rhombes, sub- to euhedral 2-4 mm	1. order blue $\delta \sim 0.020$		crystals are orientated in same direction (prismatic) Inclined extinction
Feldspar Plagioclase 20-30%	light beige	mod. (+)	an	massive, sub- to anhedral <3 mm	1. order white $\delta \sim 0.01$	often twinning in multiple directions within same mineral	more common in the sulphide-bearing part of the thin section

Thin section 525134b	PPL color (pleochroism)	Relief	Anisotropic/ Isotropic	Crystal habit	Birefringe	Twinning, structures etc.	Other
Pyroxene Clinopyroxene 2-3%	2-3%	mod. high (+)	an	prismatic, rhombes, sub- to euhedral 3-4 mm	1. order orange $\delta \sim 0.007$		more frequent in the lower part of the thin section EDS: clinopyroxene
Feldspar Alkali feldspar 1-2%	white/colorless	mod. (+)	an	massive, sub- to anhedral <3 mm	1. order white $\delta \sim 0.01$		more common in the sulphide-bearing part of the thin section
RFL Pyrrhotite 1-2%	yellow (moderate)	-	an	massive, some equant 1-4 mm	grey-dusty blue	subhedral isometric crystals are present, but rare	
RFL *Hematite* *<1%*	Greyish white	-	iso	In cracks, and as veins	-	In veins	internal reflections possible - Goethite may be present as a minor constituent

Table B4. Minerals observed in thin section 525134b during optical microscopy.

Description of thin section 525135

The overall color of the section is greenish brown. A thin (~1mm) dark brown, slightly waving, line runs throughout the length of the section. A not as defined line of a dark brown mineral runs perpendicular to this line (hematite, table B5). Prismatic minerals highlights a general orientation of the minerals in this thin section. When viewed in a microscope it is possible to see that the section has a large amount of holes/vuggs (5-10%).

A tabulated description of minerals in the thin section can be found in table B5.

Thin section 525135	PPL color (pleochroism)	Relief	Anisotropic/ Isotropic	Crystal habit	Birefringe	Twinning, structures etc.	Other
Pyroxene Orthopyroxene (90-95%)	pale pink/blue (moderate)	high (+)	an	prismatic, cubic, sub- to euhedral 2-5 mm	1. order orange $\delta \sim 0.007$	triangular pitts, 90° fractures in elongated sections	Inclined extinction
Feldspar Plagioclase 3-5%	light beige	mod. (+)	an	massive, sub- to anhedral 1-3 mm	1. order white $\delta \sim 0.01$	twinning uncommon	
Amphibole 1-2%	colorless (weak)	mod. high (+)	an	prismatic, rhombes, sub- to euhedral 1-3 mm	1. order blue $\delta \sim 0.020$	commonly less pitted that pyroxene	Inclined extinction
RFL Hematite <<1%	Greyish white	-	iso	In cracks, and as veins	-	PPL: Rusty lines on top of other minerals RFL: In cracks and as veins	Yellow internal reflections

Thin section 525135	PPL color (pleochroism)	Relief	Anisotropic/ Isotropic	Crystal habit	Birefringe	Twinning, structures etc.	Other
RFL Graphite <<1%	off-white (extreme)	-	an	fibrous <2 mm	off-white-beige		very few grains have been observed

Table B5. Minerals observed in thin section 525135 during optical microscopy.

Description of thin section 525137

The thin section is colorless with bands of a dark brown mineral (biotite, table B6). The brown mineral bands constitutes ~50% of the thin section area.

The dark brown mineral highlights a foliation in the thin section. A colorless eye-shaped structure is present in the top right corner (furthest away from the sample number). It is approx. 7mm i dia., and the only non-banding prominent non-banding structure in the section. A mineral with gold metalic luster is disseminated throughout the section, but is an overall minor component (3-4%). The golden minerals are commonly ~0,5mm in size, but single grains can get up to ~2mm. Minerals seem to be generally larger in the colorless areas of the thin section (2-3mm in dia.).

Although this section looks very similar to thin section 525138/525139 when seen with the naked eye, it looks much more ‘disturbed’ when viewed at the microscopic level. Microfracturing is extensive, and especially plagioclase and quarts looks highly fractured and partially dissolved. Chloritization of biotite and rutile in biotite is much more common in this thin section than in thin section 525138 and 525139. The foliation is highlighted by the brown platy mineral at the microscopic level as well as the macroscopic. Several microveins can be viewed at the microscopic level (~0.1mm). The veins seem to be related to the presence of biotite. The microveins are mainly quartz, with minor components of biotite, chlorite and muscovite. The microveins are also associated with opaque minerals - mainly pyrrhotite (RFL).

A tabulated description of minerals in the thin section can be found in table B6.

Thin section 525137	**PPL color (pleochroism).**	**Relief**	**Anisotropic / Isotropic**	**Crystal habit**	**Birefringe δ**	**Twinning, structures etc.**	**Other**
Feldspar Plagioclase 30-40%	light beige	mod. high (+)	an	massive, sub- to anhedral 1-4 mm	1. order white δ ~ 0.01	polysynthetic twinning - often twinning in multiple directions	symplectite
Quartz 20-25%	colorless	low (+)	an	massive, subhedral 1-3 mm	white δ <0.01		commonly undulatory extinction
Biotite 15-20%	brown (strong)	mod. high (+)	an	tabular, eu- to anhedral 2-4 mm	1. order green δ ~ 0.025	radiogenic inclusions in biotite common Highlights banding	biotite oriented with c-axis-view is common (‘smeared’ biotite? undulating extinction) - not present in the two previous sections
K-feldspar Microcline 7-10%	colorless	low neg	an	massive, anhedral 1-3 mm	1. order white δ ~ 0.01	tartan plaid - crossing - albite/pericline twinning? (Nichols, 2000)	
RFL *Pyrrhotite* *2-3%*	yellow (moderate)	-	an	massive 1-2 mm	grey-dusty blue	the surface has many holes - minerals are surrounded by smaller minerals making splash-like structures	associated with biotite and graphite

Thin section 525137	PPL color (pleochroism).	Relief	Anisotropic / Isotropic	Crystal habit	Birefringe δ	Twinning, structures etc.	Other
K-feldspar Low sanidine <1%	colorless	low neg	an	massive, sub-to anhedral 1-3 mm	1. order white δ ~ 0.008-0.01	biax neg. 2Vx = ~ 35	possibly also occurs as mineral grains in matrix as well
RFL *Graphite* *<1%*	off-white (extreme)	-	an	fibrous, euhedral 0,5-2 mm	off-white-beige	'sandwich'-structures - biotite/graphite/ muscovite layer cakes	associated with biotite looks 'dirty' in XPL +RFL Can be found as a layer in biotite
Chlorite <1%	pale green	mod. (+)	an	as substitution mineral in biotite	1. order pale orange δ ~ 0.010	found in biotite - but also as an independent mineral	chlorite is often associated with pyrrhotite (e.g. along rim)
Muscovite <1%	bluish white	mod. (+)	an	platy 0.5-1 mm	2. order green δ ~ 0.05		often found in biotite as a substitute - but can also be found independently
Zircon <<1%	colorless	high (+)	an	Prismatic <<0.5 mm	1. order grey δ ~ 0.004		only found inside biotite - creates radiohaloes
RFL *Rutile* *<<1%*	dark brown	extre me (+)	- (grains too small)	acicular, euhedral µm-size	- (grains too small)	found as an accessory mineral in chloritizied biotite	

Thin section 525137	**PPL color (pleochroism).**	**Relief**	**Anisotropic / Isotropic**	**Crystal habit**	**Birefringe δ**	**Twinning, structures etc.**	**Other**
RFL Pyrite <<1%	pale yellow	-	iso	found both as massive and cubic euhedrals 0.5-1 mm	-	surface of all grains are filled with rounded holes	associated with biotite and graphite - in rims around monazite
RFL Pyrrhotite <<1%	yellow (moderate)	-	an	massive 0.5-1 mm	grey-dusty blue		associated with biotite and graphite
Monazite <<1%	colorless	high (+)	an	rounded 0.5-2 mm	2. order green $\delta \sim 0.05$	has a golden ore mineral at rime - only two grains found	

Table B6. Minerals observed in thin section 525137 during optical microscopy.

Macroscopic description of thin section 525138

The thin section is colorless with bands of a brown mineral. The brown mineral bands constitutes ~40% of the thin section area. The section appears to be similar to 525139 and 525137 when viewed with the naked eye, but minerals with gold metallic lustre are not visible. On the microscopic scale the presence of garnet in this section sets it apart from thin section 525139/525137. Alteration and chloritization is less prominent in this section than in 525139/525137, thus rutile is also less common. Muscovite is on the contrary more common in this section than in thin section 525139, and are often found as an independent mineral. The foliation observed in the hand sample is apparent at the microscopic scale, as biotite and a thready mineral highlights the foliation by its orientation. The mineral grains seem to be generally larger in the colorless areas of the thin section.
A tabulated description of minerals in the thin section can be found in table B7.

Thin section 525138	PPL color (pleochroism).	Relief	Anisotropic/ Isotropic	Crystal habit	Birefringe	Twinning, structures etc.	Other
Quartz 30-40%	colorless	low (+)	an	massive, subhedral 2-4 mm	white <0.01		
Biotite 20-25%	Warm brown (strong)	mod. high (+)	an	tabular, eu- to subhedral 2-4 mm	1. order green δ ~ 0.025	'sandwich'-structures - biotite/ graphite/muscovite layer cakes	zircons common as inclusions - radiogenic alteration haloes.
Plagioclase 15-20%	light beige	mod. high (+)	an	massive, anhedral 1-4 mm	1. order white δ ~ 0.01	polysynthetic twinning	often very fractured
Chlorite 5-10%	pale green	mod. (+)	an	as substitution mineral in biotite	1. order pale orange δ ~ 0.010		Chloritization of biotite - not present as an independent mineral
Garnet 1-2%	fainth brown, pink tint	high (+)	iso	massive to equant 0.5-2 mm	-	has a lot of inclusionary minerals - also pyrrhotite and graphite (RFL)	pyralspite group due to isotropy (Nichols, 2000)
Muscovite 1-2%	bluish white	mod. (+)	an	platy 1-2 mm	2. order blue δ ~ 0.05	'sandwich'-structures - biotite/ graphite/muscovite layer cakes	Commonly found near or on top of biotite, but as an independent mineral

Thin section 525138	PPL color (pleochroism).	Relief	Anisotropic/ Isotropic	Crystal habit	Birefringe	Twinning, structures etc.	Other
RFL Graphite <1%	off-white (extreme)	mod. high (+)	an	fibrous, euhedral 0.5-2 mm	off-white-beige		often found as a layer in biotite - but not restricted thereto
Zircon <<1%	colorless	high (+)	an	<<0.5 mm	1. order grey $\delta \sim 0.004$		radiohaloes common
RFL *Pyrite* *<<1%*	pale yellow	-	iso	found both as massive and cubic euhedrals 0.5-1 mm	-	surface of all grains are filled with rounded holes	rims around monazite
RFL Pyrrhotite <<1%	yellow (moderate)	-	an	massive 0.5-2 mm	grey-dusty blue		associated with biotite A single garnet was also found to hold a golden ore mineral
Rutile <<1%	dark brown	extreme (+)	- (grains too small)	acicular, euhedral	- (grains too small)	needles are micrometer-size	Only found in chloritized biotite
Monazite <<1%	colorless	high (+)	an	rounded up to 3 mm	2. order green $\delta \sim 0.05$	has a golden ore mineral at rime - only two grains found	

Table B7. Minerals observed in thin section 525138 during optical microscopy.

Description of thin section 525139

The thin section is colorless with bands of a brown mineral. The brown mineral bands constitutes ~50% of the thin section area. The dark brown mineral highlights the foliation of the thin section. The top part of the section (furthest away from sample number) has a wedge-shaped structure which takes up almost 1/3 of the entire section. This wedge is dominated by a colorless minerals. Four colorless eye-shaped structures (from 3-7mm i dia.) is also present. A mineral with gold metallic luster is disseminated throughout the section, but is an overall minor component. The golden mineral is absent where the colorless mineral and thus the wedge-shaped and eye-shaped structures are present. The foliation is also recognizable at the microscopic level. Minerals seem to be generally larger in the colorless areas of the thin section.

The minerals in this section seems much more 'disturbed' than in 525137/525138, as microfractures is extensive, and especially plagioclase and quarts looks dissolved. The minerals of this section are more altered than that of 525138, and this thin section does not hold garnet. Rutile is much more common in this section, probably due to the more extensive alteration of this section compared to thin section 525137/525138.

A tabulated description of minerals in the thin section can be found in table B8.

Thin section 525139	PPL color (pleochroism)	Relief	Anisotropic / Isotropic	Crystal habit	Birefringe δ	Twinning, structures etc.	Other
Quartz 30-40%	colorless/weak grey	low (+)	an	massive, anhedral 1-3 mm	white δ ~ <0.01	undulating extinction common	Rounded bleb-like inclusions have been observed - mineralogy not determined due to very small grain size
Feldspar Plagioclase 20-30%	colorless/ light grey	mod. high (+)	an	anhedral blocky 0.5-3 mm	grey δ ~ 0.01	polysynthetic twinning common - carlsbad twinning present as a minor type	looks altered/fractures
Biotite 25-30%	brown (strong)	mod. high (+)	an	tabular, eu- to anhedral 0.5-2 mm	1. order green δ ~ 0.025	chloritization of biotite common Zircon common as an inclusionary mineral	highlights the foliation in the sample. Strong pleochroism

Thin section 525139	**PPL color (pleochroism)**	**Relief**	**Anisotropic / Isotropic**	**Crystal habit**	**Birefringe δ**	**Twinning, structures etc.**	**Other**
Chlorite 5-10%	pale green	mod. (+)	an	substitution in biotite	1. order orange δ ~ 0.015	accompanied by rutile needles when found as a substitute in biotite	chlorite-alteration of biotite - chlorite not present as an independent mineral. about 60-70% of biotite is altered
Muscovite 2-3%	bluish white	mod. (+)	an	platy, euhedral 0.5-1 mm	2. order blue δ ~ 0.04	‘sandwich’-structures - biotite/graphite/muscovite layer cakes	associated with biotite - often incorporated in biotite, but also found independently
RFL Pyrrhotite 1-3%	pale yellow	-	an	massive (blotchy apperance) <2 mm	grey-dusty blue	funny opaque structures; looks like paint splashes	pyrrhotite is associated with biotite and graphite, though not restricted to its proximity
RFL Graphite *<1%*	off-white	-	an	fibrous, euhedral 0.5-2 mm	grey-beige	‘woody’ look - deformation textures	graphite is associated with biotite Single graphite minerals has inclusions - ‘spotty’ bands of pyrrhotite (?)

Thin section 525139	**PPL color (pleochroism)**	**Relief**	**Anisotropic / Isotropic**	**Crystal habit**	**Birefringe** δ	**Twinning, structures etc.**	**Other**
RFL *Pyrite* *<<1%*	yellow	-	iso	cubic euhedrals possible - commonly anhedral <1 mm	-		not as common as pyrrhotite
Zircon <<1%	colorless	high (+)	an	prismatic - sub- to anhedral <<0.5 mm	grey $\delta \sim 0.004$	single crystals have been found to have high birefringe, but commonly the zircons are grey (low biref)	radiohaloes are common
Rutile <<1%	dark brown	extreme (+)	- (grains too small)	acicular, euhedral	- (grains too small)	needles are micrometer-size	only found in chlorite-altered biotite - exolution-Ti-mineral

Table B8. Minerals observed in thin section 525139 during optical microscopy.

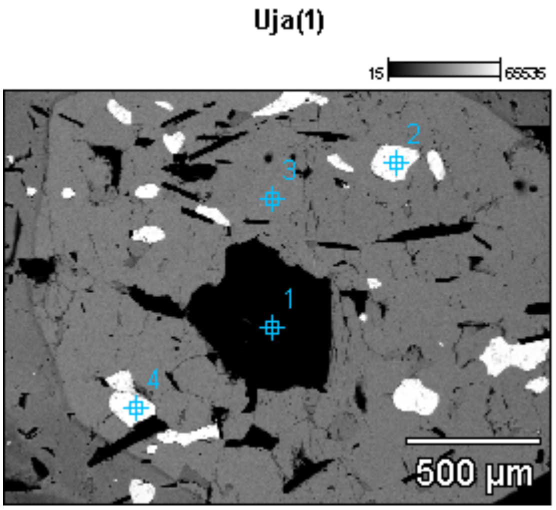

Image name: Uja(1)
Magnification: 60

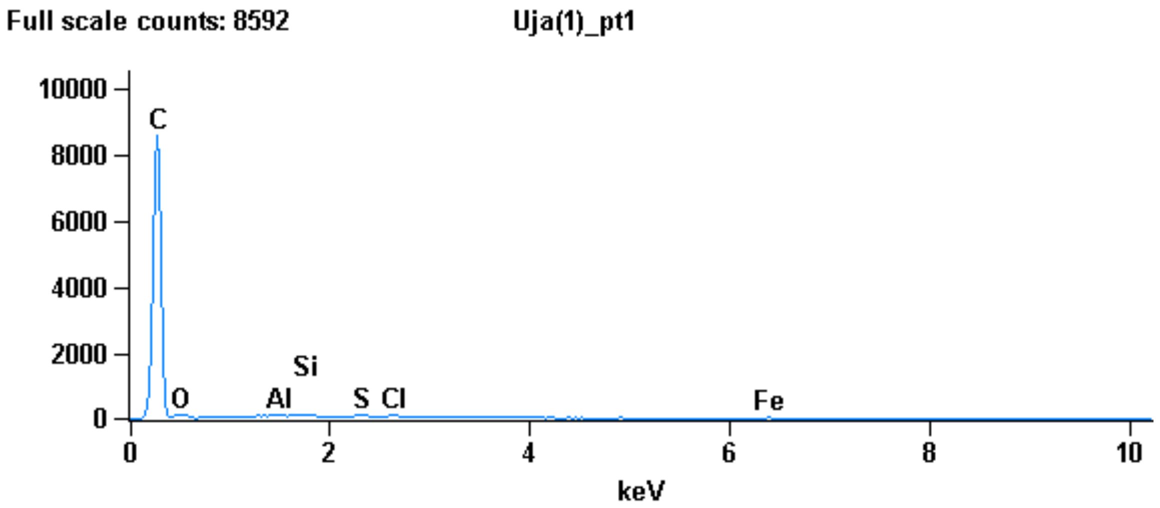

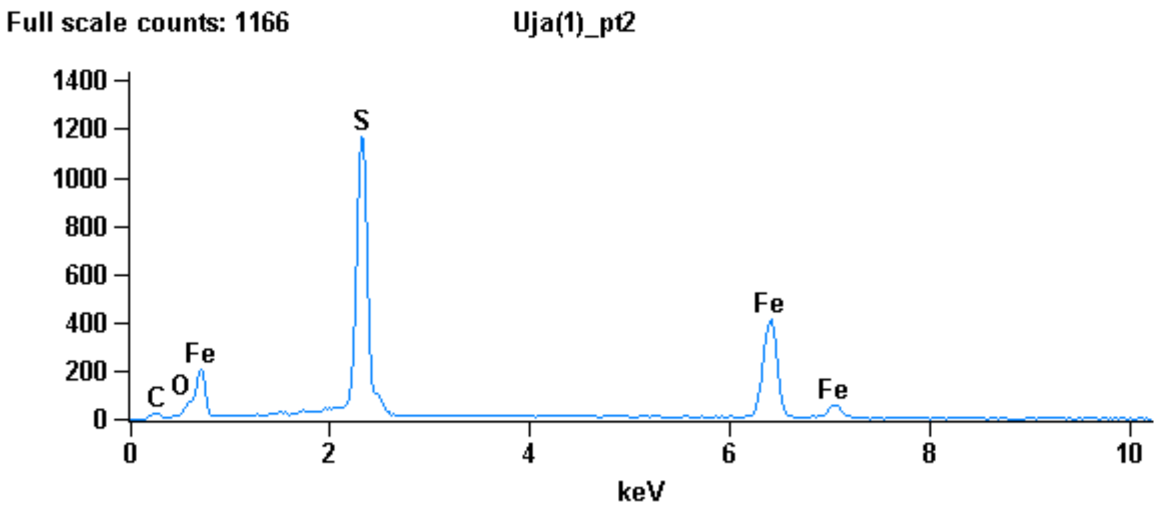

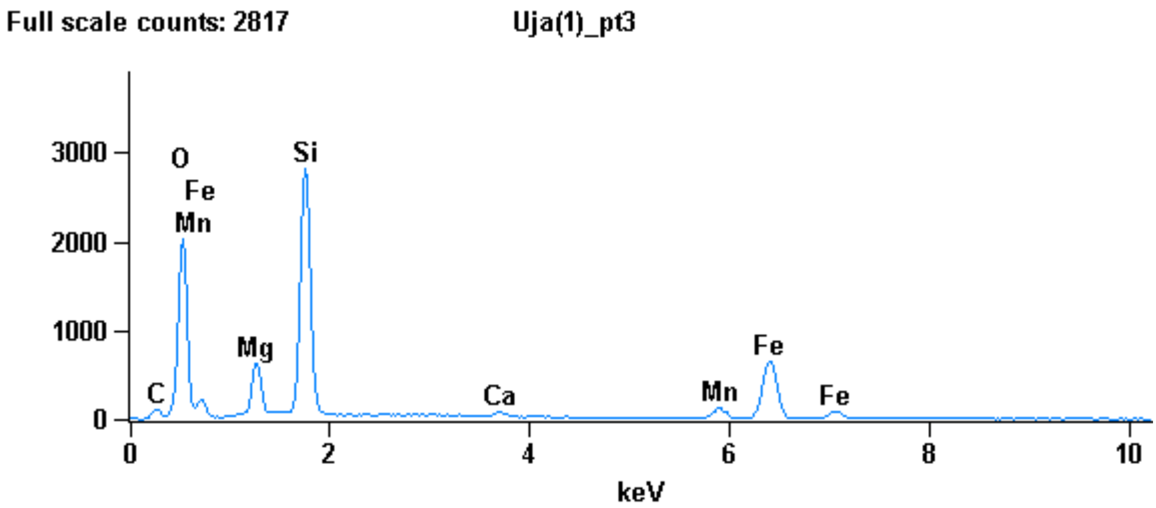

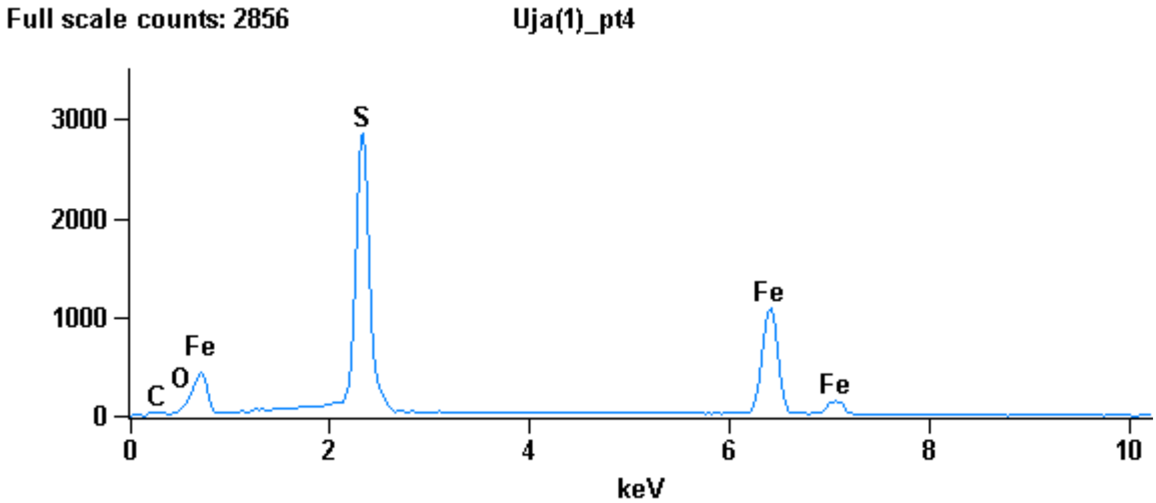

Weight %

	O-K	Mg-K	Al-K	Si-K	S-K	Cl-K	Ca-K	Mn-K	Fe-K
Uja(1)_pt1	39.83S		4.83	8.03	12.79	17.68			16.84
Uja(1)_pt2	45.73S				20.99				33.28
Uja(1)_pt3	42.07S	6.74		22.72			0.60	3.38	24.50
Uja(1)_pt4	45.63S				20.86				33.51

Atom %

	O-K	Mg-K	Al-K	Si-K	S-K	Cl-K	Ca-K	Mn-K	Fe-K
Uja(1)_pt1	59.94		4.31	6.89	9.60	12.01			7.26
Uja(1)_pt2	69.56				15.94				14.50
Uja(1)_pt3	62.15	6.55		19.12			0.35	1.45	10.37
Uja(1)_pt4	69.52				15.86				14.63

Compound %

		MgO	Al2O3	SiO2	SO3	Cl	CaO	MnO	Fe2O3
Uja(1)_pt1	0.00		9.13	17.19	31.94	17.68			24.07
Uja(1)_pt2	0.00				52.42				47.58
Uja(1)_pt3	0.00	11.18		48.60			0.84	4.36	35.02
Uja(1)_pt4	0.00				52.09				47.91

Minerals, Uja(1)
pt1: Mixed signal, hole in thin section
pt2: Pyrrhotite
pt3: Orthopyroxene - enstatite-ferrosilite
pt4: Pyrrhotite

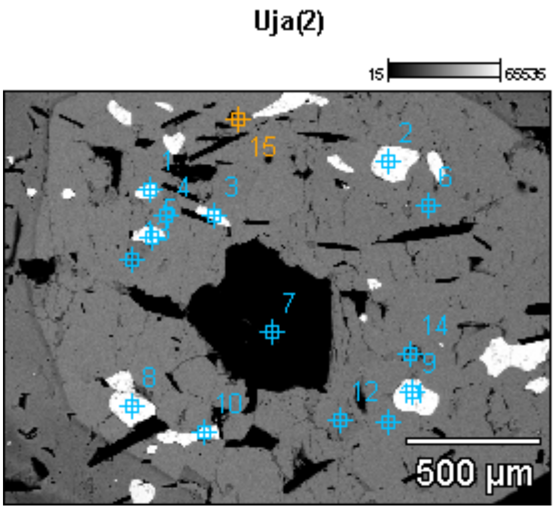

Image name: Uja(2)
Magnification: 60

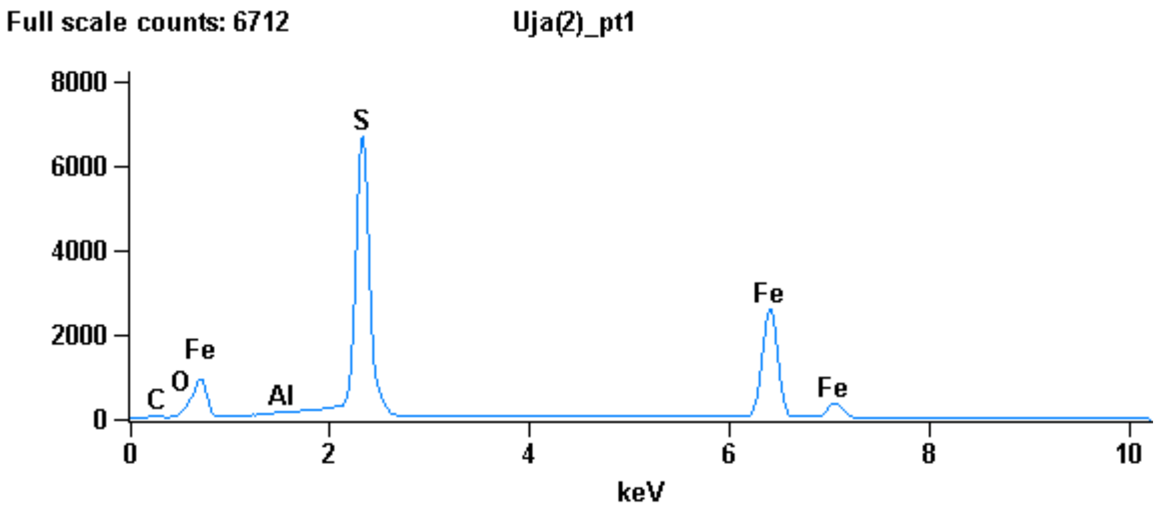

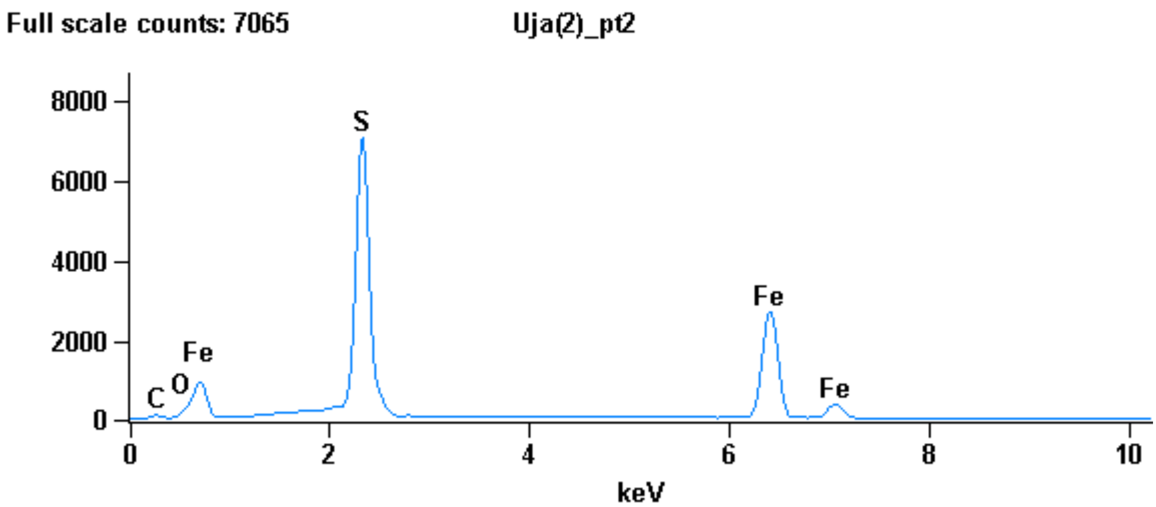

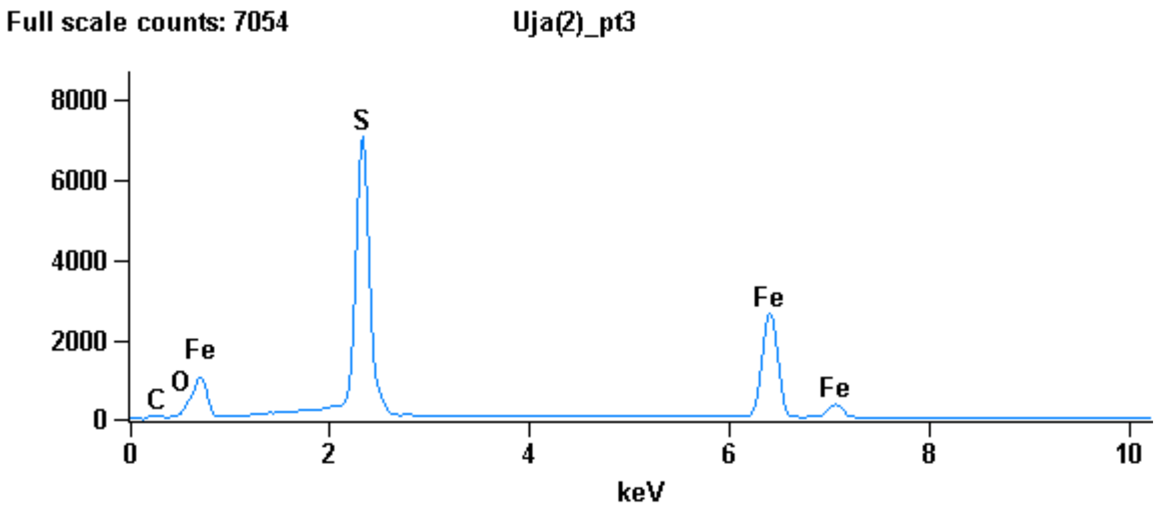
Full scale counts: 7054
Uja(2)_pt3
8000
6000
4000
2000
0
S
Fe
Fe
C
O
Fe
0
2
4
6
8
10
keV

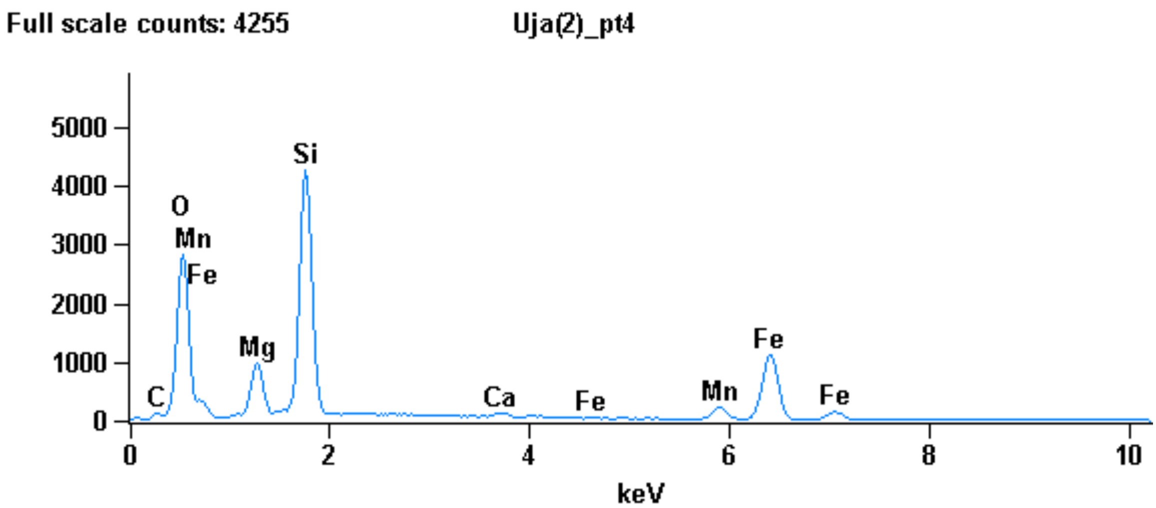
Full scale counts: 4255
Uja(2)_pt4
5000
4000
3000
2000
1000
0
Si
O
Mn
Fe
Mg
C
Ca
Fe
Mn
Fe
Fe
0
2
4
6
8
10
keV

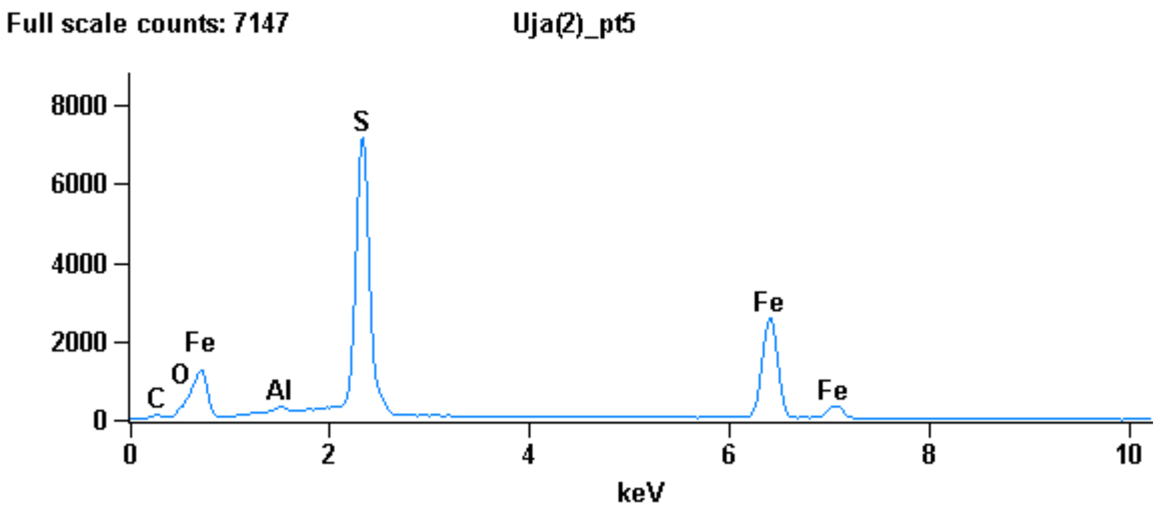
Full scale counts: 7147
Uja(2)_pt5
8000
6000
4000
2000
0
S
Fe
Fe
C
O
Al
Fe
0
2
4
6
8
10
keV

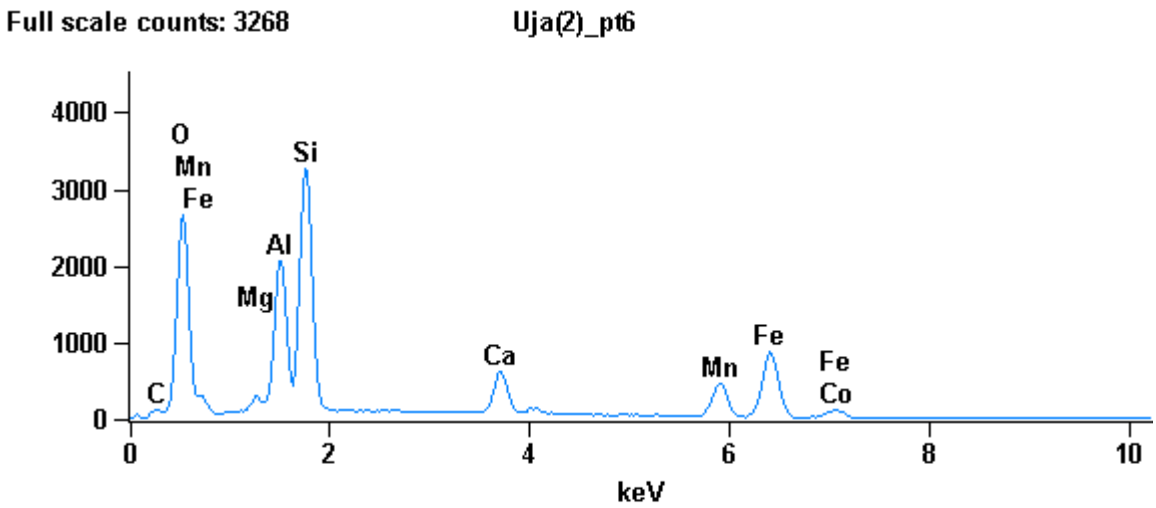
Full scale counts: 3268
Uja(2)_pt6
4000
3000
2000
1000
0
O
Mn
Fe
Si
Al
Mg
C
Ca
Mn
Fe
Fe
Co
0
2
4
6
8
10
keV

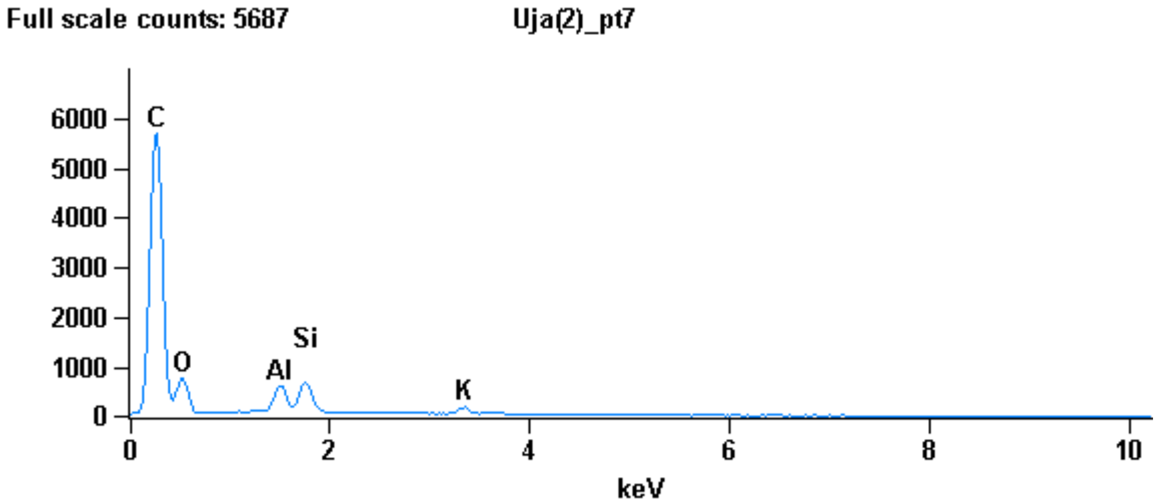
Full scale counts: 5687
Uja(2)_pt7
6000
5000
4000
3000
2000
1000
0
C
O
Al
Si
K
0
2
4
6
8
10
keV

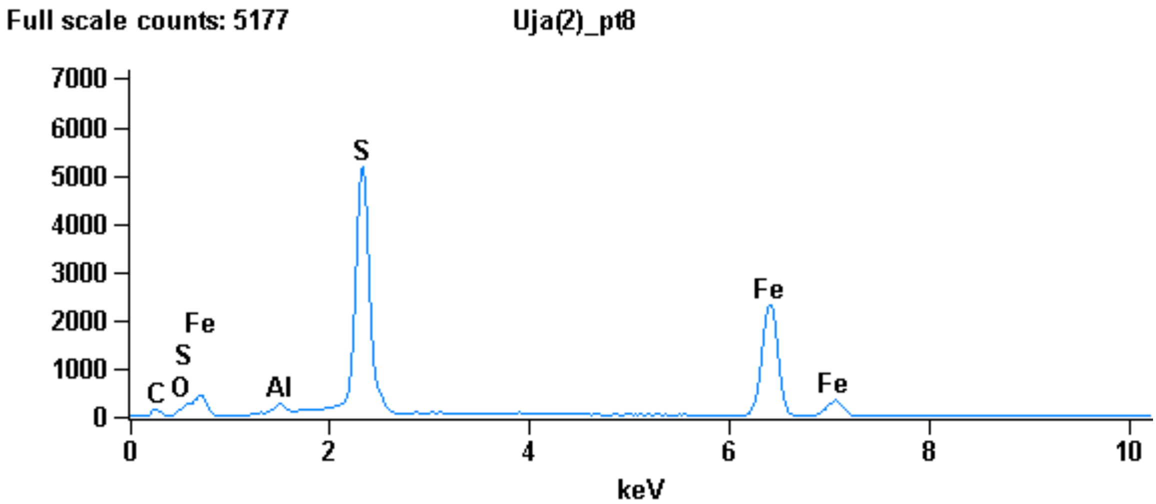
Full scale counts: 5177
Uja(2)_pt8
7000
6000
5000
4000
3000
2000
1000
0
S
Fe
Fe
S
C
O
Al
Fe
0
2
4
6
8
10
keV

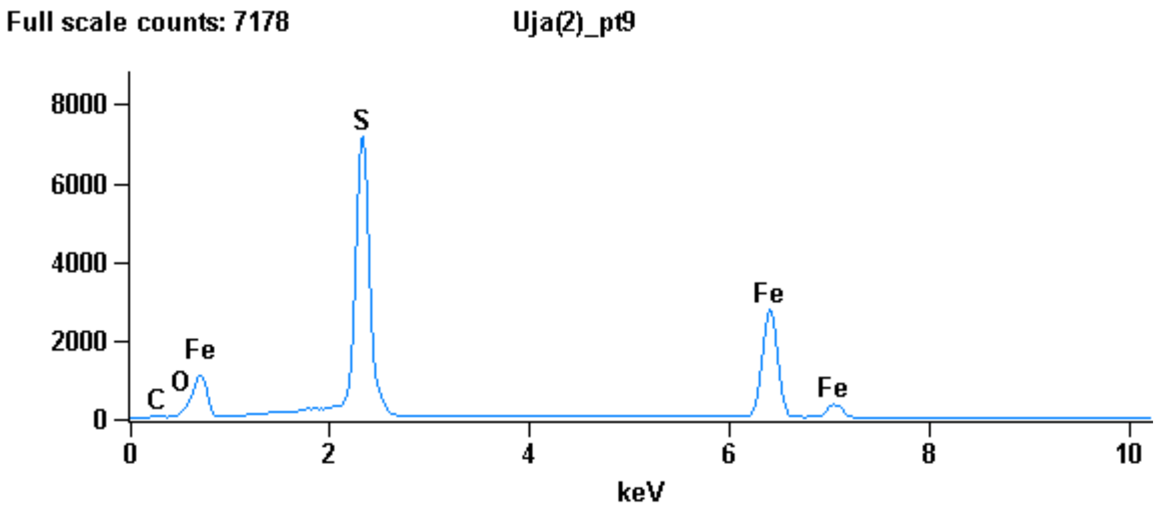
Full scale counts: 7178
Uja(2)_pt9
8000
6000
4000
2000
0
S
Fe
Fe
C
O
Fe
0
2
4
6
8
10
keV

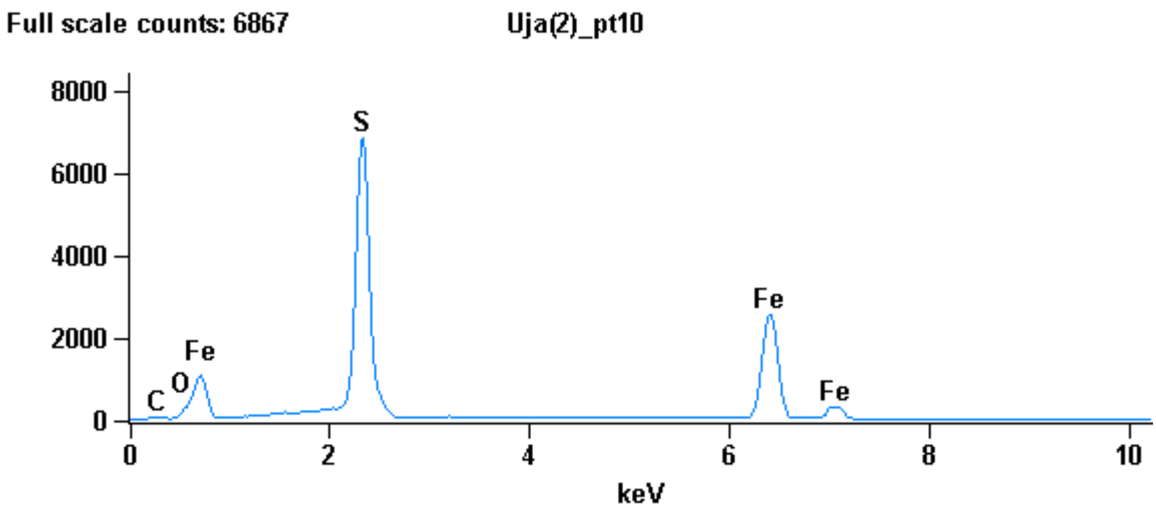
Full scale counts: 6867
Uja(2)_pt10
8000
6000
4000
2000
0
S
Fe
Fe
C
O
Fe
0
2
4
6
8
10
keV

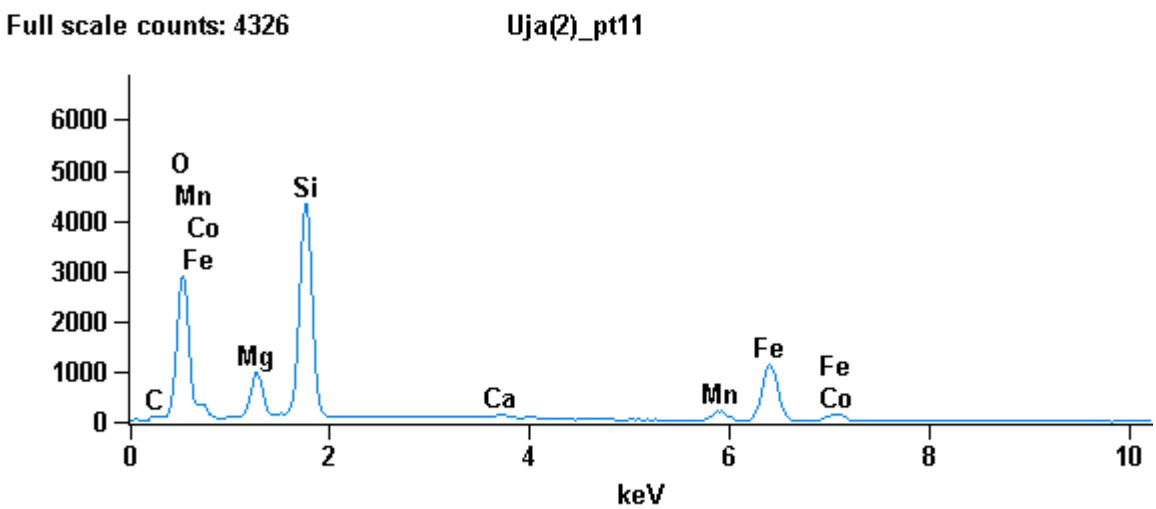
Full scale counts: 4326
Uja(2)_pt11
6000
5000
4000
3000
2000
1000
0
O
Mn
Co
Fe
Si
Mg
C
Ca
Mn
Fe
Fe
Co
0
2
4
6
8
10
keV

Full scale counts: 4633 Uja(2)_pt12

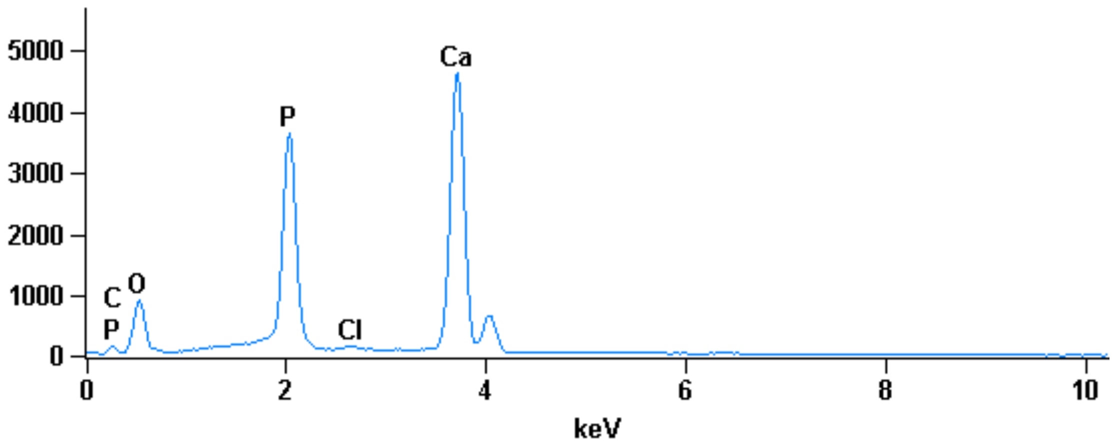

Full scale counts: 2684 Uja(2)_pt13

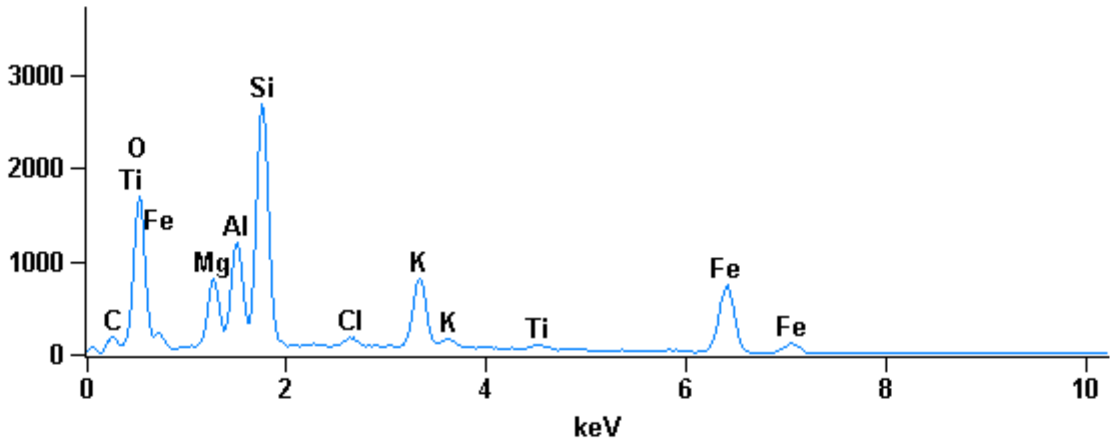

Full scale counts: 4848 Uja(2)_pt14

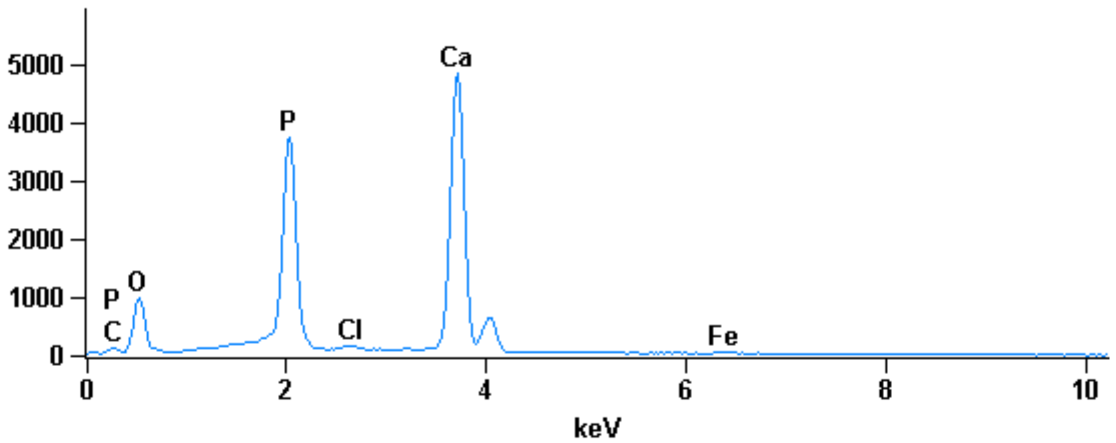

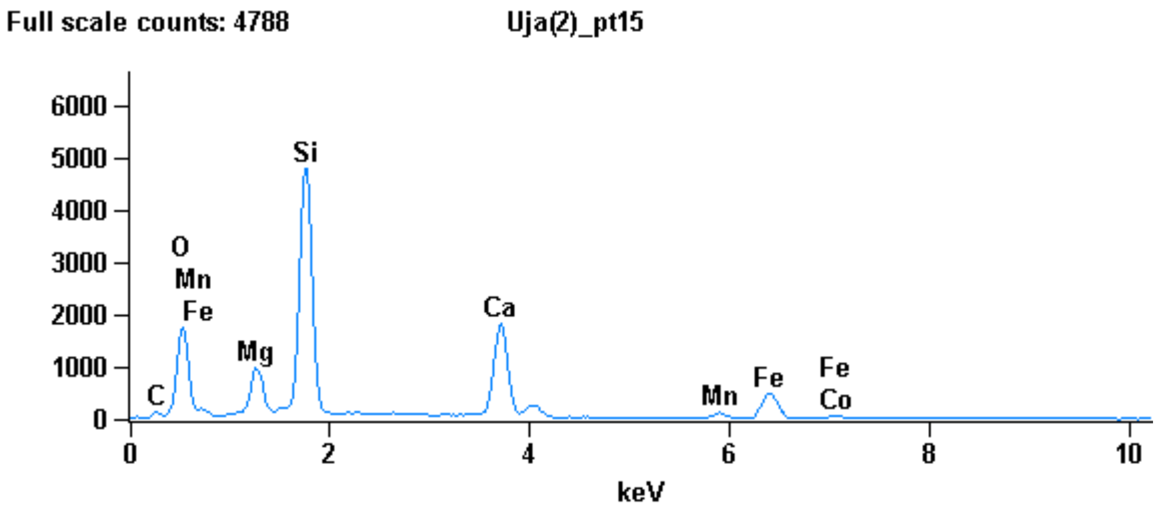

Weight %

	O-K	Mg-K	Al-K	Si-K	P-K	S-K	Cl-K	K-K	Ca-K	Ti-K	Mn-K	Fe-K	Co-K	Mo-L
Uja(2)_pt1	45.64S		0.09			20.84						33.43		
Uja(2)_pt2	45.62S		0.12			20.80						33.46		
Uja(2)_pt3	45.84S					21.15						33.01		
Uja(2)_pt4	41.92S	7.00		22.34					0.44		3.41	24.89		
Uja(2)_pt5	46.20S		0.39			21.46						31.96		
Uja(2)_pt6	41.39S	0.87	10.61	17.46					3.92		8.10	17.52	0.14	
Uja(2)_pt7	46.54S		17.40	24.12				8.08						3.87
Uja(2)_pt8	44.61S		0.59			19.24						35.56		
Uja(2)_pt9	45.84S					21.15						33.01		
Uja(2)_pt10	45.84S					21.14						33.02		
Uja(2)_pt11	42.07S	6.82		22.72					0.54		3.32	24.35	0.18	
Uja(2)_pt12	39.93S				18.07		0.43		41.57					
Uja(2)_pt13	40.93S	5.98	7.41	17.45			0.81	6.44		0.80		20.19		
Uja(2)_pt14	39.96S				18.12		0.49		40.87			0.57		
Uja(2)_pt15	42.60S	6.14		24.20					14.30		1.34	11.31	0.10	

Atom %

	O-K	Mg-K	Al-K	Si-K	P-K	S-K	Cl-K	K-K	Ca-K	Ti-K	Mn-K	Fe-K	Co-K	Mo-L
Uja(2)_pt1	69.50		0.08			15.83						14.58		
Uja(2)_pt2	69.49		0.11			15.81						14.60		
Uja(2)_pt3	69.61					16.02						14.36		
Uja(2)_pt4	62.06	6.82		18.84					0.26		1.47	10.56		
Uja(2)_pt5	69.69		0.34			16.15						13.81		
Uja(2)_pt6	61.61	0.85	9.37	14.80					2.33		3.51	7.47	0.06	
Uja(2)_pt7	62.43		13.84	18.43				4.43						0.86
Uja(2)_pt8	68.90		0.54			14.83						15.73		
Uja(2)_pt9	69.62					16.03						14.36		
Uja(2)_pt10	69.61					16.02						14.37		
Uja(2)_pt11	62.13	6.63		19.11					0.32		1.43	10.30	0.07	
Uja(2)_pt12	60.45				14.13		0.30		25.12					
Uja(2)_pt13	59.97	5.76	6.44	14.56			0.54	3.86		0.39		8.47		
Uja(2)_pt14	60.53				14.18		0.33		24.71			0.25		
Uja(2)_pt15	61.04	5.79		19.75					8.18		0.56	4.64	0.04	

Compound %

		MgO	Al2O3	SiO2	P2O5	SO3	Cl	K2O	CaO	TiO2	MnO	Fe2O3	CoO	MoO3
Uja(2)_pt1	0.00		0.18			52.03						47.79		
Uja(2)_pt2	0.00		0.23			51.94						47.83		
Uja(2)_pt3	0.00					52.80						47.20		
Uja(2)_pt4	0.00	11.61		47.79					0.61		4.41	35.59		
Uja(2)_pt5	0.00		0.73			53.58						45.69		
Uja(2)_pt6	0.00	1.44	20.05	37.35					5.48		10.45	25.05	0.18	
Uja(2)_pt7	0.00		32.87	51.60				9.73						5.80
Uja(2)_pt8	0.00		1.11			48.05						50.84		
Uja(2)_pt9	0.00					52.81						47.19		
Uja(2)_pt10	0.00					52.79						47.21		
Uja(2)_pt11	0.00	11.31		48.61					0.76		4.28	34.81	0.23	
Uja(2)_pt12	0.00				41.40		0.43		58.17					
Uja(2)_pt13	0.00	9.91	14.00	37.32			0.81	7.76		1.34		28.86		
Uja(2)_pt14	0.00				41.52		0.49		57.18			0.82		
Uja(2)_pt15	0.00	10.19		51.78					20.01		1.73	16.18	0.12	

Minerals, Uja(2)

pt1: Pyrrhotite
pt2: Pyrrhotite
pt3: Pyrrhotite
pt4: Orthopyroxene - Enstatite-ferrosilite
pt5: Pyrrhotite
pt6: Garnet - pyralspite-group
pt7: Mixed signal, hole in thin section
pt8: Pyrrhotite
pt9: Pyrrhotite
pt10: Pyrrhotite
pt11: Orthopyroxene - enstatite-ferrosilite
pt12: Apatite
pt13: Biotite
pt14: Apatite
pt15: Clinopyroxene - diopside-hedenbergite

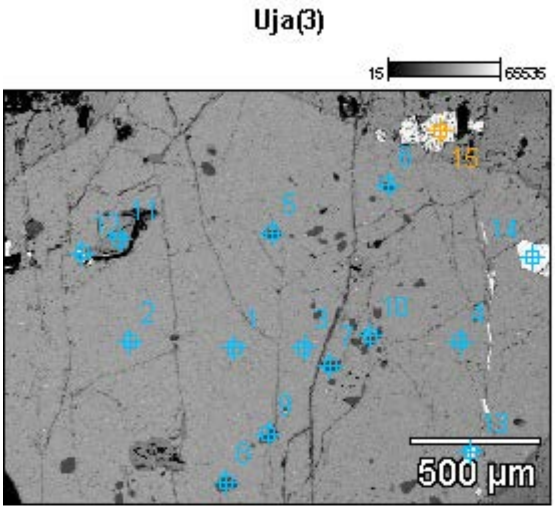

Image name: Uja(3)
Magnification: 58

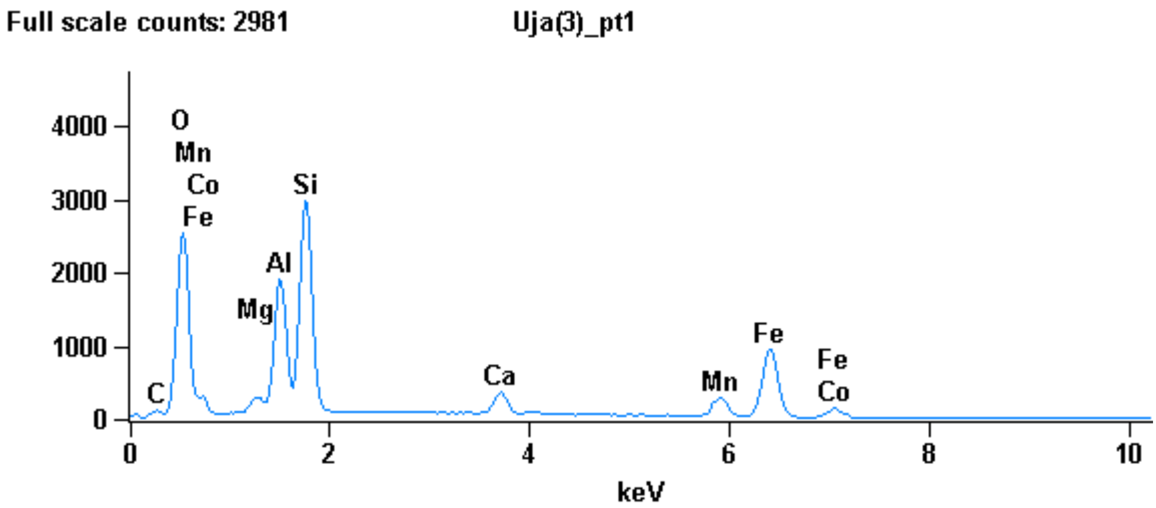

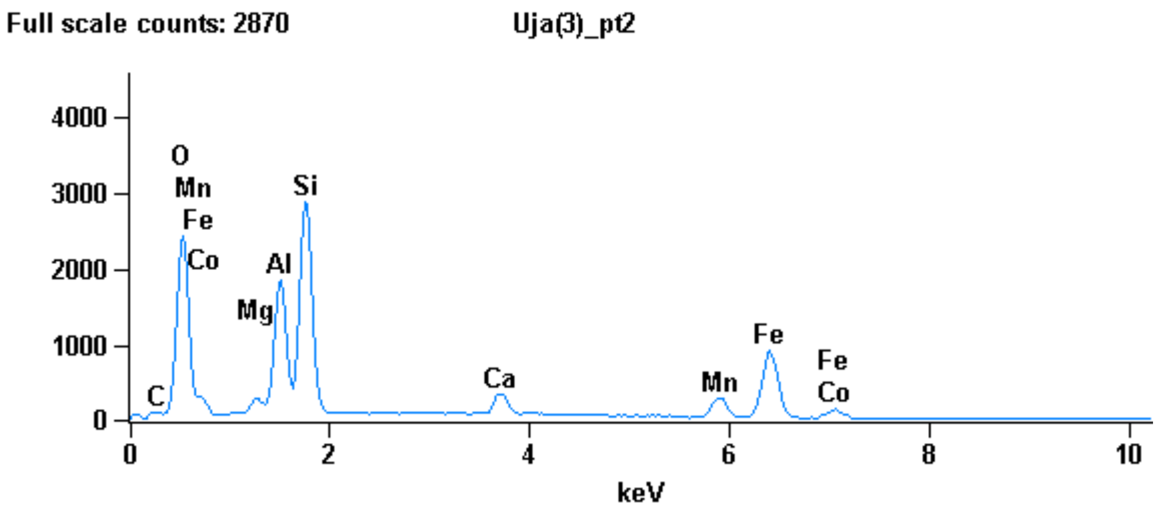

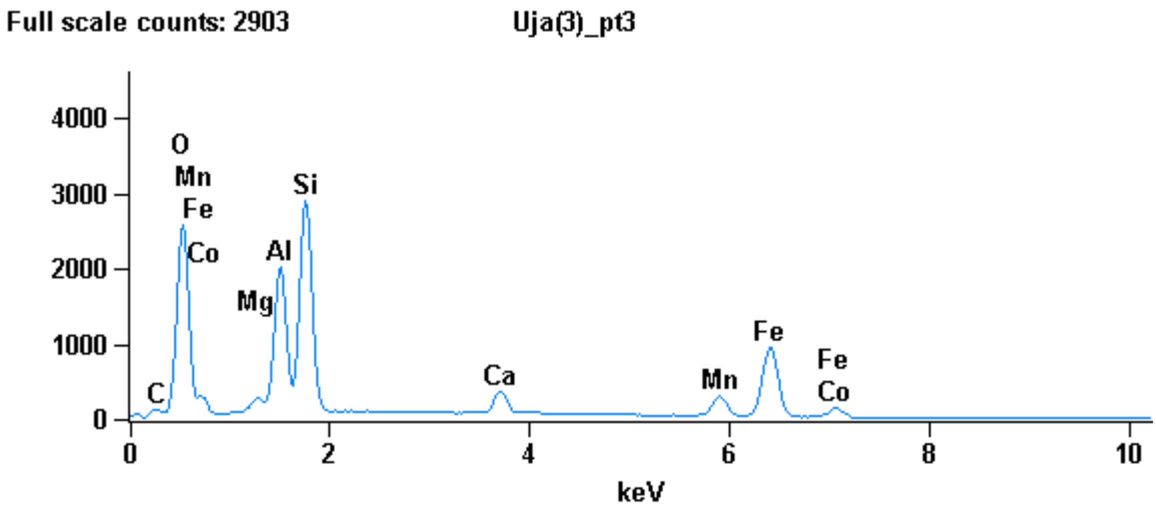
Full scale counts: 2903
Uja(3)_pt3
4000
3000
2000
1000
0
O
Mn
Fe
Co
Si
Al
Mg
C
Ca
Mn
Fe
Fe
Co
0
2
4
6
8
10
keV

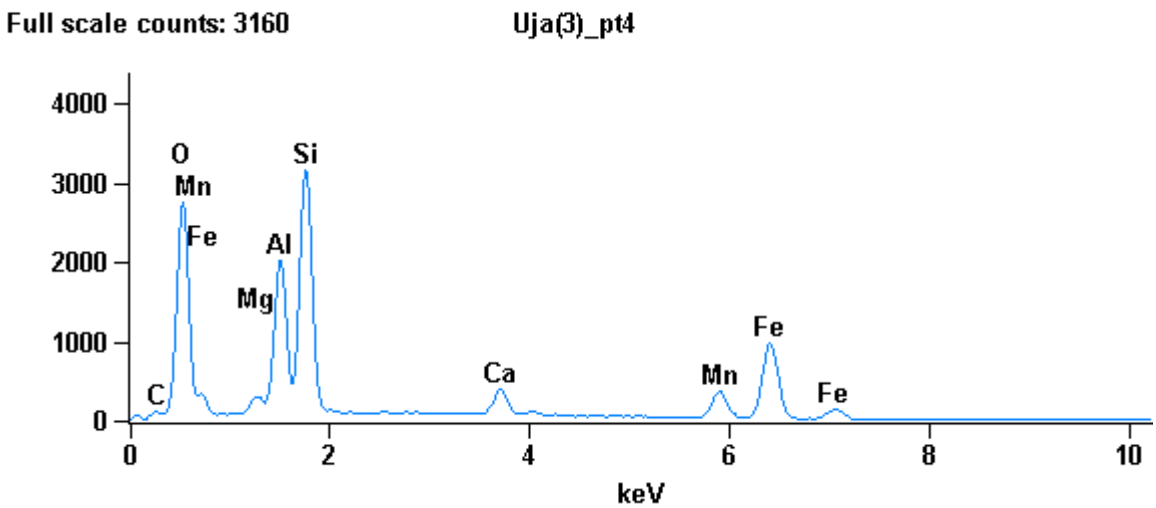
Full scale counts: 3160
Uja(3)_pt4
4000
3000
2000
1000
0
O
Mn
Fe
Si
Al
Mg
C
Ca
Mn
Fe
Fe
0
2
4
6
8
10
keV

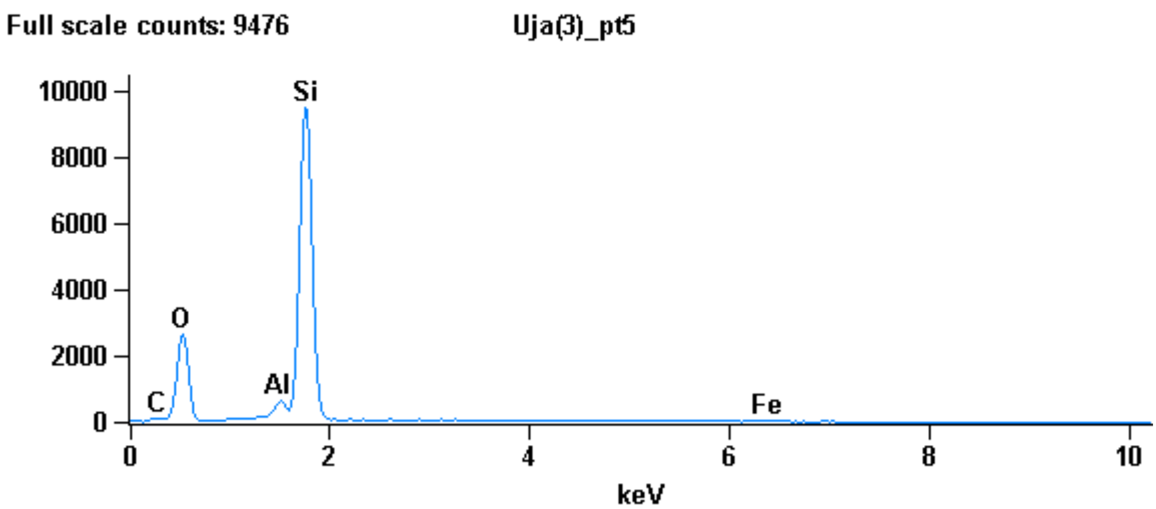
Full scale counts: 9476
Uja(3)_pt5
10000
8000
6000
4000
2000
0
Si
O
Al
C
Fe
0
2
4
6
8
10
keV

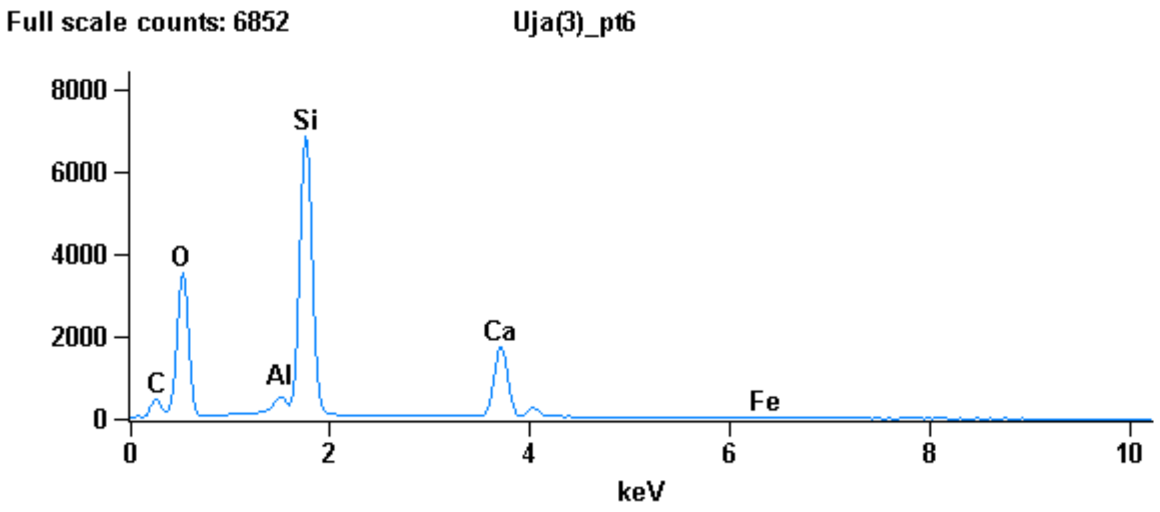
Full scale counts: 6852
Uja(3)_pt6
8000
6000
4000
2000
0
Si
O
Ca
C
Al
Fe
0
2
4
6
8
10
keV

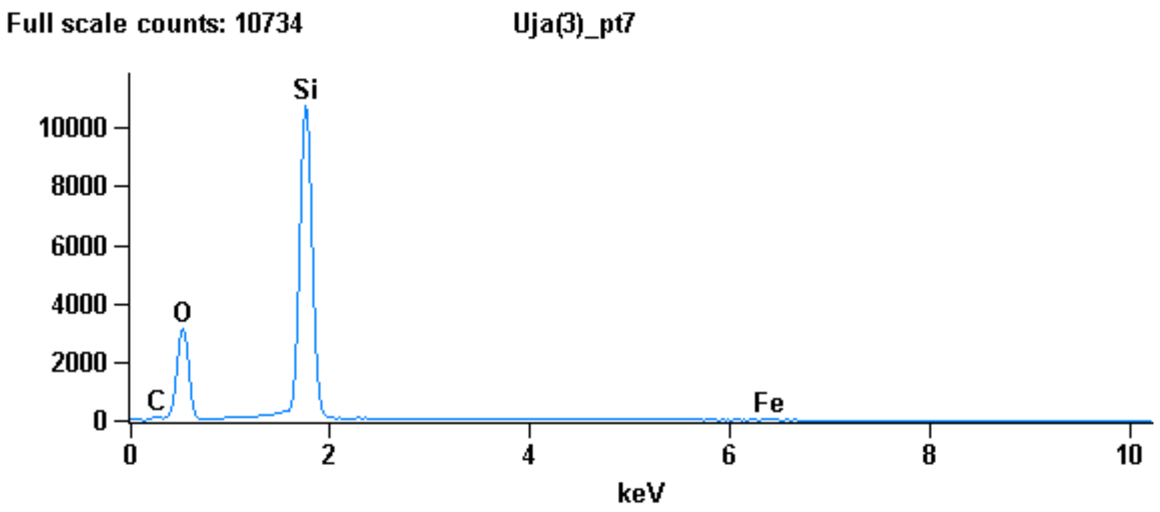
Full scale counts: 10734
Uja(3)_pt7
10000
8000
6000
4000
2000
0
Si
O
C
Fe
0
2
4
6
8
10
keV

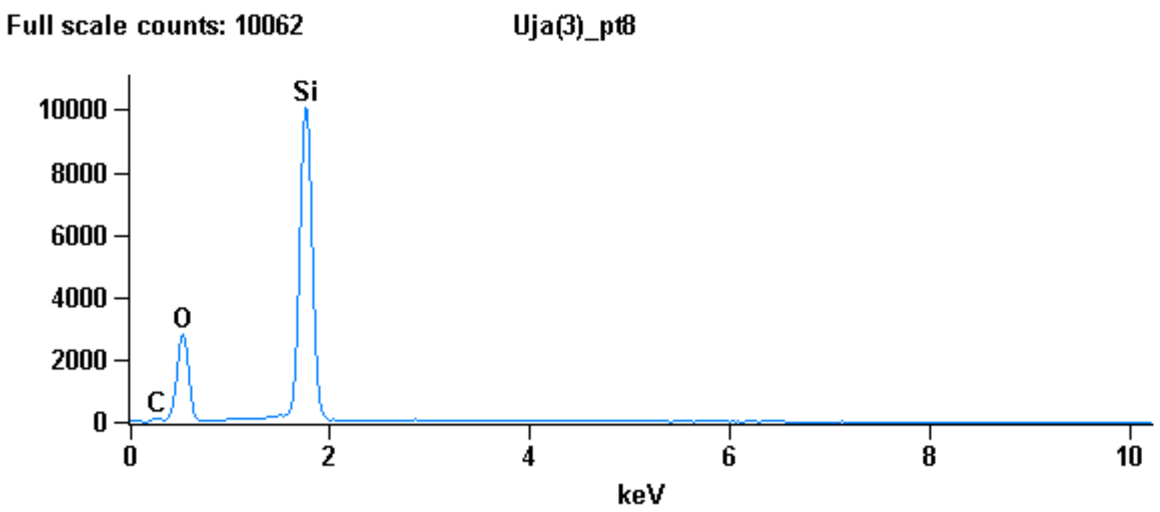
Full scale counts: 10062
Uja(3)_pt8
10000
8000
6000
4000
2000
0
Si
O
C
0
2
4
6
8
10
keV

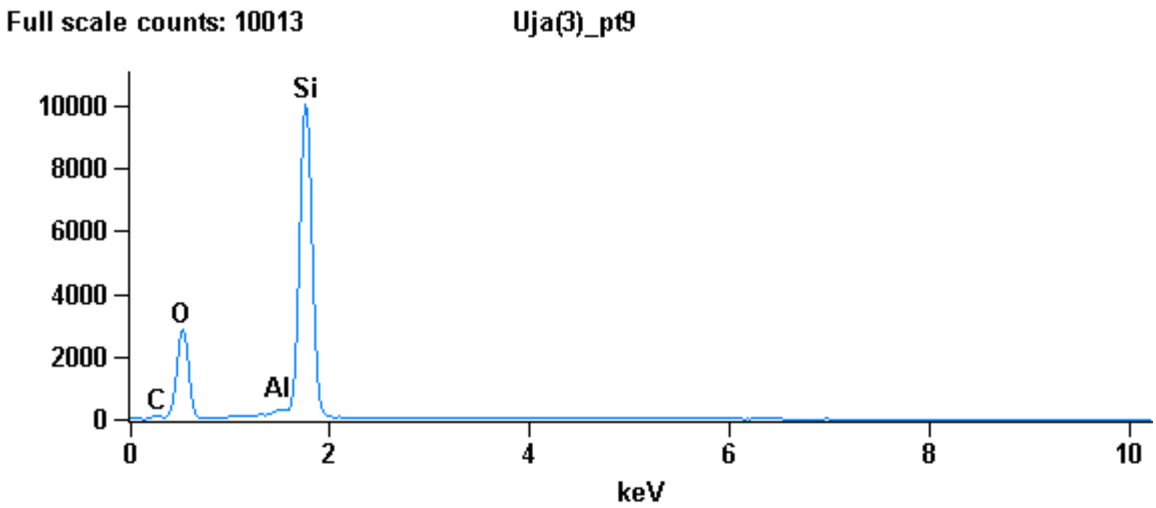
Full scale counts: 10013
Uja(3)_pt9
10000
8000
6000
4000
2000
0
Si
O
C
Al
0
2
4
6
8
10
keV

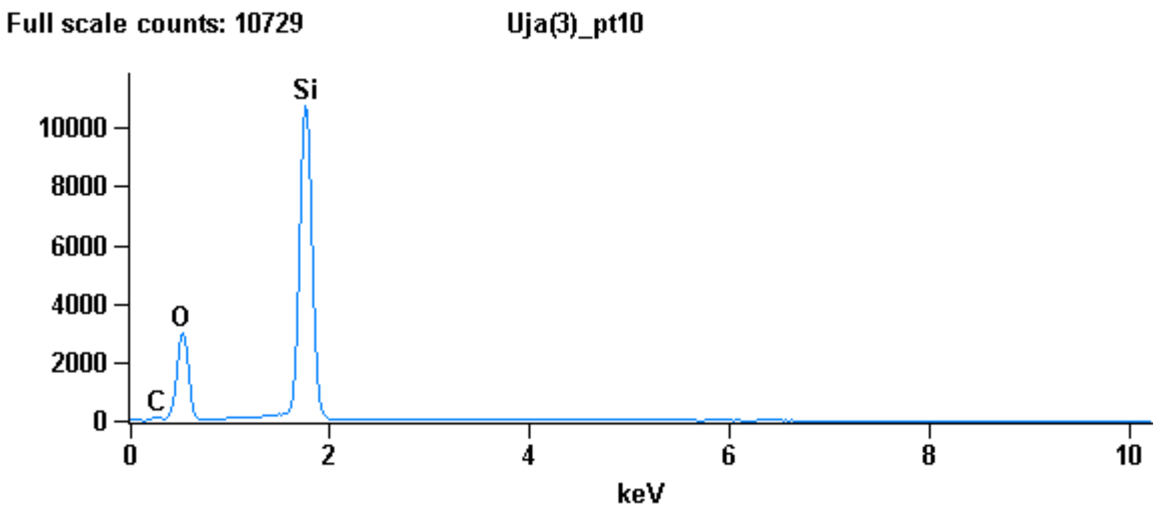
Full scale counts: 10729
Uja(3)_pt10
10000
8000
6000
4000
2000
0
Si
O
C
0
2
4
6
8
10
keV

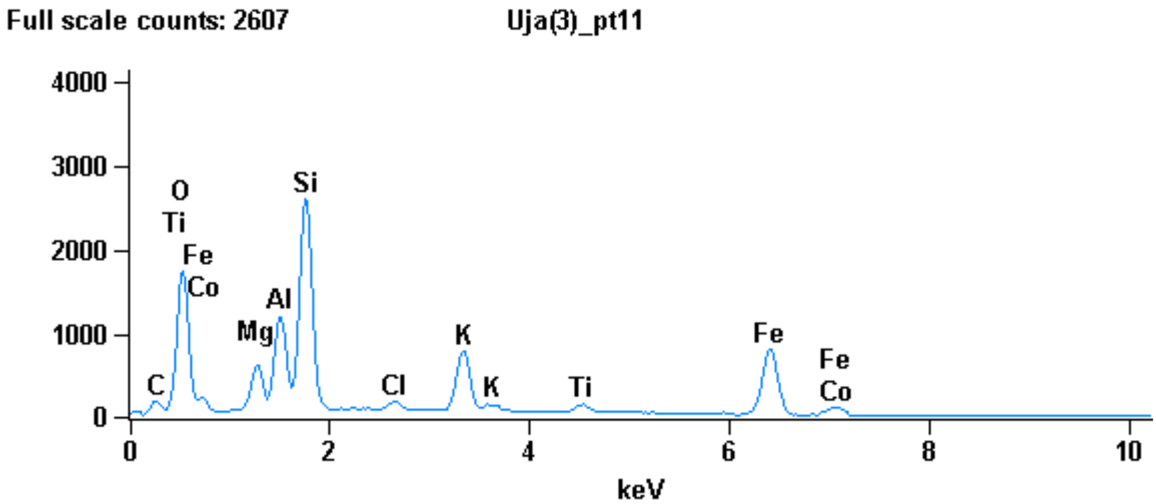
Full scale counts: 2607
Uja(3)_pt11
4000
3000
2000
1000
0
O
Ti
Fe
Co
Si
Al
Mg
C
Cl
K
K
Ti
Fe
Fe
Co
0
2
4
6
8
10
keV

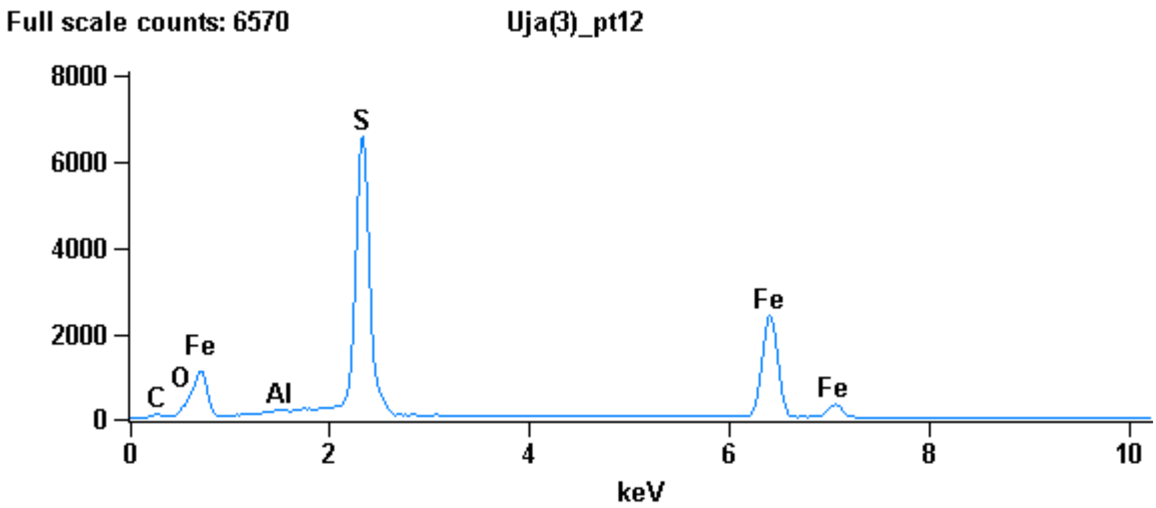
Full scale counts: 6570
Uja(3)_pt12
8000
6000
4000
2000
0
S
Fe
Fe
C
O
Al
Fe
0
2
4
6
8
10
keV

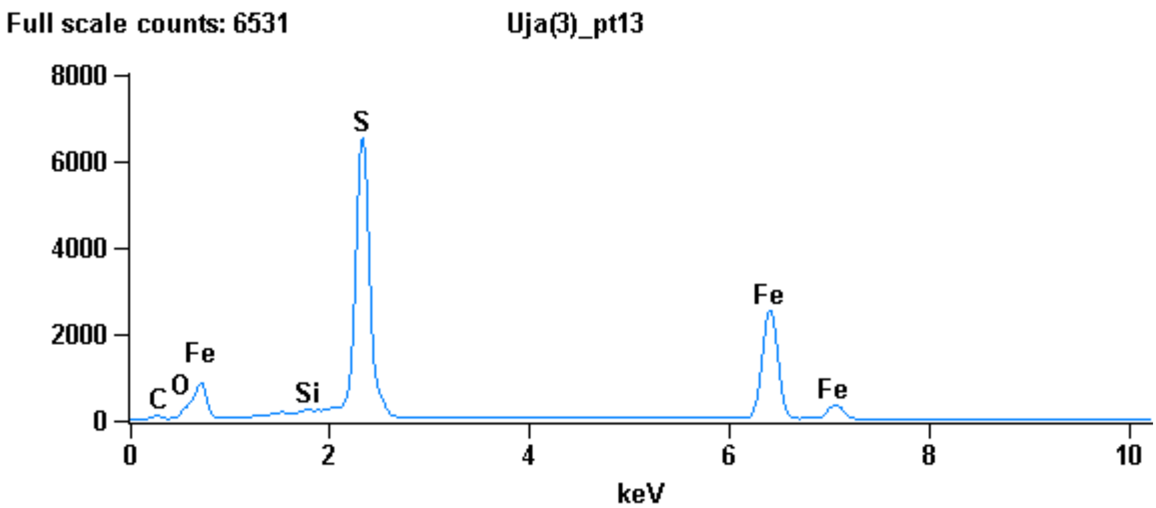
Full scale counts: 6531
Uja(3)_pt13
8000
6000
4000
2000
0
S
Fe
Fe
C
O
Si
Fe
0
2
4
6
8
10
keV

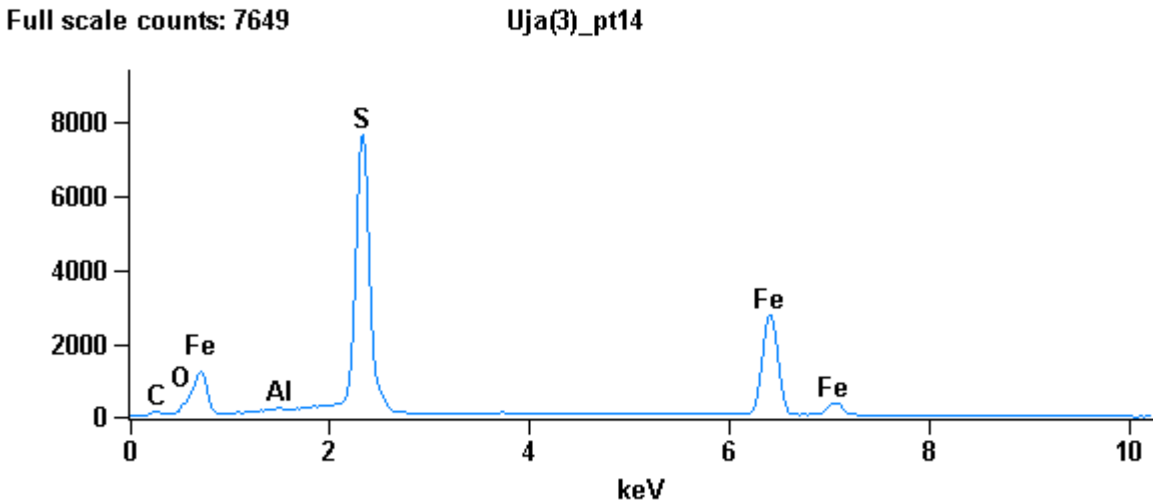
Full scale counts: 7649
Uja(3)_pt14
8000
6000
4000
2000
0
S
Fe
Fe
C
O
Al
Fe
0
2
4
6
8
10
keV

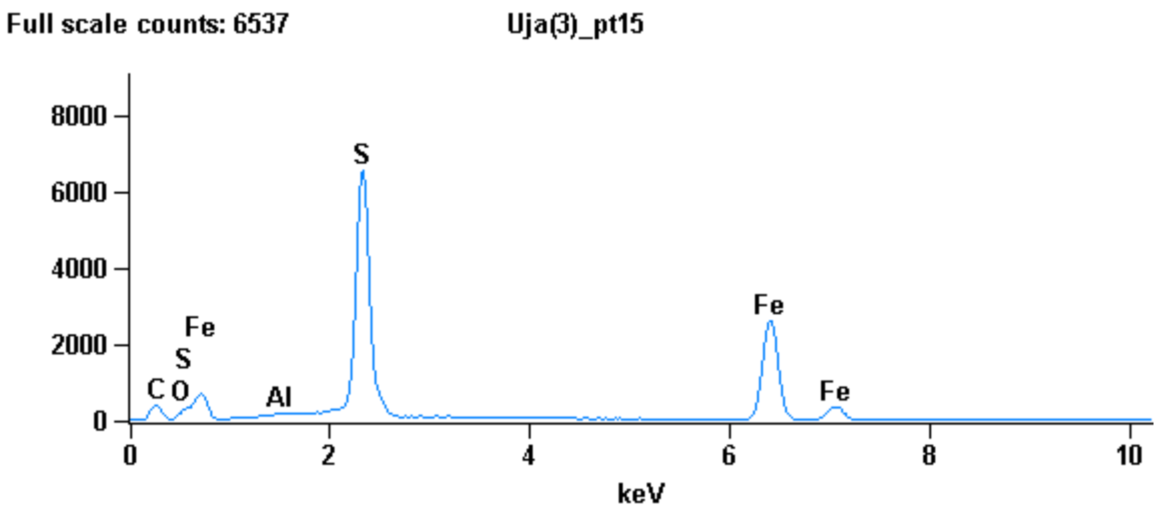

Weight %

	O-K	Mg-K	Al-K	Si-K	S-K	Cl-K	K-K	Ca-K	Ti-K	Mn-K	Fe-K	Co-K
Uja(3)_pt1	41.54S	1.49	10.62	17.02				2.41		5.50	21.18	0.24
Uja(3)_pt2	41.55S	1.23	10.49	17.23				2.34		5.76	21.21	0.19
Uja(3)_pt3	41.66S	0.98	11.13	17.06				2.30		5.65	21.23	0.00
Uja(3)_pt4	41.64S	1.36	10.77	17.27				2.42		6.32	20.22	
Uja(3)_pt5	52.79S		2.17	44.41							0.63	
Uja(3)_pt6	47.24S		1.75	34.18				16.24			0.60	
Uja(3)_pt7	53.13S			46.49							0.38	
Uja(3)_pt8	53.26S			46.74								
Uja(3)_pt9	53.19S		0.60	46.22								
Uja(3)_pt10	53.26S			46.74								
Uja(3)_pt11	40.77S	4.52	7.63	17.09		0.65	6.31		1.52		21.44	0.08
Uja(3)_pt12	45.90S		0.13		21.16						32.81	
Uja(3)_pt13	45.49S			0.06	20.63						33.81	
Uja(3)_pt14	46.07S		0.09		21.41						32.43	
Uja(3)_pt15	45.42S		0.13		20.52						33.93	

Atom %

	O-K	Mg-K	Al-K	Si-K	S-K	Cl-K	K-K	Ca-K	Ti-K	Mn-K	Fe-K	Co-K
Uja(3)_pt1	61.81	1.46	9.37	14.42				1.43		2.38	9.03	0.10
Uja(3)_pt2	61.89	1.20	9.26	14.62				1.39		2.50	9.05	0.08
Uja(3)_pt3	61.93	0.96	9.81	14.44				1.37		2.44	9.04	0.00
Uja(3)_pt4	61.82	1.33	9.48	14.60				1.43		2.73	8.60	
Uja(3)_pt5	66.36		1.62	31.80							0.23	
Uja(3)_pt6	63.49		1.40	26.17				8.71			0.23	
Uja(3)_pt7	66.64			33.22							0.14	
Uja(3)_pt8	66.67			33.33								
Uja(3)_pt9	66.59		0.44	32.97								
Uja(3)_pt10	66.67			33.33								
Uja(3)_pt11	60.36	4.40	6.70	14.41		0.44	3.82		0.75		9.09	0.03
Uja(3)_pt12	69.61		0.12		16.02						14.25	
Uja(3)_pt13	69.44			0.05	15.72						14.79	
Uja(3)_pt14	69.70		0.08		16.17						14.06	
Uja(3)_pt15	69.39		0.12		15.64						14.85	

Compound %

		MgO	Al2O3	SiO2	SO3	Cl	K2O	CaO	TiO2	MnO	Fe2O3	CoO
Uja(3)_pt1	0.00	2.48	20.06	36.41				3.37		7.10	30.28	0.31
Uja(3)_pt2	0.00	2.04	19.81	36.87				3.28		7.44	30.33	0.24
Uja(3)_pt3	0.00	1.63	21.02	36.49				3.22		7.29	30.35	0.00
Uja(3)_pt4	0.00	2.26	20.35	36.94				3.39		8.16	28.90	
Uja(3)_pt5	0.00		4.10	95.00							0.90	
Uja(3)_pt6	0.00		3.31	73.11				22.72			0.85	
Uja(3)_pt7	0.00			99.46							0.54	
Uja(3)_pt8	0.00			100.00								
Uja(3)_pt9	0.00		1.12	98.88								
Uja(3)_pt10	0.00			100.00								
Uja(3)_pt11	0.00	7.49	14.41	36.56		0.65	7.60		2.53		30.65	0.10
Uja(3)_pt12	0.00		0.25		52.84						46.91	
Uja(3)_pt13	0.00			0.13	51.53						48.34	
Uja(3)_pt14	0.00		0.17		53.47						46.37	
Uja(3)_pt15	0.00		0.25		51.24						48.52	

Minerals, Uja(3)
pt1: Garnet - pyralspite-group
pt2: Garnet - pyralspite-group
pt3: Garnet - pyralspite-group
pt4: Garnet - pyralspite-group
pt5: Quartz
pt6: Mixed signal/edge effect
pt7: Quartz
pt8: Quartz
pt9: Quartz
pt10: Quartz
pt11: Biotite
pt12: Pyrrhotite
pt13: Pyrrhotite
pt14: Pyrrhotite
pt15: Pyrrhotite

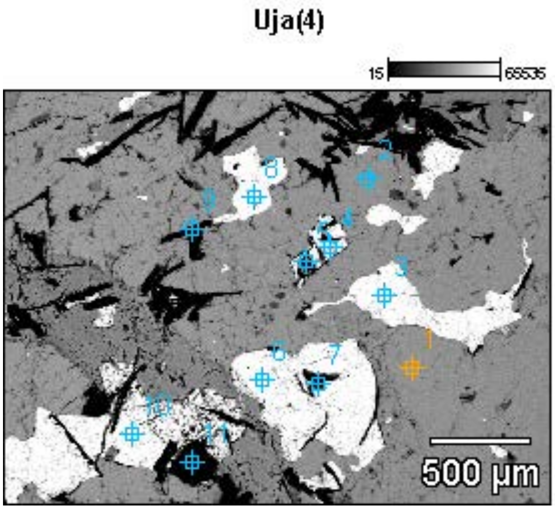

Image name: Uja(4)
Magnification: 44

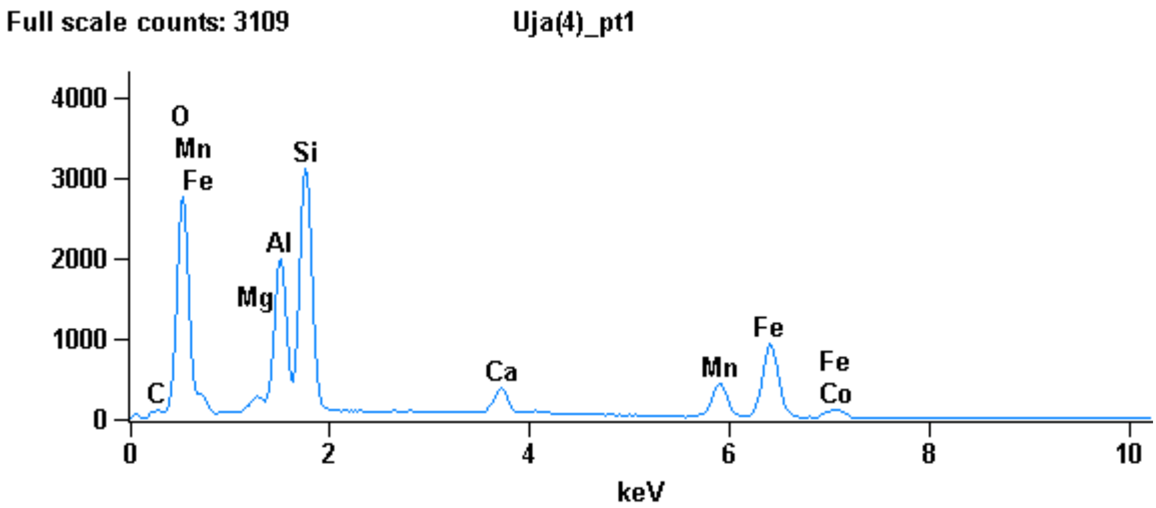

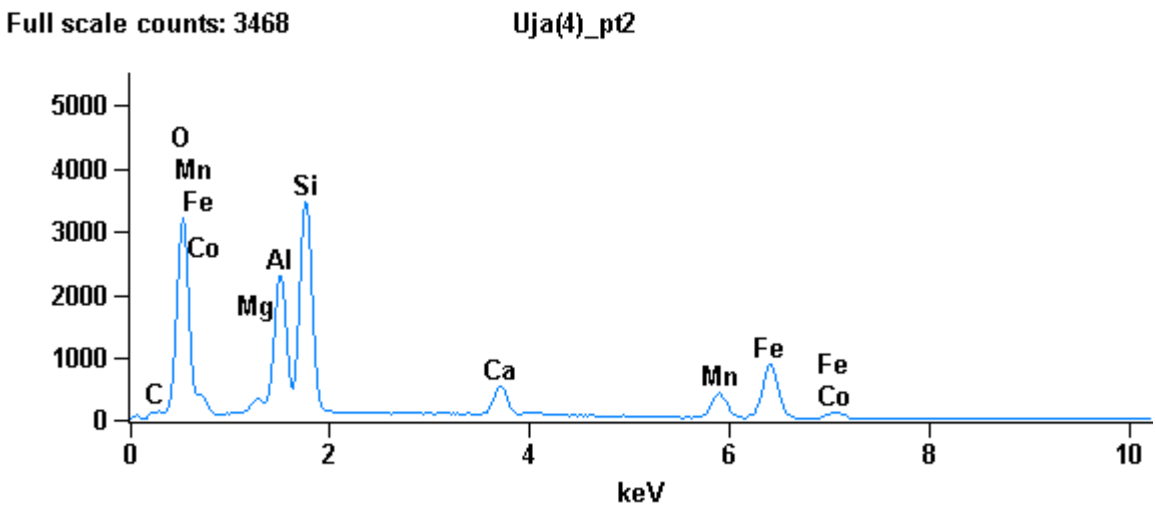

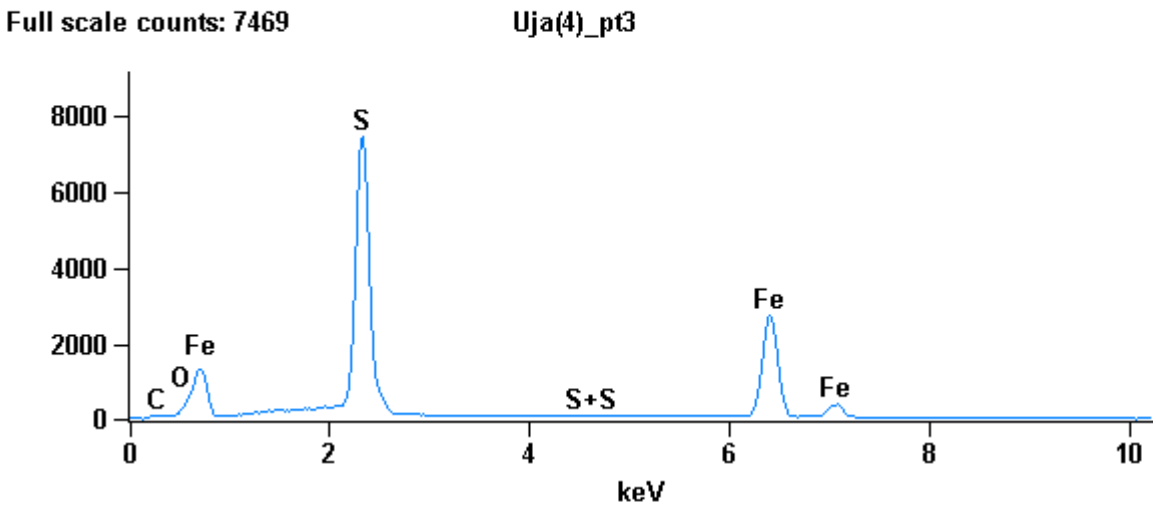
Full scale counts: 7469
Uja(4)_pt3
8000
6000
4000
2000
0
S
Fe
Fe
C
O
S+S
Fe
0
2
4
6
8
10
keV

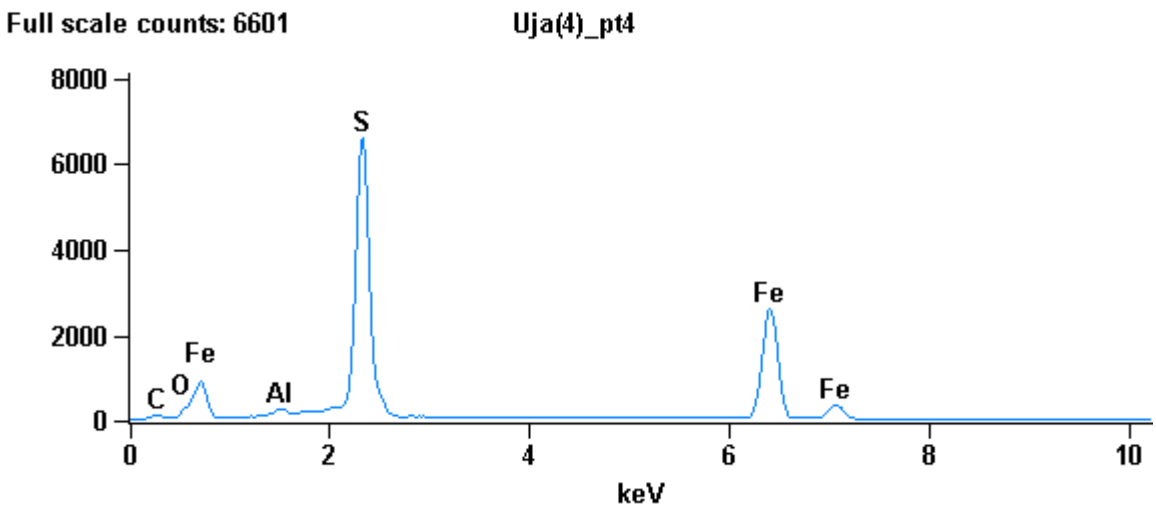
Full scale counts: 6601
Uja(4)_pt4
8000
6000
4000
2000
0
S
Fe
Fe
C
O
Al
Fe
0
2
4
6
8
10
keV

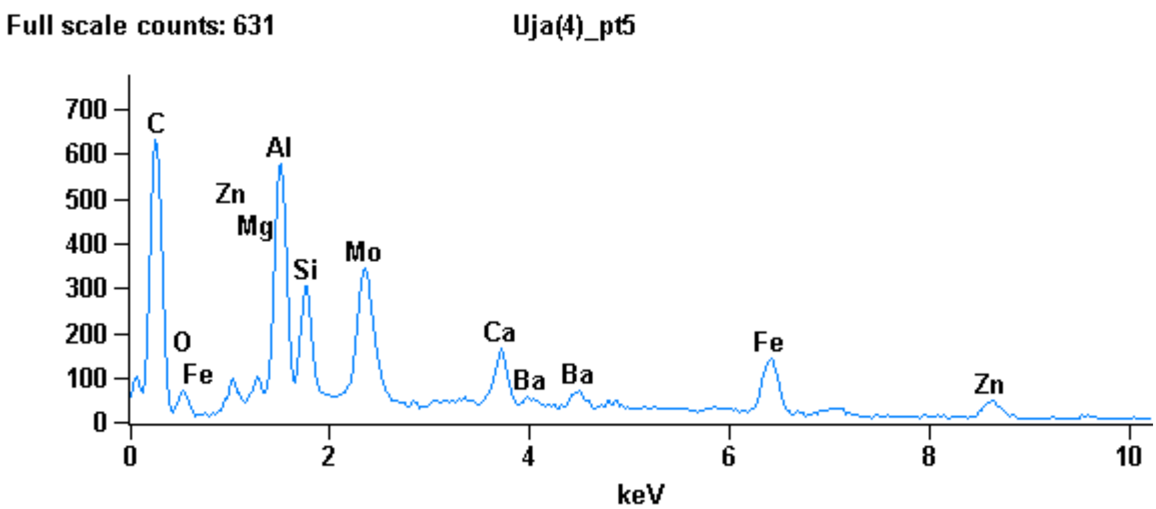
Full scale counts: 631
Uja(4)_pt5
700
600
500
400
300
200
100
0
C
Al
Zn
Mg
Si
Mo
O
Fe
Ca
Ba
Ba
Fe
Zn
0
2
4
6
8
10
keV

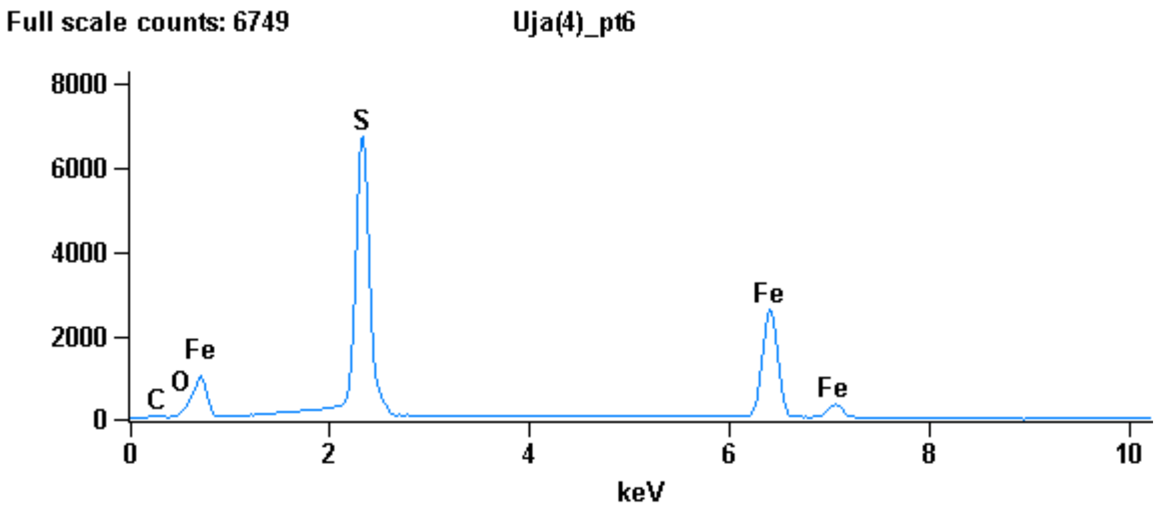
Full scale counts: 6749
Uja(4)_pt6
8000
6000
4000
2000
0
S
Fe
Fe
C
O
Fe
0
2
4
6
8
10
keV

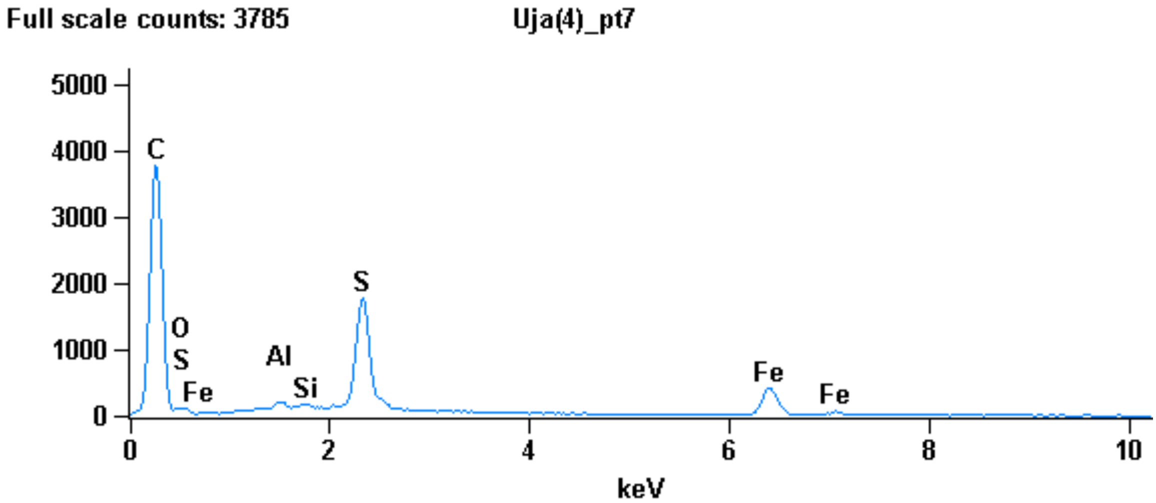
Full scale counts: 3785
Uja(4)_pt7
5000
4000
3000
2000
1000
0
C
O
S
Fe
Al
Si
S
Fe
Fe
0
2
4
6
8
10
keV

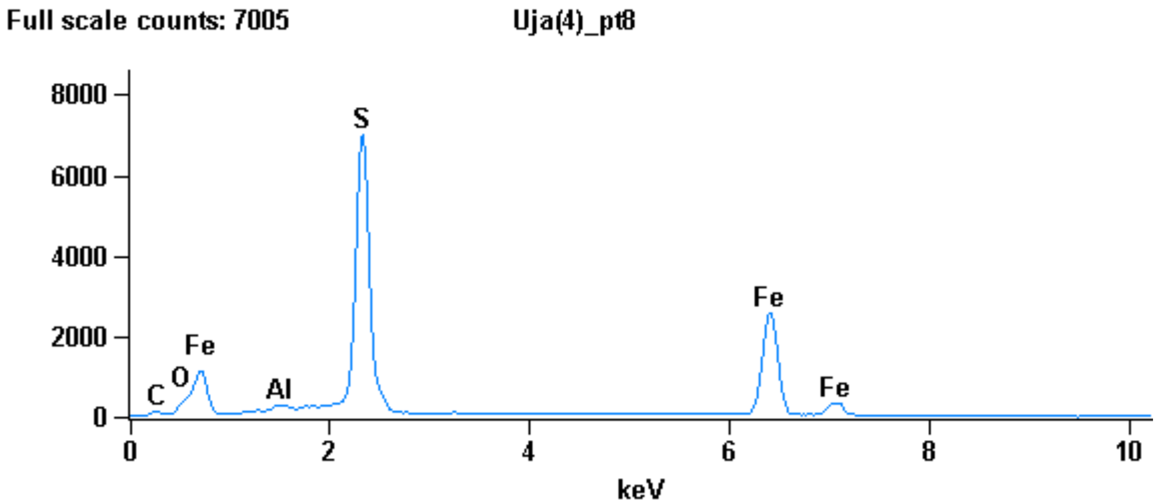
Full scale counts: 7005
Uja(4)_pt8
8000
6000
4000
2000
0
S
Fe
Fe
C
O
Al
Fe
0
2
4
6
8
10
keV

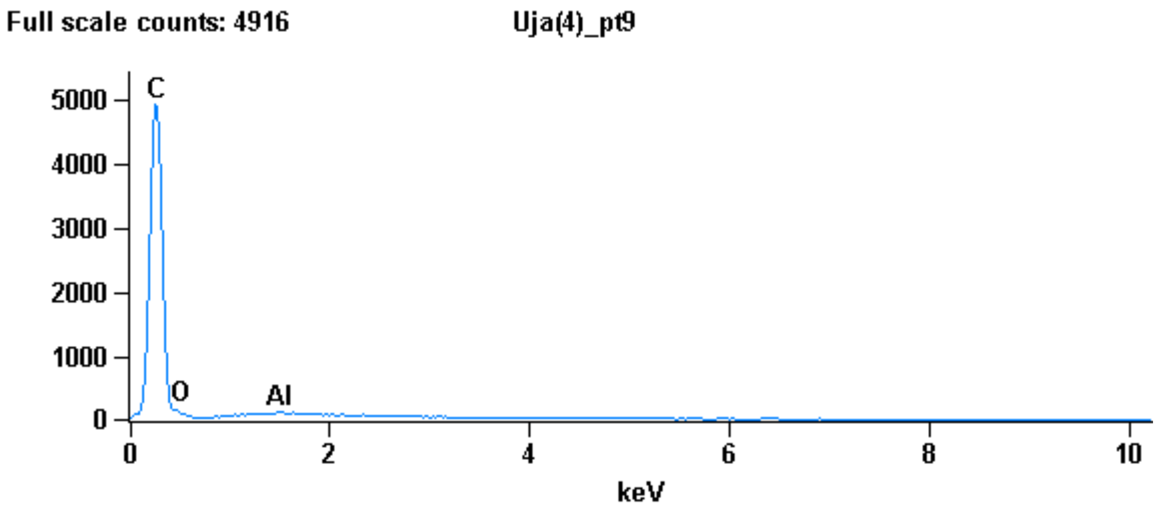
Full scale counts: 4916
Uja(4)_pt9
5000
4000
3000
2000
1000
0
C
O
Al
0
2
4
6
8
10
keV

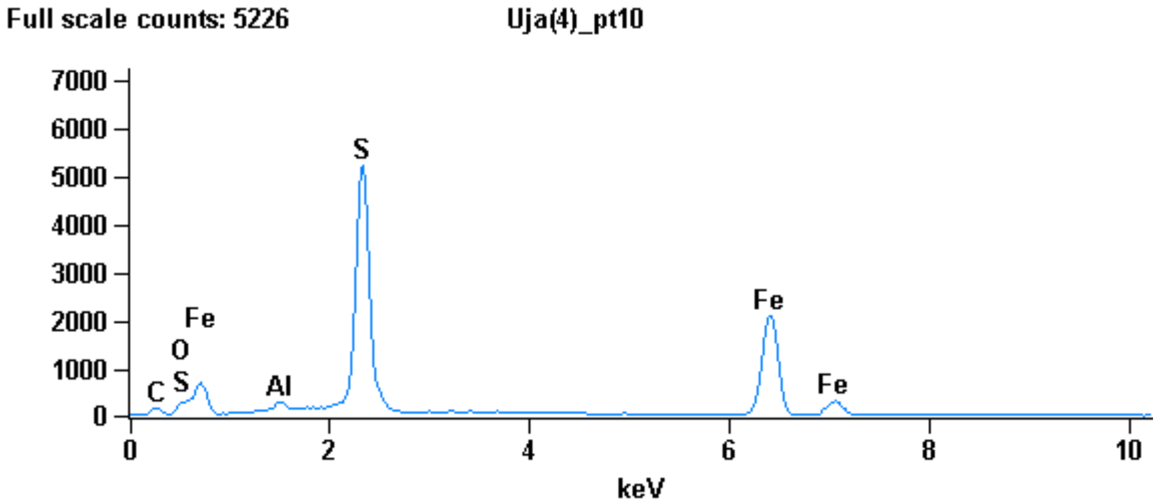
Full scale counts: 5226
Uja(4)_pt10
7000
6000
5000
4000
3000
2000
1000
0
S
Fe
O
C
S
Al
Fe
Fe
0
2
4
6
8
10
keV

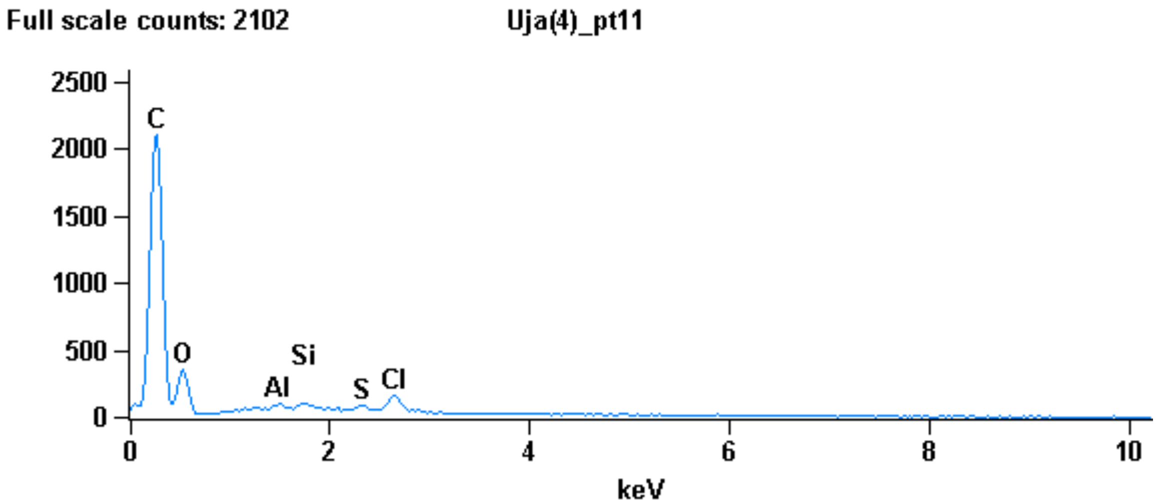
Full scale counts: 2102
Uja(4)_pt11
2500
2000
1500
1000
500
0
C
O
Si
Al
S
Cl
0
2
4
6
8
10
keV

Weight %

	O-K	Mg-K	Al-K	Si-K	S-K	Cl-K	Ca-K	Mn-K	Fe-K	Co-K	Zn-K	Mo-L	Ba-L
Uja(4)_pt1	41.36S	1.11	10.64	17.21			2.38	7.92	19.22	0.16			
Uja(4)_pt2	41.84S	1.08	11.30	17.70			3.45	7.56	17.01	0.06			
Uja(4)_pt3	46.09S				21.47				32.44				
Uja(4)_pt4	45.43S		0.36		20.43				33.78				
Uja(4)_pt5	35.93S	1.44	13.00	5.24			4.04		11.22		7.99	17.17	3.96
Uja(4)_pt6	45.82S				21.12				33.06				
Uja(4)_pt7	49.33S		1.24	0.61	24.88				23.94				
Uja(4)_pt8	45.96S		0.41		21.13				32.51				
Uja(4)_pt9	47.08S		52.92										
Uja(4)_pt10	45.27S		0.64		20.10				33.99				
Uja(4)_pt11	30.72S		5.61	9.07	10.28	44.32							

Atom %

	O-K	Mg-K	Al-K	Si-K	S-K	Cl-K	Ca-K	Mn-K	Fe-K	Co-K	Zn-K	Mo-L	Ba-L
Uja(4)_pt1	61.72	1.10	9.41	14.63			1.42	3.44	8.22	0.06			
Uja(4)_pt2	61.71	1.05	9.88	14.88			2.03	3.25	7.19	0.02			
Uja(4)_pt3	69.73				16.21				14.06				
Uja(4)_pt4	69.34		0.32		15.57				14.77				
Uja(4)_pt5	62.29	1.65	13.36	5.18			2.80		5.57		3.39	4.96	0.80
Uja(4)_pt6	69.60				16.01				14.39				
Uja(4)_pt7	70.79		1.06	0.50	17.82				9.84				
Uja(4)_pt8	69.58		0.37		15.96				14.10				
Uja(4)_pt9	60.00		40.00										
Uja(4)_pt10	69.20		0.58		15.33				14.89				
Uja(4)_pt11	47.74		5.17	8.03	7.97	31.09							

Compound %

		MgO	Al2O3	SiO2	SO3	Cl	CaO	MnO	Fe2O3	CoO	ZnO	MoO3	BaO
Uja(4)_pt1	0.00	1.85	20.10	36.81			3.33	10.22	27.48	0.20			
Uja(4)_pt2	0.00	1.79	21.35	37.88			4.82	9.76	24.32	0.07			
Uja(4)_pt3	0.00				53.62				46.38				
Uja(4)_pt4	0.00		0.68		51.03				48.30				
Uja(4)_pt5	0.00	2.40	24.56	11.22			5.65		16.04		9.95	25.76	4.43
Uja(4)_pt6	0.00				52.73				47.27				
Uja(4)_pt7	0.00		2.35	1.30	62.13				34.23				
Uja(4)_pt8	0.00		0.77		52.75				46.47				
Uja(4)_pt9	0.00		100.00										
Uja(4)_pt10	0.00		1.20		50.20				48.60				
Uja(4)_pt11	0.00		10.59	19.41	25.67	44.32							

Minerals, Uja(4)
pt1: Garnet - pyralspite-group
pt2: Garnet - pyralspite-group
pt3: Pyrrhotite
pt4: Pyrrhotite
pt5: Inclusion in mineral (pyrrhotite) - mixed signal
pt6: Pyrrhotite
pt7: Pyrite
pt8: Pyrrhotite
pt9: Al-oxide/pure Al (hole in thin section - specimen holder?)
pt10: Pyrrhotite
pt11: Mixed signal, hole in thin section

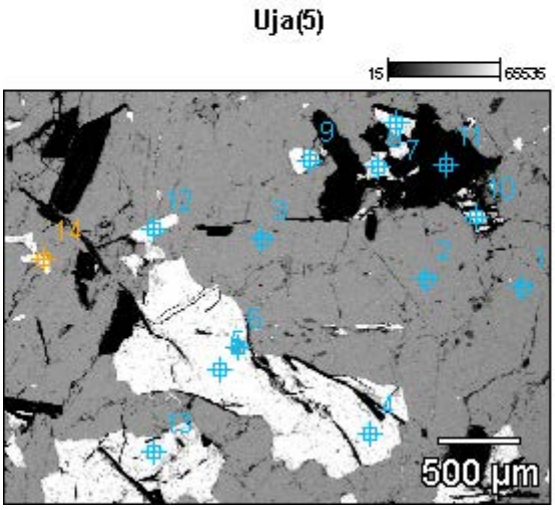

Image name: Uja(5)
Magnification: 36

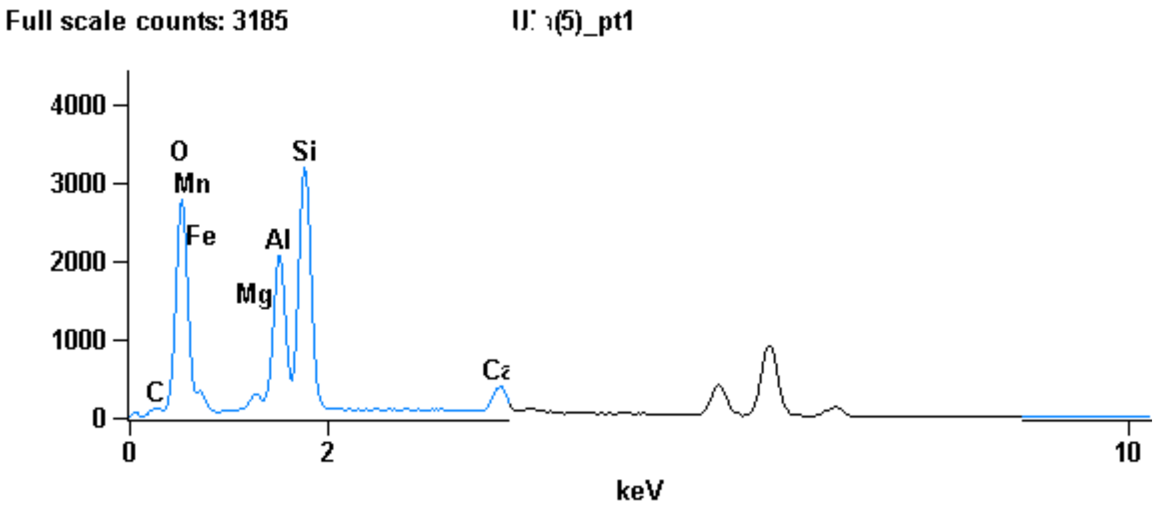

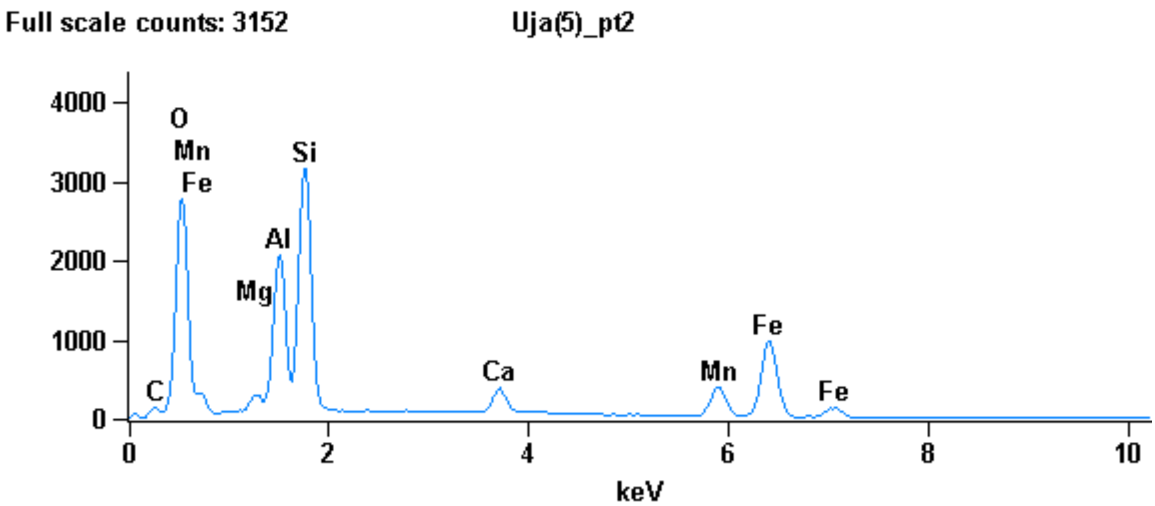

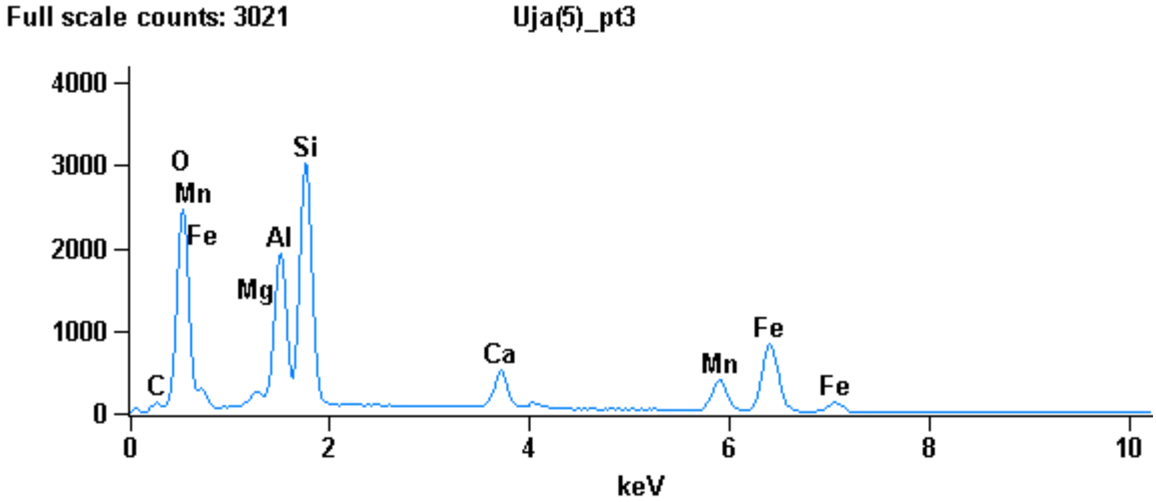
Full scale counts: 3021
Uja(5)_pt3
4000
3000
2000
1000
0
O
Mn
Fe
Si
Al
Mg
C
Ca
Mn
Fe
Fe
0
2
4
6
8
10
keV

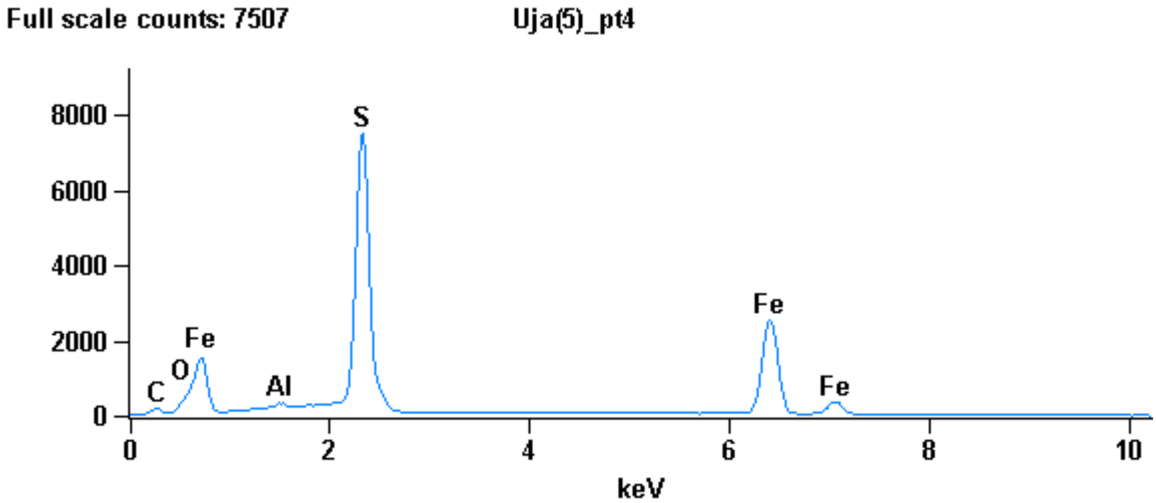
Full scale counts: 7507
Uja(5)_pt4
8000
6000
4000
2000
0
S
Fe
O
C
Al
Fe
Fe
0
2
4
6
8
10
keV

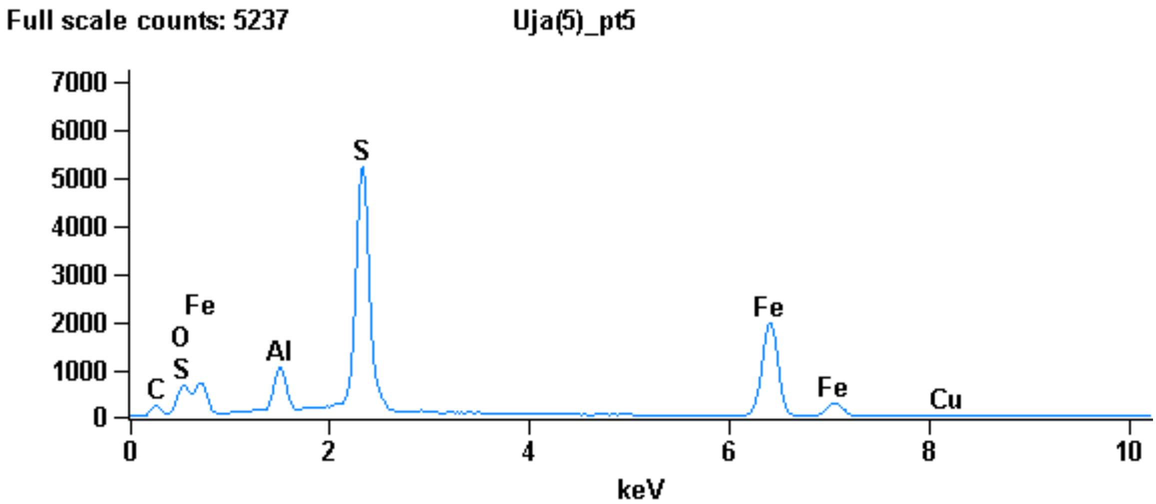
Full scale counts: 5237
Uja(5)_pt5
7000
6000
5000
4000
3000
2000
1000
0
S
Fe
O
S
C
Al
Fe
Fe
Cu
0
2
4
6
8
10
keV

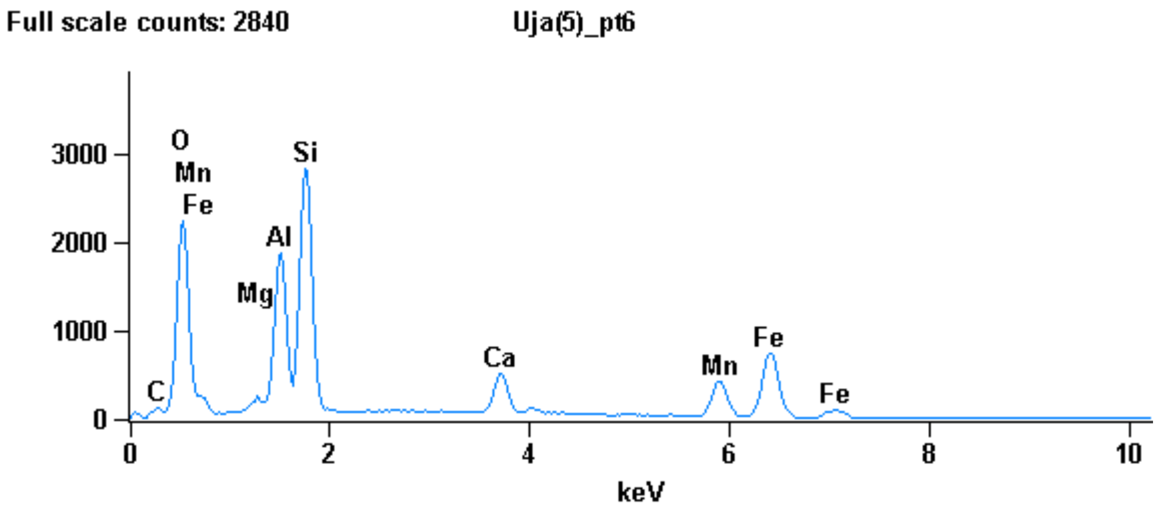
Full scale counts: 2840
Uja(5)_pt6
3000
2000
1000
0
O
Mn
Fe
Si
Al
Mg
C
Ca
Mn
Fe
Fe
0
2
4
6
8
10
keV

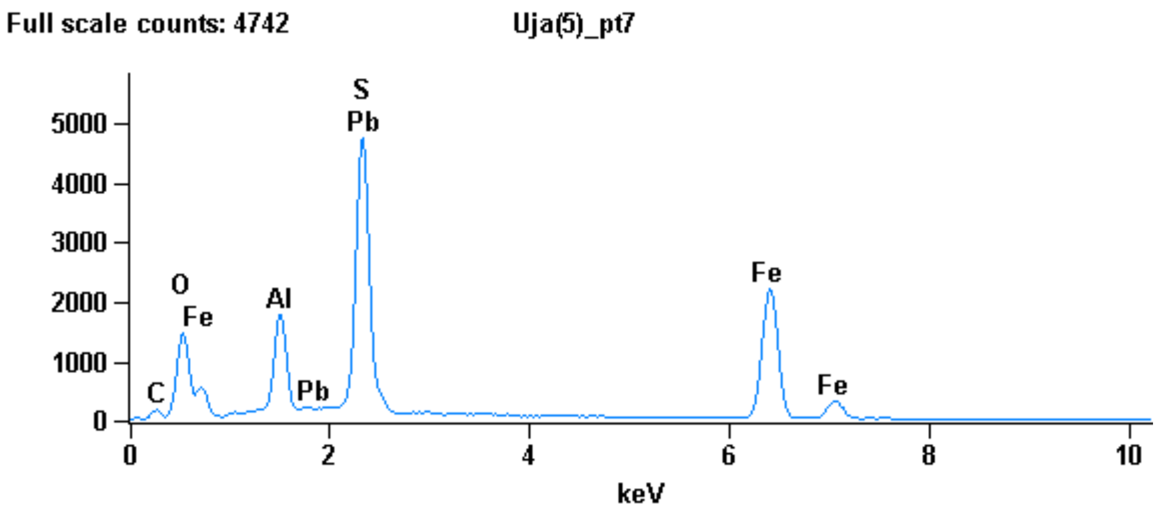
Full scale counts: 4742
Uja(5)_pt7
5000
4000
3000
2000
1000
0
S
Pb
O
Fe
Al
C
Pb
Fe
Fe
0
2
4
6
8
10
keV

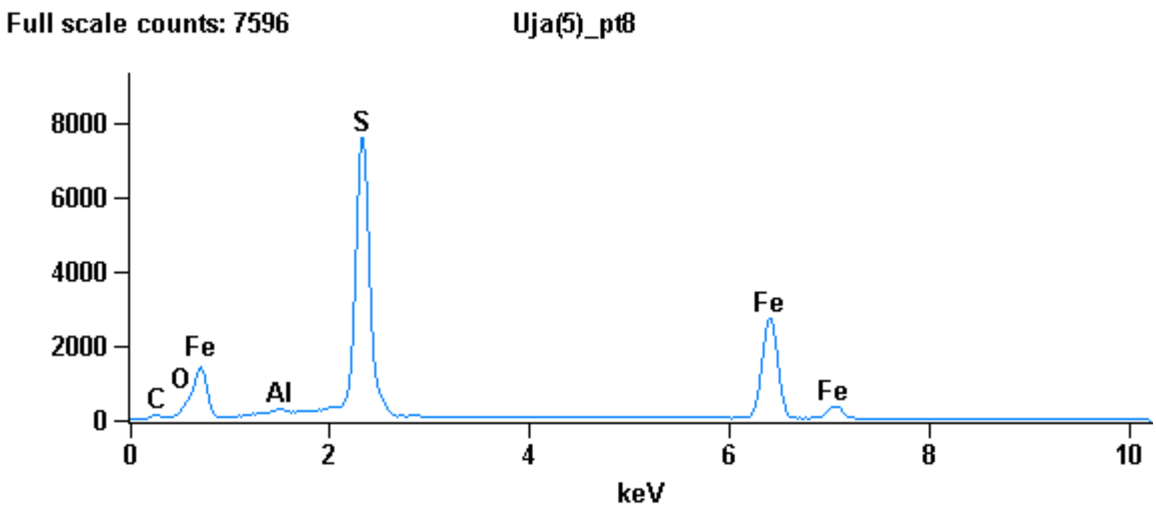
Full scale counts: 7596
Uja(5)_pt8
8000
6000
4000
2000
0
S
Fe
O
C
Al
Fe
Fe
0
2
4
6
8
10
keV

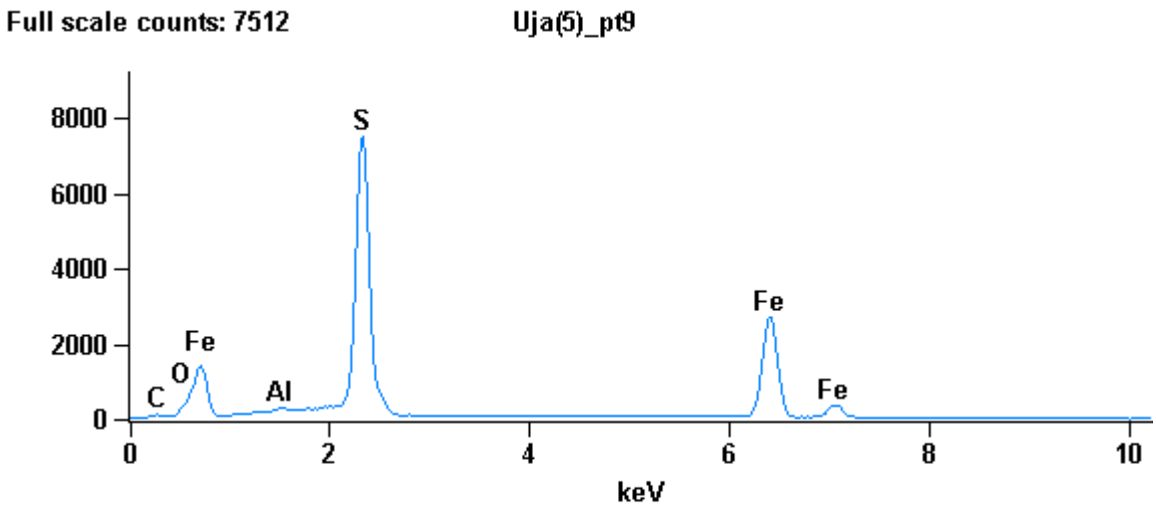
Full scale counts: 7512
Uja(5)_pt9
8000
6000
4000
2000
0
S
Fe
Fe
O
C
Al
Fe
0
2
4
6
8
10
keV

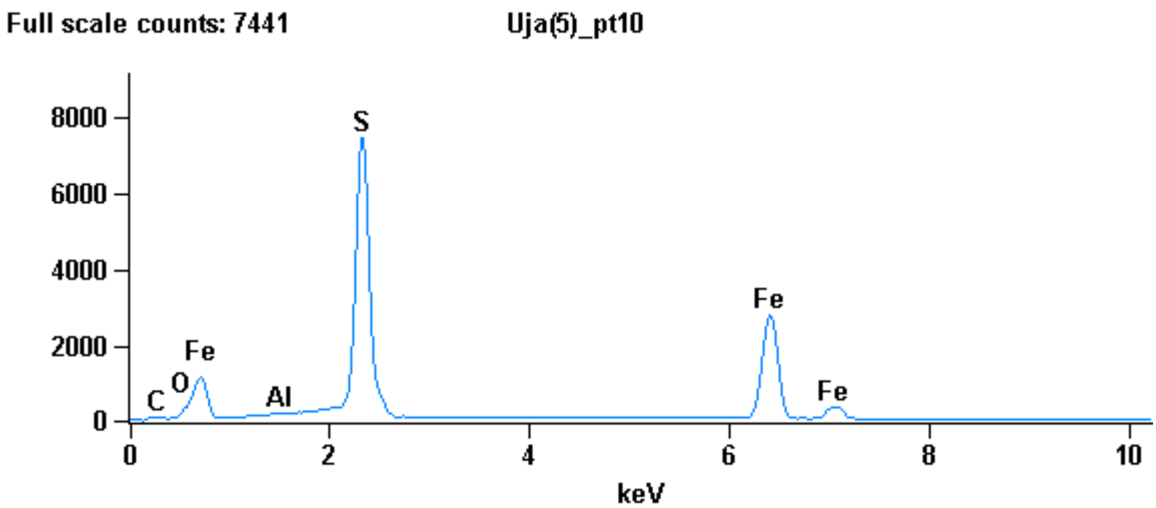
Full scale counts: 7441
Uja(5)_pt10
8000
6000
4000
2000
0
S
Fe
Fe
O
C
Al
Fe
0
2
4
6
8
10
keV

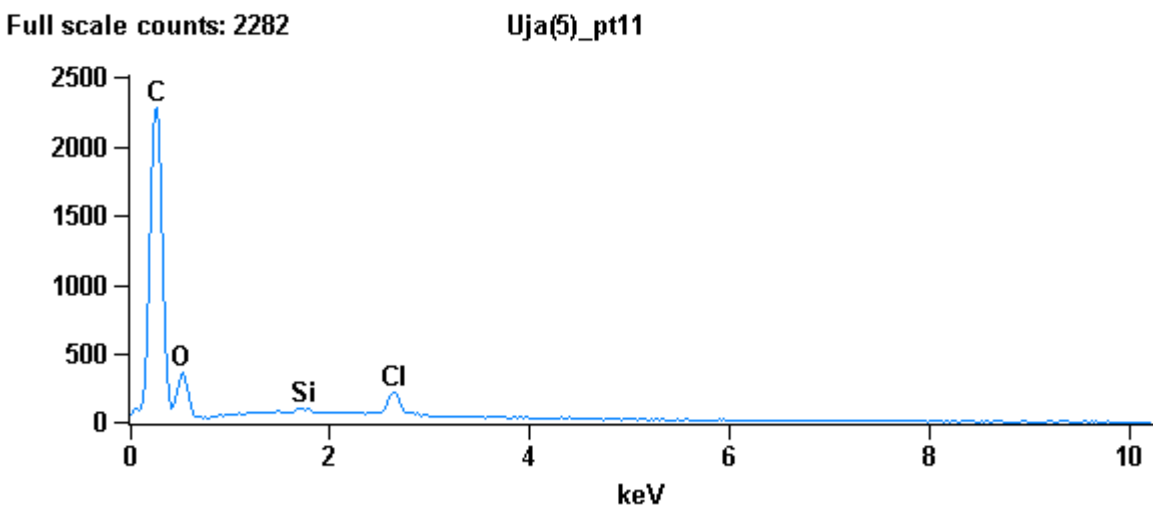
Full scale counts: 2282
Uja(5)_pt11
2500
2000
1500
1000
500
0
C
O
Si
Cl
0
2
4
6
8
10
keV

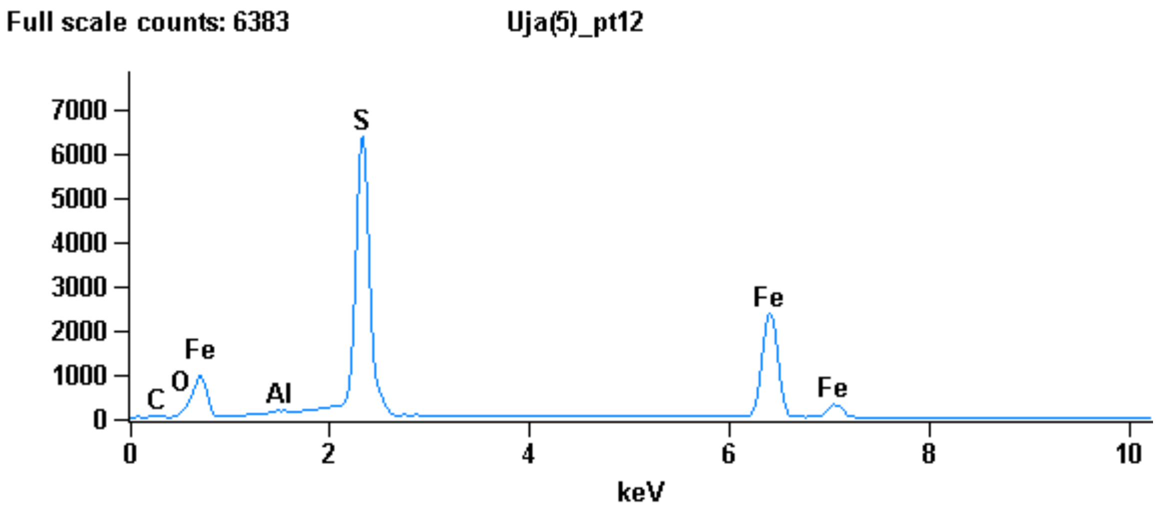
Full scale counts: 6383
Uja(5)_pt12
7000
6000
5000
4000
3000
2000
1000
0
S
Fe
Fe
C
O
Fe
Al
0
2
4
6
8
10
keV

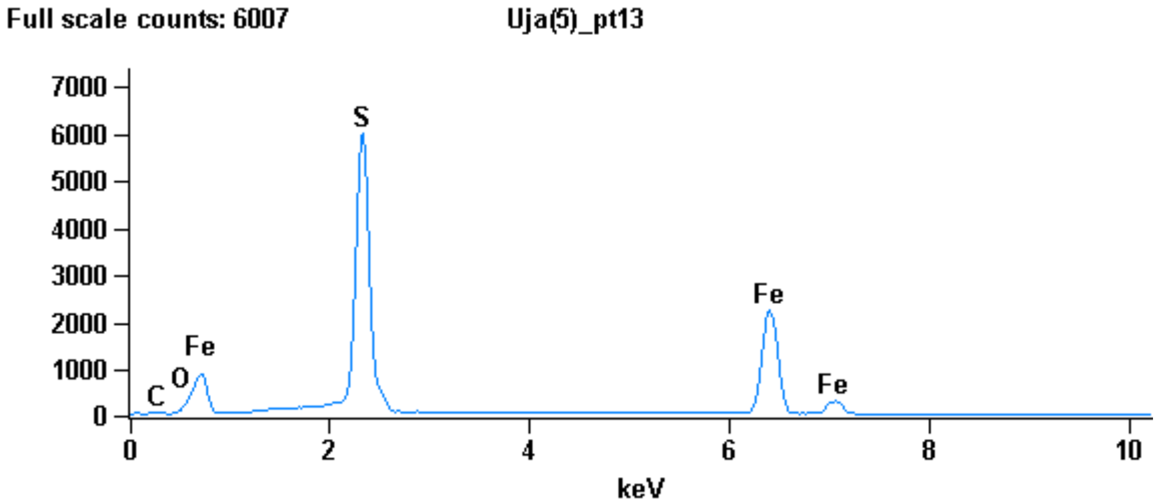
Full scale counts: 6007
Uja(5)_pt13
7000
6000
5000
4000
3000
2000
1000
0
S
Fe
Fe
C
O
Fe
0
2
4
6
8
10
keV

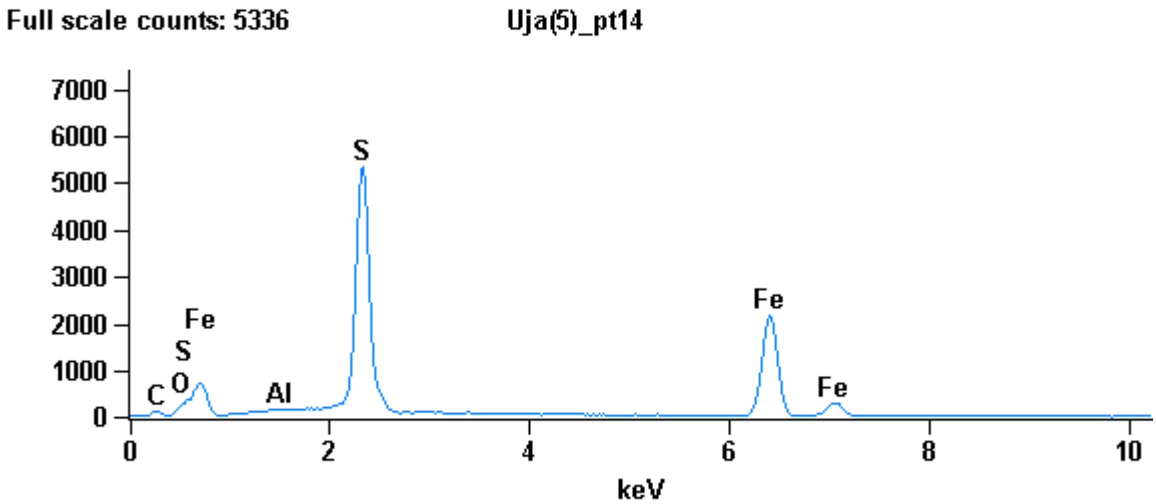
Full scale counts: 5336
Uja(5)_pt14
7000
6000
5000
4000
3000
2000
1000
0
S
Fe
Fe
Fe
S
C
O
Al
0
2
4
6
8
10
keV

Weight %

	O-K	Mg-K	Al-K	Si-K	S-K	Cl-K	Ca-K	Mn-K	Fe-K	Co-K
Uja(5)_pt1	41.37S	1.08	10.61	17.14			2.47	7.51	19.81	
Uja(5)_pt2	41.38S	1.19	10.81	17.00			2.24	7.56	19.83	0.00
Uja(5)_pt3	41.24S	0.84	10.61	17.11			3.36	8.06	18.77	
Uja(5)_pt4	46.34S		0.30		21.68				31.68	
Uja(5)_pt5	45.92S		3.83		19.60				30.65	
Uja(5)_pt6	41.26S	0.97	10.81	17.07			3.83	8.34	17.64	0.08
Uja(5)_pt7	44.65S		6.45		16.77				32.13	
Uja(5)_pt8	46.14S		0.23		21.44				32.19	
Uja(5)_pt9	46.28S		0.19		21.65				31.87	
Uja(5)_pt10	45.87S		0.07		21.15				32.91	
Uja(5)_pt11	11.59S			10.18		78.23				
Uja(5)_pt12	45.70S		0.11		20.90				33.29	
Uja(5)_pt13	45.62S				20.84				33.54	
Uja(5)_pt14	45.33S		0.15		20.40				34.13	

Atom %

	O-K	Mg-K	Al-K	Si-K	S-K	Cl-K	Ca-K	Mn-K	Fe-K	Co-K
Uja(5)_pt1	61.76	1.06	9.39	14.58			1.47	3.27	8.47	
Uja(5)_pt2	61.73	1.17	9.56	14.45			1.33	3.28	8.47	0.00
Uja(5)_pt3	61.64	0.83	9.41	14.57			2.01	3.51	8.04	
Uja(5)_pt4	69.78		0.27		16.29				13.66	
Uja(5)_pt5	68.79		3.40		14.65				13.16	
Uja(5)_pt6	61.52	0.95	9.56	14.50			2.28	3.62	7.54	0.03
Uja(5)_pt7	67.60		5.79		12.67				13.93	
Uja(5)_pt8	69.70		0.21		16.16				13.93	
Uja(5)_pt9	69.77		0.17		16.29				13.77	
Uja(5)_pt10	69.61		0.06		16.02				14.31	
Uja(5)_pt11	22.00			11.00		67.00				
Uja(5)_pt12	69.52		0.10		15.87				14.51	
Uja(5)_pt13	69.51				15.85				14.64	
Uja(5)_pt14	69.34		0.13		15.57				14.96	

Compound %

		MgO	Al2O3	SiO2	SO3	Cl	CaO	MnO	Fe2O3	CoO
Uja(5)_pt1	0.00	1.80	20.05	36.67			3.45	9.70	28.33	
Uja(5)_pt2	0.00	1.97	20.42	36.37			3.13	9.76	28.35	0.00
Uja(5)_pt3	0.00	1.40	20.06	36.60			4.70	10.41	26.83	
Uja(5)_pt4	0.00		0.56		54.15				45.29	
Uja(5)_pt5	0.00		7.23		48.94				43.82	
Uja(5)_pt6	0.00	1.60	20.43	36.51			5.37	10.76	25.22	0.10
Uja(5)_pt7	0.00		12.19		41.88				45.93	
Uja(5)_pt8	0.00		0.44		53.53				46.02	
Uja(5)_pt9	0.00		0.37		54.06				45.57	
Uja(5)_pt10	0.00		0.13		52.81				47.06	
Uja(5)_pt11	0.00			21.77		78.23				
Uja(5)_pt12	0.00		0.20		52.20				47.60	
Uja(5)_pt13	0.00				52.05				47.95	
Uja(5)_pt14	0.00		0.28		50.93				48.79	

Minerals, Uja(5)

pt1: Garnet - pyralspite-group
pt2: Garnet - pyralspite-group
pt3: Garnet - pyralspite-group
pt4: Pyrrhotite
pt5: Pyrrhotite
pt6: Garnet - pyralspite-group
pt7: Pyrrhotite
pt8: Pyrrhotite
pt9: Pyrrhotite
pt10: Pyrrhotite
pt11: Hole in thin section, mixed signal
pt12: Pyrrhotite
pt13: Pyrrhotite
pt14: Pyrrhotite

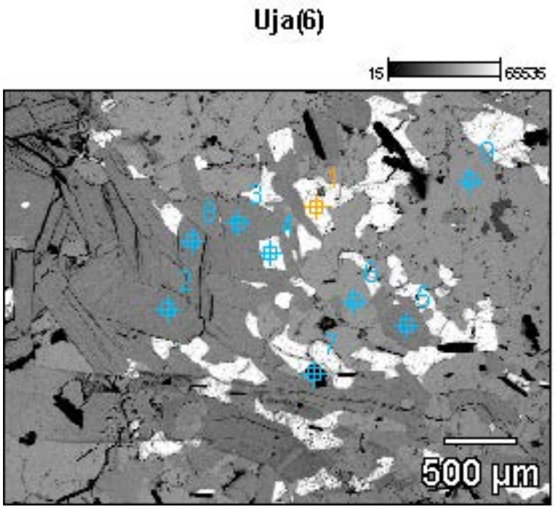

Image name: Uja(6)
Magnification: 32

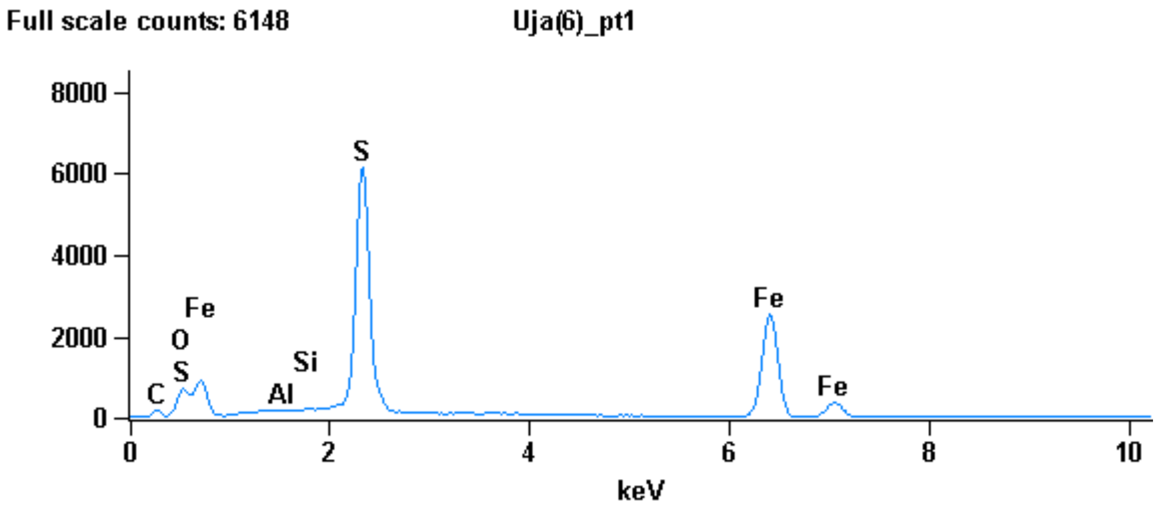

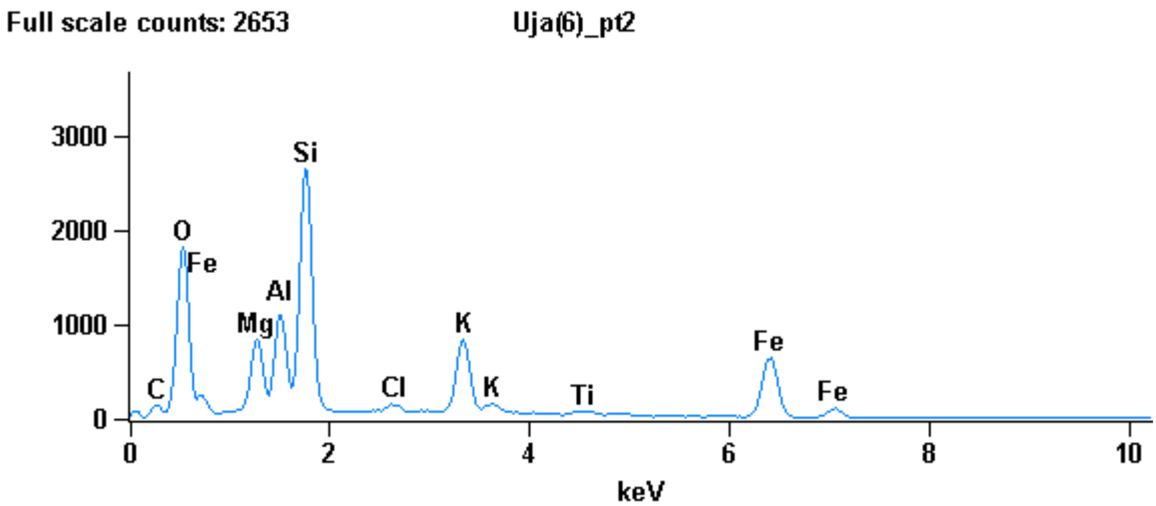

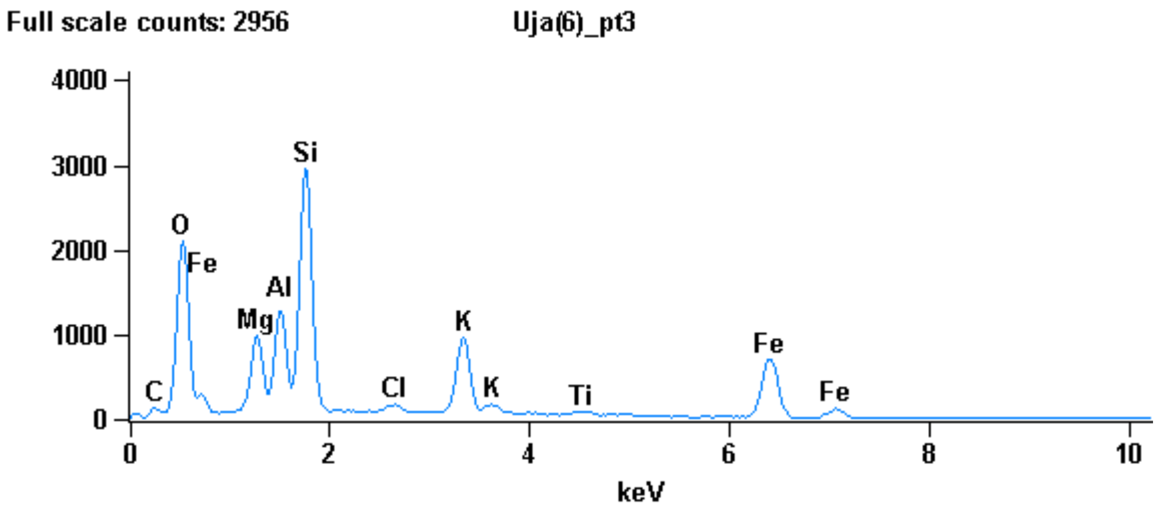
Full scale counts: 2956
Uja(6)_pt3
4000
3000
2000
1000
0
Si
O
Fe
Al
Mg
K
Fe
C
Cl
K
Ti
Fe
0
2
4
6
8
10
keV

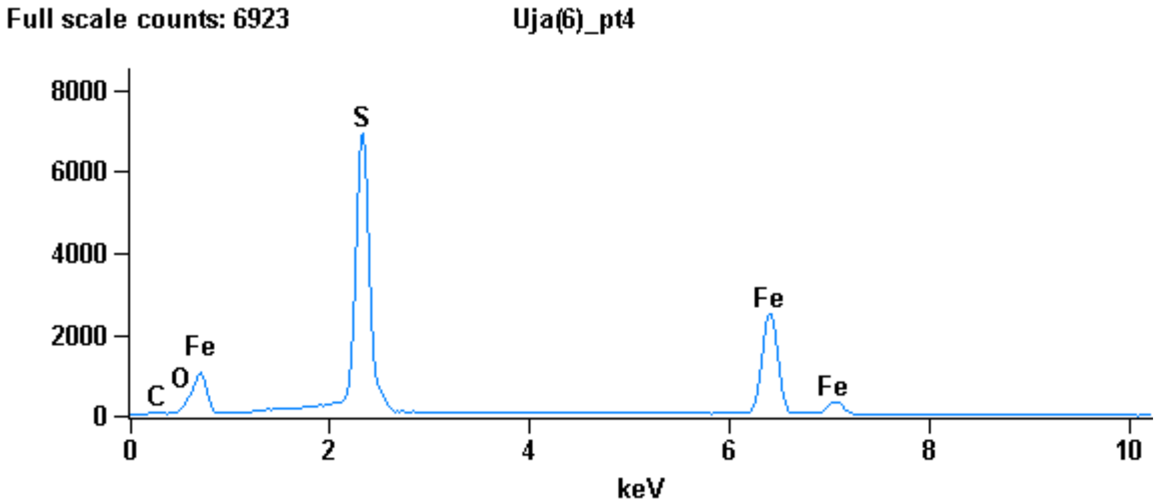
Full scale counts: 6923
Uja(6)_pt4
8000
6000
4000
2000
0
S
Fe
Fe
C
O
Fe
0
2
4
6
8
10
keV

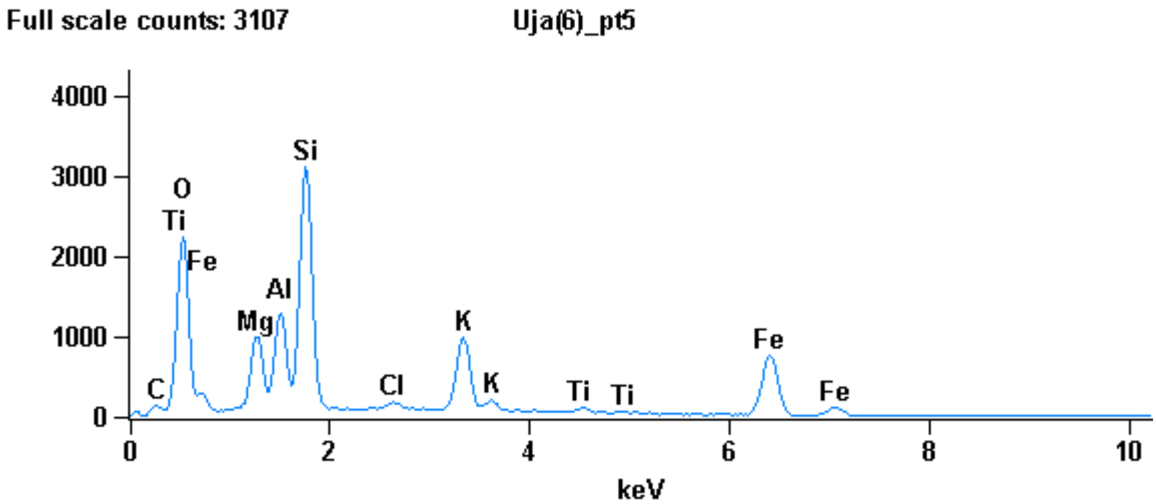
Full scale counts: 3107
Uja(6)_pt5
4000
3000
2000
1000
0
Si
O
Ti
Fe
Al
Mg
K
Fe
C
Cl
K
Ti
Ti
Fe
0
2
4
6
8
10
keV

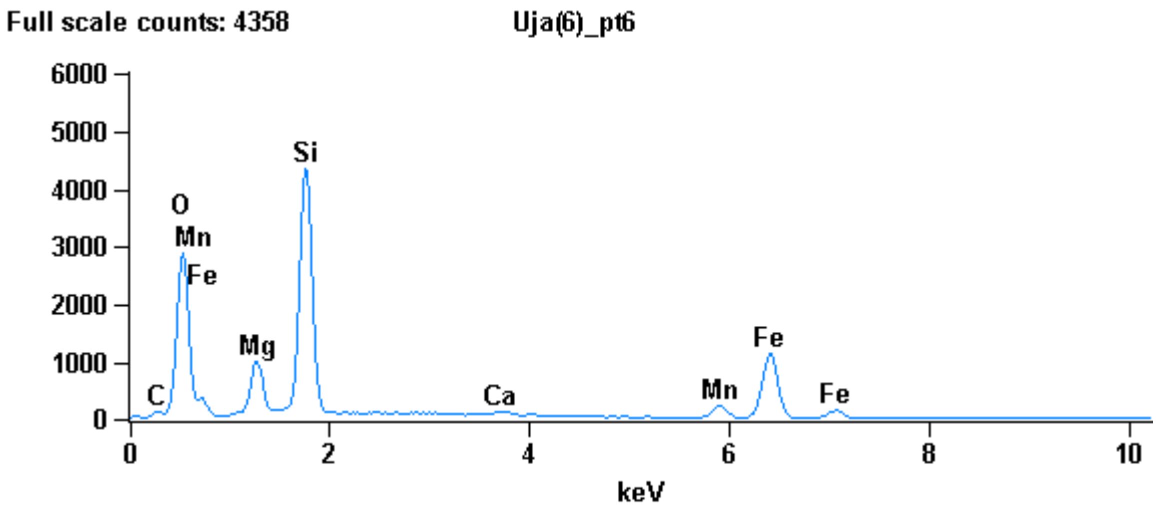
Full scale counts: 4358
Uja(6)_pt6
6000
5000
4000
3000
2000
1000
0
Si
O
Mn
Fe
Mg
C
Ca
Mn
Fe
Fe
0
2
4
6
8
10
keV

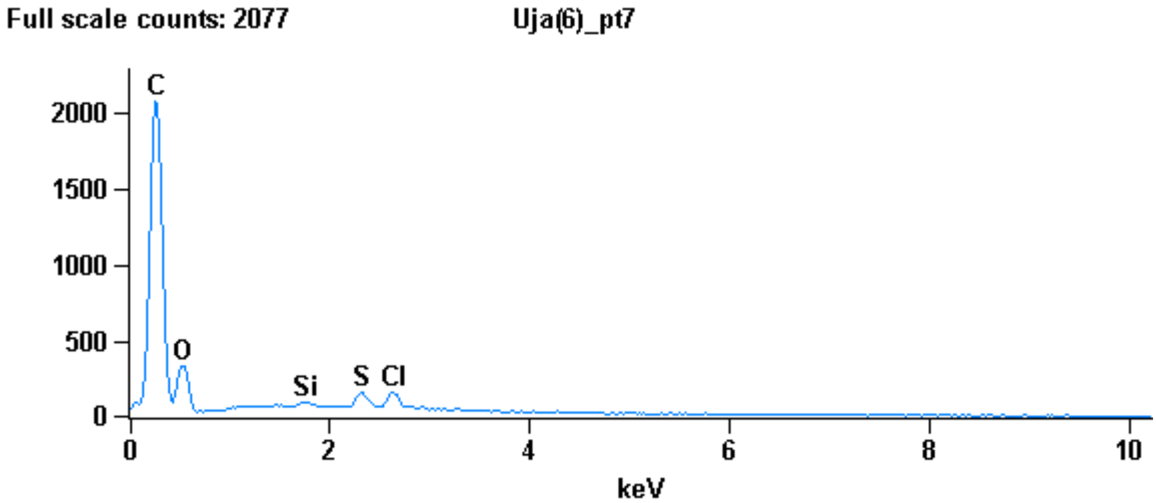
Full scale counts: 2077
Uja(6)_pt7
2000
1500
1000
500
0
C
O
Si
S
Cl
0
2
4
6
8
10
keV

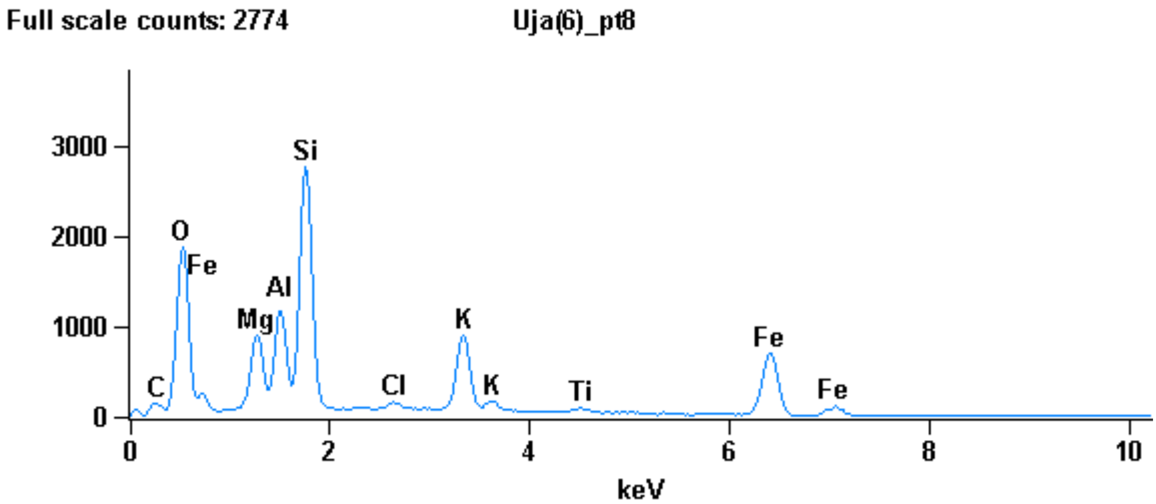
Full scale counts: 2774
Uja(6)_pt8
3000
2000
1000
0
Si
O
Fe
Al
Mg
K
C
Cl
K
Ti
Fe
Fe
0
2
4
6
8
10
keV

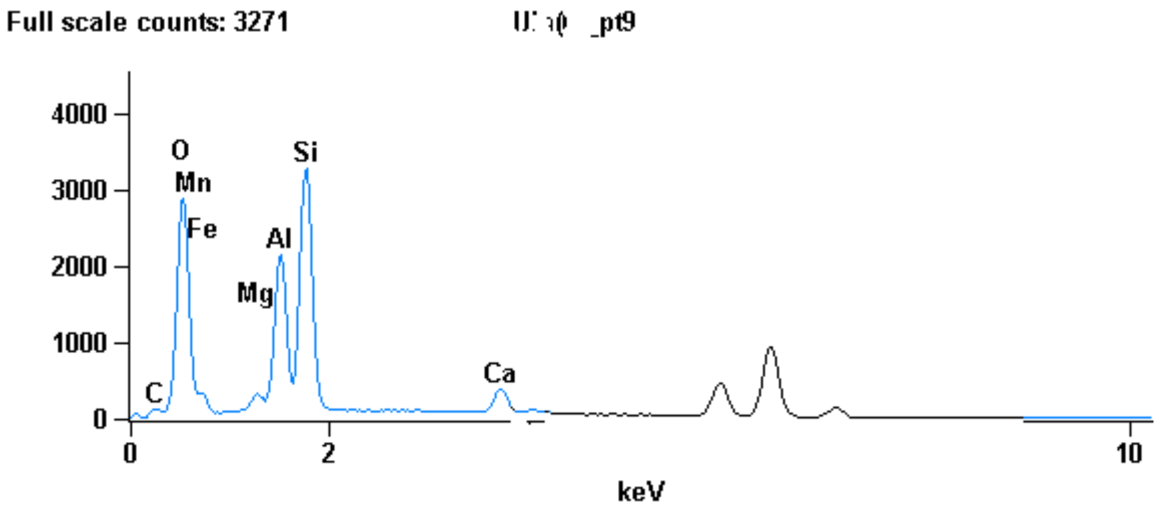

Weight %

	O-K	Mg-K	Al-K	Si-K	S-K	Cl-K	K-K	Ca-K	Ti-K	Mn-K	Fe-K
Uja(6)_pt1	45.11S		0.06	0.10	20.08						34.65
Uja(6)_pt2	41.09S	6.73	7.19	17.71		0.51	7.17		0.79		18.81
Uja(6)_pt3	41.12S	6.90	7.18	17.87		0.65	7.24		0.69		18.35
Uja(6)_pt4	45.91S				21.23						32.87
Uja(6)_pt5	41.19S	6.78	7.29	17.94		0.51	7.32		0.65		18.32
Uja(6)_pt6	42.14S	6.91		22.80				0.45		3.38	24.32
Uja(6)_pt7	39.42S			5.31	22.29	32.98					
Uja(6)_pt8	41.06S	6.85	7.20	17.73		0.49	7.31		0.57		18.78
Uja(6)_pt9	41.40S	1.08	10.69	17.29				2.38		8.27	18.89

Atom %

	O-K	Mg-K	Al-K	Si-K	S-K	Cl-K	K-K	Ca-K	Ti-K	Mn-K	Fe-K
Uja(6)_pt1	69.25		0.05	0.08	15.38						15.24
Uja(6)_pt2	59.81	6.45	6.21	14.69		0.34	4.27		0.38		7.85
Uja(6)_pt3	59.73	6.60	6.19	14.79		0.43	4.30		0.33		7.64
Uja(6)_pt4	69.64				16.07						14.28
Uja(6)_pt5	59.79	6.48	6.27	14.84		0.34	4.35		0.32		7.62
Uja(6)_pt6	62.15	6.70		19.16				0.27		1.45	10.28
Uja(6)_pt7	57.59			4.42	16.25	21.75					
Uja(6)_pt8	59.75	6.56	6.21	14.70		0.32	4.35		0.28		7.83
Uja(6)_pt9	61.72	1.06	9.46	14.69				1.41		3.59	8.07

Compound %

		MgO	Al2O3	SiO2	SO3	Cl	K2O	CaO	TiO2	MnO	Fe2O3
Uja(6)_pt1	0.00		0.11	0.21	50.14						49.54
Uja(6)_pt2	0.00	11.16	13.59	37.90		0.51	8.63		1.32		26.89
Uja(6)_pt3	0.00	11.44	13.58	38.23		0.65	8.72		1.15		26.24
Uja(6)_pt4	0.00				53.01						46.99
Uja(6)_pt5	0.00	11.24	13.76	38.38		0.51	8.82		1.09		26.20
Uja(6)_pt6	0.00	11.45		48.78				0.64		4.36	34.77
Uja(6)_pt7	0.00			11.36	55.66	32.98					
Uja(6)_pt8	0.00	11.36	13.60	37.93		0.49	8.81		0.95		26.85
Uja(6)_pt9	0.00	1.79	20.21	36.99				3.33		10.68	27.01

Minerals, Uja(6)

pt1: Pyrrhotite
pt2: Biotite
pt3: Biotite
pt4: Pyrrhotite
pt5: Biotite
pt6: Orthopyroxene - enstatite-ferrosilite
pt7: Hole in thin section, mixed signal
pt8: Biotite
pt9: Garnet - pyralspite-group

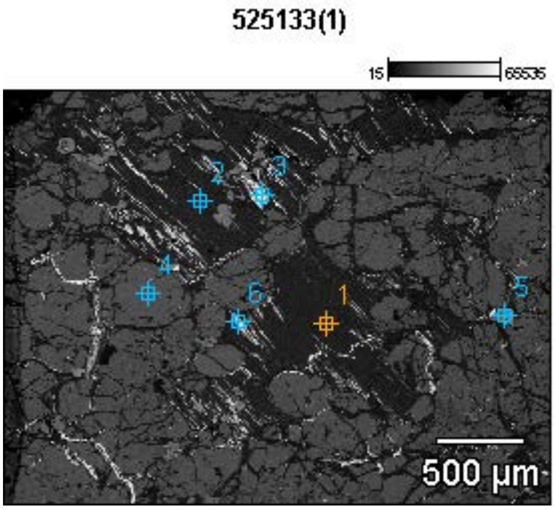

Image name: 525133(1)
Magnification: 39

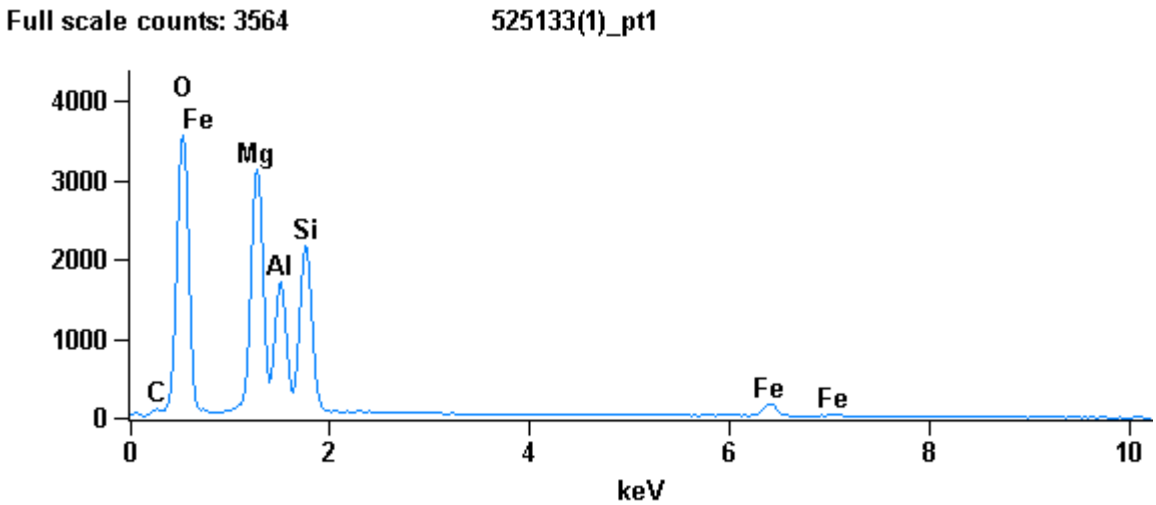

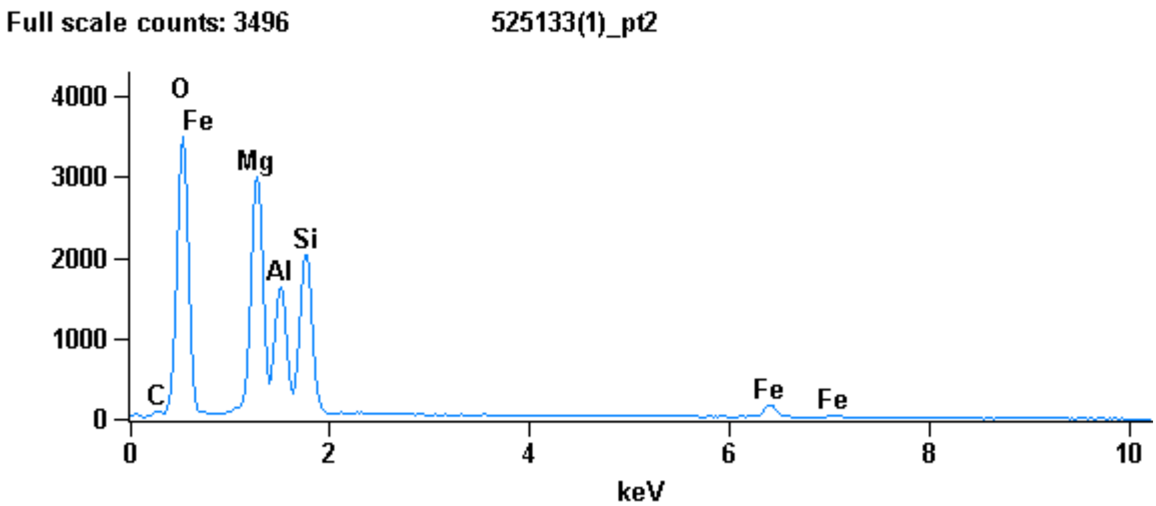

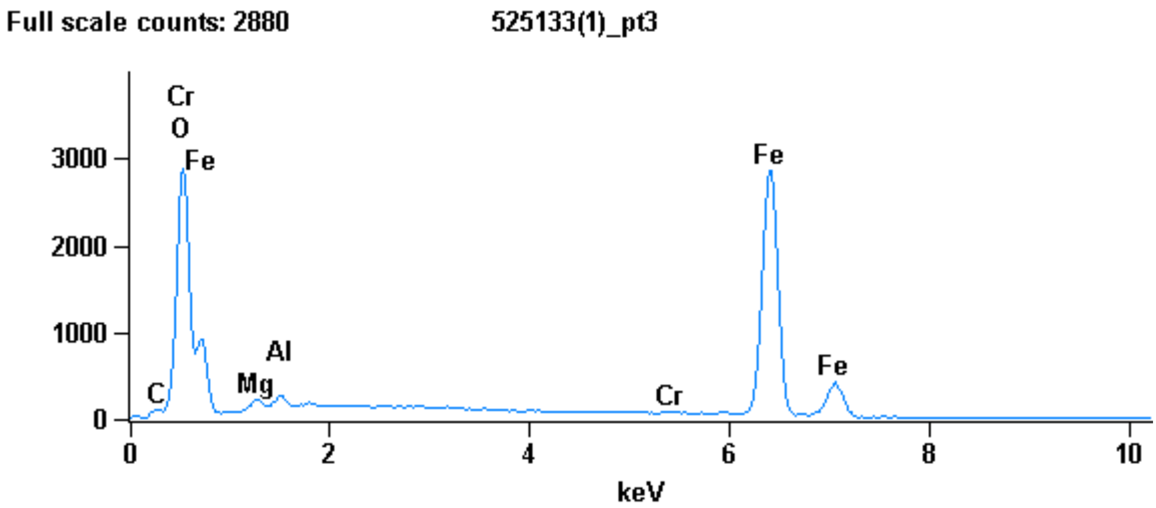
Full scale counts: 2880
525133(1)_pt3
Cr
O
Fe
Fe
Al
Mg
C
Cr
Fe
0
1000
2000
3000
0
2
4
6
8
10
keV

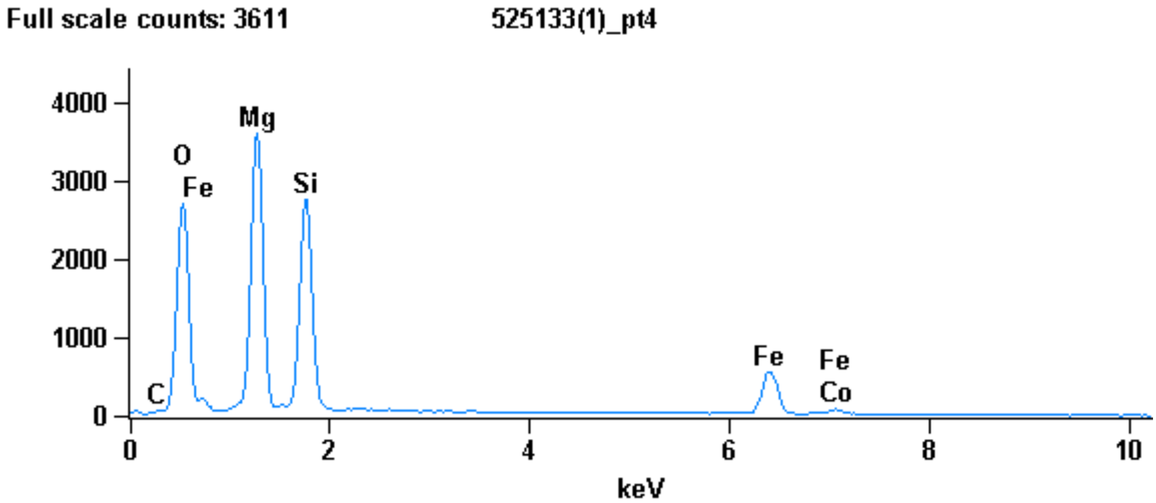
Full scale counts: 3611
525133(1)_pt4
Mg
O
Fe
Si
C
Fe
Fe
Co
0
1000
2000
3000
4000
0
2
4
6
8
10
keV

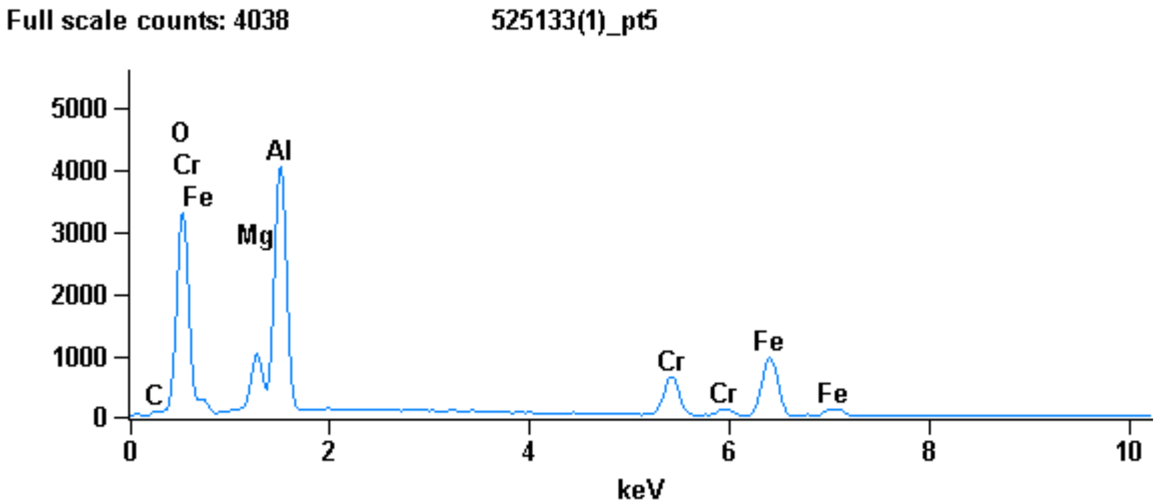
Full scale counts: 4038
525133(1)_pt5
O
Cr
Fe
Al
Mg
C
Cr
Cr
Fe
Fe
0
1000
2000
3000
4000
5000
0
2
4
6
8
10
keV

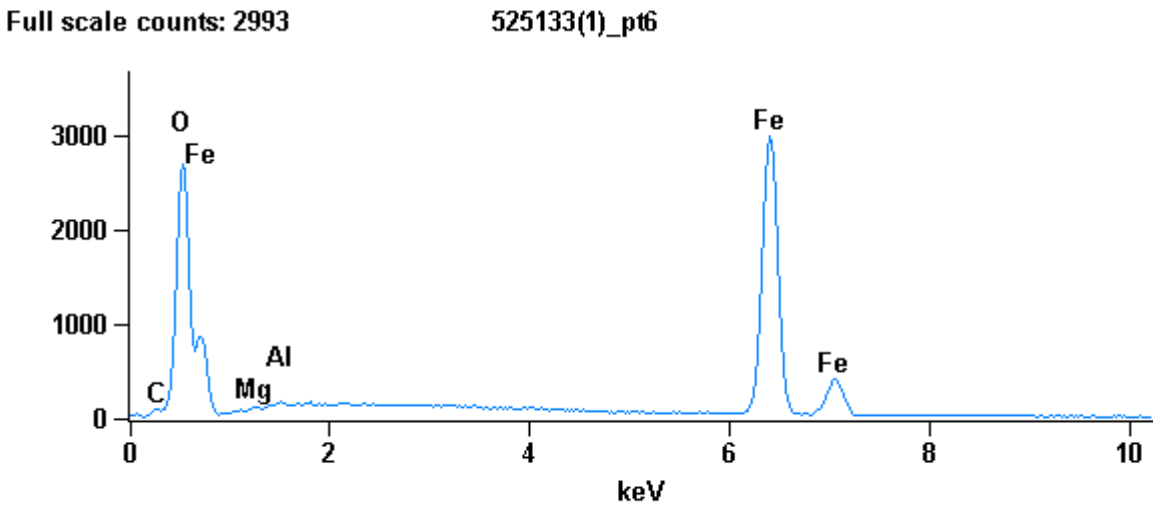

Weight %

	O-K	Mg-K	Al-K	Si-K	Cr-K	Fe-K	Co-K
525133(1)_pt1	45.49S	21.63	11.95	16.38		4.54	
525133(1)_pt2	45.65S	21.58	12.39	16.44		3.95	
525133(1)_pt3	30.65S	1.49	1.06		0.46	66.35	
525133(1)_pt4	42.78S	25.29		17.51		14.31	0.11
525133(1)_pt5	39.00S	6.19	24.15		8.75	21.81	0.10
525133(1)_pt6	30.19S	0.15	0.33			69.33	

Atom %

	O-K	Mg-K	Al-K	Si-K	Cr-K	Fe-K	Co-K
525133(1)_pt1	58.73	18.38	9.15	12.05		1.68	
525133(1)_pt2	58.75	18.28	9.45	12.05		1.46	
525133(1)_pt3	59.62	1.91	1.22		0.27	36.98	
525133(1)_pt4	58.18	22.64		13.57		5.58	0.04
525133(1)_pt5	58.76	6.14	21.58		4.06	9.42	0.04
525133(1)_pt6	59.96	0.20	0.39			39.45	

Compound %

		MgO	Al2O3	SiO2	Cr2O3	Fe2O3	CoO
525133(1)_pt1	0.00	35.87	22.59	35.05		6.50	
525133(1)_pt2	0.00	35.78	23.40	35.17		5.65	
525133(1)_pt3	0.00	2.48	2.00		0.67	94.86	
525133(1)_pt4	0.00	41.94		37.46		20.46	0.14
525133(1)_pt5	0.00	10.27	45.63		12.78	31.18	0.13
525133(1)_pt6	0.00	0.25	0.62			99.13	

Minerals, 525133(1)
pt1: Chlorite - clinochlore-chamosite series
pt2: Chlorite - clinochlore-chamosite series
pt3: Fe-oxide
pt4: Olivine - chrysolite
pt5: Spinel - picotite
pt6: Fe-oxide

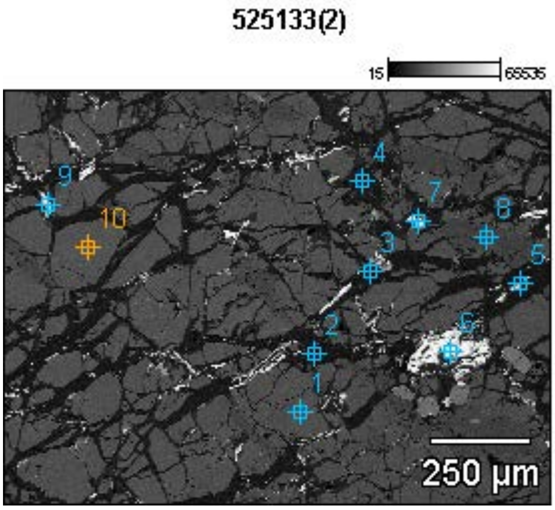

Image name: 525133(2)
Magnification: 89

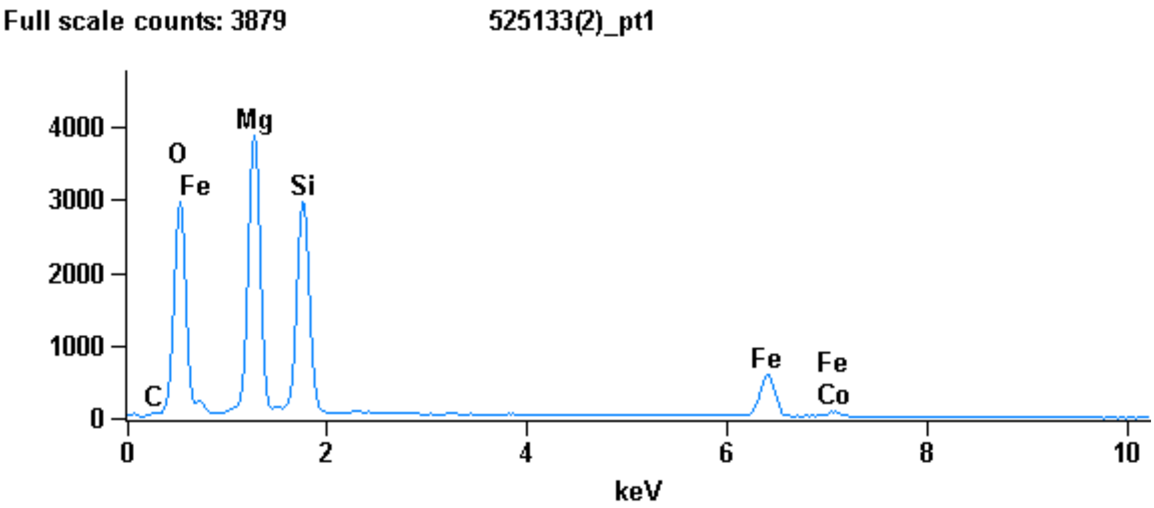

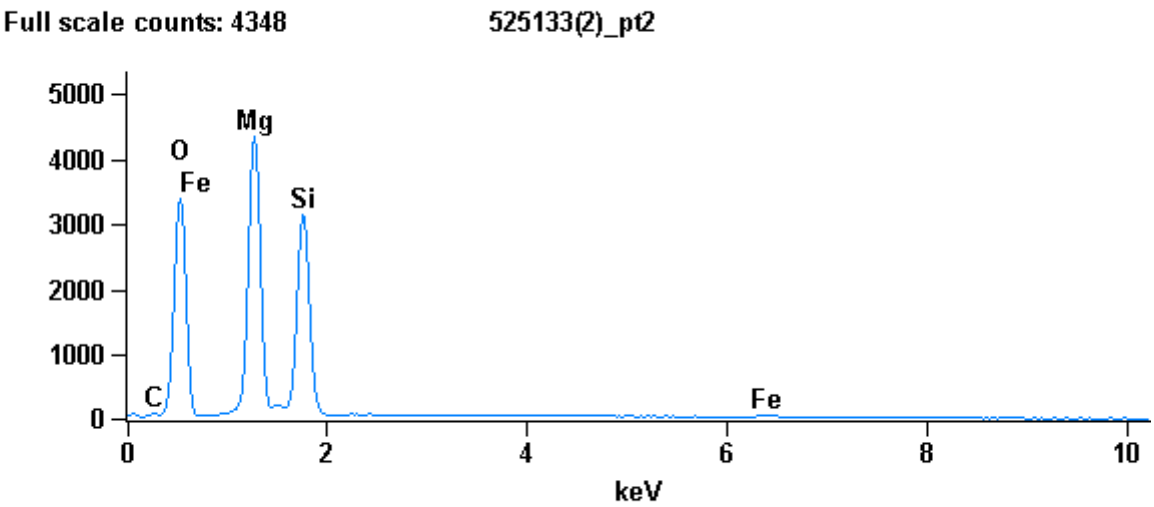

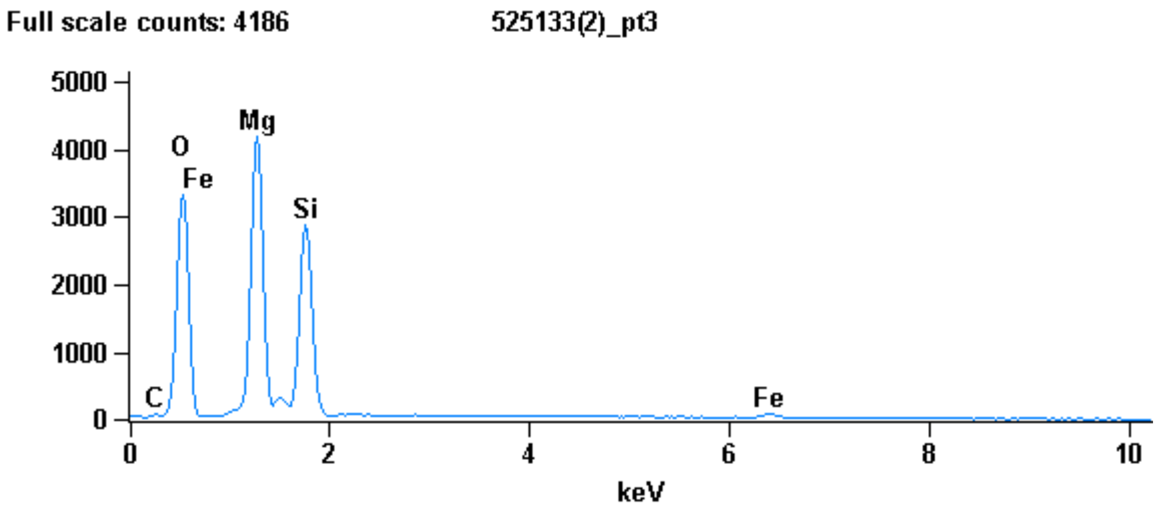
Full scale counts: 4186
525133(2)_pt3
5000
4000
3000
2000
1000
0
O
Fe
Mg
Si
C
Fe
0
2
4
6
8
10
keV

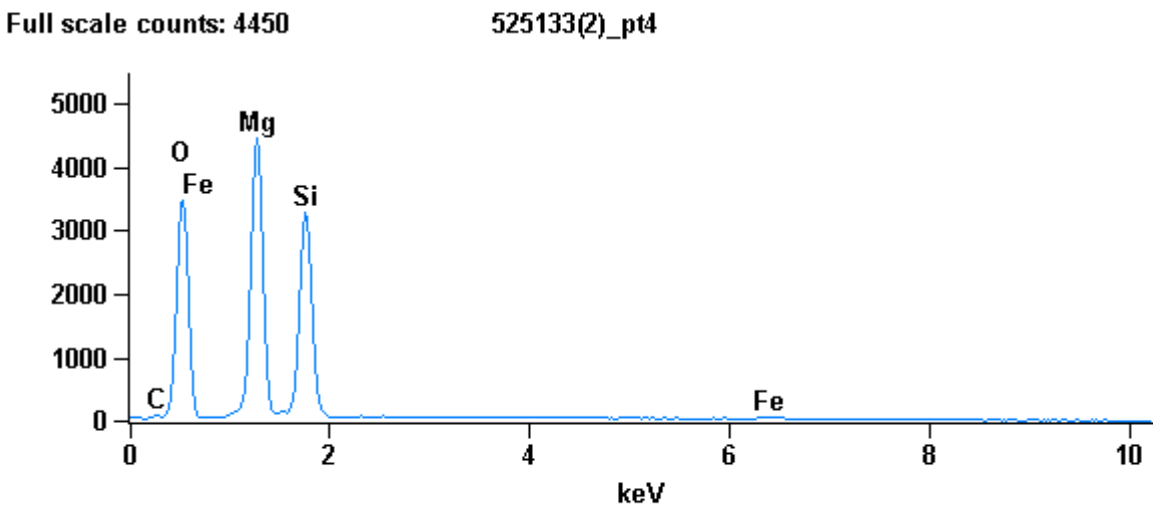
Full scale counts: 4450
525133(2)_pt4
5000
4000
3000
2000
1000
0
O
Fe
Mg
Si
C
Fe
0
2
4
6
8
10
keV

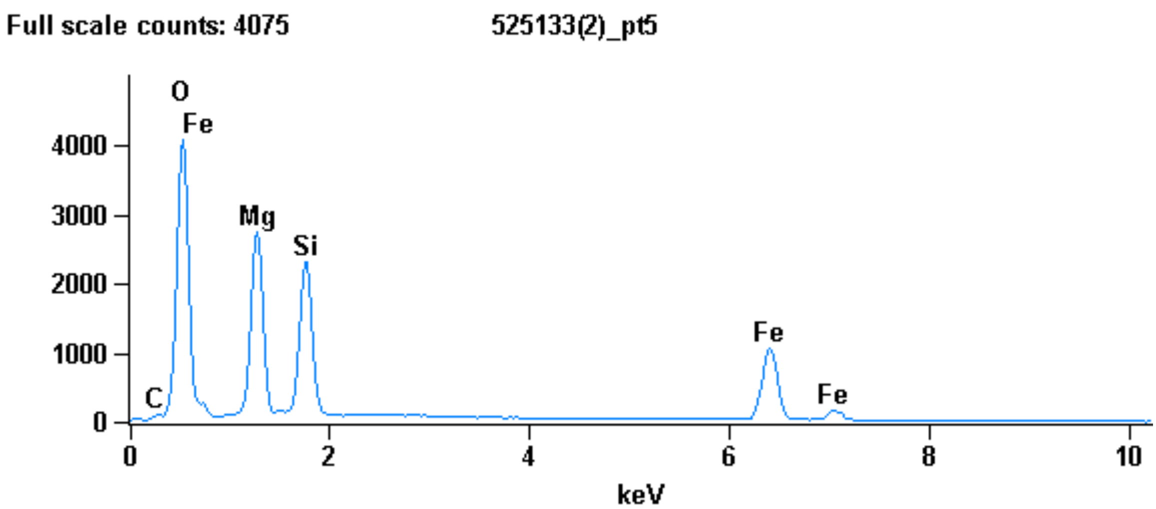
Full scale counts: 4075
525133(2)_pt5
4000
3000
2000
1000
0
O
Fe
Mg
Si
C
Fe
Fe
0
2
4
6
8
10
keV

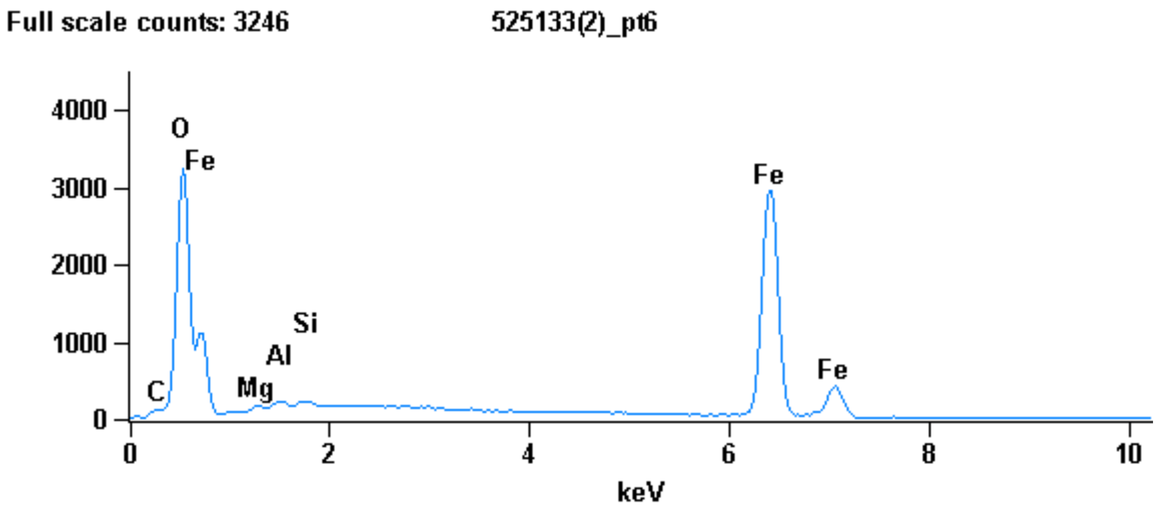
Full scale counts: 3246
525133(2)_pt6
4000
3000
2000
1000
0
O
Fe
C
Mg
Al
Si
Fe
Fe
0
2
4
6
8
10
keV

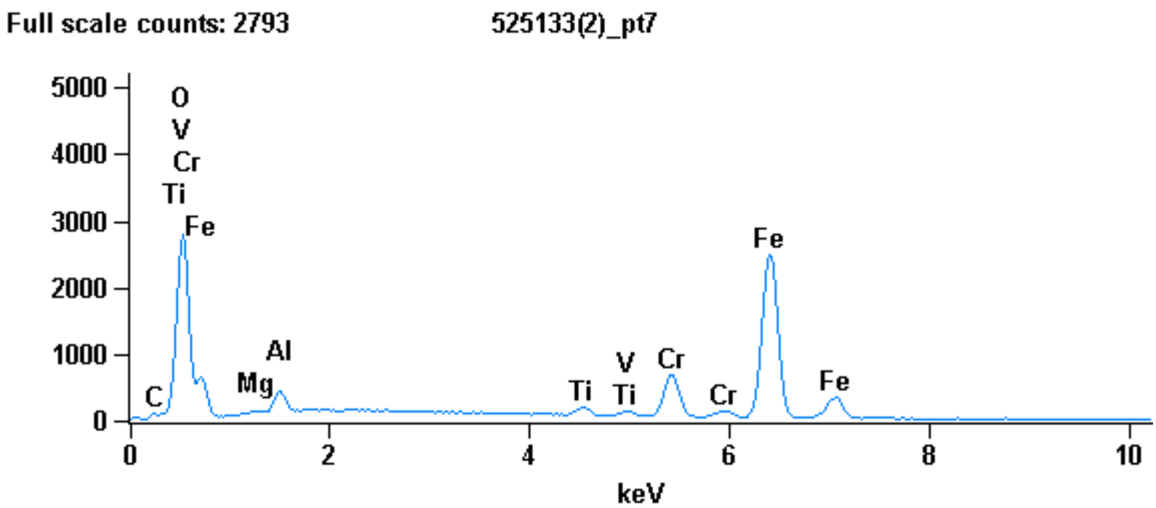
Full scale counts: 2793
525133(2)_pt7
5000
4000
3000
2000
1000
0
O
V
Cr
Ti
Fe
C
Mg
Al
Ti
V
Ti
Cr
Cr
Fe
Fe
0
2
4
6
8
10
keV

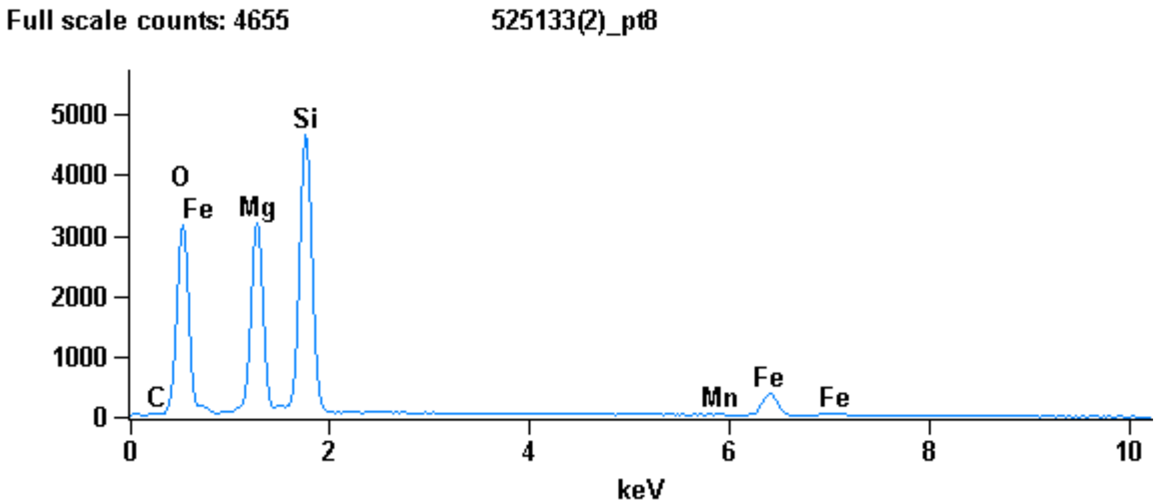
Full scale counts: 4655
525133(2)_pt8
5000
4000
3000
2000
1000
0
O
Fe
Mg
Si
C
Mn
Fe
Fe
0
2
4
6
8
10
keV

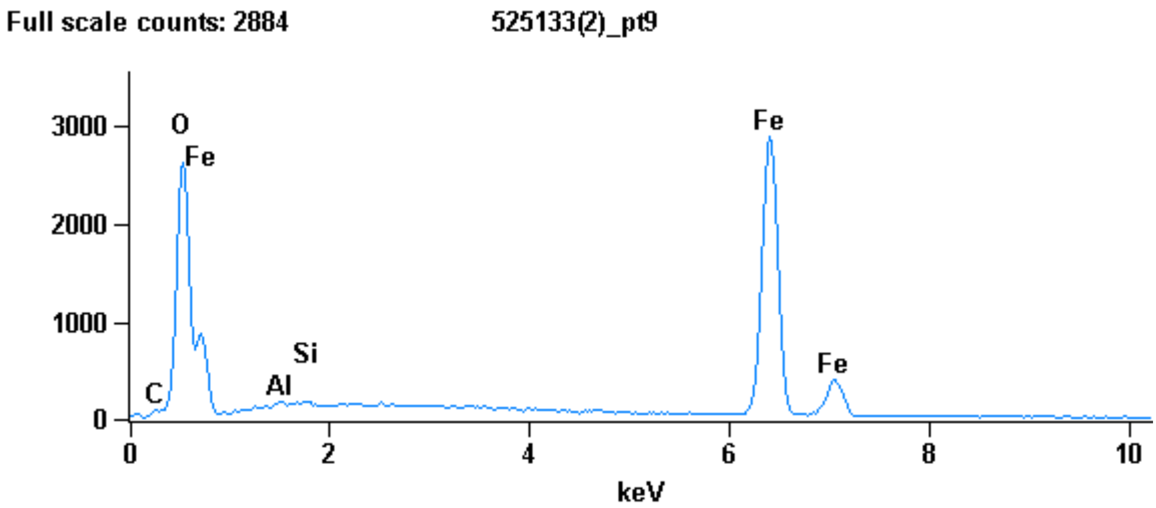
Full scale counts: 2884
525133(2)_pt9
3000
2000
1000
0
O
Fe
C
Al
Si
Fe
Fe
0
2
4
6
8
10
keV

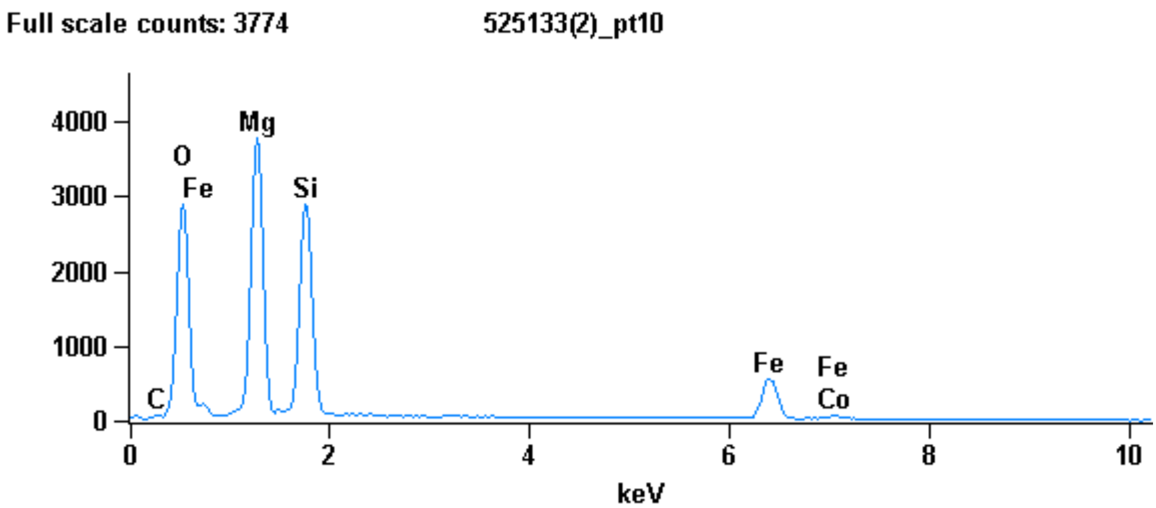
Full scale counts: 3774
525133(2)_pt10
4000
3000
2000
1000
0
O
Fe
Mg
Si
C
Fe
Fe
Co
0
2
4
6
8
10
keV

Weight %

	O-K	Mg-K	Al-K	Si-K	Ti-K	V-K	Cr-K	Mn-K	Fe-K	Co-K
525133(2)_pt1	43.00S	25.42		17.89					13.68	0.00
525133(2)_pt2	46.10S	29.74		22.75					1.42	
525133(2)_pt3	45.80S	29.74		22.14					2.33	
525133(2)_pt4	46.05S	29.04		22.88					2.02	
525133(2)_pt5	40.43S	20.87		14.18					24.52	
525133(2)_pt6	30.54S	0.48	0.62	0.41					67.94	
525133(2)_pt7	31.38S	0.37	2.27		1.24	0.55	8.58		55.62	
525133(2)_pt8	45.75S	19.42		25.45				0.30	8.92	0.16
525133(2)_pt9	30.26S		0.33	0.19					69.21	
525133(2)_pt10	43.00S	25.35		17.91					13.74	0.00

Atom %

	O-K	Mg-K	Al-K	Si-K	Ti-K	V-K	Cr-K	Mn-K	Fe-K	Co-K
525133(2)_pt1	58.23	22.66		13.80					5.31	0.00
525133(2)_pt2	58.33	24.77		16.39					0.51	
525133(2)_pt3	58.23	24.89		16.03					0.85	
525133(2)_pt4	58.46	24.27		16.54					0.74	
525133(2)_pt5	58.37	19.83		11.66					10.14	
525133(2)_pt6	59.97	0.62	0.73	0.46					38.22	
525133(2)_pt7	60.20	0.47	2.58		0.79	0.33	5.06		30.57	
525133(2)_pt8	60.42	16.88		19.15				0.12	3.38	0.06
525133(2)_pt9	60.04		0.39	0.22					39.35	
525133(2)_pt10	58.24	22.60		13.82					5.33	0.00

Compound %

		MgO	Al2O3	SiO2	TiO2	V2O5	Cr2O3	MnO	Fe2O3	CoO
525133(2)_pt1	0.00	42.16		38.28					19.56	0.00
525133(2)_pt2	0.00	49.31		48.66					2.03	
525133(2)_pt3	0.00	49.31		47.36					3.33	
525133(2)_pt4	0.00	48.16		48.95					2.89	
525133(2)_pt5	0.00	34.60		30.34					35.05	
525133(2)_pt6	0.00	0.80	1.18	0.88					97.14	
525133(2)_pt7	0.00	0.61	4.29		2.06	0.99	12.54		79.52	
525133(2)_pt8	0.00	32.21		54.45				0.39	12.75	0.20

525133(2)_pt9	0.00		0.63	0.41					98.96	
525133(2)_pt10	0.00	42.03		38.32					19.65	0.00

Minerals, 525133(2)

pt1: Olivine - chrysolite
pt2: Olivine - chrysolite
pt3: Olivine - forsterite
pt4: Olivine - chrysolite
pt5: Olivine - hyalosiderite
pt6: Fe-oxide
pt7: Spinel-series mineral
pt8: Olivine - chrysolite
pt9: Fe-oxide
pt10: Olivine - chrysolite

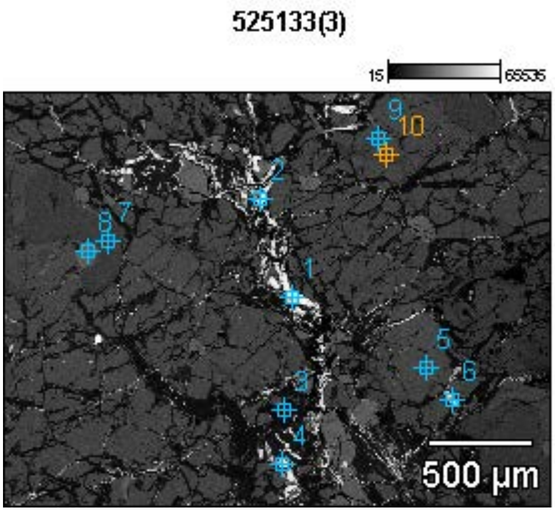

Image name: 525133(3)
Magnification: 46

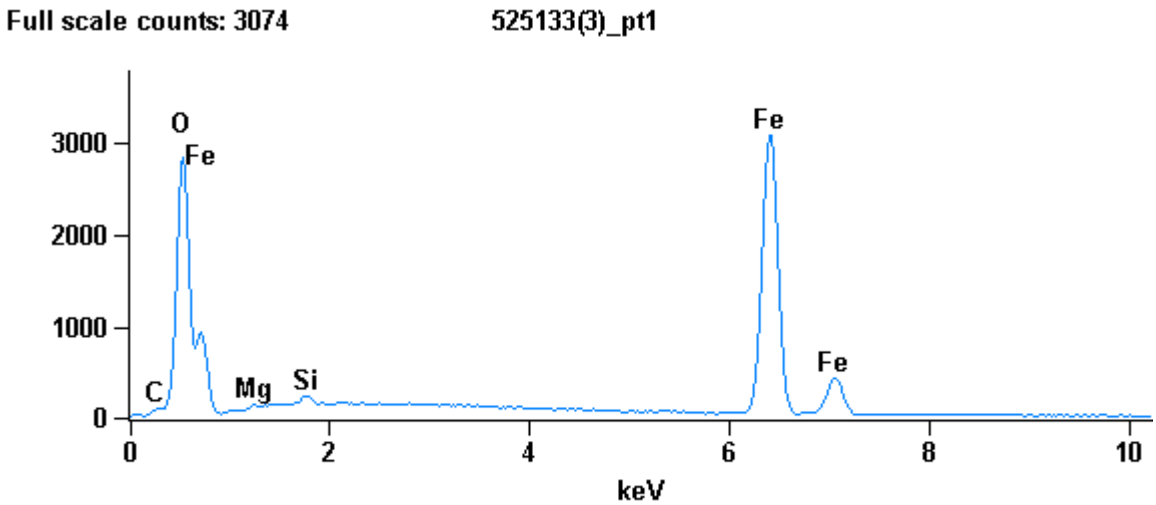

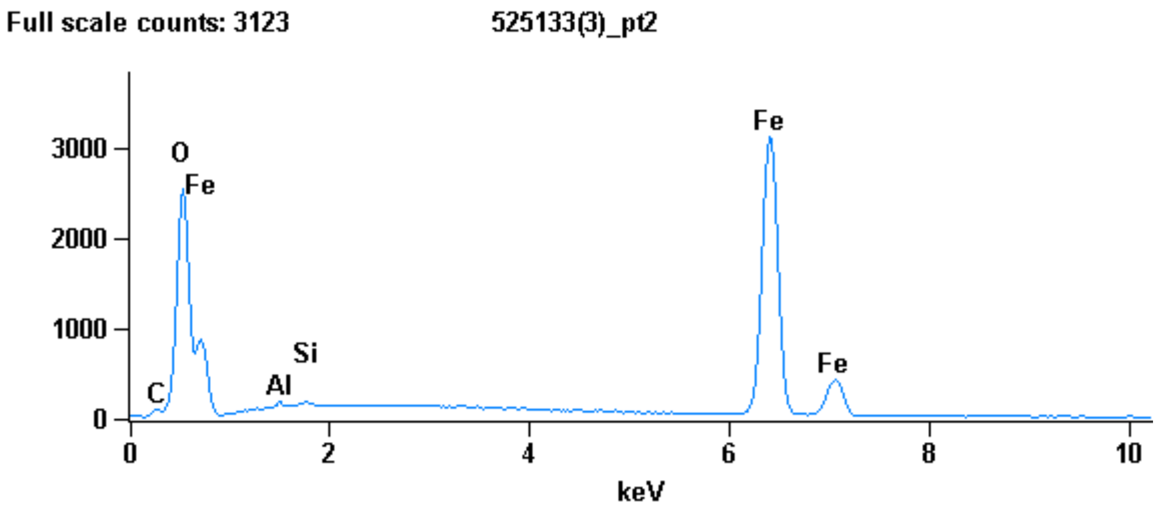

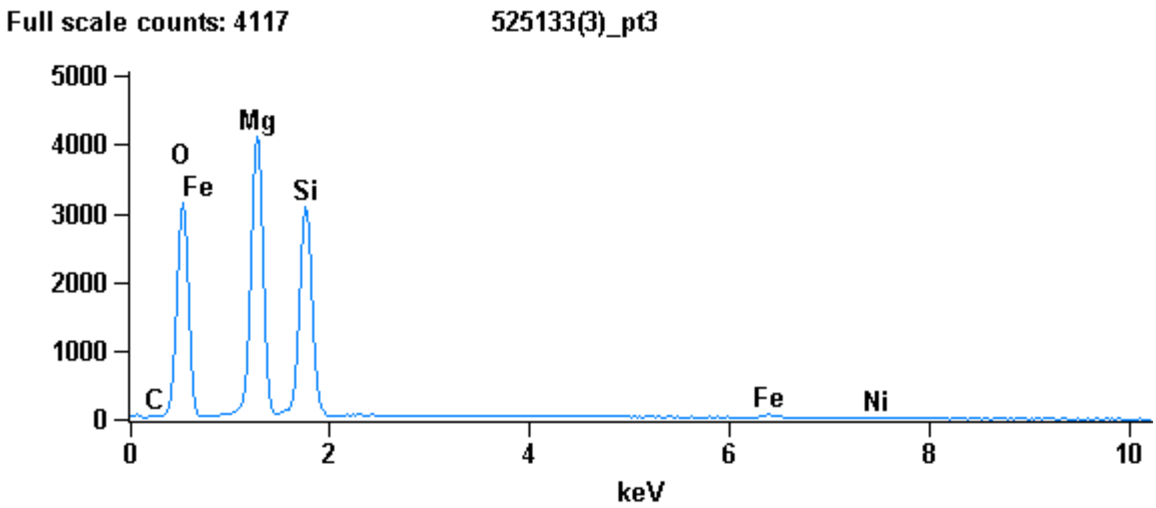
Full scale counts: 4117
525133(3)_pt3
5000
4000
3000
2000
1000
0
O
Fe
Mg
Si
C
Fe
Ni
0
2
4
6
8
10
keV

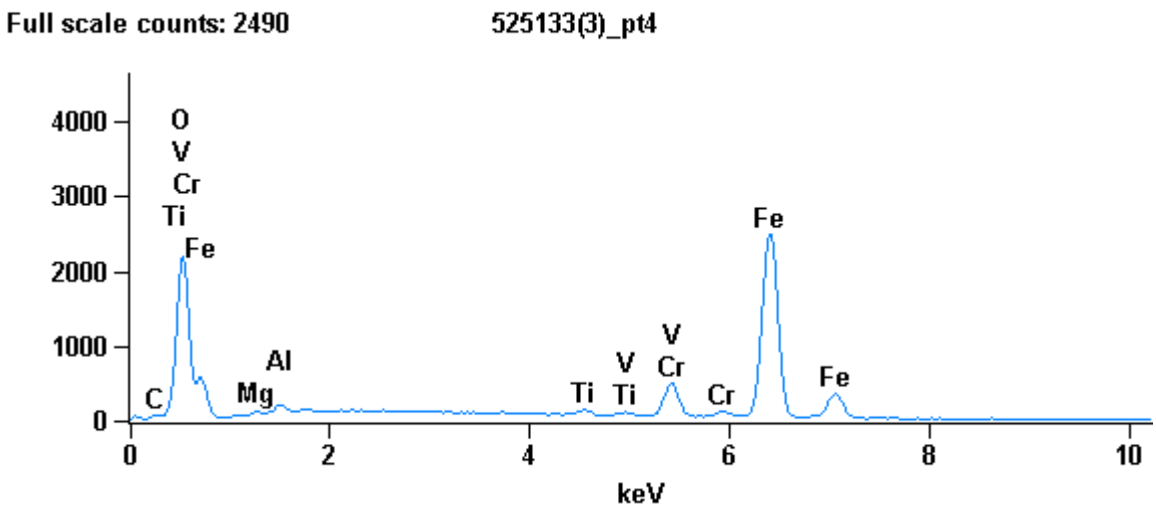
Full scale counts: 2490
525133(3)_pt4
4000
3000
2000
1000
0
O
V
Cr
Ti
Fe
Al
Mg
C
Ti
V
Ti
V
Cr
Cr
Fe
Fe
0
2
4
6
8
10
keV

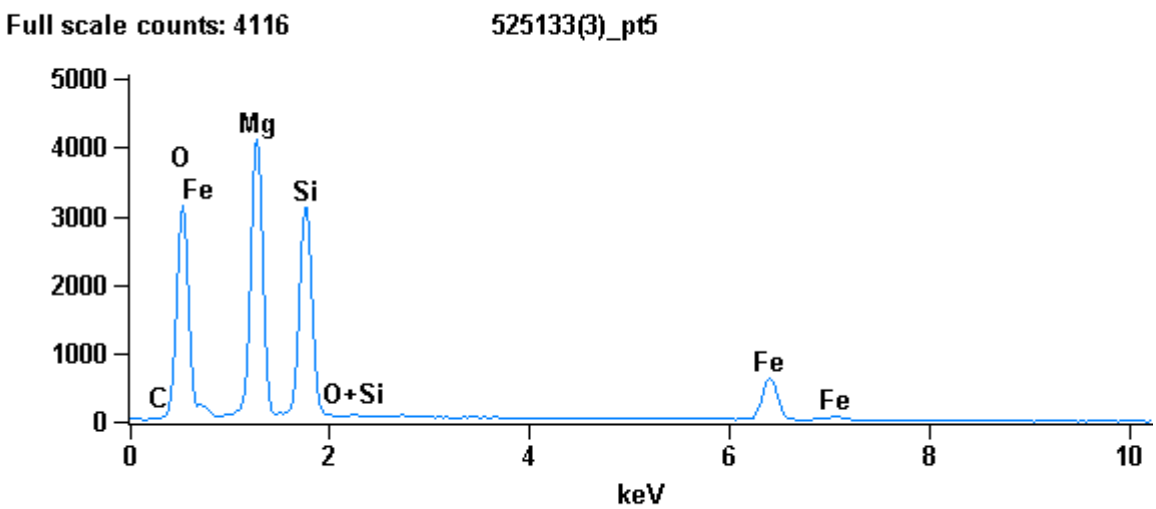
Full scale counts: 4116
525133(3)_pt5
5000
4000
3000
2000
1000
0
O
Fe
Mg
Si
C
O+Si
Fe
Fe
0
2
4
6
8
10
keV

Full scale counts: 2808 525133(3)_pt6

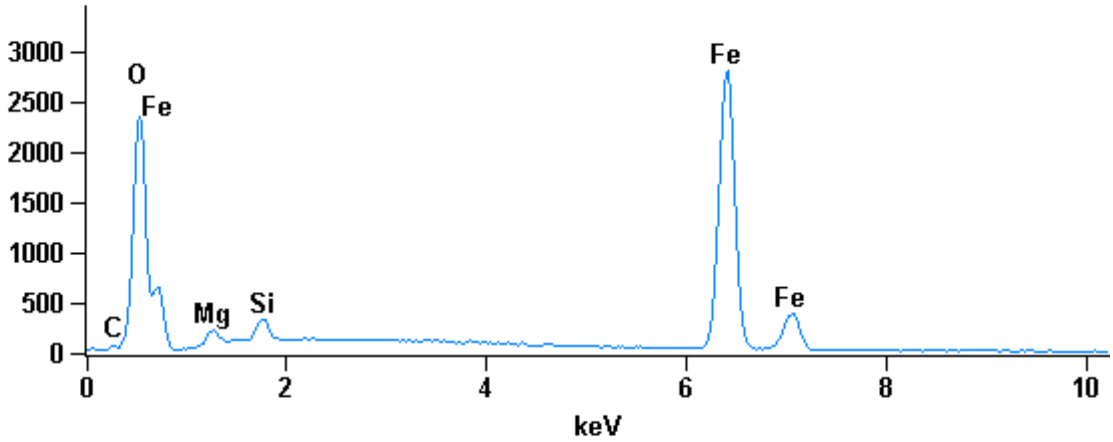

Full scale counts: 3254 525133(3)_pt7

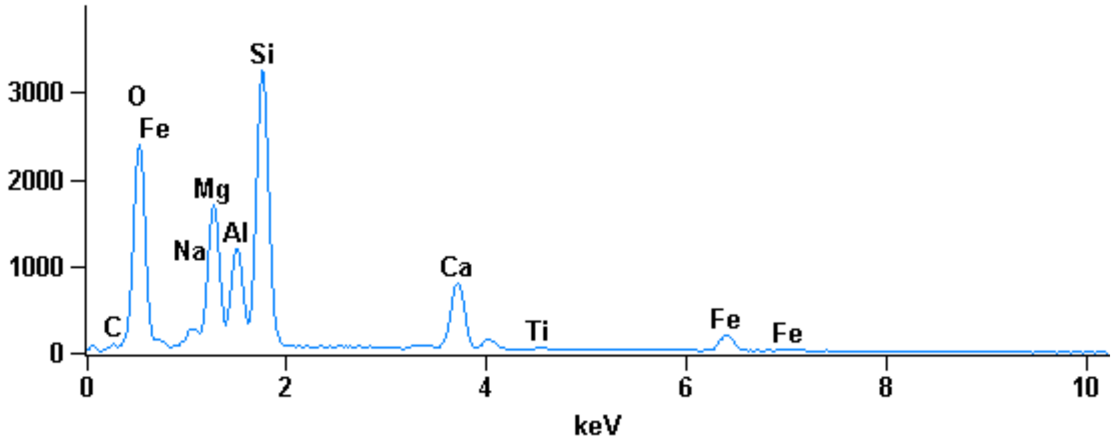

Full scale counts: 4287 525133(3)_pt8

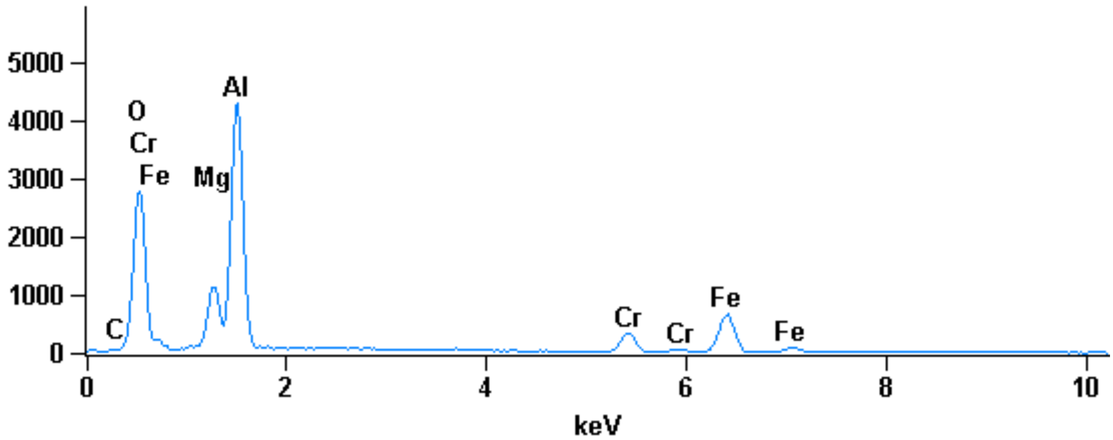

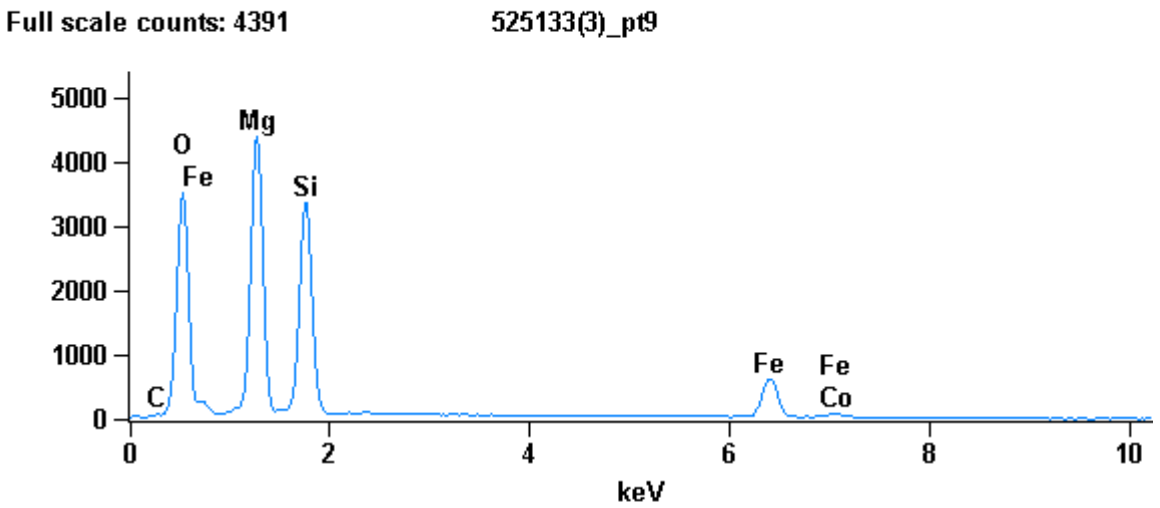

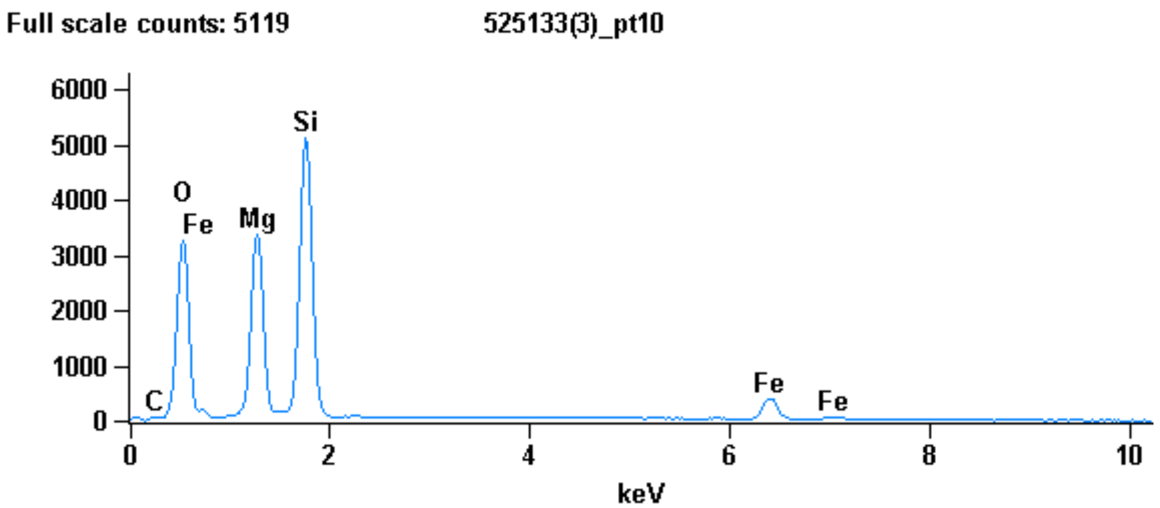

Weight %

	O-K	Na-K	Mg-K	Al-K	Si-K	Ca-K	Ti-K	V-K	Cr-K	Fe-K	Ni-K
525133(3)_pt1	30.33S		0.26		0.47					68.94	
525133(3)_pt2	30.33S			0.37	0.31					69.00	
525133(3)_pt3	45.95S		28.98		22.78					1.90	0.40
525133(3)_pt4	30.69S		0.36	0.72			0.81	0.30	6.24	60.88	
525133(3)_pt5	43.01S		25.45		17.89					13.65	
525133(3)_pt6	31.00S		1.73		1.34					65.93	
525133(3)_pt7	44.52S	1.87	11.91	7.34	20.96	7.51	0.39			5.49	
525133(3)_pt8	40.76S		8.32	28.76					5.51	16.66	
525133(3)_pt9	43.12S		25.77		18.01					13.10	
525133(3)_pt10	46.15S		19.43		26.18					8.24	

Atom %

	O-K	Na-K	Mg-K	Al-K	Si-K	Ca-K	Ti-K	V-K	Cr-K	Fe-K	Ni-K
525133(3)_pt1	60.04		0.34		0.53					39.10	
525133(3)_pt2	60.07			0.43	0.35					39.15	
525133(3)_pt3	58.42		24.25		16.50					0.69	0.14
525133(3)_pt4	60.09		0.46	0.84			0.53	0.19	3.76	34.14	
525133(3)_pt5	58.22		22.68		13.80					5.29	
525133(3)_pt6	59.86		2.20		1.47					36.47	
525133(3)_pt7	59.63	1.74	10.50	5.83	15.99	4.02	0.17			2.11	
525133(3)_pt8	58.43		7.85	24.45					2.43	6.84	
525133(3)_pt9	58.19		22.89		13.85					5.07	
525133(3)_pt10	60.56		16.78		19.56					3.10	

Compound %

		Na2O	MgO	Al2O3	SiO2	CaO	TiO2	V2O5	Cr2O3	Fe2O3	NiO
525133(3)_pt1	0.00		0.43		1.00					98.57	
525133(3)_pt2	0.00			0.69	0.66					98.65	
525133(3)_pt3	0.00		48.06		48.73					2.71	0.51
525133(3)_pt4	0.00		0.59	1.36			1.34	0.54	9.12	87.04	
525133(3)_pt5	0.00		42.21		38.28					19.51	
525133(3)_pt6	0.00		2.87		2.87					94.27	
525133(3)_pt7	0.00	2.52	19.75	13.87	44.84	10.51	0.65			7.85	
525133(3)_pt8	0.00		13.80	54.33					8.06	23.81	
525133(3)_pt9	0.00		42.73		38.53					18.74	
525133(3)_pt10	0.00		32.22		56.00					11.79	

Minerals, 525133(3)

pt1: Fe-oxide
pt2: Fe-oxide
pt3: Pyroxene - enstatite-ferrosilite
pt4: Spinel-series mineral
pt5: Olivine - chrysolite
pt6: Fe-oxide
pt7: Amphibolite - hornblende
pt8: Spinel - picotite
pt9: Olivine - chrysolite
pt10: Orthopyroxene - enstatite-ferrosilite

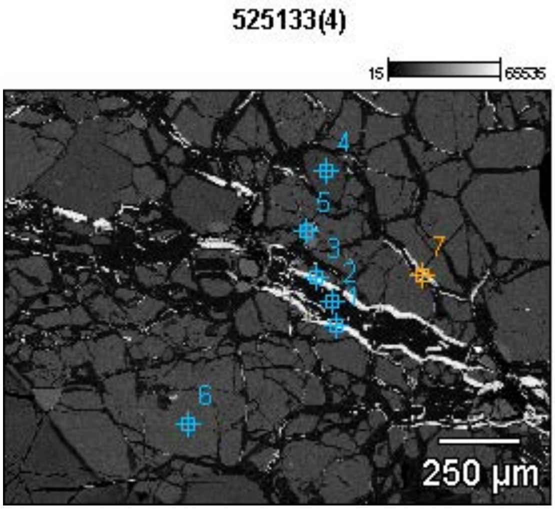

Image name: 525133(4)
Magnification: 73

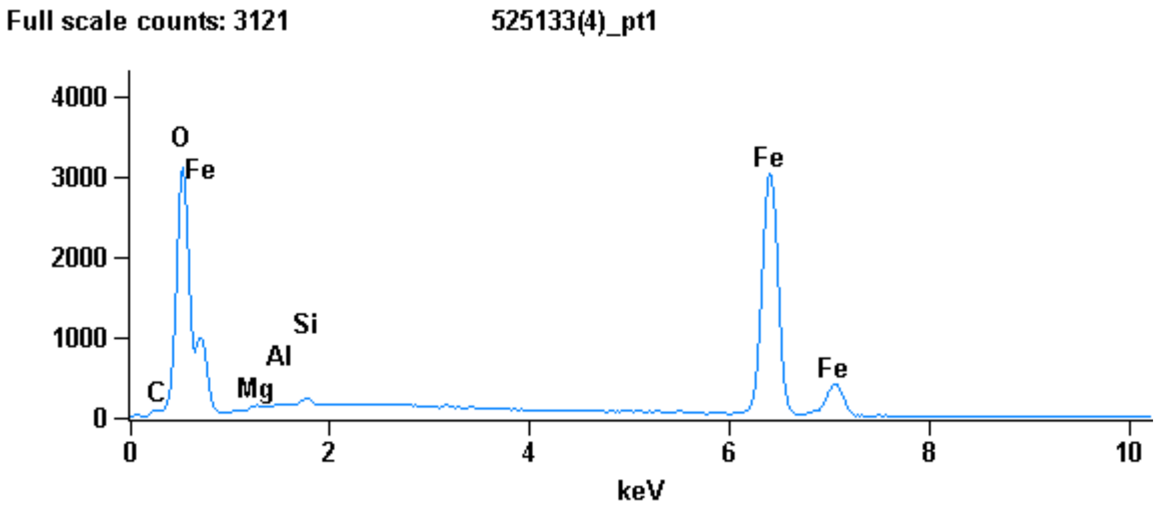

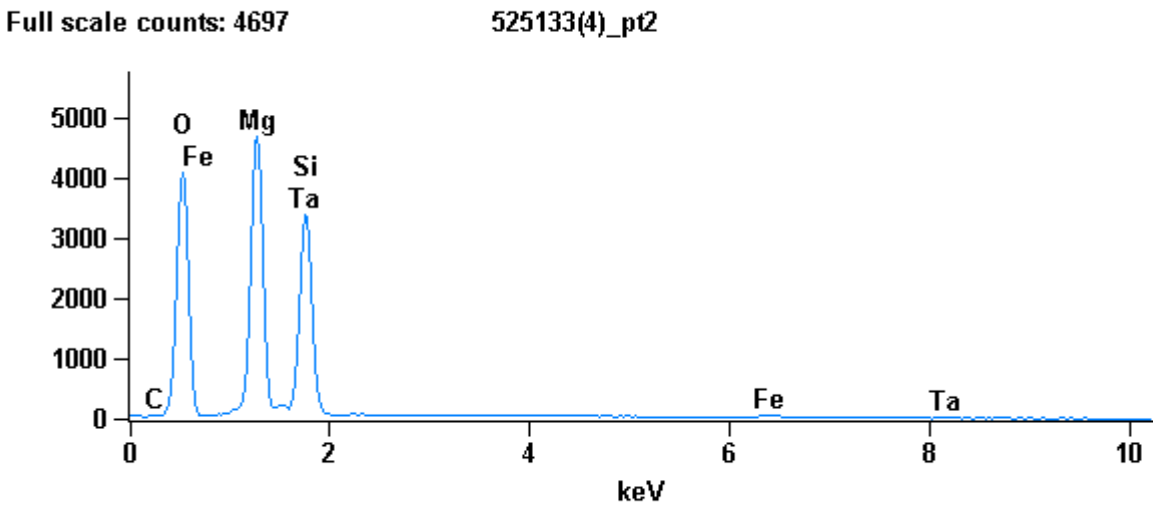

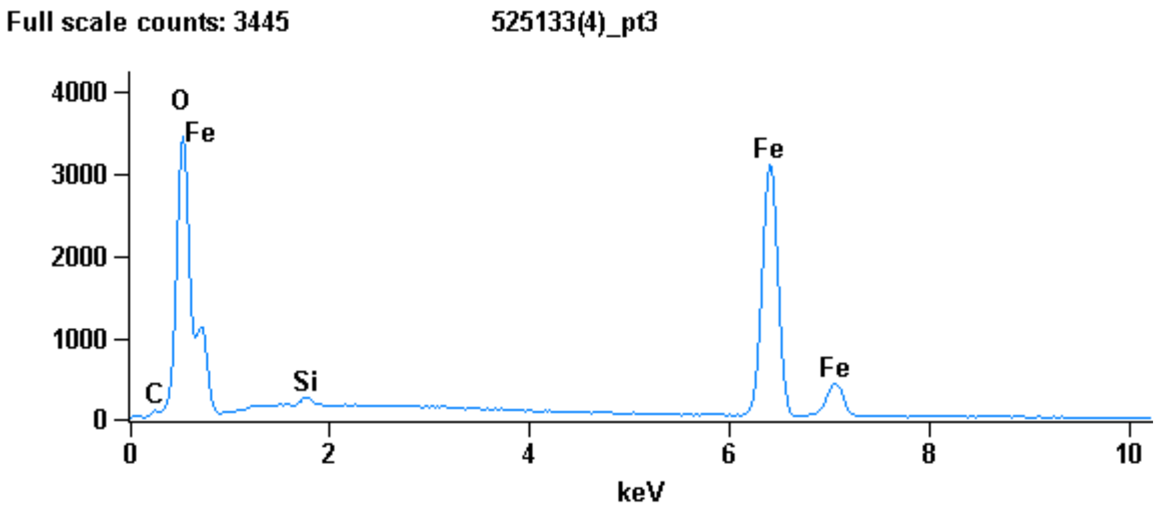

Full scale counts: 3445
525133(4)_pt3
4000
3000
2000
1000
0
O
Fe
Fe
C
Si
Fe
0
2
4
6
8
10
keV

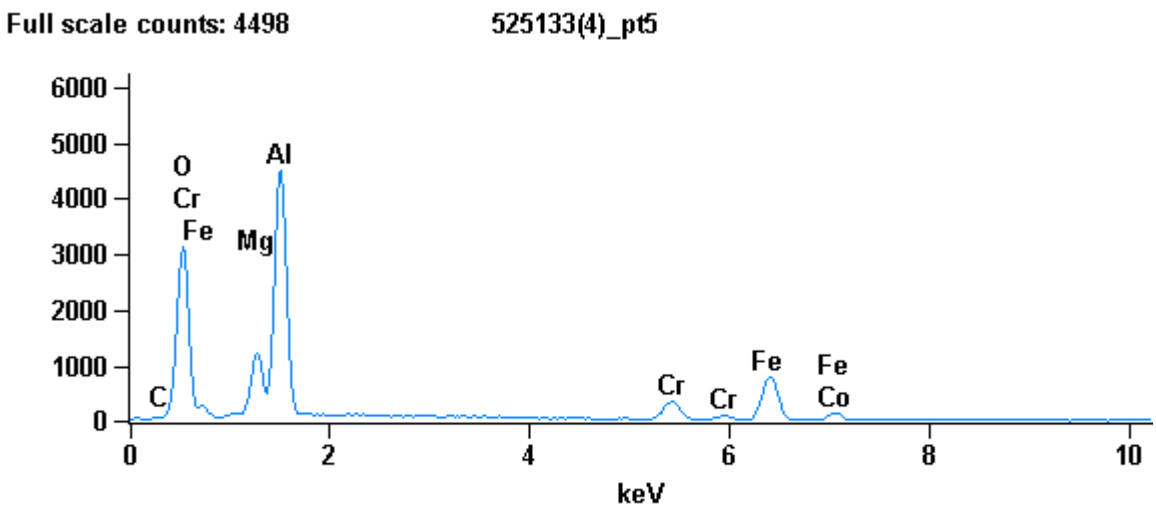

Full scale counts: 4498
525133(4)_pt5
6000
5000
4000
3000
2000
1000
0
O
Cr
Fe
Al
Mg
C
Cr
Cr
Fe
Fe
Co
0
2
4
6
8
10
keV

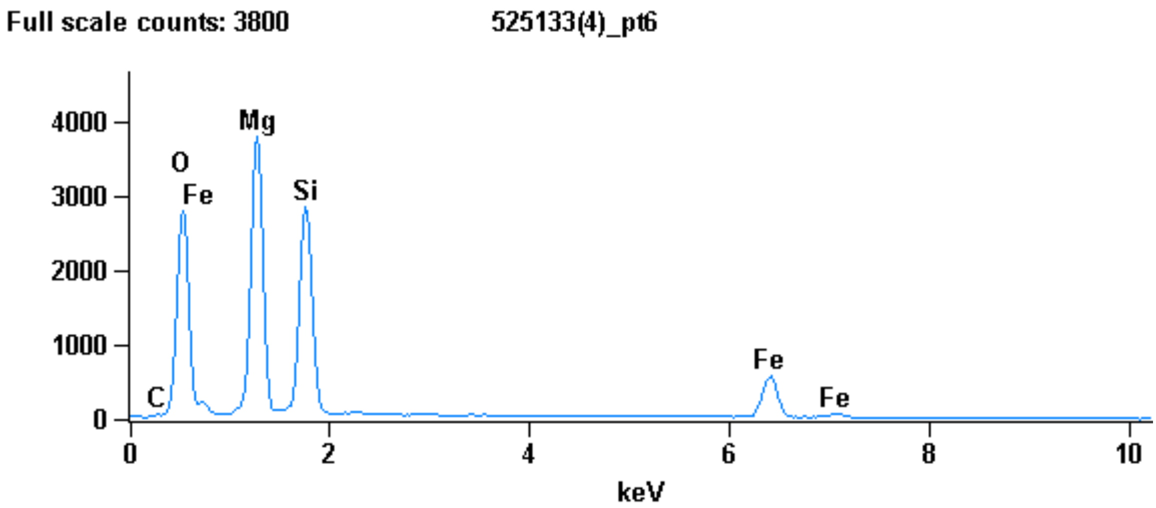
Full scale counts: 3800
525133(4)_pt6
4000
3000
2000
1000
0
O
Fe
Mg
Si
C
Fe
Fe
0
2
4
6
8
10
keV

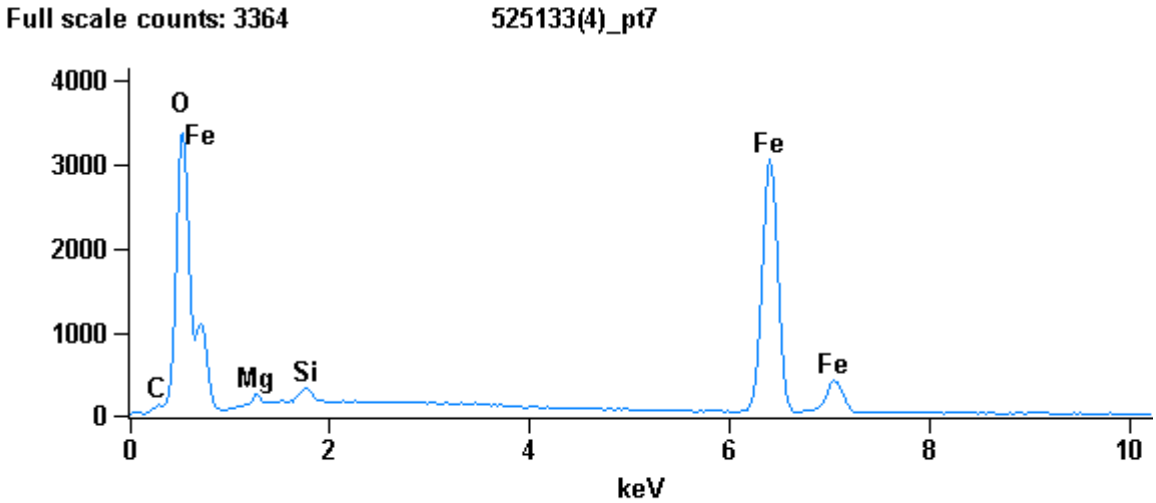
Full scale counts: 3364
525133(4)_pt7
4000
3000
2000
1000
0
O
Fe
Fe
C
Mg
Si
Fe
0
2
4
6
8
10
keV

Weight %

	O-K	Mg-K	Al-K	Si-K	Ca-K	Ti-K	Cr-K	Fe-K	Co-K	Ta-L
525133(4)_pt1	30.39S	0.34	0.20	0.42				68.65		
525133(4)_pt2	45.73S	29.49		22.43				1.19		1.16
525133(4)_pt3	30.25S			0.39				69.35		
525133(4)_pt4	45.02S	10.90	6.59	22.53	8.77	0.58	0.37	5.26		
525133(4)_pt5	40.33S	7.59	27.85				5.14	18.99	0.10	
525133(4)_pt6	42.98S	25.44		17.84				13.74		
525133(4)_pt7	30.70S	0.89		1.00				67.41		

Atom %

	O-K	Mg-K	Al-K	Si-K	Ca-K	Ti-K	Cr-K	Fe-K	Co-K	Ta-L
525133(4)_pt1	60.01	0.44	0.24	0.48				38.84		
525133(4)_pt2	58.36	24.77		16.31				0.43		0.13
525133(4)_pt3	60.09			0.45				39.47		
525133(4)_pt4	60.63	9.67	5.26	17.29	4.71	0.26	0.15	2.03		
525133(4)_pt5	58.54	7.26	23.97				2.30	7.90	0.04	
525133(4)_pt6	58.22	22.69		13.77				5.33		
525133(4)_pt7	59.99	1.15		1.12				37.74		

Compound %

		MgO	Al2O3	SiO2	CaO	TiO2	Cr2O3	Fe2O3	CoO	Ta2O5
525133(4)_pt1	0.00	0.56	0.38	0.91				98.16		
525133(4)_pt2	0.00	48.90		47.99				1.70		1.41
525133(4)_pt3	0.00			0.84				99.16		
525133(4)_pt4	0.00	18.08	12.45	48.19	12.27	0.96	0.53	7.52		
525133(4)_pt5	0.00	12.59	52.62				7.51	27.15	0.13	
525133(4)_pt6	0.00	42.19		38.16				19.65		
525133(4)_pt7	0.00	1.48		2.15				96.37		

Minerals, 525133(4)

pt1: Fe-oxide
pt2: Orthopyroxene - enstatite
pt3: Fe-oxide
pt4: Amphibole - hornblende
pt5: Spinel - pigeonite
pt6: Olivine - chrysolite
pt7: Fe-oxide

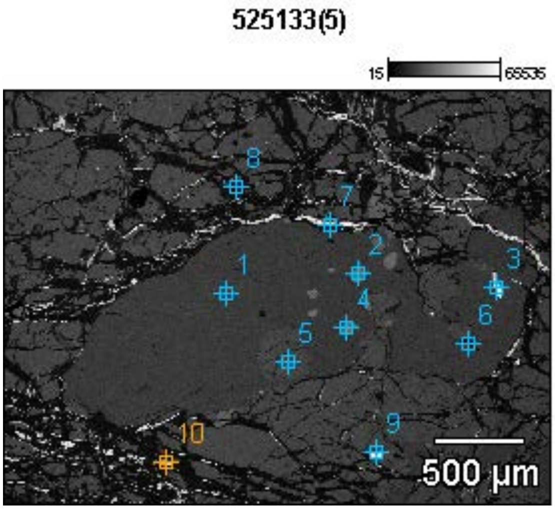

Image name: 525133(5)
Magnification: 40

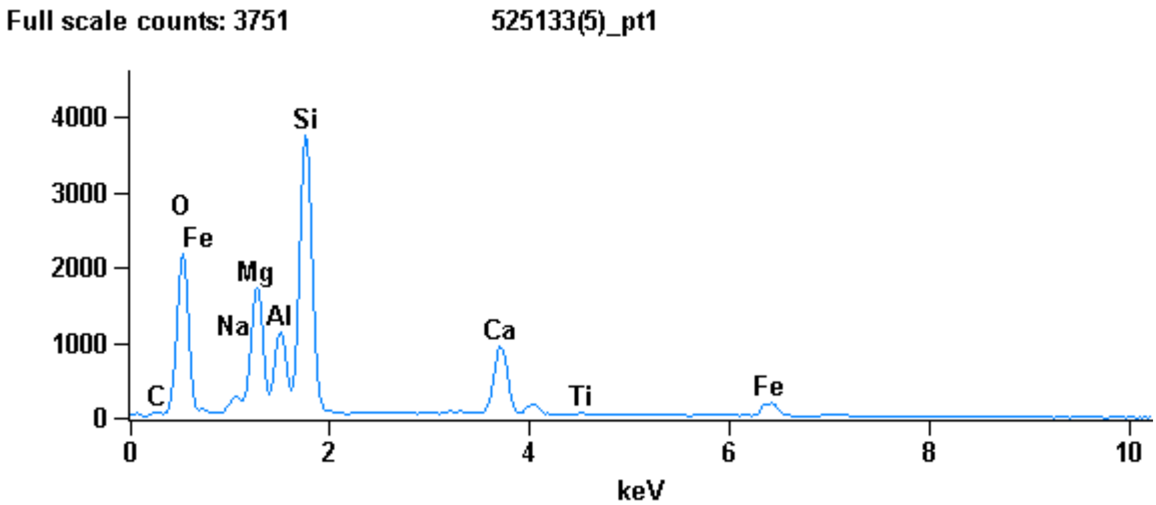

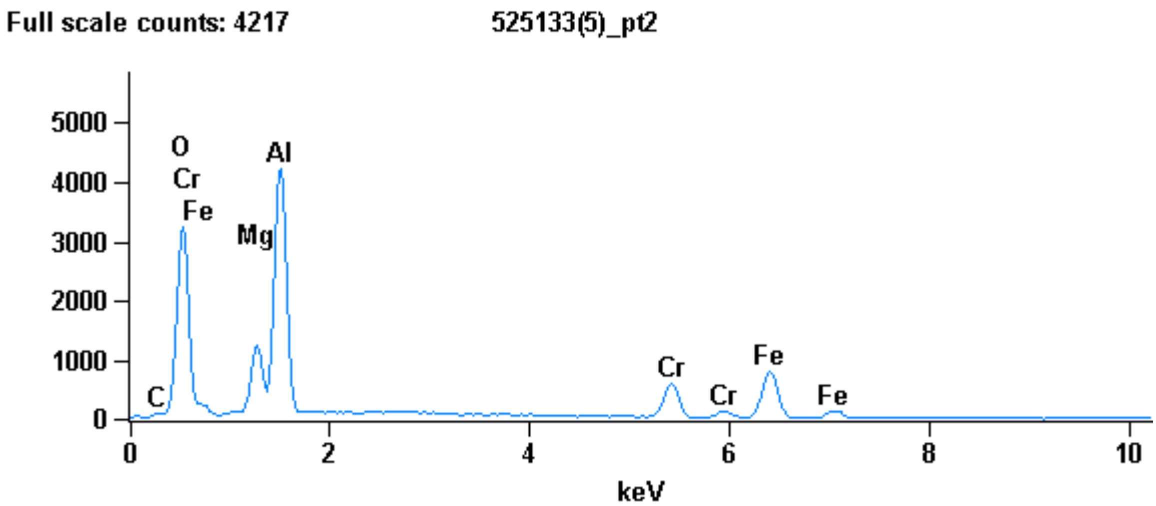

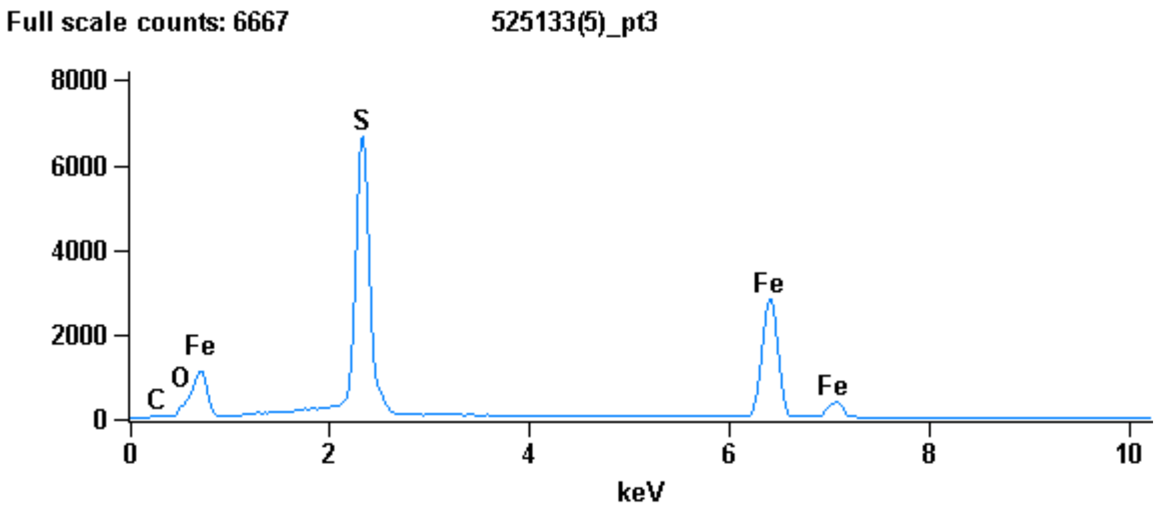
Full scale counts: 6667
525133(5)_pt3
8000
6000
4000
2000
0
S
Fe
Fe
C
O
Fe
0
2
4
6
8
10
keV

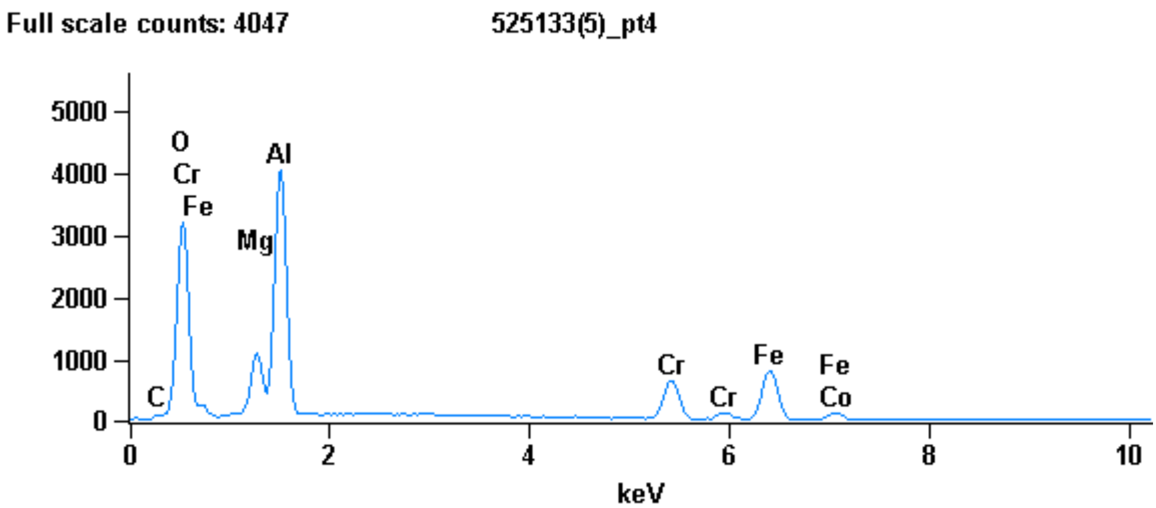
Full scale counts: 4047
525133(5)_pt4
5000
4000
3000
2000
1000
0
O
Cr
Fe
Al
Mg
C
Cr
Cr
Fe
Fe
Co
0
2
4
6
8
10
keV

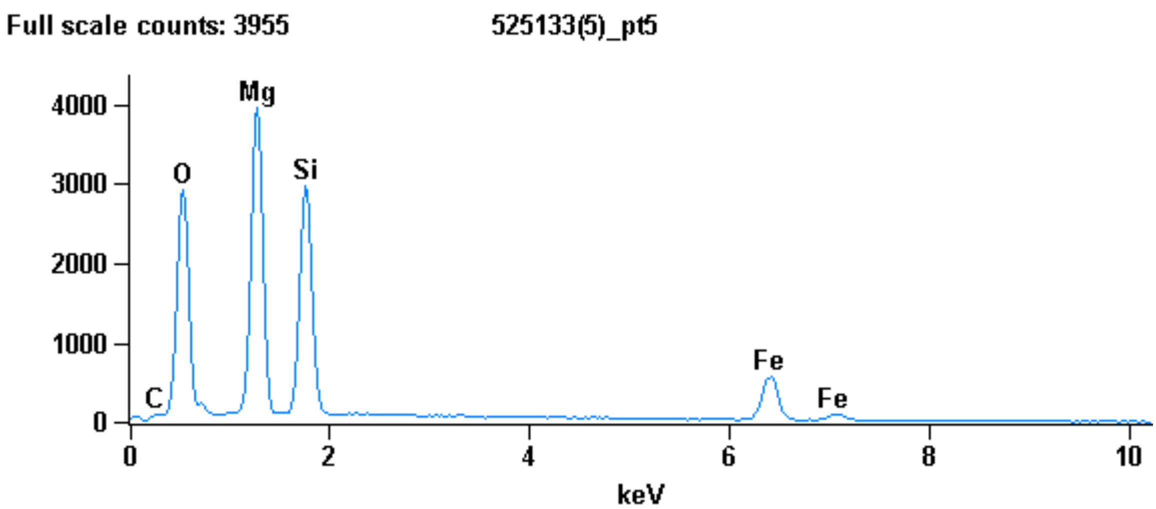
Full scale counts: 3955
525133(5)_pt5
4000
3000
2000
1000
0
Mg
O
Si
C
Fe
Fe
0
2
4
6
8
10
keV

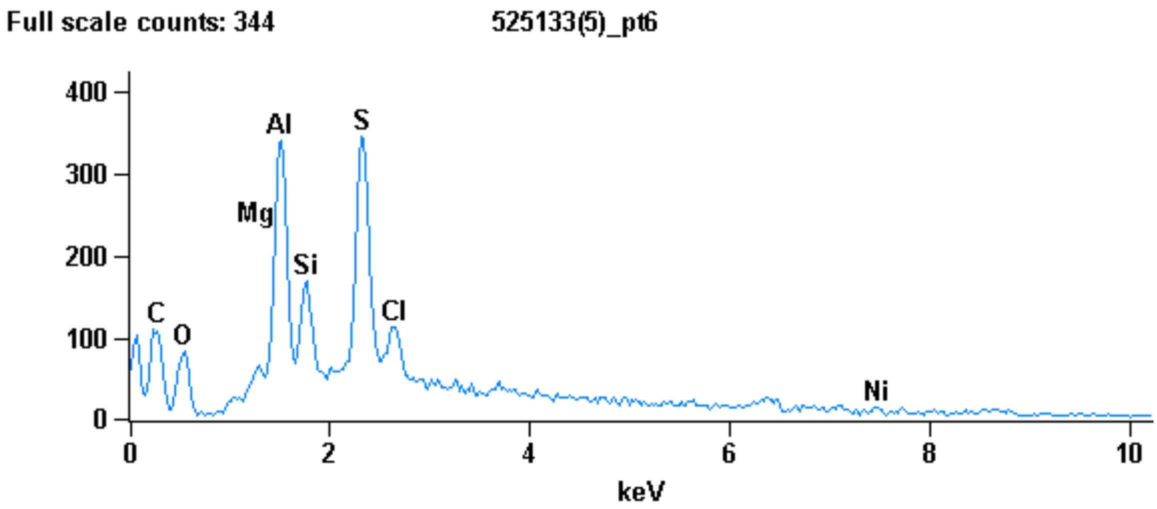
Full scale counts: 344
525133(5)_pt6
400
300
200
100
0
Al
S
Mg
Si
C
O
Cl
Ni
0
2
4
6
8
10
keV

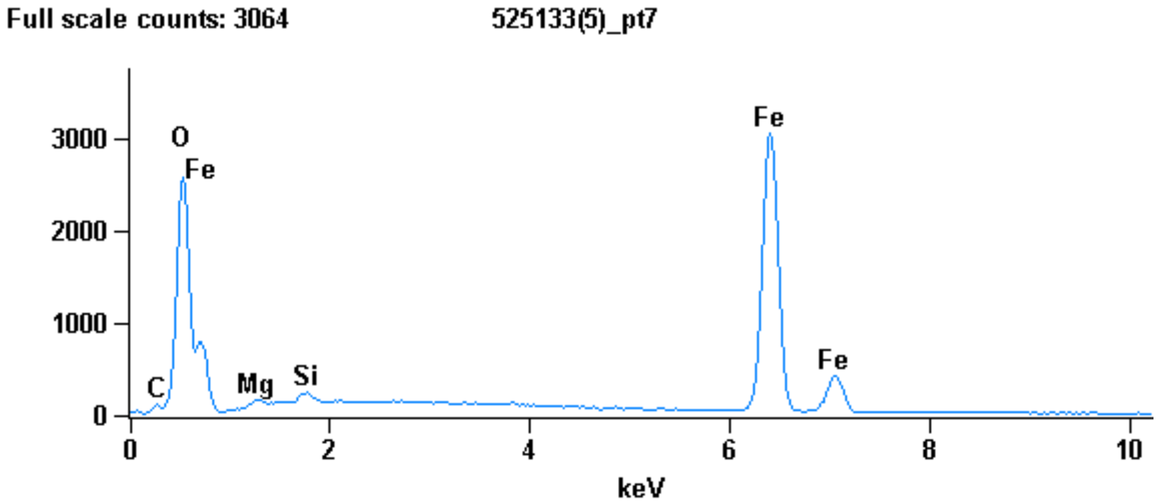
Full scale counts: 3064
525133(5)_pt7
3000
2000
1000
0
O
Fe
Fe
Fe
C
Mg
Si
0
2
4
6
8
10
keV

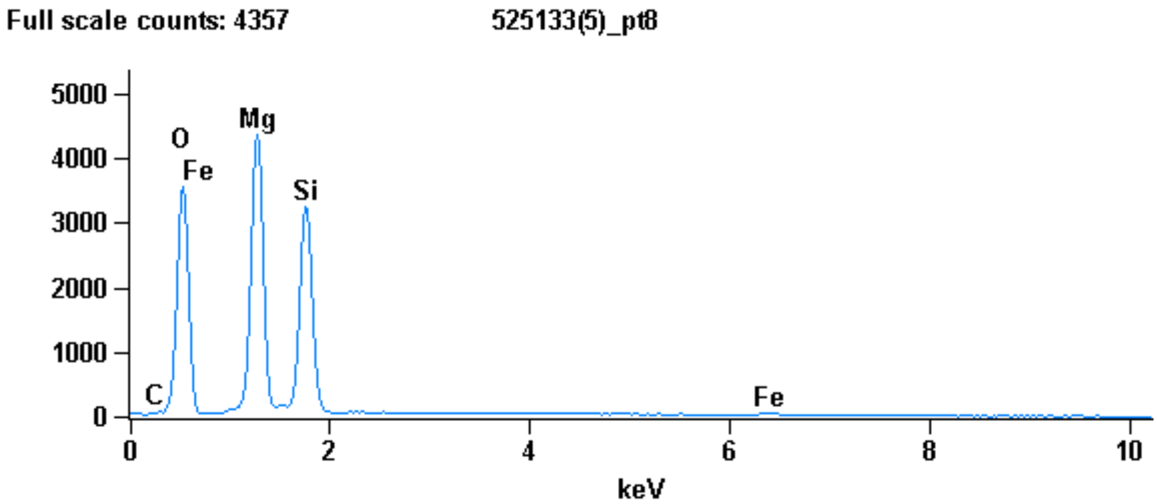
Full scale counts: 4357
525133(5)_pt8
5000
4000
3000
2000
1000
0
Mg
O
Fe
Si
C
Fe
0
2
4
6
8
10
keV

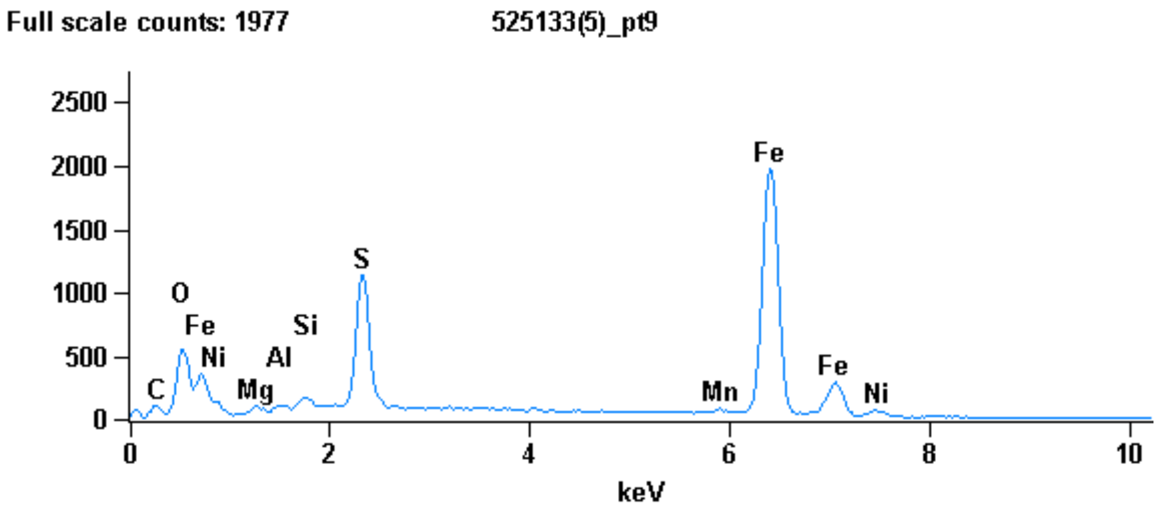

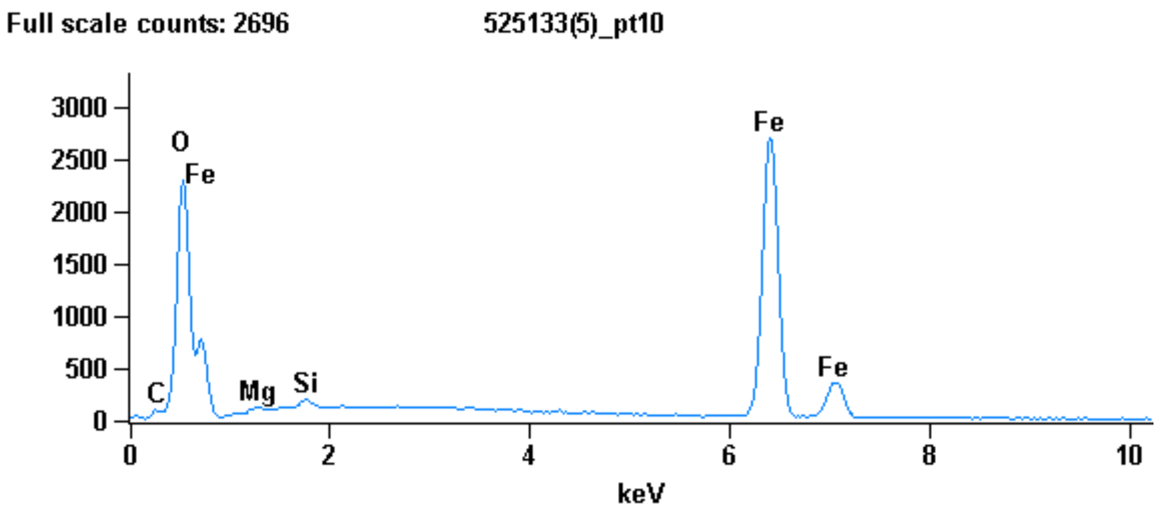

Weight %

	O-K	Na-K	Mg-K	Al-K	Si-K	S-K	Cl-K	Ca-K	Ti-K	Cr-K	Mn-K	Fe-K	Co-K	Ni-K
525133(5)_pt1	44.65S	2.01	11.62	6.16	22.14			8.24	0.35			4.85		
525133(5)_pt2	39.87S		7.78	26.06						8.47		17.83		
525133(5)_pt3	44.76S					19.69						35.55		
525133(5)_pt4	39.48S		7.04	25.16						9.50		18.76	0.06	
525133(5)_pt5	43.02S		25.57		17.88							13.53		
525133(5)_pt6	50.70S		1.46	15.44	6.53	18.69	5.04							2.14
525133(5)_pt7	30.44S		0.82		0.51							68.23		
525133(5)_pt8	46.23S		29.28		23.16							1.34		
525133(5)_pt9	36.02S		0.59	0.32	0.69	7.68					0.85	51.78		2.08
525133(5)_pt10	30.35S		0.56		0.42							68.67		

Atom %

	O-K	Na-K	Mg-K	Al-K	Si-K	S-K	Cl-K	Ca-K	Ti-K	Cr-K	Mn-K	Fe-K	Co-K	Ni-K
525133(5)_pt1	59.73	1.87	10.23	4.89	16.87			4.40	0.15			1.86		
525133(5)_pt2	58.50		7.51	22.67						3.82		7.50		
525133(5)_pt3	69.10					15.17						15.73		
525133(5)_pt4	58.62		6.88	22.15						4.34		7.98	0.03	
525133(5)_pt5	58.20		22.78		13.78							5.24		
525133(5)_pt6	66.09		1.25	11.94	4.84	12.16	2.96							0.76
525133(5)_pt7	59.90		1.06		0.57							38.47		
525133(5)_pt8	58.46		24.37		16.68							0.48		
525133(5)_pt9	63.79		0.69	0.33	0.69	6.79					0.44	26.27		1.00
525133(5)_pt10	59.95		0.72		0.47							38.86		

Compound %

		Na2O	MgO	Al2O3	SiO2	SO3	Cl	CaO	TiO2	Cr2O3	MnO	Fe2O3	CoO	NiO
525133(5)_pt1	0.00	2.70	19.26	11.64	47.36			11.53	0.58			6.93		
525133(5)_pt2	0.00		12.90	49.23						12.38		25.49		
525133(5)_pt3	0.00					49.17						50.83		
525133(5)_pt4	0.00		11.67	47.54						13.89		26.82	0.08	
525133(5)_pt5	0.00		42.41		38.25							19.35		
525133(5)_pt6	0.00		2.42	29.18	13.96	46.68	5.04							2.72
525133(5)_pt7	0.00		1.35		1.09							97.55		
525133(5)_pt8	0.00		48.55		49.54							1.91		
525133(5)_pt9	0.00		0.97	0.60	1.47	19.19					1.09	74.03		2.65
525133(5)_pt10	0.00		0.92		0.90							98.18		

Minerals, 525133(5)
pt1: Amphibole - hornblende
pt2: Spinel - picotite
pt3: Pyrite
pt4: Spinel - picotite
pt5: Olivine - chrysolite
pt6: Mixed signal/edge effect
pt7: Fe-oxide
pt8: Orthopyroxene - enstatite
pt9: Mixed signal/edge effect
pt10: Fe-oxide

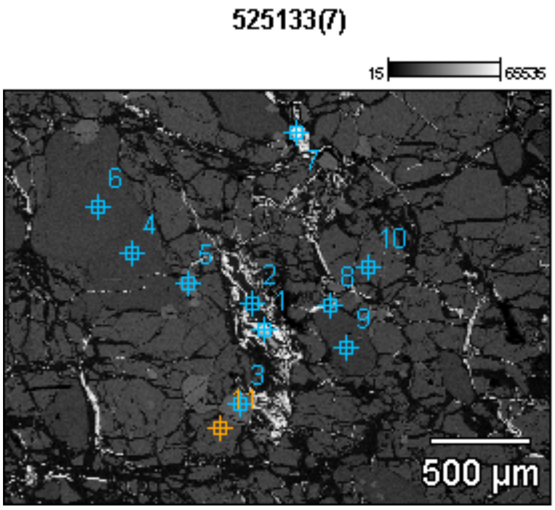

Image name: 525133(7)
Magnification: 44

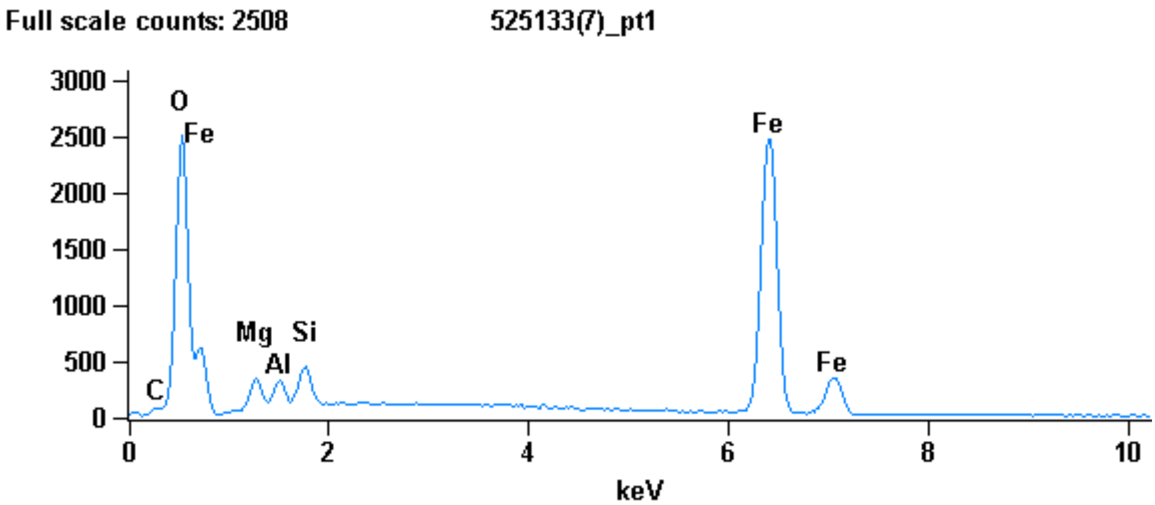

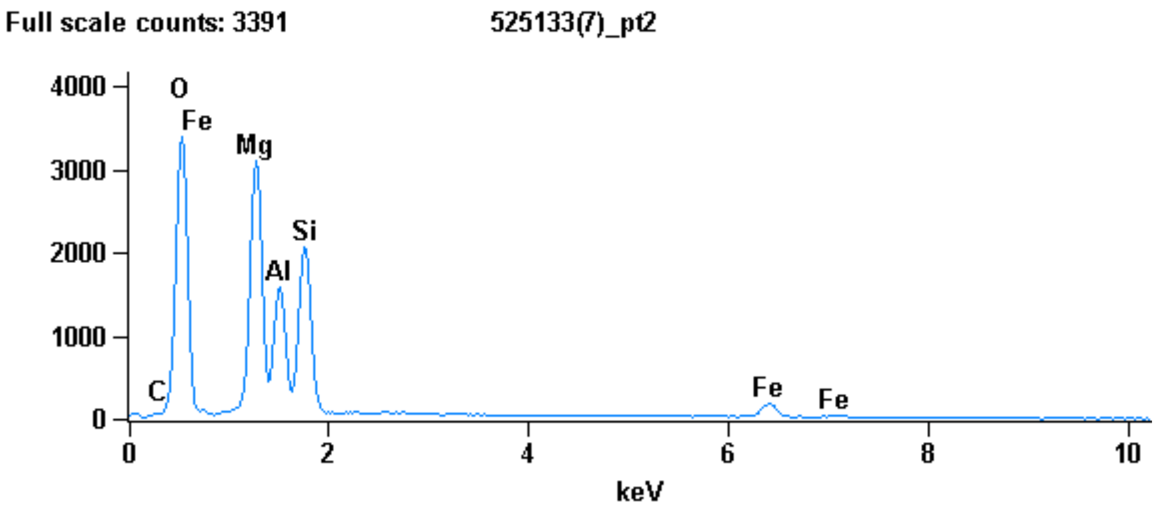

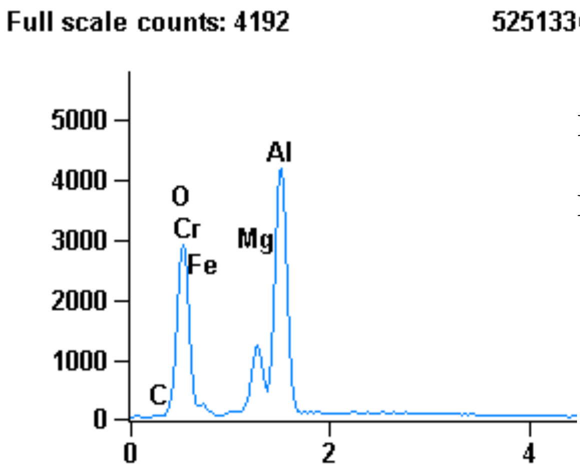

Image Name: 525138(12)

Magnification: 79

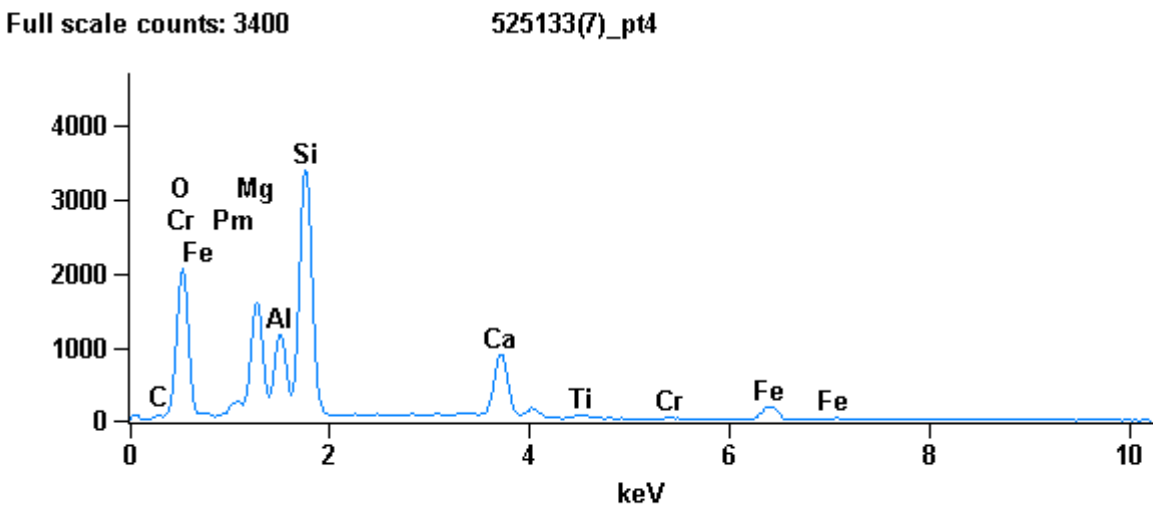

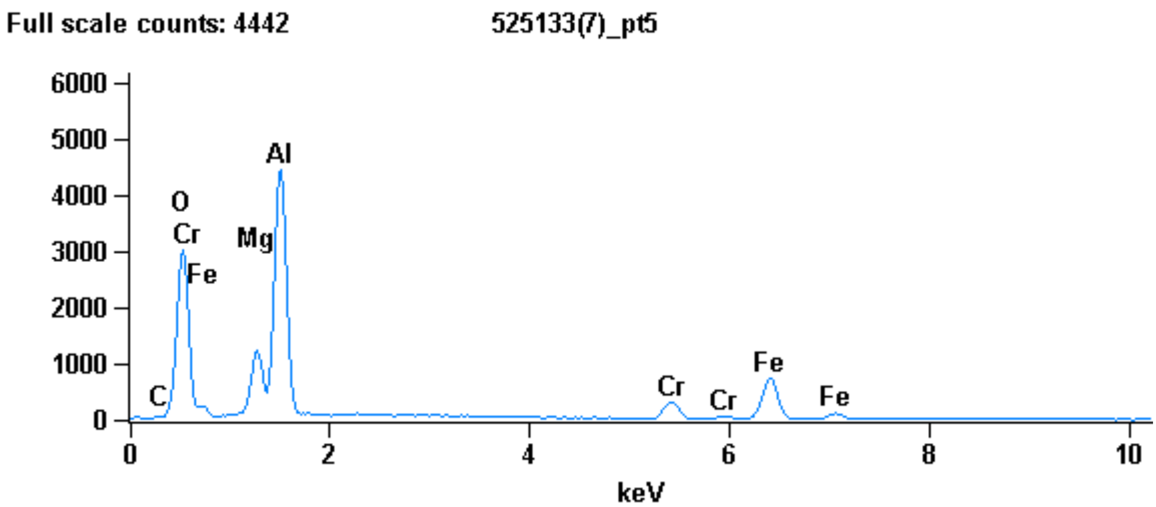

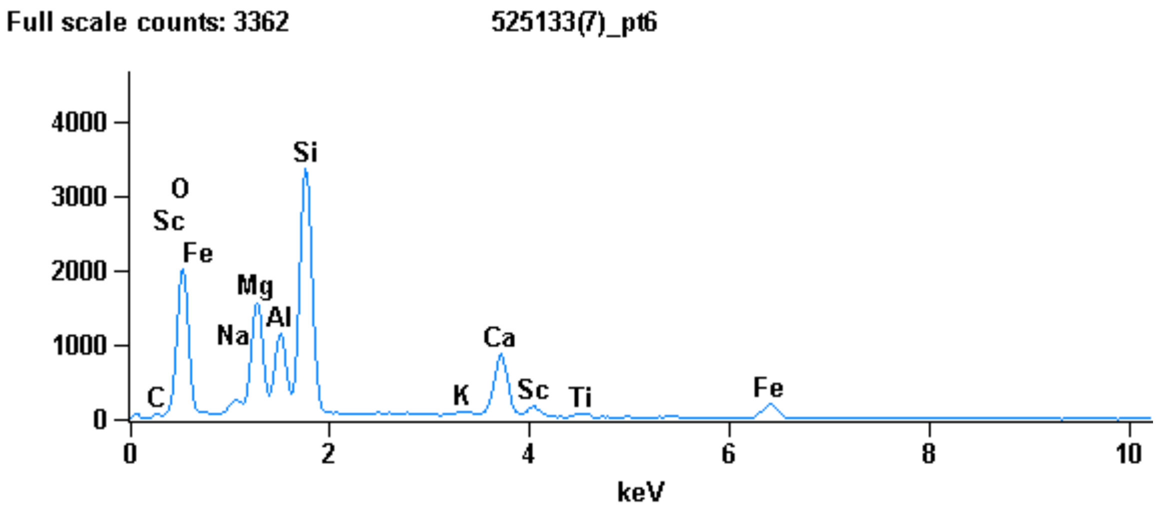
Full scale counts: 3362
525133(7)_pt6
4000
3000
2000
1000
0
O
Sc
Fe
Mg
Na
Al
Si
C
Ca
K
Sc
Ti
Fe
0
2
4
6
8
10
keV

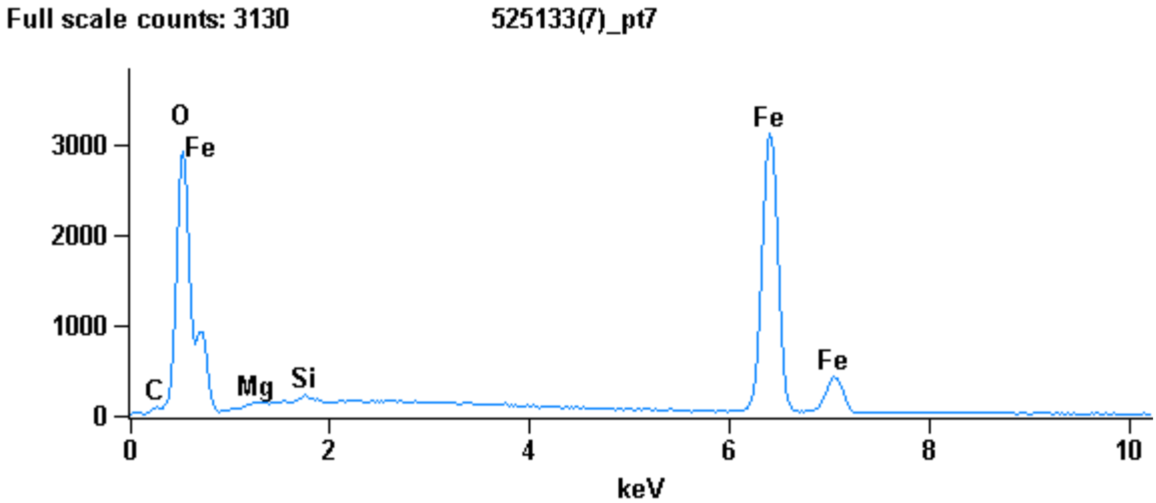
Full scale counts: 3130
525133(7)_pt7
3000
2000
1000
0
O
Fe
C
Mg
Si
Fe
Fe
0
2
4
6
8
10
keV

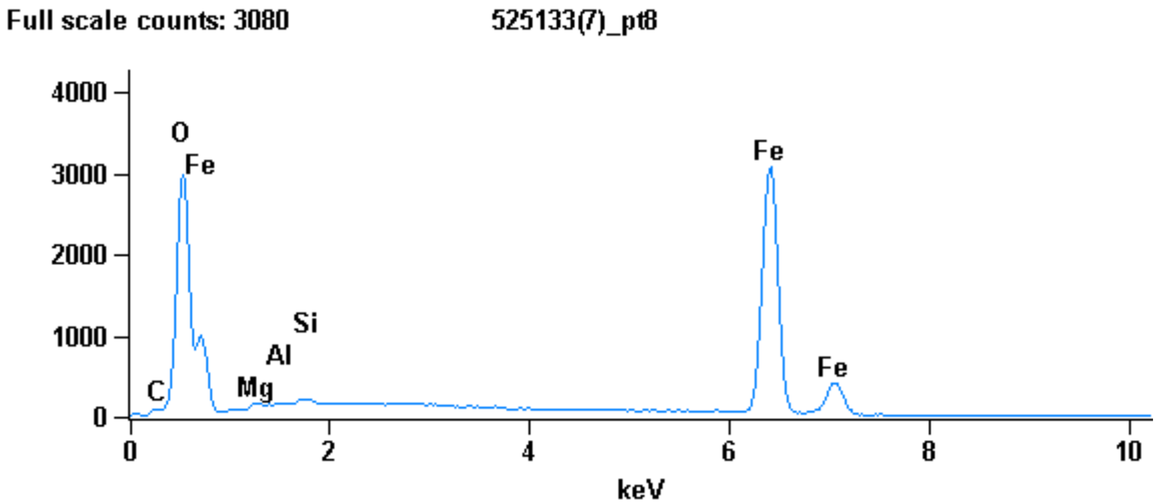
Full scale counts: 3080
525133(7)_pt8
4000
3000
2000
1000
0
O
Fe
Si
Al
Mg
C
Fe
Fe
0
2
4
6
8
10
keV

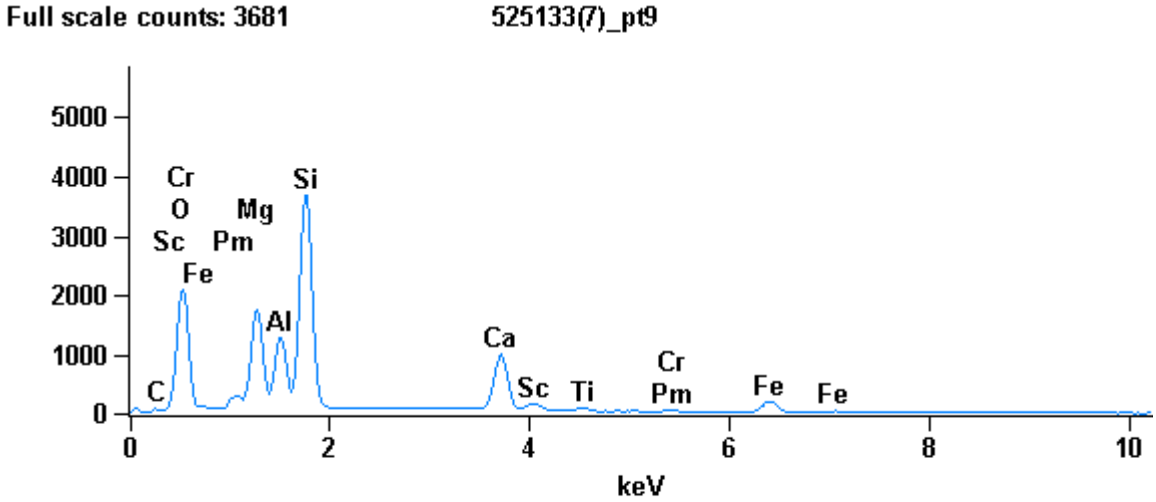
Full scale counts: 3681
525133(7)_pt9
5000
4000
3000
2000
1000
0
Cr
O
Sc
Fe
Mg
Pm
Si
Al
C
Ca
Sc
Ti
Cr
Pm
Fe
Fe
0
2
4
6
8
10
keV

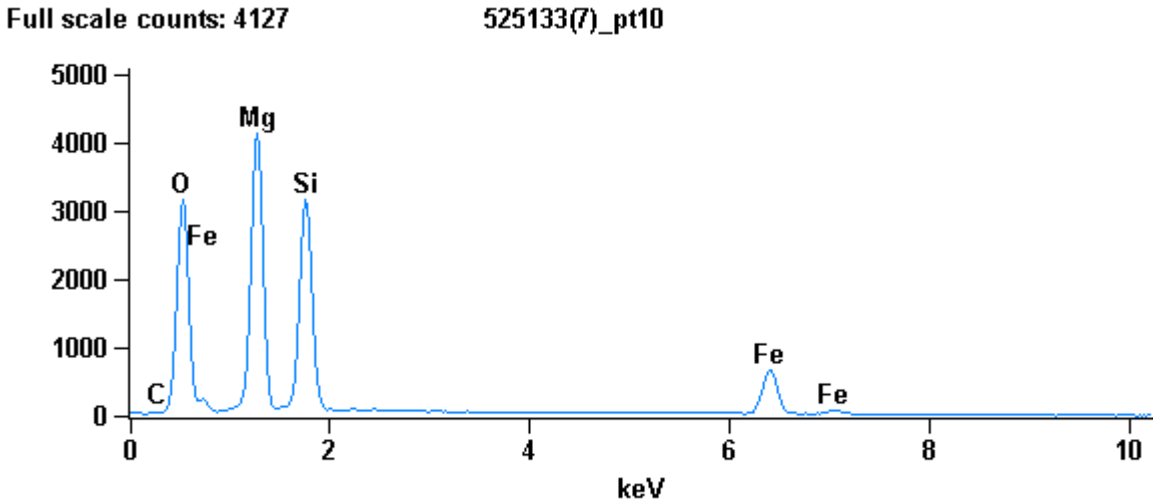
Full scale counts: 4127
525133(7)_pt10
5000
4000
3000
2000
1000
0
Mg
O
Si
Fe
C
Fe
Fe
0
2
4
6
8
10
keV

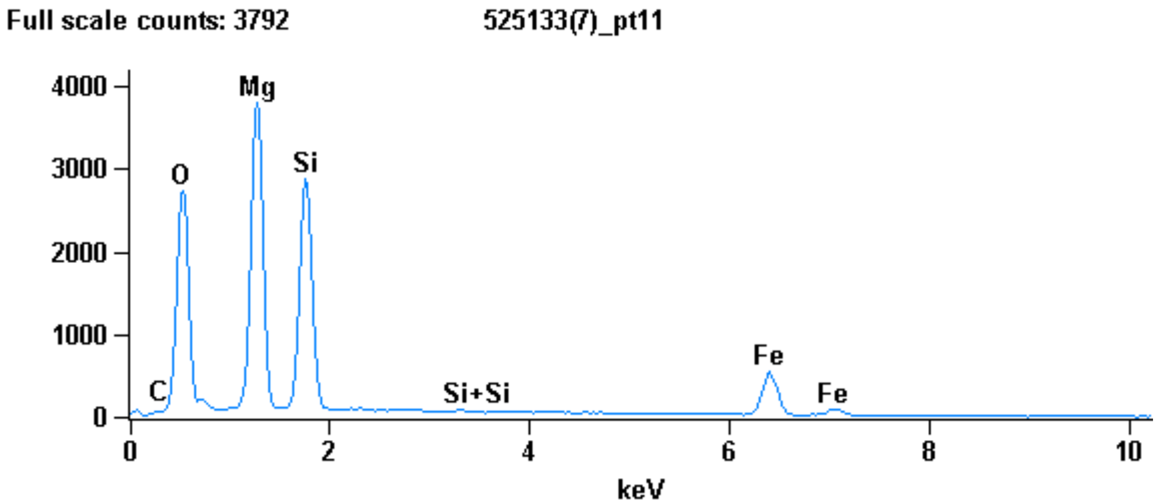
Full scale counts: 3792
525133(7)_pt11
4000
3000
2000
1000
0
Mg
O
Si
C
Si+Si
Fe
Fe
0
2
4
6
8
10
keV

Weight %

	O-K	Na-K	Mg-K	Al-K	Si-K	K-K	Ca-K	Sc-K	Ti-K	Cr-K	Fe-K	Pm-L
525133(7)_pt1	32.41S		3.10	1.94	2.48						60.07	
525133(7)_pt2	45.23S		21.84	11.70	15.96						5.27	
525133(7)_pt3	40.36S		7.99	27.64						6.21	17.81	
525133(7)_pt4	45.08S		10.77	6.89	22.52		8.80		0.51	0.51	4.92	0.00
525133(7)_pt5	40.71S		8.23	28.71						4.84	17.51	
525133(7)_pt6	44.52S	1.82	11.22	6.66	21.63	0.18	8.10	0.13	0.57		5.17	
525133(7)_pt7	30.29S		0.54		0.30						68.86	
525133(7)_pt8	30.43S		0.64	0.20	0.42						68.31	
525133(7)_pt9	44.77S		10.60	6.97	22.21		8.89	0.04	0.39	0.26	5.18	0.69
525133(7)_pt10	42.85S		25.31		17.63						14.20	
525133(7)_pt11	43.15S		25.81		18.07						12.98	

Atom %

	O-K	Na-K	Mg-K	Al-K	Si-K	K-K	Ca-K	Sc-K	Ti-K	Cr-K	Fe-K	Pm-L
525133(7)_pt1	59.77		3.77	2.12	2.61						31.74	
525133(7)_pt2	58.63		18.64	9.00	11.78						1.96	
525133(7)_pt3	58.48		7.62	23.74						2.77	7.39	
525133(7)_pt4	60.65		9.54	5.49	17.26		4.72		0.23	0.21	1.89	0.00
525133(7)_pt5	58.44		7.78	24.44						2.14	7.20	
525133(7)_pt6	59.79	1.70	9.91	5.30	16.55	0.10	4.34	0.06	0.25		1.99	
525133(7)_pt7	59.93		0.70		0.34						39.03	
525133(7)_pt8	59.93		0.83	0.24	0.47						38.54	
525133(7)_pt9	60.61		9.44	5.60	17.13		4.80	0.02	0.18	0.11	2.01	0.10
525133(7)_pt10	58.20		22.63		13.64						5.53	
525133(7)_pt11	58.19		22.91		13.88						5.01	

Compound %

		Na2O	MgO	Al2O3	SiO2	K2O	CaO	Sc2O3	TiO2	Cr2O3	Fe2O3	Pm2O3
525133(7)_pt1	0.00		5.14	3.67	5.31						85.88	
525133(7)_pt2	0.00		36.22	22.11	34.13						7.54	
525133(7)_pt3	0.00		13.25	52.22						9.07	25.46	
525133(7)_pt4	0.00		17.86	13.01	48.18		12.31		0.86	0.75	7.03	0.00
525133(7)_pt5	0.00		13.65	54.24						7.07	25.04	
525133(7)_pt6	0.00	2.45	18.60	12.58	46.27	0.22	11.33	0.21	0.94		7.39	
525133(7)_pt7	0.00		0.89		0.65						98.46	
525133(7)_pt8	0.00		1.06	0.39	0.89						97.66	
525133(7)_pt9	0.00		17.57	13.17	47.52		12.43	0.06	0.65	0.37	7.40	0.81
525133(7)_pt10	0.00		41.97		37.72						20.31	
525133(7)_pt11	0.00		42.79		38.65						18.55	

Minerals, 525133(7)

pt1: Mixed signal/edge effect
pt2: Chlorite - clinochlore-chamosite series
pt3: Spinel - picotite
pt4: Amphibole - hornblende
pt5: Spinel - picotite
pt6: Amphibole - hornblende
pt7: Fe-oxide
pt8: Fe-oxide
pt9: Amphibole - hornblende
pt10: Olivine - chrysolite
pt11: Olivine - chrysolite

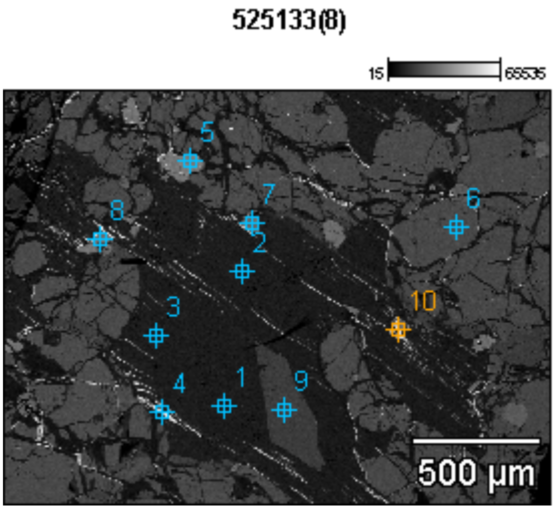

Image name: 525133(8)
Magnification: 57

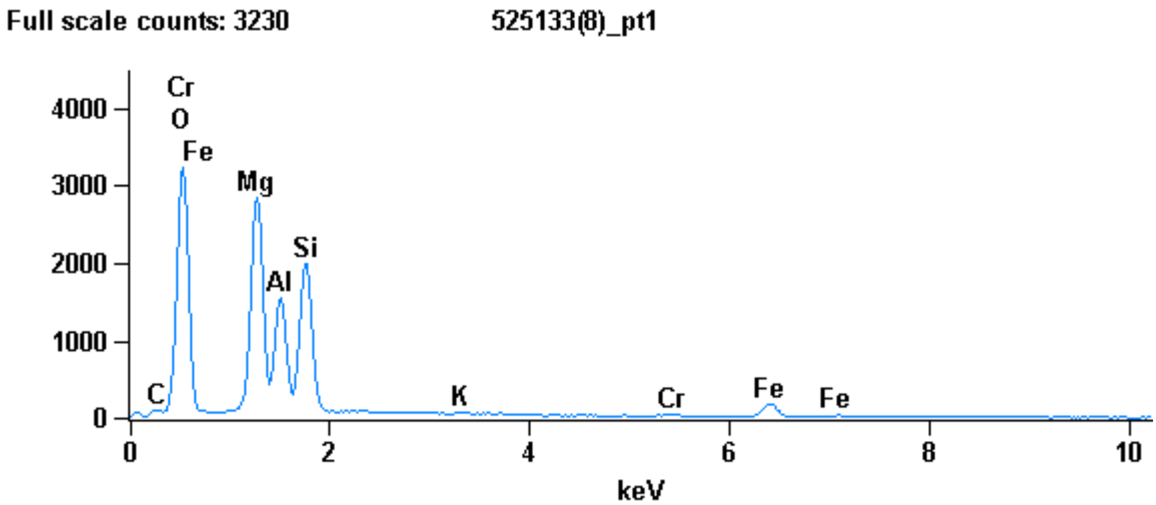

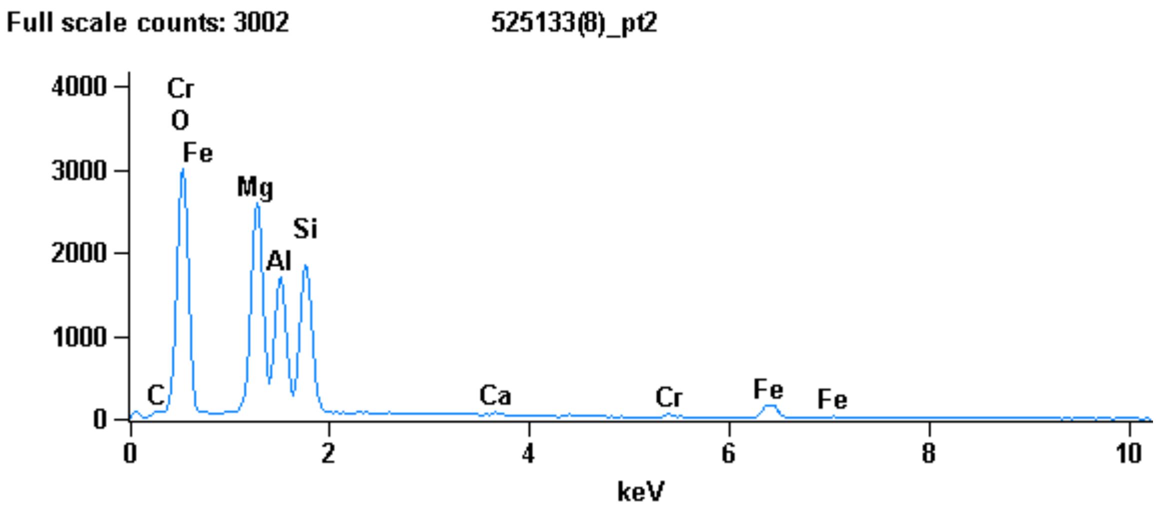

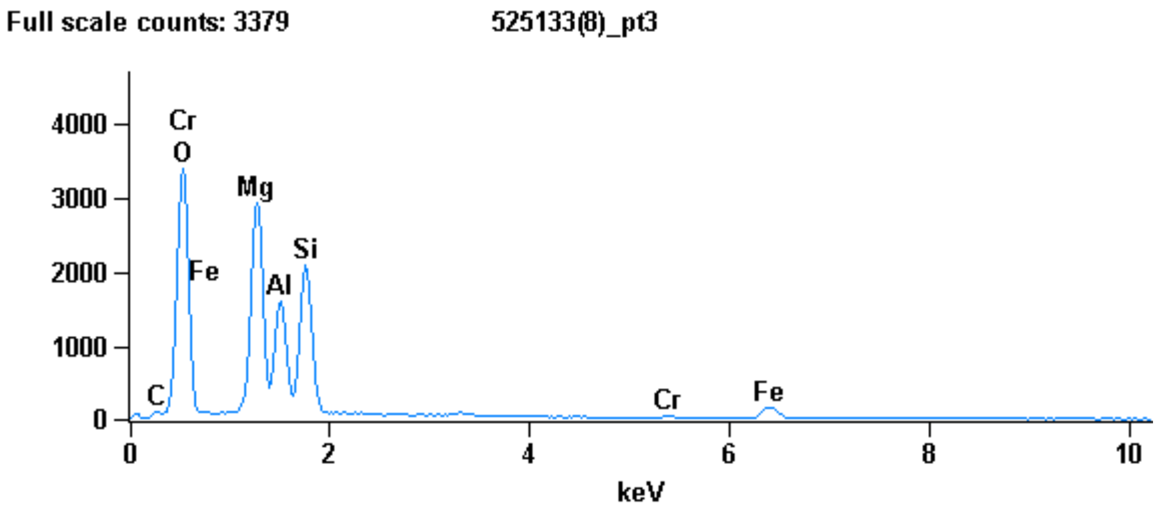
Full scale counts: 3379
525133(8)_pt3
4000
3000
2000
1000
0
Cr
O
Mg
Si
Fe
Al
C
Cr
Fe
0
2
4
6
8
10
keV

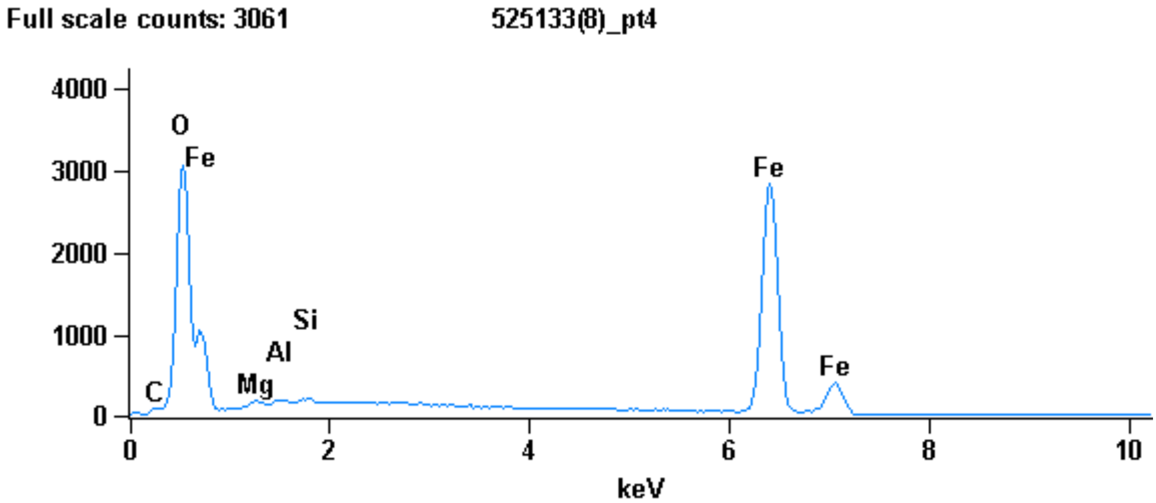
Full scale counts: 3061
525133(8)_pt4
4000
3000
2000
1000
0
O
Fe
Fe
Si
Al
Mg
C
Fe
0
2
4
6
8
10
keV

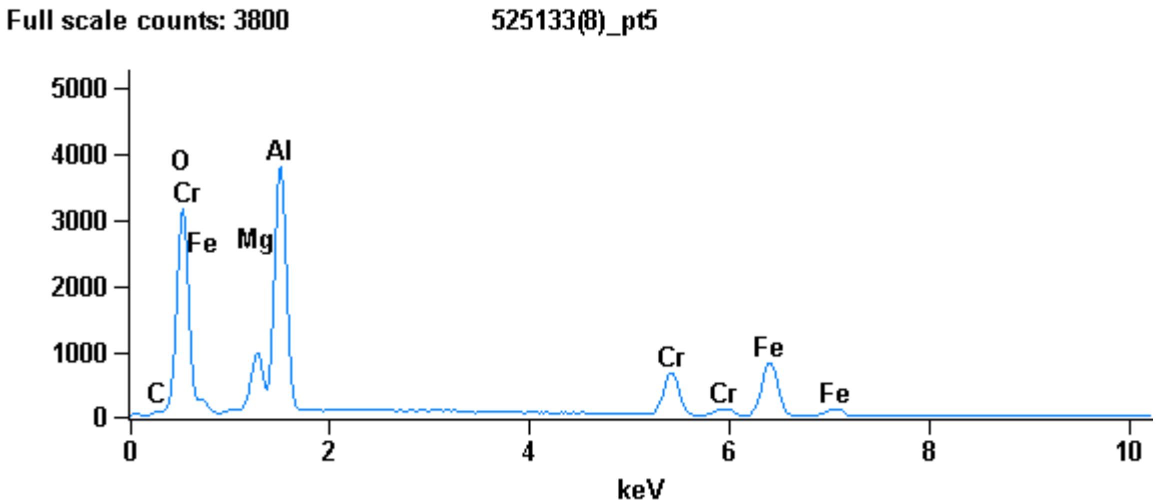
Full scale counts: 3800
525133(8)_pt5
5000
4000
3000
2000
1000
0
O
Cr
Fe
Al
Mg
C
Cr
Cr
Fe
Fe
0
2
4
6
8
10
keV

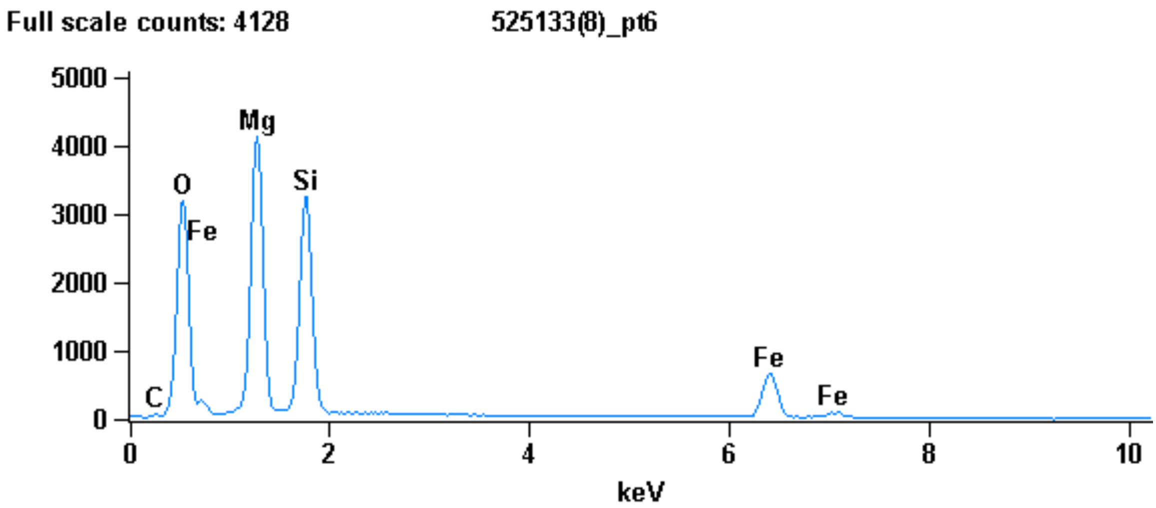

Full scale counts: 4128
525133(8)_pt6
5000
4000
3000
2000
1000
0
Mg
O
Si
Fe
C
Fe
Fe
0
2
4
6
8
10
keV

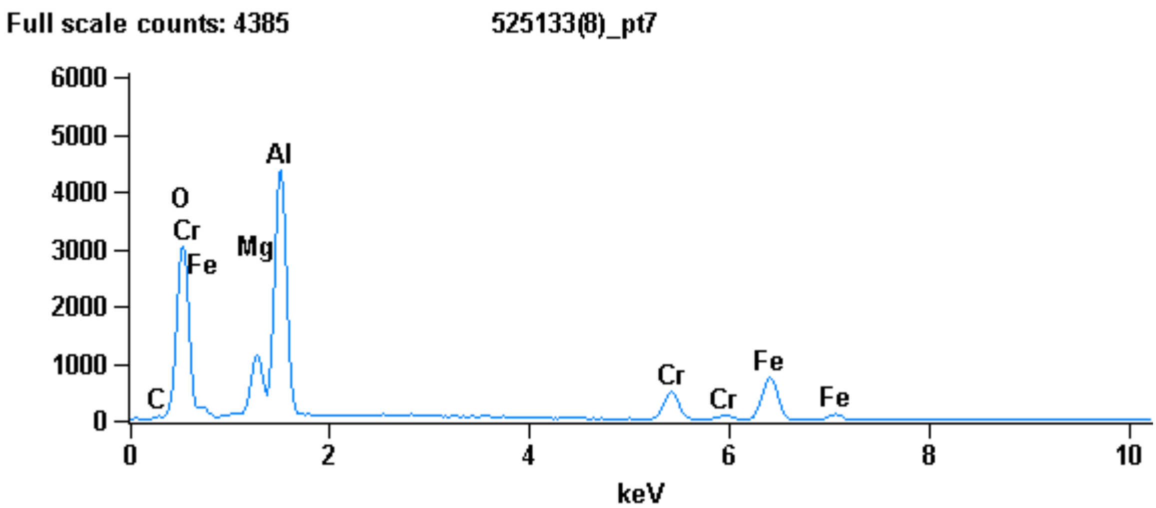

Full scale counts: 4385
525133(8)_pt7
6000
5000
4000
3000
2000
1000
0
Al
O
Cr
Mg
Fe
C
Cr
Cr
Fe
Fe
0
2
4
6
8
10
keV

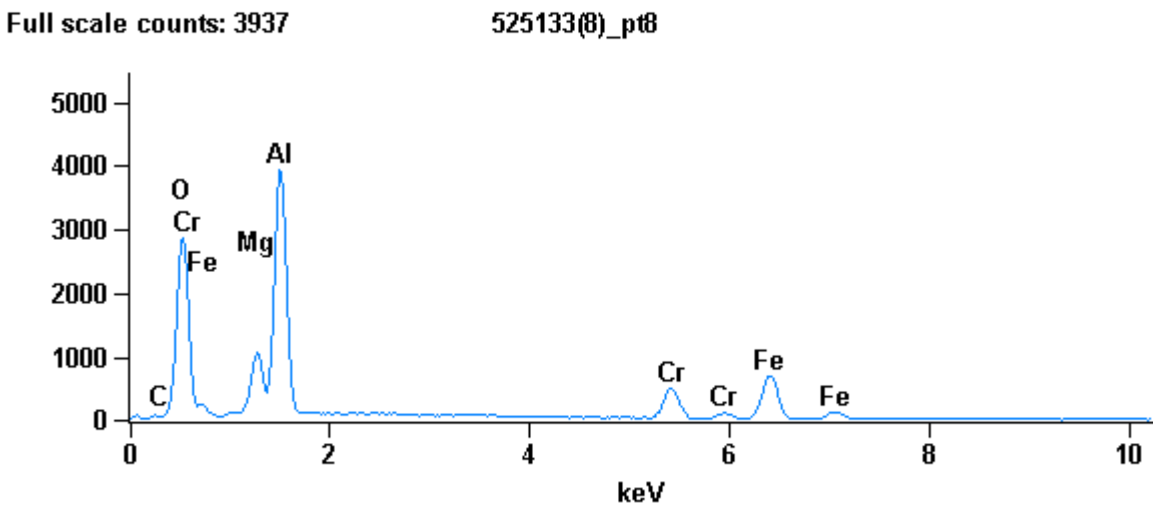

Full scale counts: 3937
525133(8)_pt8
5000
4000
3000
2000
1000
0
Al
O
Cr
Mg
Fe
C
Cr
Cr
Fe
Fe
0
2
4
6
8
10
keV

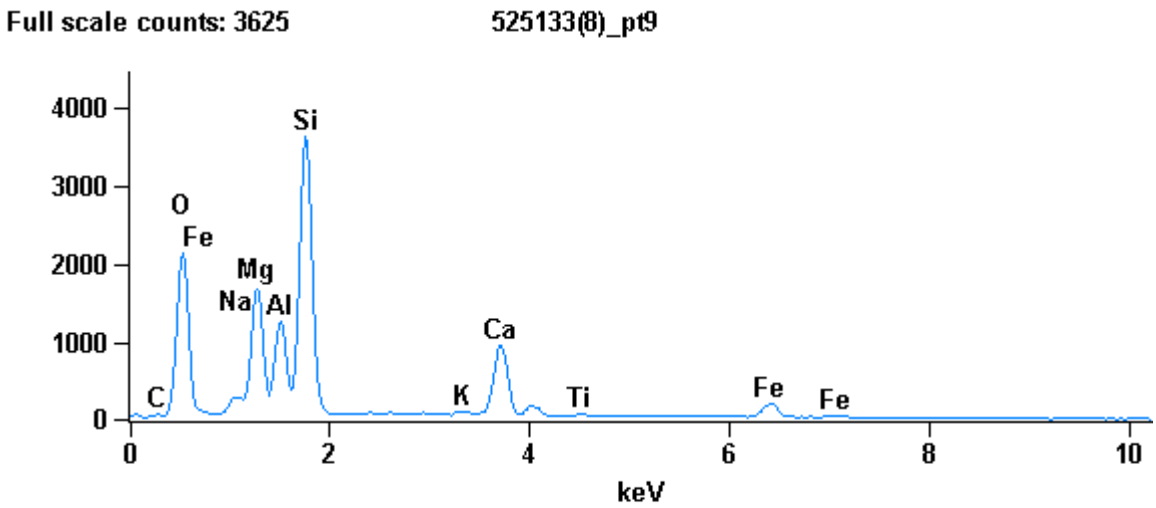

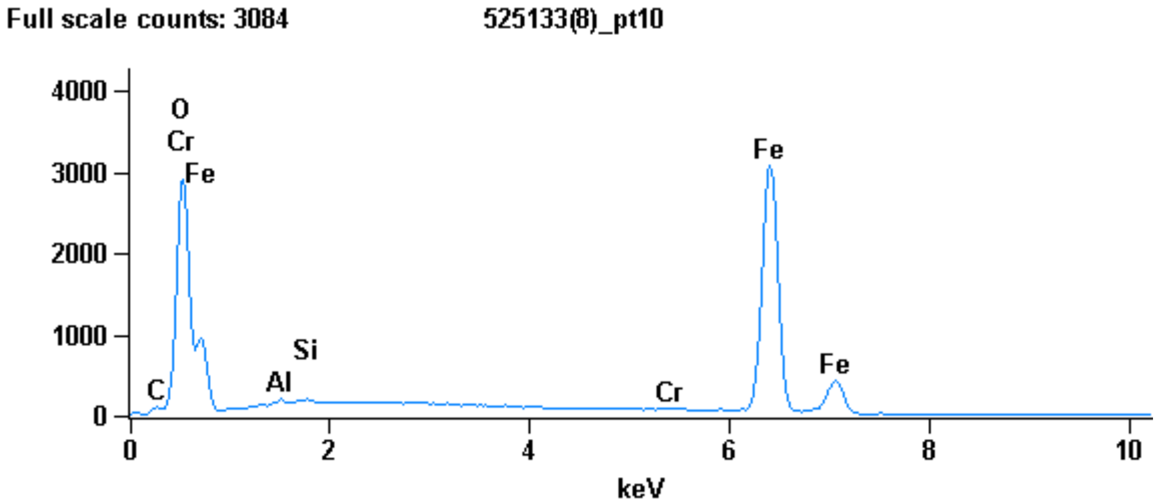

Weight %

	O-K	Na-K	Mg-K	Al-K	Si-K	K-K	Ca-K	Ti-K	Cr-K	Fe-K
525133(8)_pt1	45.28S		21.27	11.96	16.11	0.17			0.54	4.67
525133(8)_pt2	45.39S		20.15	13.54	15.62		0.10		0.49	4.72
525133(8)_pt3	45.41S		21.40	11.92	16.31				0.43	4.53
525133(8)_pt4	30.46S		0.79	0.39	0.30					68.06
525133(8)_pt5	39.08S		6.59	24.07					10.20	20.06
525133(8)_pt6	42.93S		25.19		17.83					14.05
525133(8)_pt7	40.24S		7.62	27.38					7.18	17.58
525133(8)_pt8	39.92S		7.37	26.44					8.35	17.92
525133(8)_pt9	44.55S	1.83	10.94	6.93	21.69	0.24	8.52	0.43		4.87
525133(8)_pt10	30.29S			0.36	0.23				0.34	68.78

Atom %

	O-K	Na-K	Mg-K	Al-K	Si-K	K-K	Ca-K	Ti-K	Cr-K	Fe-K
525133(8)_pt1	58.71		18.15	9.19	11.90	0.09			0.22	1.74
525133(8)_pt2	58.86		17.20	10.41	11.54		0.05		0.20	1.75
525133(8)_pt3	58.76		18.22	9.15	12.02				0.17	1.68
525133(8)_pt4	59.86		1.02	0.46	0.33					38.32
525133(8)_pt5	58.70		6.51	21.44					4.72	8.63
525133(8)_pt6	58.26		22.50		13.78					5.46
525133(8)_pt7	58.54		7.30	23.62					3.21	7.33
525133(8)_pt8	58.58		7.12	23.00					3.77	7.53
525133(8)_pt9	59.77	1.71	9.66	5.51	16.58	0.13	4.56	0.19		1.87
525133(8)_pt10	60.05			0.42	0.26				0.21	39.06

Compound %

		Na2O	MgO	Al2O3	SiO2	K2O	CaO	TiO2	Cr2O3	Fe2O3
525133(8)_pt1	0.00		35.26	22.59	34.46	0.20			0.79	6.68
525133(8)_pt2	0.00		33.41	25.58	33.43		0.13		0.72	6.74
525133(8)_pt3	0.00		35.48	22.53	34.88				0.63	6.47
525133(8)_pt4	0.00		1.31	0.74	0.64					97.31
525133(8)_pt5	0.00		10.92	45.48					14.91	28.68
525133(8)_pt6	0.00		41.77		38.13					20.09
525133(8)_pt7	0.00		12.63	51.74					10.49	25.14
525133(8)_pt8	0.00		12.22	49.96					12.20	25.62
525133(8)_pt9	0.00	2.47	18.14	13.10	46.39	0.29	11.92	0.72		6.97
525133(8)_pt10	0.00			0.67	0.49				0.50	98.34

Minerals, 525133(8)

pt1: Chlorite - clinochlore-chamosite series
pt2: Chlorite - clinochlore-chamosite series
pt3: Chlorite - clinochlore-chamosite series
pt4: Fe-oxide
pt5: Spinel - picotite
pt6: Olivine - chrysolite
pt7: Spinel - picotite
pt8: Spinel - picotite
pt9: Amphibole - hornblende
pt10: Fe-oxide

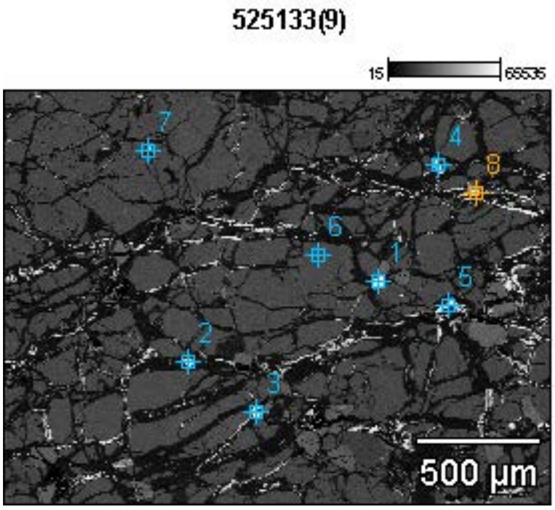

Image name: 525133(9)
Magnification: 55

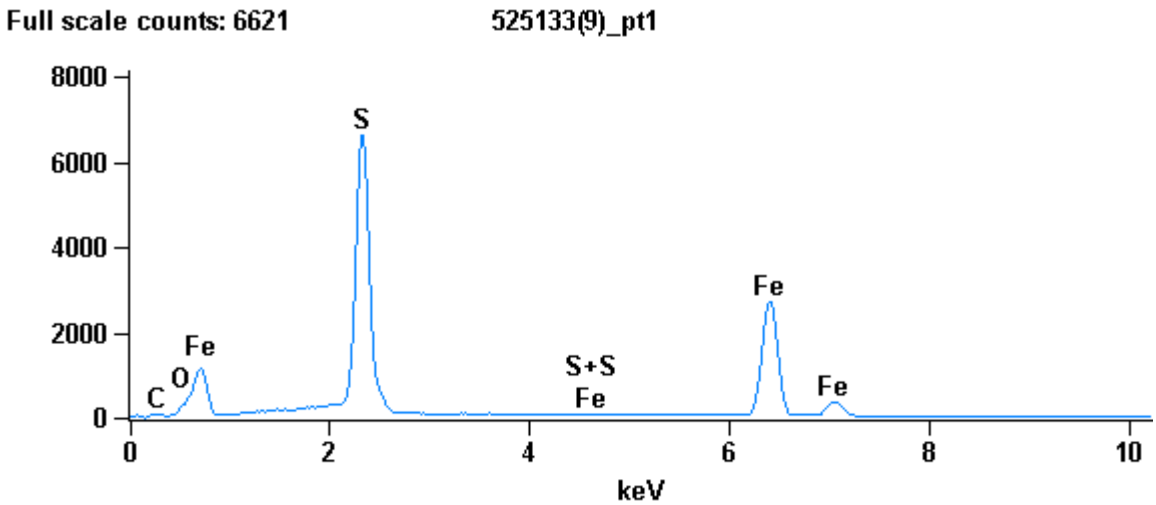

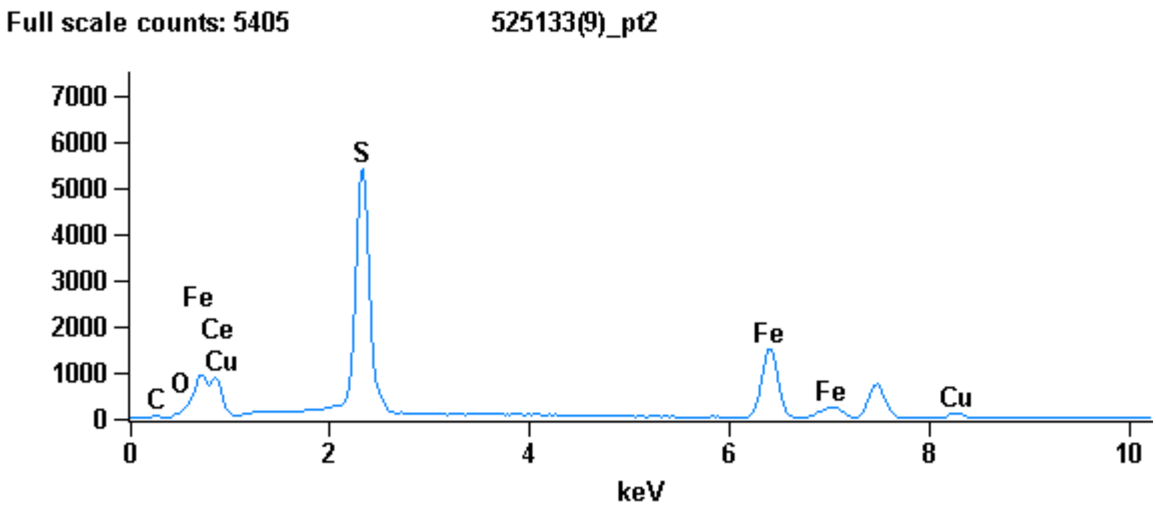

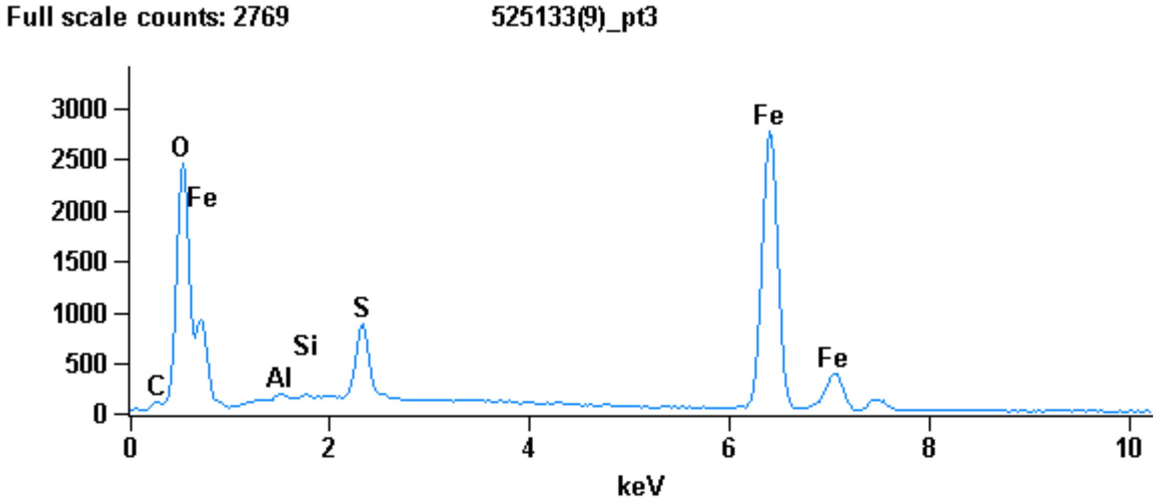
Full scale counts: 2769
525133(9)_pt3
3000
2500
2000
1500
1000
500
0
O
Fe
C
Al
Si
S
Fe
Fe
0
2
4
6
8
10
keV

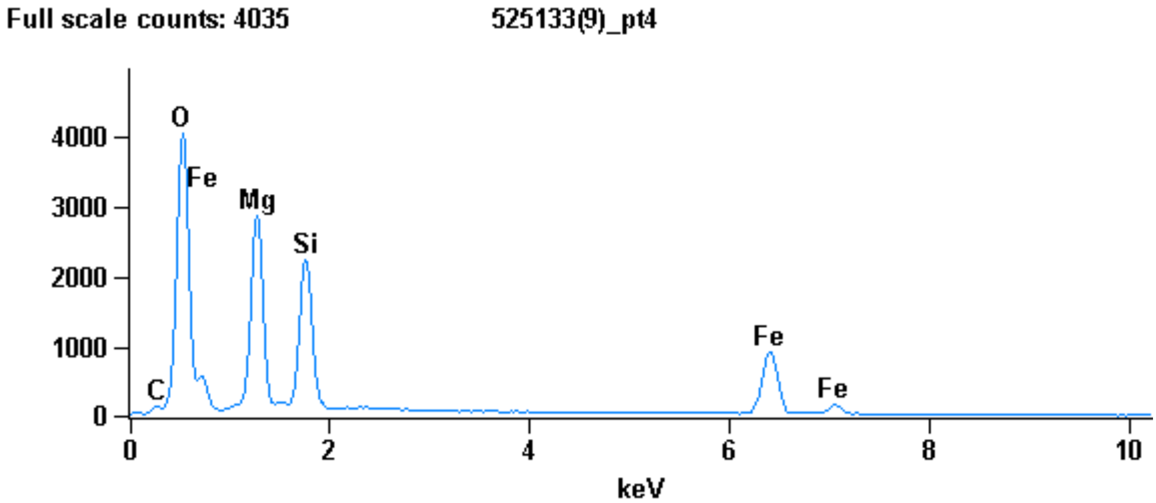
Full scale counts: 4035
525133(9)_pt4
4000
3000
2000
1000
0
O
Fe
Mg
Si
C
Fe
Fe
0
2
4
6
8
10
keV

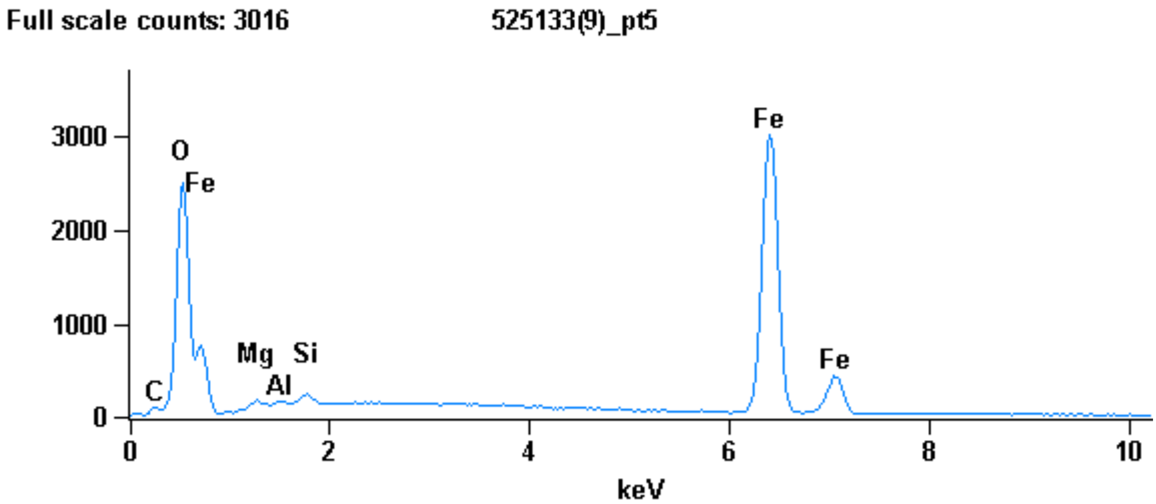
Full scale counts: 3016
525133(9)_pt5
3000
2000
1000
0
O
Fe
C
Mg
Si
Al
Fe
Fe
0
2
4
6
8
10
keV

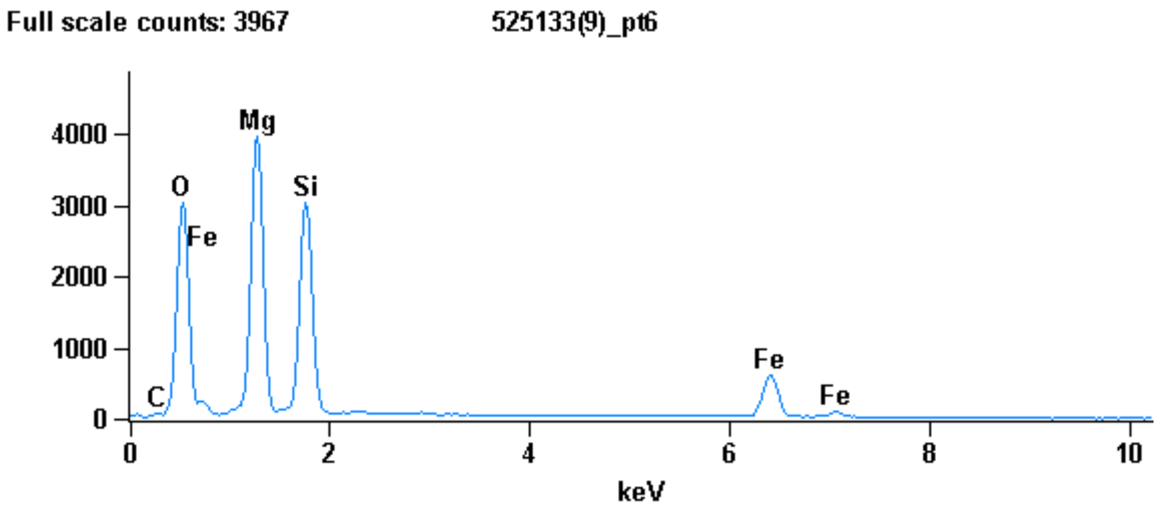
Full scale counts: 3967
525133(9)_pt6
Mg
O
Si
Fe
C
Fe
Fe
0
1000
2000
3000
4000
0
2
4
6
8
10
keV

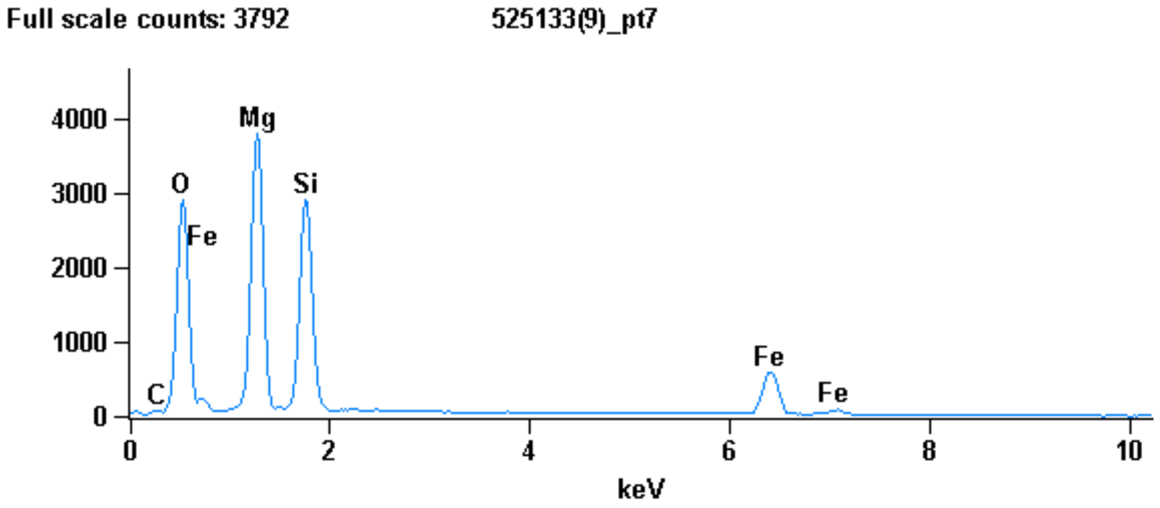
Full scale counts: 3792
525133(9)_pt7
Mg
O
Si
Fe
C
Fe
Fe
0
1000
2000
3000
4000
0
2
4
6
8
10
keV

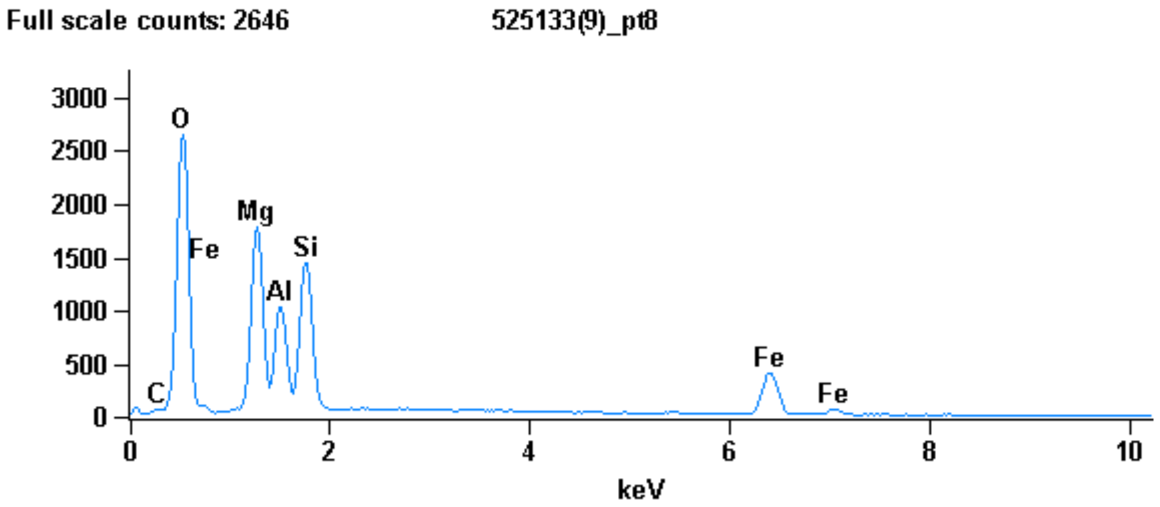
Full scale counts: 2646
525133(9)_pt8
O
Mg
Fe
Si
Al
C
Fe
Fe
0
500
1000
1500
2000
2500
3000
0
2
4
6
8
10
keV

Weight %

	O-K	Mg-K	Al-K	Si-K	S-K	Fe-K	Cu-K	Ce-L
525133(9)_pt1	45.25S				20.35	34.40		
525133(9)_pt2	47.41S				23.25	29.31	0.00	0.02
525133(9)_pt3	33.56S		0.36	0.12	4.46	61.49		
525133(9)_pt4	40.62S	21.87		14.25		23.26		
525133(9)_pt5	30.65S	0.93	0.35	0.67		67.41		
525133(9)_pt6	42.97S	25.23		17.89		13.91		
525133(9)_pt7	42.88S	25.22		17.71		14.19		
525133(9)_pt8	43.10S	18.09	9.83	14.09		14.89		

Atom %

	O-K	Mg-K	Al-K	Si-K	S-K	Fe-K	Cu-K	Ce-L
525133(9)_pt1	69.34				15.56	15.10		
525133(9)_pt2	70.33				17.21	12.46	0.00	0.00
525133(9)_pt3	62.51		0.40	0.13	4.15	32.81		
525133(9)_pt4	58.20	20.63		11.63		9.55		
525133(9)_pt5	59.91	1.20	0.40	0.74		37.75		
525133(9)_pt6	58.26	22.52		13.82		5.40		
525133(9)_pt7	58.23	22.55		13.70		5.52		
525133(9)_pt8	58.94	16.28	7.97	10.98		5.83		

Compound %

		MgO	Al2O3	SiO2	SO3	Fe2O3	Cu2O	Ce2O3
525133(9)_pt1	0.00				50.82	49.18		
525133(9)_pt2	0.00				58.07	41.91	0.00	0.03
525133(9)_pt3	0.00		0.68	0.26	11.14	87.92		
525133(9)_pt4	0.00	36.27		30.48		33.25		
525133(9)_pt5	0.00	1.54	0.65	1.43		96.37		
525133(9)_pt6	0.00	41.84		38.27		19.89		
525133(9)_pt7	0.00	41.82		37.89		20.29		
525133(9)_pt8	0.00	29.99	18.57	30.15		21.28		

Minerals, 525133(9)
pt1: Pyrite
pt2: Pyrite
pt3: Mixed signal/edge effect
pt4: Olivine - hortonolite
pt5: Fe-oxide
pt6: Olivine - chrysolite
pt7: Olivine - chrysolite
pt8: Chlorite - clinochlore-chamosite

525134a(1)

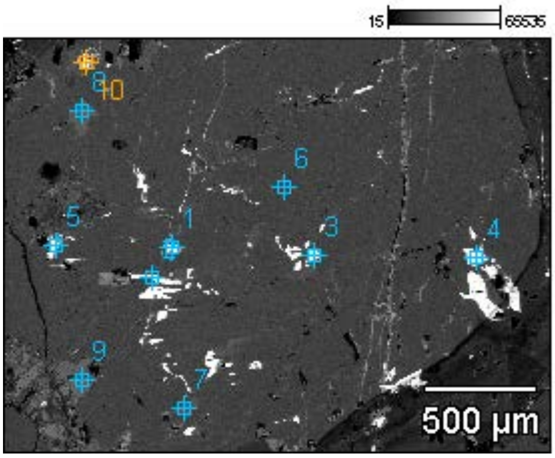

Image name: (1)
Magnification: 50

Full scale counts: 5632 525134a(1)_pt1

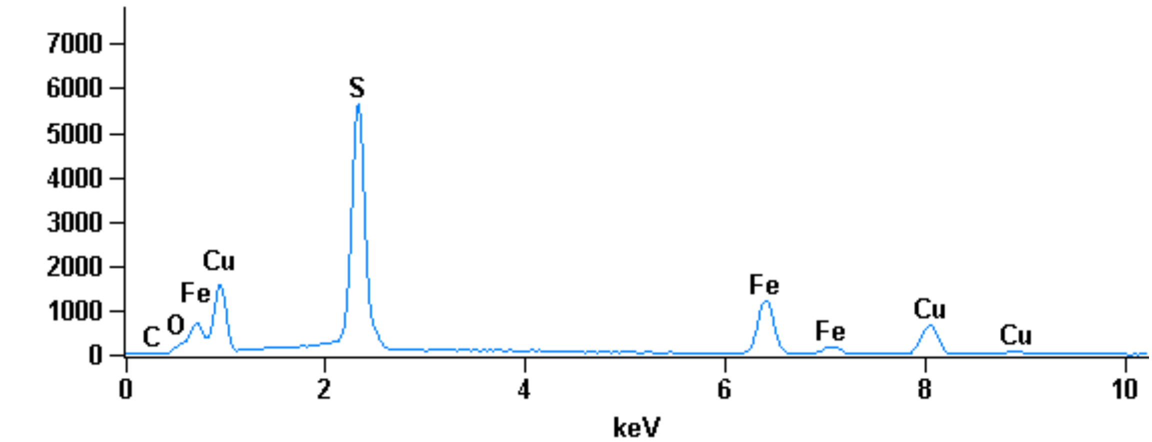

Full scale counts: 5659 525134a(1)_pt2

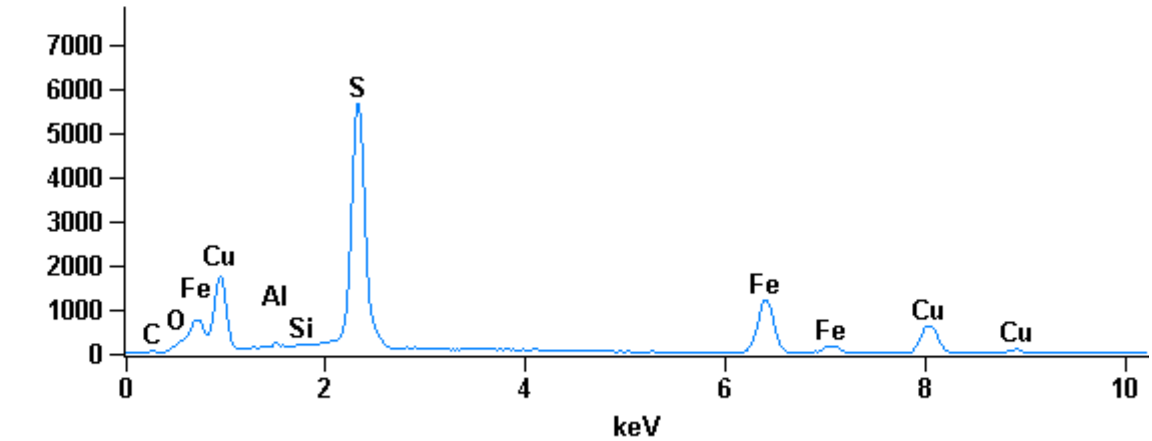

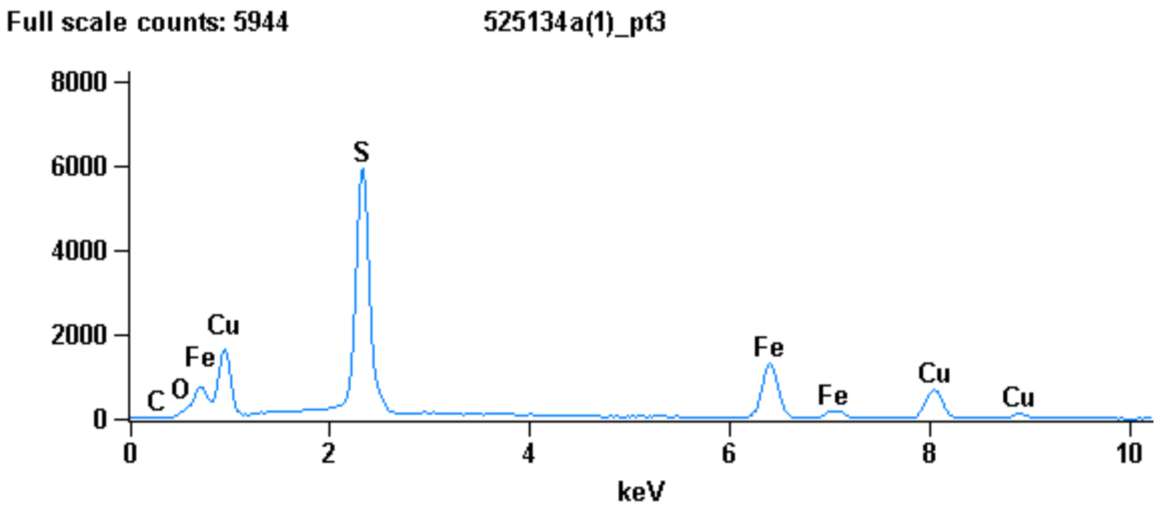
Full scale counts: 5944
525134a(1)_pt3
8000
6000
4000
2000
0
S
Cu
Fe
C
O
Fe
Fe
Cu
Cu
0
2
4
6
8
10
keV

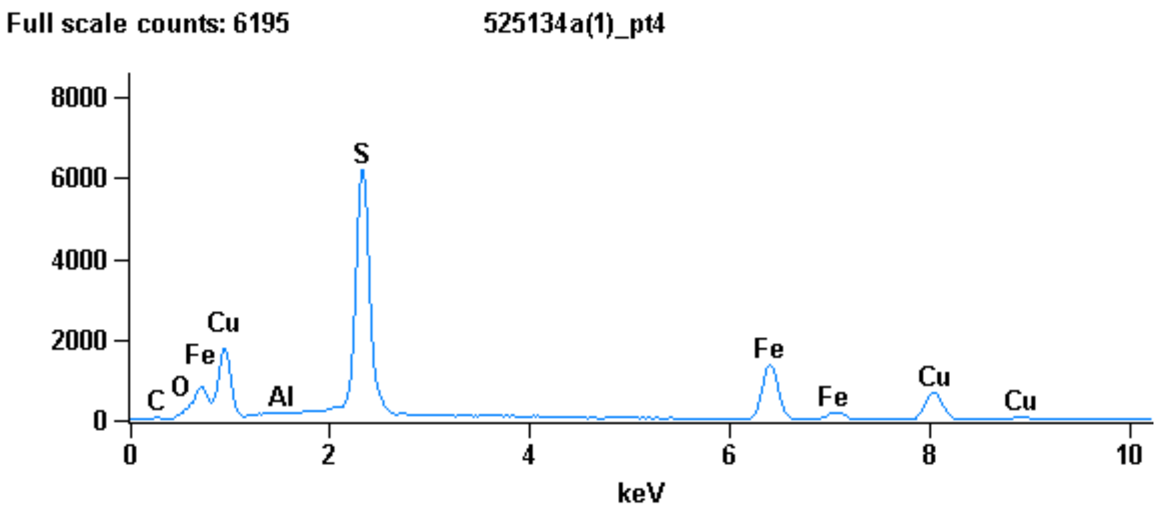
Full scale counts: 6195
525134a(1)_pt4
8000
6000
4000
2000
0
S
Cu
Fe
C
O
Al
Fe
Fe
Cu
Cu
0
2
4
6
8
10
keV

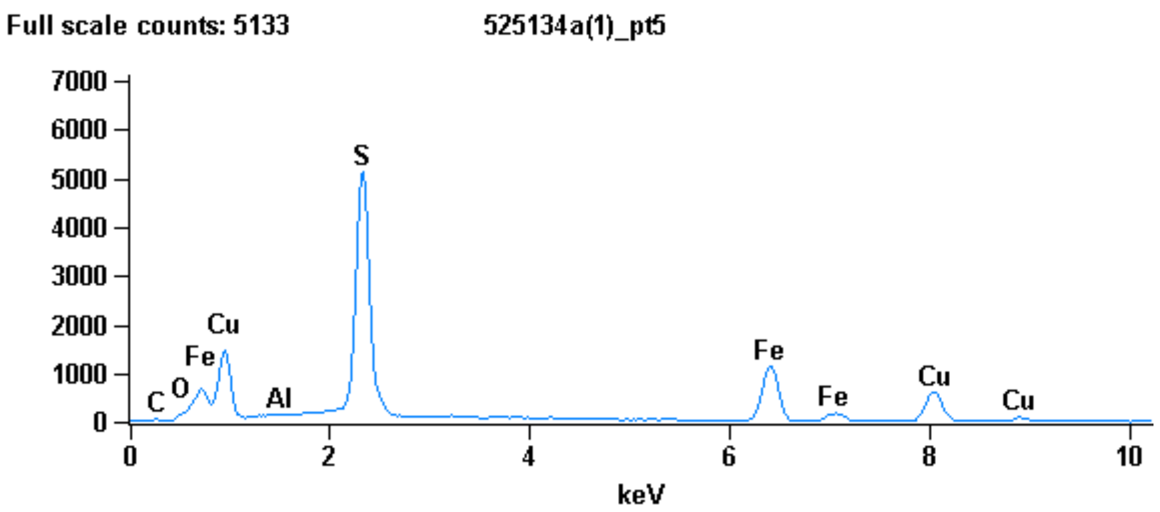
Full scale counts: 5133
525134a(1)_pt5
7000
6000
5000
4000
3000
2000
1000
0
S
Cu
Fe
C
O
Al
Fe
Fe
Cu
Cu
0
2
4
6
8
10
keV

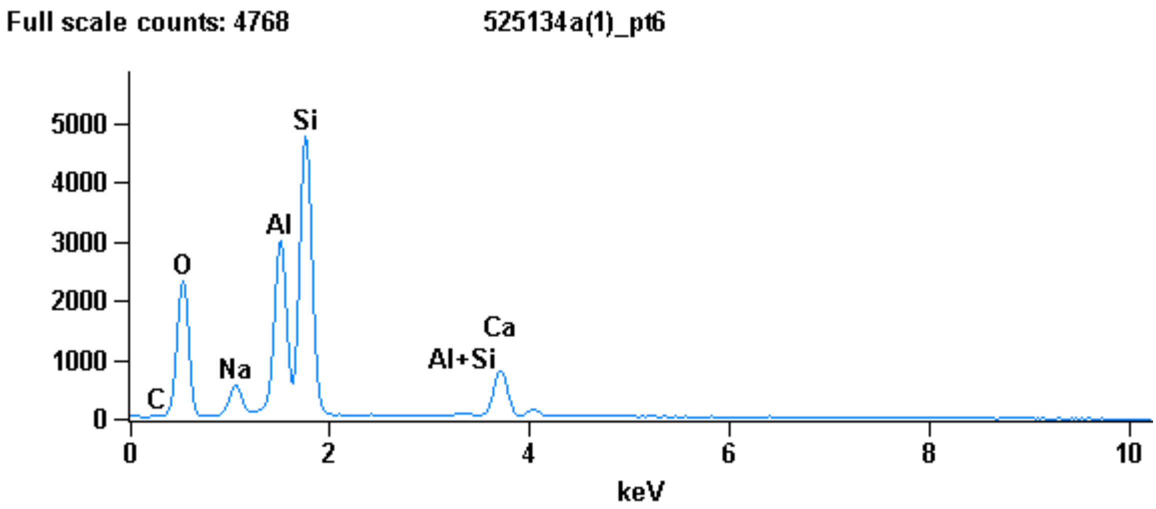
Full scale counts: 4768
525134a(1)_pt6
5000
4000
3000
2000
1000
0
Si
Al
O
Na
C
Ca
Al+Si
0
2
4
6
8
10
keV

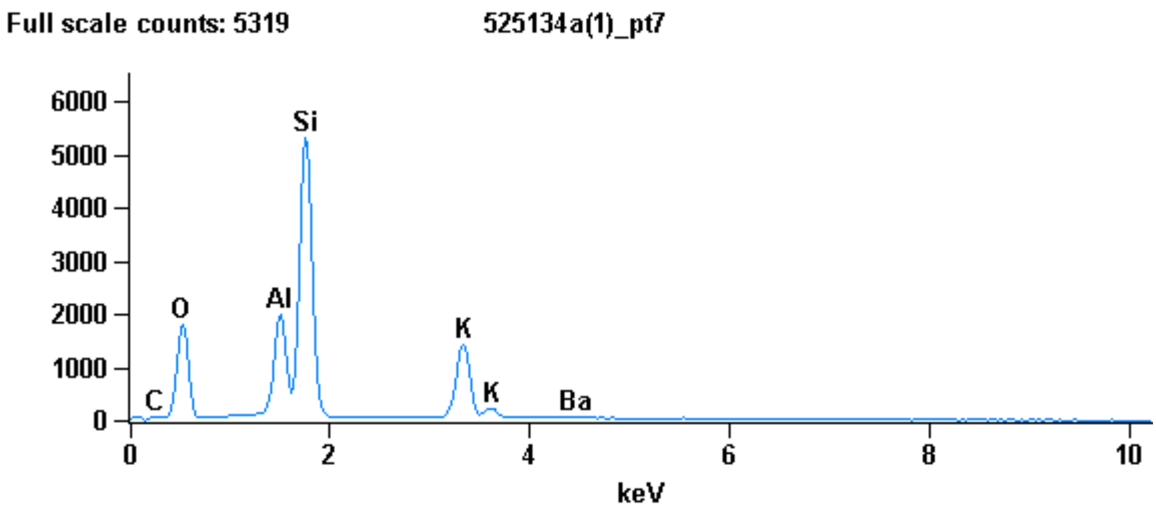
Full scale counts: 5319
525134a(1)_pt7
6000
5000
4000
3000
2000
1000
0
Si
Al
O
C
K
K
Ba
0
2
4
6
8
10
keV

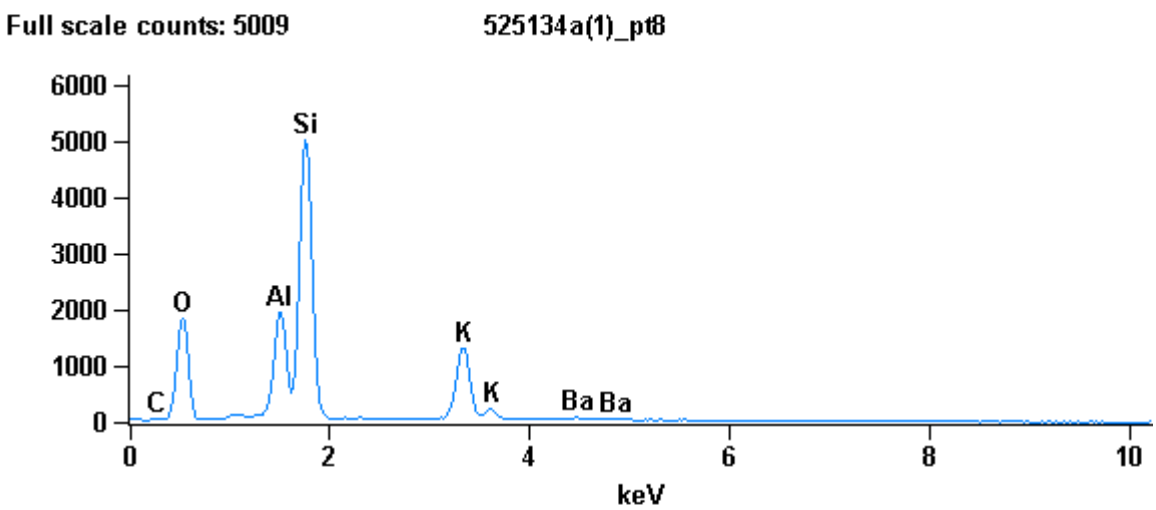
Full scale counts: 5009
525134a(1)_pt8
6000
5000
4000
3000
2000
1000
0
Si
Al
O
C
K
K
Ba Ba
0
2
4
6
8
10
keV

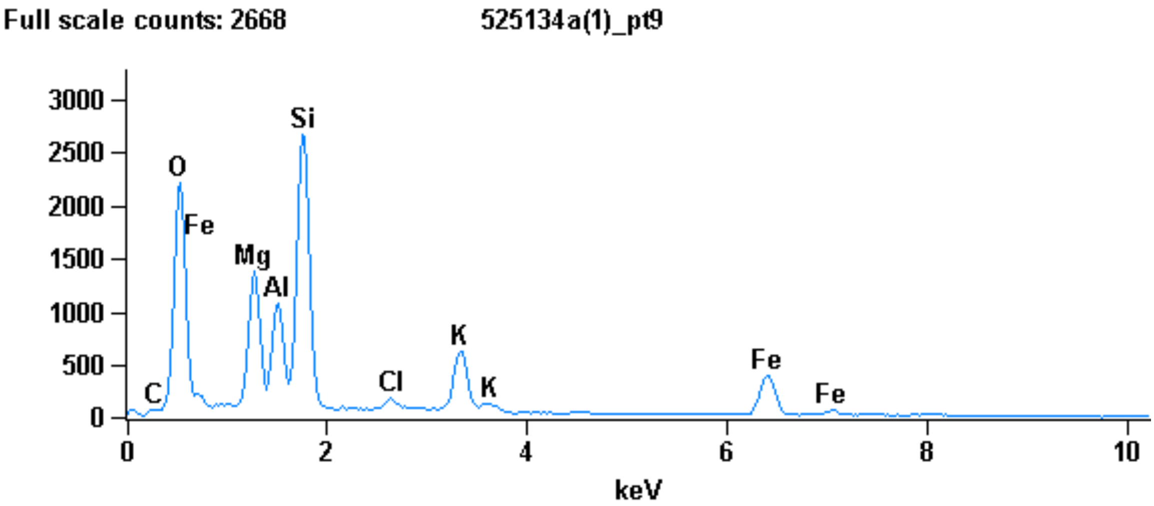

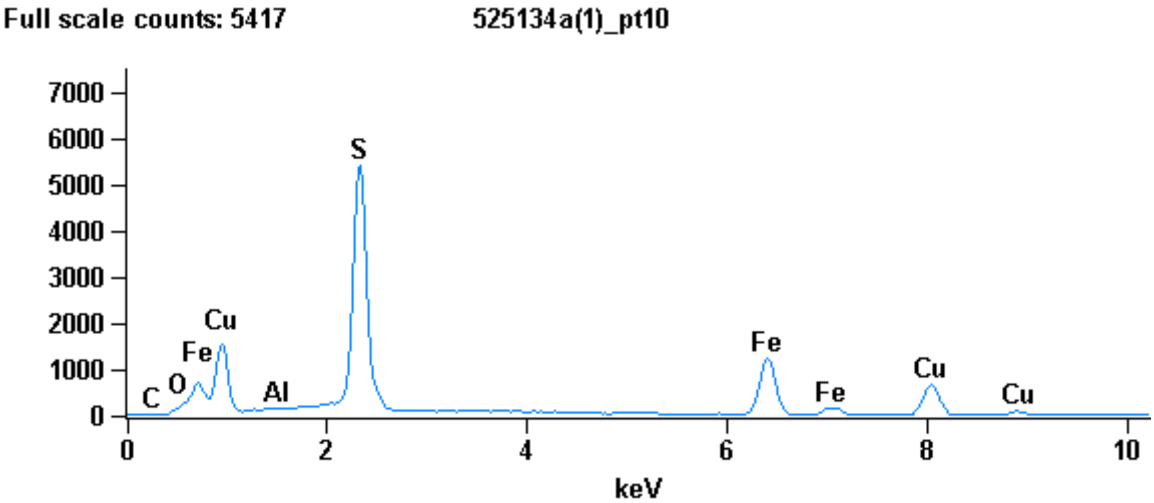

Weight %

	O-K	Na-K	Mg-K	Al-K	Si-K	S-K	Cl-K	K-K	Ca-K	Fe-K	Cu-K	Ba-L
525134a(1)_pt1	41.51S					21.03				17.48	19.98	
525134a(1)_pt2	41.73S			0.25	0.10	21.01				17.46	19.45	
525134a(1)_pt3	41.60S					21.09				17.54	19.78	
525134a(1)_pt4	41.80S			0.11		21.17				17.65	19.27	
525134a(1)_pt5	41.63S			0.14		21.00				17.71	19.52	
525134a(1)_pt6	47.45S	4.50		14.35	26.57				7.13			
525134a(1)_pt7	46.29S			9.91	30.59			12.36				0.84
525134a(1)_pt8	45.95S			10.31	29.99			11.52				2.24
525134a(1)_pt9	42.93S		11.19	7.44	19.82		0.84	5.64		12.14		
525134a(1)_pt10	41.38S			0.13		20.74				17.98	19.77	

Atom %

	O-K	Na-K	Mg-K	Al-K	Si-K	S-K	Cl-K	K-K	Ca-K	Fe-K	Cu-K	Ba-L
525134a(1)_pt1	66.91					16.91				8.07	8.11	
525134a(1)_pt2	66.97			0.23	0.09	16.82				8.03	7.86	
525134a(1)_pt3	66.96					16.94				8.09	8.01	
525134a(1)_pt4	67.05			0.11		16.94				8.11	7.78	
525134a(1)_pt5	66.95			0.13		16.86				8.16	7.90	
525134a(1)_pt6	61.56	4.06		11.04	19.64				3.69			
525134a(1)_pt7	61.93			7.86	23.31			6.77				0.13
525134a(1)_pt8	62.00			8.24	23.05			6.36				0.35
525134a(1)_pt9	59.49		10.20	6.11	15.65		0.52	3.20		4.82		
525134a(1)_pt10	66.81			0.12		16.71				8.32	8.04	

Compound %

		Na2O	MgO	Al2O3	SiO2	SO3	Cl	K2O	CaO	Fe2O3	Cu2O	BaO
525134a(1)_pt1	0.00					52.51				25.00	22.49	
525134a(1)_pt2	0.00			0.46	0.21	52.46				24.97	21.90	
525134a(1)_pt3	0.00					52.66				25.08	22.27	
525134a(1)_pt4	0.00			0.22		52.86				25.23	21.70	
525134a(1)_pt5	0.00			0.26		52.45				25.31	21.98	
525134a(1)_pt6	0.00	6.06		27.12	56.84				9.98			
525134a(1)_pt7	0.00			18.72	65.45			14.89				0.94
525134a(1)_pt8	0.00			19.47	64.15			13.88				2.50
525134a(1)_pt9	0.00		18.55	14.06	42.40		0.84	6.80		17.36		
525134a(1)_pt10	0.00			0.24		51.79				25.71	22.26	

Minerals, 525134a(1)

pt1: Chalcopyrite
pt2: Chalcopyrite
pt3: Chalcopyrite
pt4: Chalcopyrite
pt5: Chalcopyrite
pt6: Feldspar - plagioclase
pt7: Feldspar - alkali feldspar
pt8: Feldspar - alkali feldspar
pt9: Biotite
pt10: Chalcopyrite

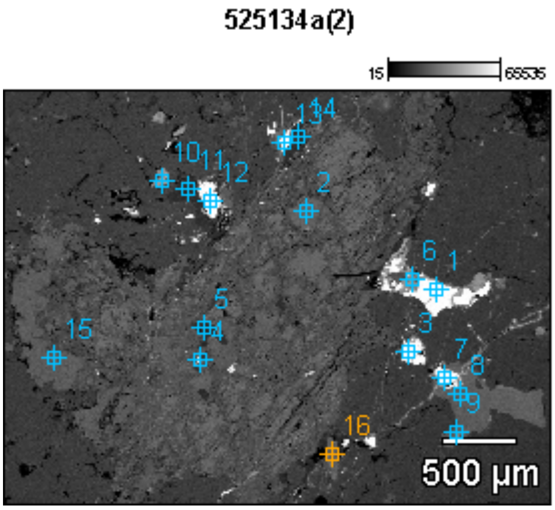

Image name: 525134a(2)
Magnification: 33

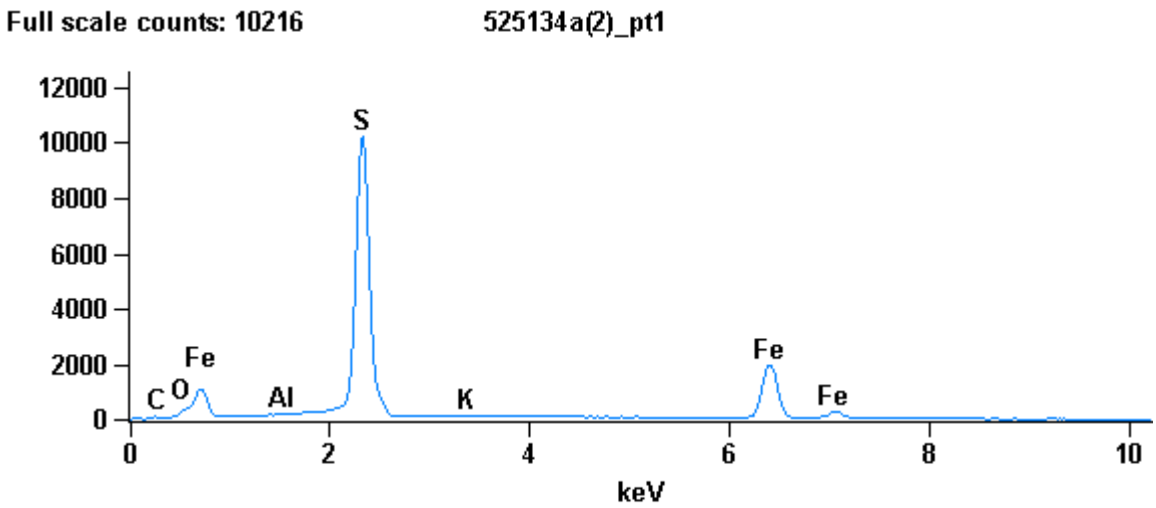

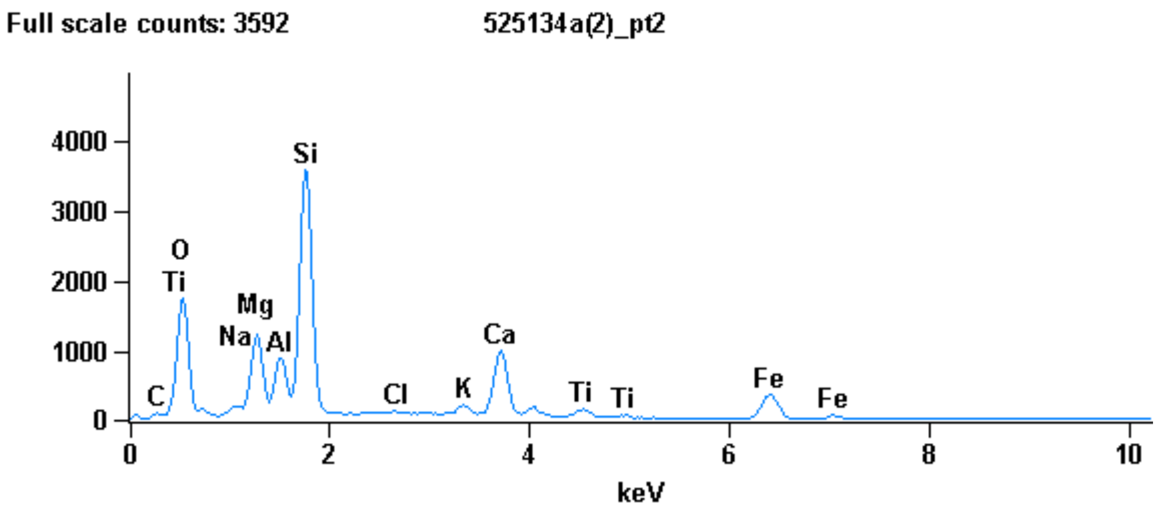

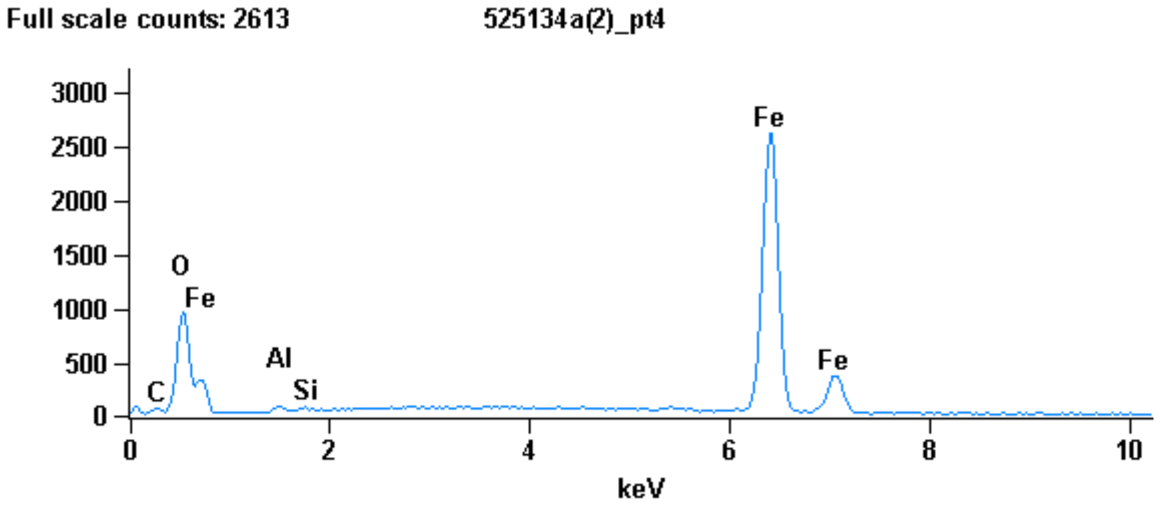
Full scale counts: 2613
525134a(2)_pt4
3000
2500
2000
1500
1000
500
0
Fe
O
Fe
Al
Si
C
Fe
0
2
4
6
8
10
keV

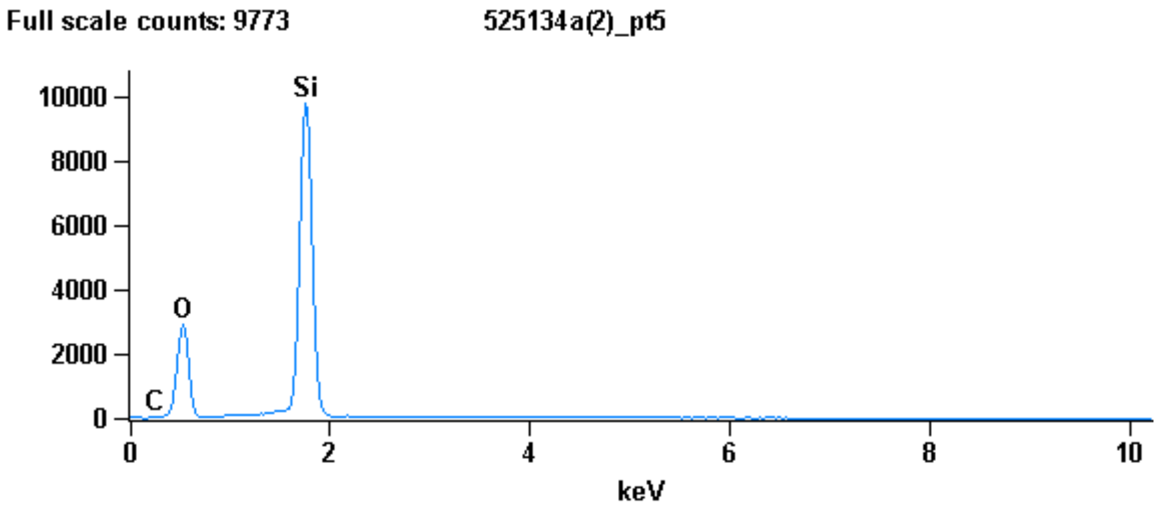
Full scale counts: 9773
525134a(2)_pt5
10000
8000
6000
4000
2000
0
Si
O
C
0
2
4
6
8
10
keV

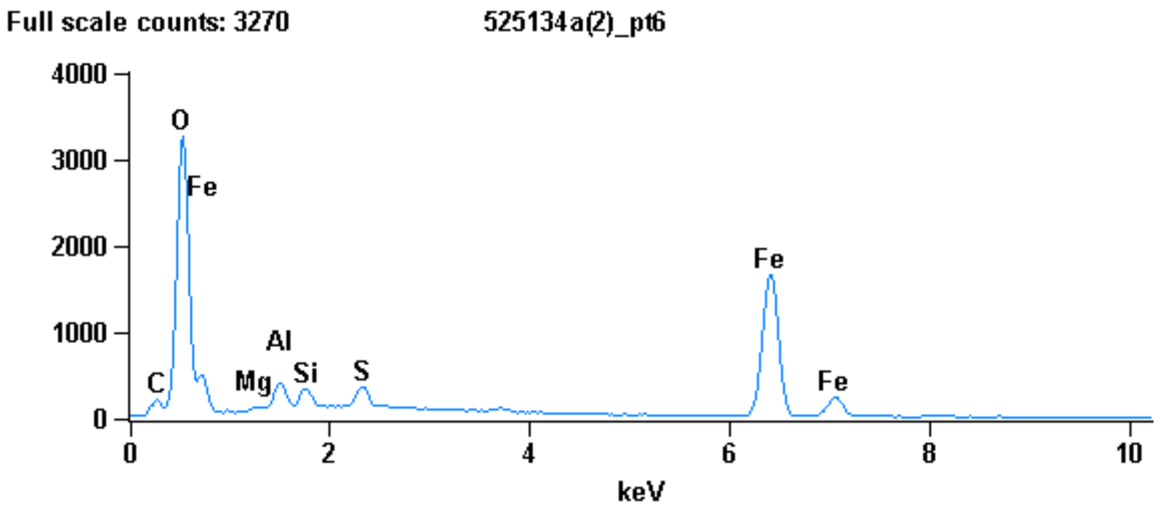
Full scale counts: 3270
525134a(2)_pt6
4000
3000
2000
1000
0
O
Fe
C
Mg
Al
Si
S
Fe
Fe
0
2
4
6
8
10
keV

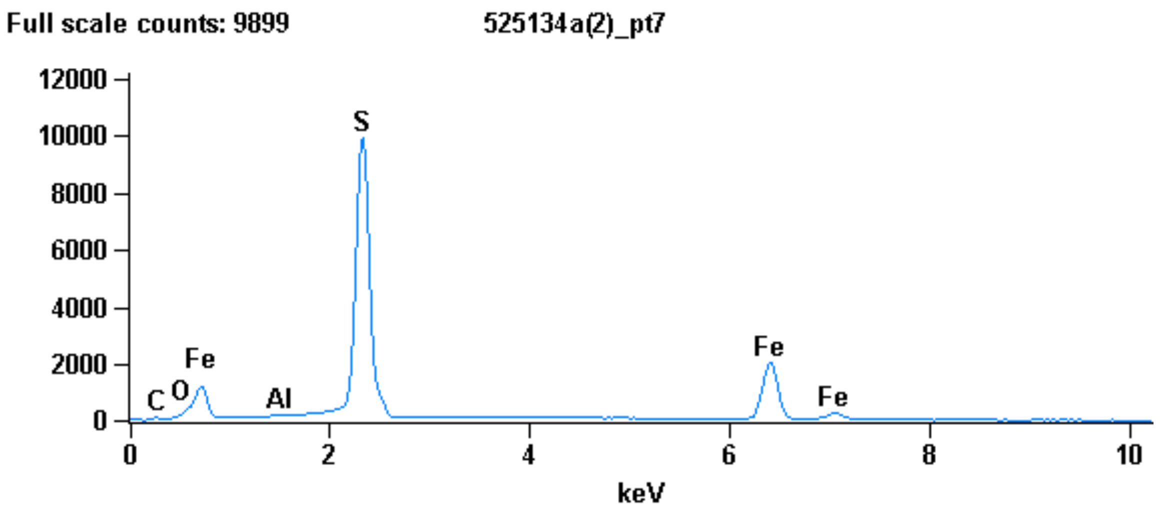
Full scale counts: 9899
525134a(2)_pt7
12000
10000
8000
6000
4000
2000
0
S
Fe
C
O
Al
Fe
Fe
0
2
4
6
8
10
keV

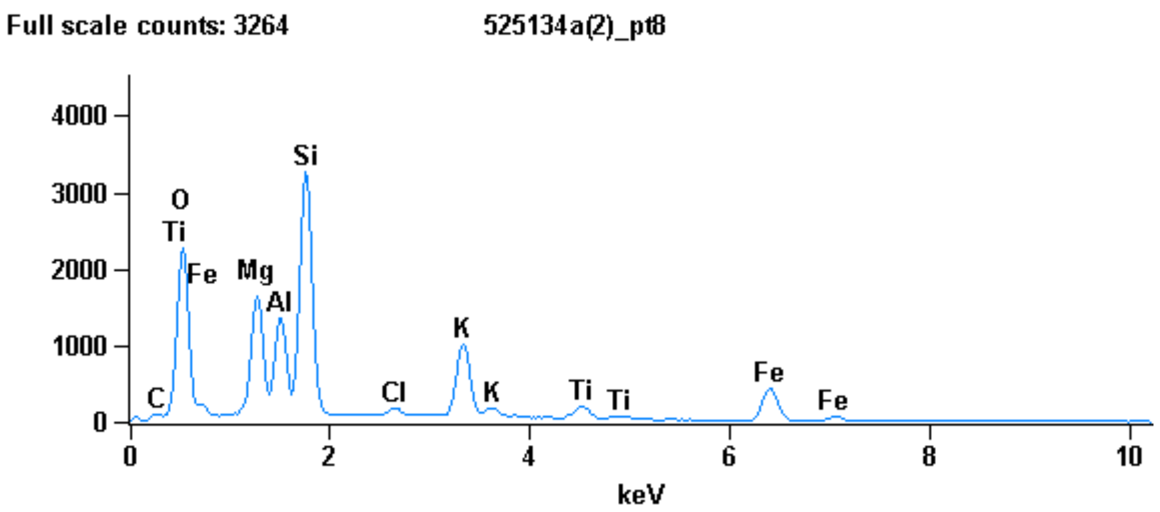
Full scale counts: 3264
525134a(2)_pt8
4000
3000
2000
1000
0
Si
O
Ti
Fe
Mg
Al
K
C
Cl
K
Ti
Ti
Fe
Fe
0
2
4
6
8
10
keV

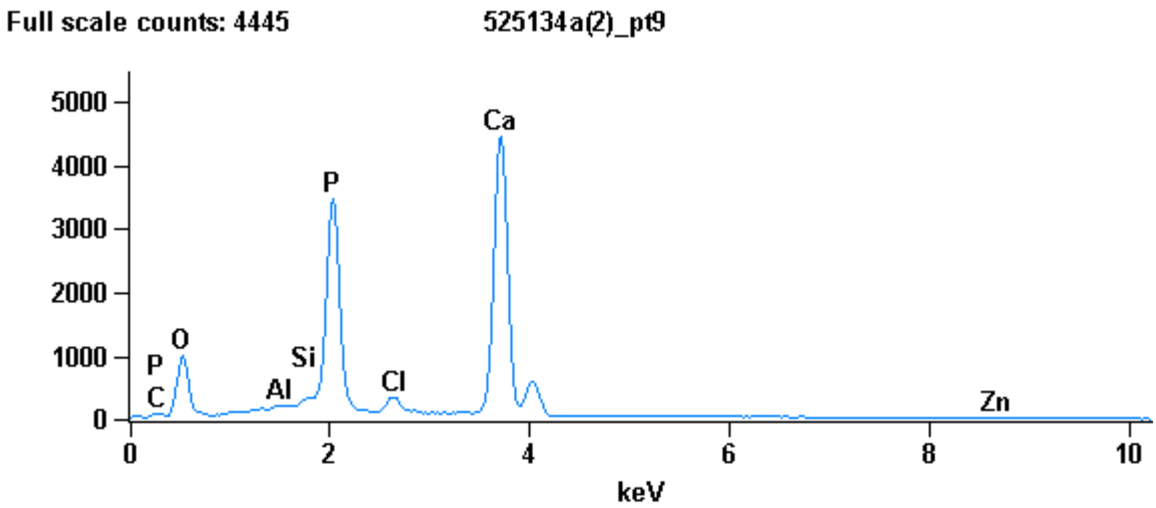
Full scale counts: 4445
525134a(2)_pt9
5000
4000
3000
2000
1000
0
Ca
P
O
P
C
Al
Si
Cl
Zn
0
2
4
6
8
10
keV

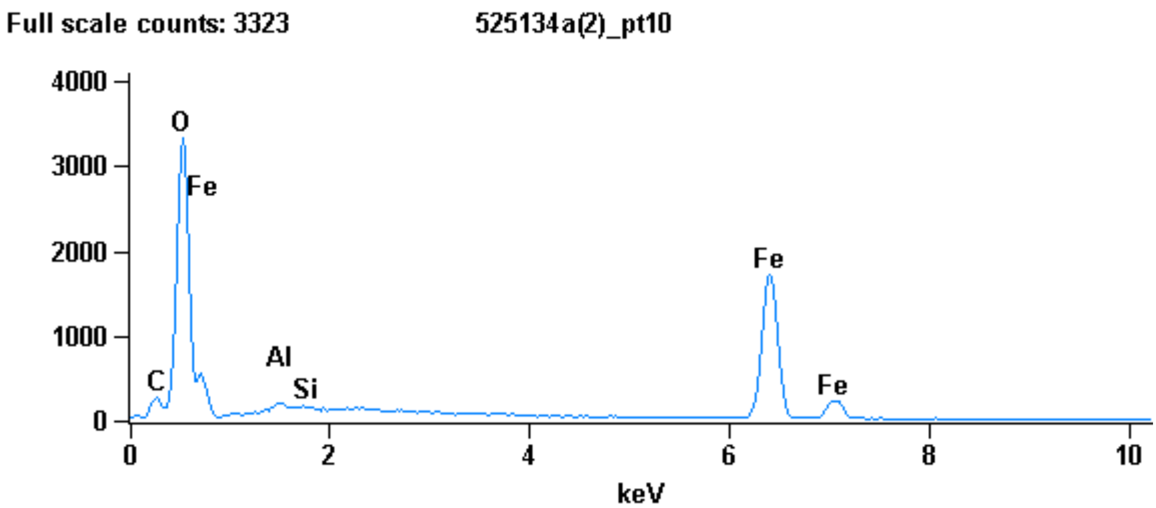
Full scale counts: 3323
525134a(2)_pt10
4000
3000
2000
1000
0
O
Fe
C
Al
Si
Fe
Fe
0
2
4
6
8
10
keV

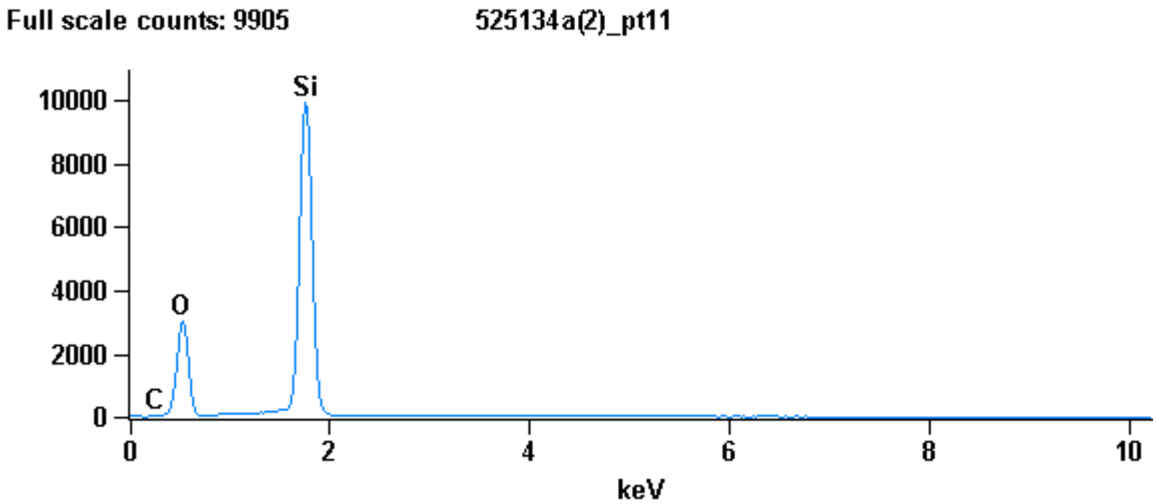
Full scale counts: 9905
525134a(2)_pt11
10000
8000
6000
4000
2000
0
Si
O
C
0
2
4
6
8
10
keV

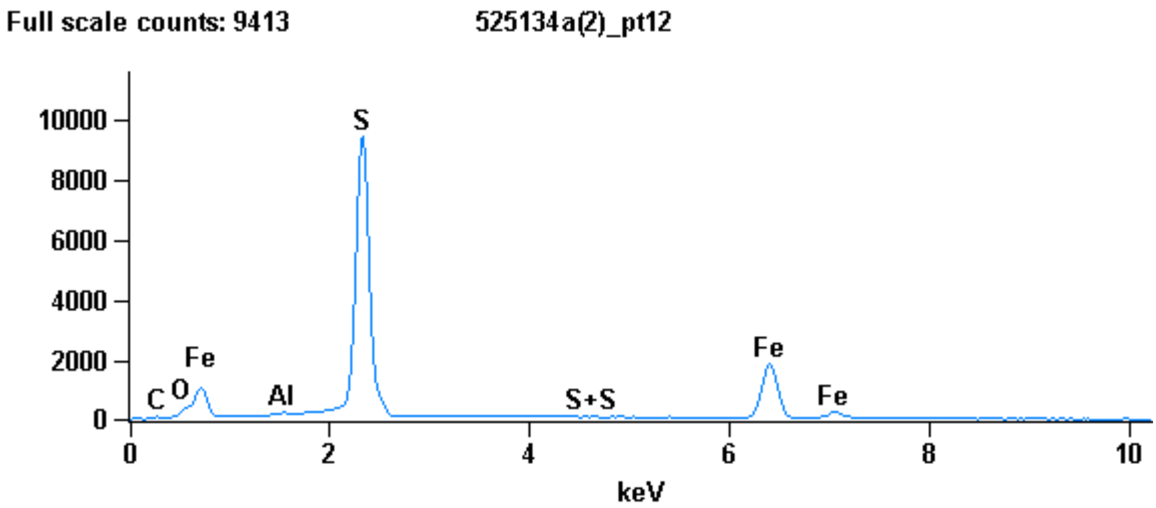
Full scale counts: 9413
525134a(2)_pt12
10000
8000
6000
4000
2000
0
S
Fe
C
O
Al
S+S
Fe
Fe
0
2
4
6
8
10
keV

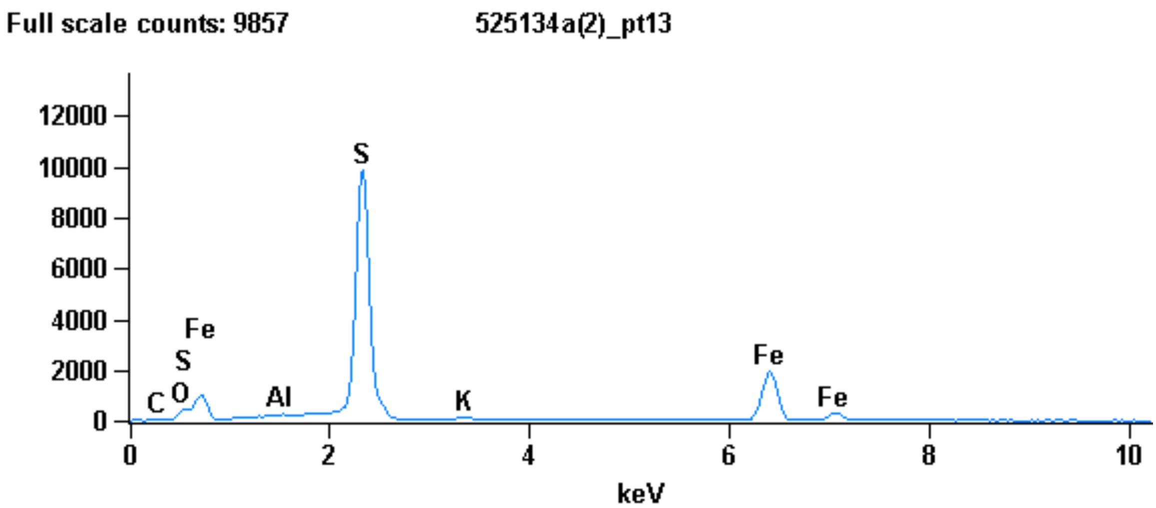
Full scale counts: 9857
525134a(2)_pt13
12000
10000
8000
6000
4000
2000
0
S
Fe
S
C
O
Al
K
Fe
Fe
0
2
4
6
8
10
keV

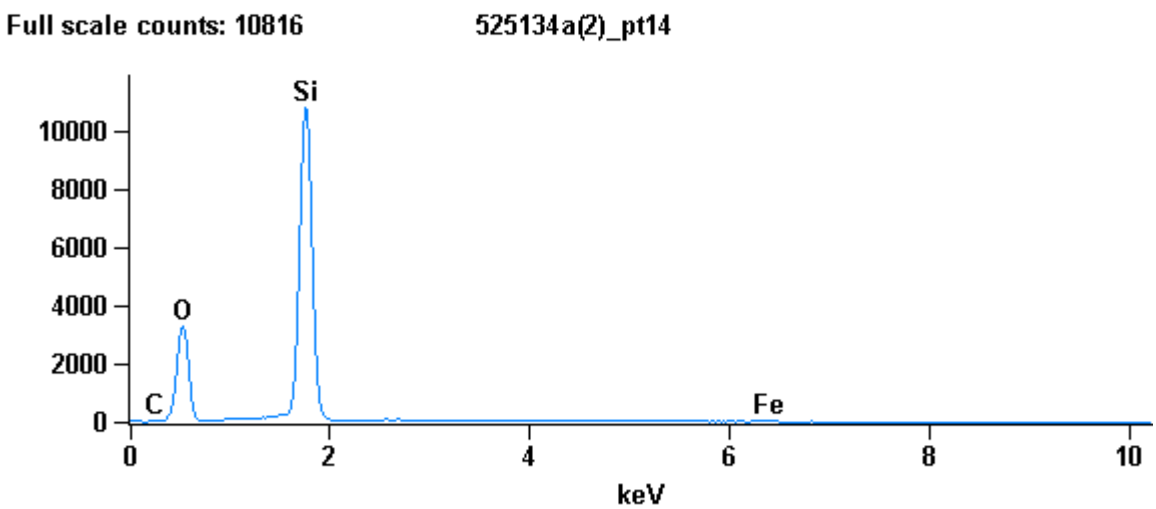
Full scale counts: 10816
525134a(2)_pt14
10000
8000
6000
4000
2000
0
Si
O
C
Fe
0
2
4
6
8
10
keV

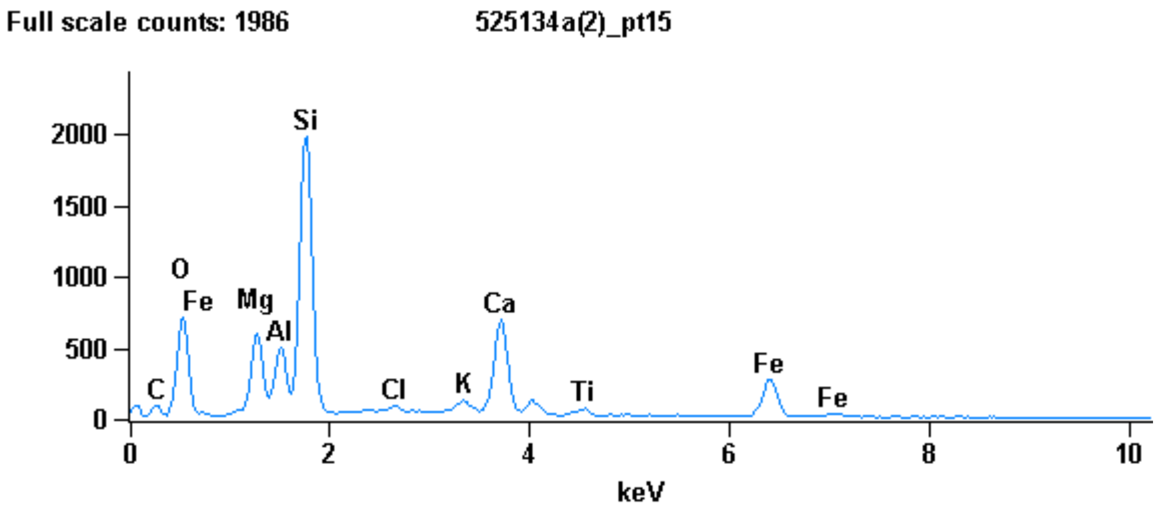
Full scale counts: 1986
525134a(2)_pt15
2000
1500
1000
500
0
Si
O
Fe
Mg
Al
Ca
C
Cl
K
Ti
Fe
Fe
0
2
4
6
8
10
keV

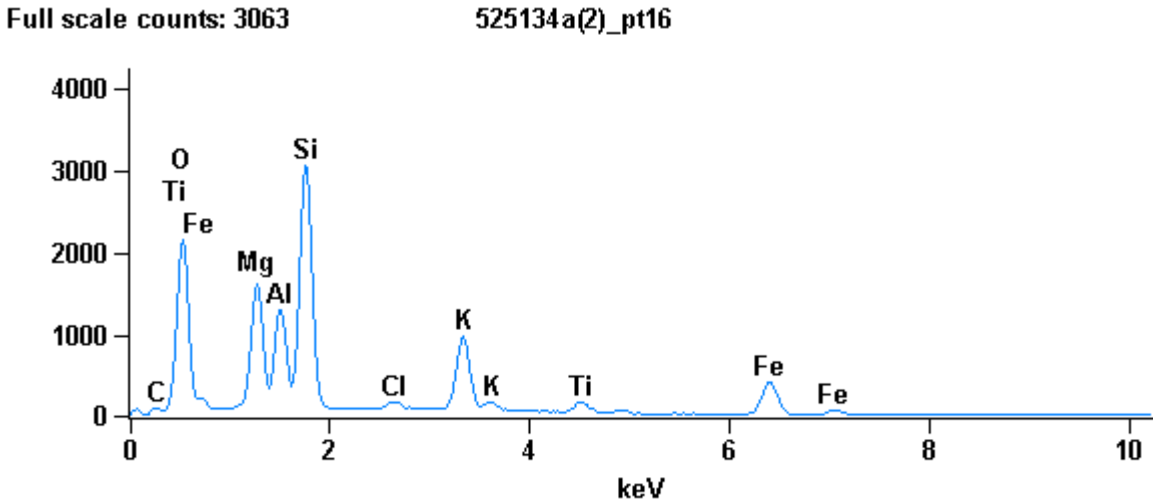
Full scale counts: 3063
525134a(2)_pt16
4000
3000
2000
1000
0
O
Ti
Fe
Si
Mg
Al
K
C
Cl
K
Ti
Fe
Fe
0
2
4
6
8
10
keV

Weight %

	O-K	Na-K	Mg-K	Al-K	Si-K	P-K	S-K	Cl-K	K-K	Ca-K	Ti-K	Fe-K	Zn-K
525134a(2)_pt1	50.37S			0.06			27.20		0.05			22.31	
525134a(2)_pt2	43.22S	1.19	8.65	4.60	21.32			0.24	1.06	8.74	1.30	9.67	
525134a(2)_pt3	50.31S			0.09			27.09					22.51	
525134a(2)_pt4	30.24S			0.35	0.14							69.27	
525134a(2)_pt5	53.26S				46.74								
525134a(2)_pt6	34.15S		0.55	3.64	2.16		2.36					57.14	
525134a(2)_pt7	50.31S			0.08			27.09					22.53	
525134a(2)_pt8	42.48S		10.80	7.36	18.81			0.52	7.58		2.10	10.34	
525134a(2)_pt9	39.42S			0.11	0.28	17.70		1.79		40.10			0.60
525134a(2)_pt10	30.76S			1.35	0.55							67.34	
525134a(2)_pt11	53.26S				46.74								
525134a(2)_pt12	50.25S			0.10			27.00					22.65	
525134a(2)_pt13	50.27S			0.07			27.10		0.21			22.35	
525134a(2)_pt14	53.15S				46.52							0.33	
525134a(2)_pt15	42.77S		7.11	4.72	20.96			0.38	1.18	10.30	1.06	11.52	
525134a(2)_pt16	42.59S		10.96	7.63	18.97			0.59	7.42		1.54	10.31	

Atom %

	O-K	Na-K	Mg-K	Al-K	Si-K	P-K	S-K	Cl-K	K-K	Ca-K	Ti-K	Fe-K	Zn-K
525134a(2)_pt1	71.56			0.05			19.28		0.03			9.08	
525134a(2)_pt2	60.15	1.15	7.93	3.80	16.90			0.15	0.60	4.86	0.60	3.86	
525134a(2)_pt3	71.53			0.08			19.22					9.17	
525134a(2)_pt4	60.03			0.42	0.16							39.39	
525134a(2)_pt5	66.67				33.33								
525134a(2)_pt6	61.59		0.65	3.89	2.22		2.12					29.52	
525134a(2)_pt7	71.53			0.07			19.22					9.18	
525134a(2)_pt8	59.27		9.92	6.09	14.95			0.33	4.33		0.98	4.13	
525134a(2)_pt9	59.96			0.10	0.24	13.90		1.23		24.35			0.22
525134a(2)_pt10	60.12			1.57	0.61							37.70	
525134a(2)_pt11	66.67				33.33								
525134a(2)_pt12	71.51			0.08			19.18					9.24	
525134a(2)_pt13	71.49			0.05			19.23		0.12			9.10	
525134a(2)_pt14	66.65				33.23							0.12	
525134a(2)_pt15	60.57		6.63	3.96	16.91			0.24	0.69	5.83	0.50	4.68	
525134a(2)_pt16	59.23		10.03	6.30	15.03			0.37	4.22		0.72	4.11	

Compound %

		Na2O	MgO	Al2O3	SiO2	P2O5	SO3	Cl	K2O	CaO	TiO2	Fe2O3	ZnO
525134a(2)_pt1	0.00			0.12			67.92		0.06			31.90	
525134a(2)_pt2	0.00	1.60	14.35	8.69	45.61			0.24	1.28	12.23	2.17	13.83	
525134a(2)_pt3	0.00			0.17			67.65					32.18	
525134a(2)_pt4	0.00			0.67	0.30							99.03	
525134a(2)_pt5	0.00				100.00								
525134a(2)_pt6	0.00		0.90	6.88	4.63		5.89					81.69	
525134a(2)_pt7	0.00			0.16			67.64					32.21	
525134a(2)_pt8	0.00		17.92	13.90	40.24			0.52	9.13		3.50	14.79	
525134a(2)_pt9	0.00			0.20	0.60	40.55		1.79		56.11			0.75
525134a(2)_pt10	0.00			2.56	1.17							96.28	
525134a(2)_pt11	0.00				100.00								
525134a(2)_pt12	0.00			0.18			67.43					32.39	
525134a(2)_pt13	0.00			0.12			67.66		0.26			31.95	
525134a(2)_pt14	0.00				99.52							0.48	
525134a(2)_pt15	0.00		11.79	8.91	44.83			0.38	1.42	14.42	1.76	16.48	
525134a(2)_pt16	0.00		18.17	14.42	40.58			0.59	8.93		2.57	14.74	

Minerals, 525134a(2)

pt1: Pyrite
pt2: Amphibole - hornblende
pt3: Pyrite
pt4: Fe-oxide
pt5: Quartz
pt6: Mixed signal/edge effect
pt7: Pyrite
pt8: Biotite
pt9: Apatite
pt10: Fe-oxide
pt11: Quartz
pt12: Pyrite
pt13: Pyrite
pt14: Quartz
pt15: Amphibolite - hornblende
pt16: Biotite

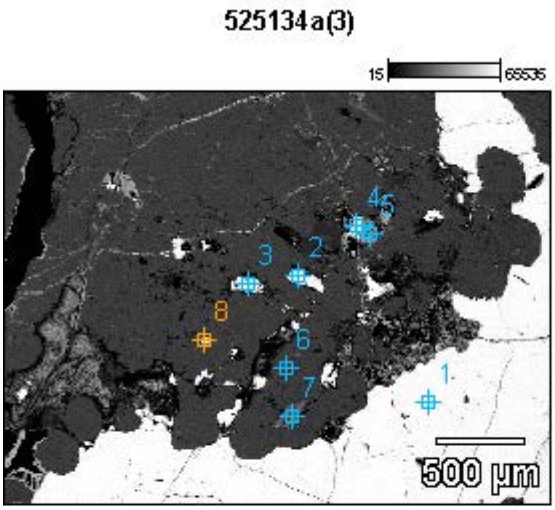

Image name: 525134a(3)
Magnification: 39

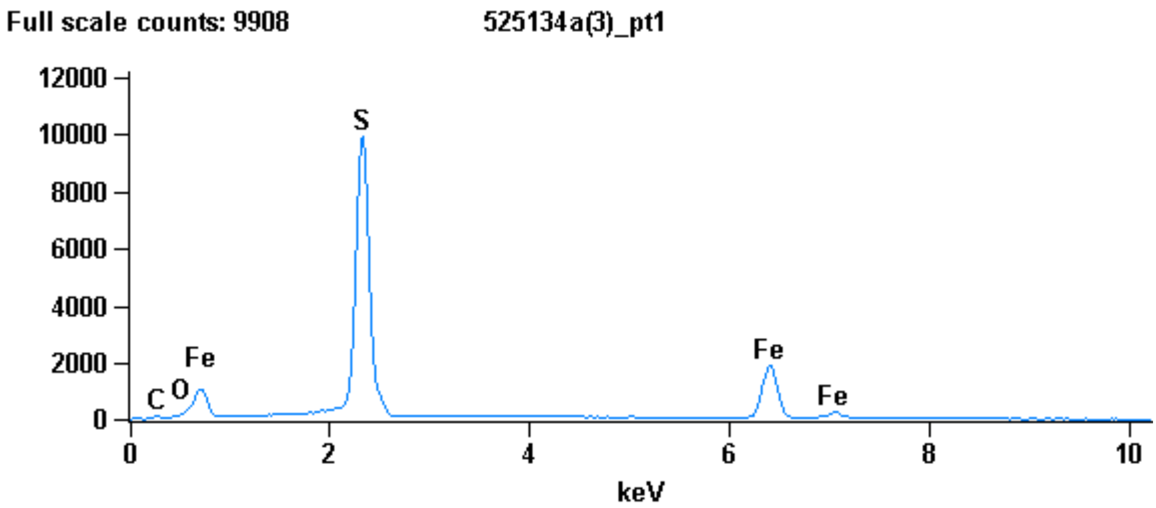

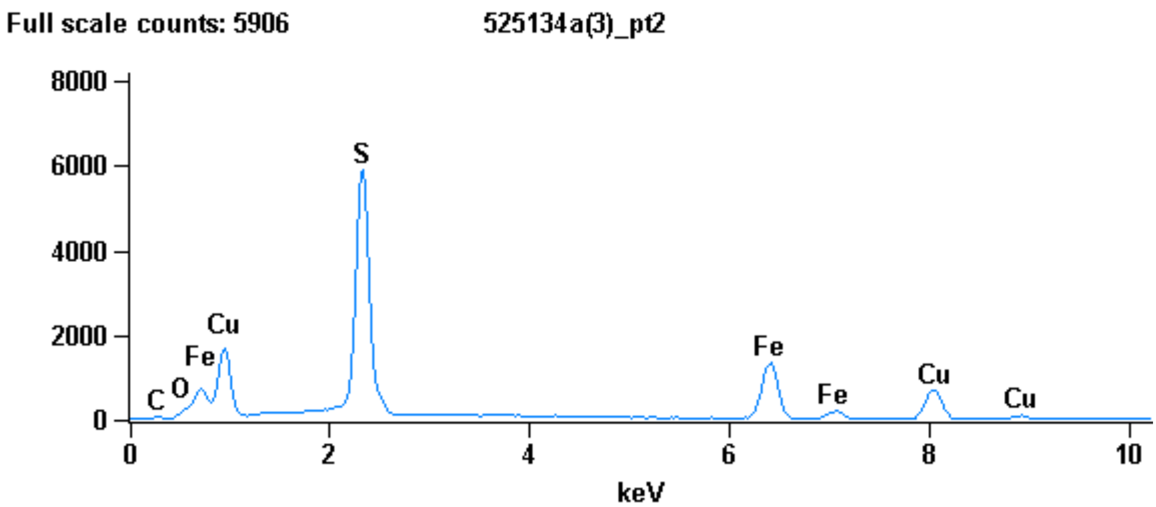

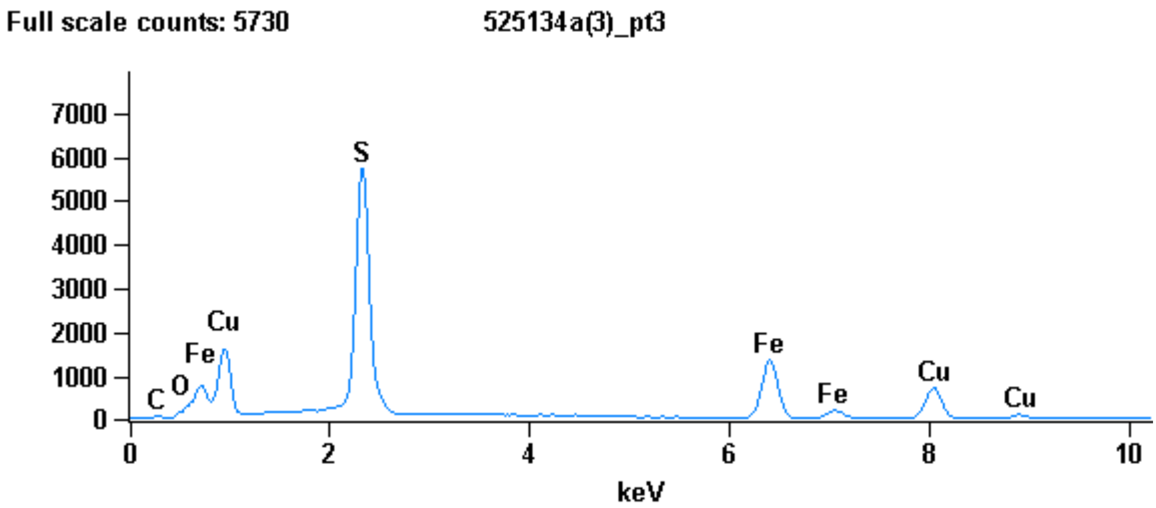
Full scale counts: 5730
525134a(3)_pt3
7000
6000
5000
4000
3000
2000
1000
0
S
Cu
Fe
O
C
Fe
Fe
Cu
Cu
0
2
4
6
8
10
keV

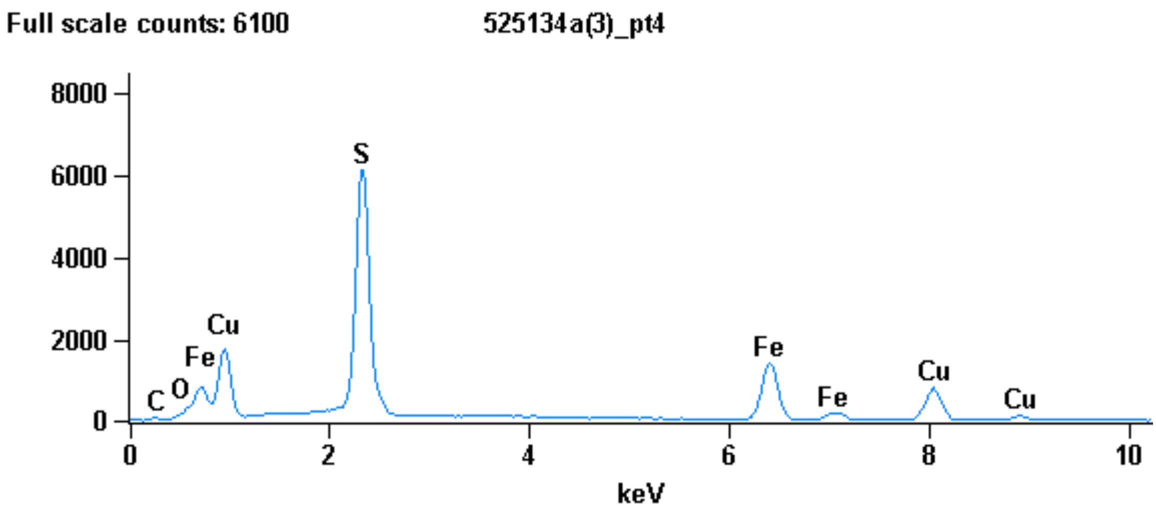
Full scale counts: 6100
525134a(3)_pt4
8000
6000
4000
2000
0
S
Cu
Fe
O
C
Fe
Fe
Cu
Cu
0
2
4
6
8
10
keV

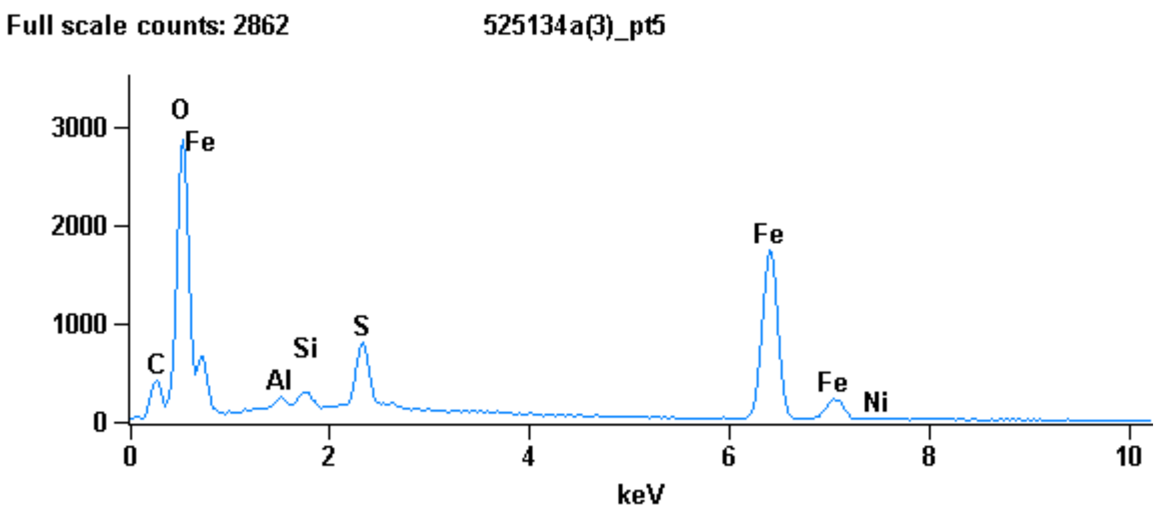
Full scale counts: 2862
525134a(3)_pt5
3000
2000
1000
0
O
Fe
C
Al
Si
S
Fe
Fe
Ni
0
2
4
6
8
10
keV

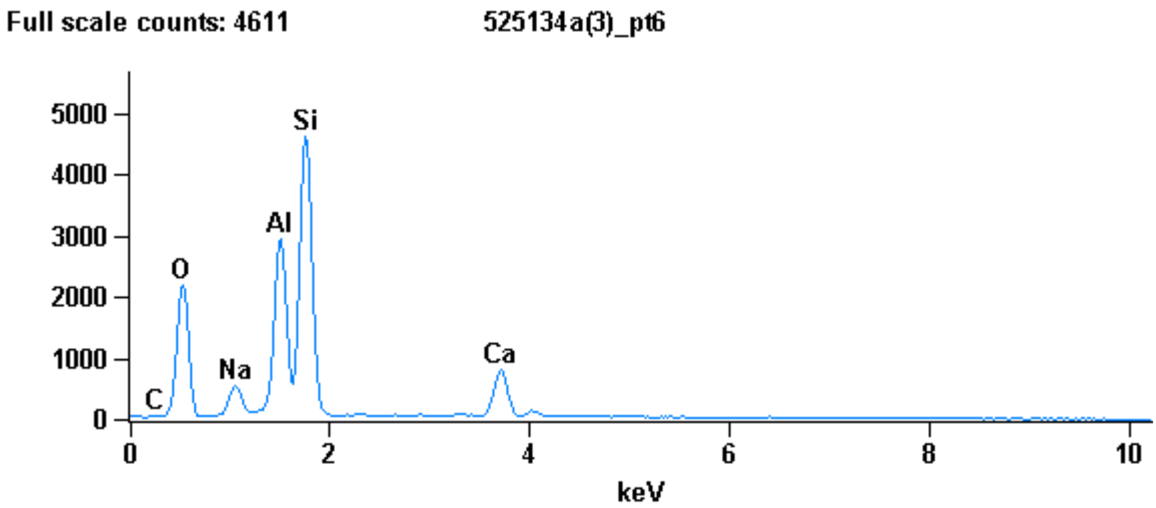
Full scale counts: 4611
525134a(3)_pt6
5000
4000
3000
2000
1000
0
Si
Al
O
Na
C
Ca
0
2
4
6
8
10
keV

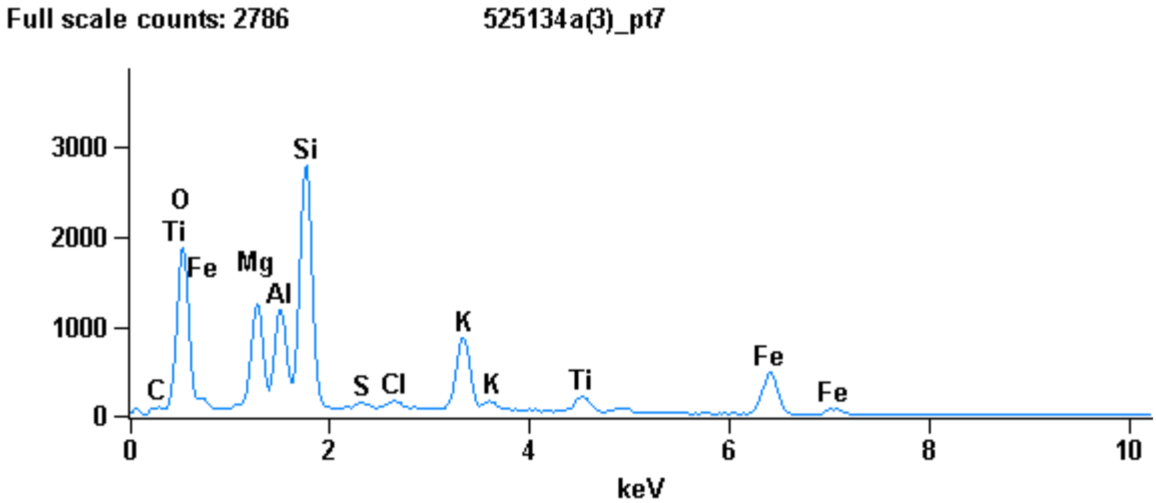
Full scale counts: 2786
525134a(3)_pt7
3000
2000
1000
0
Si
O
Ti
Fe
Mg
Al
K
C
S
Cl
K
Ti
Fe
Fe
0
2
4
6
8
10
keV

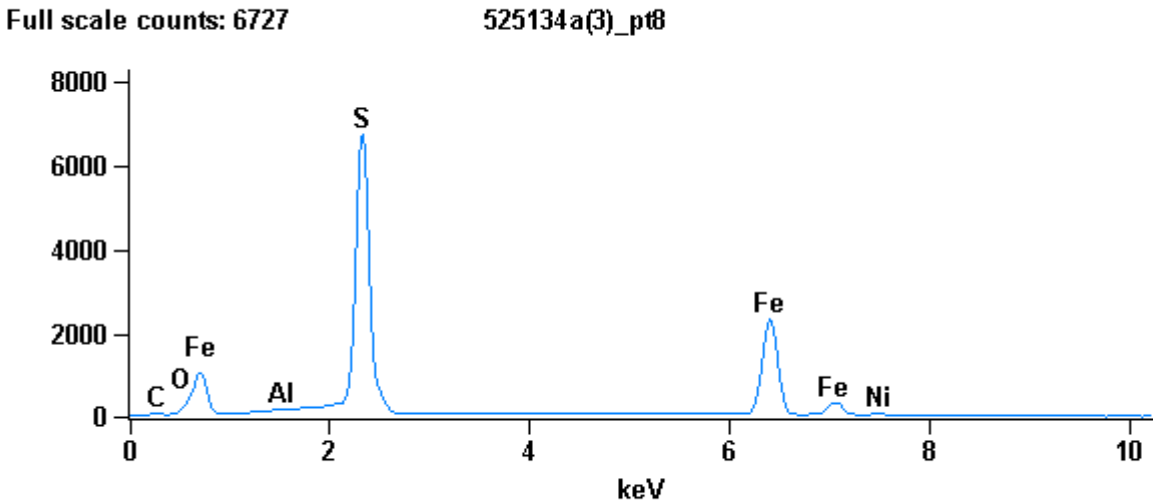
Full scale counts: 6727
525134a(3)_pt8
8000
6000
4000
2000
0
S
Fe
Fe
C
O
Al
Fe
Ni
0
2
4
6
8
10
keV

Weight %

	O-K	Na-K	Mg-K	Al-K	Si-K	S-K	Cl-K	K-K	Ca-K	Ti-K	Fe-K	Ni-K	Cu-K
525134a(3)_pt1	50.53S					27.43					22.04		
525134a(3)_pt2	41.47S					20.82					18.26		19.44
525134a(3)_pt3	41.21S					20.58					18.40		19.81
525134a(3)_pt4	41.45S					20.91					17.79		19.85
525134a(3)_pt5	35.48S			0.87	1.37	6.11					55.34	0.83	
525134a(3)_pt6	47.49S	4.55		14.59	26.49				6.88				
525134a(3)_pt7	42.20S		9.15	7.35	18.04	0.30	0.60	7.14		2.63	12.58		
525134a(3)_pt8	46.29S			0.08		21.82					31.04	0.78	

Atom %

	O-K	Na-K	Mg-K	Al-K	Si-K	S-K	Cl-K	K-K	Ca-K	Ti-K	Fe-K	Ni-K	Cu-K
525134a(3)_pt1	71.64					19.41					8.95		
525134a(3)_pt2	66.90					16.76					8.44		7.90
525134a(3)_pt3	66.75					16.64					8.54		8.08
525134a(3)_pt4	66.88					16.84					8.22		8.06
525134a(3)_pt5	63.47			0.92	1.39	5.45					28.36	0.40	
525134a(3)_pt6	61.56	4.10		11.22	19.56				3.56				
525134a(3)_pt7	59.70		8.52	6.17	14.54	0.21	0.38	4.13		1.24	5.10		
525134a(3)_pt8	69.79			0.07		16.42					13.41	0.32	

Compound %

		Na2O	MgO	Al2O3	SiO2	SO3	Cl	K2O	CaO	TiO2	Fe2O3	NiO	Cu2O
525134a(3)_pt1	0.00					68.49					31.51		
525134a(3)_pt2	0.00					52.00					26.11		21.89
525134a(3)_pt3	0.00					51.40					26.30		22.30
525134a(3)_pt4	0.00					52.21					25.44		22.35
525134a(3)_pt5	0.00			1.64	2.92	15.25					79.12	1.06	
525134a(3)_pt6	0.00	6.13		27.57	56.67				9.63				
525134a(3)_pt7	0.00		15.18	13.90	38.60	0.76	0.60	8.60		4.38	17.99		
525134a(3)_pt8	0.00			0.15		54.48					44.38	0.99	

Minerals, 525134a(3)

pt1: Pyrite
pt2: Chalcopyrite
pt3: Chalcopyrite
pt4: Chalcopyrite
pt5: Mixed signal/edge effect
pt6: Feldspar - plagioclase
pt7: Biotite (+ edge effect)
pt8: Pyrrhotite

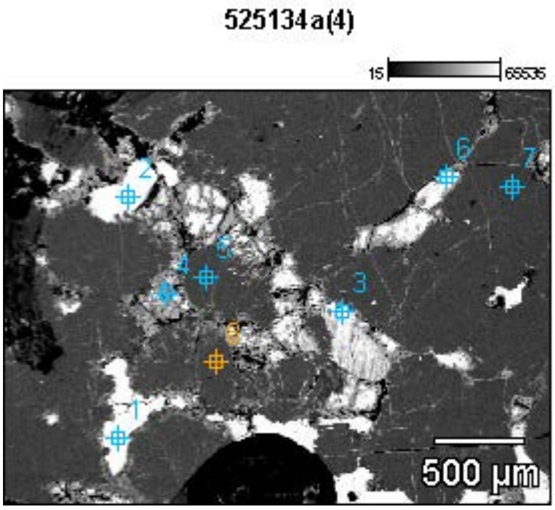

Image name: 525134a(4)
Magnification: 40

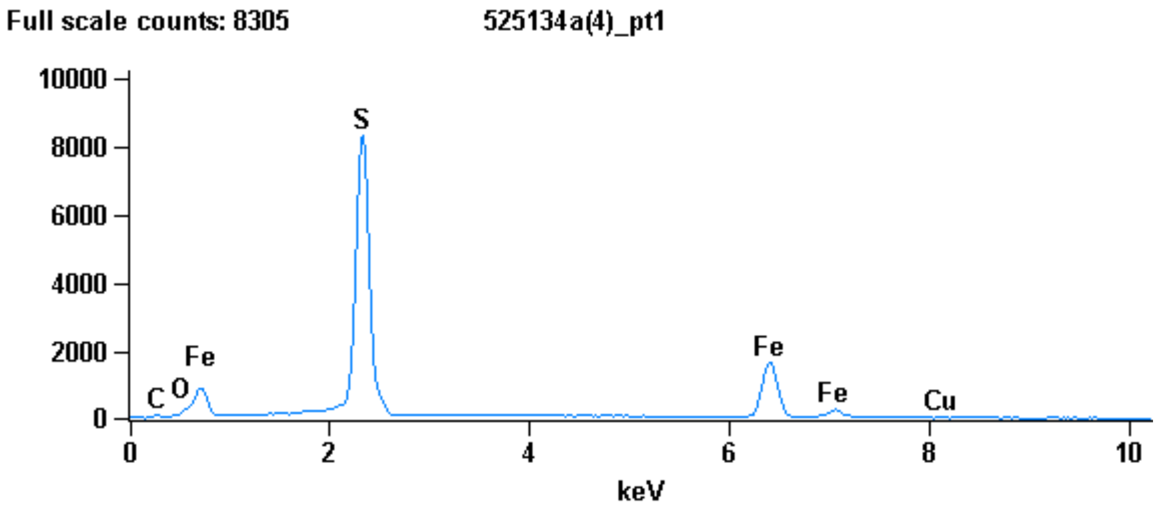

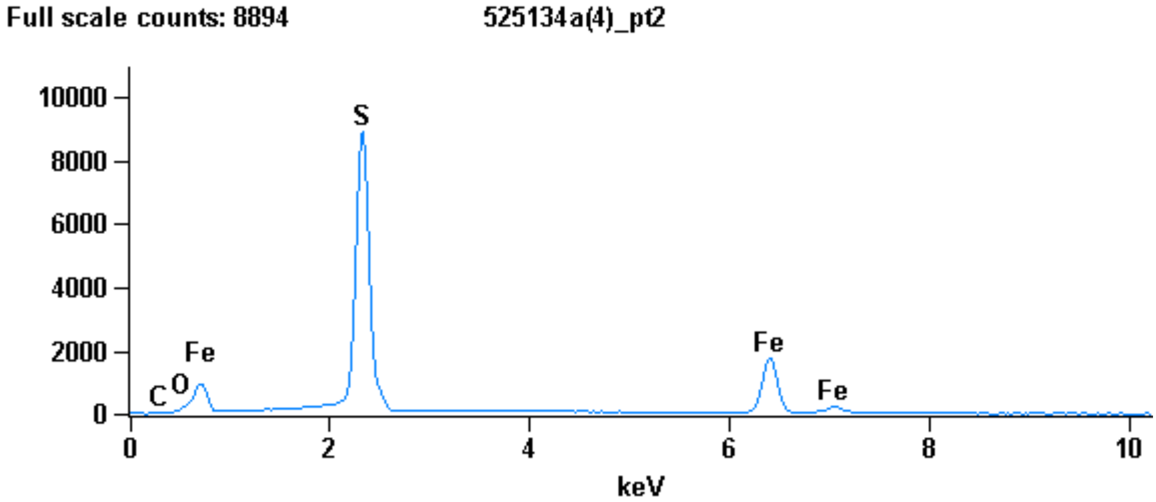

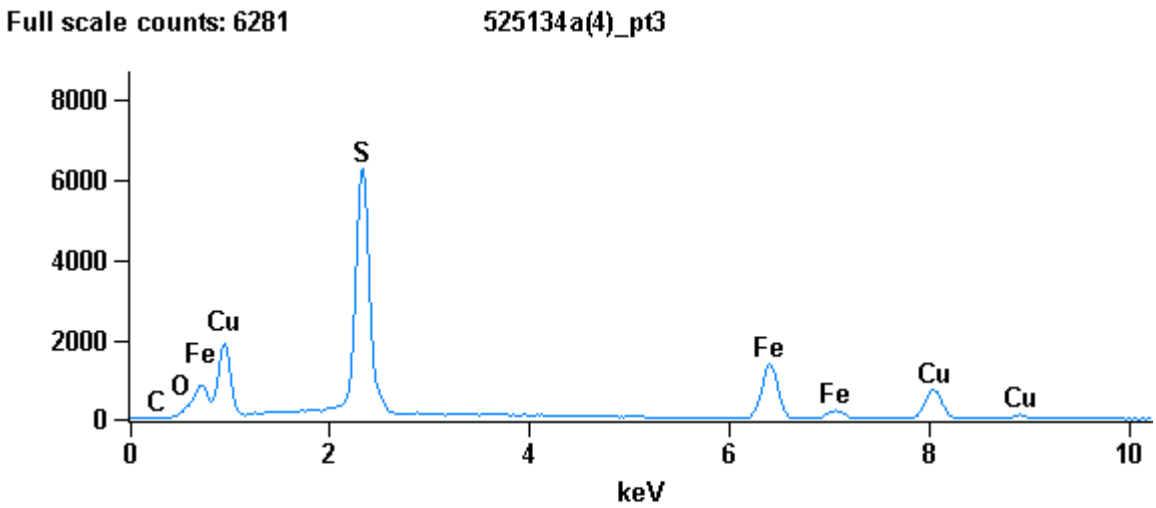
Full scale counts: 6281
525134a(4)_pt3
8000
6000
4000
2000
0
S
Cu
Fe
O
C
Fe
Fe
Cu
Cu
0
2
4
6
8
10
keV

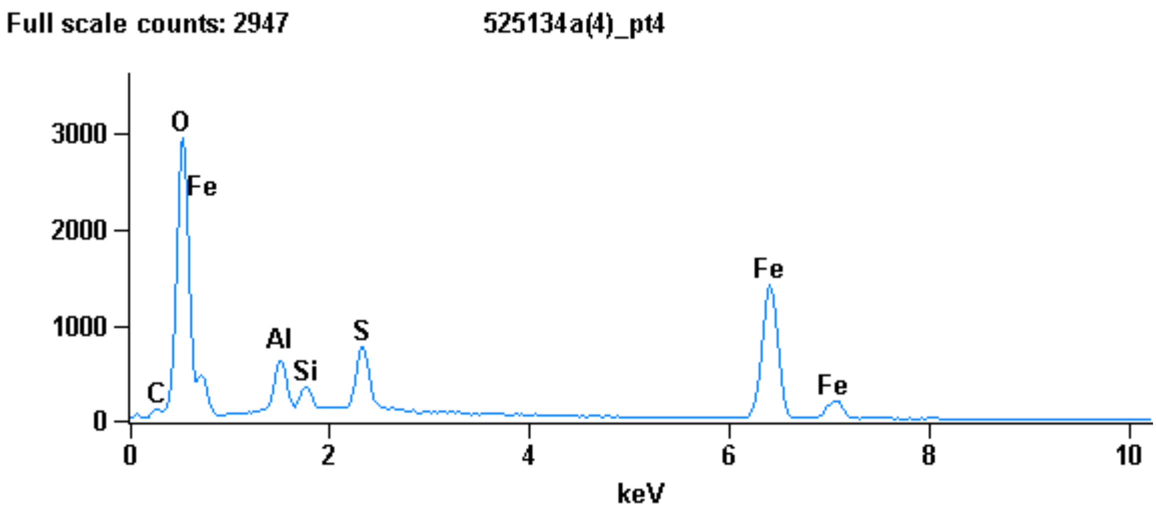
Full scale counts: 2947
525134a(4)_pt4
3000
2000
1000
0
O
Fe
Al
Si
S
C
Fe
Fe
0
2
4
6
8
10
keV

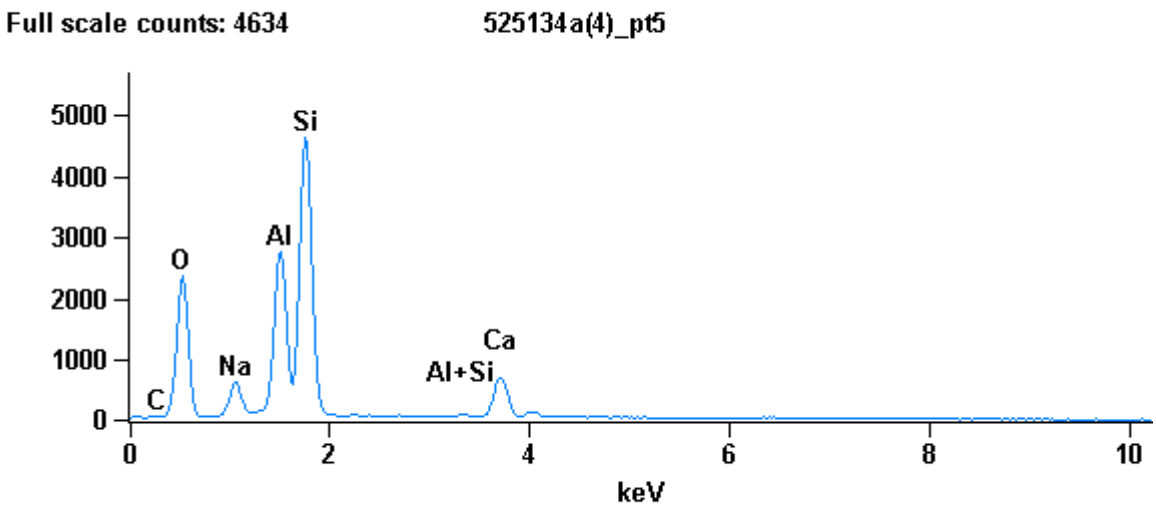
Full scale counts: 4634
525134a(4)_pt5
5000
4000
3000
2000
1000
0
Si
Al
O
Na
C
Ca
Al+Si
0
2
4
6
8
10
keV

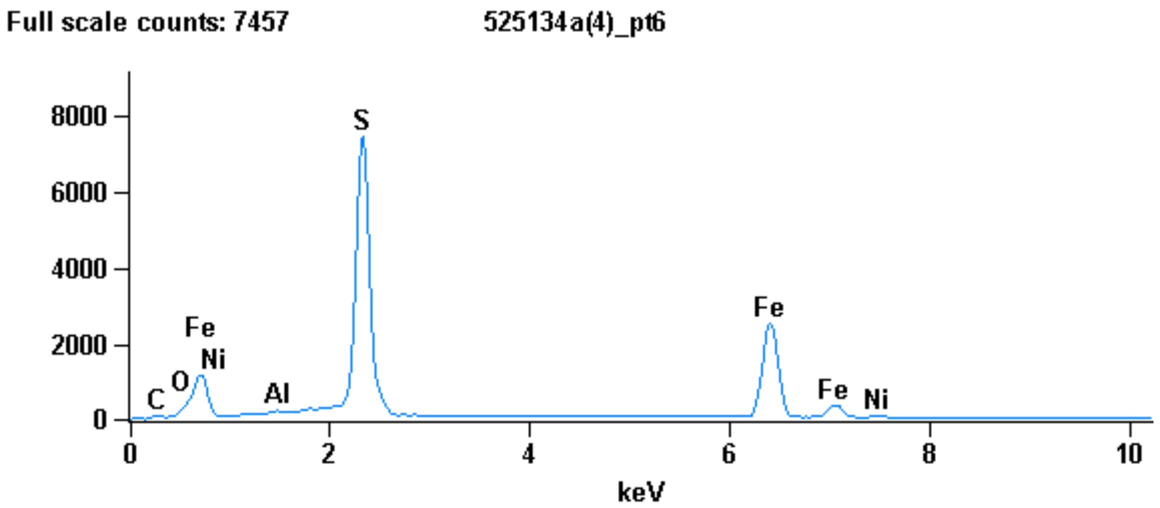
Full scale counts: 7457
525134a(4)_pt6
8000
6000
4000
2000
0
S
Fe
Ni
C
O
Al
Fe
Fe
Ni
0
2
4
6
8
10
keV

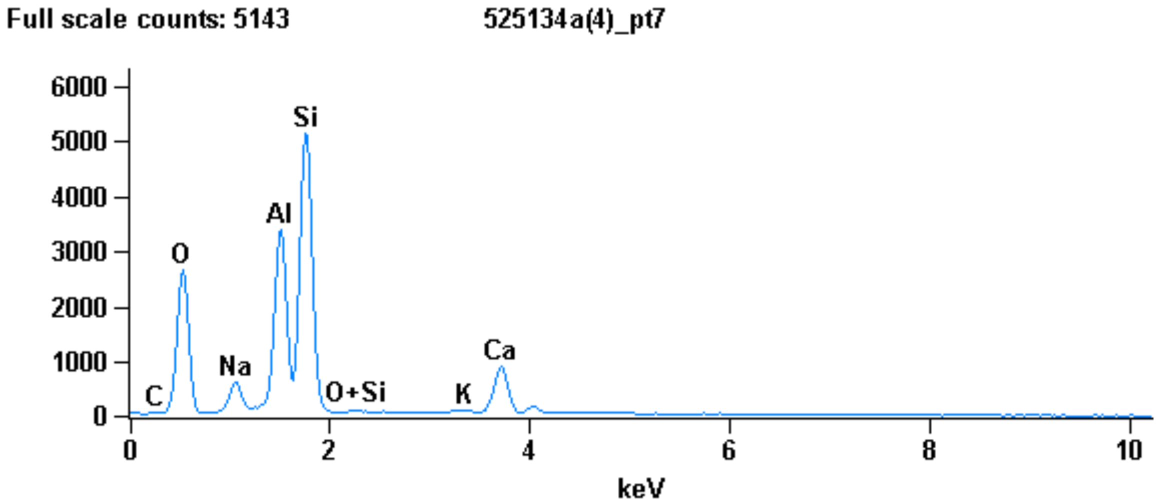
Full scale counts: 5143
525134a(4)_pt7
6000
5000
4000
3000
2000
1000
0
Si
Al
O
Na
C
O+Si
K
Ca
0
2
4
6
8
10
keV

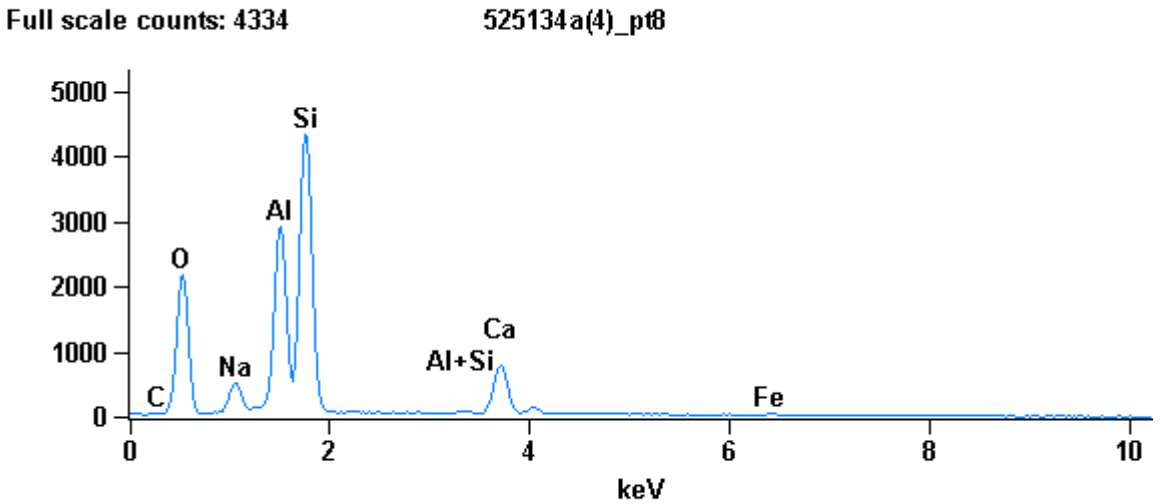
Full scale counts: 4334
525134a(4)_pt8
5000
4000
3000
2000
1000
0
Si
Al
O
Na
C
Ca
Al+Si
Fe
0
2
4
6
8
10
keV

Weight %

	O-K	Na-K	Al-K	Si-K	S-K	K-K	Ca-K	Fe-K	Ni-K	Cu-K
525134a(4)_pt1	50.22S				27.03			22.68		0.07
525134a(4)_pt2	50.33S				27.16			22.51		
525134a(4)_pt3	41.74S				21.18			17.65		19.42
525134a(4)_pt4	37.77S		5.83	2.25	6.33			47.82		
525134a(4)_pt5	47.66S	4.83	14.27	27.04			6.20			
525134a(4)_pt6	46.33S		0.10		21.86			30.97	0.73	
525134a(4)_pt7	47.46S	4.35	14.81	26.33		0.19	6.86			
525134a(4)_pt8	47.30S	4.26	14.84	25.93			7.25	0.42		

Atom %

	O-K	Na-K	Al-K	Si-K	S-K	K-K	Ca-K	Fe-K	Ni-K	Cu-K
525134a(4)_pt1	71.51				19.21			9.25		0.03
525134a(4)_pt2	71.56				19.27			9.17		
525134a(4)_pt3	67.05				16.98			8.12		7.85
525134a(4)_pt4	63.62		5.82	2.16	5.32			23.08		
525134a(4)_pt5	61.60	4.35	10.94	19.91			3.20			
525134a(4)_pt6	69.80		0.09		16.44			13.37	0.30	
525134a(4)_pt7	61.57	3.92	11.39	19.46		0.10	3.55			
525134a(4)_pt8	61.55	3.85	11.45	19.22			3.76	0.16		

Compound %

		Na2O	Al2O3	SiO2	SO3	K2O	CaO	Fe2O3	NiO	Cu2O
525134a(4)_pt1	0.00				67.50			32.42		0.08
525134a(4)_pt2	0.00				67.81			32.19		
525134a(4)_pt3	0.00				52.90			25.24		21.87
525134a(4)_pt4	0.00		11.01	4.82	15.80			68.38		
525134a(4)_pt5	0.00	6.51	26.96	57.85			8.68			
525134a(4)_pt6	0.00		0.19		54.60			44.28	0.94	
525134a(4)_pt7	0.00	5.86	27.98	56.32		0.23	9.60			
525134a(4)_pt8	0.00	5.74	28.05	55.47			10.14	0.60		

Minerals, 525134a(4)
pt1: Pyrite
pt2: Pyrite
pt3: Chalcopyrite
pt4: Mixed signal/edge effect
pt5: Feldspar - plagioclase
pt6: Pyrrhotite
pt7: Feldspar - plagioclase
pt8: Feldspar - plagioclase

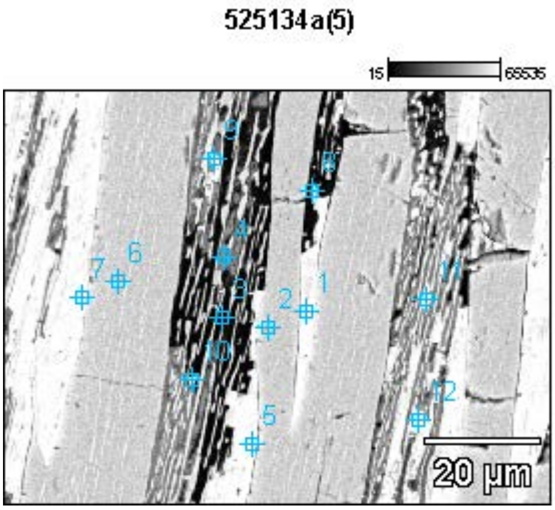

Image name: 525134a(5)
Magnification: 1295

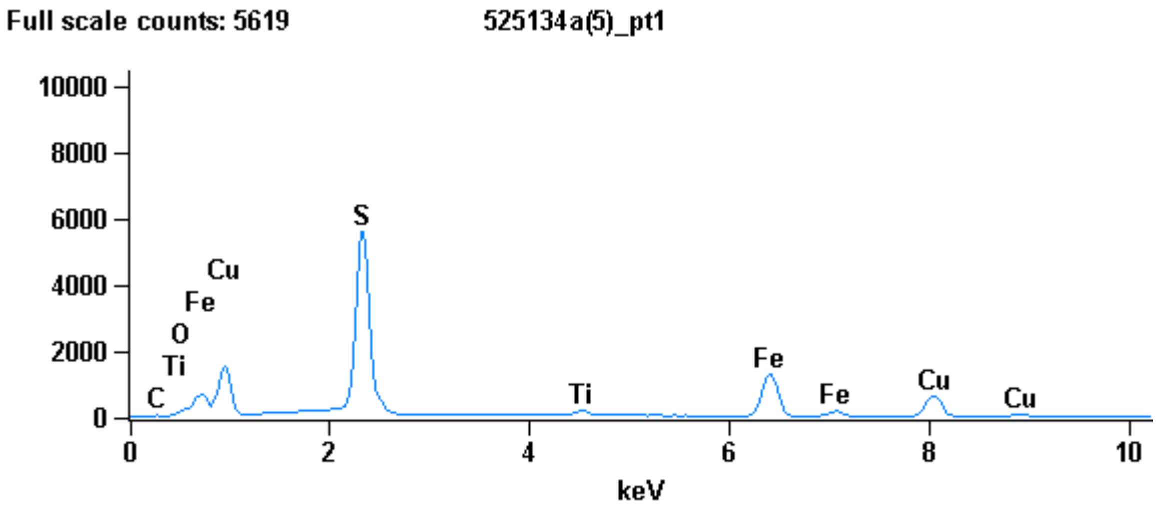

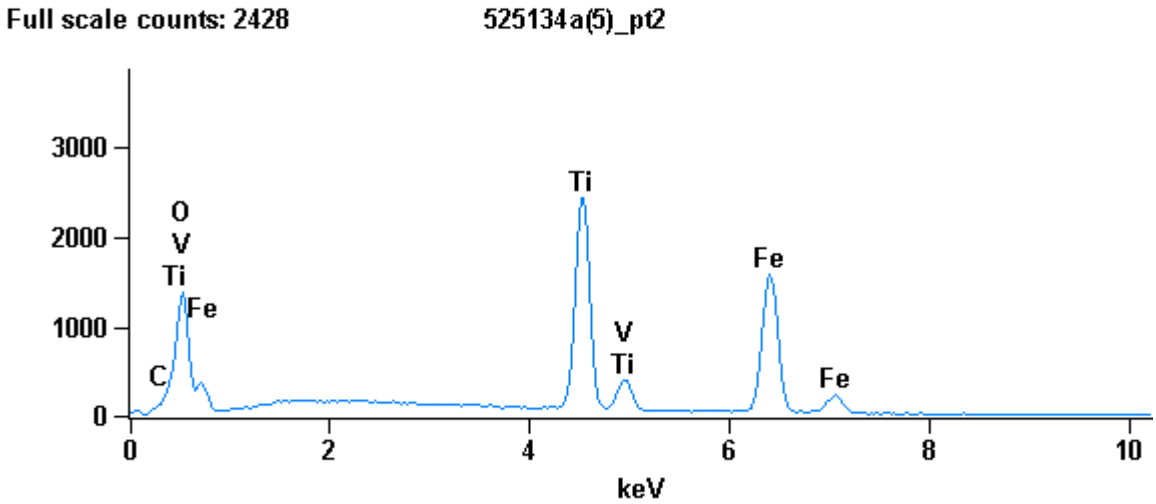

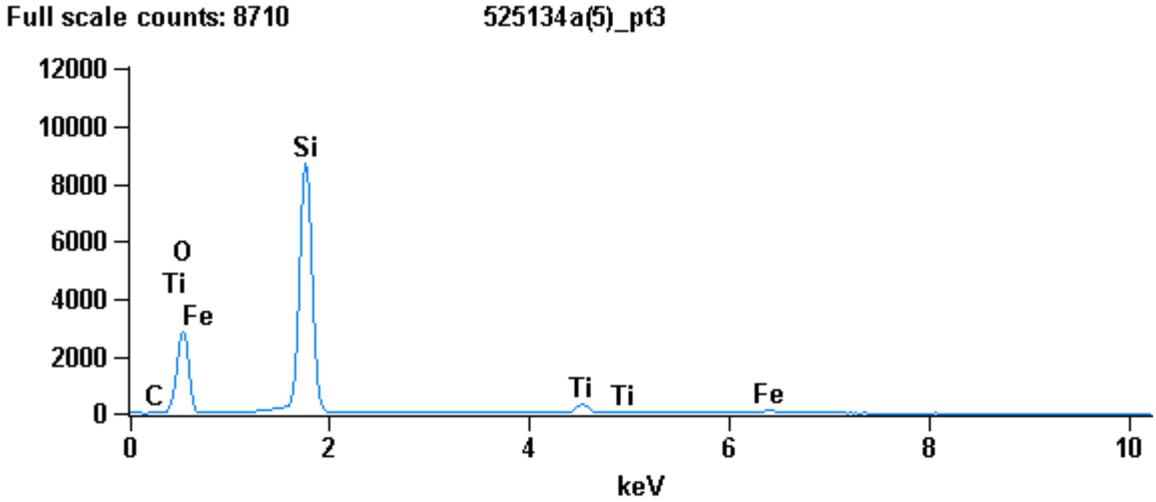
Full scale counts: 8710
525134a(5)_pt3
12000
10000
8000
6000
4000
2000
0
Si
O
Ti
Fe
C
Ti
Ti
Fe
0
2
4
6
8
10
keV

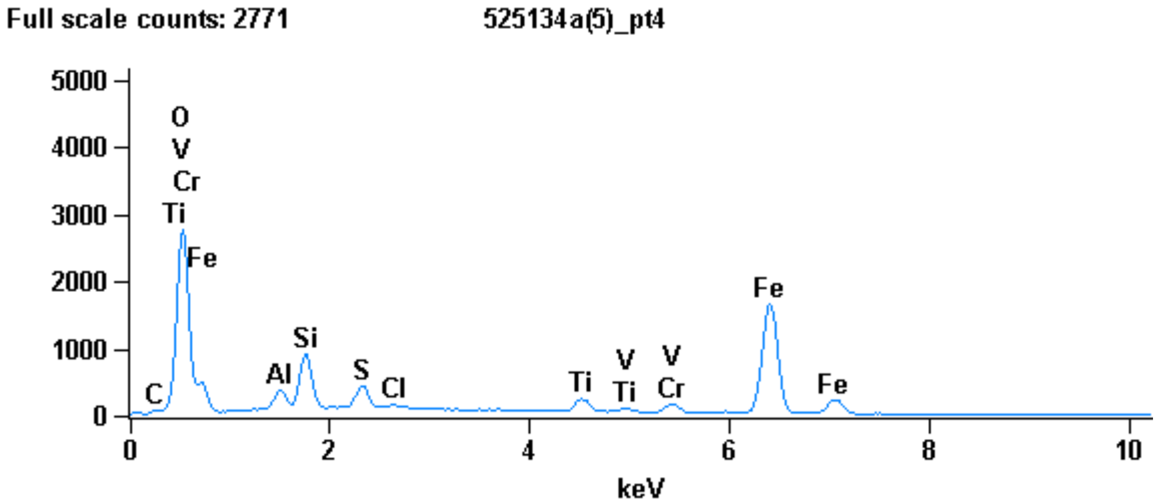
Full scale counts: 2771
525134a(5)_pt4
5000
4000
3000
2000
1000
0
O
V
Cr
Ti
Fe
C
Al
Si
S
Cl
Ti
V
Ti
V
Cr
Fe
Fe
0
2
4
6
8
10
keV

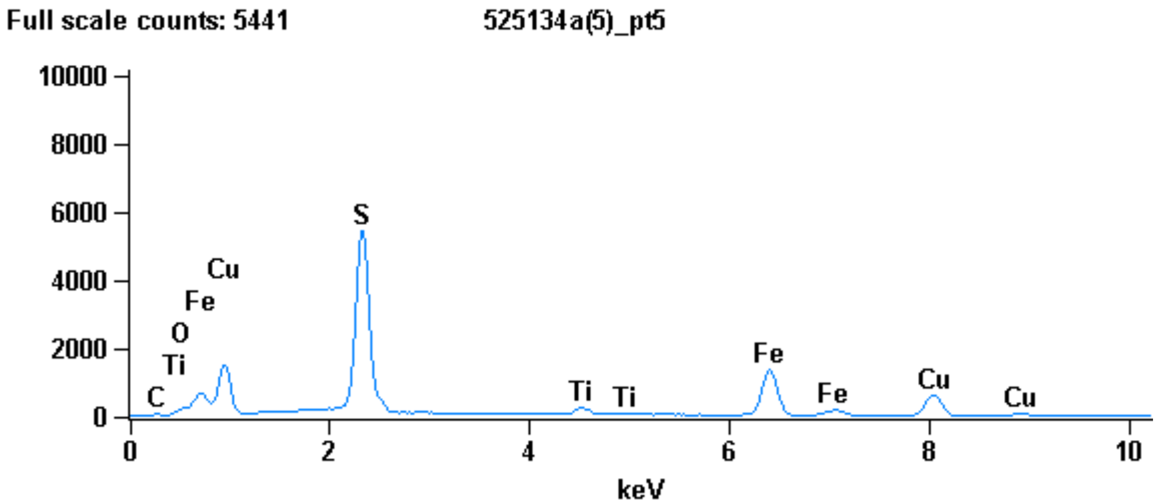
Full scale counts: 5441
525134a(5)_pt5
10000
8000
6000
4000
2000
0
S
Cu
Fe
O
Ti
C
Ti
Ti
Fe
Fe
Cu
Cu
0
2
4
6
8
10
keV

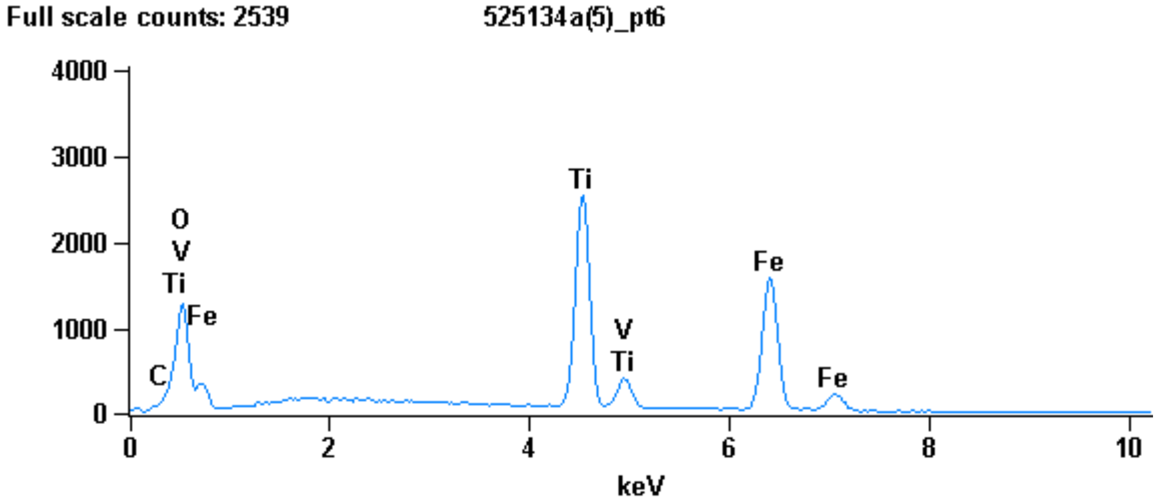
Full scale counts: 2539
525134a(5)_pt6
4000
3000
2000
1000
0
O
V
Ti
Fe
C
Ti
V
Ti
Fe
Fe
0
2
4
6
8
10
keV

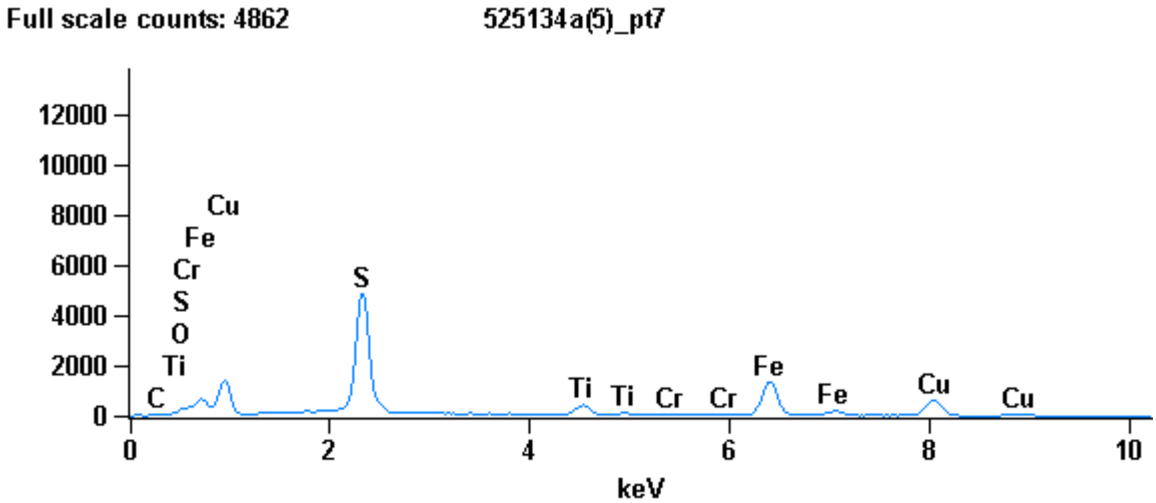
Full scale counts: 4862
525134a(5)_pt7
12000
10000
8000
6000
4000
2000
0
Cu
Fe
Cr
S
O
Ti
C
S
Ti
Ti
Cr
Cr
Fe
Fe
Cu
Cu
0
2
4
6
8
10
keV

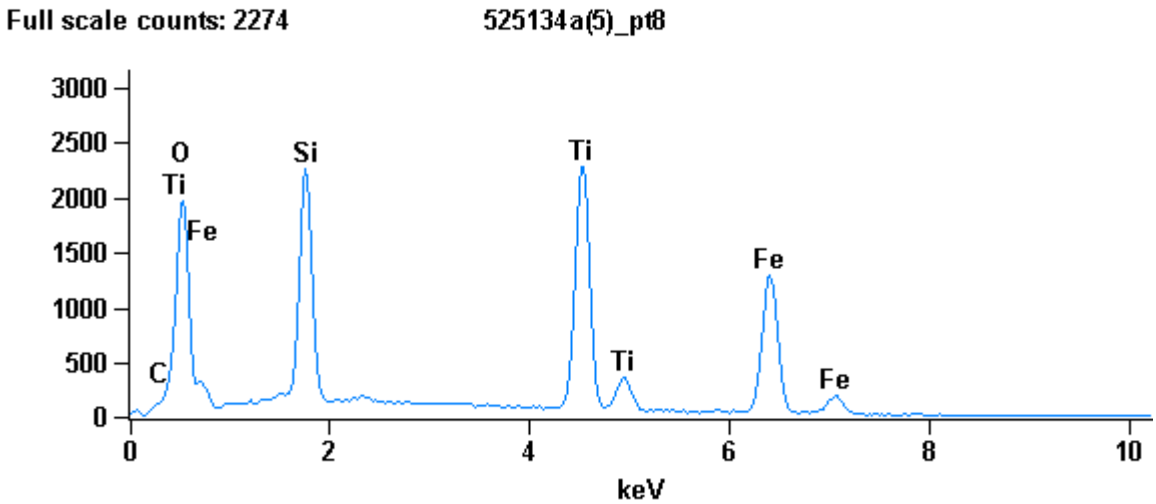
Full scale counts: 2274
525134a(5)_pt8
3000
2500
2000
1500
1000
500
0
O
Ti
Fe
C
Si
Ti
Ti
Fe
Fe
0
2
4
6
8
10
keV

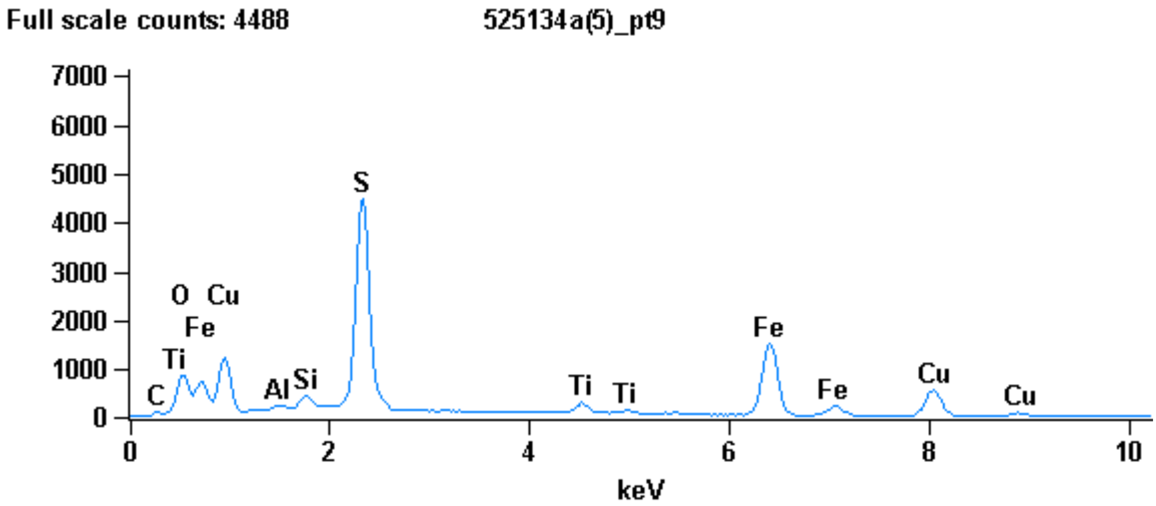
Full scale counts: 4488
525134a(5)_pt9
7000
6000
5000
4000
3000
2000
1000
0
S
O Cu
Fe
Ti
C
Al Si
Ti Ti
Fe
Fe
Cu
Cu
0
2
4
6
8
10
keV

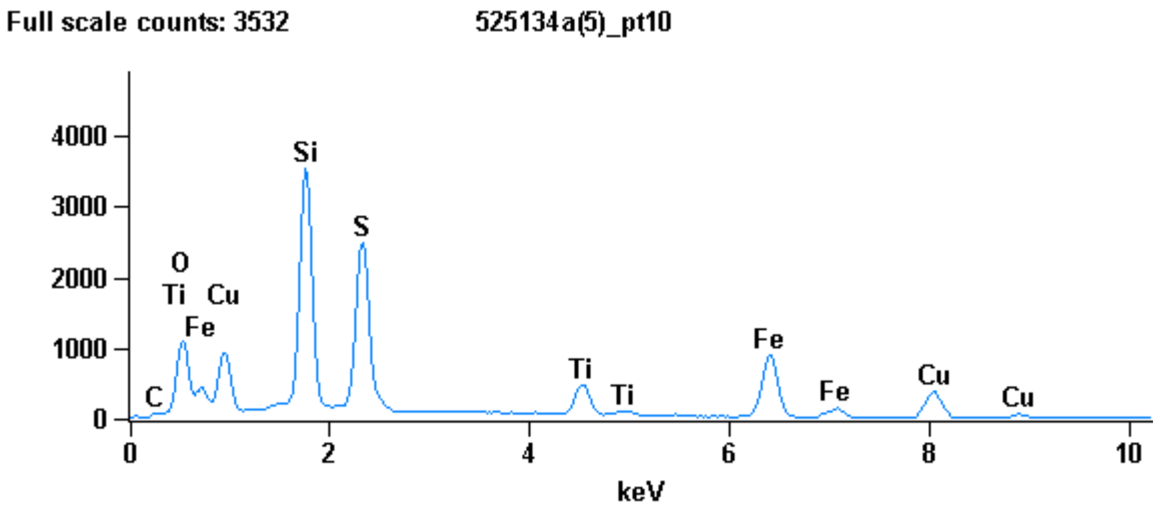
Full scale counts: 3532
525134a(5)_pt10
4000
3000
2000
1000
0
Si
S
O
Ti Cu
Fe
C
Ti
Ti
Fe
Fe
Cu
Cu
0
2
4
6
8
10
keV

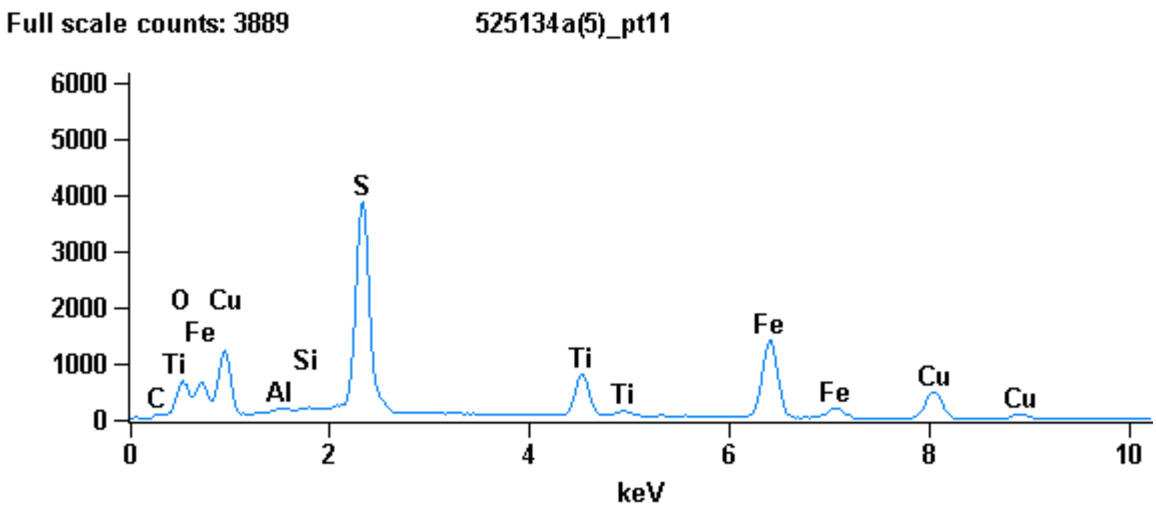
Full scale counts: 3889
525134a(5)_pt11
6000
5000
4000
3000
2000
1000
0
S
O Cu
Fe
Ti
C
Al
Si
Ti
Ti
Fe
Fe
Cu
Cu
0
2
4
6
8
10
keV

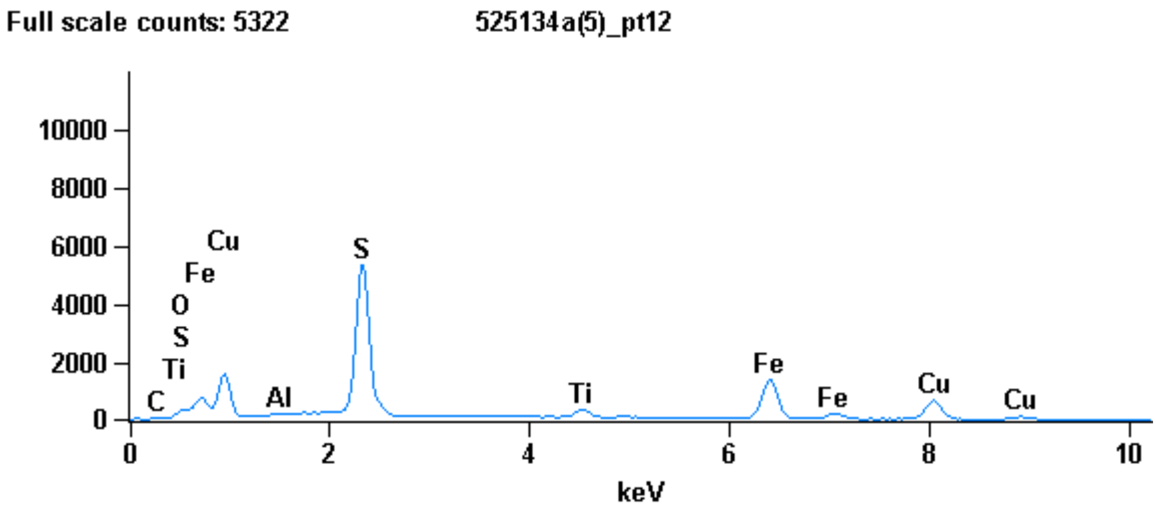

Weight %

	O-K	Al-K	Si-K	S-K	Cl-K	Ti-K	V-K	Cr-K	Fe-K	Cu-K
525134a(5)_pt1	41.44S			20.33		0.91			18.72	18.60
525134a(5)_pt2	34.68S					26.89	0.57		37.87	
525134a(5)_pt3	51.40S		41.77			3.69			3.13	
525134a(5)_pt4	36.17S	2.32	6.04	2.54	0.40	2.76	0.34	2.05	47.38	
525134a(5)_pt5	41.14S			19.89		1.49			18.60	18.89
525134a(5)_pt6	34.79S					27.96	0.28		36.98	
525134a(5)_pt7	40.25S			18.48		2.71			19.49	19.07
525134a(5)_pt8	39.26S		10.76			23.15			26.83	
525134a(5)_pt9	40.74S	0.35	0.98	17.77		1.65			22.27	16.24
525134a(5)_pt10	43.47S		13.80	11.63		3.79			14.37	12.94
525134a(5)_pt11	39.55S	0.23	0.12	15.96		5.78			21.79	16.57
525134a(5)_pt12	41.22S	0.15		19.65		1.97			18.72	18.30

Atom %

	O-K	Al-K	Si-K	S-K	Cl-K	Ti-K	V-K	Cr-K	Fe-K	Cu-K
525134a(5)_pt1	66.91			16.38		0.49			8.66	7.56
525134a(5)_pt2	63.41					16.42	0.32		19.84	
525134a(5)_pt3	66.47		30.77			1.59			1.16	
525134a(5)_pt4	62.72	2.39	5.97	2.20	0.32	1.60	0.18	1.09	23.54	
525134a(5)_pt5	66.73			16.10		0.81			8.64	7.72
525134a(5)_pt6	63.47					17.04	0.16		19.33	
525134a(5)_pt7	66.24			15.18		1.49			9.19	7.90
525134a(5)_pt8	64.56		10.08			12.72			12.64	
525134a(5)_pt9	66.36	0.34	0.91	14.44		0.90			10.39	6.66
525134a(5)_pt10	66.09		11.95	8.83		1.92			6.26	4.95
525134a(5)_pt11	65.84	0.23	0.11	13.26		3.22			10.39	6.95
525134a(5)_pt12	66.76	0.14		15.89		1.06			8.69	7.46

Compound %

		Al2O3	SiO2	SO3	Cl	TiO2	V2O5	Cr2O3	Fe2O3	Cu2O
525134a(5)_pt1	0.00			50.78		1.52			26.76	20.94
525134a(5)_pt2	0.00					44.85	1.01		54.14	
525134a(5)_pt3	0.00		89.37			6.15			4.48	
525134a(5)_pt4	0.00	4.39	12.92	6.35	0.40	4.60	0.60	2.99	67.74	
525134a(5)_pt5	0.00			49.66		2.48			26.59	21.27
525134a(5)_pt6	0.00					46.64	0.49		52.87	
525134a(5)_pt7	0.00			46.14		4.52			27.87	21.47
525134a(5)_pt8	0.00		23.02			38.62			38.37	
525134a(5)_pt9	0.00	0.66	2.09	44.37		2.75			31.84	18.29
525134a(5)_pt10	0.00		29.53	29.05		6.32			20.54	14.57
525134a(5)_pt11	0.00	0.44	0.26	39.84		9.65			31.15	18.66
525134a(5)_pt12	0.00	0.28		49.08		3.28			26.76	20.60

Minerals, 525134a(5)
pt1: Pyrrhotite
pt2: Ilmenite
pt3: Mixed signal/edge effect
pt4: Mixed signal/edge effect
pt5: Chalcopyrite
pt6: Ilmenite
pt7: Chalcopyrite
pt8: Mixed signal/edge effect
pt9: Chalcopyrite
pt10: Mixed signal/edge effect
pt11: Chalcopyrite
pt12: Chalcopyrite

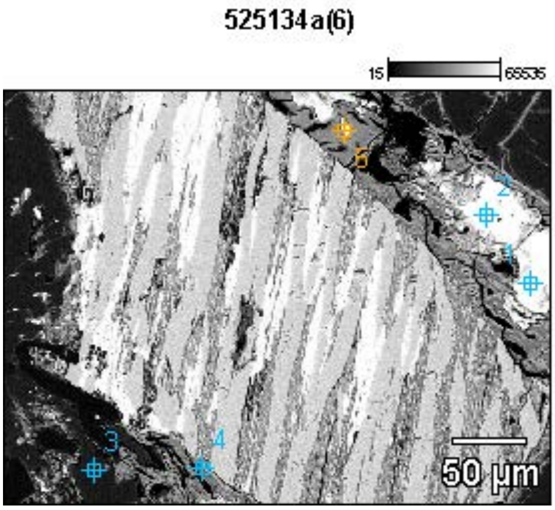

Image name: 525134a(6)
Magnification: 323

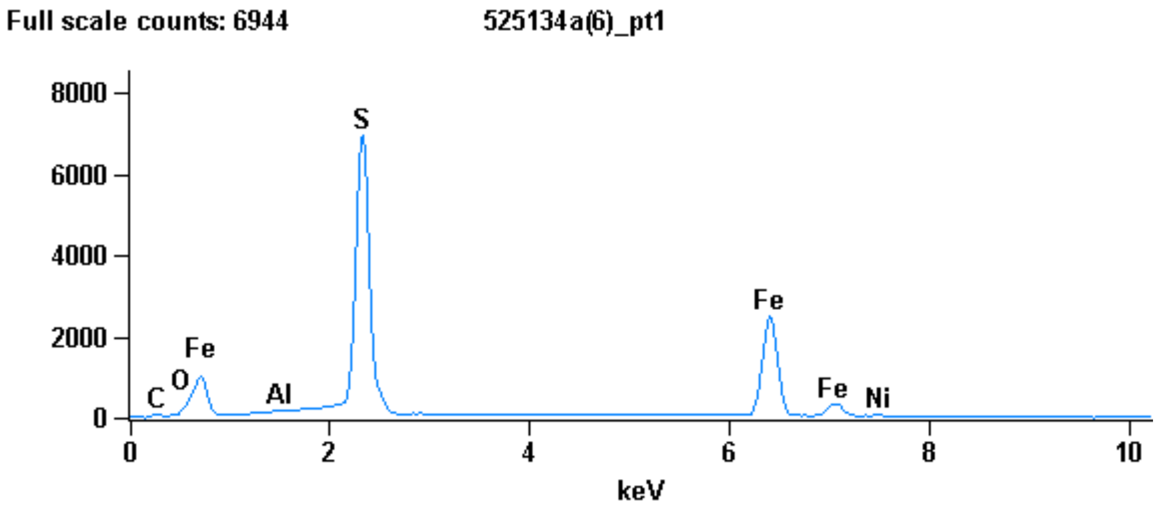

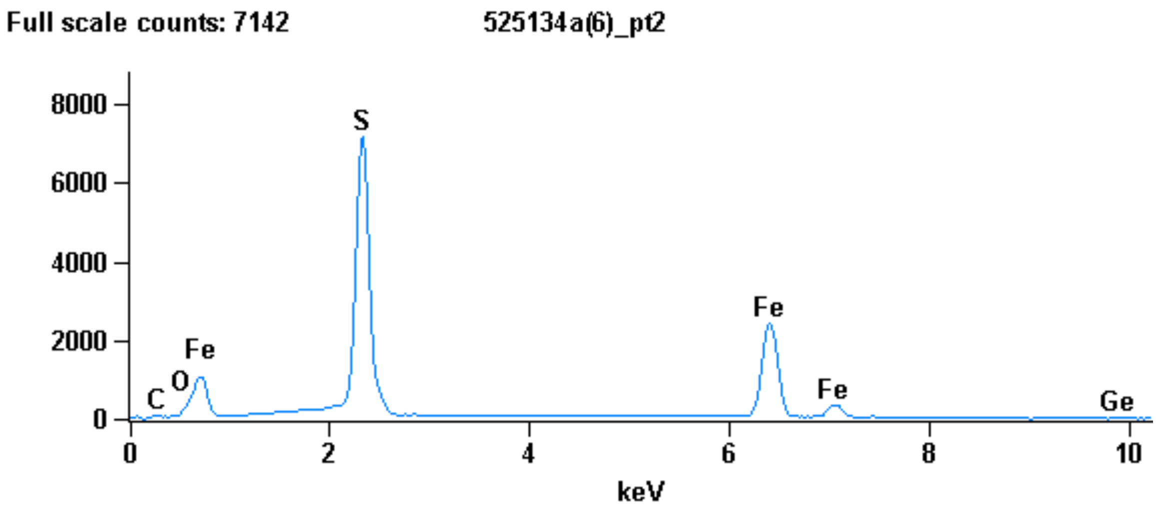

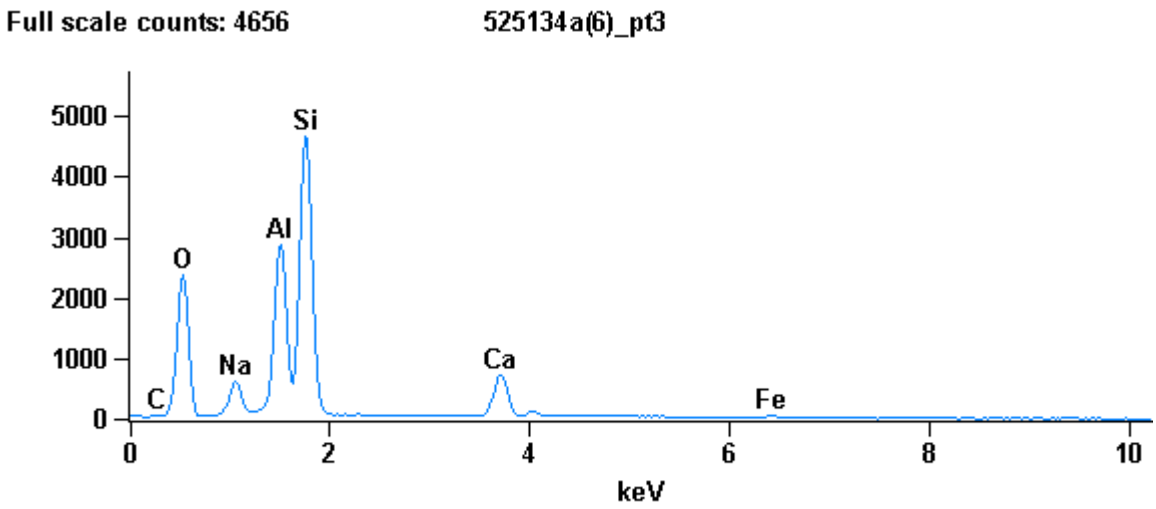
Full scale counts: 4656
525134a(6)_pt3
5000
4000
3000
2000
1000
0
Si
Al
O
Na
C
Ca
Fe
0
2
4
6
8
10
keV

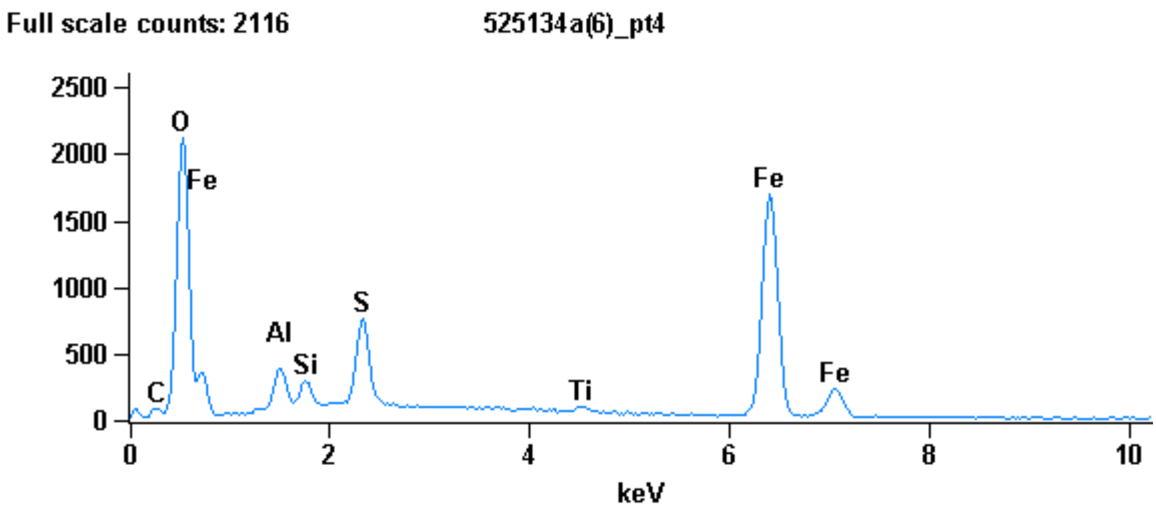
Full scale counts: 2116
525134a(6)_pt4
2500
2000
1500
1000
500
0
O
Fe
Fe
S
Al
Si
C
Ti
Fe
0
2
4
6
8
10
keV

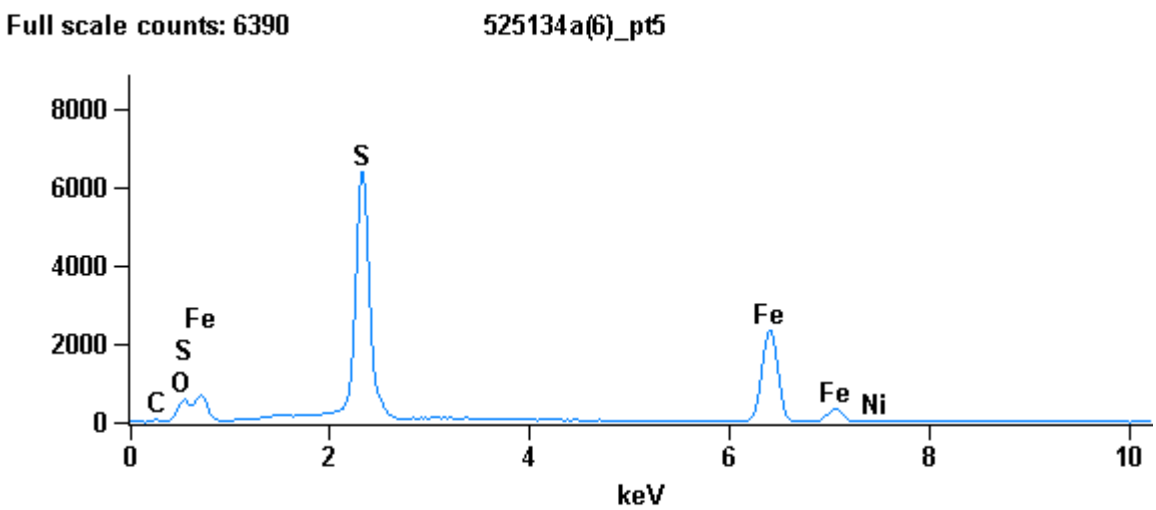
Full scale counts: 6390
525134a(6)_pt5
8000
6000
4000
2000
0
S
Fe
S
O
C
Fe
Fe
Ni
0
2
4
6
8
10
keV

Weight %

	O-K	Na-K	Al-K	Si-K	S-K	Ca-K	Ti-K	Fe-K	Ni-K	Ge-K	Au-L
525134a(6)_pt1	46.38S		0.07		21.90			31.23	0.42		
525134a(6)_pt2	46.37S				21.85			31.16		0.62	
525134a(6)_pt3	47.46S	4.88	14.46	26.53		6.25		0.42			
525134a(6)_pt4	36.27S		3.19	1.65	5.75		0.45	52.68			0.00
525134a(6)_pt5	45.82S				21.20			32.35	0.63		

Atom %

	O-K	Na-K	Al-K	Si-K	S-K	Ca-K	Ti-K	Fe-K	Ni-K	Ge-K	Au-L
525134a(6)_pt1	69.84		0.06		16.46			13.47	0.17		
525134a(6)_pt2	69.90				16.44			13.46		0.20	
525134a(6)_pt3	61.51	4.40	11.11	19.59		3.24		0.16			
525134a(6)_pt4	63.39		3.31	1.64	5.02		0.26	26.37			0.00
525134a(6)_pt5	69.59				16.07			14.08	0.26		

Compound %

		Na2O	Al2O3	SiO2	SO3	CaO	TiO2	Fe2O3	NiO	GeO2	Au
525134a(6)_pt1	0.00		0.12		54.69			44.66	0.53		
525134a(6)_pt2	0.00				54.56			44.56		0.89	
525134a(6)_pt3	0.00	6.57	27.32	56.75		8.75		0.61			
525134a(6)_pt4	0.00		6.04	3.53	14.37		0.76	75.31			0.00
525134a(6)_pt5	0.00				52.94			46.25	0.80		

Minerals, 525134a(6)

pt1: Pyrrhotite
pt2: Pyrrhotite
pt3: Feldspar - plagioclase
pt4: Mixed signal/edge effect
pt5: Pyrrhotite

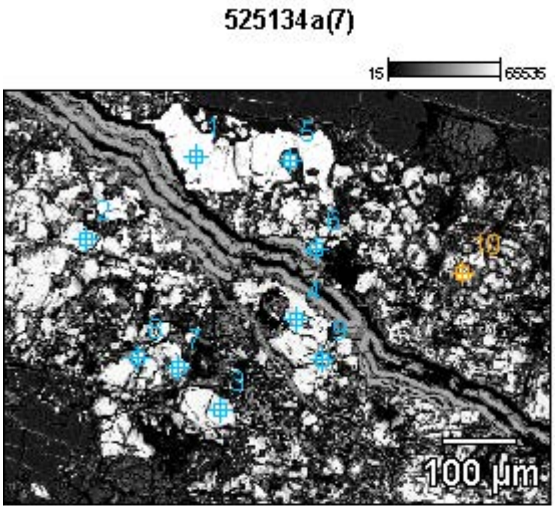

Image name: 525134a(7)
Magnification: 161

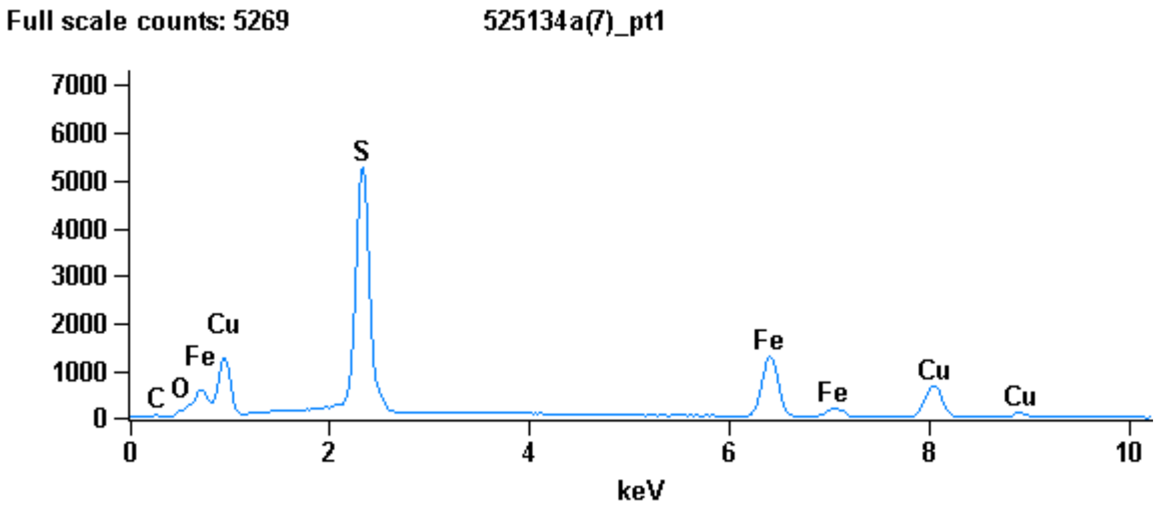

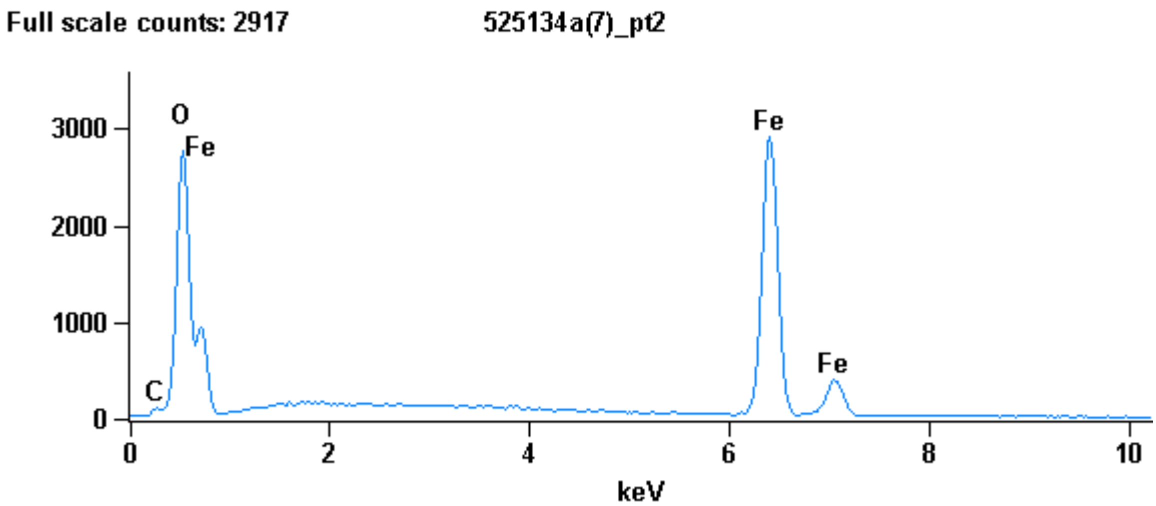

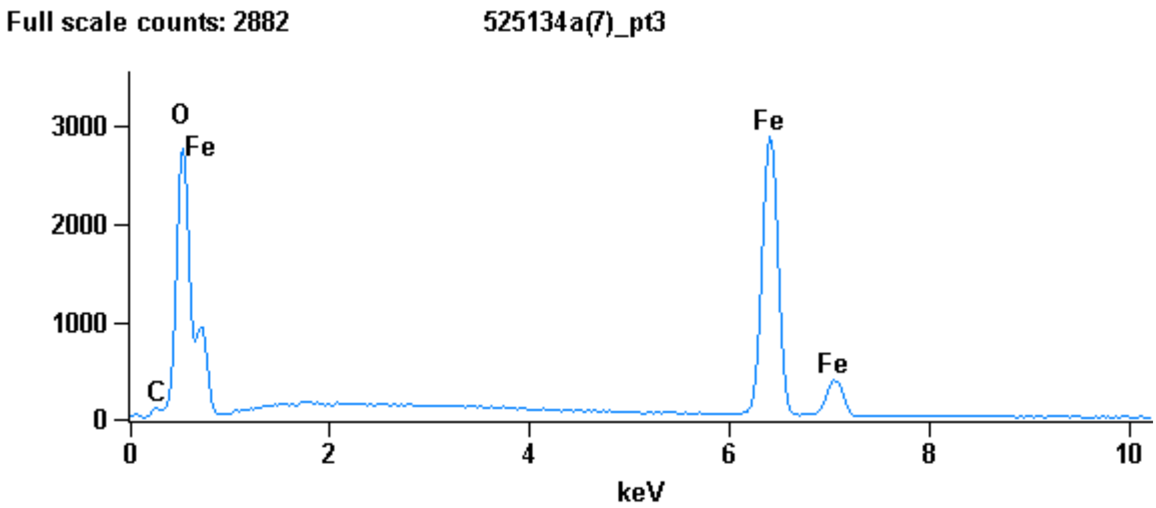
Full scale counts: 2882
525134a(7)_pt3
3000
2000
1000
0
O
Fe
Fe
Fe
C
0
2
4
6
8
10
keV

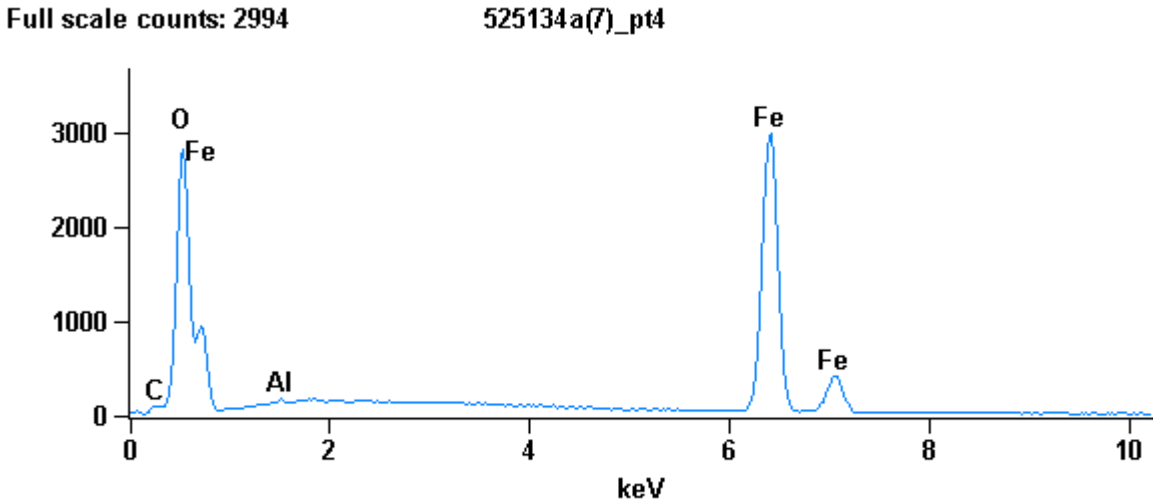
Full scale counts: 2994
525134a(7)_pt4
3000
2000
1000
0
O
Fe
Fe
Fe
C
Al
0
2
4
6
8
10
keV

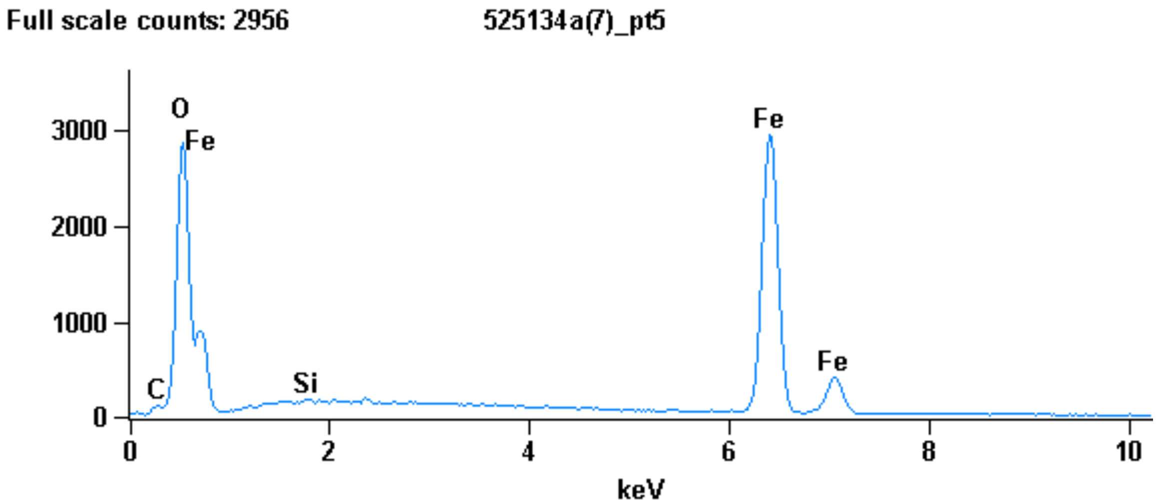
Full scale counts: 2956
525134a(7)_pt5
3000
2000
1000
0
O
Fe
Fe
Fe
C
Si
0
2
4
6
8
10
keV

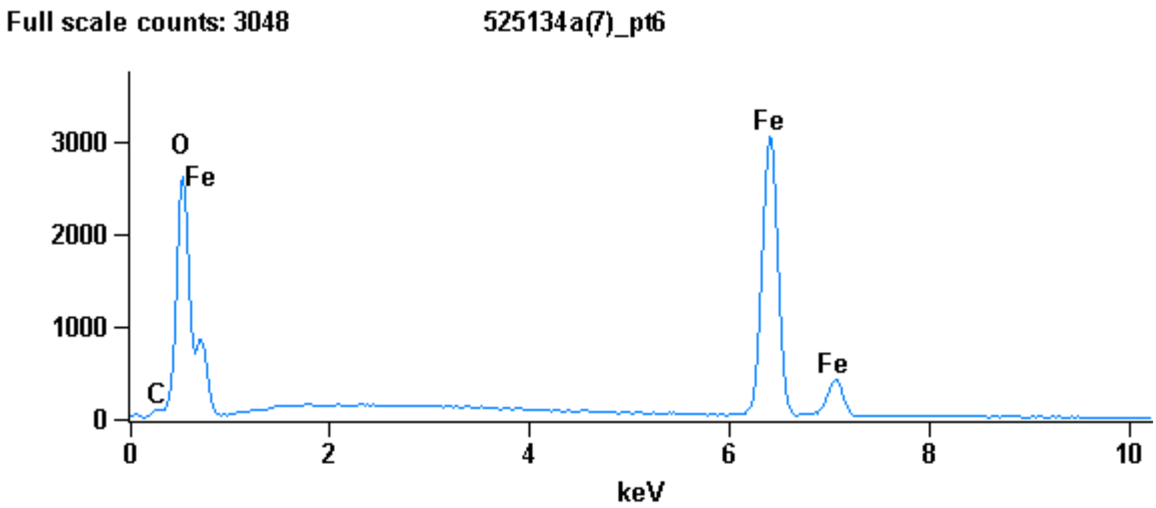
Full scale counts: 3048
525134a(7)_pt6
O
Fe
C
Fe
Fe
keV

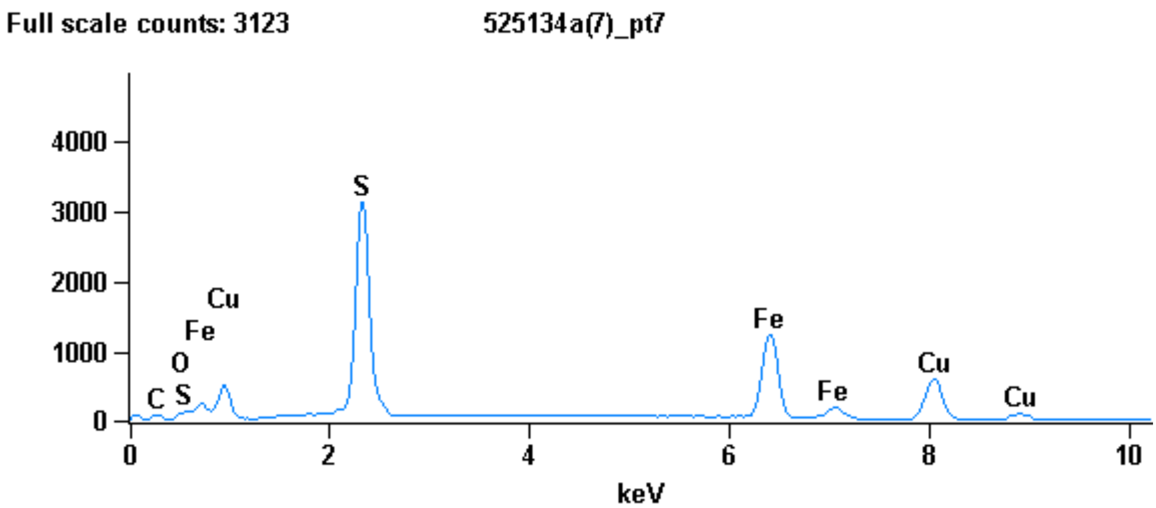
Full scale counts: 3123
525134a(7)_pt7
S
Cu
Fe
O
C S
Fe
Fe
Cu
Cu
keV

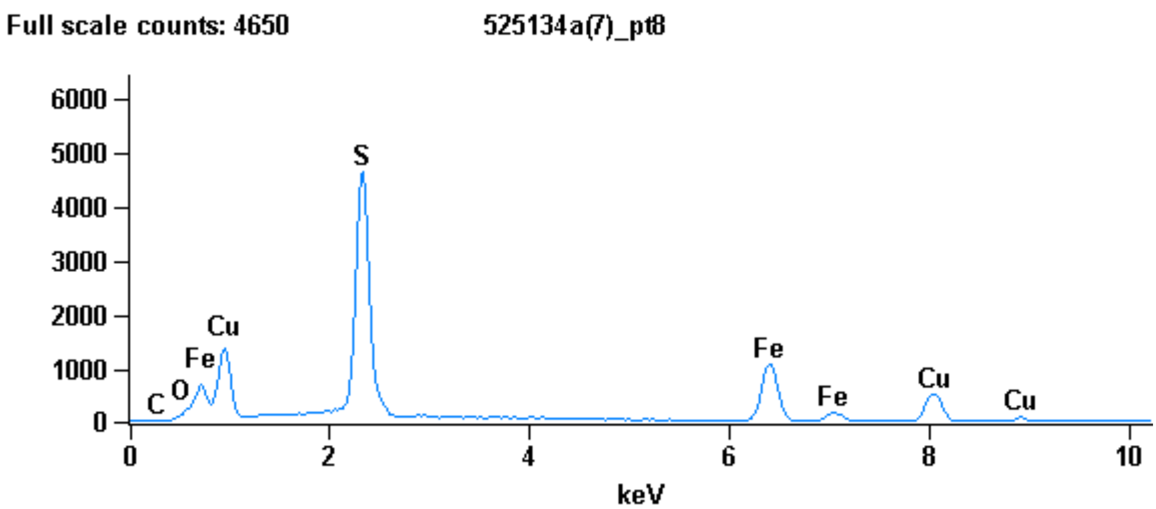
Full scale counts: 4650
525134a(7)_pt8
S
Cu
Fe
C O
Fe
Fe
Cu
Cu
keV

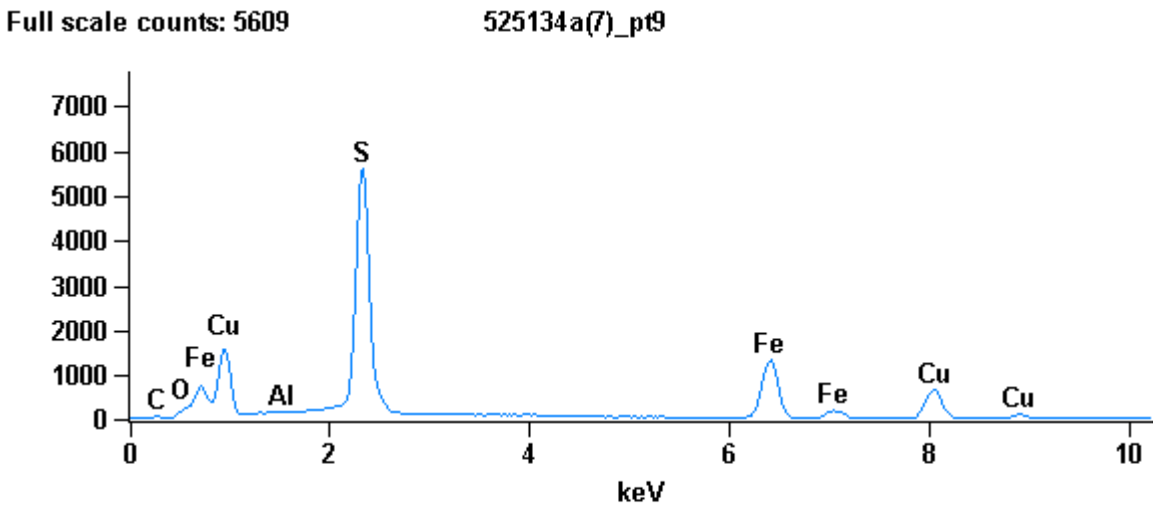

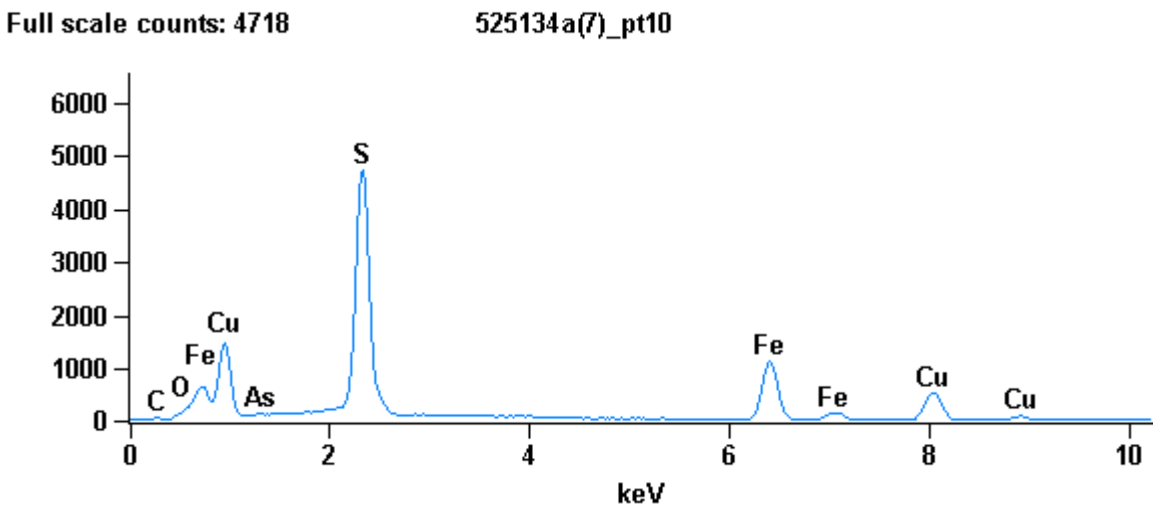

Weight %

	O-K	*Al-K*	*Si-K*	*S-K*	*Fe-K*	*Cu-K*	*As-K*
525134b(0)_pt1	40.72S			20.17	18.41	20.70	
525134b(0)_pt2	30.06S				69.94		
525134b(0)_pt3	30.06S				69.94		
525134b(0)_pt4	30.16S	0.32			69.52		
525134b(0)_pt5	30.10S		0.08		69.82		
525134b(0)_pt6	30.06S				69.94		
525134b(0)_pt7	37.16S			16.23	23.01	23.61	
525134b(0)_pt8	41.72S			20.91	18.79	18.58	
525134b(0)_pt9	41.54S	0.06		20.71	18.88	18.81	
525134b(0)_pt10	42.08S			21.35	18.11	18.45	0.00

Atom %

	O-K	Al-K	Si-K	S-K	Fe-K	Cu-K	As-K
525134b(0)_pt1	66.46			16.43	8.61	8.51	
525134b(0)_pt2	60.00				40.00		
525134b(0)_pt3	60.00				40.00		
525134b(0)_pt4	60.00	0.38			39.62		
525134b(0)_pt5	60.02		0.09		39.89		
525134b(0)_pt6	60.00				40.00		
525134b(0)_pt7	64.29			14.01	11.41	10.29	
525134b(0)_pt8	67.06			16.77	8.65	7.52	
525134b(0)_pt9	66.94	0.06		16.65	8.72	7.63	
525134b(0)_pt10	67.25			17.03	8.29	7.43	0.00

Compound %

		Al2O3	SiO2	SO3	Fe2O3	Cu2O	As2O3
525134b(0)_pt1	0.00			50.37	26.32	23.31	
525134b(0)_pt2	0.00				100.00		
525134a(7)_pt3	0.00				100.00		
525134a(7)_pt4	0.00	0.61			99.39		
525134a(7)_pt5	0.00		0.17		99.83		
525134a(7)_pt6	0.00				100.00		
525134a(7)_pt7	0.00			40.52	32.90	26.58	
525134a(7)_pt8	0.00			52.22	26.86	20.92	
525134a(7)_pt9	0.00	0.12		51.70	27.00	21.18	
525134a(7)_pt10	0.00			53.32	25.90	20.78	0.00

Minerals, 525134a(7)
pt1: Chalcopyrite
pt2: Fe-oxide
pt3: Fe-oxide
pt4: Fe-oxide
pt5: Fe-oxide
pt6: Fe-oxide
pt7: Chalcopyrite
pt8: Chalcopyrite
pt9: Chalcopyrite
pt10: Chalcopyrite

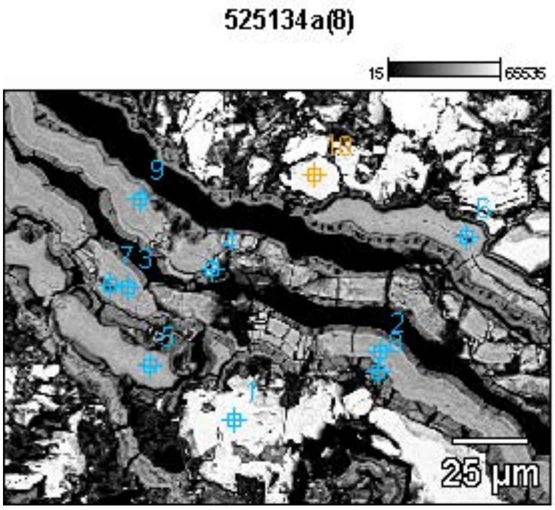

Image name: 525134a(8)
Magnification: 677

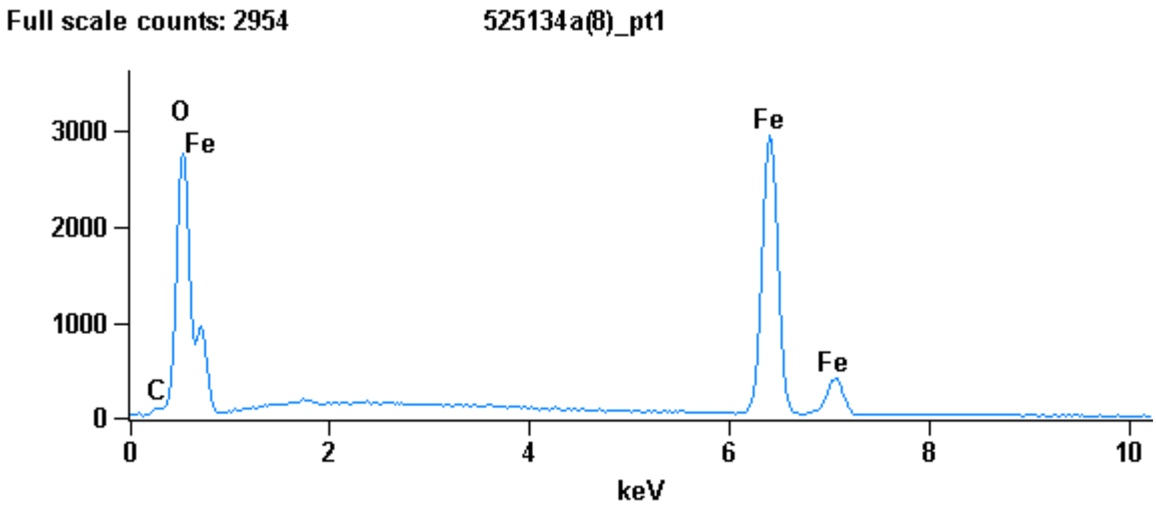

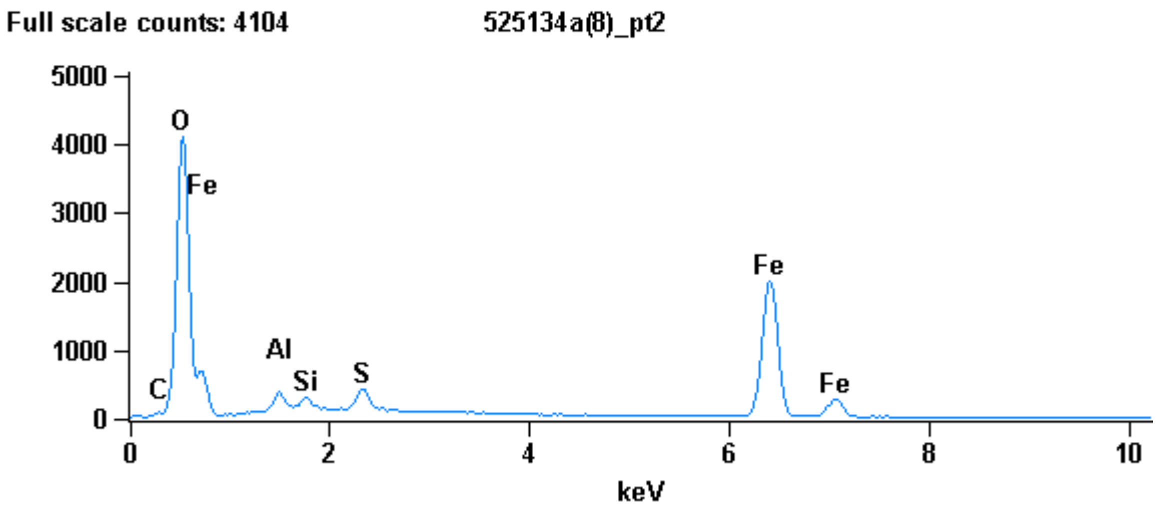

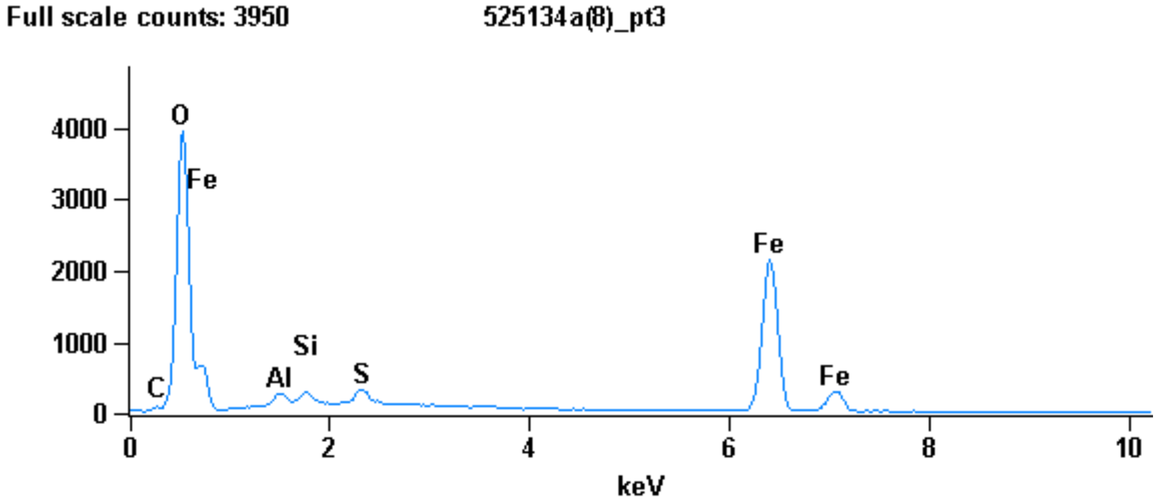
Full scale counts: 3950
525134a(8)_pt3
4000
3000
2000
1000
0
O
Fe
C
Al
Si
S
Fe
Fe
0
2
4
6
8
10
keV

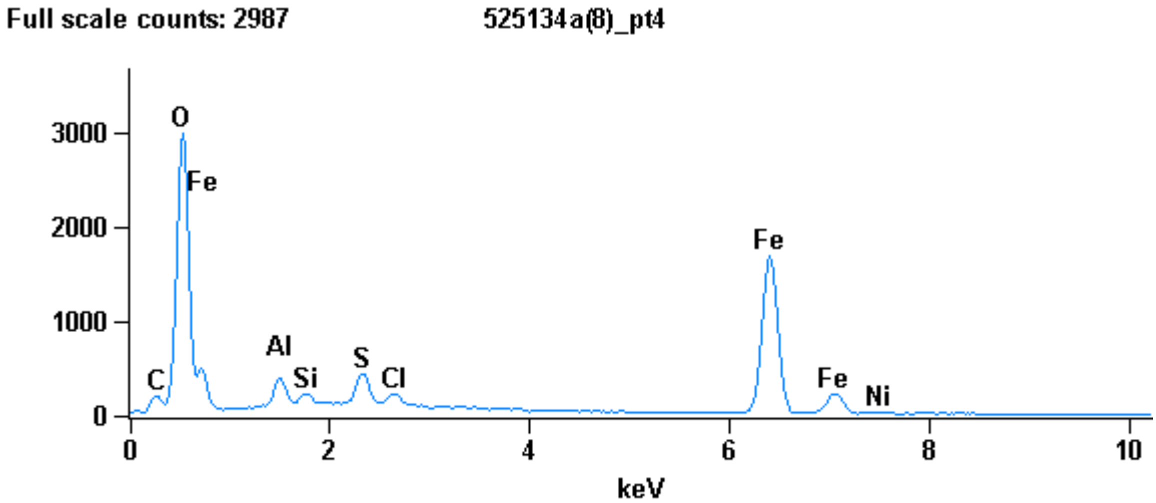
Full scale counts: 2987
525134a(8)_pt4
3000
2000
1000
0
O
Fe
C
Al
Si
S
Cl
Fe
Fe
Ni
0
2
4
6
8
10
keV

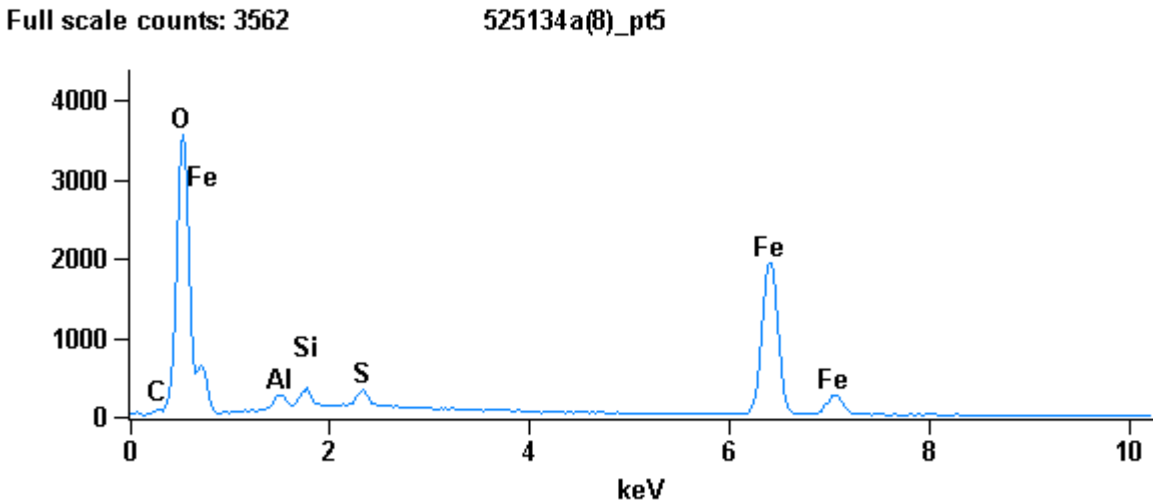
Full scale counts: 3562
525134a(8)_pt5
4000
3000
2000
1000
0
O
Fe
C
Al
Si
S
Fe
Fe
0
2
4
6
8
10
keV

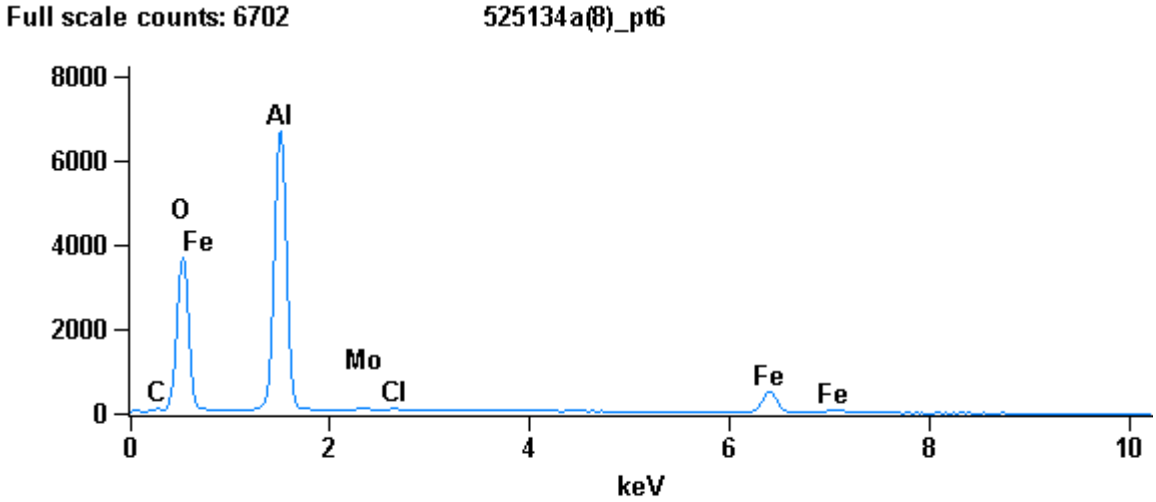
Full scale counts: 6702
525134a(8)_pt6
8000
6000
4000
2000
0
Al
O
Fe
C
Mo
Cl
Fe
Fe
0
2
4
6
8
10
keV

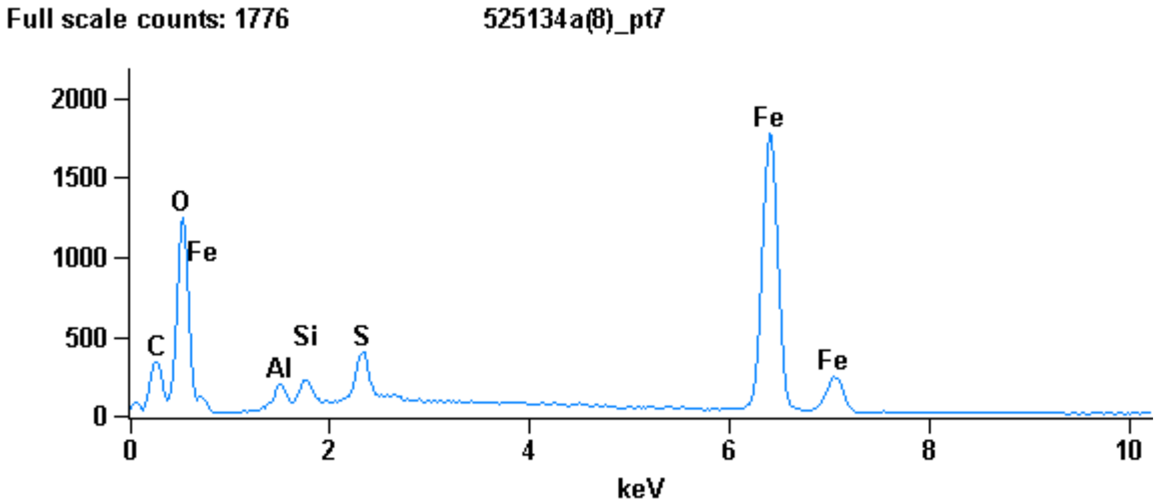
Full scale counts: 1776
525134a(8)_pt7
2000
1500
1000
500
0
Fe
O
Fe
C
Al
Si
S
Fe
0
2
4
6
8
10
keV

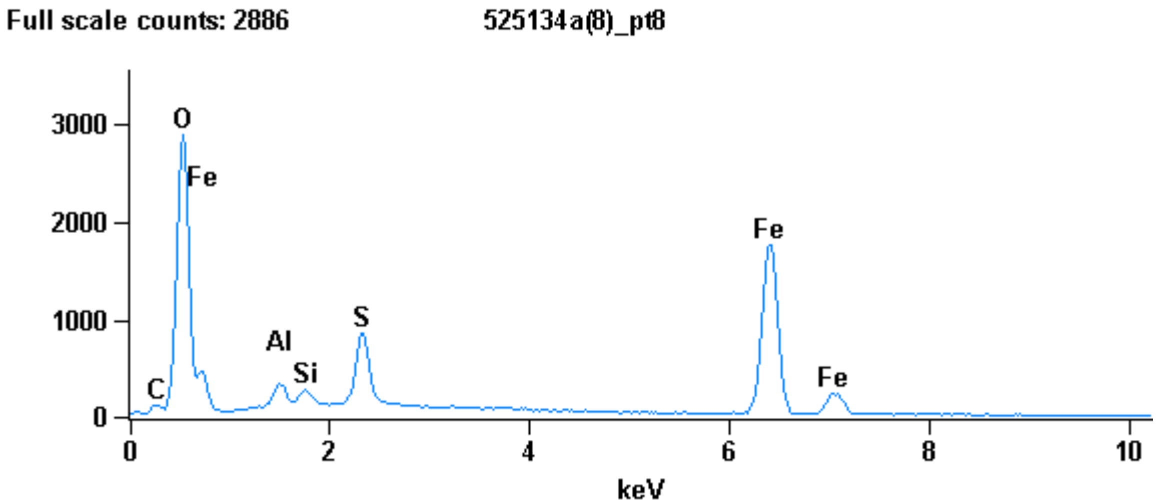
Full scale counts: 2886
525134a(8)_pt8
3000
2000
1000
0
O
Fe
C
Al
Si
S
Fe
Fe
0
2
4
6
8
10
keV

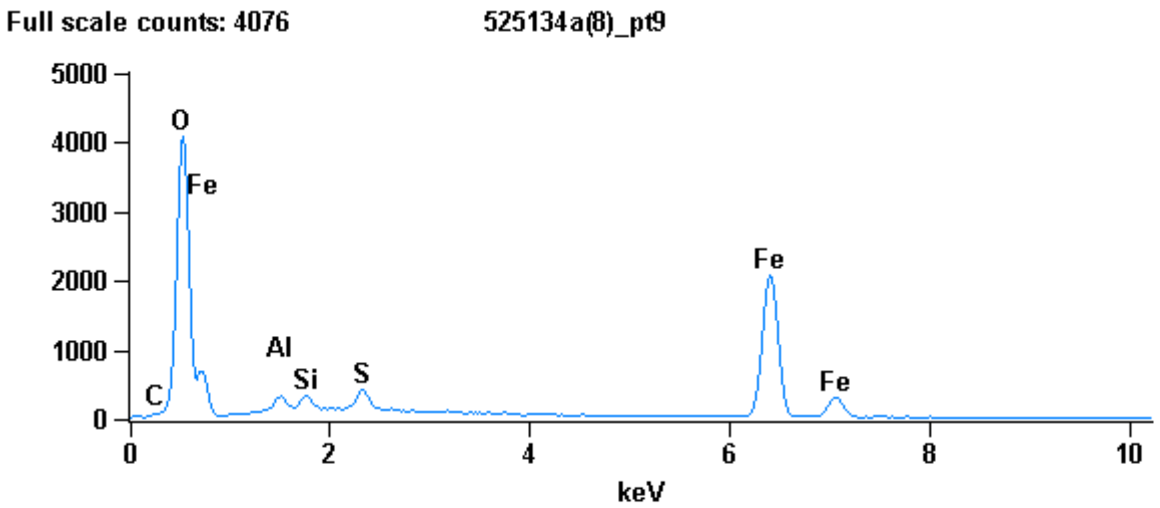

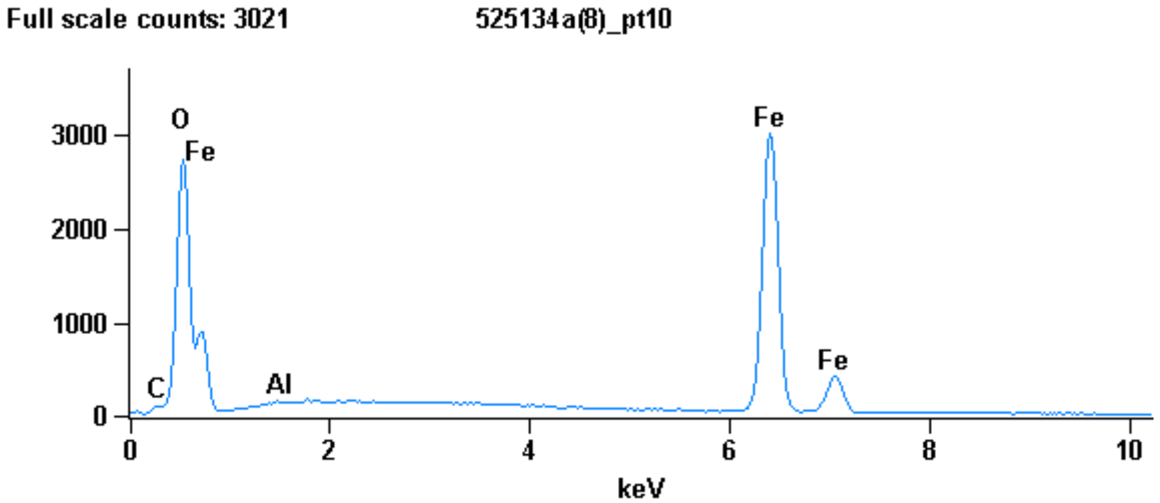

Weight %

	O-K	Al-K	Si-K	S-K	Cl-K	Fe-K	Ni-K	Mo-L
525134a(8)_pt1	30.06S					69.94		
525134a(8)_pt2	33.40S	2.31	1.27	2.64		60.38		
525134a(8)_pt3	32.59S	1.66	1.48	1.70		62.58		
525134a(8)_pt4	33.49S	3.23	0.88	3.39	1.42	56.32	1.27	
525134a(8)_pt5	33.15S	1.94	2.11	1.90		60.90		
525134a(8)_pt6	43.30S	41.43			0.46	13.60		1.21
525134a(8)_pt7	33.57S	1.69	1.50	2.99		60.25		
525134a(8)_pt8	36.24S	2.58	1.42	6.23		53.53		
525134a(8)_pt9	33.17S	1.82	1.40	2.46		61.15		
525134a(8)_pt10	30.14S	0.27				69.59		

Atom %

	O-K	Al-K	Si-K	S-K	Cl-K	Fe-K	Ni-K	Mo-L
525134a(8)_pt1	60.00					40.00		
525134a(8)_pt2	61.73	2.53	1.33	2.44		31.97		
525134a(8)_pt3	61.27	1.85	1.58	1.59		33.70		
525134a(8)_pt4	61.20	3.50	0.91	3.09	1.17	29.49	0.63	
525134a(8)_pt5	61.50	2.14	2.24	1.76		32.37		
525134a(8)_pt6	59.99	34.04			0.29	5.40		0.28
525134a(8)_pt7	61.97	1.85	1.58	2.75		31.86		
525134a(8)_pt8	63.55	2.69	1.42	5.45		26.89		
525134a(8)_pt9	61.67	2.01	1.49	2.28		32.56		
525134a(8)_pt10	60.00	0.31				39.69		

Compound %

		Al2O3	SiO2	SO3	Cl	Fe2O3	NiO	MoO3
525134a(8)_pt1	0.00					100.00		
525134a(8)_pt2	0.00	4.36	2.71	6.60		86.33		
525134a(8)_pt3	0.00	3.14	3.16	4.23		89.47		
525134a(8)_pt4	0.00	6.10	1.88	8.45	1.42	80.53	1.62	
525134a(8)_pt5	0.00	3.67	4.52	4.74		87.07		
525134a(8)_pt6	0.00	78.28			0.46	19.44		1.82
525134a(8)_pt7	0.00	3.19	3.21	7.46		86.15		
525134a(8)_pt8	0.00	4.88	3.04	15.55		76.53		
525134a(8)_pt9	0.00	3.44	3.00	6.14		87.42		
525134a(8)_pt10	0.00	0.50				99.50		

Minerals, 525134a(8)

pt1: Fe-oxide
pt2: Fe-oxide, goethite (structure) +mixed signal/edge effect
pt3: Fe-oxide, goethite (structure) +mixed signal/edge effect
pt4: Fe-oxide (+mixed signal/edge effect)
pt5: Fe-oxide, goethite (structure) +mixed signal/edge effect
pt6: Fe-bearing Al-oxide
pt7: Fe-oxide (+mixed signal/edge effect)
pt8: Fe-oxide (+mixed signal/edge effect)
pt9: Fe-oxide, goethite (structure) +mixed signal/edge effect
pt10: Fe-oxide

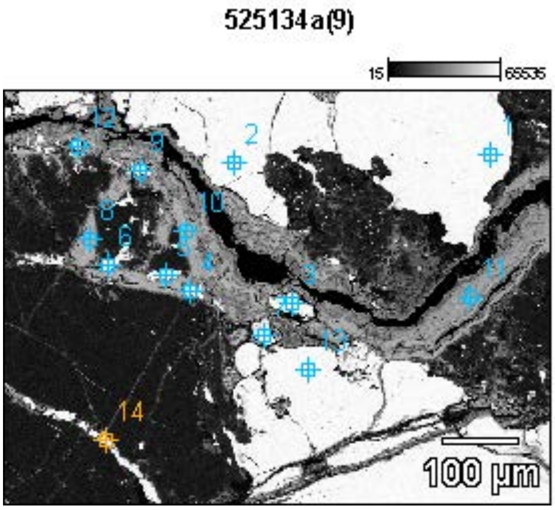

Image name: 525134a(9)
Magnification: 169

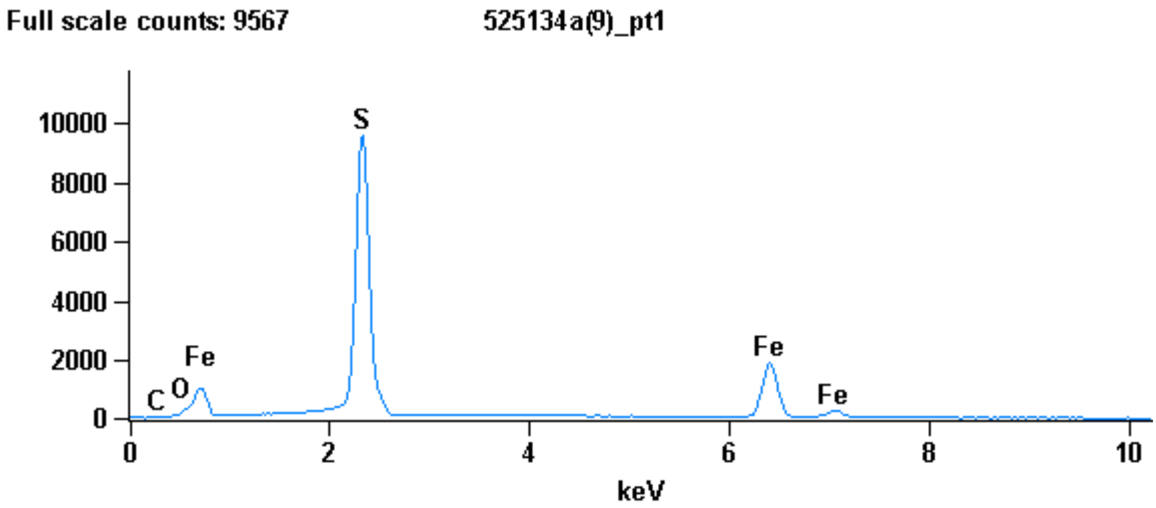

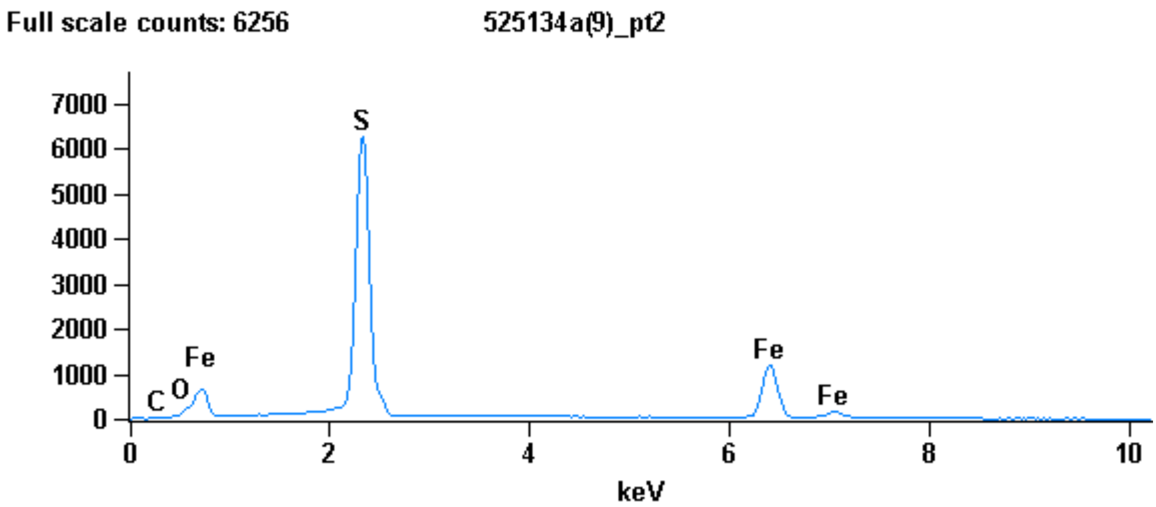

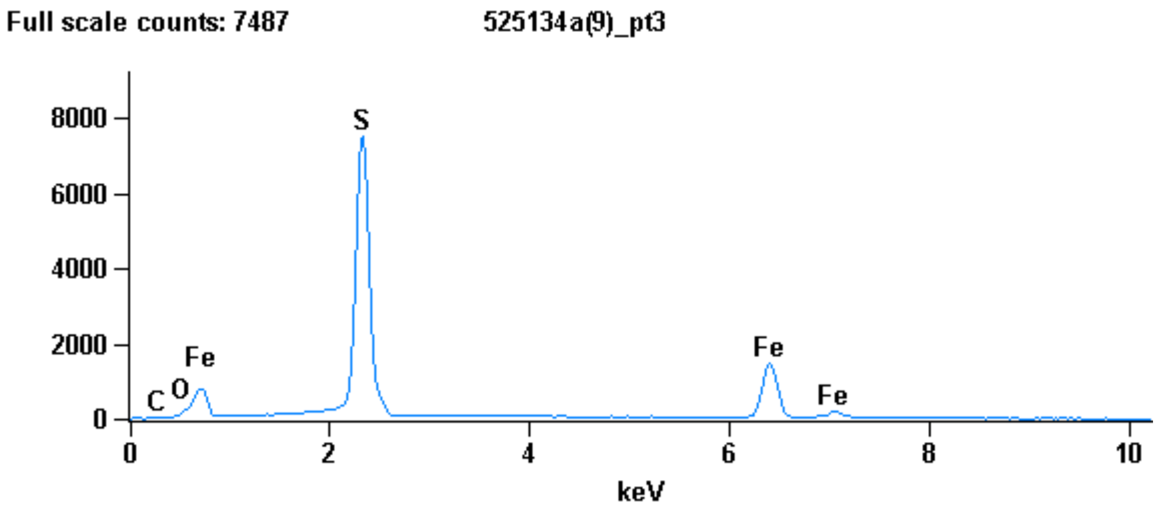
Full scale counts: 7487
525134a(9)_pt3
8000
6000
4000
2000
0
S
Fe
C
O
Fe
Fe
0
2
4
6
8
10
keV

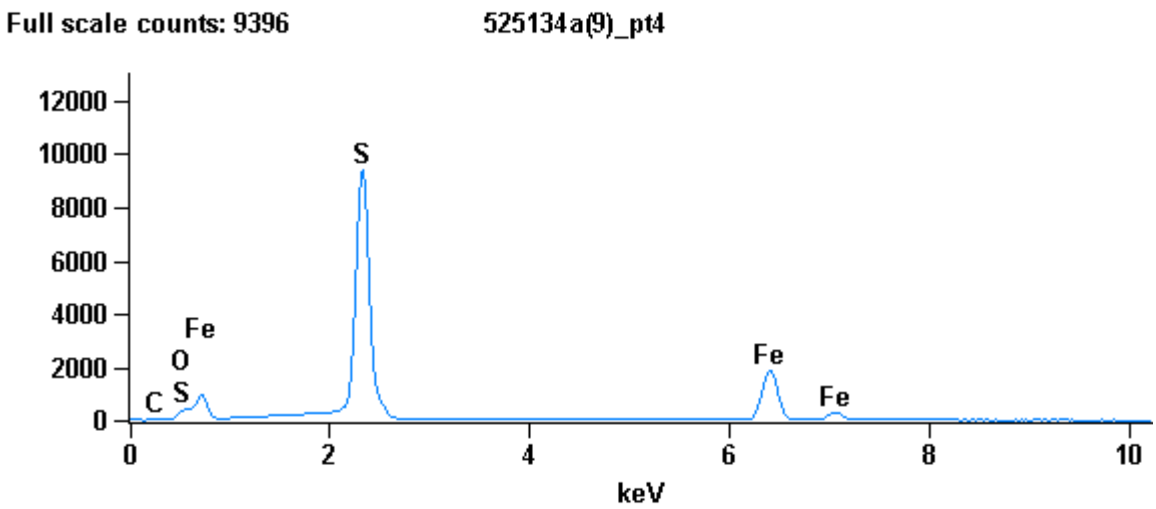
Full scale counts: 9396
525134a(9)_pt4
12000
10000
8000
6000
4000
2000
0
S
Fe
O
C
S
Fe
Fe
0
2
4
6
8
10
keV

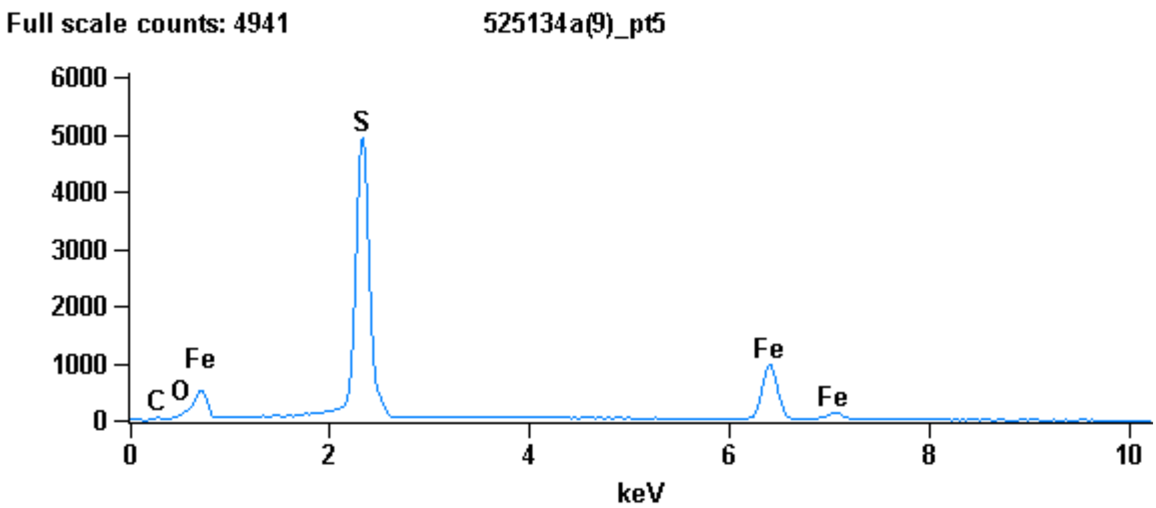
Full scale counts: 4941
525134a(9)_pt5
6000
5000
4000
3000
2000
1000
0
S
Fe
C
O
Fe
Fe
0
2
4
6
8
10
keV

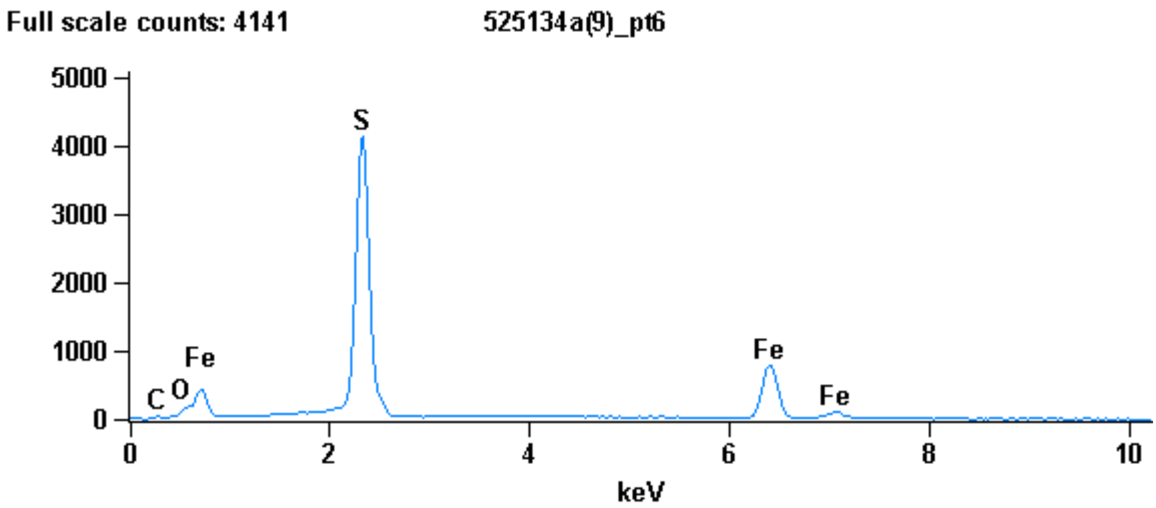
Full scale counts: 4141
525134a(9)_pt6
5000
4000
3000
2000
1000
0
S
Fe
C
O
Fe
Fe
0
2
4
6
8
10
keV

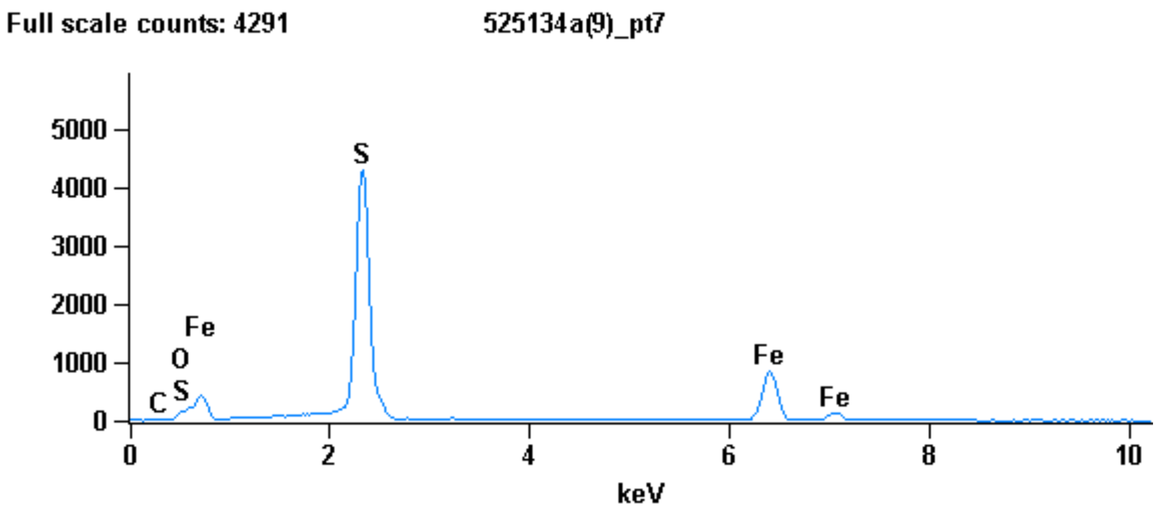
Full scale counts: 4291
525134a(9)_pt7
5000
4000
3000
2000
1000
0
S
Fe
O
C
S
Fe
Fe
0
2
4
6
8
10
keV

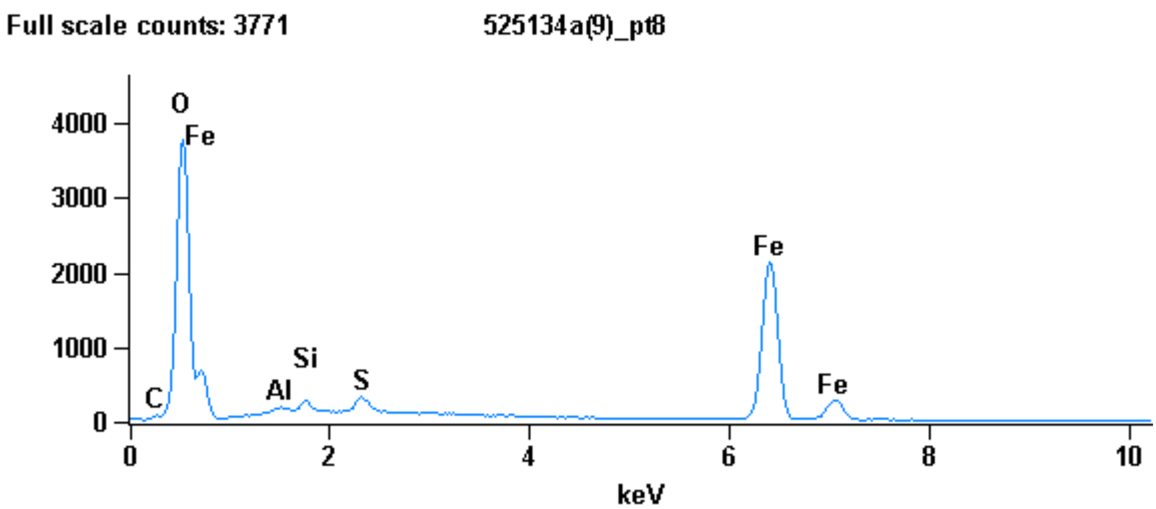
Full scale counts: 3771
525134a(9)_pt8
4000
3000
2000
1000
0
O
Fe
Fe
Si
Al
S
C
Fe
0
2
4
6
8
10
keV

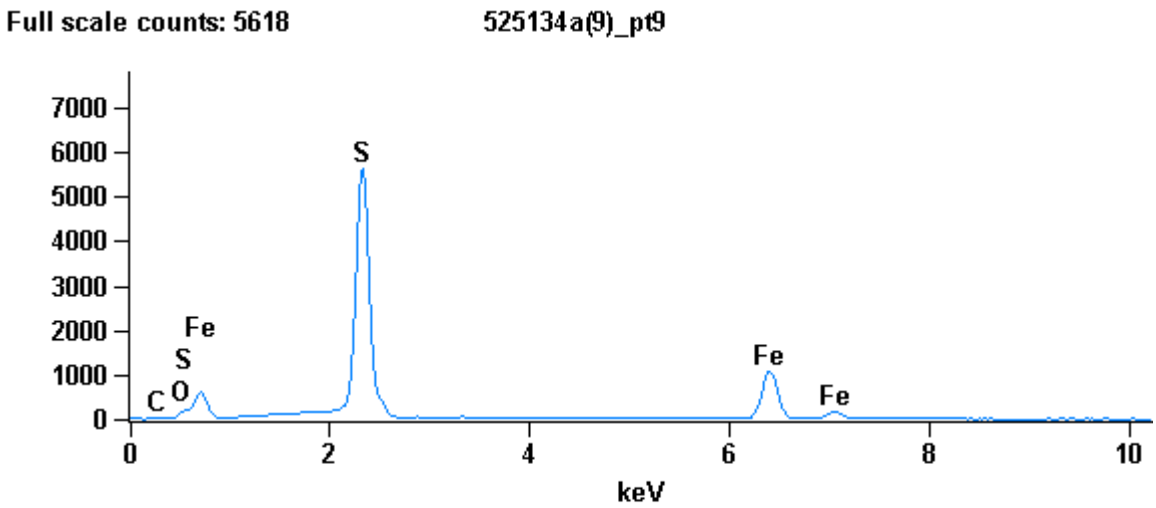
Full scale counts: 5618
525134a(9)_pt9
7000
6000
5000
4000
3000
2000
1000
0
S
Fe
S
C
O
Fe
Fe
0
2
4
6
8
10
keV

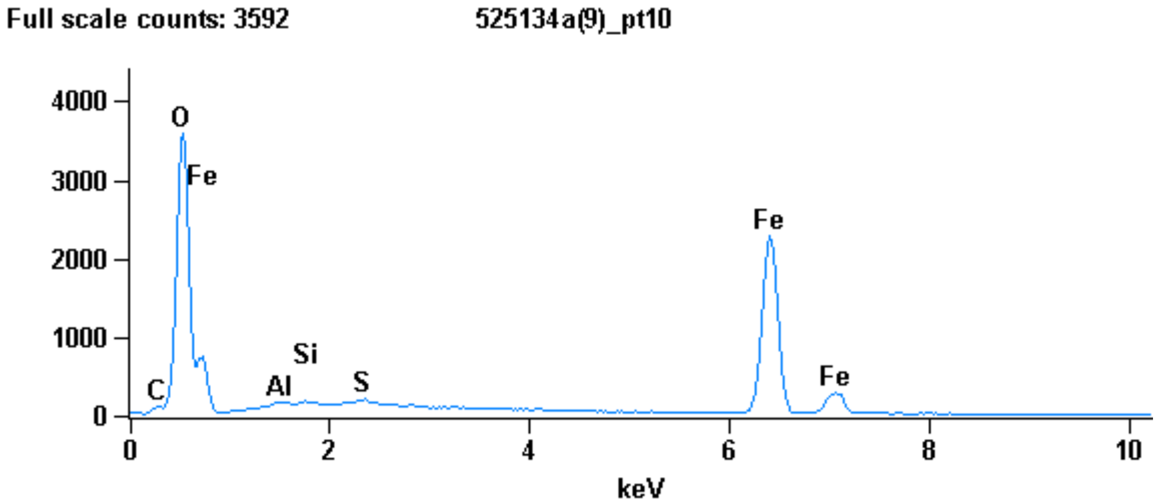
Full scale counts: 3592
525134a(9)_pt10
4000
3000
2000
1000
0
O
Fe
Fe
Si
C
Al
S
Fe
0
2
4
6
8
10
keV

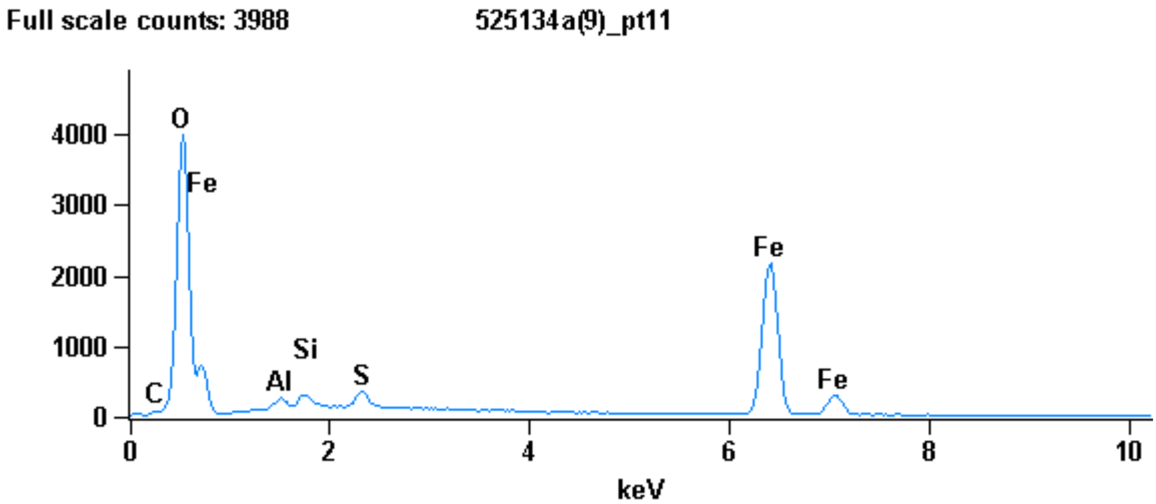
Full scale counts: 3988
525134a(9)_pt11
4000
3000
2000
1000
0
O
Fe
Fe
Si
C
Al
S
Fe
0
2
4
6
8
10
keV

Full scale counts: 7038 525134a(9)_pt12

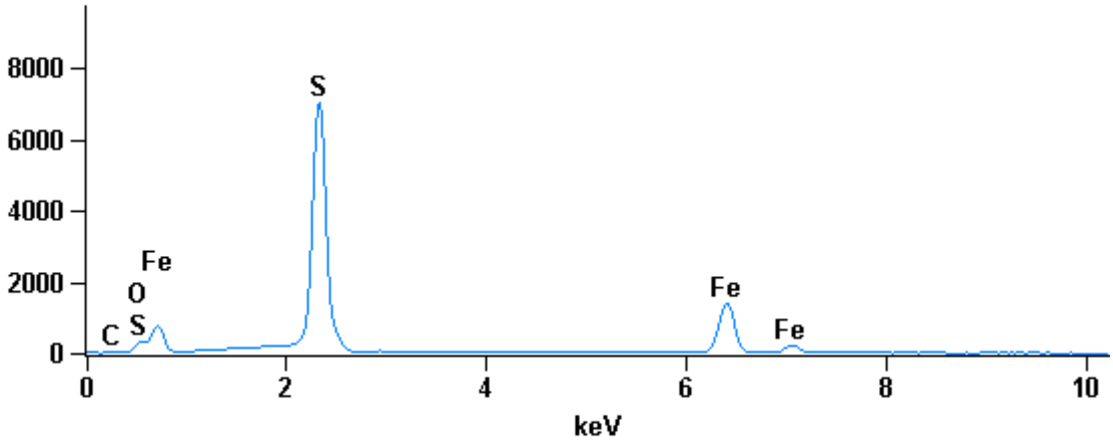

Full scale counts: 4744 525134a(9)_pt13

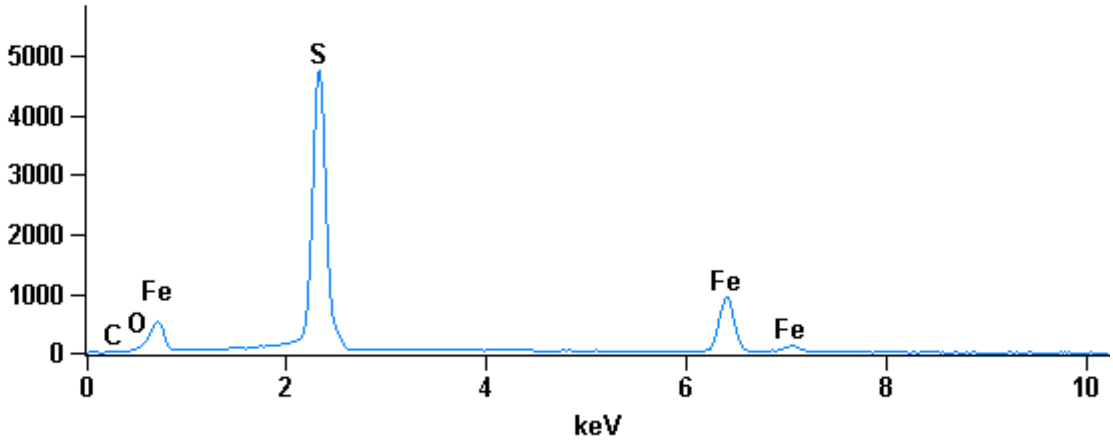

Full scale counts: 3284 525134a(9)_pt14

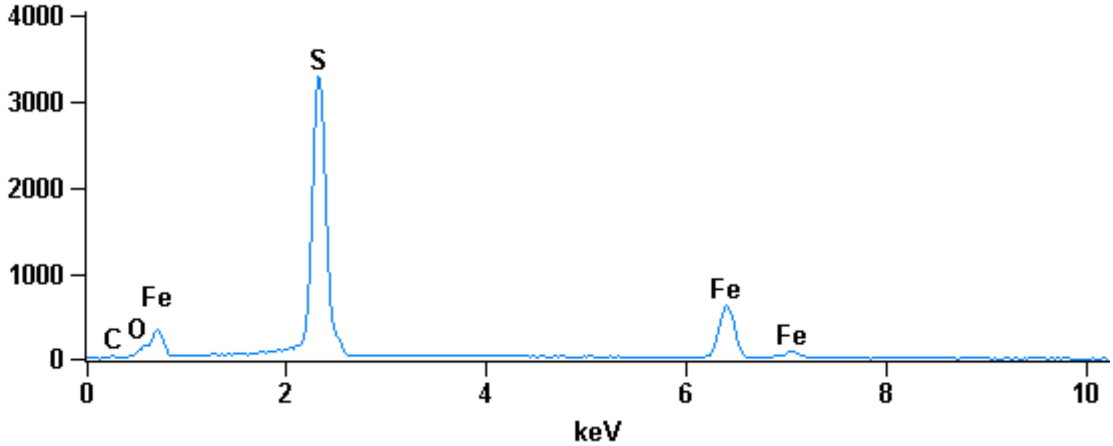

Weight %

	O-K	Al-K	Si-K	S-K	Fe-K
525134a(9)_pt1	50.40S			27.25	22.35
525134a(9)_pt2	50.49S			27.37	22.14
525134a(9)_pt3	50.44S			27.30	22.26
525134a(9)_pt4	50.14S			26.90	22.95
525134a(9)_pt5	50.31S			27.13	22.57
525134a(9)_pt6	50.35S			27.18	22.48
525134a(9)_pt7	50.46S			27.33	22.21
525134a(9)_pt8	32.19S	0.88	1.07	1.76	64.10
525134a(9)_pt9	50.39S			27.23	22.38
525134a(9)_pt10	30.95S	0.47	0.42	0.71	67.45
525134a(9)_pt11	32.71S	1.31	1.47	2.01	62.51
525134a(9)_pt12	50.30S			27.11	22.59
525134a(9)_pt13	50.38S			27.23	22.39
525134a(9)_pt14	50.46S			27.33	22.22

Atom %

	O-K	Al-K	Si-K	S-K	Fe-K
525134a(9)_pt1	71.59			19.31	9.10
525134a(9)_pt2	71.63			19.38	9.00
525134a(9)_pt3	71.60			19.34	9.06
525134a(9)_pt4	71.48			19.14	9.37
525134a(9)_pt5	71.55			19.25	9.19
525134a(9)_pt6	71.57			19.28	9.15
525134a(9)_pt7	71.61			19.36	9.03
525134a(9)_pt8	61.24	0.99	1.16	1.67	34.94
525134a(9)_pt9	71.58			19.31	9.11
525134a(9)_pt10	60.51	0.54	0.47	0.69	37.78
525134a(9)_pt11	61.45	1.46	1.57	1.89	33.64
525134a(9)_pt12	71.55			19.25	9.21
525134a(9)_pt13	71.58			19.30	9.11
525134a(9)_pt14	71.61			19.35	9.03

Compound %

		Al2O3	*SiO2*	*SO3*	*Fe2O3*
525134a(9)_pt1	0.00			68.04	31.96
525134a(9)_pt2	0.00			68.34	31.66
525134a(9)_pt3	0.00			68.17	31.83
525134a(9)_pt4	0.00			67.19	32.81
525134a(9)_pt5	0.00			67.74	32.26
525134a(9)_pt6	0.00			67.86	32.14
525134a(9)_pt7	0.00			68.24	31.76
525134a(9)_pt8	0.00	1.66	2.29	4.40	91.65
525134a(9)_pt9	0.00			68.01	31.99
525134a(9)_pt10	0.00	0.88	0.90	1.77	96.44
525134a(9)_pt11	0.00	2.47	3.14	5.02	89.37
525134a(9)_pt12	0.00			67.70	32.30
525134a(9)_pt13	0.00			67.99	32.01
525134a(9)_pt14	0.00			68.23	31.77

Minerals, 525134a(14)

pt1: Pyrite
pt2: Pyrite
pt3: Pyrite
pt4: Pyrite
pt5: Pyrite
pt6: Pyrite
pt7: Pyrite
pt8: Fe-oxide, goethite (structure)
pt9: Pyrite
pt10: Fe-oxide, goethite (structure)
pt11: Fe-oxide, goethite (structure)
pt12: Pyrite
pt13: Pyrite
pt14: Pyrite

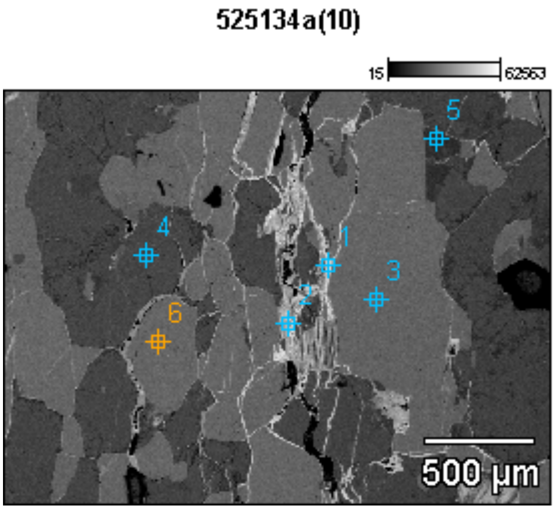

Image name: 525134a(10)
Magnification: 49

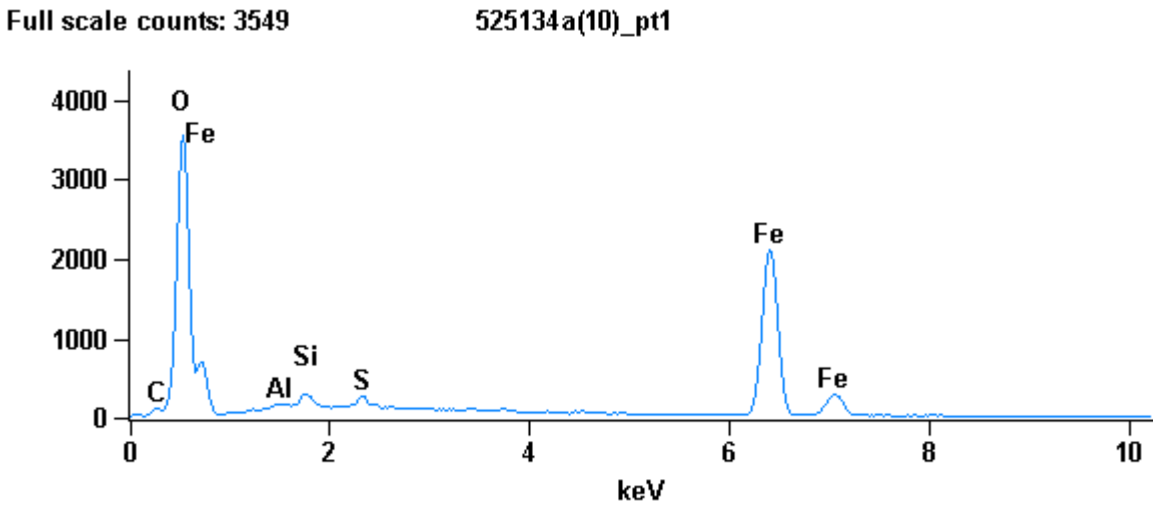

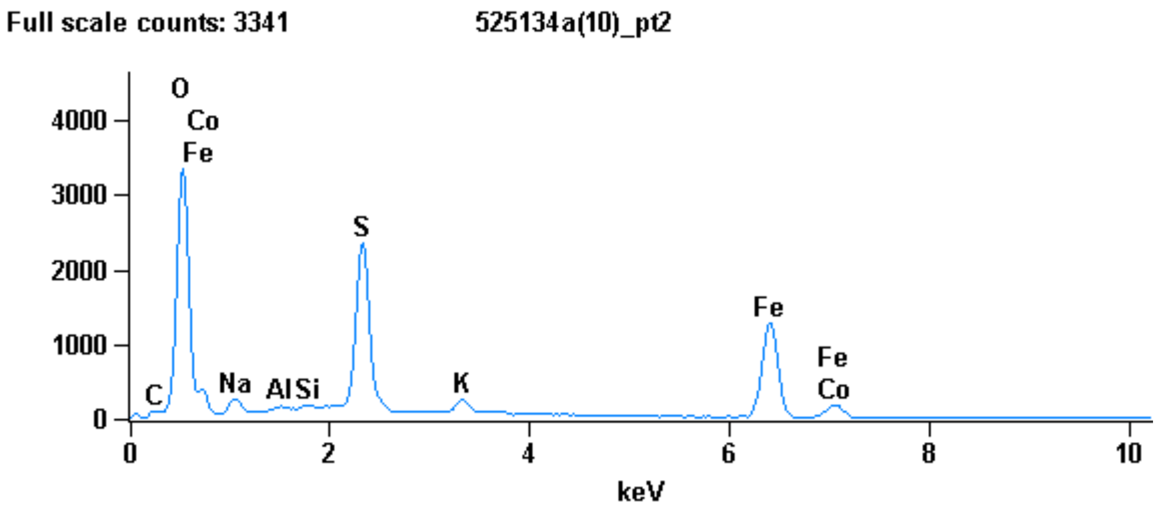

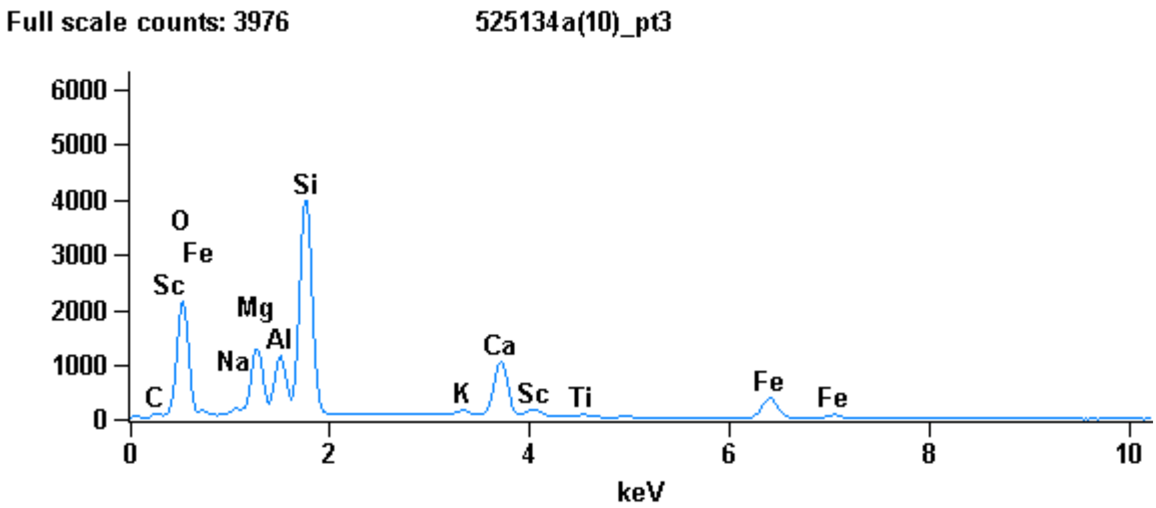

Full scale counts: 3976
525134a(10)_pt3
6000
5000
4000
3000
2000
1000
0
Si
O
Fe
Sc
Mg
Al
Na
C
Ca
K
Sc
Ti
Fe
Fe
0
2
4
6
8
10
keV

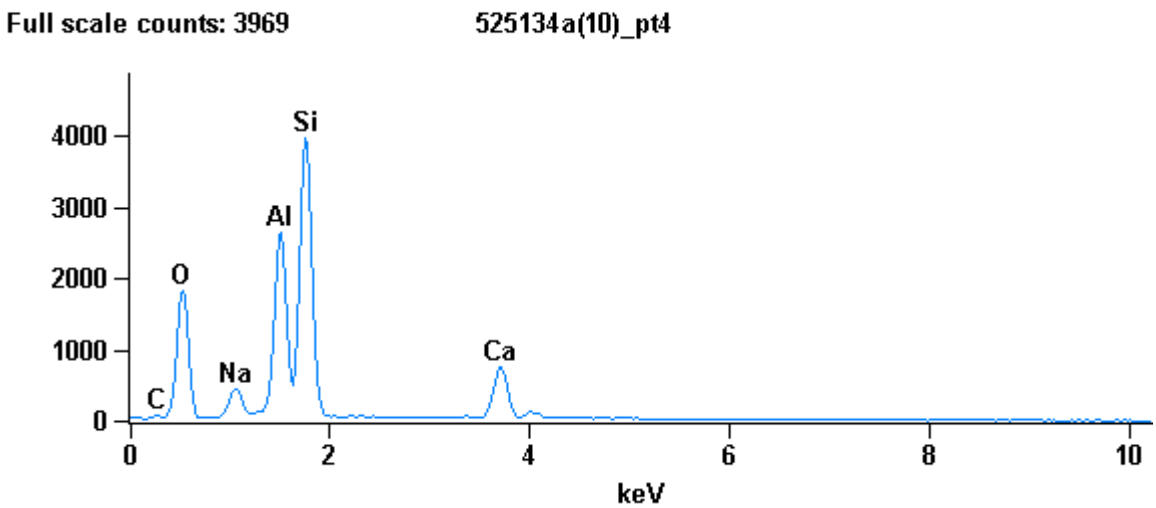

Full scale counts: 3969
525134a(10)_pt4
4000
3000
2000
1000
0
Si
Al
O
Na
C
Ca
0
2
4
6
8
10
keV

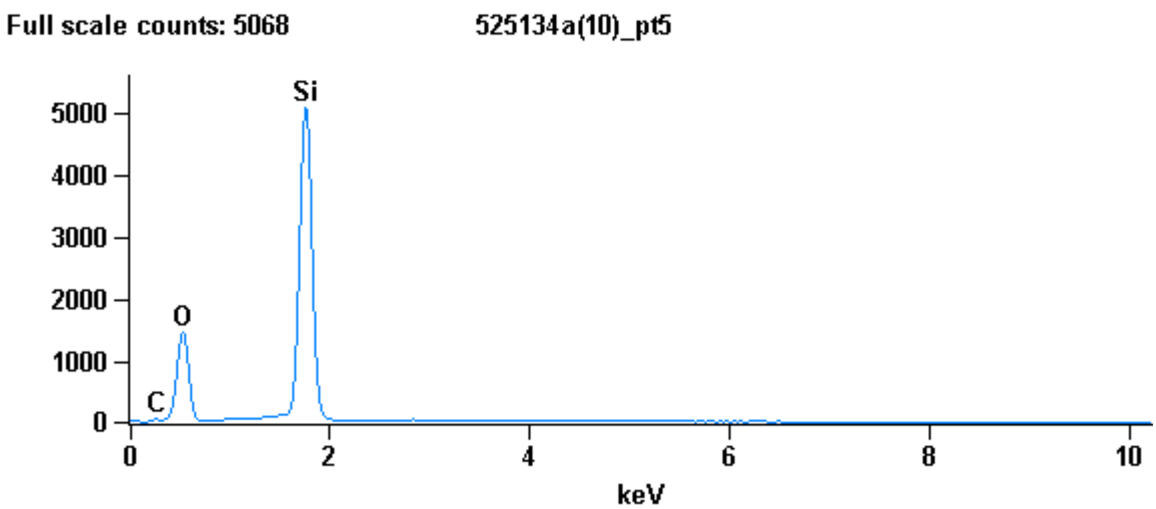

Full scale counts: 5068
525134a(10)_pt5
5000
4000
3000
2000
1000
0
Si
O
C
0
2
4
6
8
10
keV

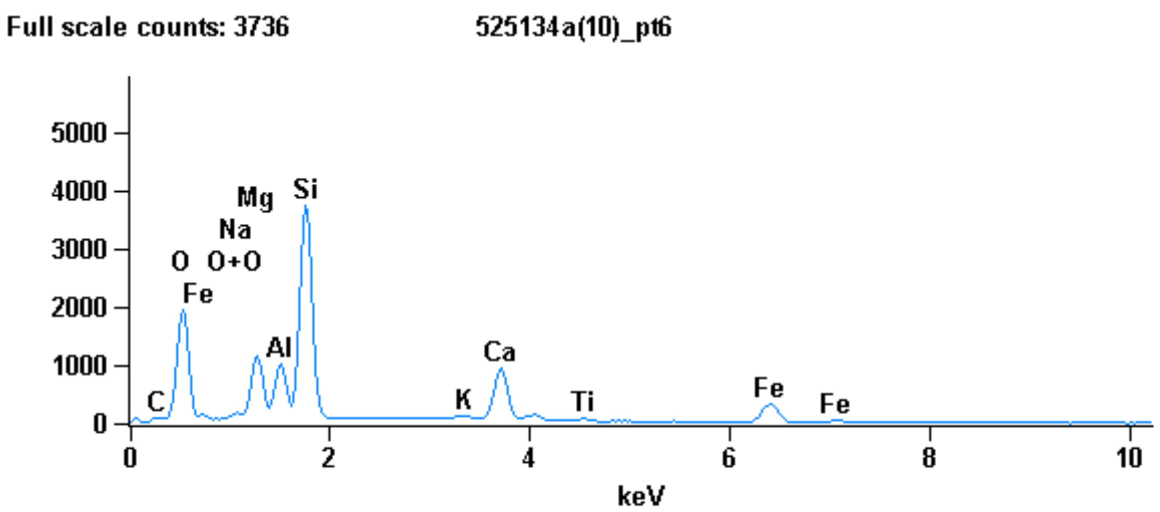

Weight %

	O-K	Na-K	Mg-K	Al-K	Si-K	S-K	K-K	Ca-K	Sc-K	Ti-K	Fe-K	Co-K
525134a(10)_pt1	31.72S			0.66	1.54	0.92					65.16	
525134a(10)_pt2	41.67S	4.30		0.26	0.13	16.06	1.58				35.79	0.21
525134a(10)_pt3	43.98S	0.89	8.14	5.56	22.40		0.72	8.61	0.05	0.38	9.27	
525134a(10)_pt4	47.29S	4.32		14.97	25.84			7.58				
525134a(10)_pt5	53.26S				46.74							
525134a(10)_pt6	44.08S	0.77	8.15	5.48	22.62		0.79	8.45		0.51	9.14	

Atom %

	O-K	Na-K	Mg-K	Al-K	Si-K	S-K	K-K	Ca-K	Sc-K	Ti-K	Fe-K	Co-K
525134a(10)_pt1	60.87			0.75	1.68	0.88					35.82	
525134a(10)_pt2	65.25	4.69		0.24	0.11	12.55	1.01				16.05	0.09
525134a(10)_pt3	60.62	0.85	7.39	4.54	17.59		0.41	4.74	0.03	0.17	3.66	
525134a(10)_pt4	61.48	3.91		11.54	19.14			3.93				
525134a(10)_pt5	66.67				33.33							
525134a(10)_pt6	60.71	0.74	7.39	4.48	17.74		0.45	4.64		0.24	3.61	

Compound %

		Na2O	MgO	Al2O3	SiO2	SO3	K2O	CaO	Sc2O3	TiO2	Fe2O3	CoO
525134a(10)_pt1	0.00			1.24	3.29	2.30					93.17	
525134a(10)_pt2	0.00	5.80		0.49	0.27	40.10	1.90				51.17	0.27
525134a(10)_pt3	0.00	1.20	13.50	10.50	47.92		0.87	12.04	0.08	0.63	13.26	
525134a(10)_pt4	0.00	5.83		28.29	55.28			10.60				
525134a(10)_pt5	0.00				100.00							
525134a(10)_pt6	0.00	1.04	13.52	10.36	48.38		0.96	11.82		0.85	13.07	

Minerals, 525134a(10)
pt1: Fe-oxide
pt2: Pyrrhotite
pt3: Amphibole - hornblende
pt4: Feldspar - plagioclase
pt5: Quartz
pt6: Amphibole - hornblende

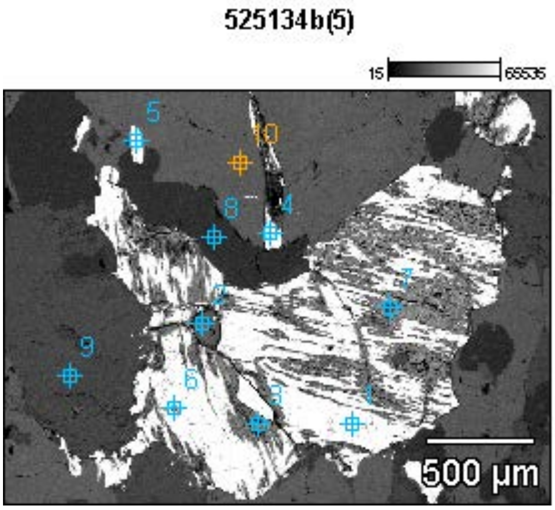

Image name: 525134b(5)
Magnification: 48

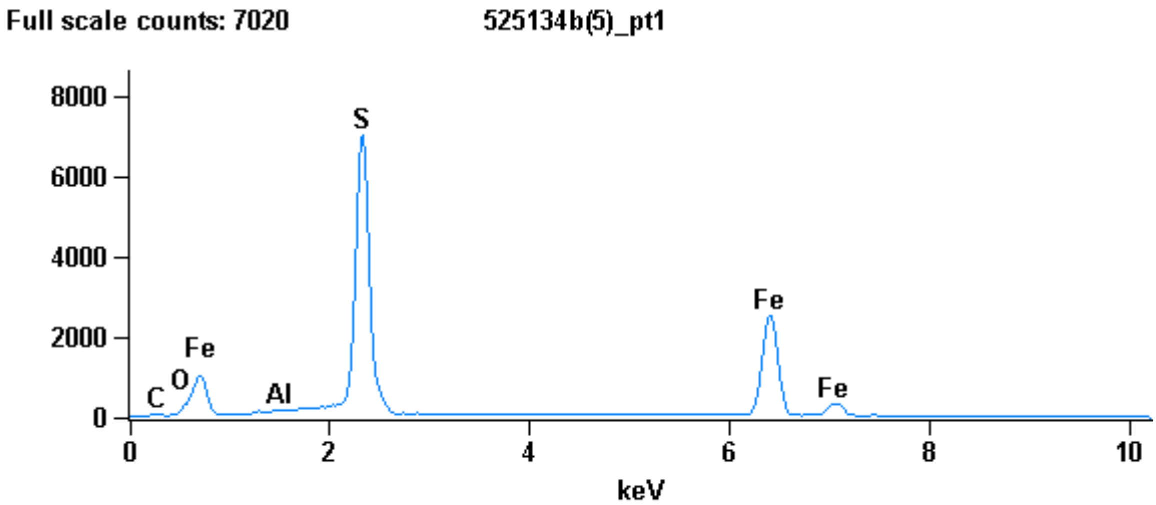

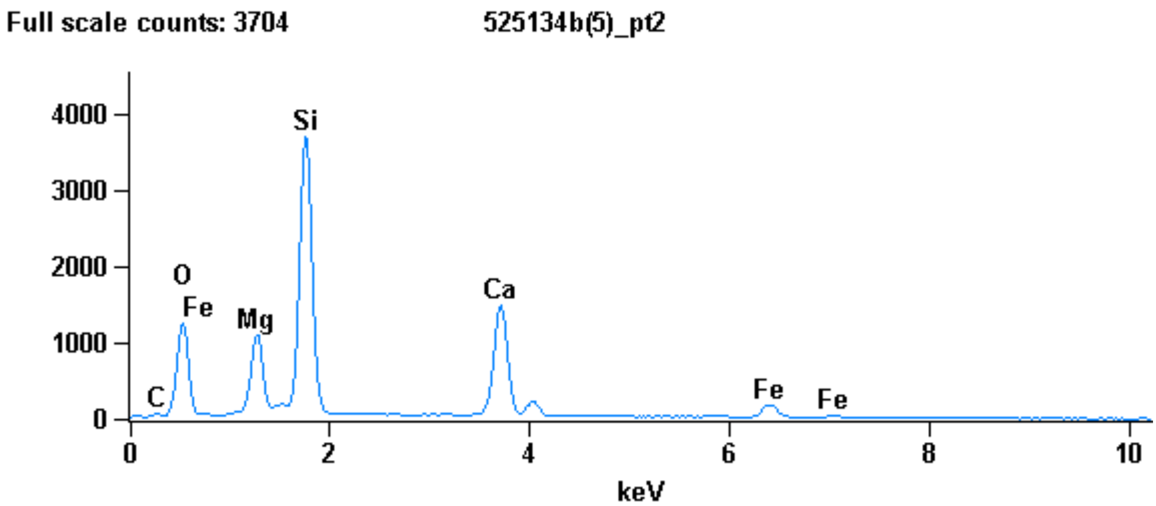

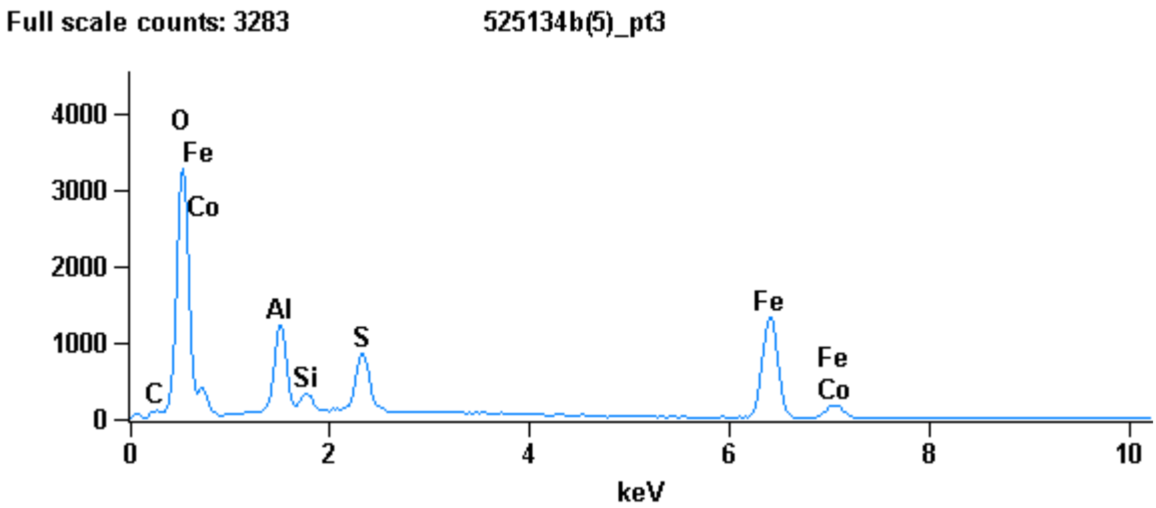
Full scale counts: 3283
525134b(5)_pt3
4000
3000
2000
1000
0
O
Fe
Co
Al
Si
S
C
Fe
Fe
Co
0
2
4
6
8
10
keV

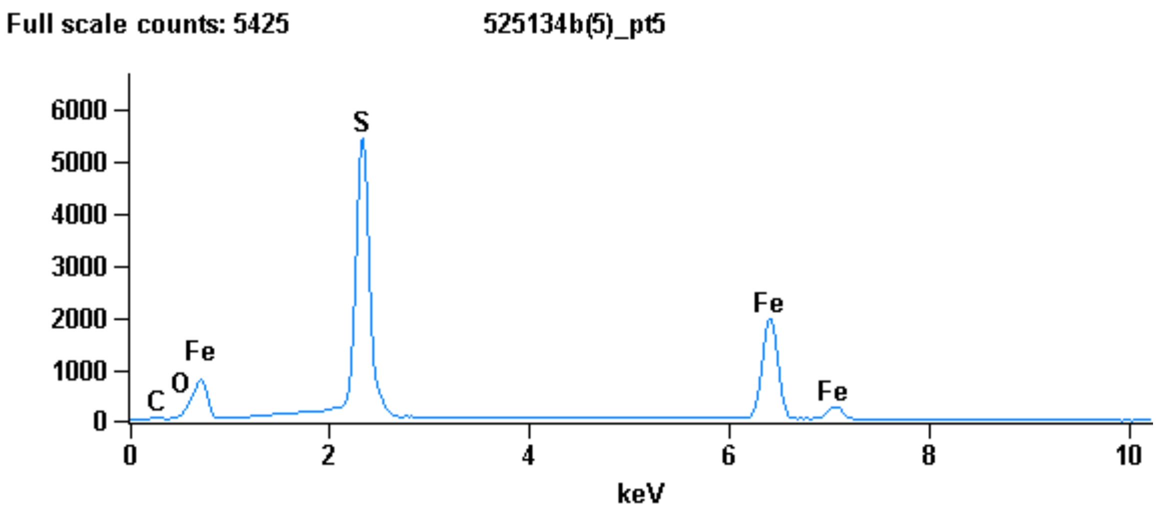
Full scale counts: 5425
525134b(5)_pt5
6000
5000
4000
3000
2000
1000
0
S
Fe
C
O
Fe
Fe
0
2
4
6
8
10
keV

Full scale counts: 3593 525134b(5)_pt6

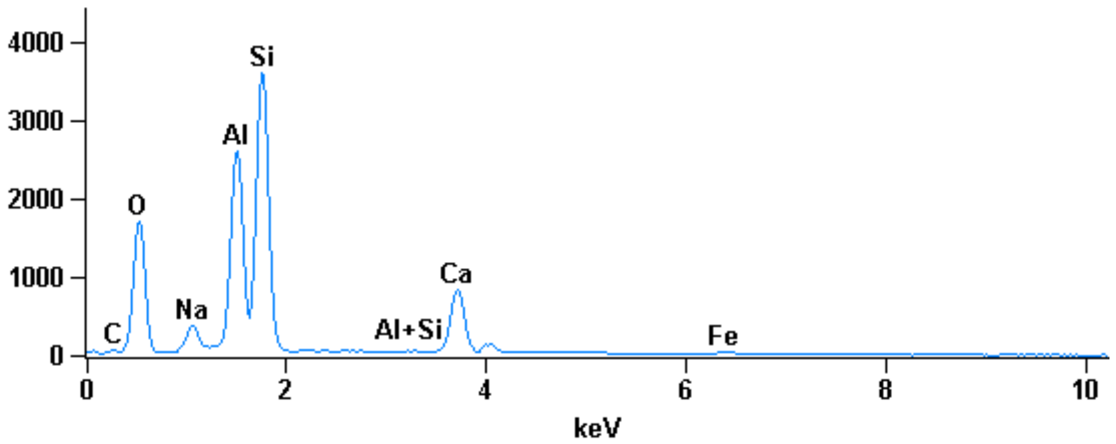

Full scale counts: 4144 525134b(5)_pt7

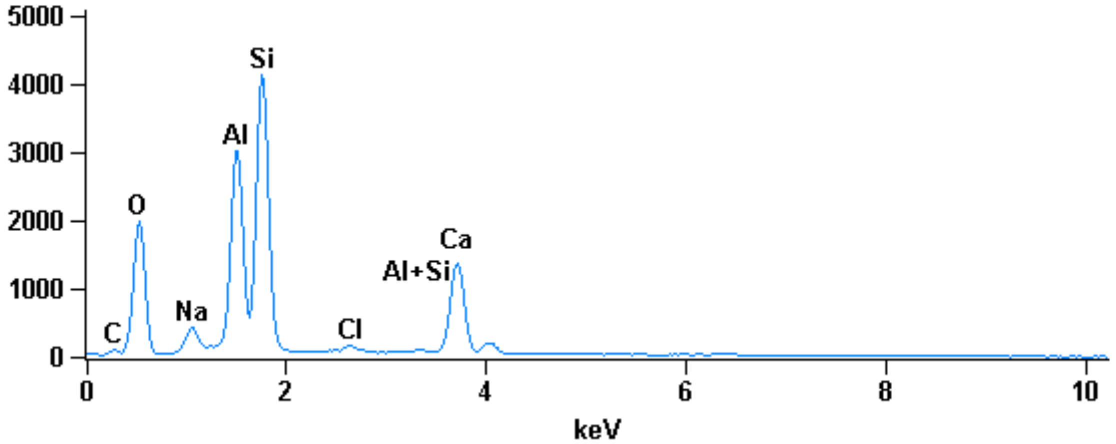

Full scale counts: 4216 525134b(5)_pt8

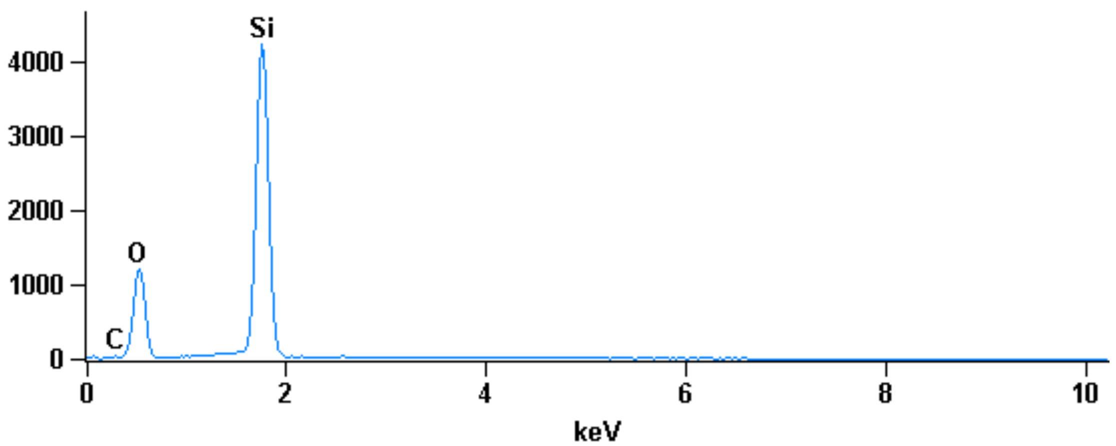

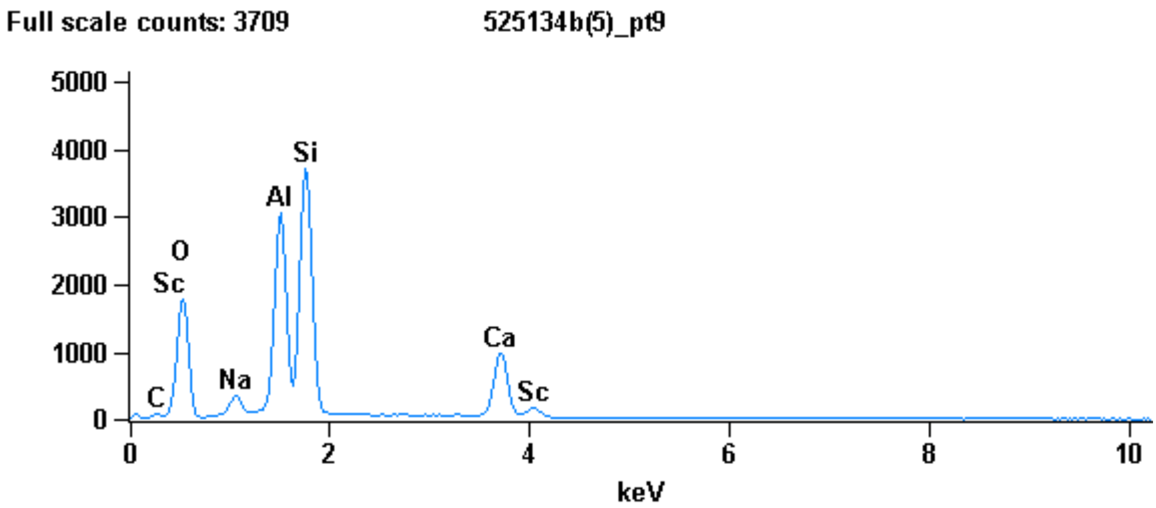

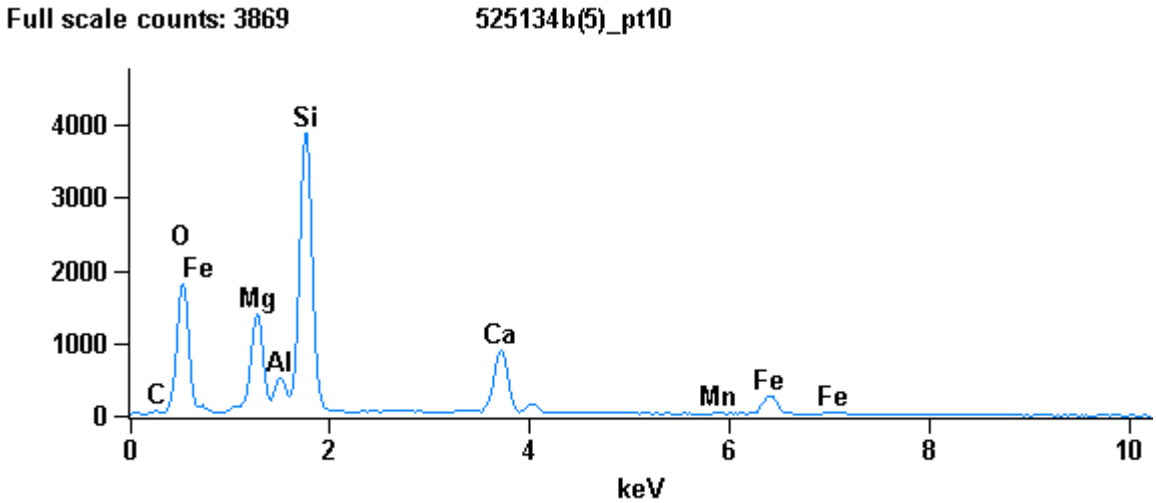

Weight %

	O-K	Na-K	Mg-K	Al-K	Si-K	S-K	Cl-K	Ca-K	Sc-K	Mn-K	Fe-K	Co-K
525134b(5)_pt1	46.10S			0.08		21.46					32.36	
525134b(5)_pt2	43.52S		8.76		25.03			16.71			5.99	
525134b(5)_pt3	39.43S			10.51	2.17	6.64					40.91	0.33
525134b(5)_pt4	39.76S			0.17		12.92					47.15	
525134b(5)_pt5	45.96S					21.31					32.73	
525134b(5)_pt6	47.05S	3.30		15.70	24.81			8.49			0.65	
525134b(5)_pt7	45.74S	3.25		14.83	23.24		0.56	12.38				
525134b(5)_pt8	53.26S				46.74							
525134b(5)_pt9	46.96S	2.77		16.39	24.16			9.62	0.09			
525134b(5)_pt10	44.91S		10.15	2.30	25.63			9.23		0.29	7.49	

Atom %

	O-K	Na-K	Mg-K	Al-K	Si-K	S-K	Cl-K	Ca-K	Sc-K	Mn-K	Fe-K	Co-K
525134b(5)_pt1	69.72			0.07		16.19					14.02	
525134b(5)_pt2	60.51		8.01		19.82			9.27			2.39	
525134b(5)_pt3	63.58			10.05	1.99	5.34					18.90	0.14
525134b(5)_pt4	66.47			0.17		10.78					22.58	
525134b(5)_pt5	69.67					16.12					14.21	
525134b(5)_pt6	61.61	3.01		12.19	18.51			4.44			0.24	
525134b(5)_pt7	60.80	3.01		11.69	17.60		0.33	6.57				
525134b(5)_pt8	66.67				33.33							
525134b(5)_pt9	61.59	2.53		12.75	18.05			5.04	0.04			
525134b(5)_pt10	61.13		9.09	1.86	19.87			5.02		0.12	2.92	

Compound %

		Na2O	MgO	Al2O3	SiO2	SO3	Cl	CaO	Sc2O3	MnO	Fe2O3	CoO
525134b(5)_pt1	0.00			0.15		53.59					46.27	
525134b(5)_pt2	0.00		14.52		53.54			23.38			8.57	
525134b(5)_pt3	0.00			19.86	4.64	16.58					58.50	0.42
525134b(5)_pt4	0.00			0.32		32.27					67.41	
525134b(5)_pt5	0.00					53.20					46.80	
525134b(5)_pt6	0.00	4.45		29.66	53.07			11.89			0.93	
525134b(5)_pt7	0.00	4.39		28.01	49.72		0.56	17.33				
525134b(5)_pt8	0.00				100.00							
525134b(5)_pt9	0.00	3.74		30.97	51.69			13.46	0.14			
525134b(5)_pt10	0.00		16.83	4.35	54.82			12.92		0.38	10.71	

Minerals, 525134b(5)

pt1: Pyrrhotite
pt2: Clinopyroxene - diopside-hedenbergite (inclusion in pyrrhotite)
pt3: Mixed signal/edge effect
pt4: Pyrite
pt5: Pyrrhotite
pt6: Feldspar - plagioclase (inclusion/microxenolith?)
pt7: Feldspar - plagioclase (inclusion/microxenolith?)
pt8: Quartz
pt9: Feldspar - plagioclase
pt10: Amphibole - hornblende

525134b(6)

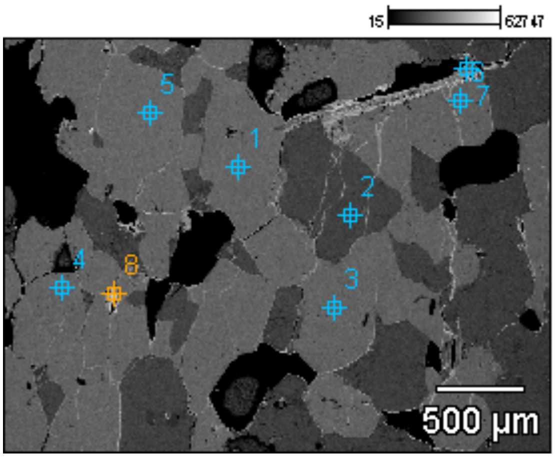

Image name: 525134b(6)
Magnification: 39

Full scale counts: 3424 525134b(6)_pt1

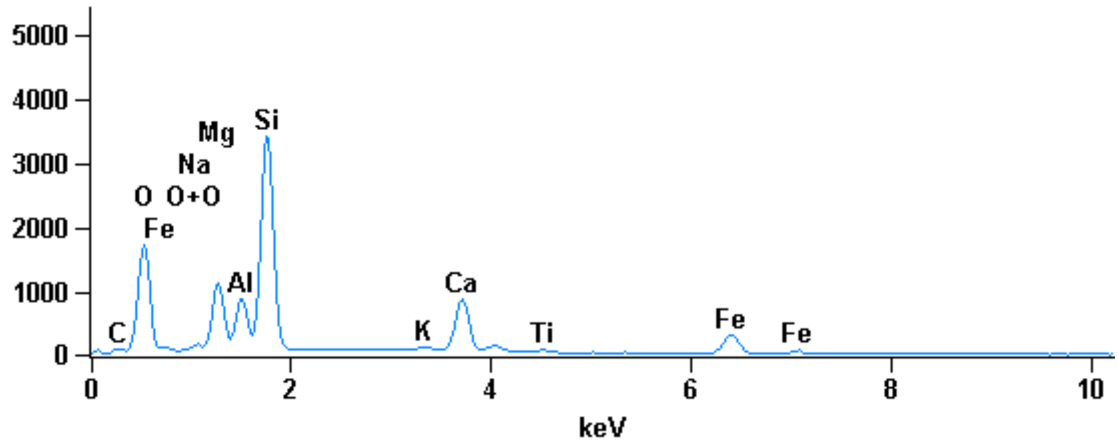

Full scale counts: 3644 525134b(6)_pt2

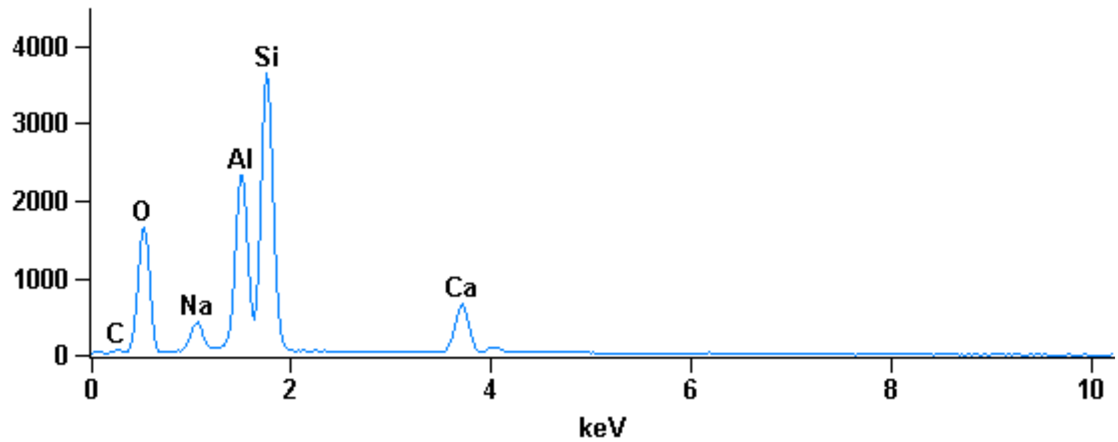

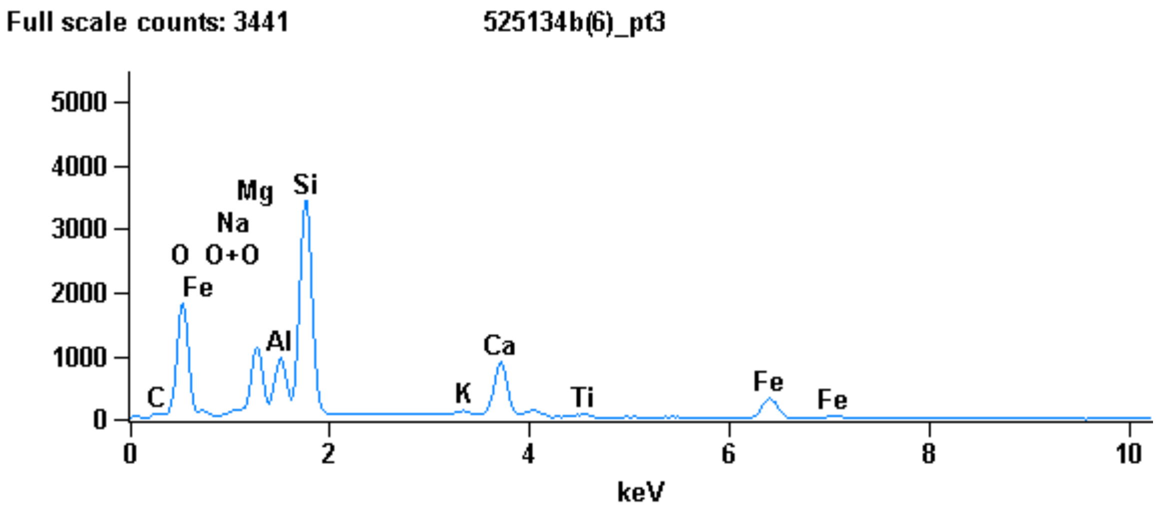
Full scale counts: 3441
525134b(6)_pt3
5000
4000
3000
2000
1000
0
C
O
Fe
O+O
Na
Mg
Si
Al
K
Ca
Ti
Fe
Fe
0
2
4
6
8
10
keV

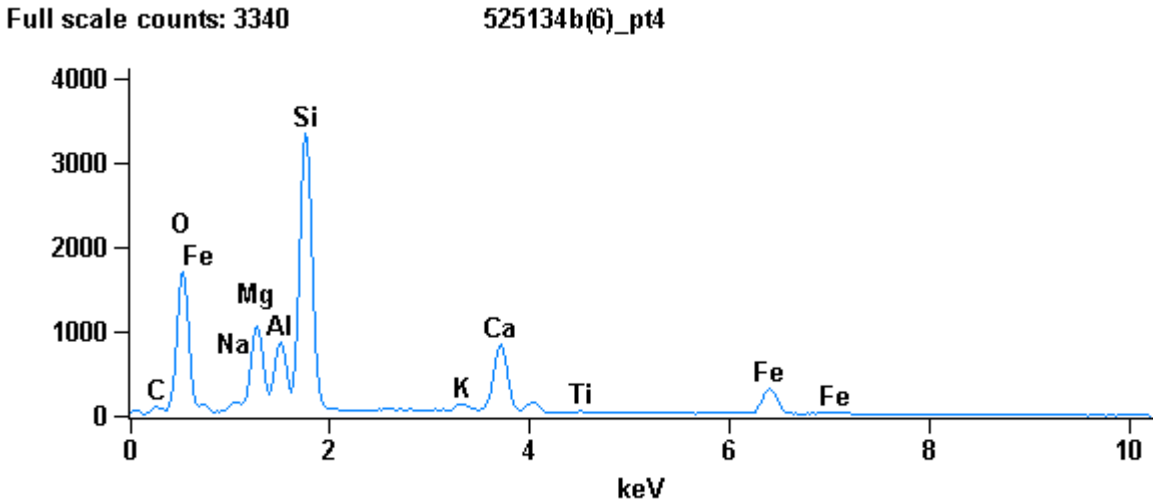
Full scale counts: 3340
525134b(6)_pt4
4000
3000
2000
1000
0
C
O
Fe
Na
Mg
Al
Si
K
Ca
Ti
Fe
Fe
0
2
4
6
8
10
keV

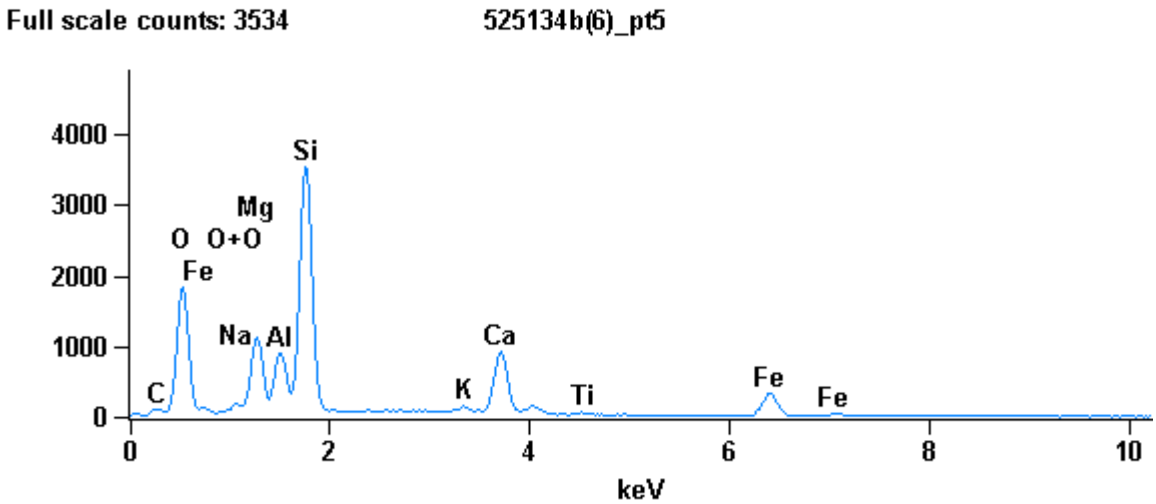
Full scale counts: 3534
525134b(6)_pt5
4000
3000
2000
1000
0
C
O
Fe
O+O
Mg
Na
Al
Si
K
Ca
Ti
Fe
Fe
0
2
4
6
8
10
keV

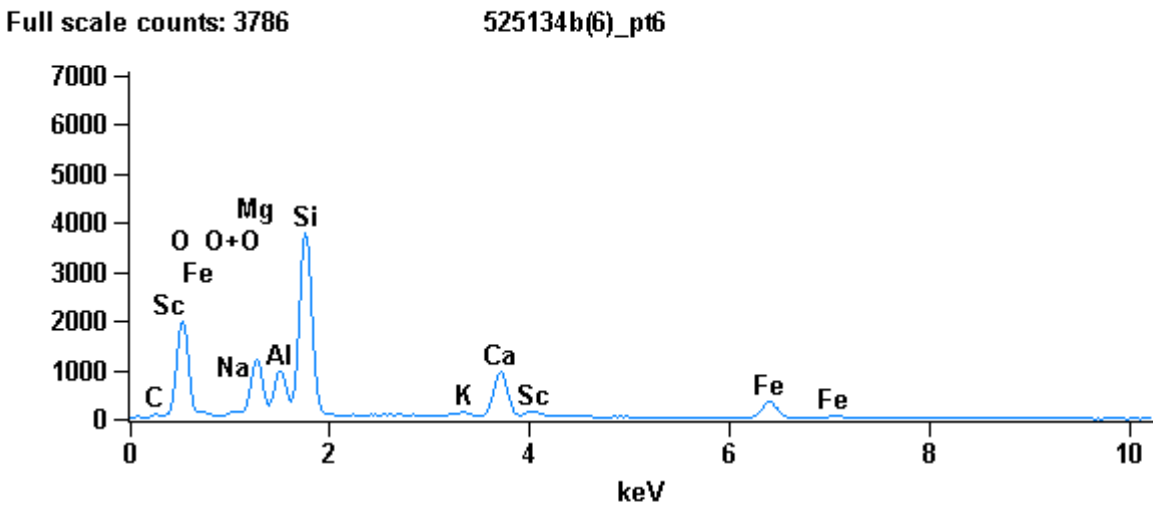
Full scale counts: 3786
525134b(6)_pt6
7000
6000
5000
4000
3000
2000
1000
0
C
Sc
O
Fe
O+O
Mg
Na
Al
Si
K
Ca
Sc
Fe
Fe
0
2
4
6
8
10
keV

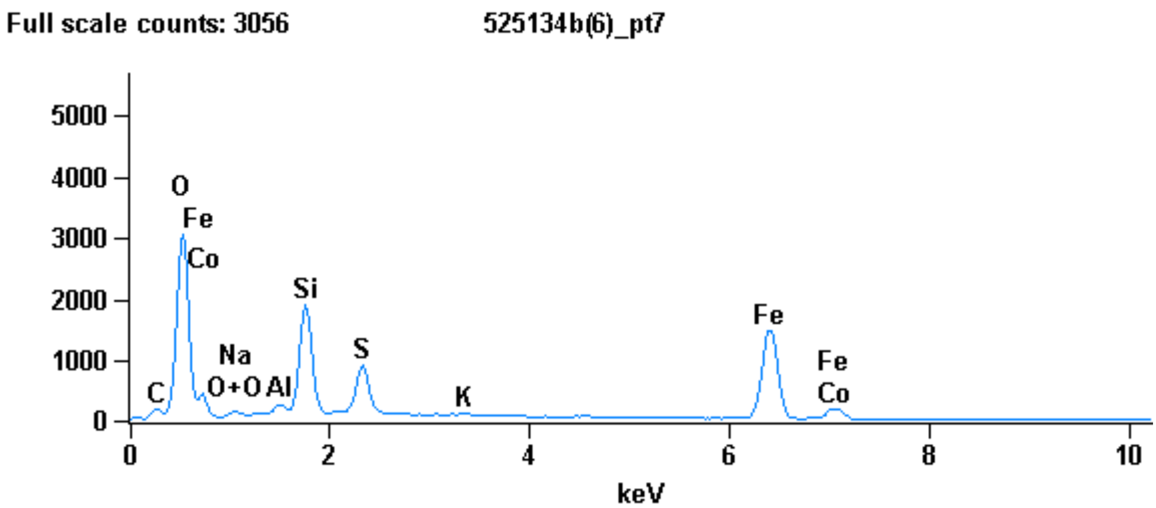
Full scale counts: 3056
525134b(6)_pt7
5000
4000
3000
2000
1000
0
C
O
Fe
Co
Na
O+O
Al
Si
S
K
Fe
Fe
Co
0
2
4
6
8
10
keV

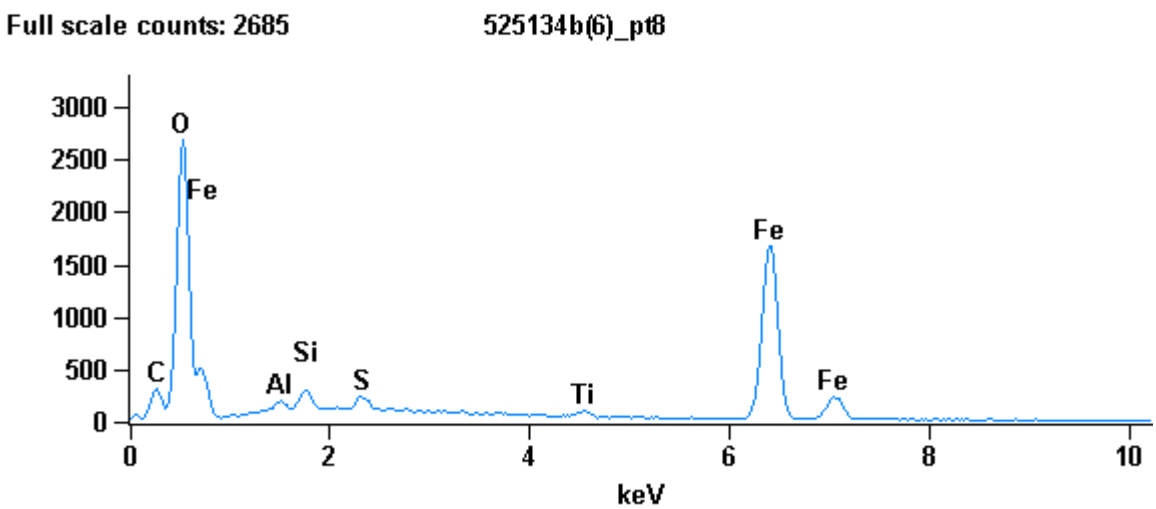
Full scale counts: 2685
525134b(6)_pt8
3000
2500
2000
1500
1000
500
0
C
O
Fe
Al
Si
S
Ti
Fe
Fe
0
2
4
6
8
10
keV

Weight %

	O-K	Na-K	Mg-K	Al-K	Si-K	S-K	K-K	Ca-K	Sc-K	Ti-K	Fe-K	Co-K
525134b(6)_pt1	44.12S	0.83	8.34	4.93	22.96		0.60	8.54		0.44	9.22	
525134b(6)_pt2	47.41S	4.39		15.04	26.04			7.12				
525134b(6)_pt3	44.12S	0.80	8.24	5.80	22.40		0.57	8.32		0.48	9.26	
525134b(6)_pt4	44.11S	1.10	8.68	5.48	22.52		0.55	8.26		0.33	8.97	
525134b(6)_pt5	44.14S	1.07	8.45	5.38	22.73		0.55	8.55		0.32	8.80	
525134b(6)_pt6	44.10S	0.82	8.33	5.17	22.91		0.59	8.57	0.12		9.39	
525134b(6)_pt7	40.33S	1.24		0.89	11.74	5.72	0.28				39.79	0.00
525134b(6)_pt8	32.71S			1.23	2.15	1.44				0.71	61.76	

Atom %

	O-K	Na-K	Mg-K	Al-K	Si-K	S-K	K-K	Ca-K	Sc-K	Ti-K	Fe-K	Co-K
525134b(6)_pt1	60.74	0.80	7.56	4.03	18.01		0.34	4.69		0.20	3.64	
525134b(6)_pt2	61.53	3.97		11.57	19.25			3.69				
525134b(6)_pt3	60.71	0.76	7.46	4.73	17.56		0.32	4.57		0.22	3.65	
525134b(6)_pt4	60.53	1.05	7.84	4.46	17.60		0.31	4.53		0.15	3.53	
525134b(6)_pt5	60.59	1.02	7.64	4.38	17.77		0.31	4.68		0.15	3.46	
525134b(6)_pt6	60.69	0.79	7.55	4.22	17.96		0.33	4.71	0.06		3.70	
525134b(6)_pt7	64.23	1.38		0.85	10.65	4.55	0.18				18.16	0.00
525134b(6)_pt8	61.36			1.37	2.30	1.35				0.44	33.19	

Compound %

		Na2O	MgO	Al2O3	SiO2	SO3	K2O	CaO	Sc2O3	TiO2	Fe2O3	CoO
525134b(6)_pt1	0.00	1.12	13.83	9.32	49.13		0.73	11.94		0.73	13.19	
525134b(6)_pt2	0.00	5.92		28.42	55.70			9.96				
525134b(6)_pt3	0.00	1.08	13.66	10.96	47.93		0.69	11.64		0.80	13.24	
525134b(6)_pt4	0.00	1.48	14.39	10.36	48.17		0.66	11.56		0.55	12.82	
525134b(6)_pt5	0.00	1.44	14.02	10.16	48.63		0.66	11.96		0.54	12.59	
525134b(6)_pt6	0.00	1.11	13.82	9.76	49.00		0.71	11.99	0.19		13.43	
525134b(6)_pt7	0.00	1.67		1.69	25.12	14.29	0.34				56.89	0.00
525134b(6)_pt8	0.00			2.32	4.60	3.59				1.18	88.31	

Minerals, 525134b(6)
pt1: Amphibolite - hornblende
pt2: Feldspar - plagioclase
pt3: Amphibolite - hornblende
pt4: Amphibolite - hornblende
pt5: Amphibolite - hornblende
pt6: Amphibolite - hornblende
pt7: Mixed signal/edge effect
pt8: Fe-oxide + mixed signal/edge effect

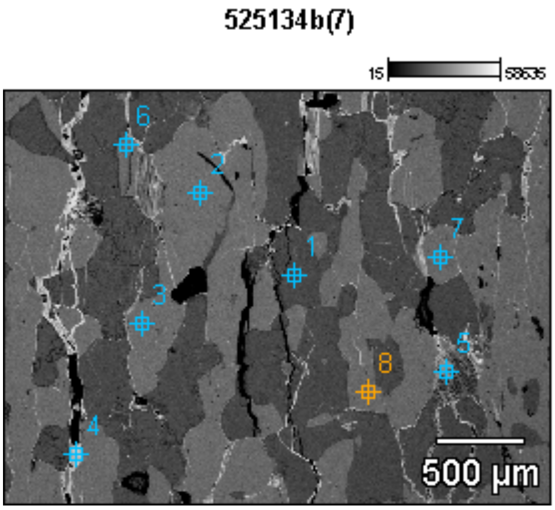

Image name: 525134b(7)
Magnification: 39

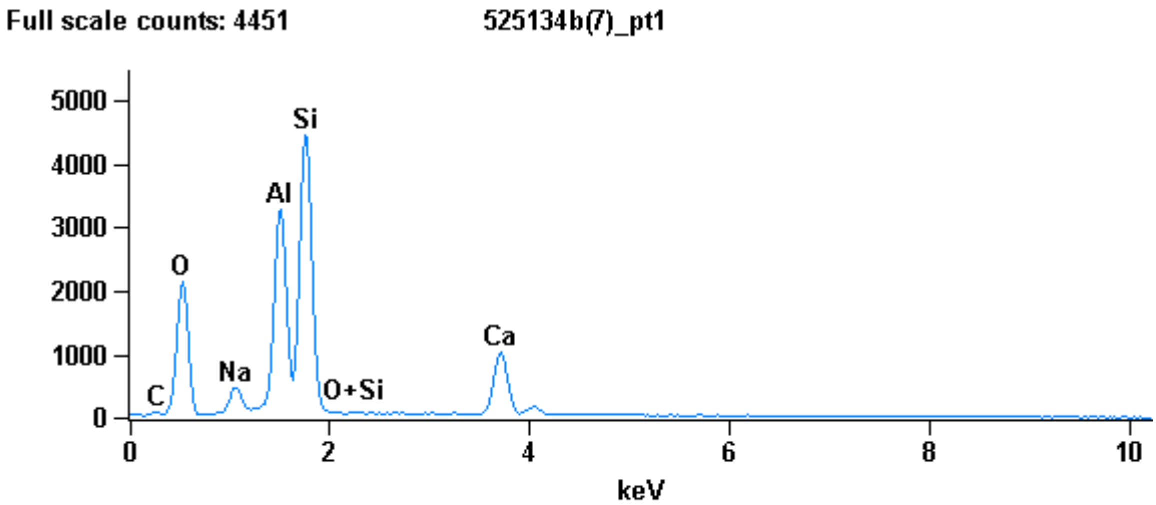

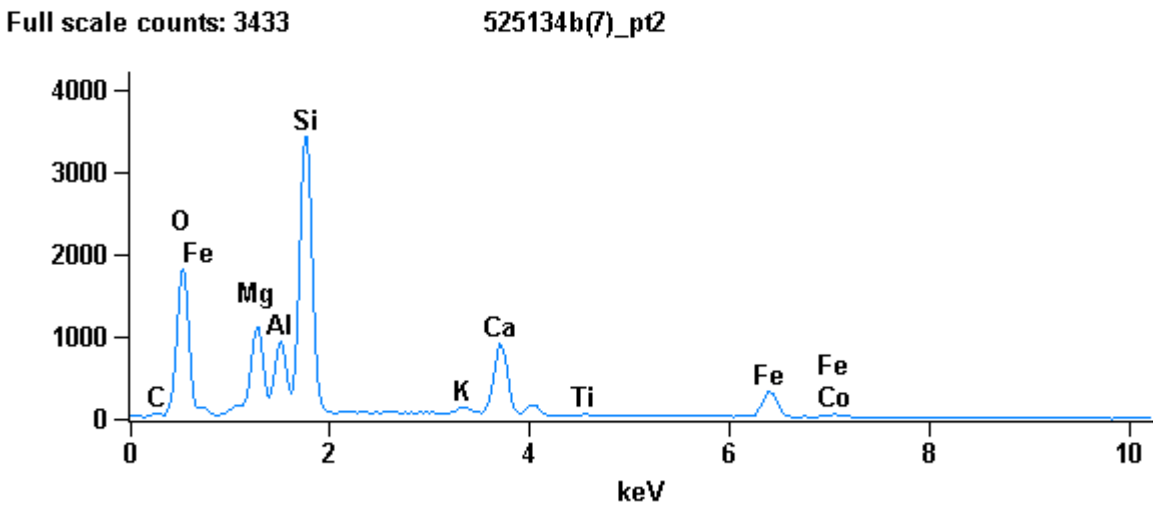

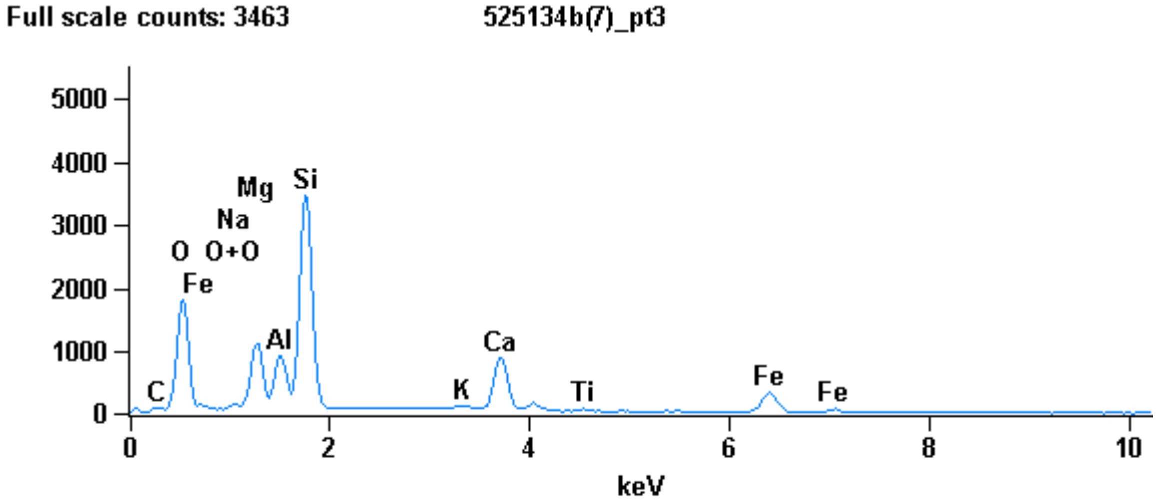
Full scale counts: 3463
525134b(7)_pt3
5000
4000
3000
2000
1000
0
Mg
Si
Na
O
O+O
Fe
Al
C
K
Ca
Ti
Fe
Fe
0
2
4
6
8
10
keV

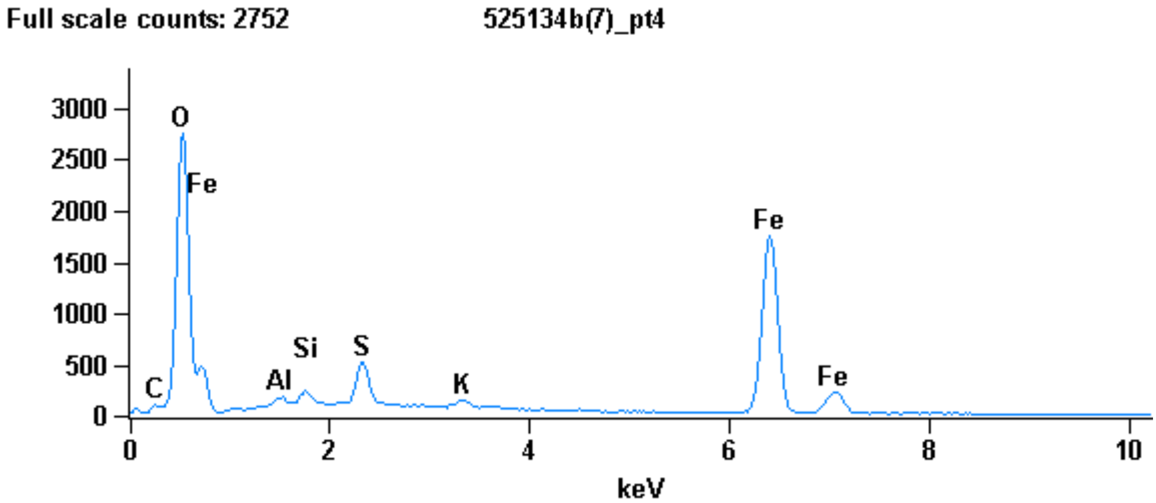
Full scale counts: 2752
525134b(7)_pt4
3000
2500
2000
1500
1000
500
0
O
Fe
Fe
Si
S
C
Al
K
Fe
0
2
4
6
8
10
keV

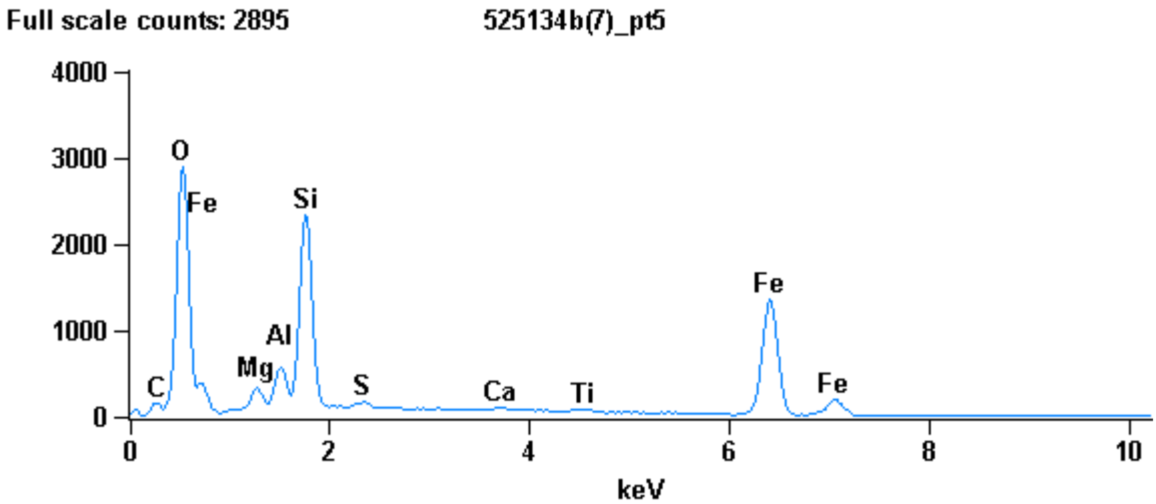
Full scale counts: 2895
525134b(7)_pt5
4000
3000
2000
1000
0
O
Fe
Si
Fe
Al
Mg
C
S
Ca
Ti
Fe
0
2
4
6
8
10
keV

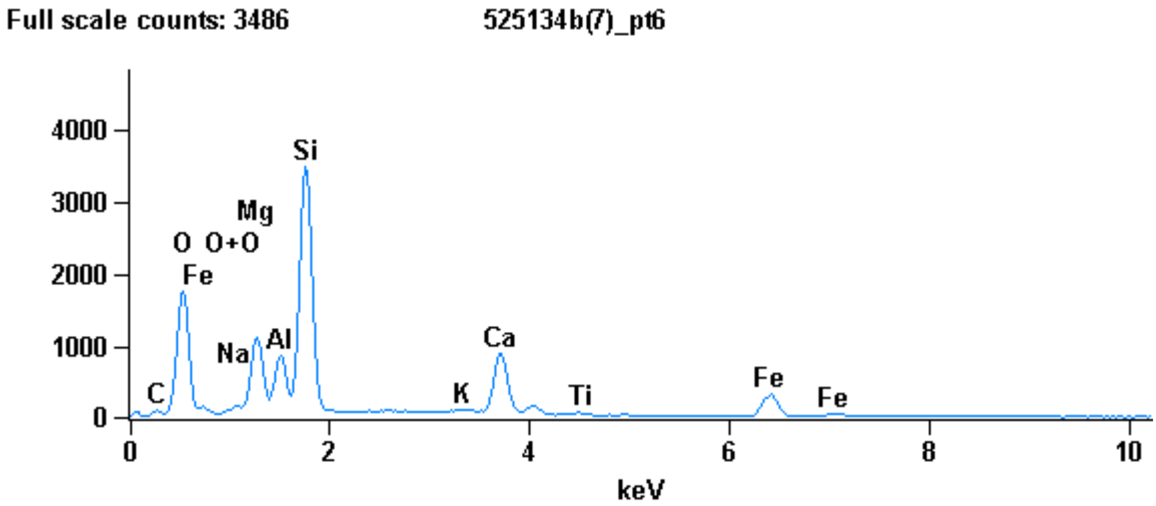
Full scale counts: 3486
525134b(7)_pt6
4000
3000
2000
1000
0
Si
Mg
O O+O
Fe
Na Al
C
Ca
K
Ti
Fe
Fe
0
2
4
6
8
10
keV

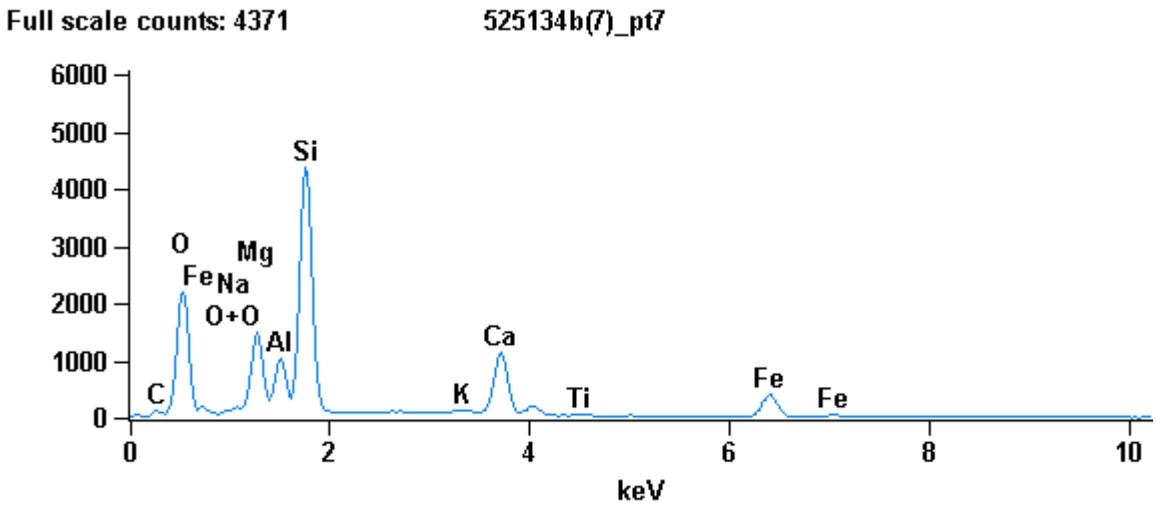
Full scale counts: 4371
525134b(7)_pt7
6000
5000
4000
3000
2000
1000
0
Si
O
Mg
Fe
Na
O+O
Al
C
Ca
K
Ti
Fe
Fe
0
2
4
6
8
10
keV

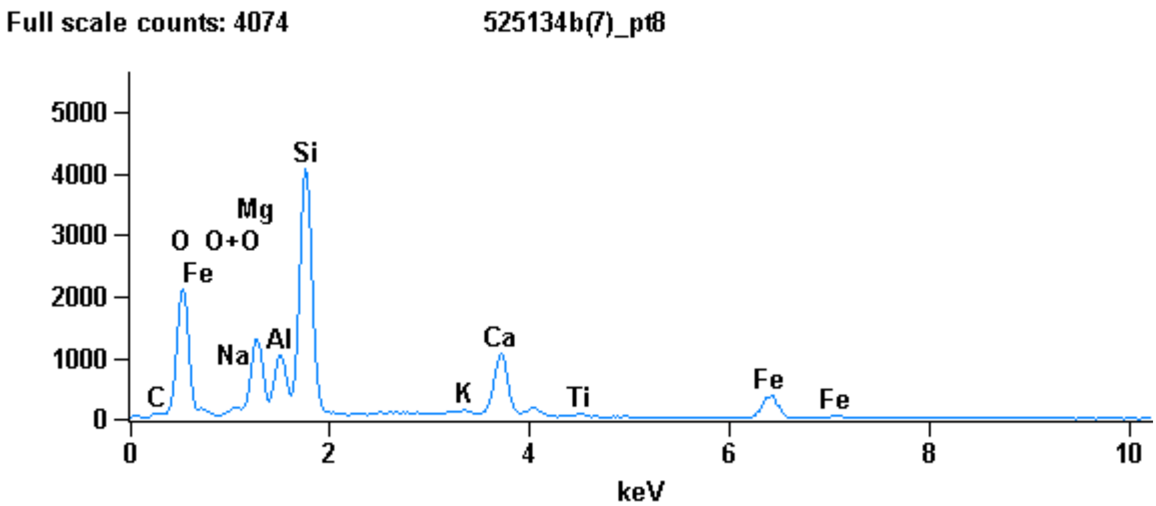
Full scale counts: 4074
525134b(7)_pt8
5000
4000
3000
2000
1000
0
Si
Mg
O O+O
Fe
Na Al
C
Ca
K
Ti
Fe
Fe
0
2
4
6
8
10
keV

Weight %

	O-K	Na-K	Mg-K	Al-K	Si-K	S-K	K-K	Ca-K	Ti-K	Fe-K	Co-K
525134b(7)_pt1	47.10S	3.55		15.69	24.96			8.69			
525134b(7)_pt2	44.30S		7.77	5.33	23.21		0.60	8.90	0.32	9.58	0.00
525134b(7)_pt3	44.04S	0.83	8.46	5.53	22.38		0.52	8.62	0.31	9.31	
525134b(7)_pt4	33.81S			0.97	1.15	3.99	0.67			59.41	
525134b(7)_pt5	40.03S		2.13	3.44	16.14	0.56		0.34	0.62	36.75	
525134b(7)_pt6	44.14S	0.84	8.58	5.01	22.91		0.52	8.71	0.29	8.99	
525134b(7)_pt7	44.19S	0.82	9.08	4.78	22.96		0.45	8.83	0.33	8.56	
525134b(7)_pt8	43.97S	0.85	8.38	5.27	22.45		0.59	8.68	0.37	9.44	

Atom %

	O-K	Na-K	Mg-K	Al-K	Si-K	S-K	K-K	Ca-K	Ti-K	Fe-K	Co-K
525134b(7)_pt1	61.52	3.23		12.15	18.57			4.53			
525134b(7)_pt2	61.15		7.06	4.36	18.25		0.34	4.90	0.15	3.79	0.00
525134b(7)_pt3	60.62	0.79	7.67	4.52	17.55		0.29	4.74	0.14	3.67	
525134b(7)_pt4	62.24			1.06	1.21	3.66	0.50			31.33	
525134b(7)_pt5	62.73		2.19	3.20	14.41	0.44		0.21	0.32	16.50	
525134b(7)_pt6	60.67	0.81	7.76	4.09	17.94		0.29	4.78	0.13	3.54	
525134b(7)_pt7	60.60	0.78	8.20	3.89	17.94		0.25	4.83	0.15	3.36	
525134b(7)_pt8	60.63	0.81	7.61	4.31	17.63		0.33	4.78	0.17	3.73	

Compound %

		Na2O	MgO	Al2O3	SiO2	SO3	K2O	CaO	TiO2	Fe2O3	CoO
525134b(7)_pt1	0.00	4.79		29.65	53.39			12.17			
525134b(7)_pt2	0.00		12.89	10.07	49.65		0.72	12.45	0.54	13.69	0.00
525134b(7)_pt3	0.00	1.11	14.03	10.46	47.88		0.63	12.06	0.52	13.31	
525134b(7)_pt4	0.00			1.83	2.46	9.95	0.80			84.94	
525134b(7)_pt5	0.00		3.53	6.51	34.52	1.41		0.47	1.03	52.54	
525134b(7)_pt6	0.00	1.14	14.23	9.47	49.01		0.62	12.18	0.48	12.86	
525134b(7)_pt7	0.00	1.10	15.06	9.04	49.12		0.54	12.36	0.55	12.23	
525134b(7)_pt8	0.00	1.14	13.90	9.95	48.03		0.71	12.15	0.62	13.50	

Minerals, 525134b(x)
pt1: Feldspar - plagioclase
pt2: Amphibole - hornblende
pt3: Amphibole - hornblende
pt4: Fe-oxide + mixed signal/edge effect
pt5: Mixed signal/edge effect
pt6: Amphibole - hornblende
pt7: Amphibole - hornblende
pt8: Amphibole - hornblende

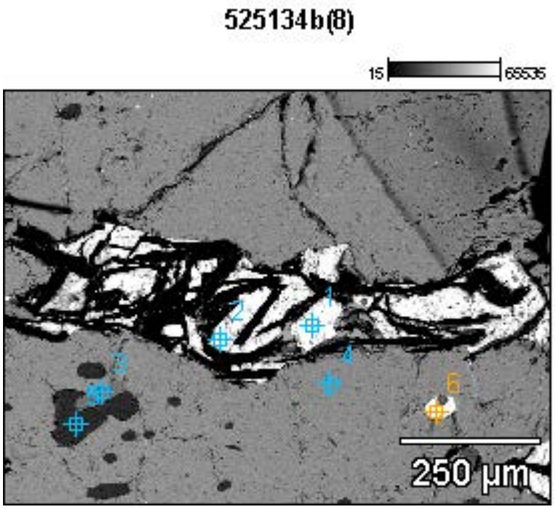

Image name: 525134b(8)
Magnification: 124

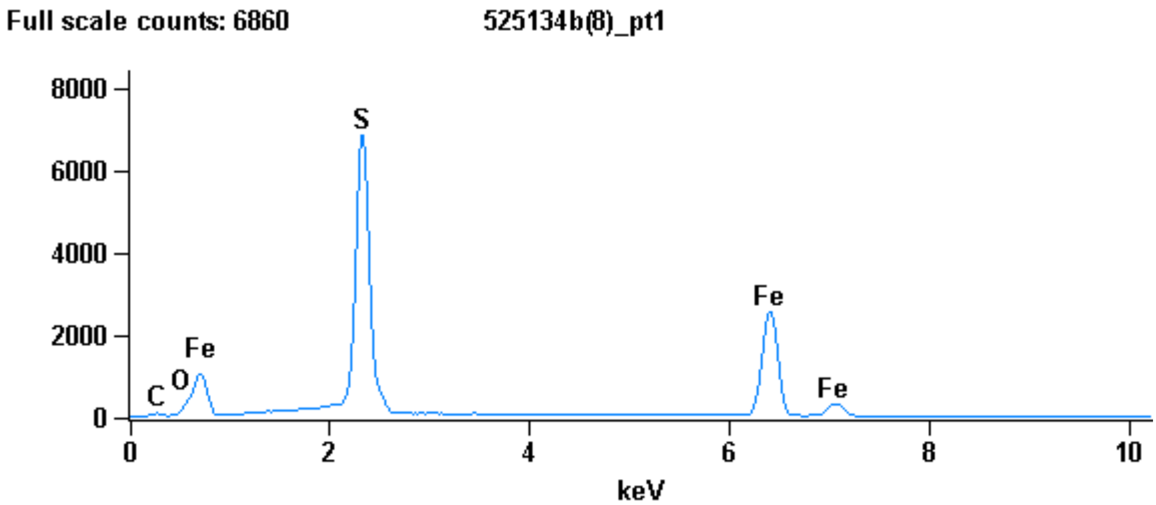

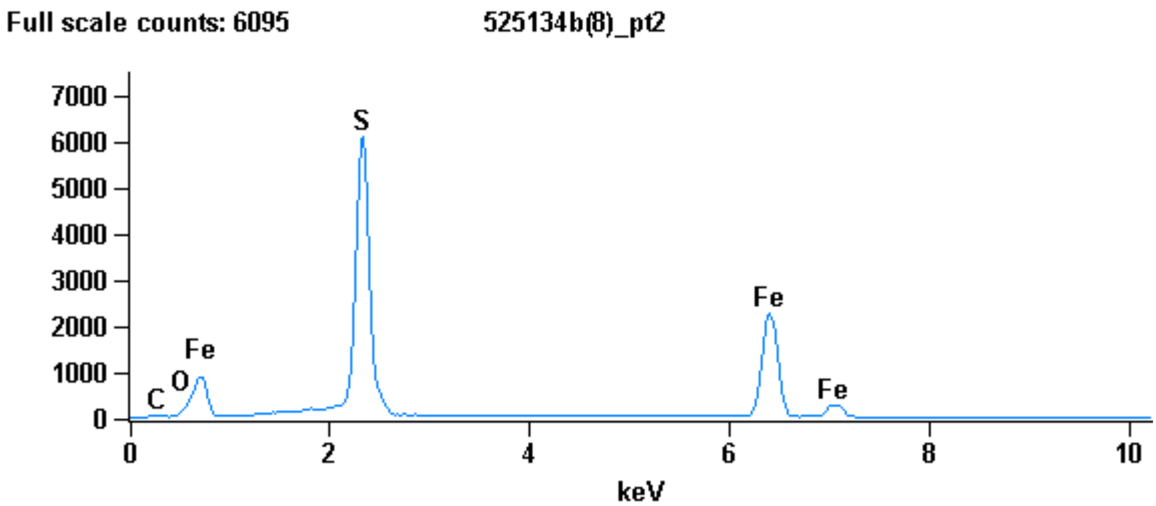

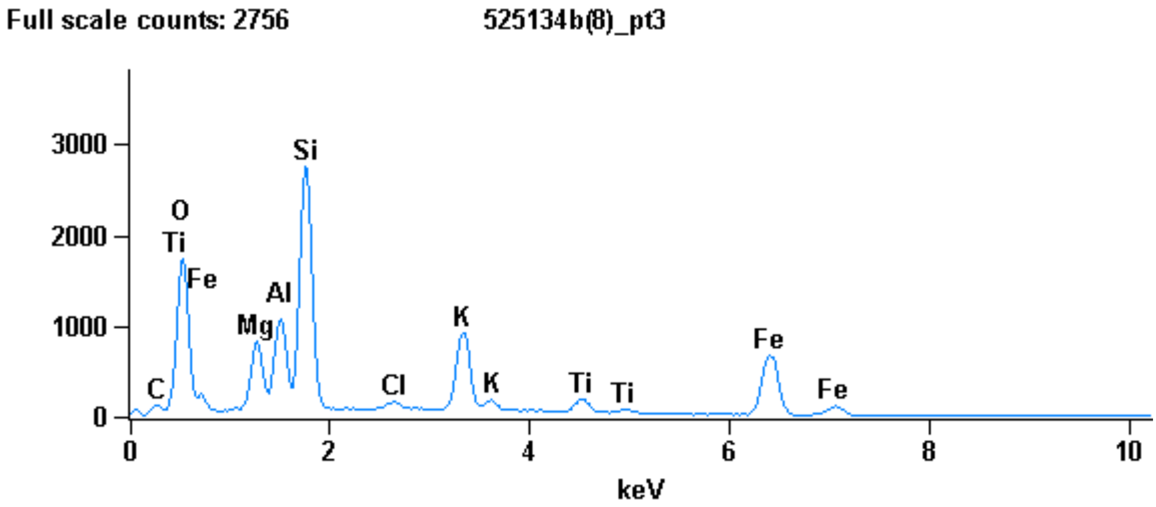
Full scale counts: 2756
525134b(8)_pt3
3000
2000
1000
0
0
2
4
6
8
10
keV
O
Ti
Fe
C
Mg
Al
Si
Cl
K
K
Ti
Ti
Fe
Fe

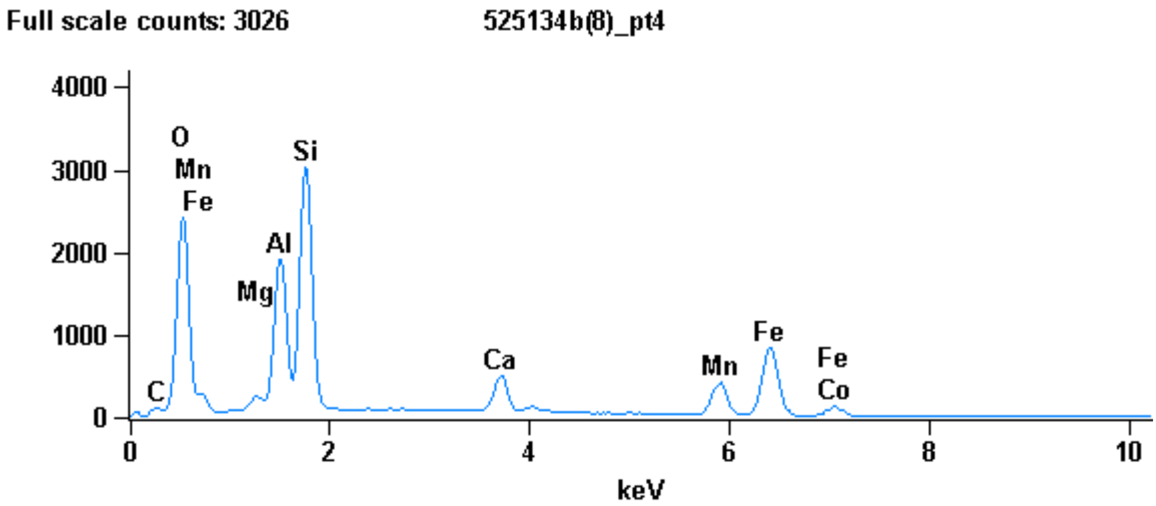
Full scale counts: 3026
525134b(8)_pt4
4000
3000
2000
1000
0
0
2
4
6
8
10
keV
O
Mn
Fe
C
Mg
Al
Si
Ca
Mn
Fe
Fe
Co

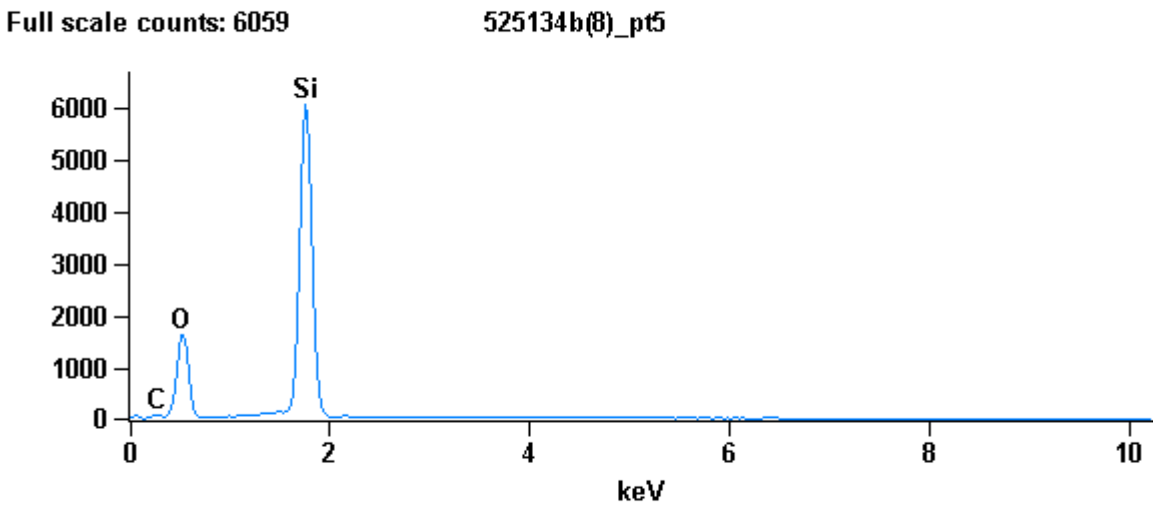
Full scale counts: 6059
525134b(8)_pt5
6000
5000
4000
3000
2000
1000
0
0
2
4
6
8
10
keV
Si
O
C

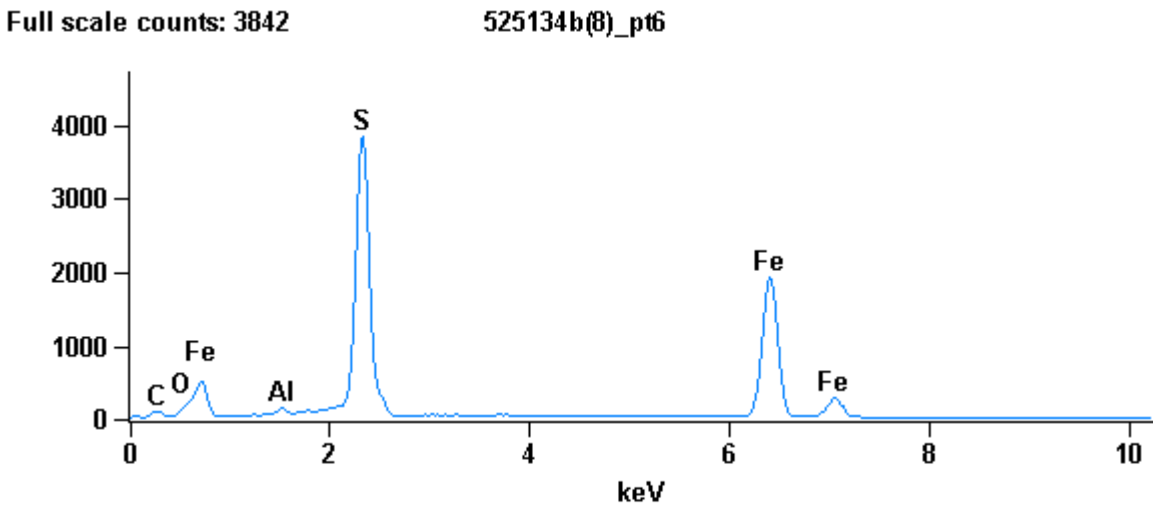

Weight %

	O-K	Mg-K	Al-K	Si-K	S-K	Cl-K	K-K	Ca-K	Ti-K	Mn-K	Fe-K	Co-K
525134b(8)_pt1	45.83S				21.13						33.04	
525134b(8)_pt2	45.79S				21.07						33.14	
525134b(8)_pt3	40.89S	6.02	6.86	17.40		0.48	7.38		2.05		18.93	
525134b(8)_pt4	41.42S	0.93	10.82	17.27				3.38		7.79	18.30	0.09
525134b(8)_pt5	53.26S			46.74								
525134b(8)_pt6	44.08S		0.26		18.66						37.00	

Atom %

	O-K	Mg-K	Al-K	Si-K	S-K	Cl-K	K-K	Ca-K	Ti-K	Mn-K	Fe-K	Co-K
525134b(8)_pt1	69.61				16.02						14.37	
525134b(8)_pt2	69.59				15.98						14.43	
525134b(8)_pt3	59.98	5.81	5.97	14.54		0.32	4.43		1.00		7.96	
525134b(8)_pt4	61.66	0.91	9.56	14.64				2.01		3.38	7.81	0.04
525134b(8)_pt5	66.67			33.33								
525134b(8)_pt6	68.71		0.24		14.52						16.52	

Compound %

		MgO	Al2O3	SiO2	SO3	Cl	K2O	CaO	TiO2	MnO	Fe2O3	CoO
525134b(8)_pt1	0.00				52.77						47.23	
525134b(8)_pt2	0.00				52.62						47.38	
525134b(8)_pt3	0.00	9.98	12.96	37.22		0.48	8.88		3.42		27.07	
525134b(8)_pt4	0.00	1.54	20.45	36.94				4.73		10.06	26.17	0.11
525134b(8)_pt5	0.00			100.00								
525134b(8)_pt6	0.00		0.50		46.60						52.90	

Minerals, 525134b(8)
pt1: Pyrrhotite
pt2: Pyrrhotite
pt3: Biotite
pt4: Garnet - pyralspite-group
pt5: Quartz
pt6: Pyrrhotite

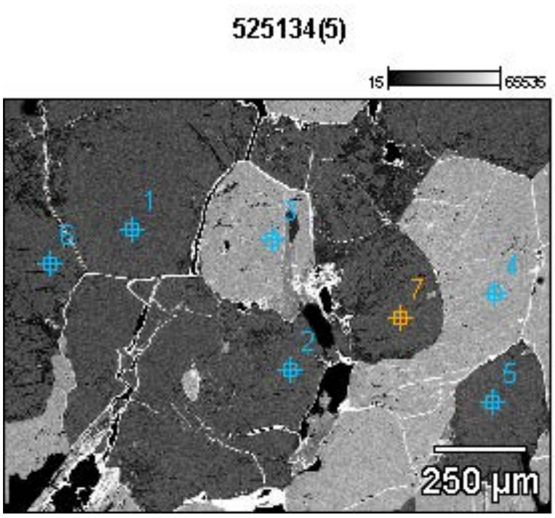

Image name: 525134a(5) (Data from 13/03/13)
Magnification: 82

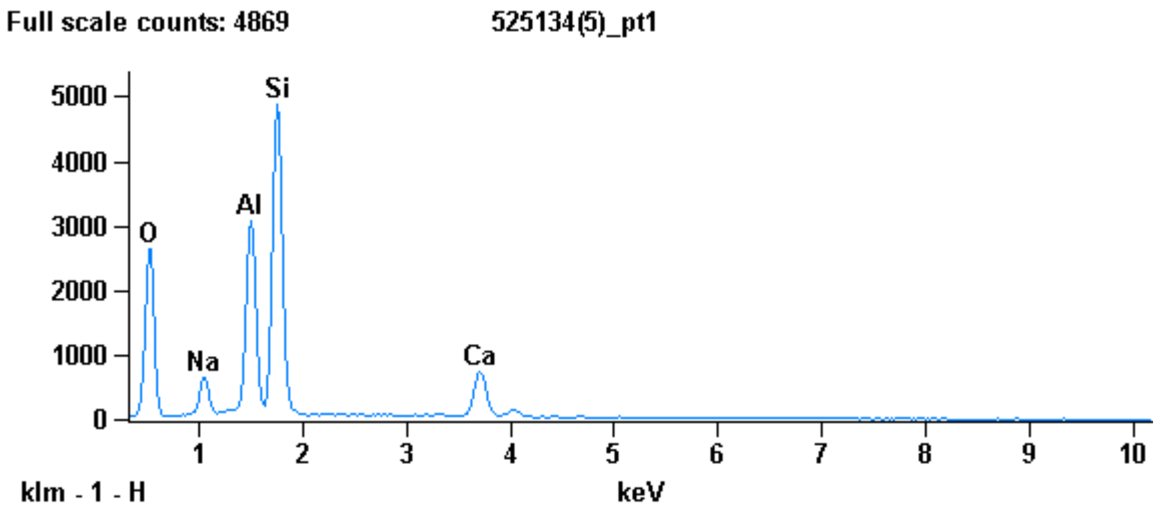

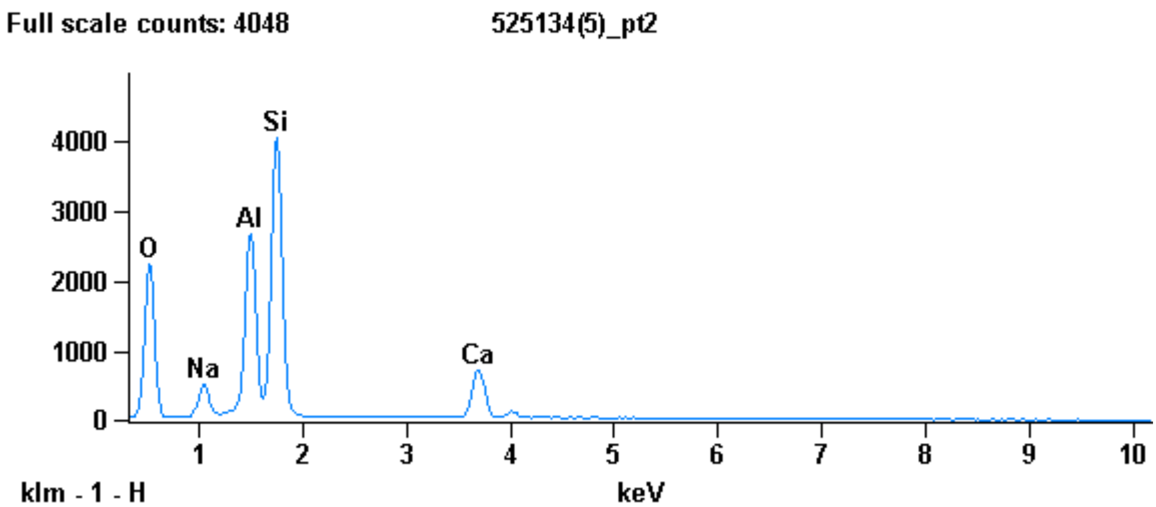

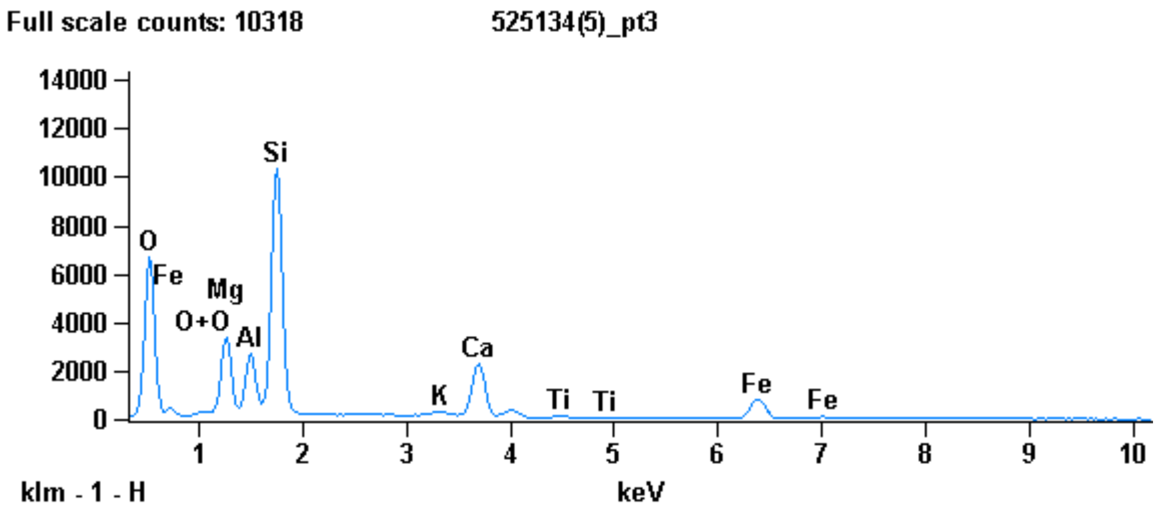
Full scale counts: 10318
525134(5)_pt3
14000
12000
10000
8000
6000
4000
2000
0
O
Fe
Mg
O+O
Al
Si
K
Ca
Ti
Ti
Fe
Fe
1 2 3 4 5 6 7 8 9 10
klm - 1 - H
keV

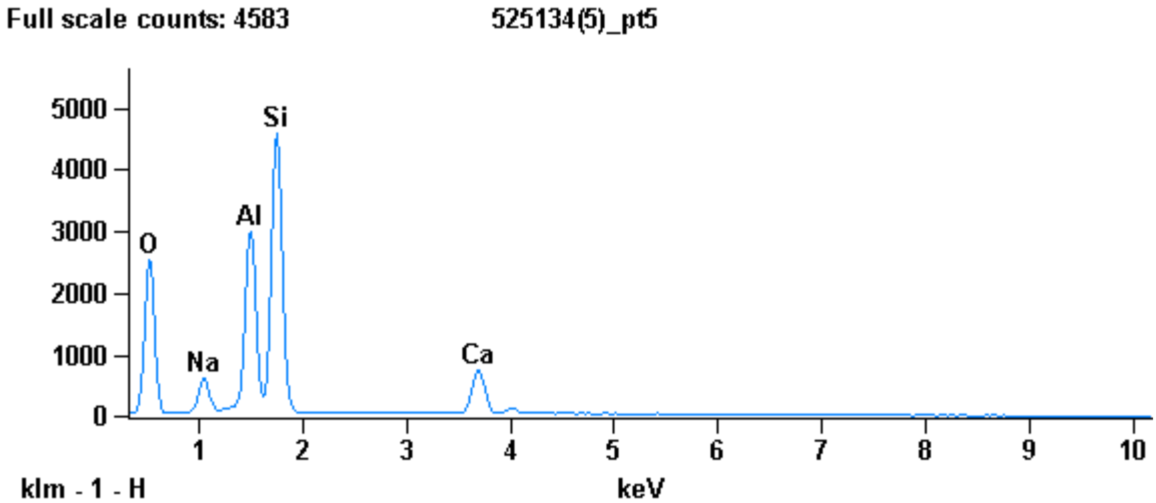
Full scale counts: 4583
525134(5)_pt5
5000
4000
3000
2000
1000
0
O
Na
Al
Si
Ca
1 2 3 4 5 6 7 8 9 10
klm - 1 - H
keV

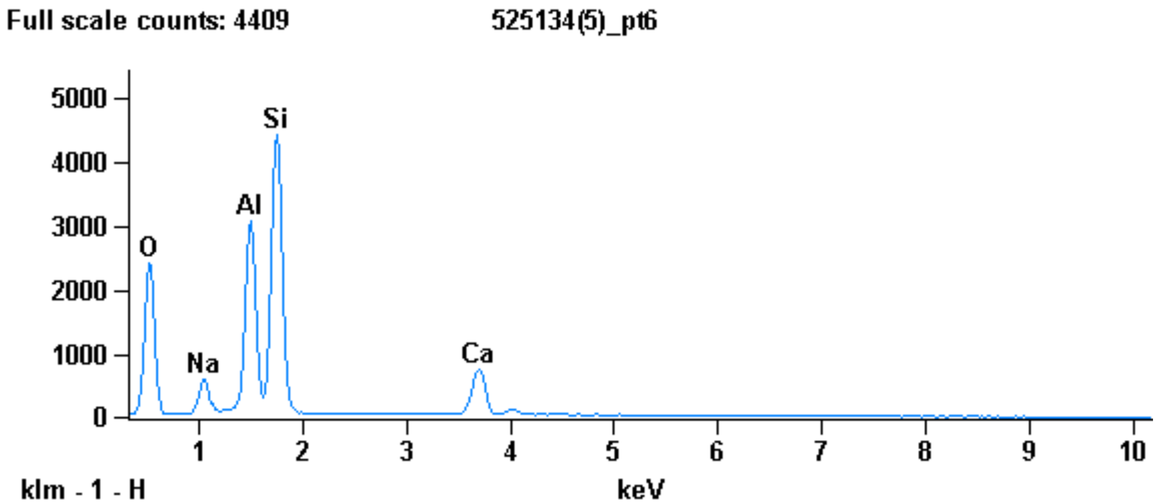
Full scale counts: 4409
525134(5)_pt6
5000
4000
3000
2000
1000
0
O
Na
Al
Si
Ca
1 2 3 4 5 6 7 8 9 10
klm - 1 - H
keV

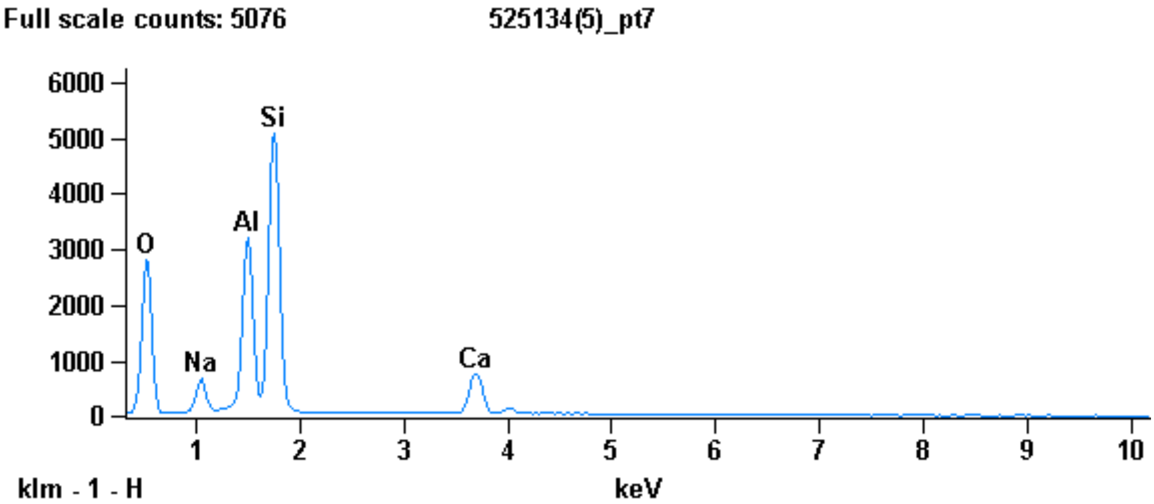

Weight %

	O-K	Na-K	Mg-K	Al-K	Si-K	K-K	Ca-K	Ti-K	Fe-K
525134(5)_pt1	47.51S	4.93		14.69	26.49		6.39		
525134(5)_pt2	47.32S	4.66		14.84	26.02		7.16		
525134(5)_pt3	44.66S		8.56	5.33	23.61	0.50	7.91	0.32	9.11
525134(5)_pt4	44.65S		8.58	5.79	23.27	0.52	8.39	0.44	8.36
525134(5)_pt5	47.46S	4.87		14.85	26.29		6.52		
525134(5)_pt6	47.43S	4.74		15.16	26.00		6.67		
525134(5)_pt7	47.58S	4.82		14.17	26.96		6.47		

Atom %

	O-K	Na-K	Mg-K	Al-K	Si-K	K-K	Ca-K	Ti-K	Fe-K
525134(5)_pt1	61.47	4.44		11.27	19.52		3.30		
525134(5)_pt2	61.42	4.21		11.42	19.24		3.71		
525134(5)_pt3	61.19		7.72	4.33	18.42	0.28	4.33	0.15	3.58
525134(5)_pt4	61.09		7.73	4.70	18.14	0.29	4.58	0.20	3.28
525134(5)_pt5	61.45	4.39		11.40	19.39		3.37		
525134(5)_pt6	61.44	4.27		11.65	19.19		3.45		
525134(5)_pt7	61.57	4.34		10.87	19.87		3.34		

Compound %

		Na2O	***MgO***	***Al2O3***	***SiO2***	***K2O***	***CaO***	***TiO2***	***Fe2O3***
525134(5)_pt1	0.00	6.65		27.75	56.67		8.94		
525134(5)_pt2	0.00	6.28		28.05	55.66		10.02		
525134(5)_pt3	0.00		14.20	10.07	50.50	0.60	11.07	0.53	13.02
525134(5)_pt4	0.00		14.23	10.94	49.79	0.63	11.73	0.73	11.95
525134(5)_pt5	0.00	6.56		28.06	56.25		9.13		
525134(5)_pt6	0.00	6.39		28.65	55.63		9.33		
525134(5)_pt7	0.00	6.50		26.77	57.67		9.05		

Minerals, 525134a(5)
pt1: Feldspar - plagioclase
pt2: Feldspar - plagioclase
pt3: Amphibole - hornblende
pt4: Amphibole - hornblende
pt5: Feldspar - plagioclase
pt6: Feldspar - plagioclase
pt7: Feldspar - plagioclase
pt8: Feldspar - plagioclase
pt9: Feldspar - plagioclase

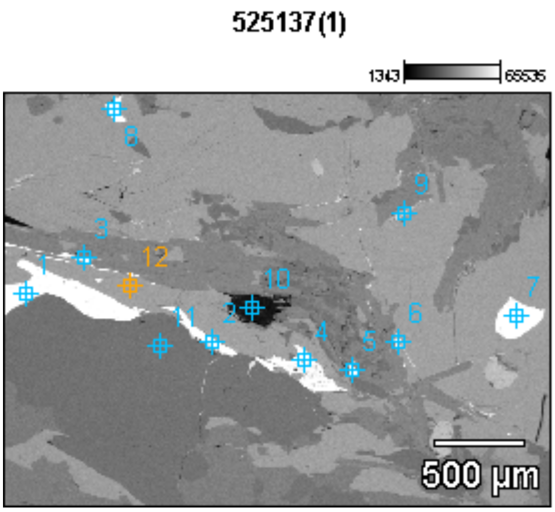

Image name: 525137(1)
Magnification: 40

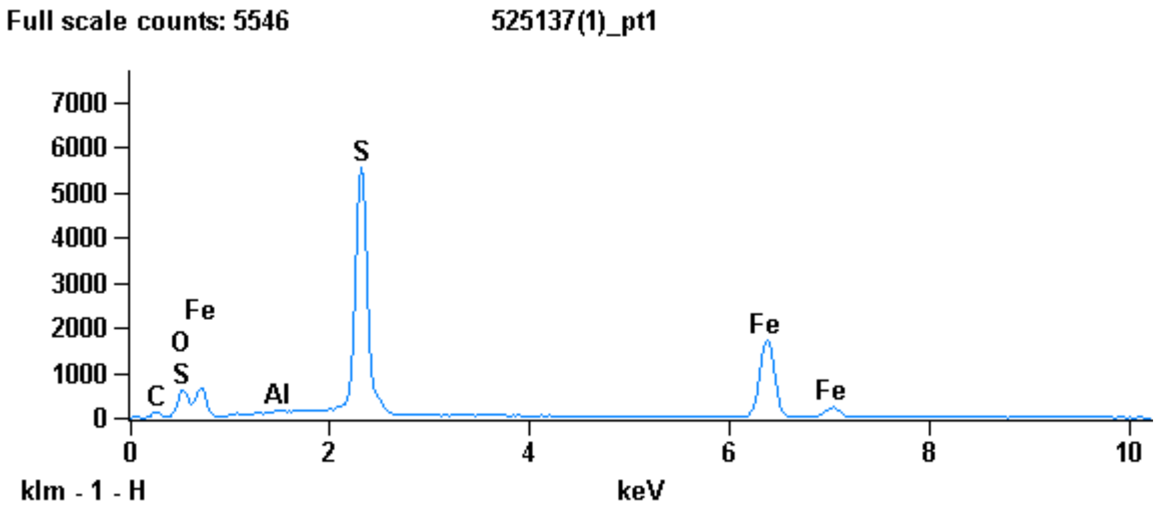

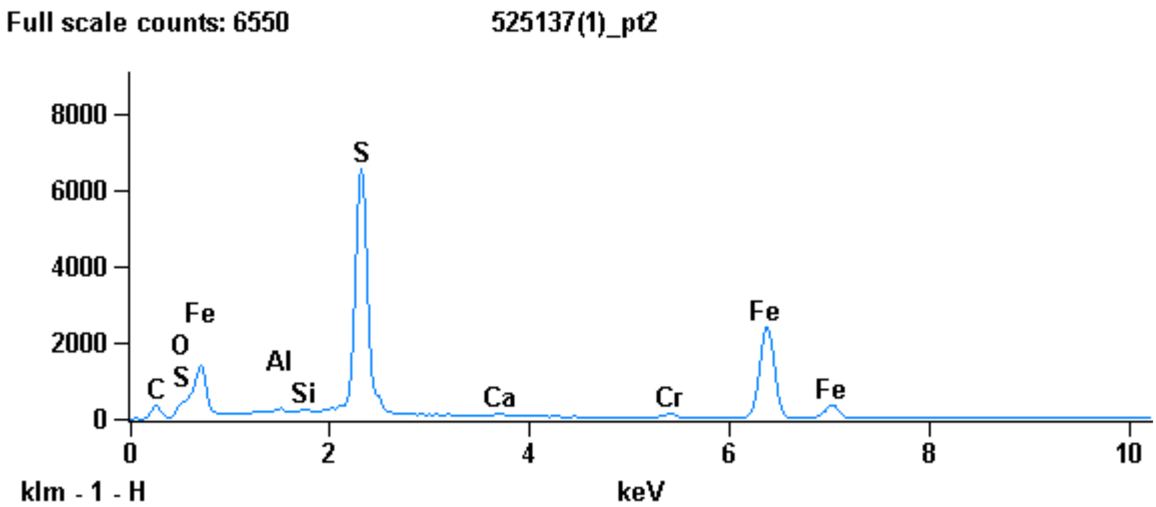

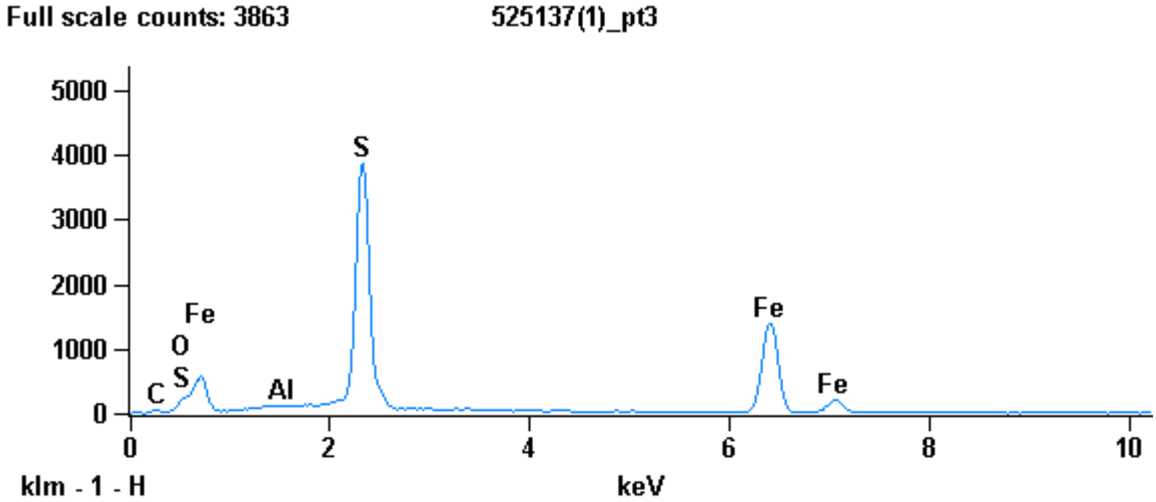
Full scale counts: 3863
525137(1)_pt3
5000
4000
3000
2000
1000
0
S
Fe
O
S
C
Al
Fe
Fe
0
2
4
6
8
10
klm - 1 - H
keV

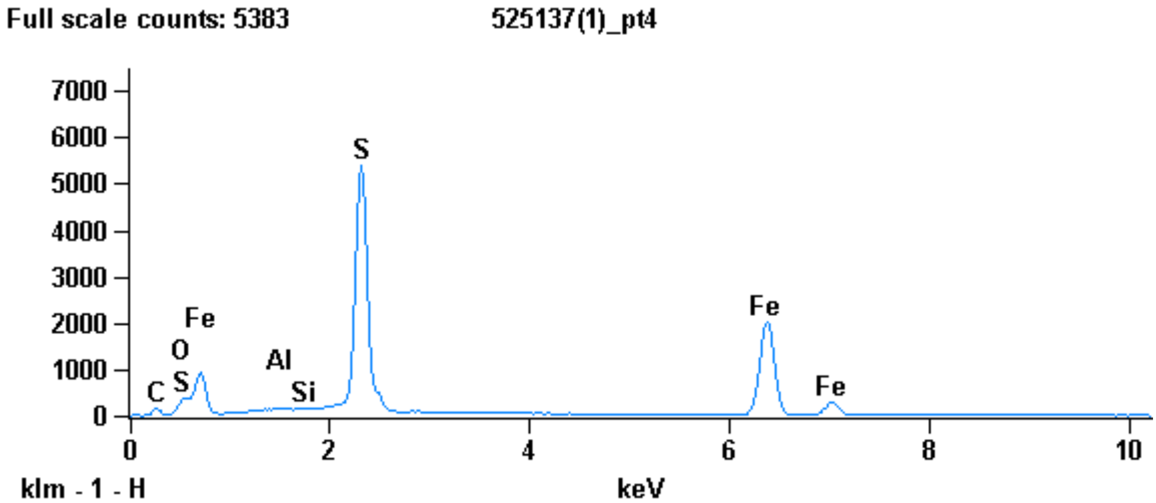
Full scale counts: 5383
525137(1)_pt4
7000
6000
5000
4000
3000
2000
1000
0
S
Fe
O
S
C
Al
Si
Fe
Fe
0
2
4
6
8
10
klm - 1 - H
keV

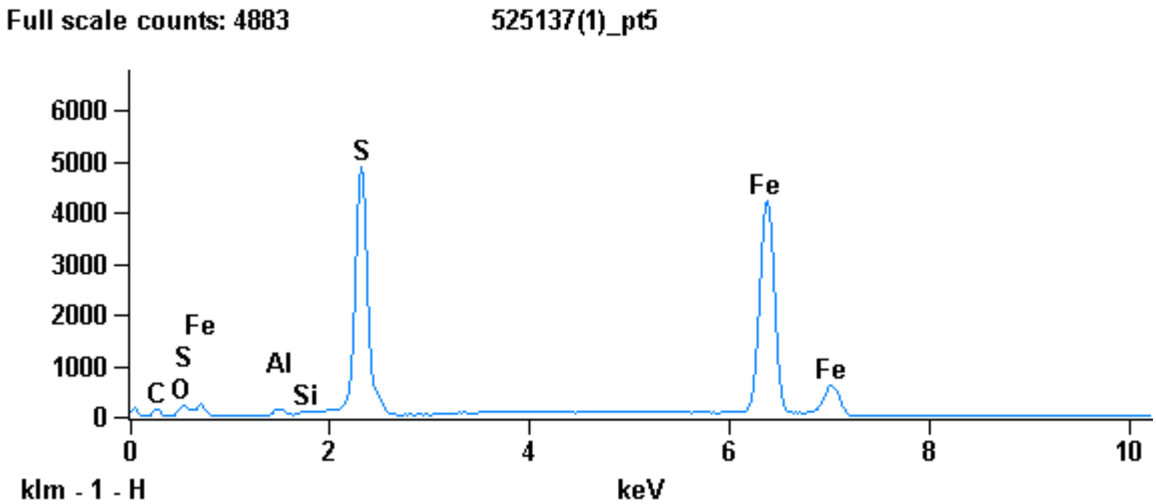
Full scale counts: 4883
525137(1)_pt5
6000
5000
4000
3000
2000
1000
0
S
Fe
Fe
S
C
O
Al
Si
Fe
0
2
4
6
8
10
klm - 1 - H
keV

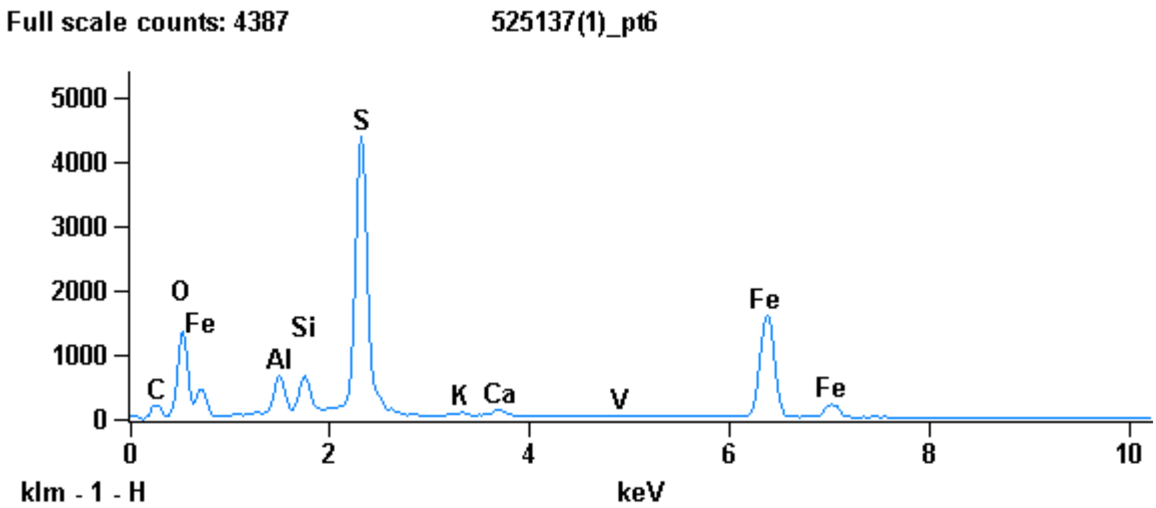
Full scale counts: 4387
525137(1)_pt6
5000
4000
3000
2000
1000
0
S
O
Fe
Si
Al
C
K
Ca
V
Fe
Fe
0
2
4
6
8
10
klm - 1 - H
keV

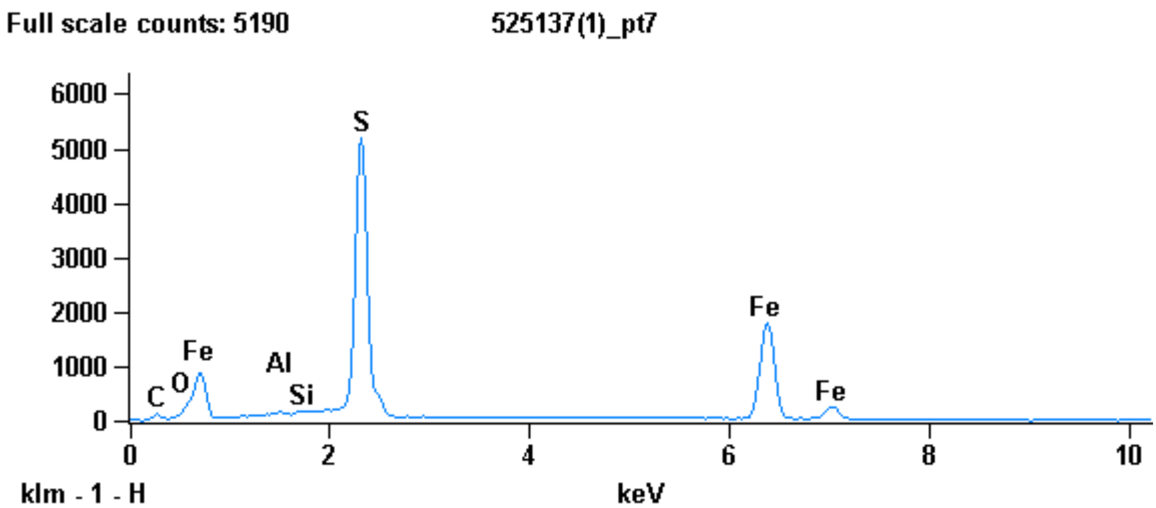
Full scale counts: 5190
525137(1)_pt7
6000
5000
4000
3000
2000
1000
0
S
Fe
Al
C
O
Si
Fe
Fe
0
2
4
6
8
10
klm - 1 - H
keV

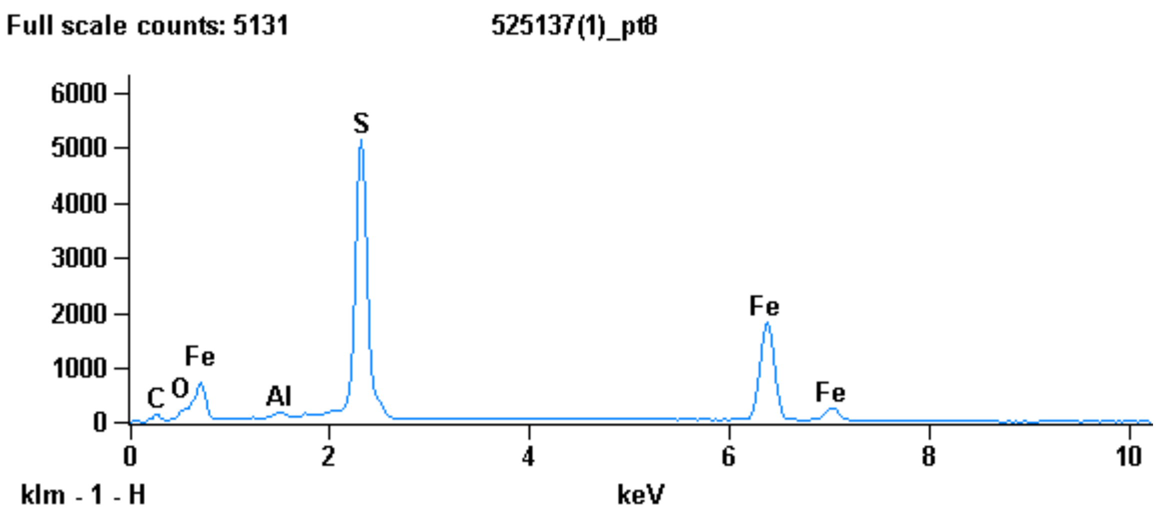
Full scale counts: 5131
525137(1)_pt8
6000
5000
4000
3000
2000
1000
0
S
Fe
C
O
Al
Fe
Fe
0
2
4
6
8
10
klm - 1 - H
keV

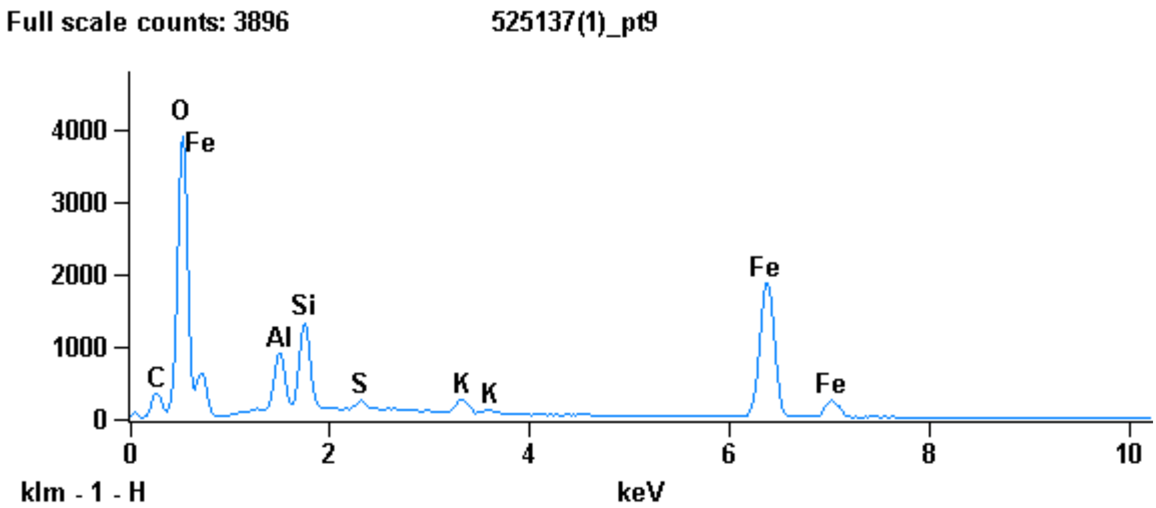
Full scale counts: 3896
525137(1)_pt9
O
Fe
C
Al
Si
S
K
K
Fe
Fe
4000
3000
2000
1000
0
0
2
4
6
8
10
klm - 1 - H
keV

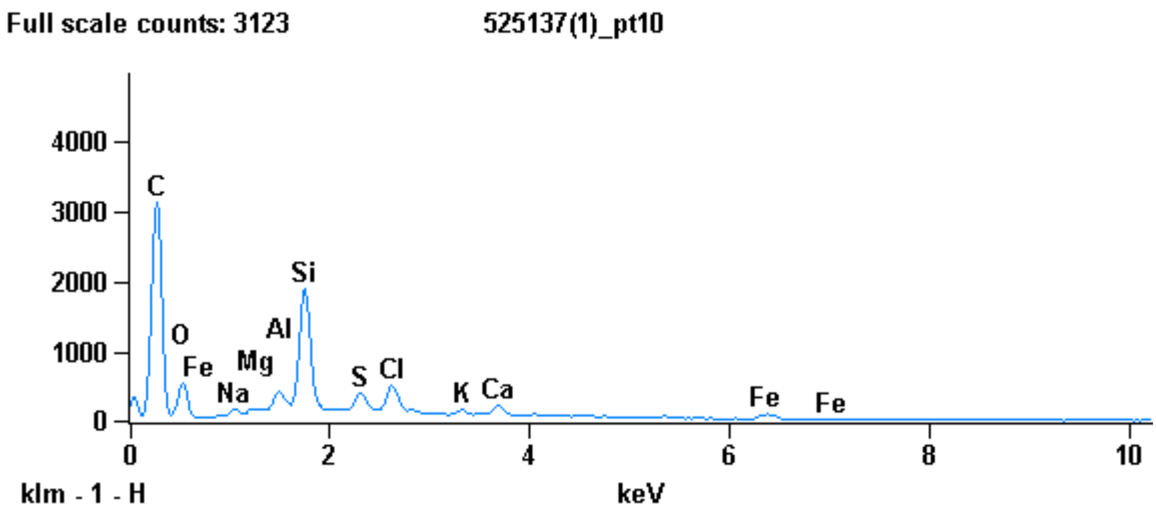
Full scale counts: 3123
525137(1)_pt10
C
O
Fe
Na
Mg
Al
Si
S
Cl
K
Ca
Fe
Fe
4000
3000
2000
1000
0
0
2
4
6
8
10
klm - 1 - H
keV

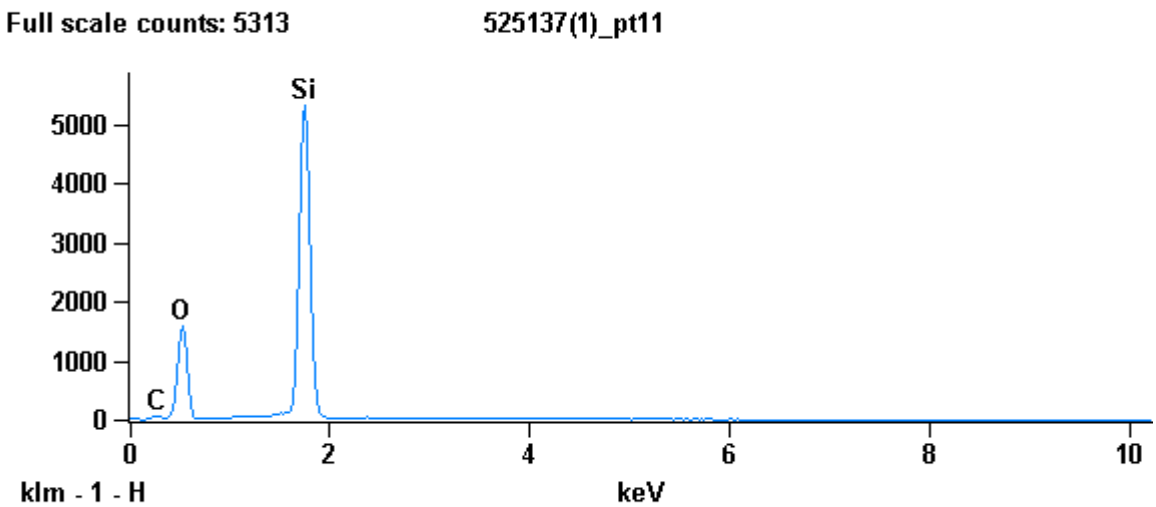
Full scale counts: 5313
525137(1)_pt11
Si
O
C
5000
4000
3000
2000
1000
0
0
2
4
6
8
10
klm - 1 - H
keV

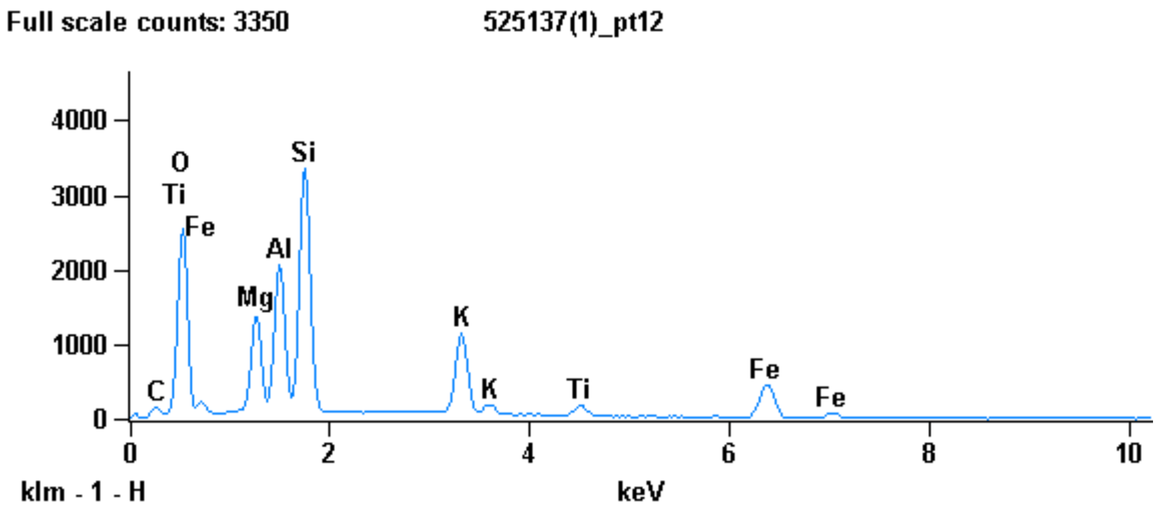

Weight %

	O-K	Na-K	Mg-K	Al-K	Si-K	S-K	Cl-K	K-K	Ca-K	Ti-K	V-K	Cr-K	Fe-K
525137(1)_pt1	46.67S			0.12		22.20							31.02
525137(1)_pt2	45.43S			0.23	0.13	20.39			0.15			0.71	32.98
525137(1)_pt3	46.10S			0.12		21.43							32.35
525137(1)_pt4	45.49S			0.21	0.07	20.54							33.69
525137(1)_pt5	39.80S			0.41	0.07	12.83							46.88
525137(1)_pt6	46.02S			2.67	2.27	18.73		0.15	0.37		0.09		29.70
525137(1)_pt7	46.08S			0.10	0.08	21.36							32.38
525137(1)_pt8	45.81S			0.40		20.92							32.87
525137(1)_pt9	36.13S			5.74	7.74	0.83		1.43					48.14
525137(1)_pt10	44.85S	2.20	1.16	3.70	25.08	5.13	8.26	1.22	2.69				5.71
525137(1)_pt11	53.26S				46.74								
525137(1)_pt12	42.66S		7.92	10.30	18.30			8.21		1.38			11.24

Atom %

	O-K	Na-K	Mg-K	Al-K	Si-K	S-K	Cl-K	K-K	Ca-K	Ti-K	V-K	Cr-K	Fe-K
525137(1)_pt1	69.96			0.11		16.61							13.32
525137(1)_pt2	69.32			0.21	0.11	15.52			0.09			0.33	14.42
525137(1)_pt3	69.71			0.10		16.18							14.02
525137(1)_pt4	69.39			0.19	0.06	15.63							14.72
525137(1)_pt5	66.43			0.40	0.07	10.69							22.41
525137(1)_pt6	68.69			2.36	1.93	13.96		0.09	0.22		0.04		12.70
525137(1)_pt7	69.69			0.09	0.07	16.13							14.03
525137(1)_pt8	69.51			0.36		15.84							14.29
525137(1)_pt9	61.52			5.79	7.50	0.70		0.99					23.48
525137(1)_pt10	61.34	2.09	1.05	3.00	19.54	3.50	5.10	0.68	1.47				2.24
525137(1)_pt11	66.67				33.33								
525137(1)_pt12	59.71		7.30	8.55	14.59			4.70		0.64			4.51

Compound %

		Na2O	*MgO*	*Al2O3*	*SiO2*	*SO3*	*Cl*	*K2O*	*CaO*	*TiO2*	*V2O5*	*Cr2O3*	*Fe2O3*
525137(1)_pt1	0.00			0.23		55.43							44.35
525137(1)_pt2	0.00			0.44	0.27	50.91			0.21			1.03	47.15
525137(1)_pt3	0.00			0.22		53.52							46.26
525137(1)_pt4	0.00			0.40	0.15	51.28							48.17
525137(1)_pt5	0.00			0.77	0.16	32.04							67.03
525137(1)_pt6	0.00			5.04	4.86	46.78		0.18	0.52		0.16		42.46
525137(1)_pt7	0.00			0.18	0.17	53.35							46.30
525137(1)_pt8	0.00			0.75		52.25							47.00
525137(1)_pt9	0.00			10.84	16.55	2.06		1.72					68.83
525137(1)_pt10	0.00	2.97	1.93	6.99	53.66	12.82	8.26	1.47	3.76				8.16
525137(1)_pt11	0.00				100.00								
525137(1)_pt12	0.00		13.13	19.46	39.15			9.89		2.30			16.07

Minerals, 525137(1)

pt1: Pyrrhotite
pt2: Pyrrhotite
pt3: Pyrrhotite
pt4: Pyrrhotite
pt5: Pyrite
pt6: Pyrrhotite
pt7: Pyrrhotite
pt8: Pyrrhotite
pt9: Mixed signal/edge effect
pt10: Mixed signal/edge effect
pt11: Quartz
pt12: Biotite

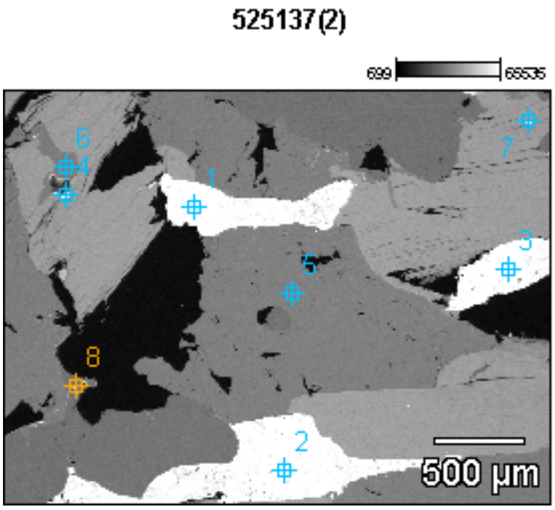

Image name: 525137(2)
Magnification: 40

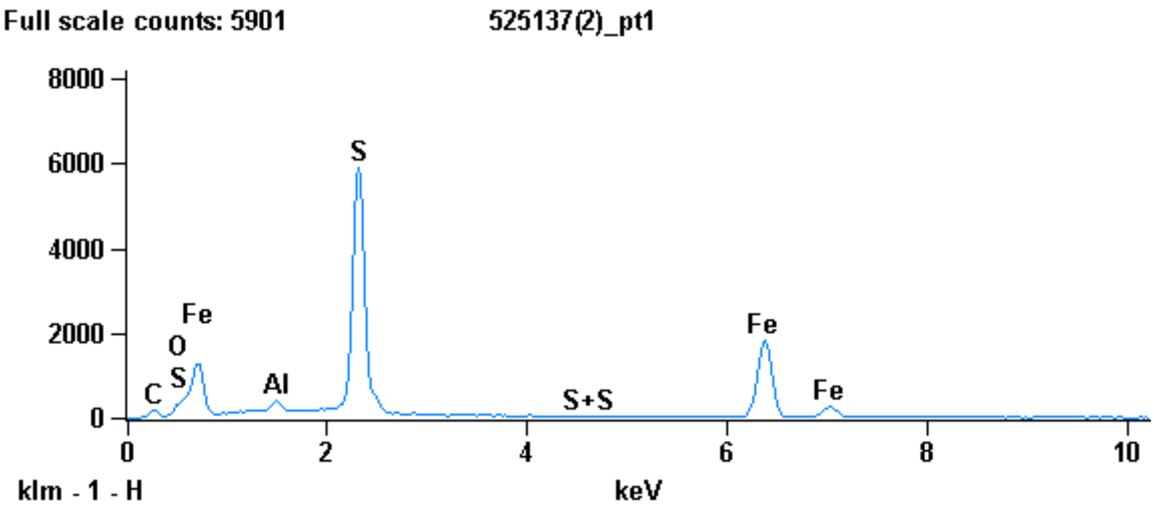

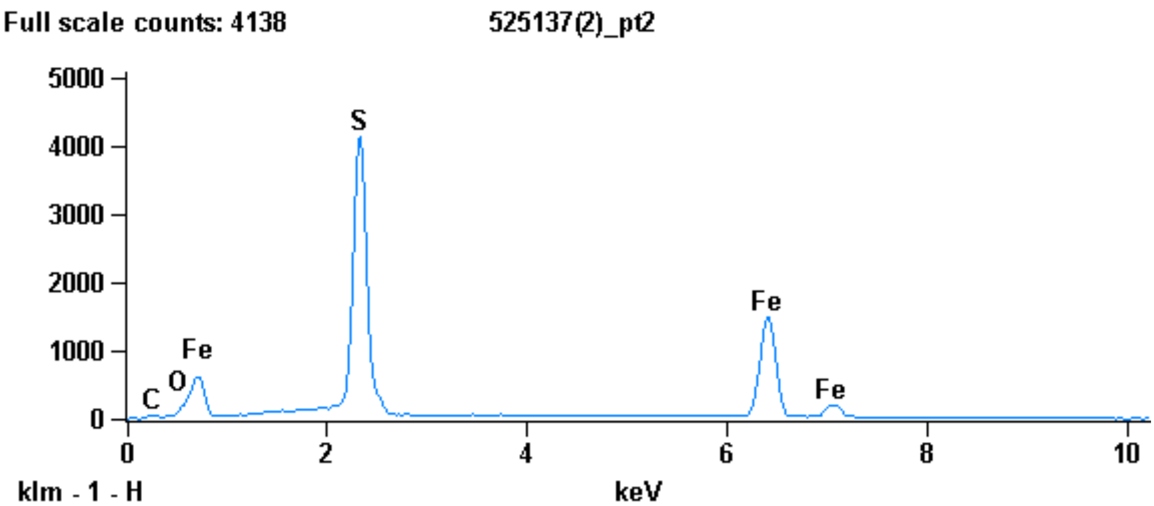

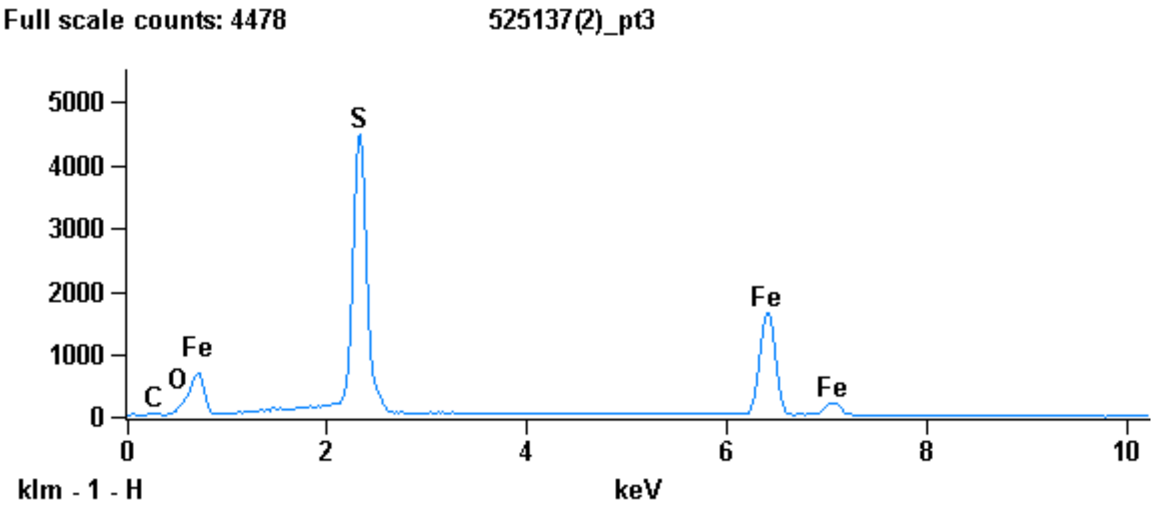
Full scale counts: 4478
525137(2)_pt3
5000
4000
3000
2000
1000
0
S
Fe
Fe
C
O
Fe
0
2
4
6
8
10
klm - 1 - H
keV

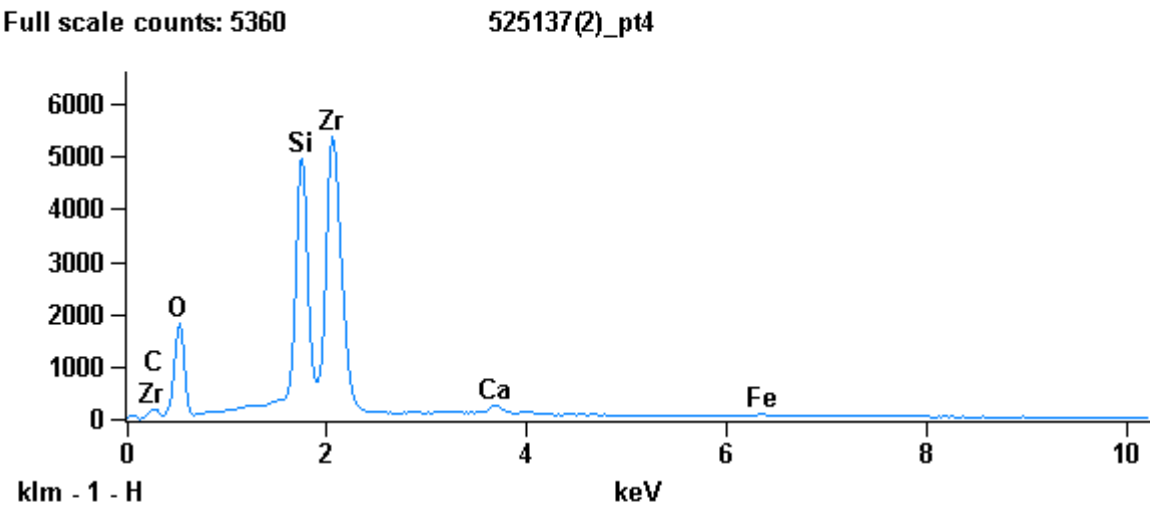
Full scale counts: 5360
525137(2)_pt4
6000
5000
4000
3000
2000
1000
0
Si
Zr
O
C
Zr
Ca
Fe
0
2
4
6
8
10
klm - 1 - H
keV

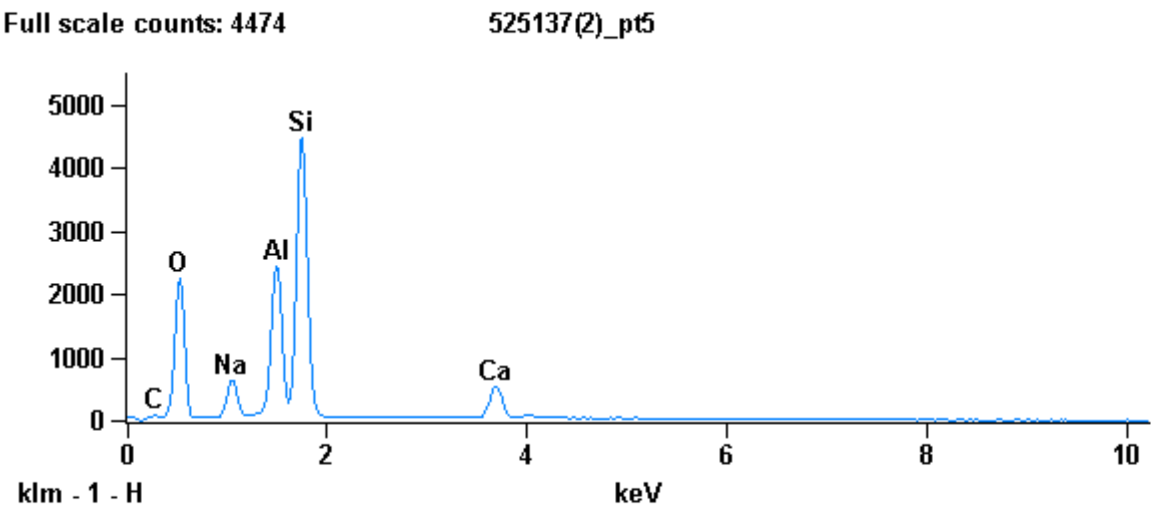
Full scale counts: 4474
525137(2)_pt5
5000
4000
3000
2000
1000
0
Si
Al
O
Na
C
Ca
0
2
4
6
8
10
klm - 1 - H
keV

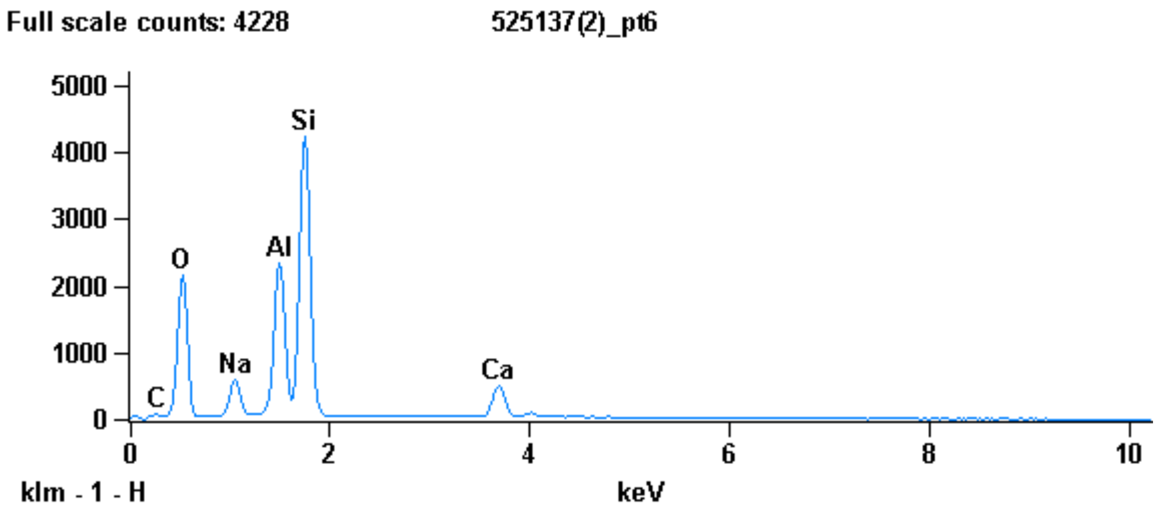
Full scale counts: 4228
525137(2)_pt6
5000
4000
3000
2000
1000
0
Si
O
Al
Na
Ca
C
0
2
4
6
8
10
klm - 1 - H
keV

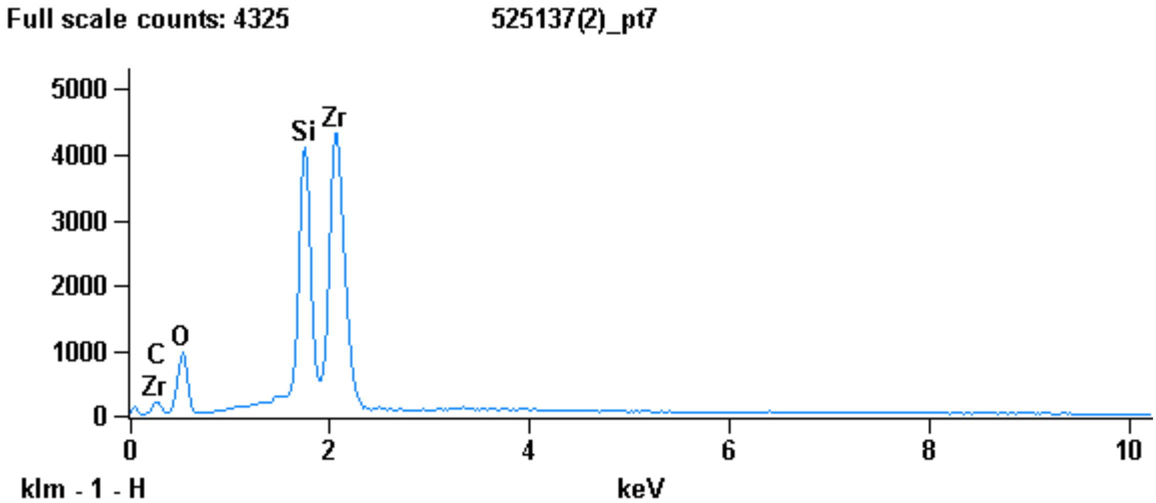
Full scale counts: 4325
525137(2)_pt7
5000
4000
3000
2000
1000
0
Si
Zr
C
O
Zr
0
2
4
6
8
10
klm - 1 - H
keV

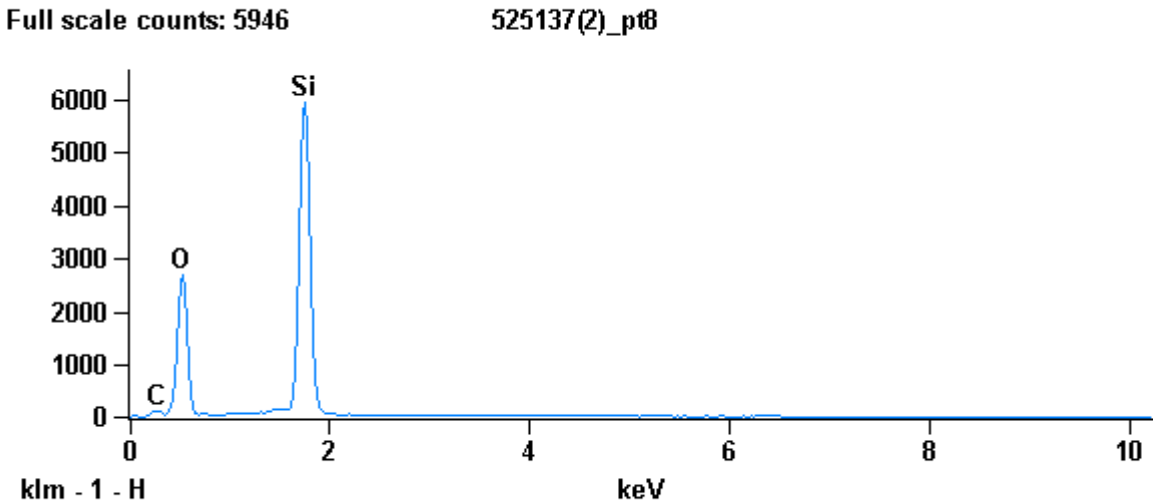
Full scale counts: 5946
525137(2)_pt8
6000
5000
4000
3000
2000
1000
0
Si
O
C
0
2
4
6
8
10
klm - 1 - H
keV

Weight %

	O-K	Na-K	Al-K	Si-K	S-K	Ca-K	Fe-K	Zr-L
525137(2)_pt1	46.81S		0.94		22.03		30.22	
525137(2)_pt2	46.02S				21.38		32.59	
525137(2)_pt3	45.91S				21.23		32.86	
525137(2)_pt4	34.52S			14.51		0.94	0.78	49.25
525137(2)_pt5	47.76S	5.77	13.50	27.82		5.15		
525137(2)_pt6	47.69S	5.75	13.40	27.74		5.42		
525137(2)_pt7	34.74S			15.03				50.22
525137(2)_pt8	53.26S			46.74				

Atom %

	O-K	Na-K	Al-K	Si-K	S-K	Ca-K	Fe-K	Zr-L
525137(2)_pt1	69.84		0.83		16.41		12.92	
525137(2)_pt2	69.70				16.16		14.14	
525137(2)_pt3	69.64				16.07		14.28	
525137(2)_pt4	66.35			15.89		0.72	0.43	16.60
525137(2)_pt5	61.48	5.17	10.30	20.40		2.64		
525137(2)_pt6	61.45	5.16	10.24	20.36		2.79		
525137(2)_pt7	66.67			16.43				16.90
525137(2)_pt8	66.67			33.33				

Compound %

		Na2O	Al2O3	SiO2	SO3	CaO	Fe2O3	ZrO2
525137(2)_pt1	0.00		1.78		55.01		43.21	
525137(2)_pt2	0.00				53.40		46.60	
525137(2)_pt3	0.00				53.02		46.98	
525137(2)_pt4	0.00			31.04		1.32	1.12	66.52
525137(2)_pt5	0.00	7.78	25.51	59.51		7.20		
525137(2)_pt6	0.00	7.75	25.33	59.34		7.58		
525137(2)_pt7	0.00			32.16				67.84
525137(2)_pt8	0.00			100.00				

Minerals, 525137(2)
pt1: Pyrrhotite
pt2: Pyrrhotite
pt3: Pyrrhotite
pt4: Zircon
pt5: Feldspar - plagioclase
pt6: Feldspar - plagioclase
pt7: Zircon
pt8: Quartz

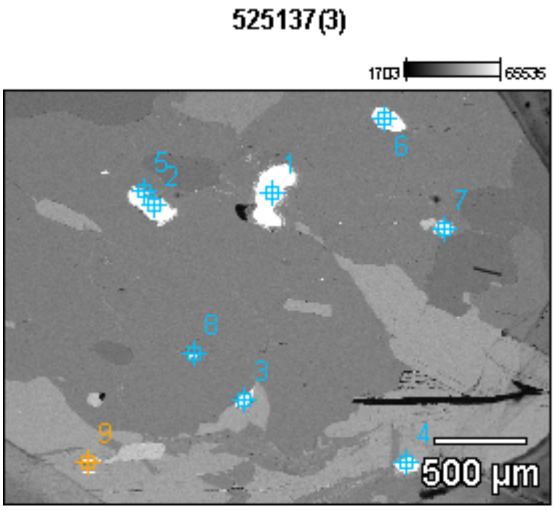

Image name: 525137(3)
Magnification: 41

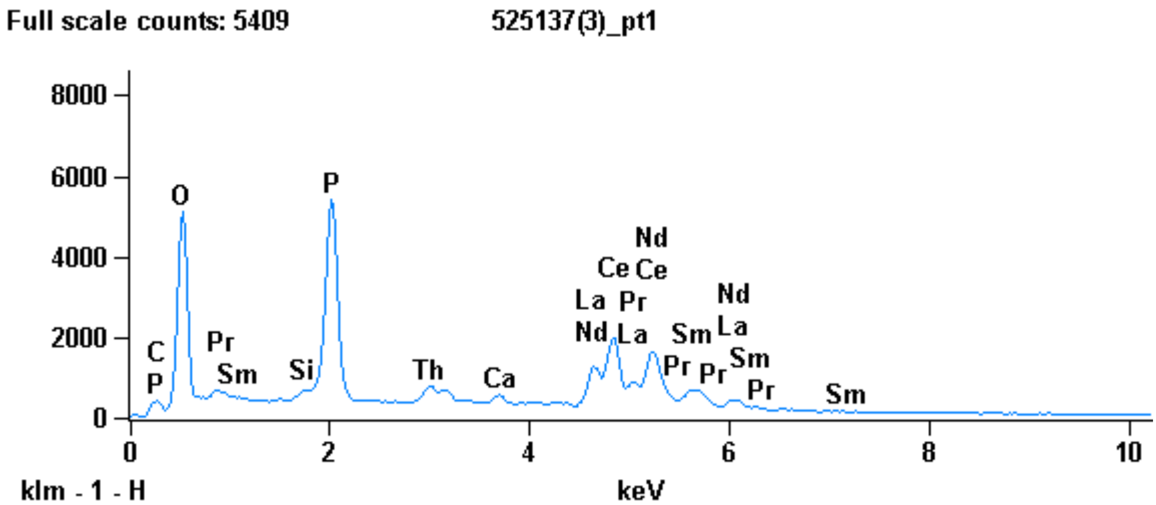

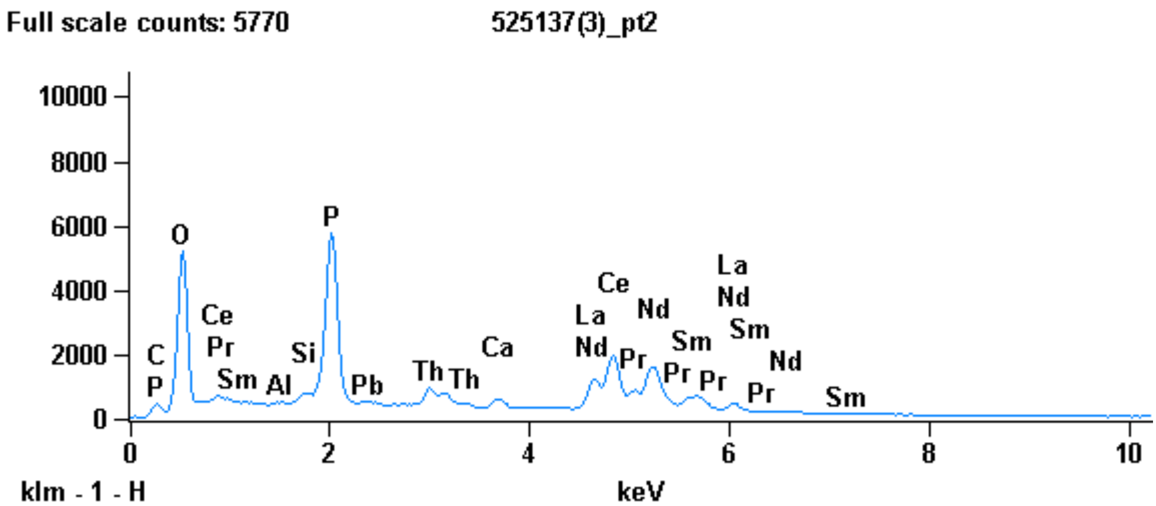

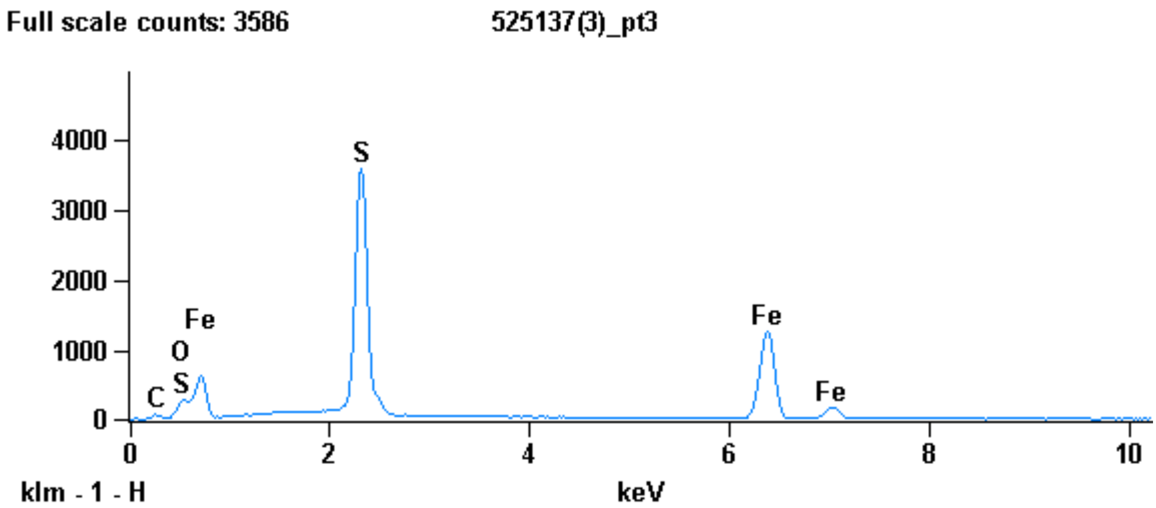
Full scale counts: 3586
525137(3)_pt3
4000
3000
2000
1000
0
S
Fe
O
S
C
Fe
Fe
0
2
4
6
8
10
klm - 1 - H
keV

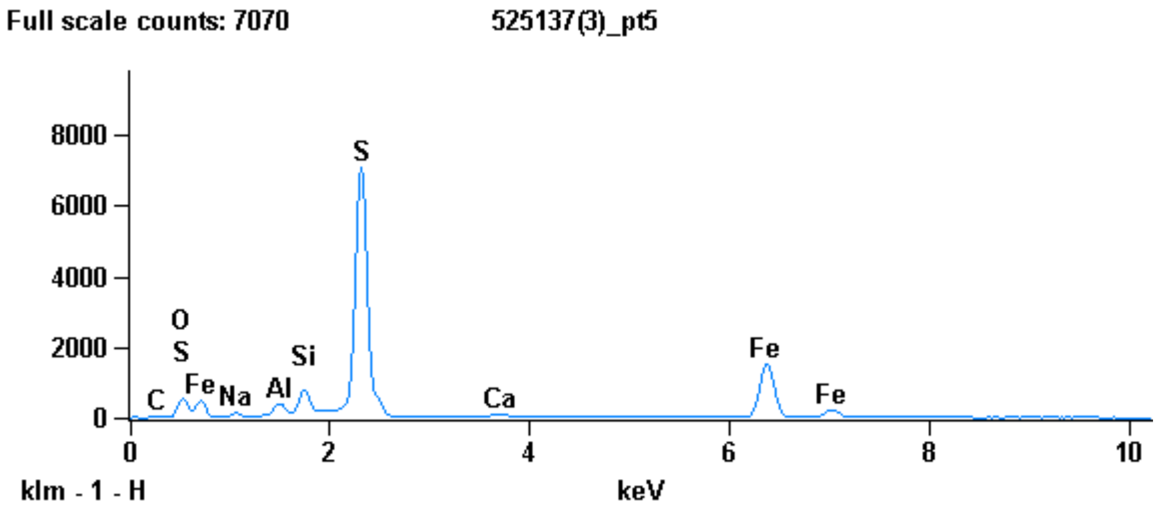
Full scale counts: 7070
525137(3)_pt5
8000
6000
4000
2000
0
S
O
S
Si
C
Fe
Na
Al
Ca
Fe
Fe
0
2
4
6
8
10
klm - 1 - H
keV

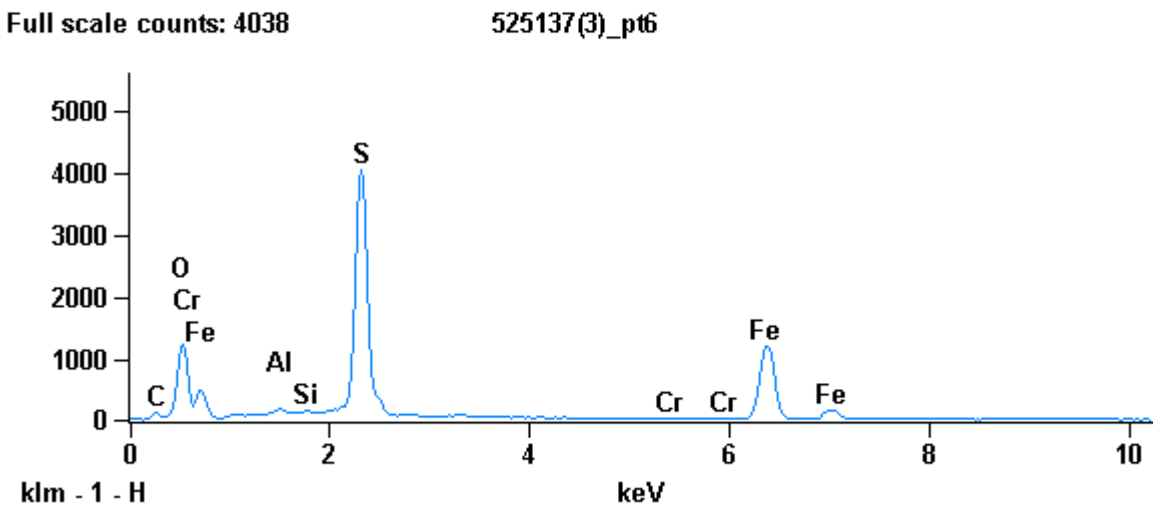
Full scale counts: 4038
525137(3)_pt6
5000
4000
3000
2000
1000
0
S
O
Cr
Fe
Al
Si
C
Cr
Cr
Fe
Fe
0
2
4
6
8
10
klm - 1 - H
keV

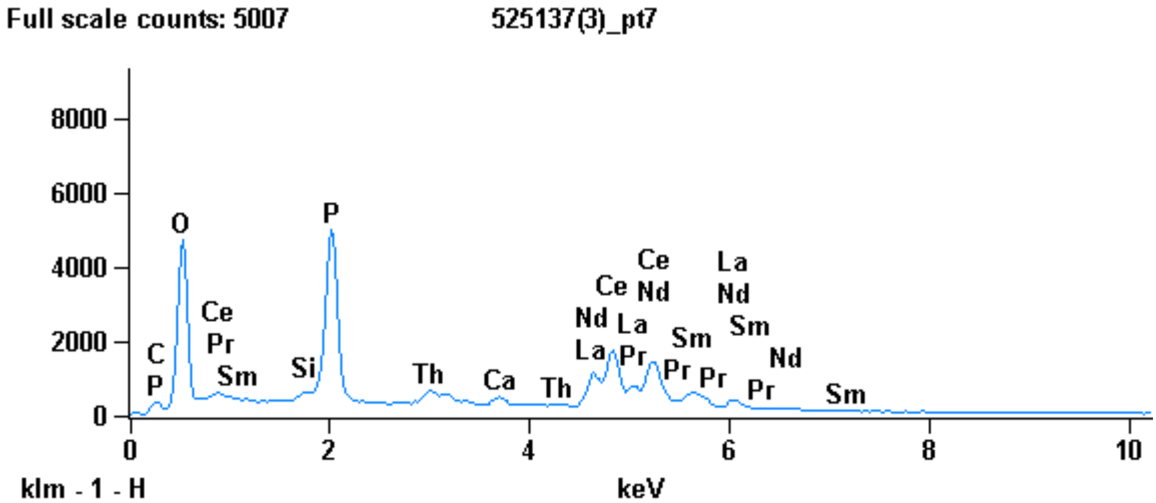
Full scale counts: 5007
525137(3)_pt7
8000
6000
4000
2000
0
O
P
C
P
Ce
Pr
Sm
Si
Th
Ca
Th
Nd
La
Ce
La
Pr
Ce
Nd
Sm
Pr
Pr
La
Nd
Sm
Nd
Pr
Sm
0
2
4
6
8
10
klm - 1 - H
keV

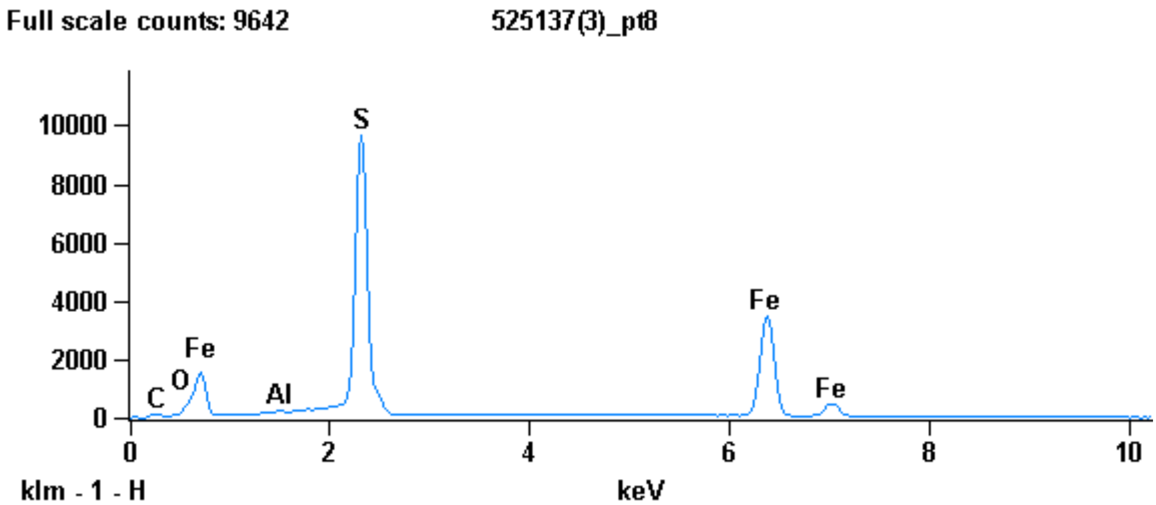
Full scale counts: 9642
525137(3)_pt8
10000
8000
6000
4000
2000
0
C
O
Fe
Al
S
Fe
Fe
0
2
4
6
8
10
klm - 1 - H
keV

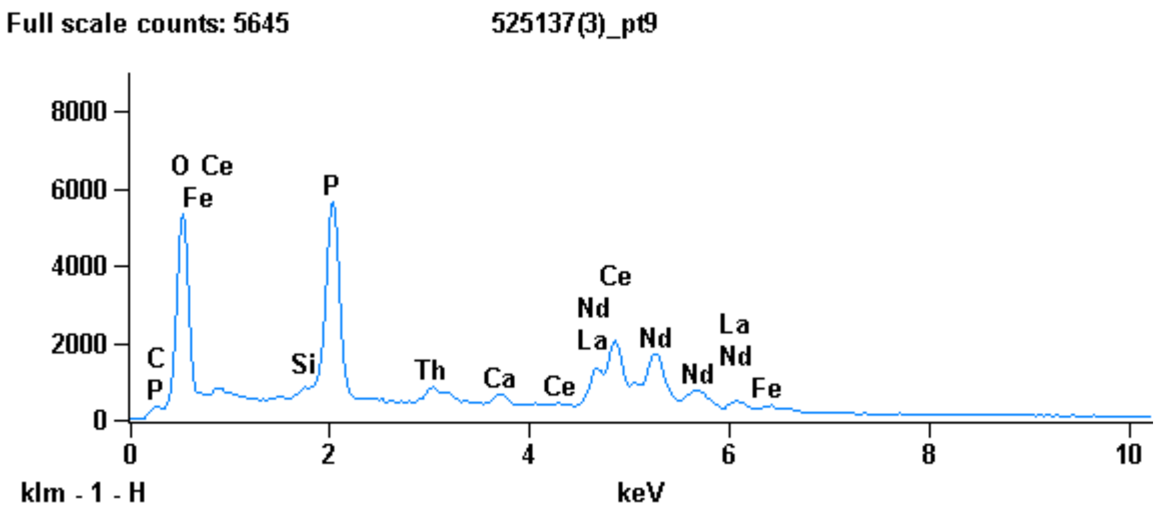
Full scale counts: 5645
525137(3)_pt9
8000
6000
4000
2000
0
O Ce
Fe
P
C
P
Si
Th
Ca
Ce
Ce
Nd
La
Nd
Nd
La
Nd
Fe
0
2
4
6
8
10
klm - 1 - H
keV

Weight %

	O-K	Na-K	Al-K	Si-K	P-K	S-K	Ca-K	Cr-K	Fe-K	La-L	Ce-L	Pr-L	Nd-L	Sm-L	Pb-L
525137(3)_pt1	32.14S			0.05	18.08		1.04			11.32	28.39		8.98		
525137(3)_pt2	31.39S		0.09	0.12	17.21		1.01			9.89	27.75	1.89	9.57	1.03	0.04
525137(3)_pt3	46.03S					21.40			32.57						
525137(3)_pt4	32.32S				18.35		0.90			10.96	28.50		8.96		
525137(3)_pt5	49.13S	0.77	1.06	1.88		23.92	0.34		22.90						
525137(3)_pt6	47.03S		0.39	0.12		22.49		0.00	29.96						
525137(3)_pt7	32.39S			0.09	18.36		0.83			11.28	27.84		9.21		
525137(3)_pt8	45.82S		0.05			21.09			33.05						
525137(3)_pt9	32.86S			0.35	18.29		1.27		1.03	11.62	25.56		9.02		

Atom %

	O-K	Na-K	Al-K	Si-K	P-K	S-K	Ca-K	Cr-K	Fe-K	La-L	Ce-L	Pr-L	Nd-L	Sm-L	Pb-L
525137(3)_pt1	67.71			0.06	19.67		0.88			2.75	6.83		2.10		
525137(3)_pt2	67.50		0.11	0.15	19.12		0.86			2.45	6.82	0.46	2.28	0.24	0.01
525137(3)_pt3	69.70					16.17			14.13						
525137(3)_pt4	67.80				19.88		0.75			2.65	6.83		2.09		
525137(3)_pt5	70.19	0.77	0.90	1.53		17.05	0.20		9.37						
525137(3)_pt6	70.05		0.35	0.10		16.72		0.00	12.79						
525137(3)_pt7	67.82			0.11	19.86		0.70			2.72	6.65		2.14		
525137(3)_pt8	69.59		0.04			15.99			14.38						
525137(3)_pt9	67.65			0.41	19.45		1.05		0.61	2.75	6.01		2.06		

Compound %

		Na2O	Al2O3	SiO2	P2O5	SO3	CaO	Cr2O3	Fe2O3	La2O3	Ce2O3	Pr2O3	Nd2O3	Sm2O3	PbO
525137(3)_pt1	0.00			0.12	41.42		1.46			13.27	33.26		10.47		
525137(3)_pt2	0.00		0.17	0.26	39.44		1.41			11.60	32.51	2.21	11.16	1.20	0.04
525137(3)_pt3	0.00					53.44			46.56						
525137(3)_pt4	0.00				42.05		1.26			12.85	33.38		10.45		
525137(3)_pt5	0.00	1.04	2.01	4.02		59.72	0.48		32.73						
525137(3)_pt6	0.00		0.74	0.25		56.17		0.01	42.84						
525137(3)_pt7	0.00			0.20	42.07		1.17			13.23	32.60		10.74		
525137(3)_pt8	0.00		0.09			52.66			47.25						
525137(3)_pt9	0.00			0.75	41.91		1.78		1.48	13.62	29.93		10.52		

Minerals, 525137(3)

pt1: Monazite
pt2: Monazite
pt3: Pyrrhotite
pt4: Monazite
pt5: Pyrite
pt6: Pyrite
pt7: Monazite
pt8: Pyrrhotite
pt9: Monazite

525138(1)

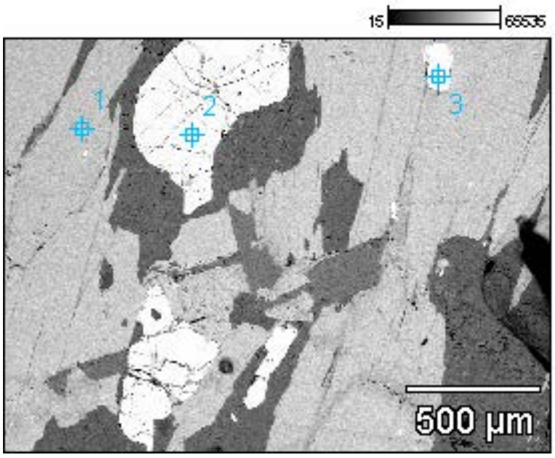
15
65535
1
2
3
500 µm

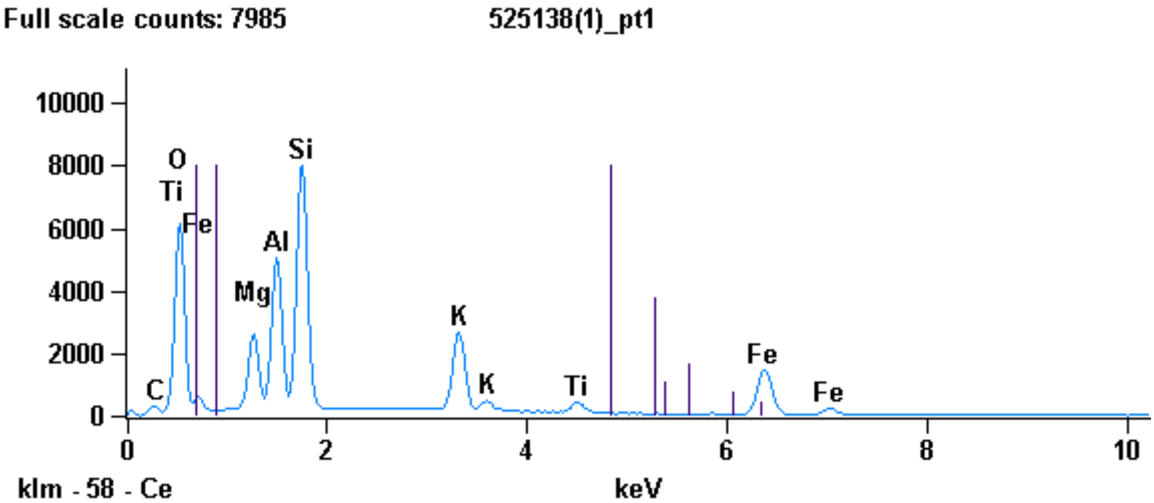
Full scale counts: 7985
525138(1)_pt1
10000
8000
6000
4000
2000
0
O
Ti
Fe
Si
Al
Mg
K
C
K
Ti
Fe
Fe
0
2
4
6
8
10
klm - 58 - Ce
keV

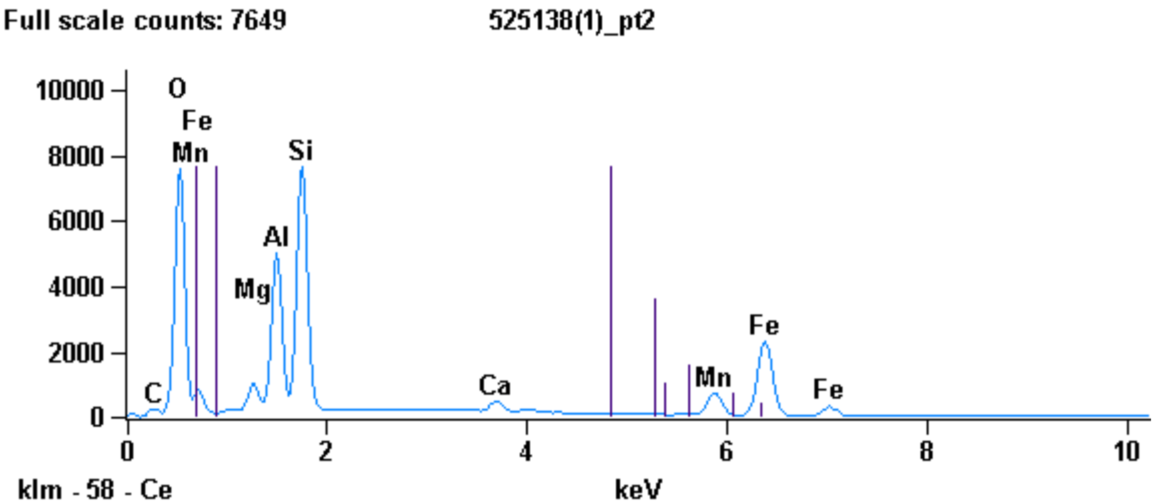
Full scale counts: 7649
525138(1)_pt2
10000
8000
6000
4000
2000
0
O
Fe
Mn
Si
Al
Mg
C
Ca
Mn
Fe
Fe
0
2
4
6
8
10
klm - 58 - Ce
keV

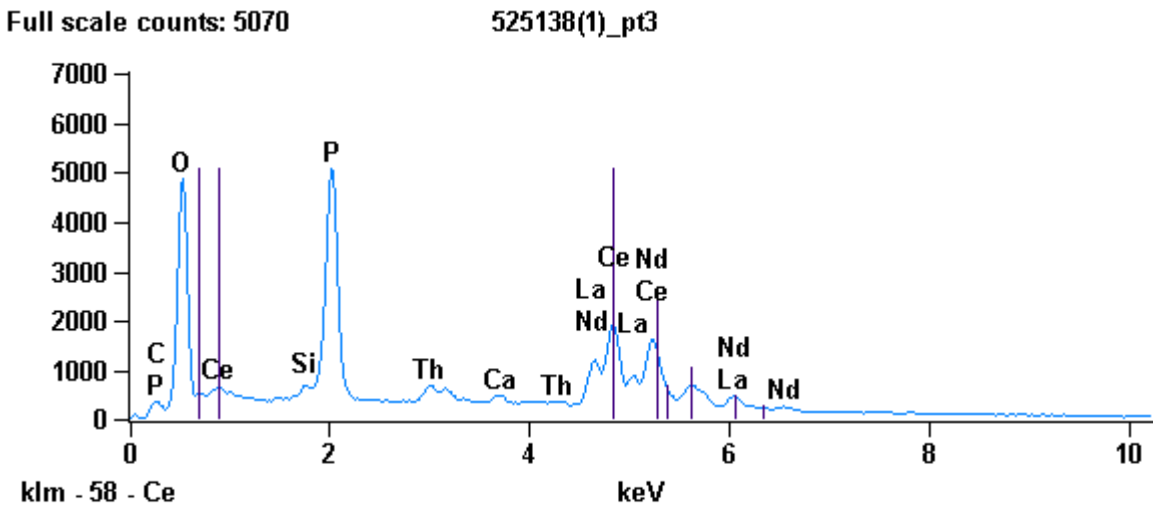

Weight %

	O-K	Mg-K	Al-K	Si-K	P-K	K-K	Ca-K	Ti-K	Mn-K	Fe-K	La-L	Ce-L	Nd-L	Th-L
525138(1)_pt1	42.16S	6.07	10.40	17.71		7.75		1.31		14.61				
525138(1)_pt2	41.67S	2.11	10.60	17.01			1.09		5.71	21.81				
525138(1)_pt3	31.98S			0.18	17.87		0.76				10.29	29.53	9.38	0.00

Atom %

	O-K	Mg-K	Al-K	Si-K	P-K	K-K	Ca-K	Ti-K	Mn-K	Fe-K	La-L	Ce-L	Nd-L	Th-L
525138(1)_pt1	60.05	5.70	8.78	14.37		4.51		0.62		5.96				
525138(1)_pt2	61.84	2.06	9.33	14.38			0.65		2.47	9.27				
525138(1)_pt3	67.73			0.22	19.55		0.64				2.51	7.14	2.20	0.00

Compound %

		MgO	Al2O3	SiO2	P2O5	K2O	CaO	TiO2	MnO	Fe2O3	La2O3	Ce2O3	Nd2O3	ThO2
525138(1)_pt1	0.00	10.07	19.65	37.88		9.33		2.18		20.89				
525138(1)_pt2	0.00	3.50	20.03	36.40			1.53		7.37	31.18				
525138(1)_pt3	0.00			0.39	40.95		1.07				12.07	34.59	10.93	0.00

Minerals, 525138(1)
pt1: Biotite
pt2: Garnet, pyralspite-group
pt3: Monazite

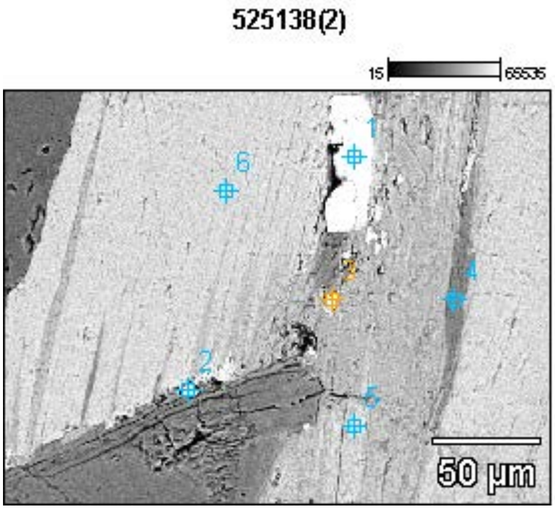

Image name: 525138(2)
Magnification: 480

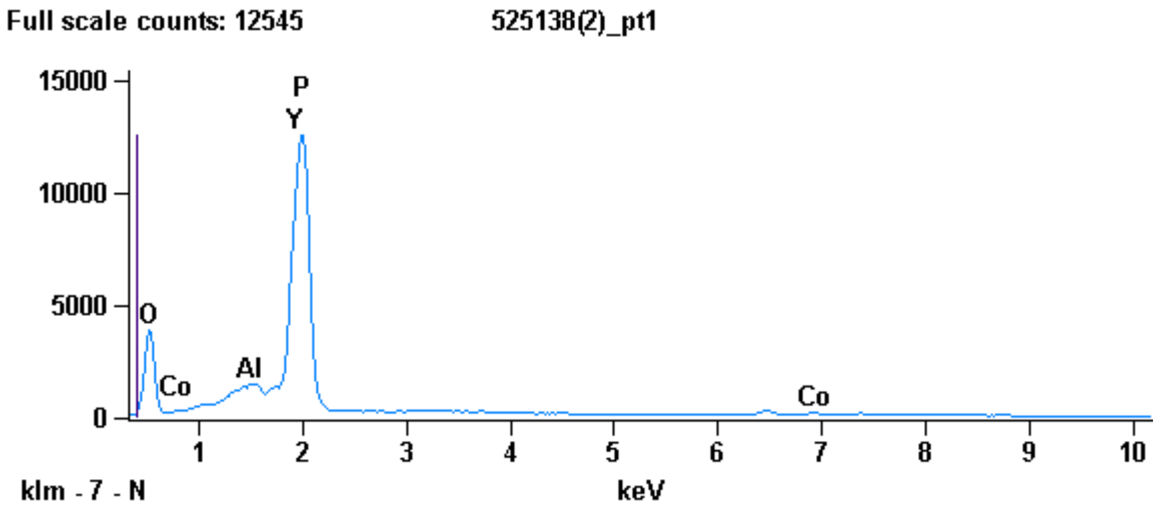

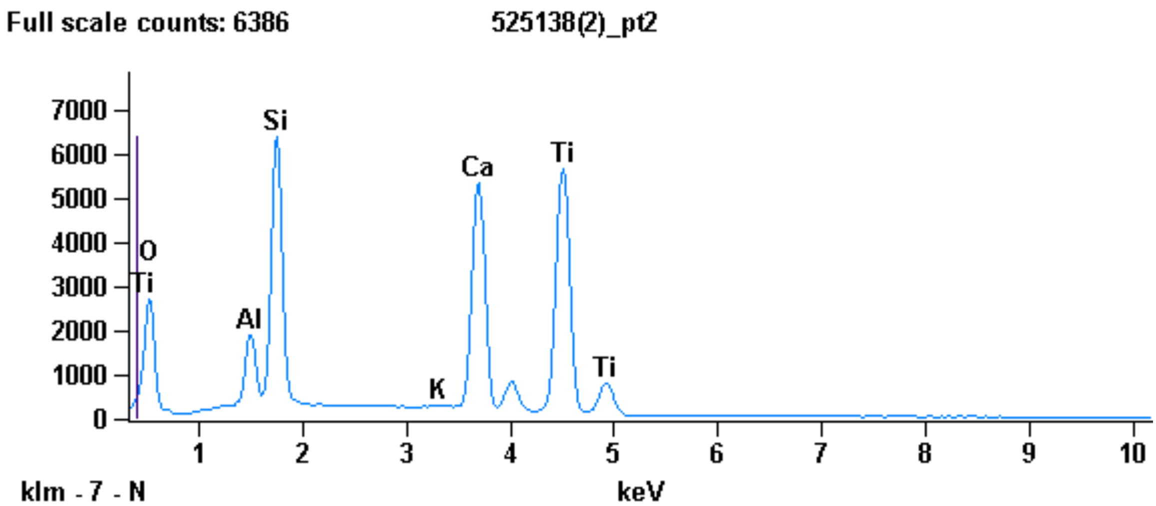

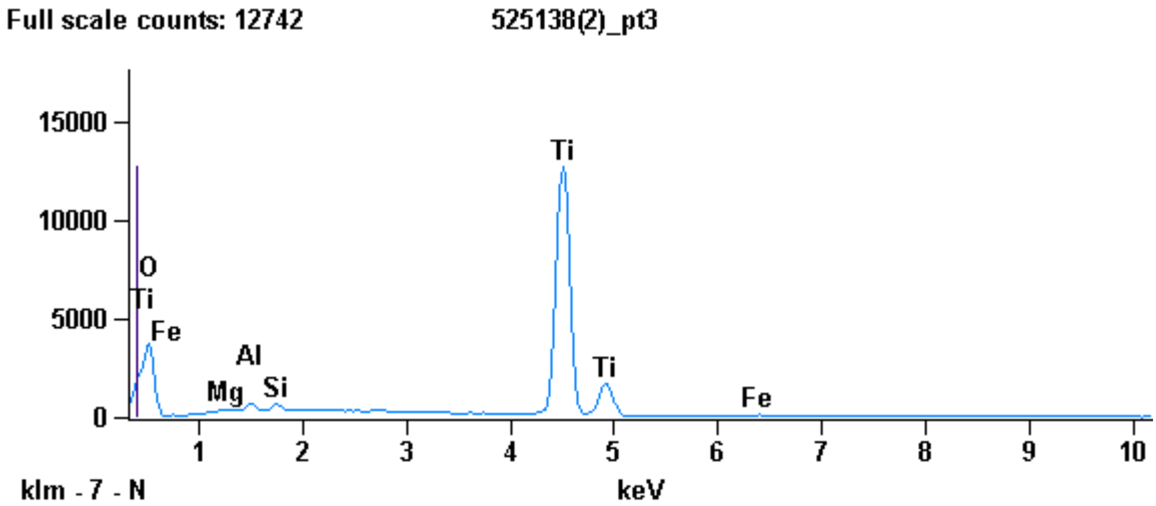
Full scale counts: 12742
525138(2)_pt3
15000
10000
5000
0
O
Ti
Fe
Mg
Al
Si
Ti
Ti
Fe
1 2 3 4 5 6 7 8 9 10
klm - 7 - N
keV

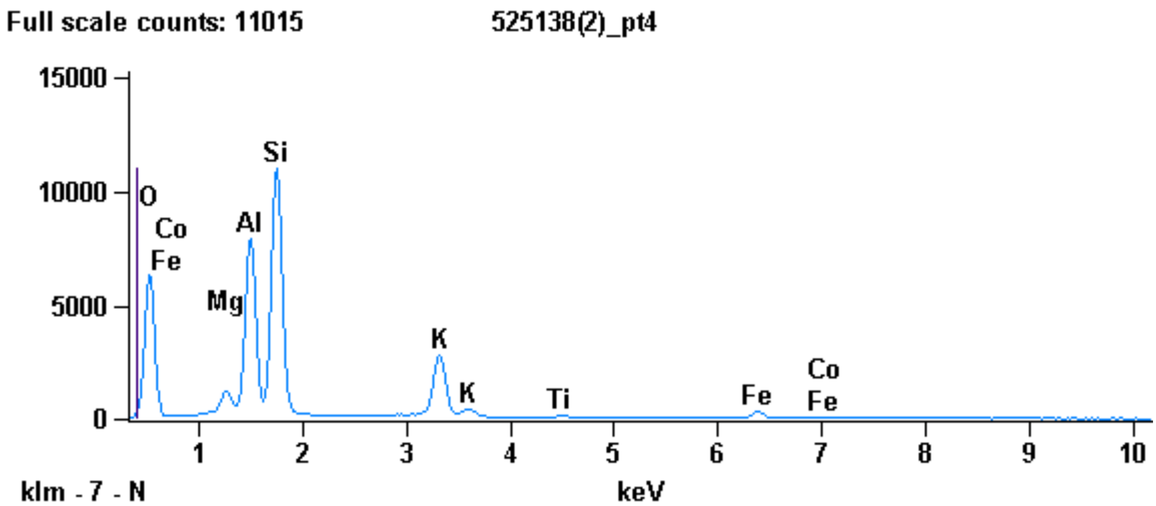
Full scale counts: 11015
525138(2)_pt4
15000
10000
5000
0
O
Co
Fe
Mg
Al
Si
K
K
Ti
Fe
Co
Fe
1 2 3 4 5 6 7 8 9 10
klm - 7 - N
keV

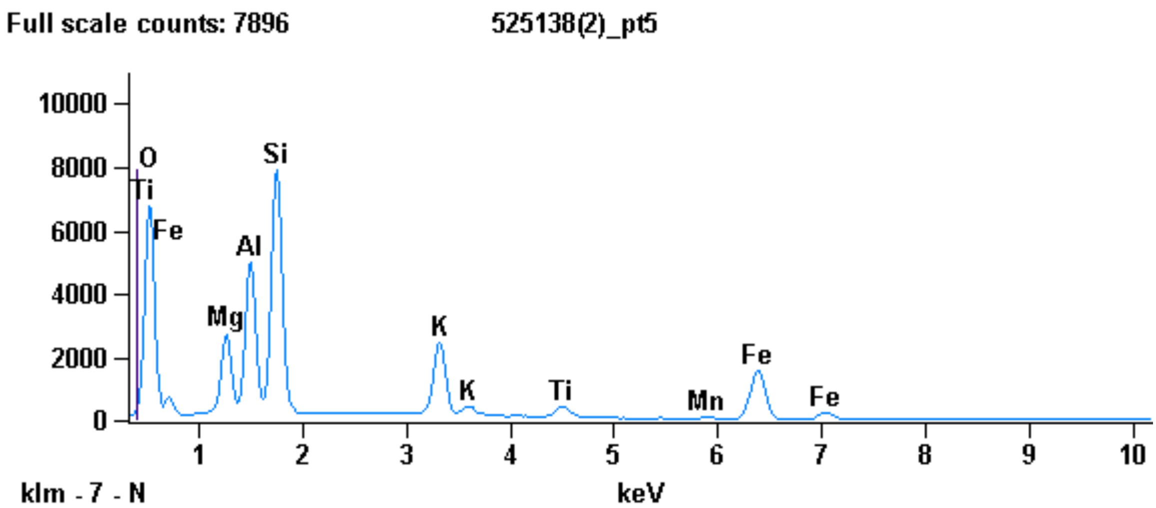
Full scale counts: 7896
525138(2)_pt5
10000
8000
6000
4000
2000
0
O
Ti
Fe
Mg
Al
Si
K
K
Ti
Mn
Fe
Fe
1 2 3 4 5 6 7 8 9 10
klm - 7 - N
keV

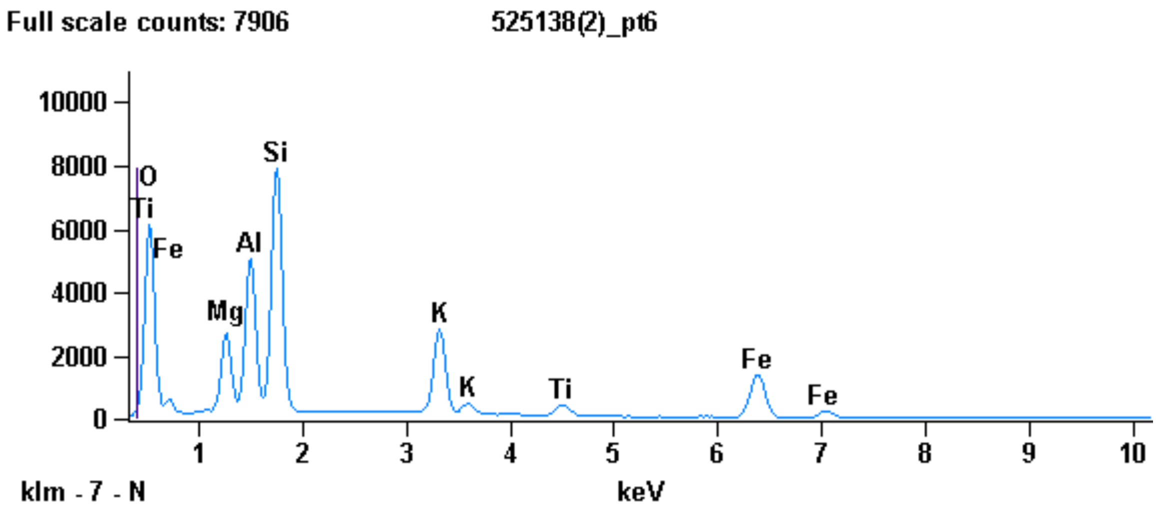

Weight %

	O-K	Mg-K	Al-K	Si-K	P-K	K-K	Ca-K	Ti-K	Mn-K	Fe-K	Co-K	Y-L
525138(2)_pt1	34.92S		1.19		16.27						1.87	45.74
525138(2)_pt2	41.13S		3.19	11.68		0.17	16.12	27.72				
525138(2)_pt3	40.15S	0.27	0.65	0.54				57.46		0.93		
525138(2)_pt4	46.16S	2.04	15.13	24.72		8.95		0.32		2.61	0.07	
525138(2)_pt5	42.05S	6.23	10.15	17.40		6.97		1.34	0.33	15.53		
525138(2)_pt6	42.12S	6.21	10.35	17.66		7.98		1.41		14.27		

Atom %

	O-K	Mg-K	Al-K	Si-K	P-K	K-K	Ca-K	Ti-K	Mn-K	Fe-K	Co-K	Y-L
525138(2)_pt1	66.18		1.34		15.92						0.96	15.60
525138(2)_pt2	62.85		2.89	10.17		0.10	9.83	14.15				
525138(2)_pt3	66.39	0.29	0.64	0.51				31.73		0.44		
525138(2)_pt4	61.47	1.79	11.95	18.76		4.88		0.14		1.00	0.02	
525138(2)_pt5	60.13	5.87	8.61	14.17		4.08		0.64	0.14	6.36		
525138(2)_pt6	59.98	5.82	8.74	14.32		4.65		0.67		5.82		

Compound %

		MgO	Al2O3	SiO2	P2O5	K2O	CaO	TiO2	MnO	Fe2O3	CoO	Y2O3
525138(2)_pt1	0.00		2.26		37.27						2.38	58.09
525138(2)_pt2	0.00		6.03	24.99		0.20	22.55	46.23				
525138(2)_pt3	0.00	0.45	1.23	1.15				95.85		1.33		
525138(2)_pt4	0.00	3.39	28.58	52.89		10.78		0.54		3.73	0.09	
525138(2)_pt5	0.00	10.34	19.18	37.22		8.39		2.23	0.43	22.20		
525138(2)_pt6	0.00	10.29	19.56	37.78		9.61		2.35		20.40		

Minerals, 525138(2)
pt1: Xenotime
pt2: Sphene
pt3: Rutile
pt4: Chlorite
pt5: Biotite
pt6: Biotite

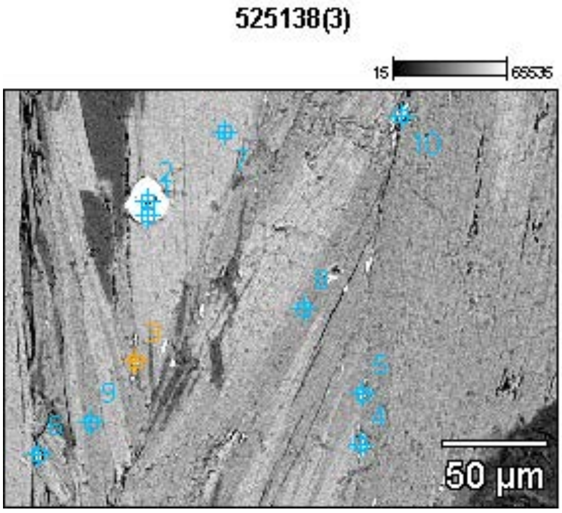

Image name: 525138(3)
Magnification: 463

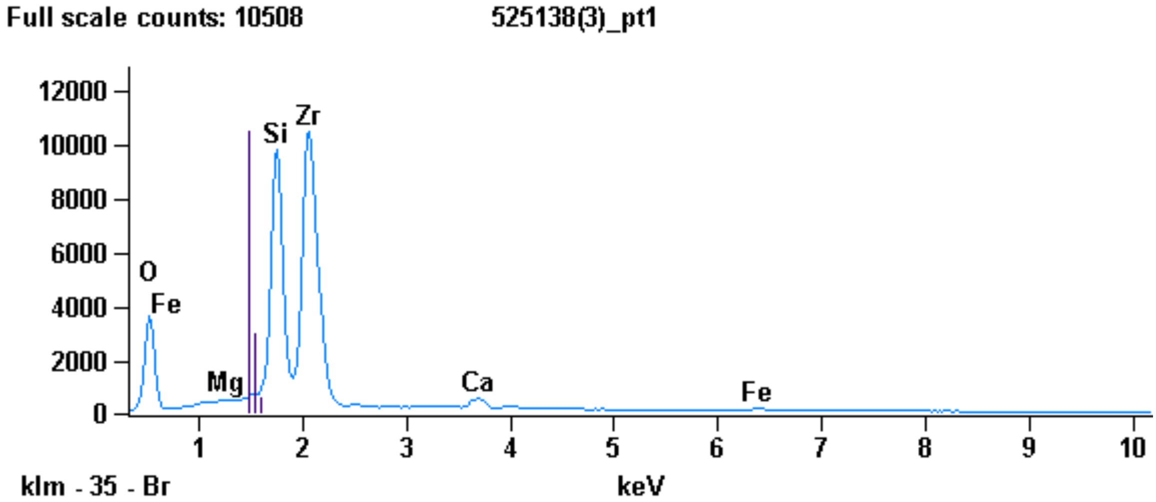

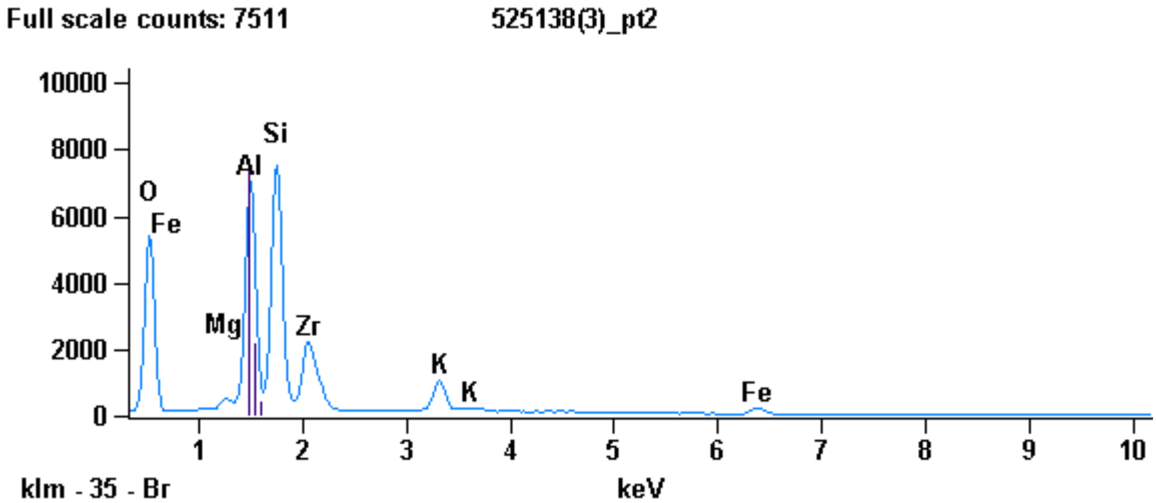

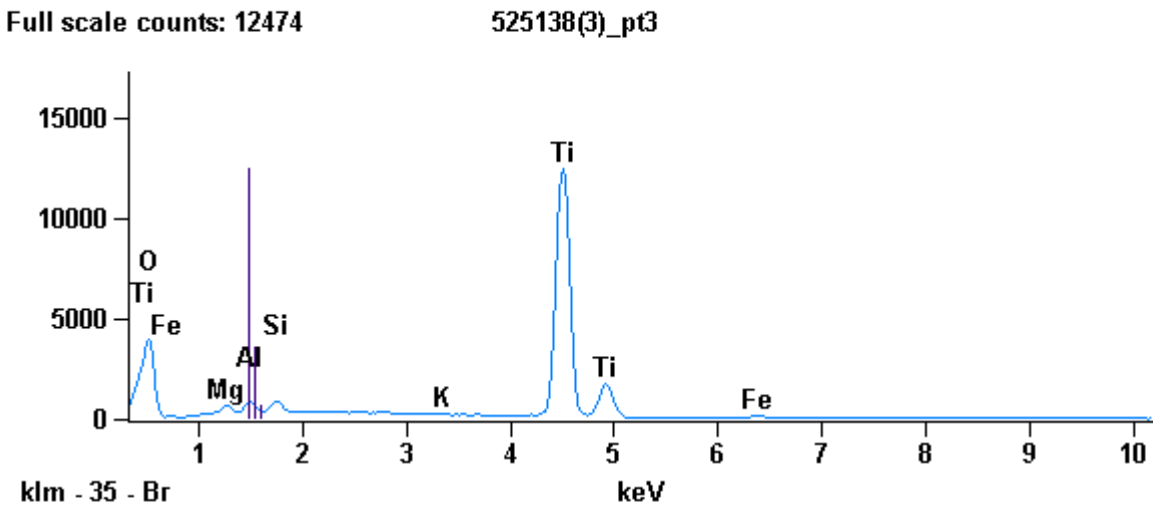
Full scale counts: 12474
525138(3)_pt3
15000
10000
5000
0
O
Ti
Fe
Mg
Al
Si
K
Ti
Ti
Fe
1
2
3
4
5
6
7
8
9
10
klm - 35 - Br
keV

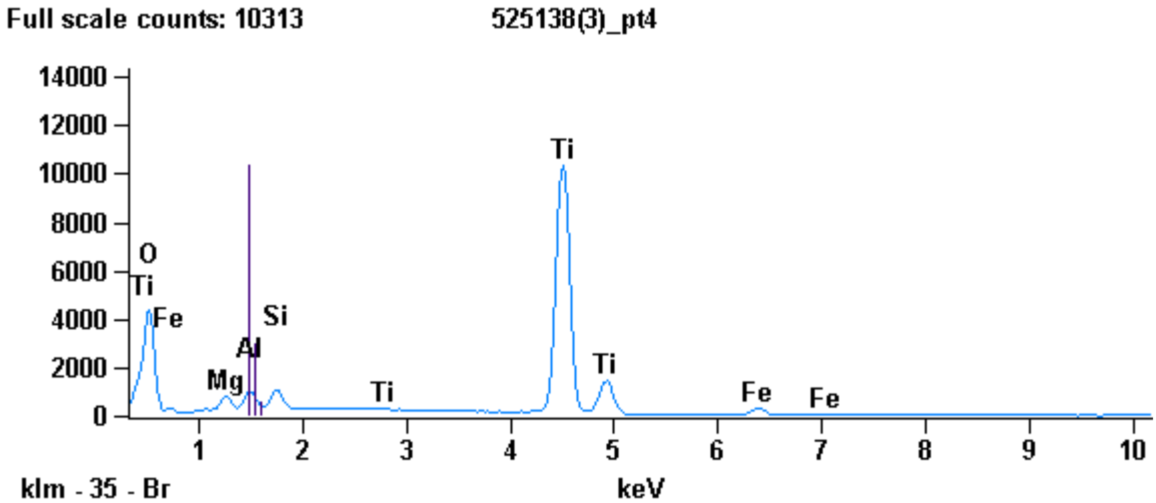
Full scale counts: 10313
525138(3)_pt4
14000
12000
10000
8000
6000
4000
2000
0
O
Ti
Fe
Mg
Al
Si
Ti
Ti
Ti
Fe
Fe
1
2
3
4
5
6
7
8
9
10
klm - 35 - Br
keV

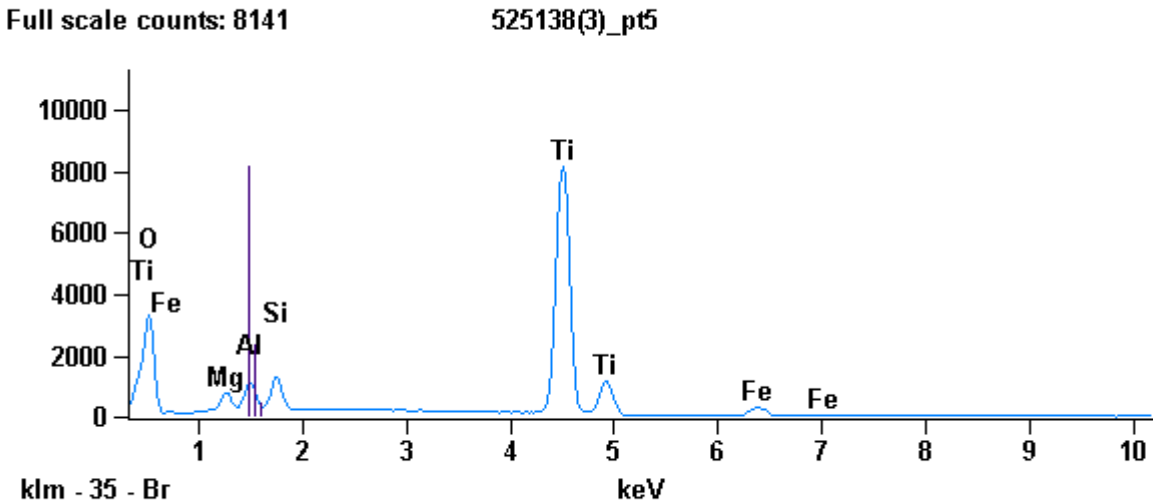
Full scale counts: 8141
525138(3)_pt5
10000
8000
6000
4000
2000
0
O
Ti
Fe
Mg
Al
Si
Ti
Ti
Fe
Fe
1
2
3
4
5
6
7
8
9
10
klm - 35 - Br
keV

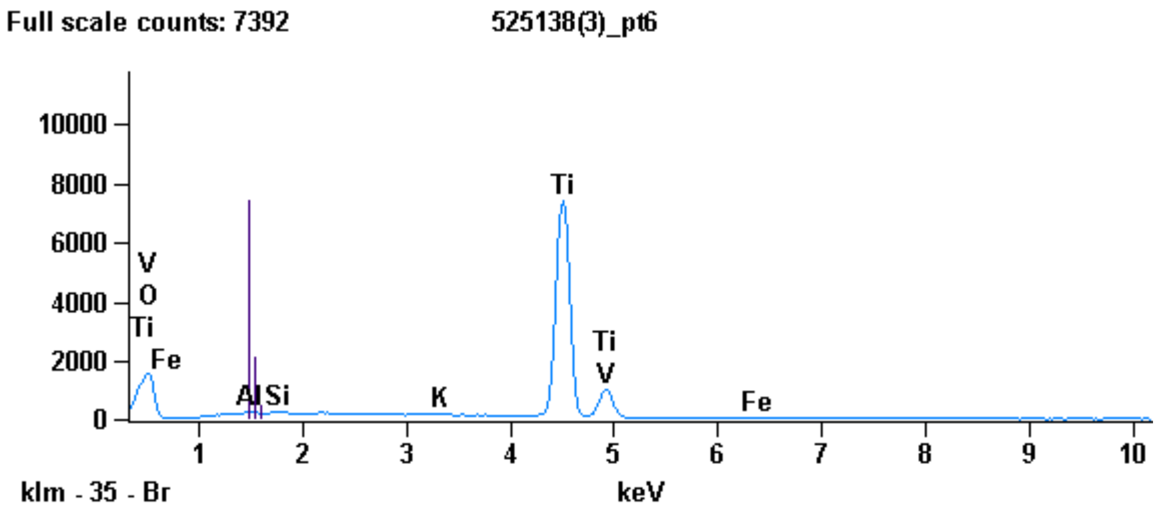
Full scale counts: 7392
525138(3)_pt6
10000
8000
6000
4000
2000
0
V
O
Ti
Fe
Al
Si
K
Ti
Ti
V
Fe
1
2
3
4
5
6
7
8
9
10
klm - 35 - Br
keV

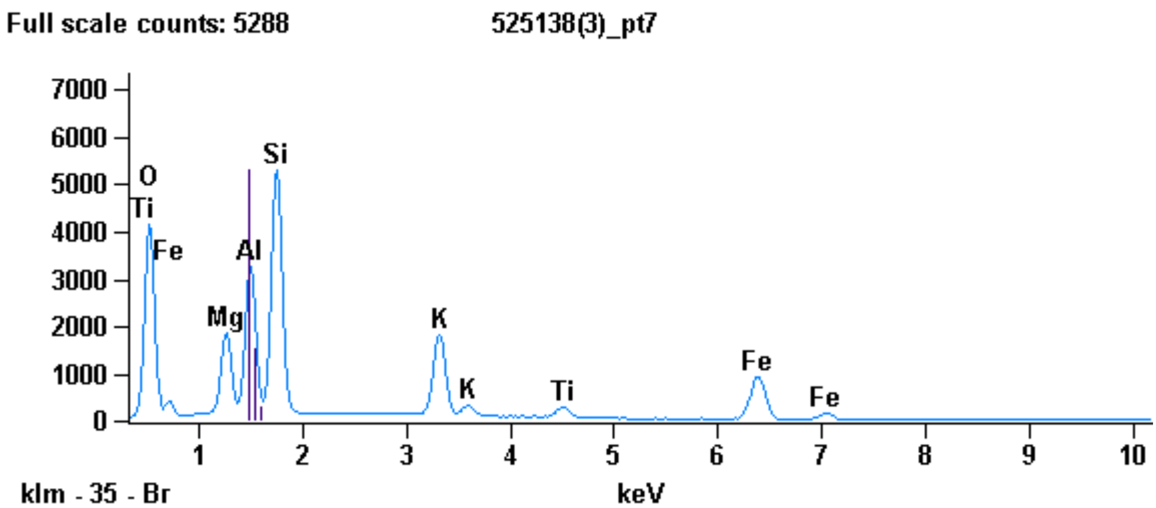
Full scale counts: 5288
525138(3)_pt7
7000
6000
5000
4000
3000
2000
1000
0
O
Ti
Fe
Mg
Al
Si
K
K
Ti
Fe
Fe
1
2
3
4
5
6
7
8
9
10
klm - 35 - Br
keV

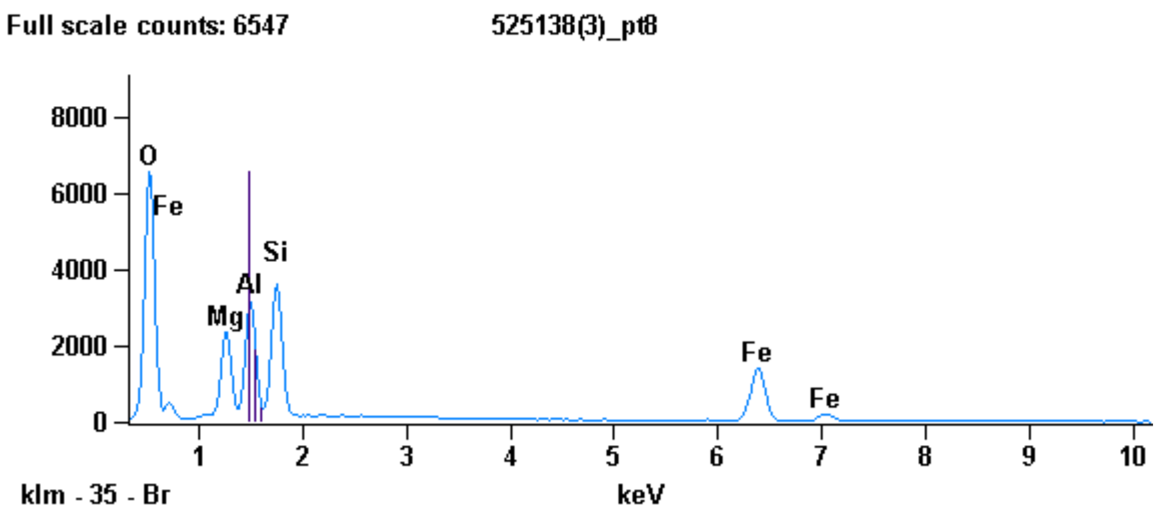
Full scale counts: 6547
525138(3)_pt8
8000
6000
4000
2000
0
O
Fe
Mg
Al
Si
Fe
Fe
1
2
3
4
5
6
7
8
9
10
klm - 35 - Br
keV

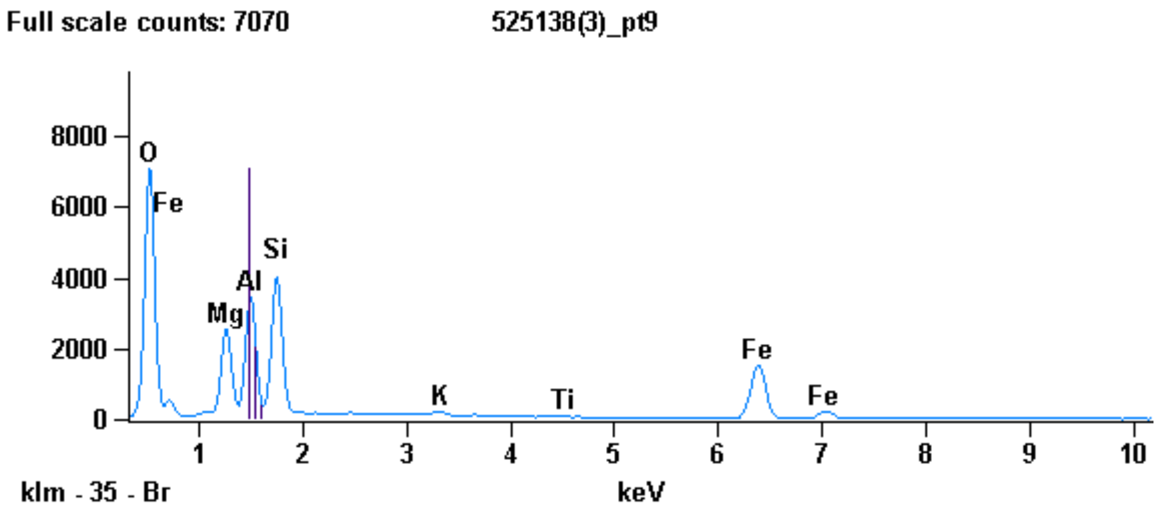

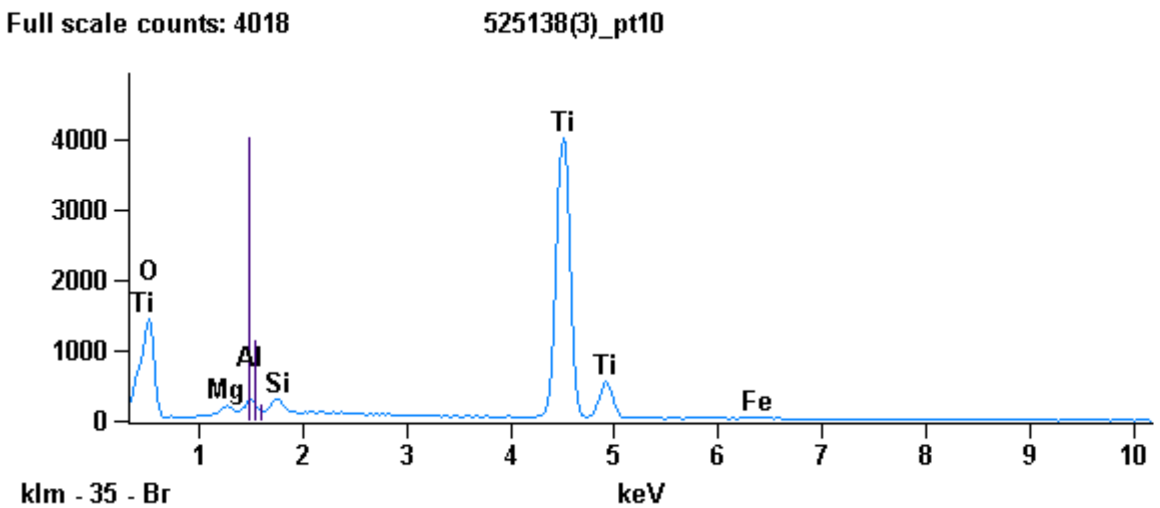

Weight %

	O-K	Mg-K	Al-K	Si-K	K-K	Ca-K	Ti-K	V-K	Fe-K	Zr-L
525138(3)_pt1	34.55S	0.11		14.48		1.26			0.89	48.71
525138(3)_pt2	43.22S	0.40	15.64	19.26	3.96				1.90	15.63
525138(3)_pt3	40.25S	0.95	1.00	1.05	0.10		55.26		1.39	
525138(3)_pt4	40.41S	1.82	1.83	1.70			51.78		2.48	
525138(3)_pt5	40.64S	2.21	2.57	2.69			48.37		3.52	
525138(3)_pt6	39.99S		0.18	0.26	0.14		58.61	0.00	0.83	
525138(3)_pt7	42.17S	6.65	10.18	17.75	7.98		1.36		13.92	
525138(3)_pt8	42.22S	9.99	11.59	13.79					22.41	
525138(3)_pt9	42.15S	9.76	11.58	13.79	0.34		0.10		22.29	
525138(3)_pt10	40.38S	1.00	1.23	1.18			55.10		1.12	

Atom %

	O-K	Mg-K	Al-K	Si-K	K-K	Ca-K	Ti-K	V-K	Fe-K	Zr-L
525138(3)_pt1	66.22	0.14		15.81		0.96			0.49	16.38
525138(3)_pt2	62.98	0.38	13.52	15.98	2.36				0.79	3.99
525138(3)_pt3	66.02	1.03	0.97	0.98	0.07		30.28		0.65	
525138(3)_pt4	65.54	1.94	1.76	1.57			28.05		1.15	
525138(3)_pt5	65.21	2.34	2.45	2.46			25.93		1.62	
525138(3)_pt6	66.52		0.18	0.24	0.10		32.57	0.00	0.39	
525138(3)_pt7	59.90	6.21	8.57	14.36	4.64		0.65		5.66	
525138(3)_pt8	60.37	9.40	9.82	11.23					9.18	
525138(3)_pt9	60.34	9.20	9.83	11.25	0.20		0.05		9.14	
525138(3)_pt10	66.02	1.08	1.19	1.10			30.09		0.52	

Compound %

		MgO	Al2O3	SiO2	K2O	CaO	TiO2	V2O5	Fe2O3	ZrO2
525138(3)_pt1	0.00	0.19		30.98		1.76			1.27	65.80
525138(3)_pt2	0.00	0.66	29.56	41.20	4.76				2.72	21.11
525138(3)_pt3	0.00	1.58	1.89	2.24	0.12		92.18		1.99	
525138(3)_pt4	0.00	3.01	3.45	3.63			86.37		3.54	
525138(3)_pt5	0.00	3.67	4.86	5.76			80.69		5.03	
525138(3)_pt6	0.00		0.34	0.55	0.17		97.76	0.00	1.18	
525138(3)_pt7	0.00	11.02	19.23	37.97	9.61		2.27		19.90	
525138(3)_pt8	0.00	16.56	21.90	29.50					32.04	
525138(3)_pt9	0.00	16.18	21.87	29.50	0.41		0.17		31.87	
525138(3)_pt10	0.00	1.66	2.32	2.52			91.91		1.60	

Minerals, 525138(3)
pt1: Zircon
pt2: Mixed signal/edge effect (biotite nucleus of zircon?)
pt3: Rutile (+ mixed signal, biotite)
pt4: Rutile (+ mixed signal, biotite)
pt5: Rutile (+ mixed signal, biotite)
pt6: Rutile
pt7: Biotite
pt8: Chlorite
pt9: Chlorite
pt10: Rutile

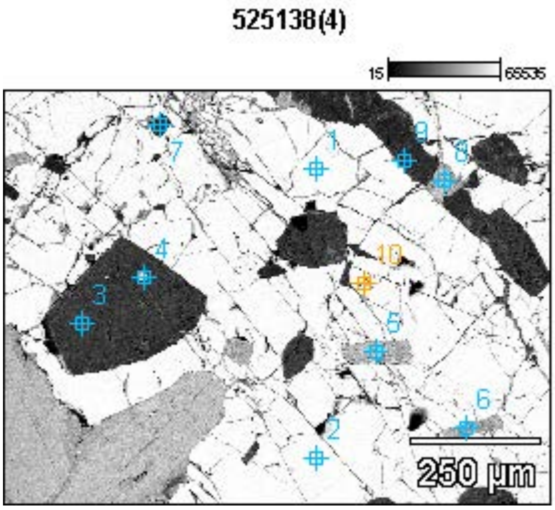

Image name: 525138(4)
Magnification: 115

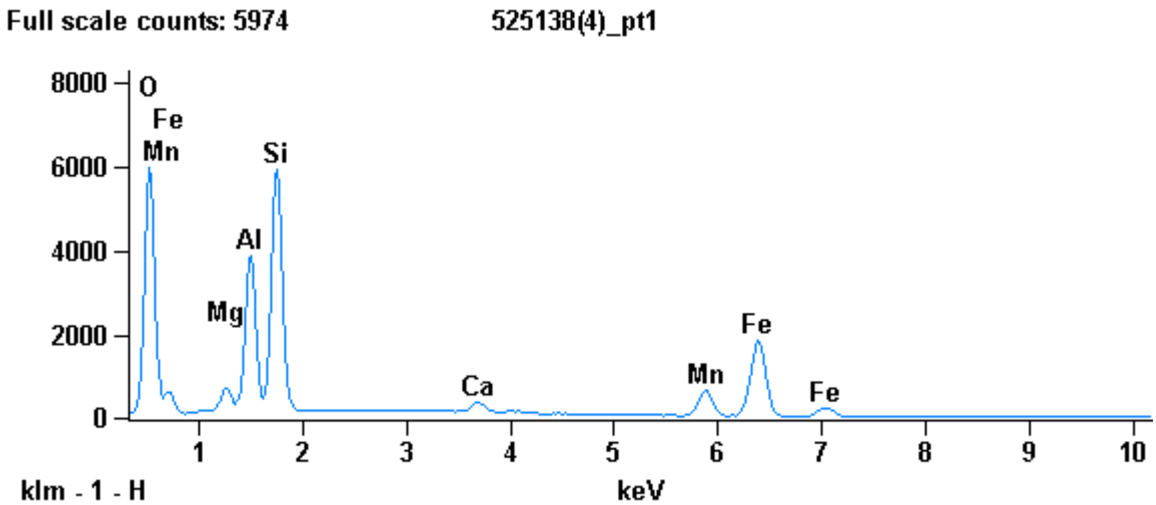

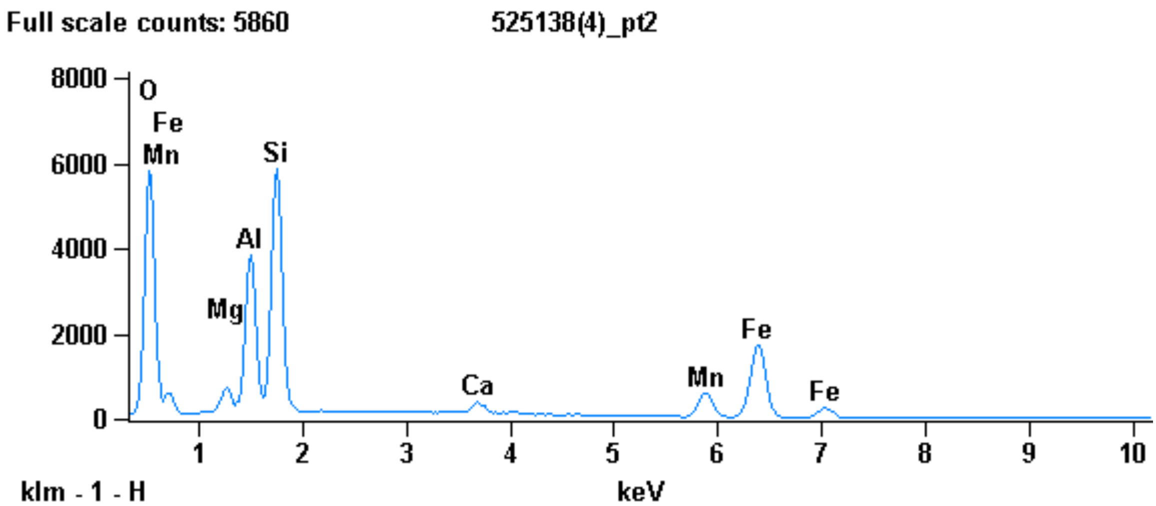

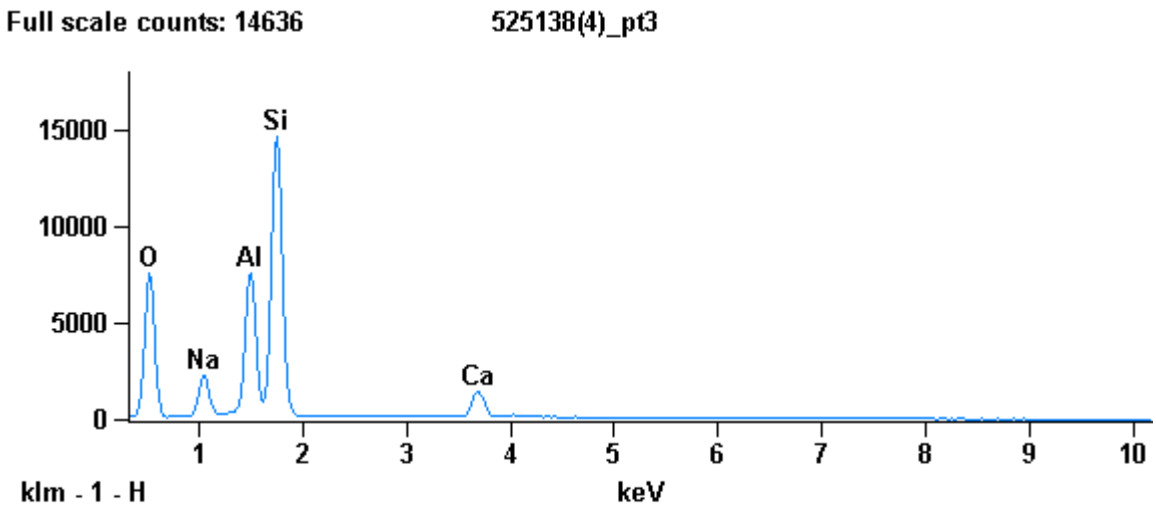
Full scale counts: 14636
525138(4)_pt3
15000
10000
5000
0
Si
O
Al
Na
Ca
1 2 3 4 5 6 7 8 9 10
klm - 1 - H
keV

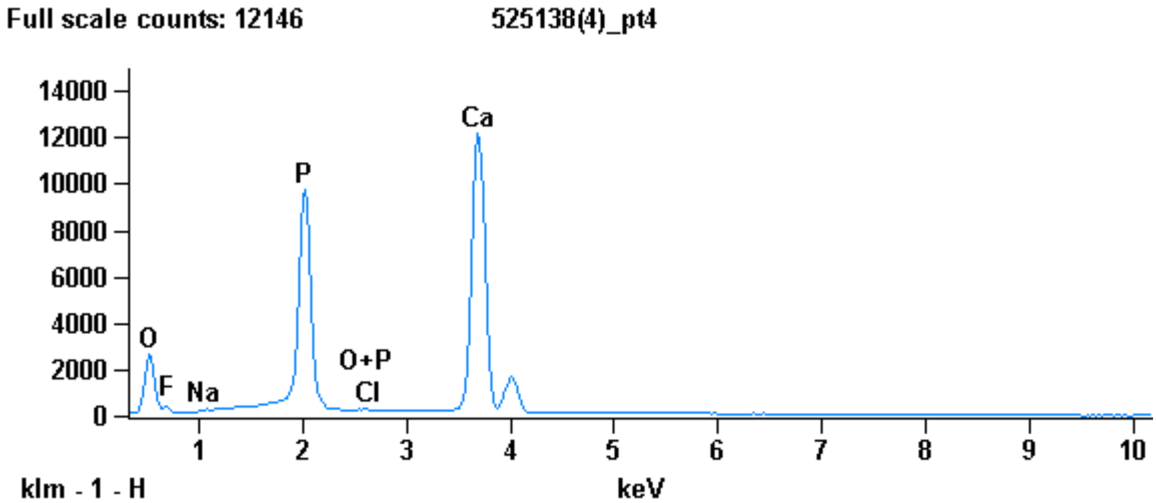
Full scale counts: 12146
525138(4)_pt4
14000
12000
10000
8000
6000
4000
2000
0
Ca
P
O
O+P
F
Na
Cl
1 2 3 4 5 6 7 8 9 10
klm - 1 - H
keV

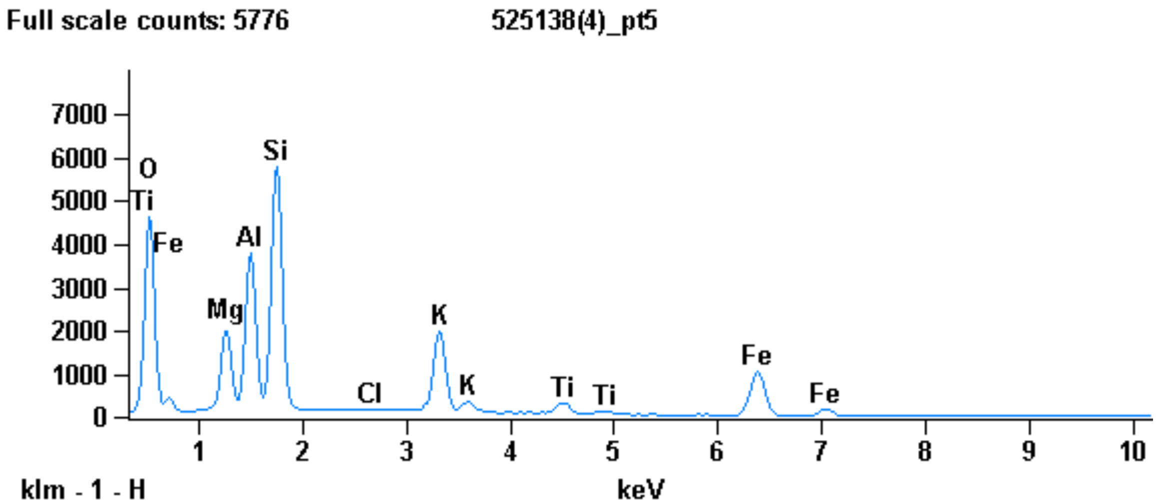
Full scale counts: 5776
525138(4)_pt5
7000
6000
5000
4000
3000
2000
1000
0
Si
O
Ti
Fe
Al
Mg
K
Fe
Cl
K
Ti
Ti
Fe
1 2 3 4 5 6 7 8 9 10
klm - 1 - H
keV

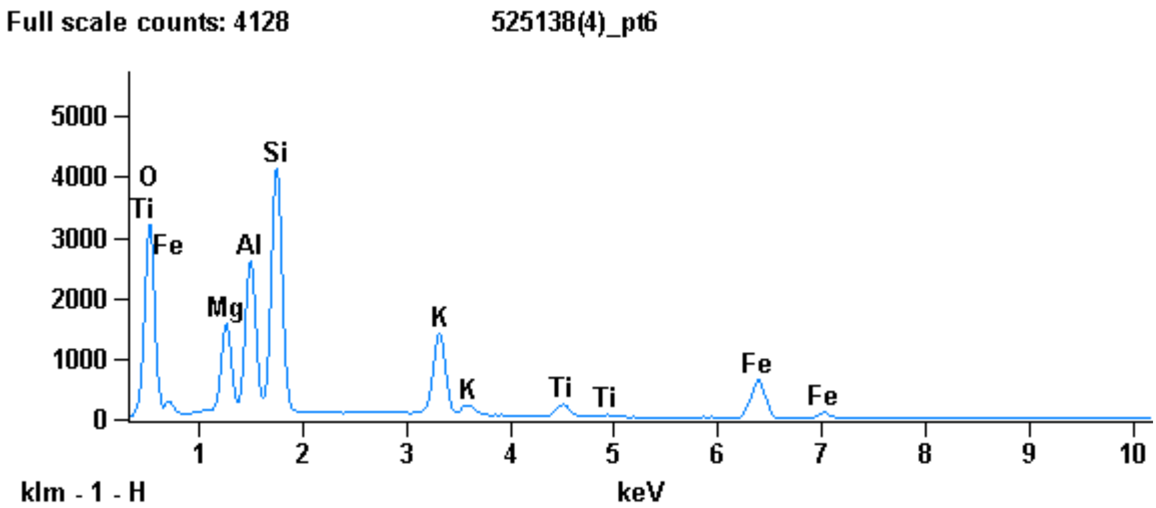
Full scale counts: 4128
525138(4)_pt6
5000
4000
3000
2000
1000
0
O
Ti
Fe
Mg
Al
Si
K
K
Ti
Ti
Fe
Fe
1
2
3
4
5
6
7
8
9
10
klm - 1 - H
keV

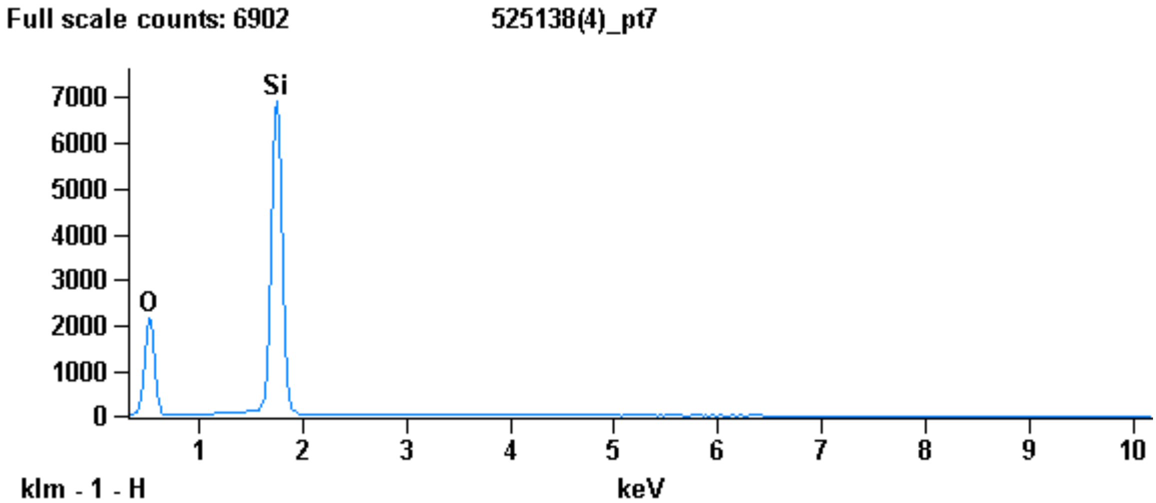
Full scale counts: 6902
525138(4)_pt7
7000
6000
5000
4000
3000
2000
1000
0
O
Si
1
2
3
4
5
6
7
8
9
10
klm - 1 - H
keV

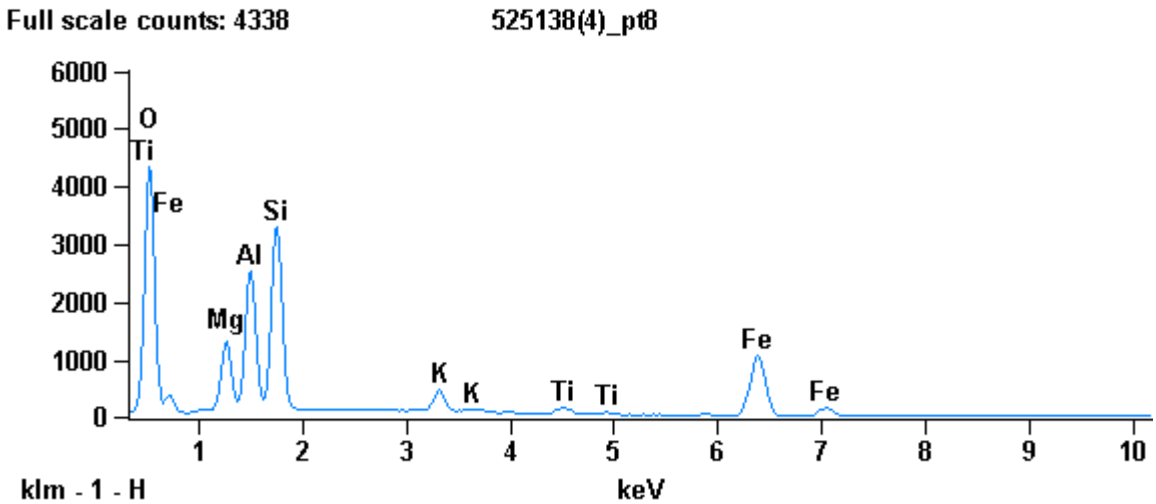
Full scale counts: 4338
525138(4)_pt8
6000
5000
4000
3000
2000
1000
0
O
Ti
Fe
Mg
Al
Si
K
K
Ti
Ti
Fe
Fe
1
2
3
4
5
6
7
8
9
10
klm - 1 - H
keV

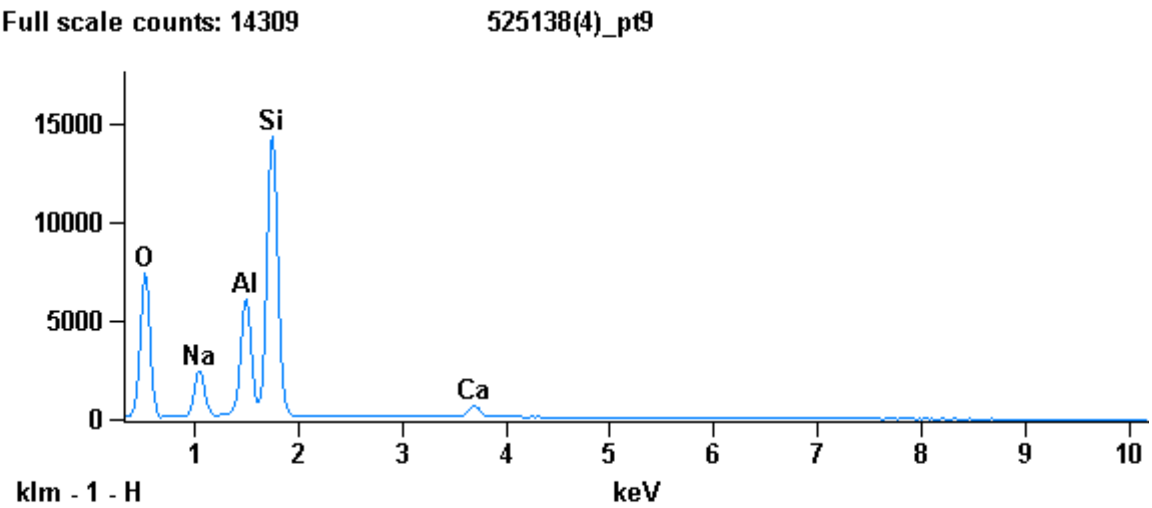

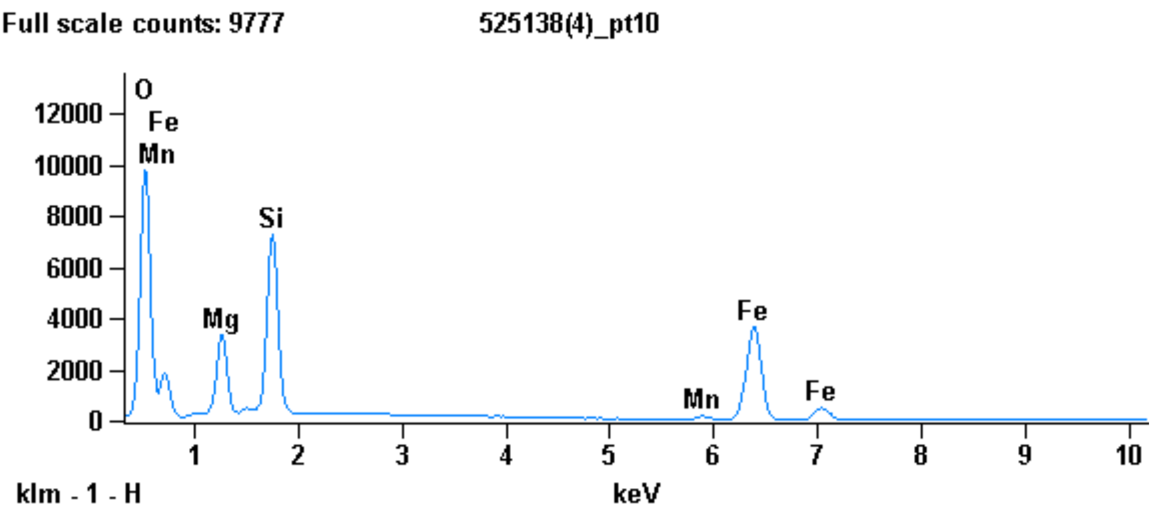

Weight %

	O-K	*F-K*	*Na-K*	*Mg-K*	*Al-K*	*Si-K*	*P-K*	*Cl-K*	*K-K*	*Ca-K*	*Ti-K*	*Mn-K*	*Fe-K*
525138(4)_pt1	41.38S			1.77	10.52	16.77				1.01		6.60	21.95
525138(4)_pt2	41.60S			1.79	10.73	17.01				1.00		6.28	21.59
525138(4)_pt3	47.90S		6.45		12.88	28.53				4.25			
525138(4)_pt4	37.88S	5.96	0.12				17.33			38.71			
525138(4)_pt5	42.21S			6.36	10.58	17.48		0.08	7.58		1.63		14.08
525138(4)_pt6	42.57S			7.05	10.59	18.06			8.02		1.67		12.04
525138(4)_pt7	53.26S					46.74							
525138(4)_pt8	42.20S			6.57	11.23	15.44			2.11		0.93		21.52
525138(4)_pt9	48.31S		7.93		11.36	30.42				1.98			
525138(4)_pt10	39.47S			9.95		15.90						0.75	33.92

Atom %

	O-K	F-K	Na-K	Mg-K	Al-K	Si-K	P-K	Cl-K	K-K	Ca-K	Ti-K	Mn-K	Fe-K
525138(4)_pt1	61.81			1.74	9.31	14.27				0.60		2.87	9.39
525138(4)_pt2	61.87			1.75	9.46	14.41				0.60		2.72	9.20
525138(4)_pt3	61.43		5.76		9.80	20.84				2.17			
525138(4)_pt4	56.21	7.44	0.13				13.29			22.93			
525138(4)_pt5	60.00			5.96	8.92	14.16		0.05	4.41		0.77		5.73
525138(4)_pt6	59.90			6.53	8.84	14.48			4.62		0.78		4.85
525138(4)_pt7	66.67					33.33							
525138(4)_pt8	60.88			6.24	9.60	12.69			1.24		0.45		8.90
525138(4)_pt9	61.40		7.01		8.56	22.03				1.00			
525138(4)_pt10	60.70			10.08		13.93						0.34	14.95

Compound %

		F	Na2O	MgO	Al2O3	SiO2	P2O5	Cl	K2O	CaO	TiO2	MnO	Fe2O3
525138(4)_pt1	0.00			2.93	19.87	35.87				1.42		8.52	31.39
525138(4)_pt2	0.00			2.96	20.28	36.38				1.40		8.11	30.86
525138(4)_pt3	0.00		8.70		24.34	61.03				5.94			
525138(4)_pt4	0.00	5.96	0.17				39.71			54.17			
525138(4)_pt5	0.00			10.55	20.00	37.40		0.08	9.13		2.72		20.13
525138(4)_pt6	0.00			11.70	20.01	38.65			9.66		2.78		17.21
525138(4)_pt7	0.00					100.00							
525138(4)_pt8	0.00			10.89	21.21	33.04			2.54		1.55		30.77
525138(4)_pt9	0.00		10.68		21.46	65.08				2.77			
525138(4)_pt10	0.00			16.50		34.02						0.97	48.50

Minerals, 525138(4)

pt1: Garnet - pyralspite-group
pt2: Garnet - pyralspite-group
pt3: Feldspar - plagioclase
pt4: Apatite
pt5: Biotite
pt6: Biotite
pt7: Quartz
pt8: Biotite
pt9: Feldspar - plagioclase
pt10: Olivine

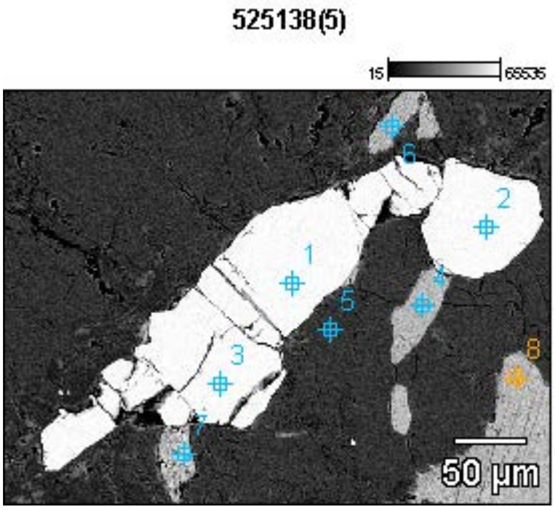

Image name: 525138(5)
Magnification: 320

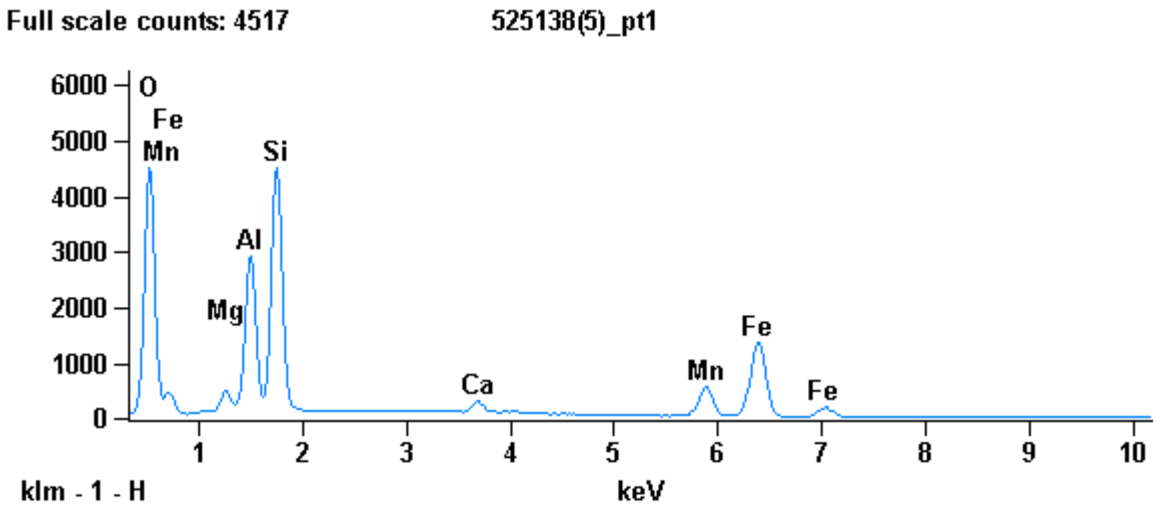

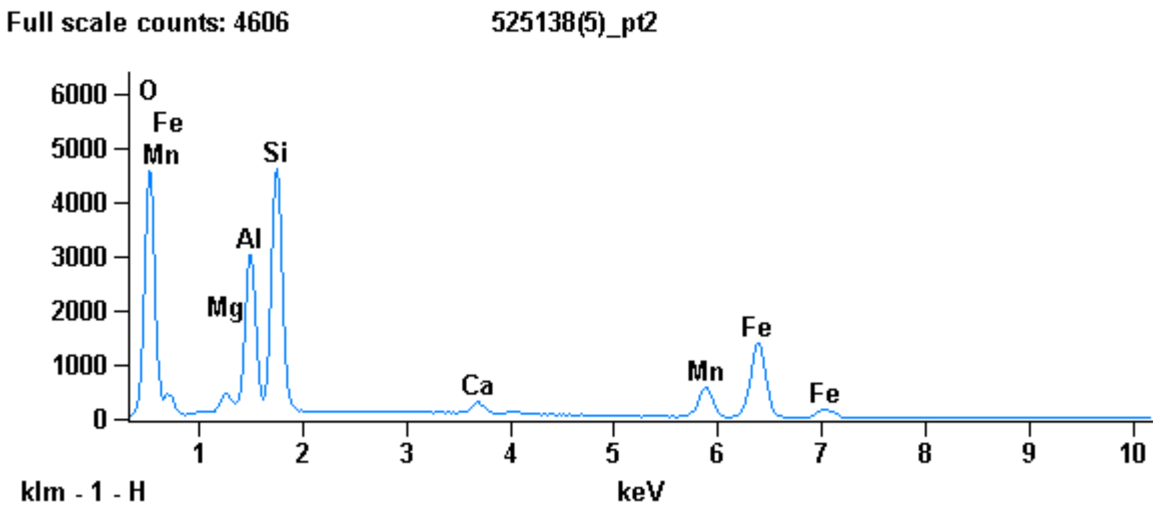

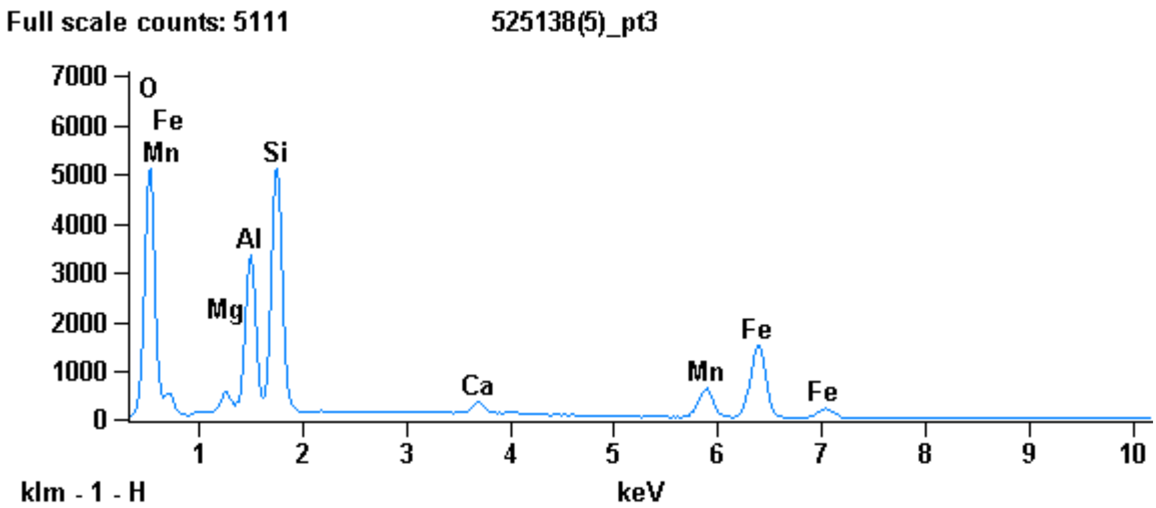
Full scale counts: 5111
525138(5)_pt3
7000
6000
5000
4000
3000
2000
1000
0
O
Fe
Mn
Si
Al
Mg
Ca
Mn
Fe
Fe
1
2
3
4
5
6
7
8
9
10
klm - 1 - H
keV

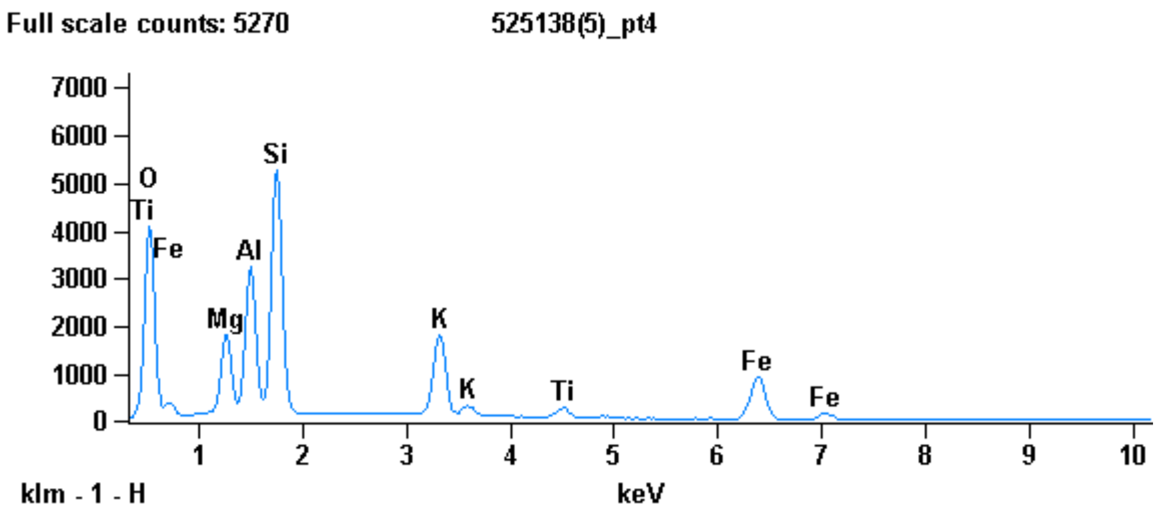
Full scale counts: 5270
525138(5)_pt4
7000
6000
5000
4000
3000
2000
1000
0
Si
O
Ti
Fe
Al
Mg
K
K
Ti
Fe
Fe
1
2
3
4
5
6
7
8
9
10
klm - 1 - H
keV

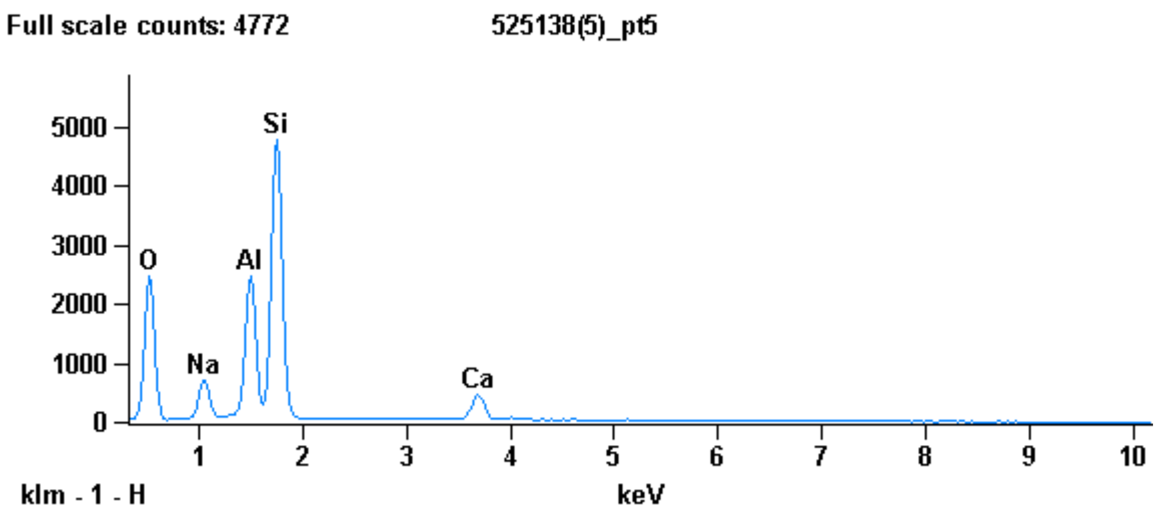
Full scale counts: 4772
525138(5)_pt5
5000
4000
3000
2000
1000
0
Si
O
Al
Na
Ca
1
2
3
4
5
6
7
8
9
10
klm - 1 - H
keV

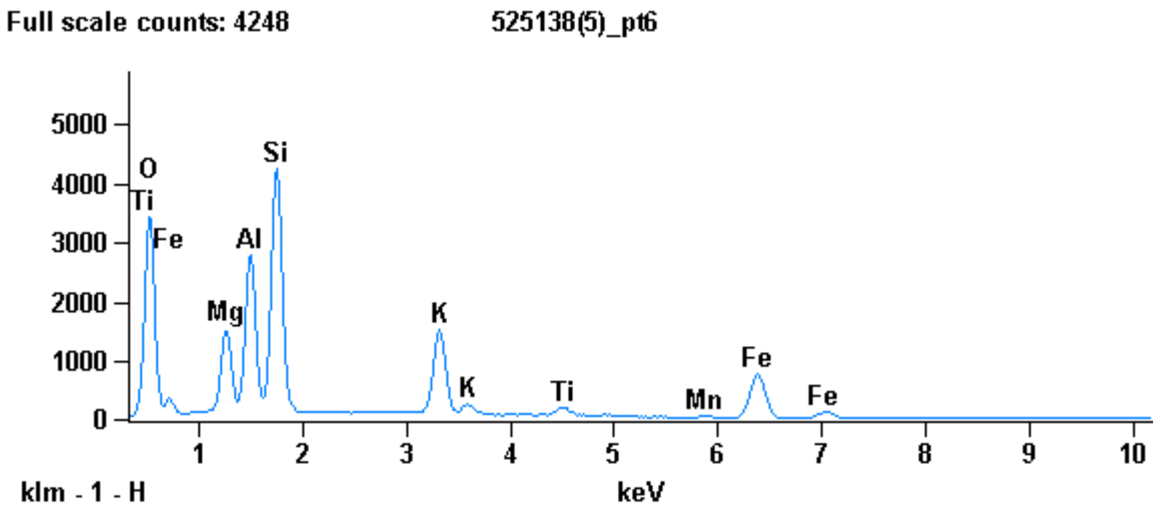
Full scale counts: 4248
525138(5)_pt6
5000
4000
3000
2000
1000
0
O
Ti
Fe
Mg
Al
Si
K
K
Ti
Mn
Fe
Fe
1 2 3 4 5 6 7 8 9 10
klm - 1 - H
keV

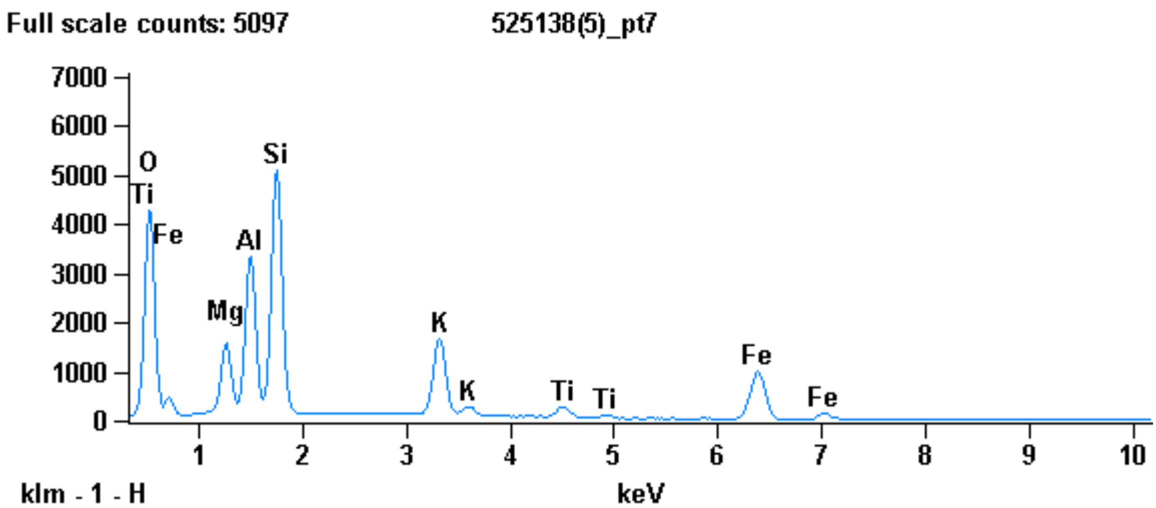
Full scale counts: 5097
525138(5)_pt7
7000
6000
5000
4000
3000
2000
1000
0
O
Ti
Fe
Mg
Al
Si
K
K
Ti
Ti
Fe
Fe
1 2 3 4 5 6 7 8 9 10
klm - 1 - H
keV

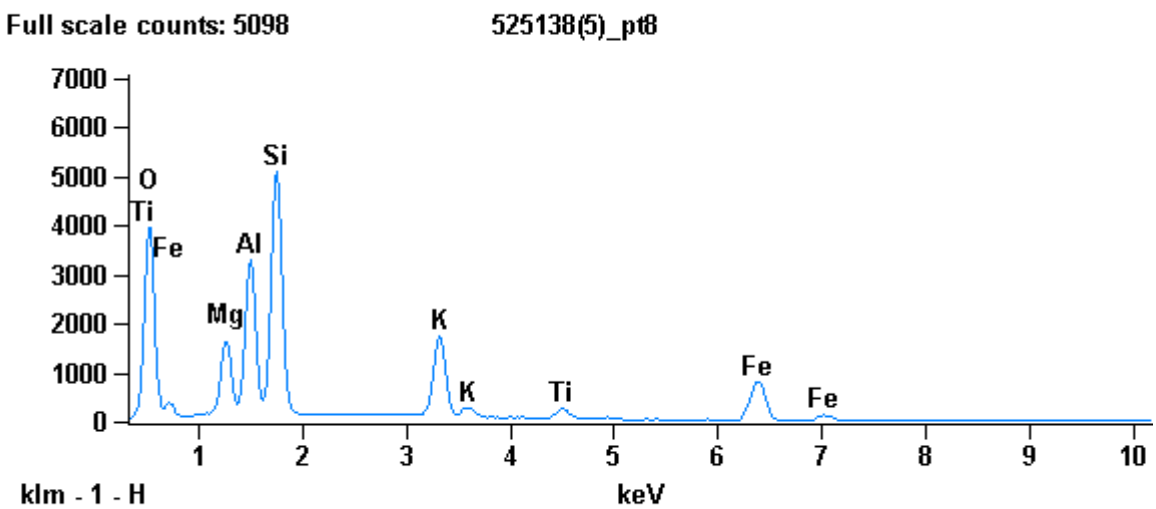
Full scale counts: 5098
525138(5)_pt8
7000
6000
5000
4000
3000
2000
1000
0
O
Ti
Fe
Mg
Al
Si
K
K
Ti
Fe
Fe
1 2 3 4 5 6 7 8 9 10
klm - 1 - H
keV

Weight %

	O-K	Na-K	Mg-K	Al-K	Si-K	K-K	Ca-K	Ti-K	Mn-K	Fe-K
525138(5)_pt1	41.43S		1.48	10.56	16.98		1.01		6.83	21.72
525138(5)_pt2	41.40S		1.28	10.75	16.96		1.10		7.38	21.12
525138(5)_pt3	41.43S		1.52	10.69	16.99		1.07		7.35	20.95
525138(5)_pt4	42.14S		6.56	10.19	17.74	7.95		1.23		14.18
525138(5)_pt5	47.91S	6.40		12.78	28.61		4.31			
525138(5)_pt6	41.96S		6.52	10.36	17.34	7.96		1.17	0.25	14.44
525138(5)_pt7	42.09S		5.64	10.65	17.47	7.57		1.38		15.21
525138(5)_pt8	42.36S		6.14	10.72	17.91	7.94		1.43		13.50

Atom %

	O-K	Na-K	Mg-K	Al-K	Si-K	K-K	Ca-K	Ti-K	Mn-K	Fe-K
525138(5)_pt1	61.88		1.46	9.35	14.44		0.60		2.97	9.29
525138(5)_pt2	61.86		1.26	9.53	14.44		0.65		3.21	9.04
525138(5)_pt3	61.82		1.50	9.46	14.44		0.64		3.19	8.95
525138(5)_pt4	59.91		6.14	8.59	14.37	4.63		0.58		5.78
525138(5)_pt5	61.46	5.71		9.72	20.91		2.21			
525138(5)_pt6	59.83		6.12	8.76	14.09	4.64		0.56	0.10	5.90
525138(5)_pt7	60.14		5.31	9.02	14.22	4.43		0.66		6.23
525138(5)_pt8	60.04		5.73	9.01	14.46	4.61		0.67		5.48

Compound %

		Na2O	MgO	Al2O3	SiO2	K2O	CaO	TiO2	MnO	Fe2O3
525138(5)_pt1	0.00		2.45	19.95	36.32		1.41		8.82	31.05
525138(5)_pt2	0.00		2.13	20.32	36.29		1.53		9.53	30.20
525138(5)_pt3	0.00		2.53	20.20	36.34		1.49		9.49	29.95
525138(5)_pt4	0.00		10.88	19.26	37.96	9.58		2.05		20.27
525138(5)_pt5	0.00	8.62		24.14	61.21		6.03			
525138(5)_pt6	0.00		10.82	19.58	37.10	9.59		1.95	0.32	20.64
525138(5)_pt7	0.00		9.35	20.12	37.37	9.12		2.30		21.74
525138(5)_pt8	0.00		10.18	20.26	38.31	9.57		2.38		19.30

Minerals, 525138(5)
pt1: Garnet, pyralspite-group
pt2: Garnet, pyralspite-group
pt3: Garnet, pyralspite-group
pt4: Biotite
pt5: Feldspar - plagioclase
pt6: Biotite
pt7: Biotite
pt8: Biotite

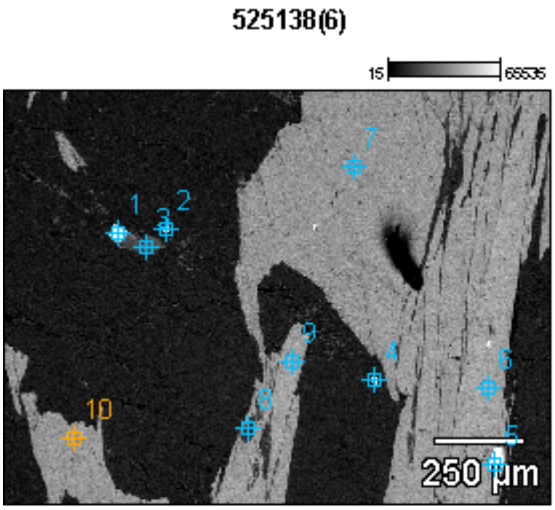

Image name: 525138(6)
Magnification: 80

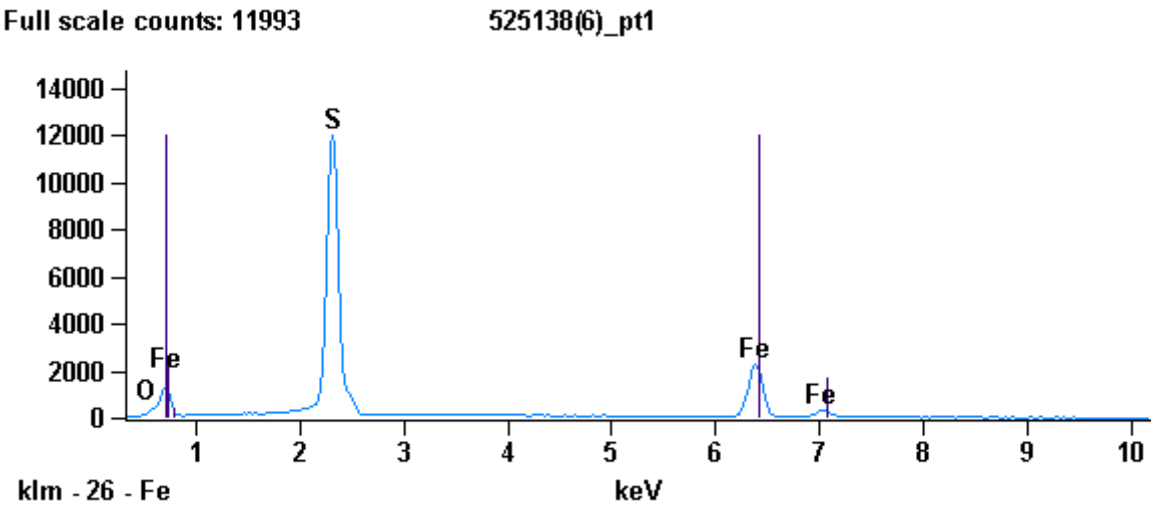

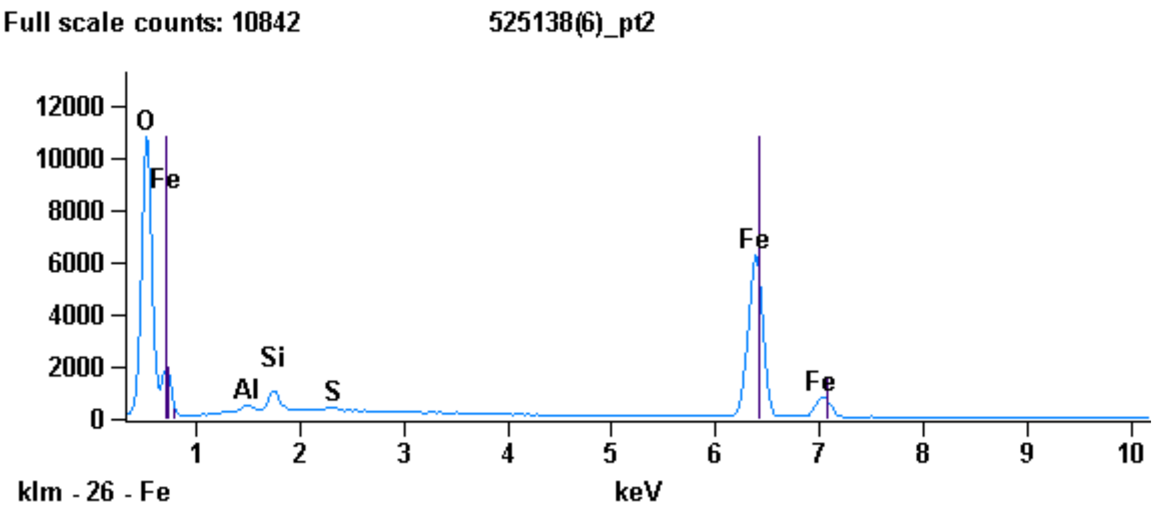

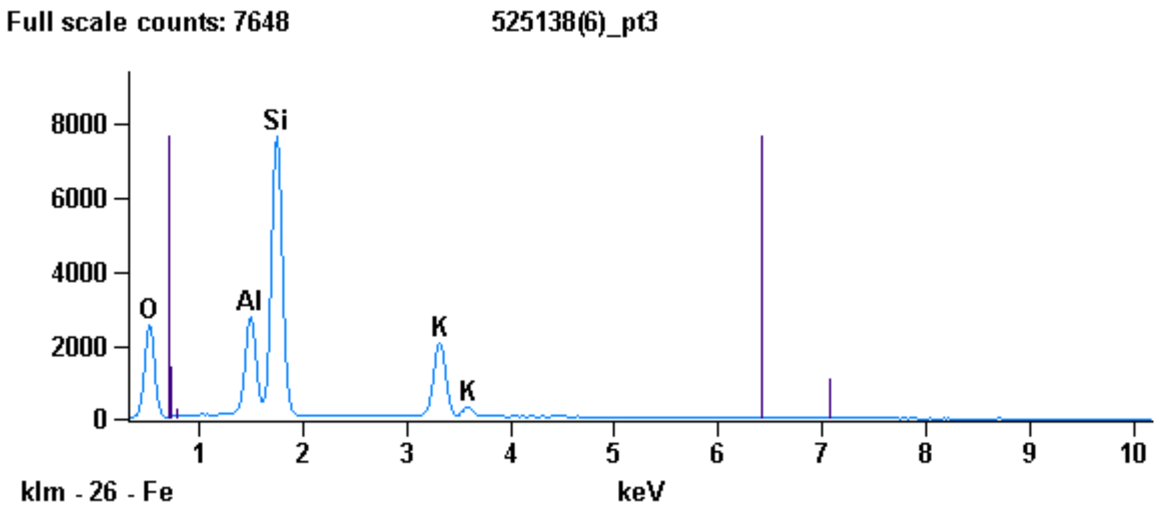
Full scale counts: 7648
525138(6)_pt3
8000
6000
4000
2000
0
Si
O
Al
K
K
1
2
3
4
5
6
7
8
9
10
klm - 26 - Fe
keV

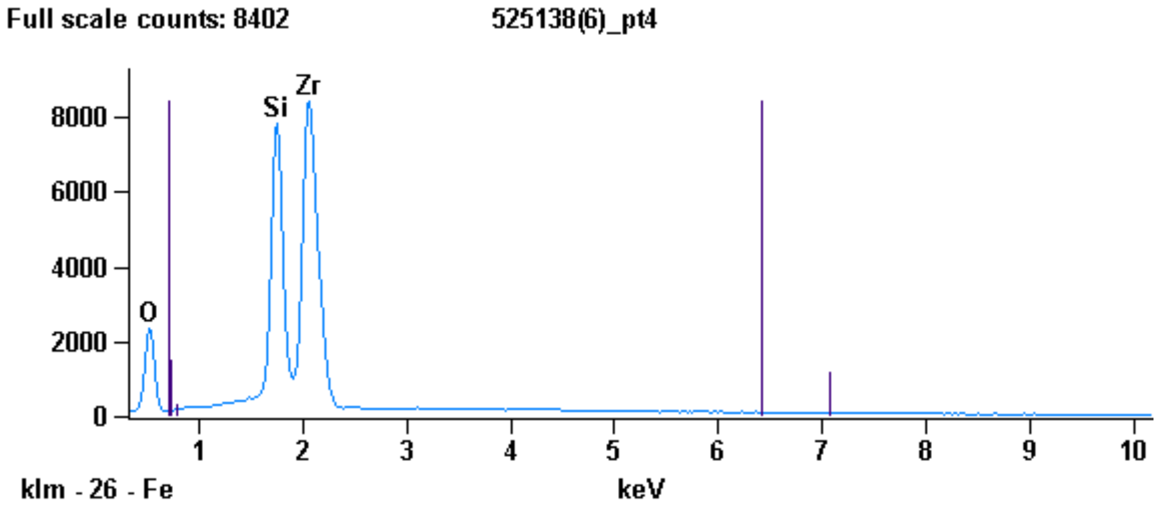
Full scale counts: 8402
525138(6)_pt4
8000
6000
4000
2000
0
Zr
Si
O
1
2
3
4
5
6
7
8
9
10
klm - 26 - Fe
keV

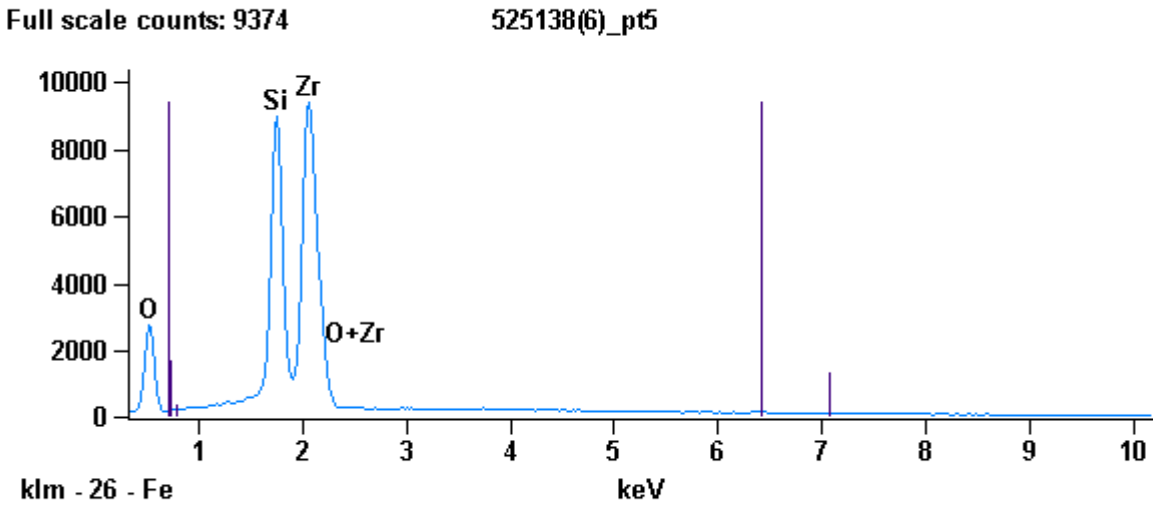
Full scale counts: 9374
525138(6)_pt5
10000
8000
6000
4000
2000
0
Si
Zr
O
O+Zr
1
2
3
4
5
6
7
8
9
10
klm - 26 - Fe
keV

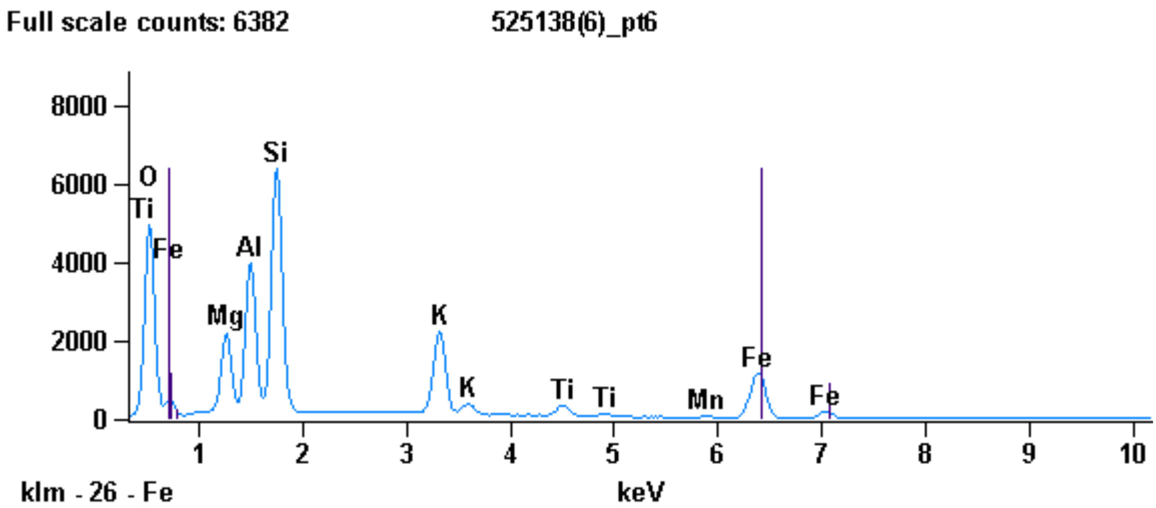
Full scale counts: 6382
525138(6)_pt6
8000
6000
4000
2000
0
O
Ti
Fe
Mg
Al
Si
K
K
Ti
Ti
Mn
Fe
Fe
1
2
3
4
5
6
7
8
9
10
klm - 26 - Fe
keV

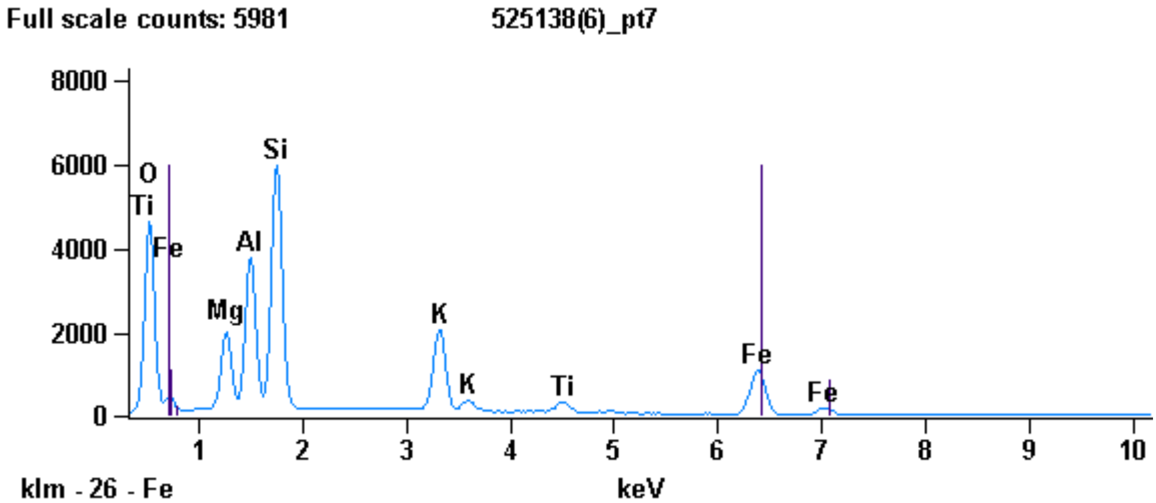
Full scale counts: 5981
525138(6)_pt7
8000
6000
4000
2000
0
O
Ti
Fe
Mg
Al
Si
K
K
Ti
Fe
Fe
1
2
3
4
5
6
7
8
9
10
klm - 26 - Fe
keV

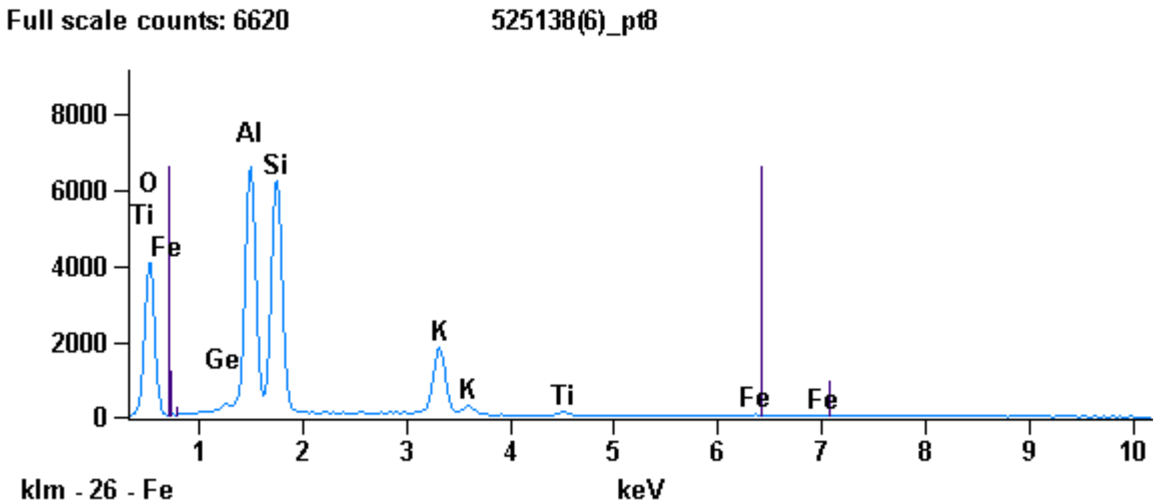
Full scale counts: 6620
525138(6)_pt8
8000
6000
4000
2000
0
O
Ti
Fe
Ge
Al
Si
K
K
Ti
Fe
Fe
1
2
3
4
5
6
7
8
9
10
klm - 26 - Fe
keV

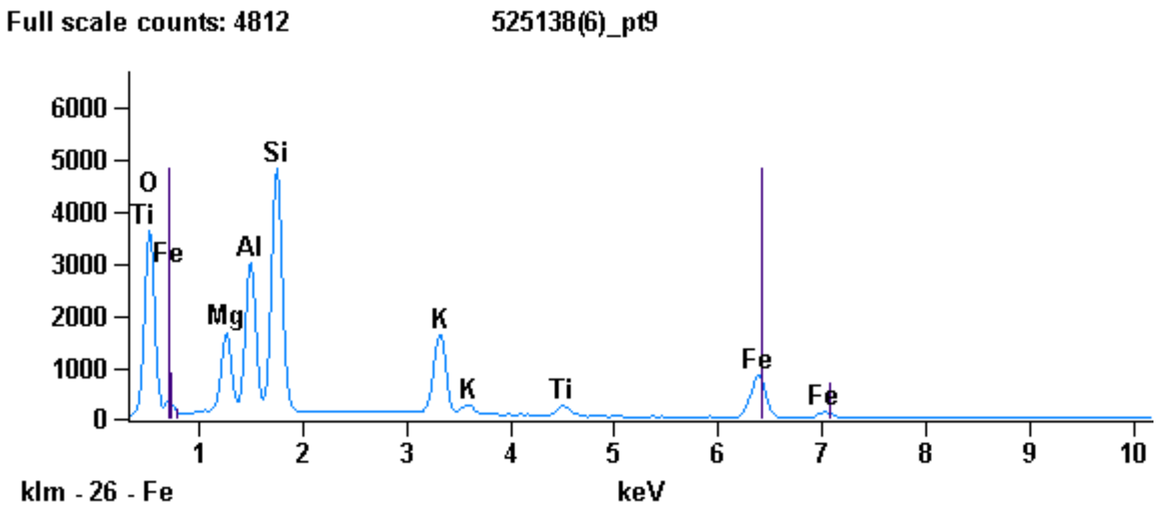

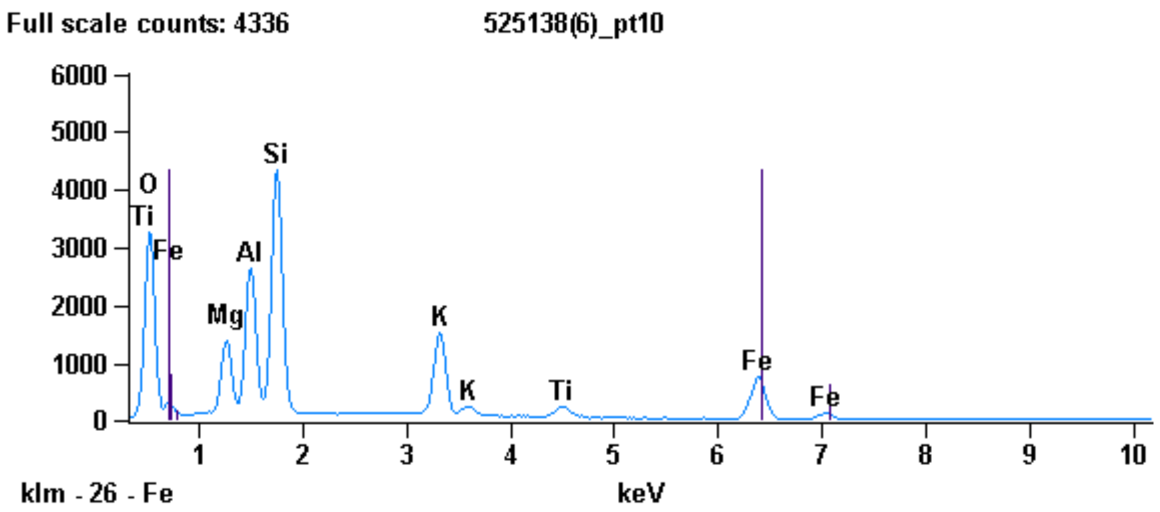

Weight %

	O-K	*Mg-K*	*Al-K*	*Si-K*	*S-K*	*K-K*	*Ti-K*	*Mn-K*	*Fe-K*	*Zr-L*
525138(6)_pt1	49.99S				26.70				23.31	
525138(6)_pt2	31.52S		0.63	2.13	0.27				65.46	
525138(6)_pt3	46.35S		9.61	30.80		13.24				
525138(6)_pt4	34.65S			14.87						50.48
525138(6)_pt5	34.74S			15.03						50.23
525138(6)_pt6	41.90S	6.39	10.05	17.34		7.82	1.46	0.33	14.72	
525138(6)_pt7	42.07S	6.27	10.24	17.56		7.85	1.44		14.58	
525138(6)_pt8	46.46S		19.52	23.14		9.28	0.62		0.96	
525138(6)_pt9	42.21S	6.42	10.37	17.73		7.88	1.38		14.01	
525138(6)_pt10	42.24S	6.14	10.30	17.90		7.94	1.52		13.95	

Atom %

	O-K	Mg-K	Al-K	Si-K	S-K	K-K	Ti-K	Mn-K	Fe-K	Zr-L
525138(6)_pt1	71.42				19.04				9.54	
525138(6)_pt2	60.62		0.72	2.33	0.26				36.07	
525138(6)_pt3	61.79		7.60	23.39		7.22				
525138(6)_pt4	66.67			16.30						17.03
525138(6)_pt5	66.67			16.43						16.91
525138(6)_pt6	59.91	6.01	8.52	14.12		4.57	0.70	0.14	6.03	
525138(6)_pt7	59.98	5.88	8.65	14.26		4.58	0.69		5.96	
525138(6)_pt8	61.54		15.33	17.46		5.03	0.28		0.37	
525138(6)_pt9	59.97	6.01	8.74	14.35		4.58	0.65		5.70	
525138(6)_pt10	60.05	5.75	8.69	14.50		4.62	0.72		5.68	

Compound %

		MgO	Al2O3	SiO2	SO3	K2O	TiO2	MnO	Fe2O3	ZrO2
525138(6)_pt1	0.00				66.67				33.33	
525138(6)_pt2	0.00		1.19	4.56	0.67				93.58	
525138(6)_pt3	0.00		18.16	65.89		15.95				
525138(6)_pt4	0.00			31.81						68.19
525138(6)_pt5	0.00			32.15						67.85
525138(6)_pt6	0.00	10.59	19.00	37.09		9.42	2.44	0.42	21.05	
525138(6)_pt7	0.00	10.40	19.34	37.56		9.45	2.40		20.85	
525138(6)_pt8	0.00		36.89	49.51		11.18	1.04		1.38	
525138(6)_pt9	0.00	10.65	19.60	37.94		9.49	2.30		20.03	
525138(6)_pt10	0.00	10.19	19.47	38.30		9.57	2.53		19.95	

Minerals, 525138(6)

pt1: Pyrite
pt2: Magnetite
pt3: Alkali feldspar - microcline
pt4: Zircon
pt5: Zircon
pt6: Biotite
pt7: Biotite
pt8: Muscovite (+mixed signal/edge effect)
pt9: Biotite
pt10: Biotite

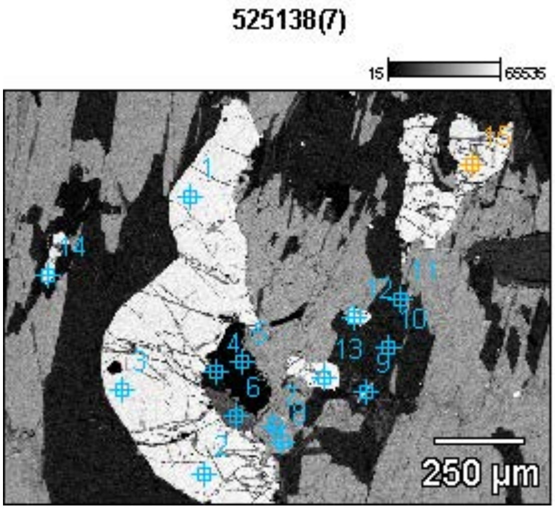

Image name: 525138(7)
Magnification: 80

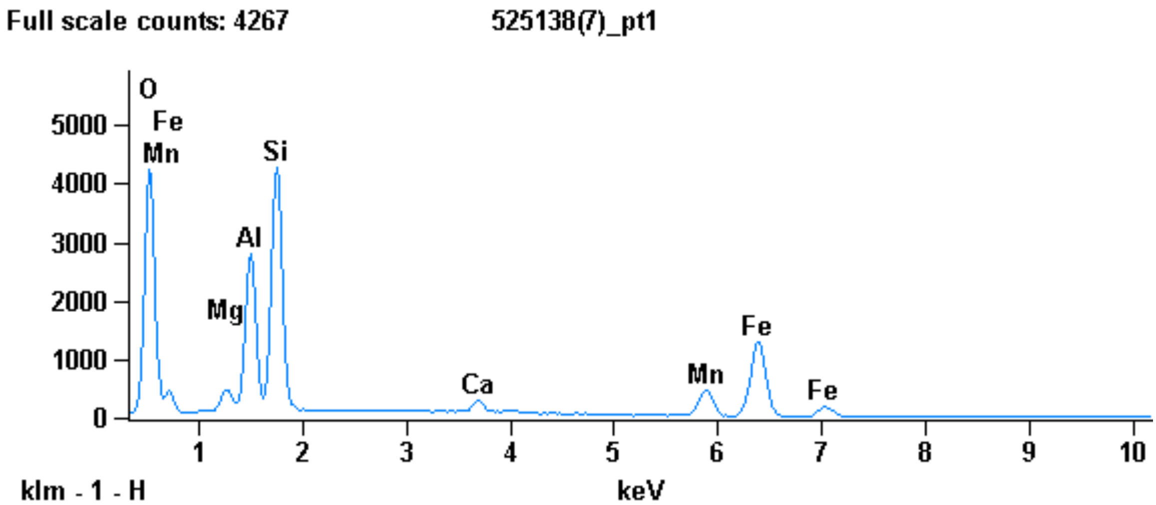

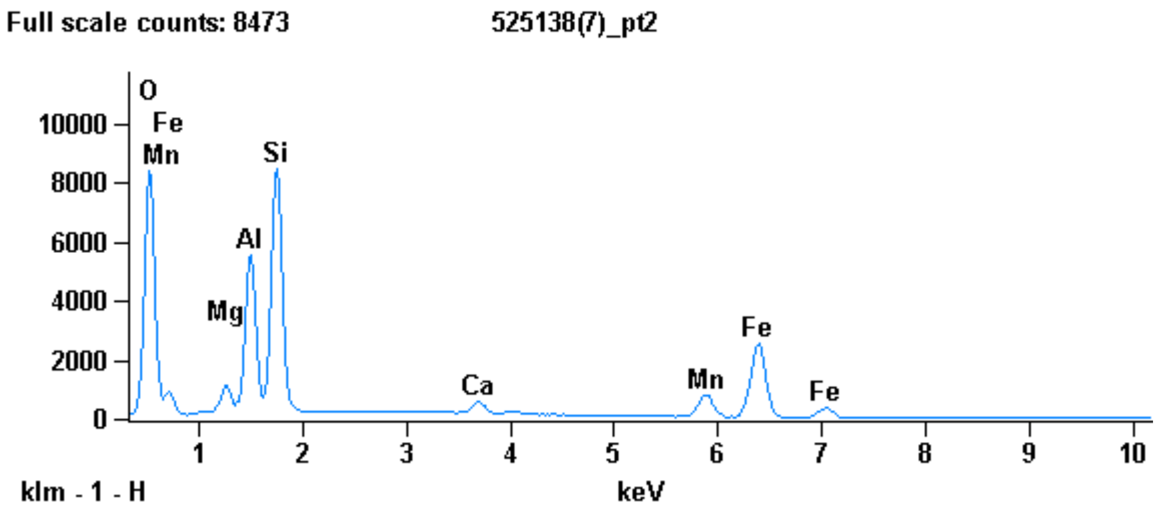

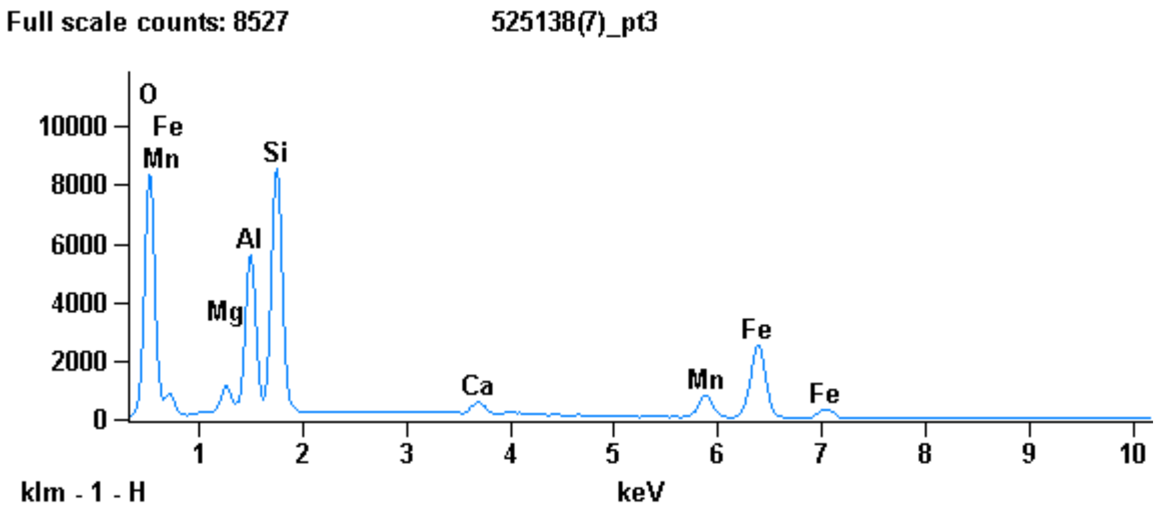
Full scale counts: 8527
525138(7)_pt3
O
Fe
Mn
Si
Al
Mg
Ca
Mn
Fe
Fe
10000
8000
6000
4000
2000
0
1 2 3 4 5 6 7 8 9 10
klm - 1 - H
keV

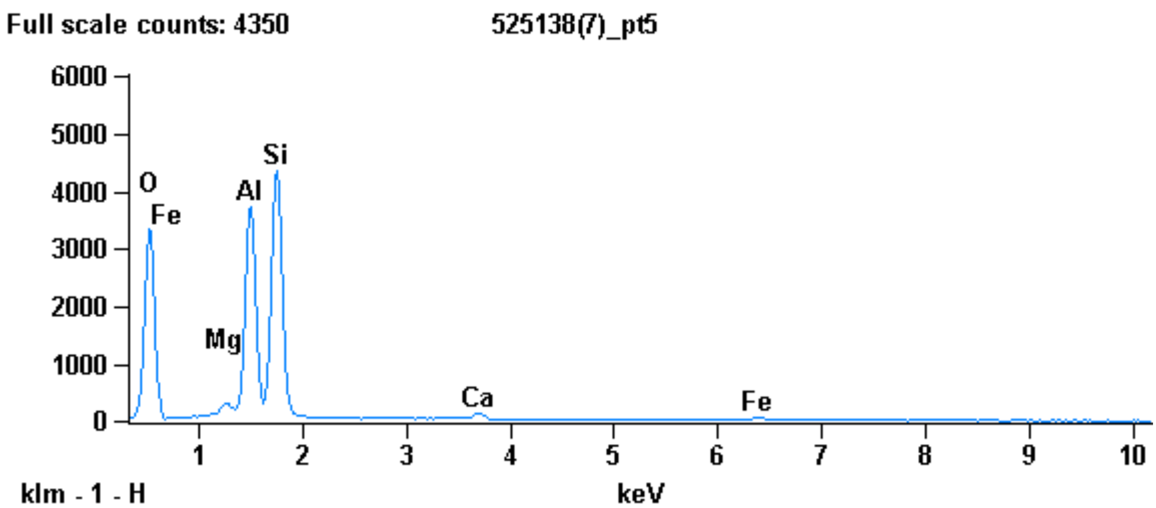
Full scale counts: 4350
525138(7)_pt5
Si
O
Al
Fe
Mg
Ca
Fe
6000
5000
4000
3000
2000
1000
0
1 2 3 4 5 6 7 8 9 10
klm - 1 - H
keV

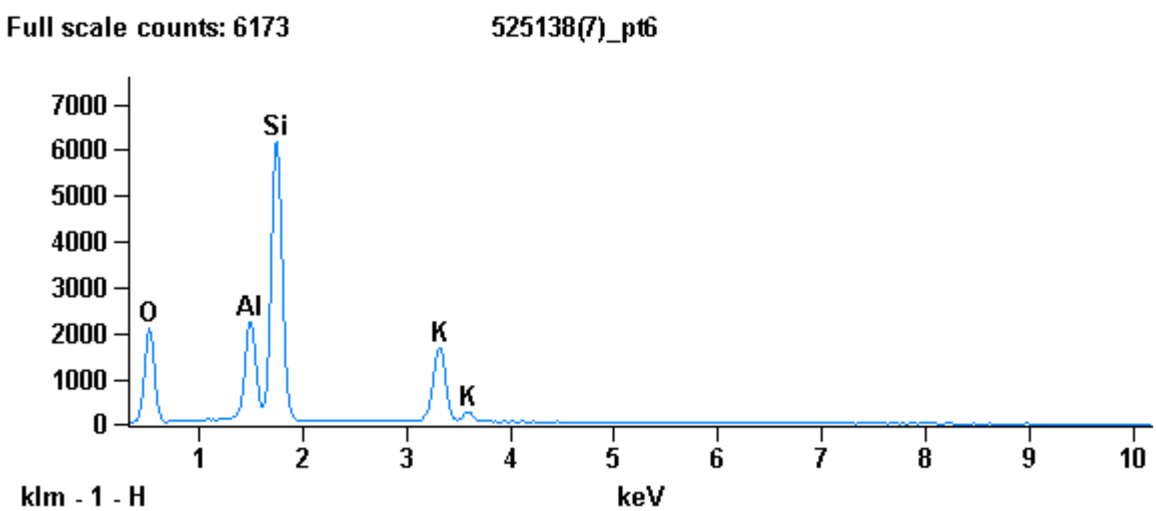
Full scale counts: 6173
525138(7)_pt6
Si
O
Al
K
K
7000
6000
5000
4000
3000
2000
1000
0
1 2 3 4 5 6 7 8 9 10
klm - 1 - H
keV

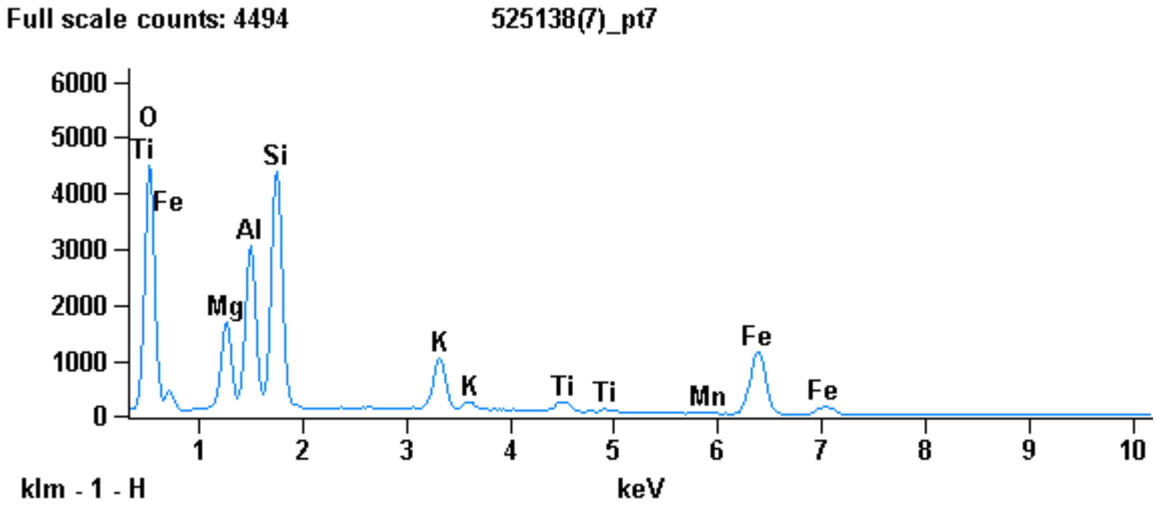
Full scale counts: 4494
525138(7)_pt7
O
Ti
Fe
Si
Al
Mg
K
K
Ti
Ti
Mn
Fe
Fe
klm - 1 - H
keV

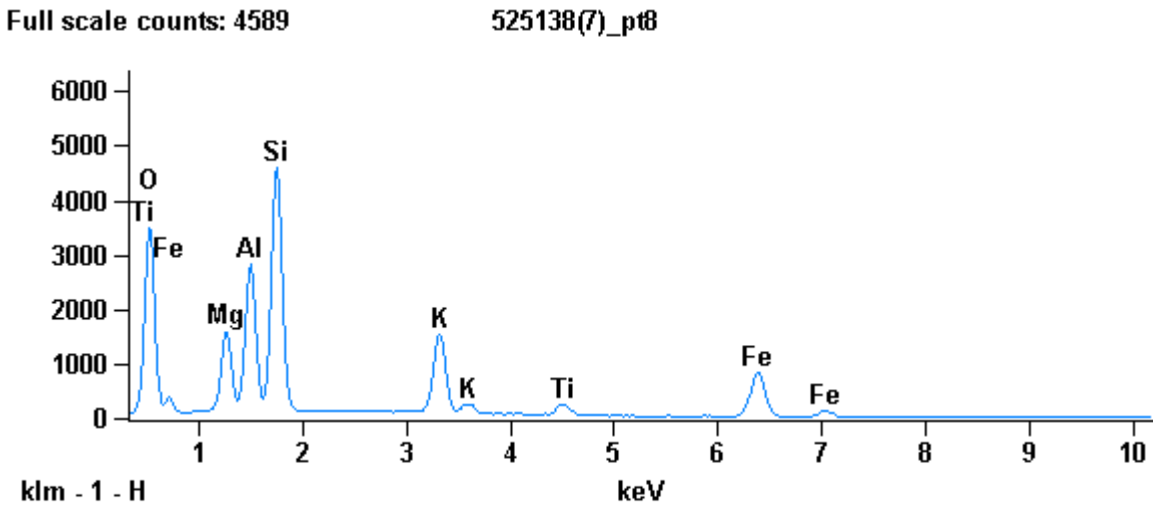
Full scale counts: 4589
525138(7)_pt8
Si
O
Ti
Fe
Al
Mg
K
K
Ti
Fe
Fe
klm - 1 - H
keV

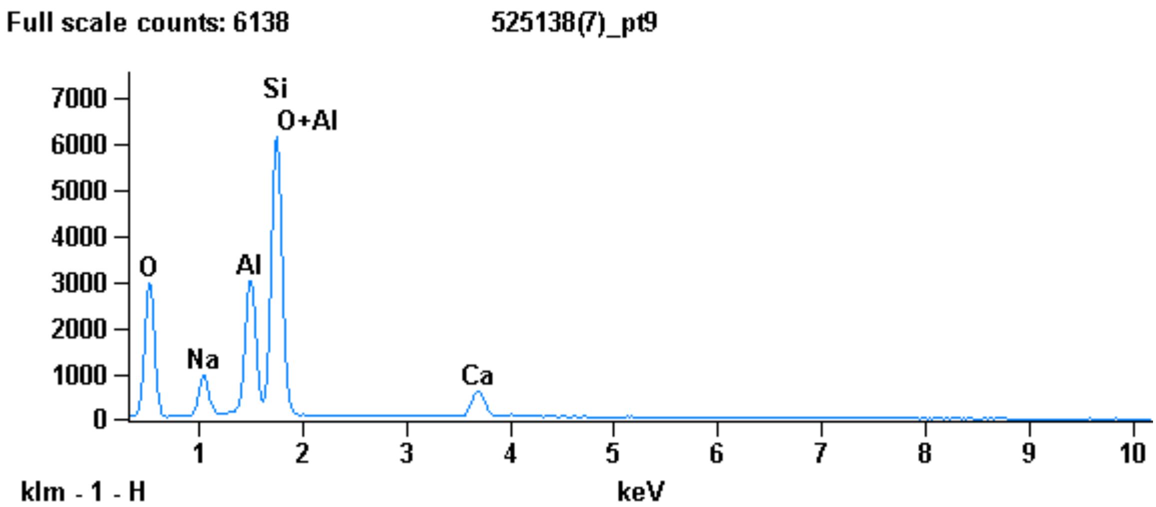
Full scale counts: 6138
525138(7)_pt9
Si
O+Al
O
Al
Na
Ca
klm - 1 - H
keV

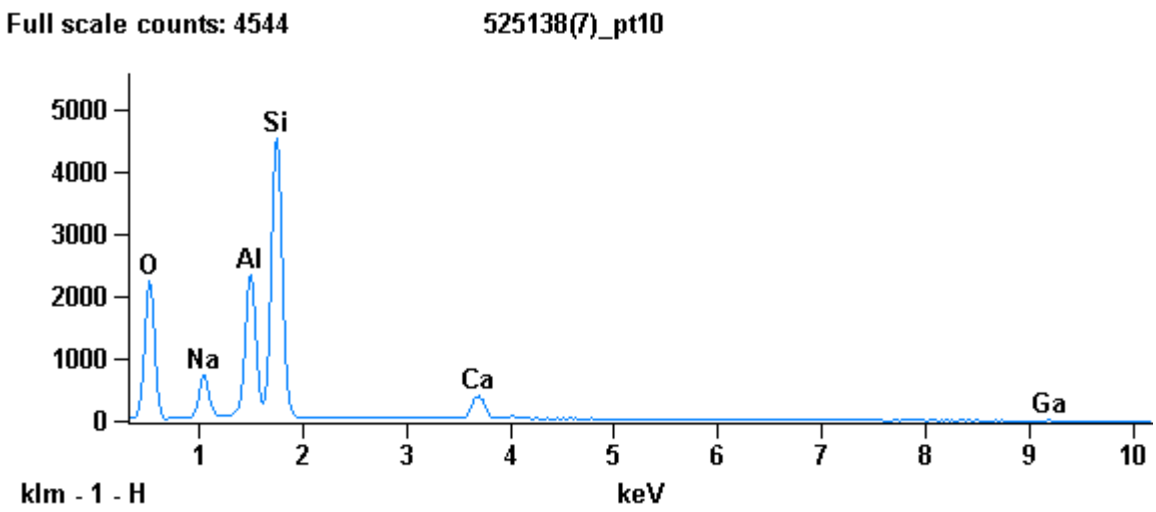
Full scale counts: 4544
525138(7)_pt10
5000
4000
3000
2000
1000
0
O
Na
Al
Si
Ca
Ga
1
2
3
4
5
6
7
8
9
10
klm - 1 - H
keV

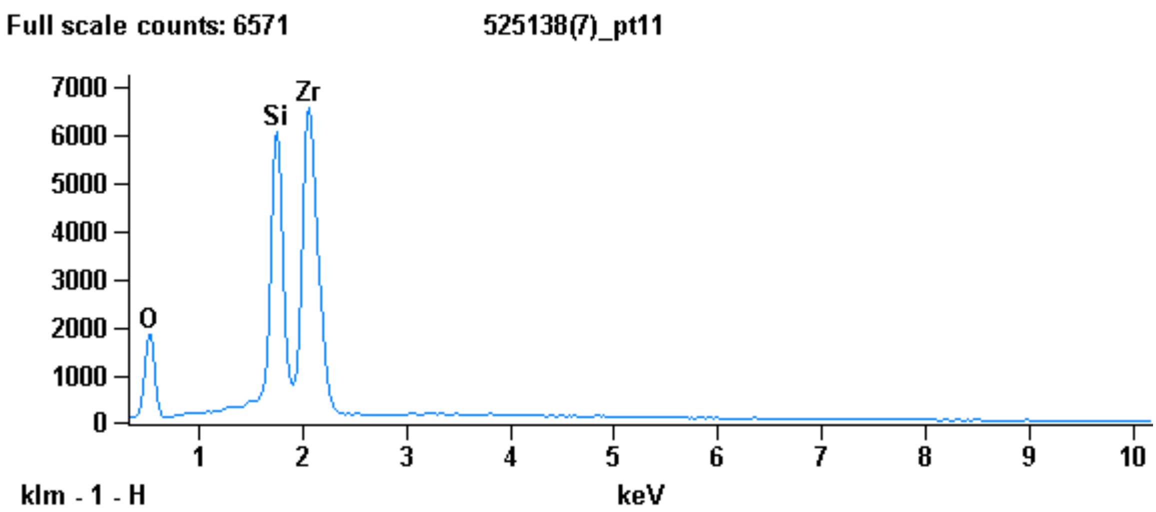
Full scale counts: 6571
525138(7)_pt11
7000
6000
5000
4000
3000
2000
1000
0
O
Si
Zr
1
2
3
4
5
6
7
8
9
10
klm - 1 - H
keV

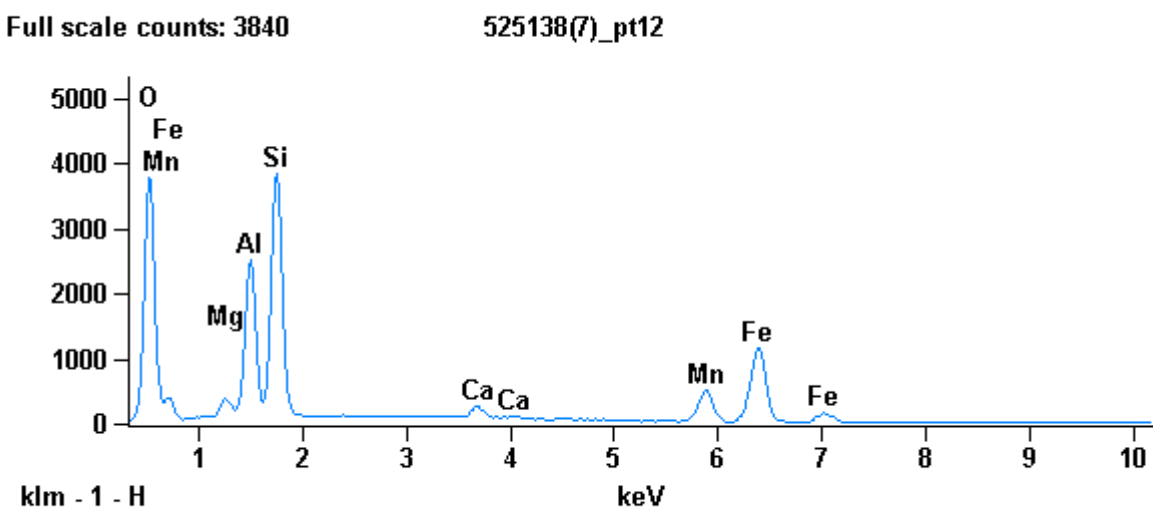
Full scale counts: 3840
525138(7)_pt12
5000
4000
3000
2000
1000
0
O
Fe
Mn
Mg
Al
Si
Ca
Ca
Mn
Fe
Fe
1
2
3
4
5
6
7
8
9
10
klm - 1 - H
keV

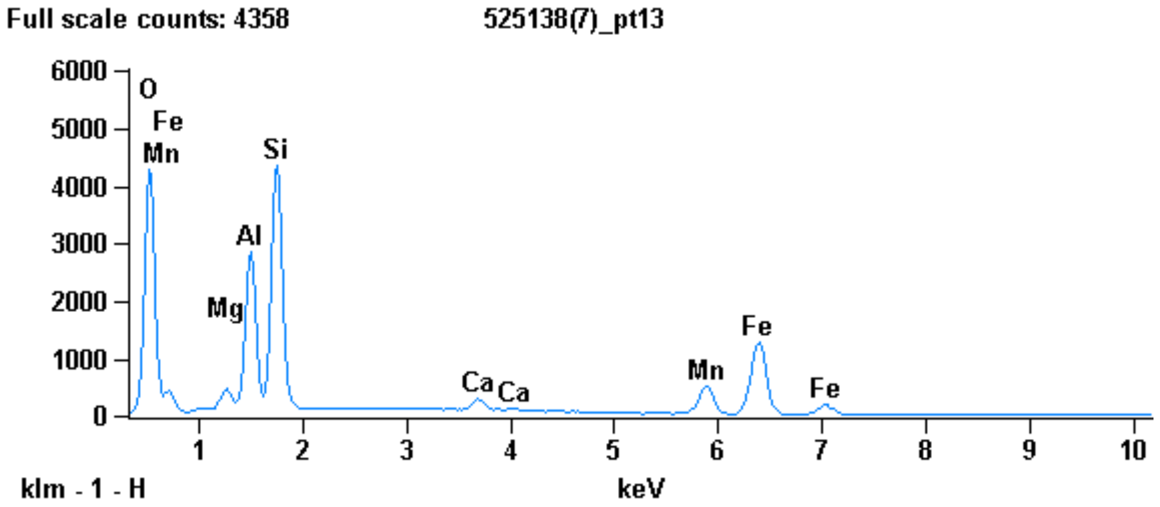
Full scale counts: 4358
525138(7)_pt13
6000
5000
4000
3000
2000
1000
0
O
Fe
Mn
Si
Al
Mg
Ca Ca
Mn
Fe
Fe
1 2 3 4 5 6 7 8 9 10
klm - 1 - H
keV

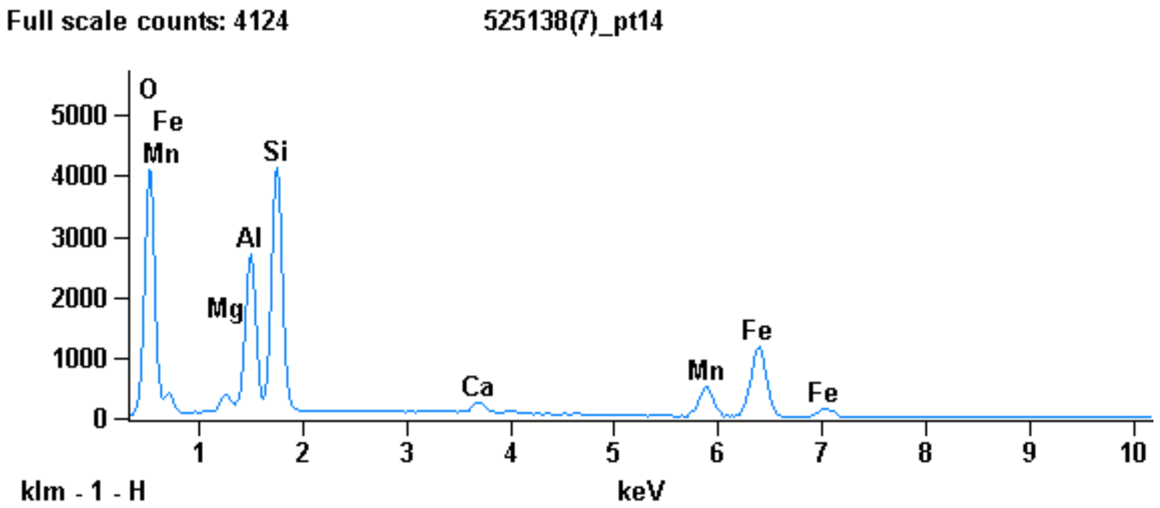
Full scale counts: 4124
525138(7)_pt14
5000
4000
3000
2000
1000
0
O
Fe
Mn
Si
Al
Mg
Ca
Mn
Fe
Fe
1 2 3 4 5 6 7 8 9 10
klm - 1 - H
keV

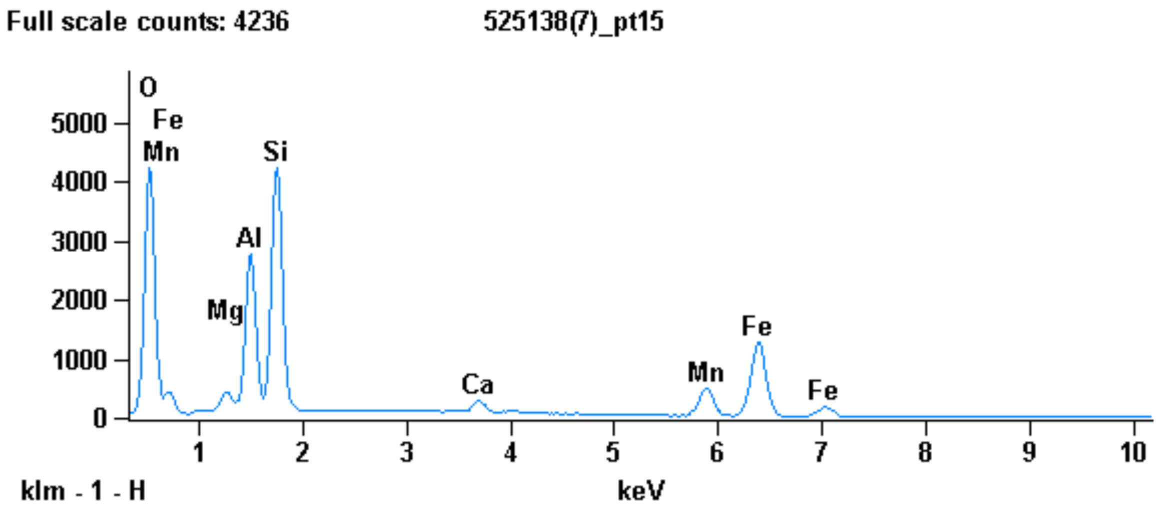
Full scale counts: 4236
525138(7)_pt15
5000
4000
3000
2000
1000
0
O
Fe
Mn
Si
Al
Mg
Ca
Mn
Fe
Fe
1 2 3 4 5 6 7 8 9 10
klm - 1 - H
keV

Weight %

	O-K	Na-K	Mg-K	Al-K	Si-K	K-K	Ca-K	Ti-K	Mn-K	Fe-K	Ga-K	Zr-L
525138(7)_pt1	41.56S		1.74	10.70	16.99		0.99		6.44	21.57		
525138(7)_pt2	41.73S		2.02	10.69	17.12		1.19		5.82	21.43		
525138(7)_pt3	41.78S		2.06	10.73	17.13		1.20		5.53	21.57		
525138(7)_pt4	53.26S				46.74							
525138(7)_pt5	50.17S		0.86	18.84	28.07		0.69			1.38		
525138(7)_pt6	46.26S			9.60	30.70	13.44						
525138(7)_pt7	41.97S		6.62	10.39	16.10	4.44		1.48	0.27	18.74		
525138(7)_pt8	42.05S		6.51	10.01	17.55	7.79		1.52		14.57		
525138(7)_pt9	47.89S	6.33		12.56	28.72		4.51					
525138(7)_pt10	48.04S	6.23		12.77	28.87		3.85				0.25	
525138(7)_pt11	34.68S				14.93							50.39
525138(7)_pt12	41.25S		1.30	10.54	16.90		1.11		7.95	20.94		
525138(7)_pt13	41.40S		1.52	10.52	17.01		1.06		7.27	21.21		
525138(7)_pt14	41.34S		1.15	10.74	16.97		1.09		7.71	21.00		
525138(7)_pt15	41.37S		1.44	10.47	16.98		1.04		7.11	21.58		

Atom %

	O-K	Na-K	Mg-K	Al-K	Si-K	K-K	Ca-K	Ti-K	Mn-K	Fe-K	Ga-K	Zr-L
525138(7)_pt1	61.86		1.71	9.45	14.41		0.59		2.79	9.20		
525138(7)_pt2	61.85		1.97	9.40	14.46		0.71		2.51	9.10		
525138(7)_pt3	61.87		2.01	9.43	14.45		0.71		2.39	9.15		
525138(7)_pt4	66.67				33.33							
525138(7)_pt5	63.86		0.72	14.22	20.35		0.35			0.50		
525138(7)_pt6	61.73			7.60	23.33	7.34						
525138(7)_pt7	60.46		6.28	8.88	13.21	2.61		0.71	0.11	7.73		
525138(7)_pt8	59.96		6.11	8.46	14.26	4.54		0.72		5.95		
525138(7)_pt9	61.48	5.66		9.56	21.00		2.31					
525138(7)_pt10	61.60	5.56		9.71	21.09		1.97				0.07	
525138(7)_pt11	66.67				16.35							16.99
525138(7)_pt12	61.80		1.28	9.37	14.42		0.67		3.47	8.99		
525138(7)_pt13	61.84		1.50	9.32	14.48		0.63		3.16	9.07		
525138(7)_pt14	61.86		1.13	9.53	14.46		0.65		3.36	9.00		
525138(7)_pt15	61.87		1.42	9.29	14.47		0.62		3.10	9.25		

Compound %

		Na2O	*MgO*	*Al2O3*	*SiO2*	*K2O*	*CaO*	*TiO2*	*MnO*	*Fe2O3*	*Ga2O3*	*ZrO2*
525138(7)_pt1	0.00		2.89	20.22	36.35		1.39		8.31	30.84		
525138(7)_pt2	0.00		3.34	20.20	36.63		1.67		7.51	30.64		
525138(7)_pt3	0.00		3.41	20.28	36.65		1.67		7.14	30.85		
525138(7)_pt4	0.00				100.00							
525138(7)_pt5	0.00		1.42	35.61	60.04		0.96			1.97		
525138(7)_pt6	0.00			18.15	65.67	16.18						
525138(7)_pt7	0.00		10.97	19.64	34.44	5.34		2.46	0.35	26.79		
525138(7)_pt8	0.00		10.79	18.91	37.55	9.38		2.53		20.83		
525138(7)_pt9	0.00	8.54		23.73	61.43		6.30					
525138(7)_pt10	0.00	8.39		24.13	61.76		5.39				0.33	
525138(7)_pt11	0.00				31.94							68.06
525138(7)_pt12	0.00		2.16	19.92	36.16		1.56		10.27	29.94		
525138(7)_pt13	0.00		2.52	19.89	36.40		1.49		9.39	30.32		
525138(7)_pt14	0.00		1.90	20.29	36.30		1.53		9.96	30.02		
525138(7)_pt15	0.00		2.39	19.79	36.33		1.45		9.18	30.85		

Minerals, 525138(7)

pt1: Garnet - pyralspite-group
pt2: Garnet - pyralspite-group
pt3: Garnet - pyralspite-group
pt4: Quartz
pt5: Mixed signal/edge effect
pt6: Alkali feldspar - microcline
pt7: Biotite
pt8: Biotite
pt9: Feldspar - plagioclase
pt10: Feldspar - plagioclase
pt11: Zircon
pt12: Garnet - pyralspite-group
pt13: Garnet - pyralspite-group
pt14: Garnet - pyralspite-group
pt15: Garnet - pyralspite-group

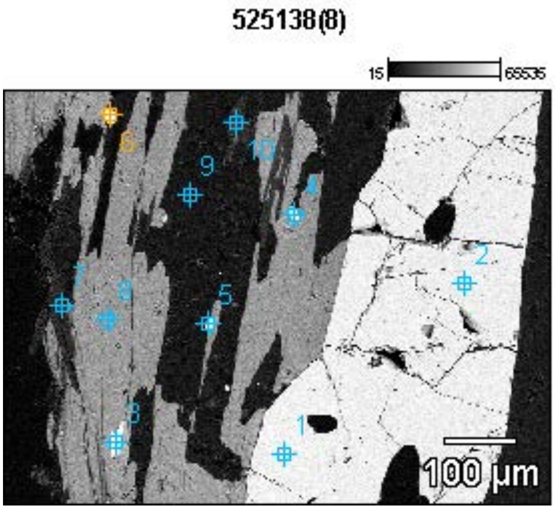

Image name: 525138(8)
Magnification: 160

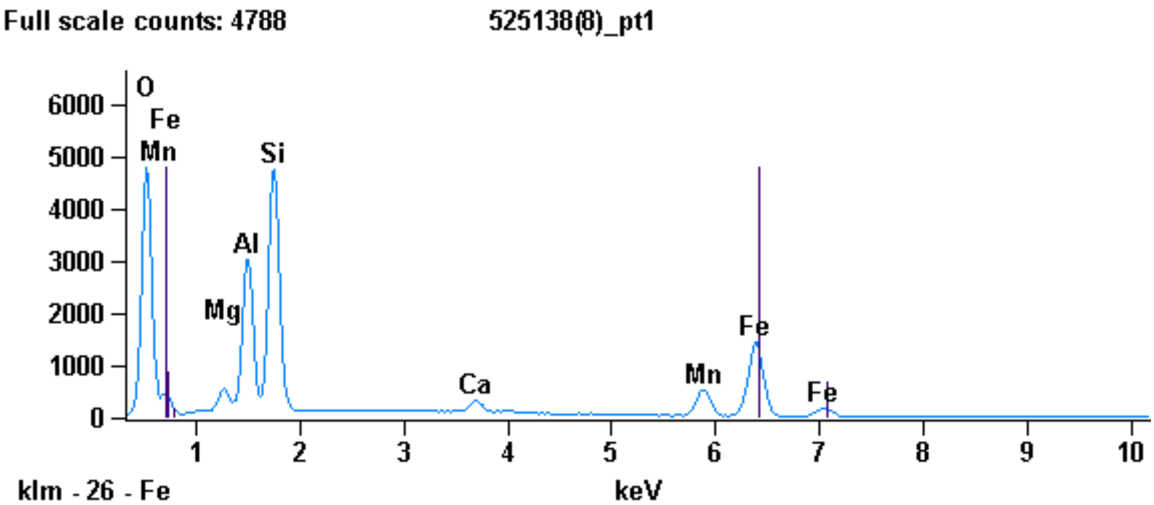

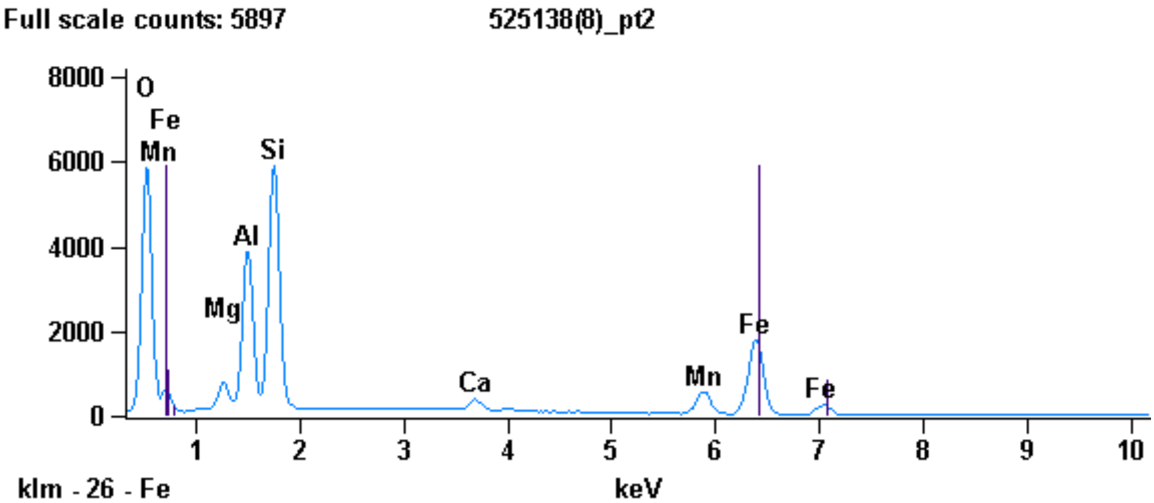

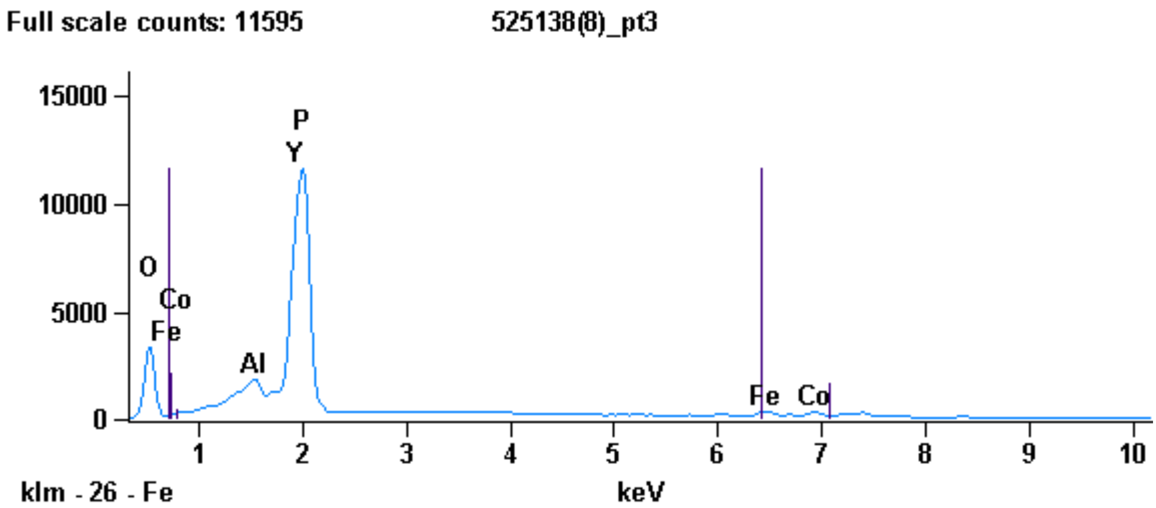
Full scale counts: 11595
525138(8)_pt3
15000
10000
5000
0
P
Y
O
Co
Fe
Al
Fe Co
1 2 3 4 5 6 7 8 9 10
klm - 26 - Fe
keV

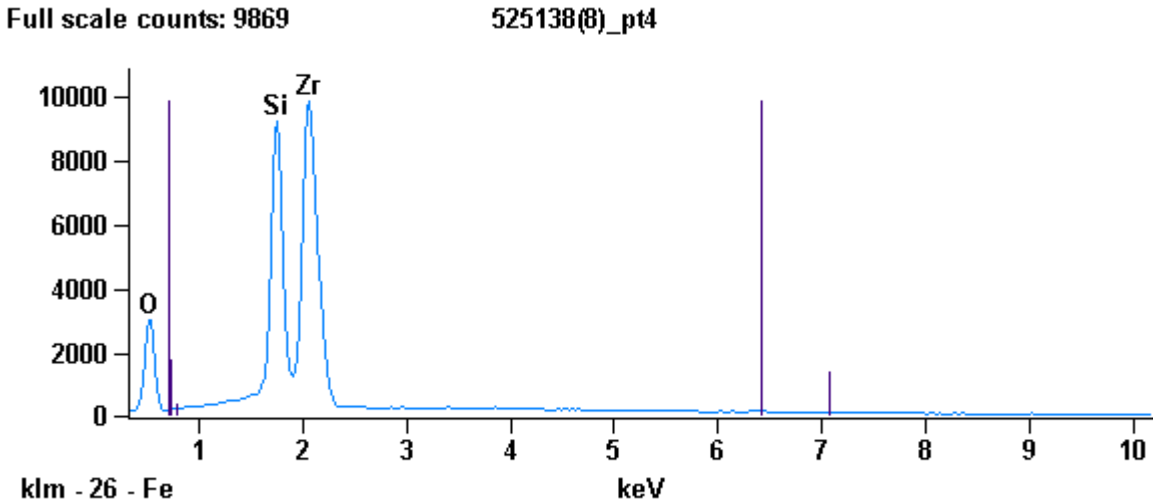
Full scale counts: 9869
525138(8)_pt4
10000
8000
6000
4000
2000
0
Si
Zr
O
1 2 3 4 5 6 7 8 9 10
klm - 26 - Fe
keV

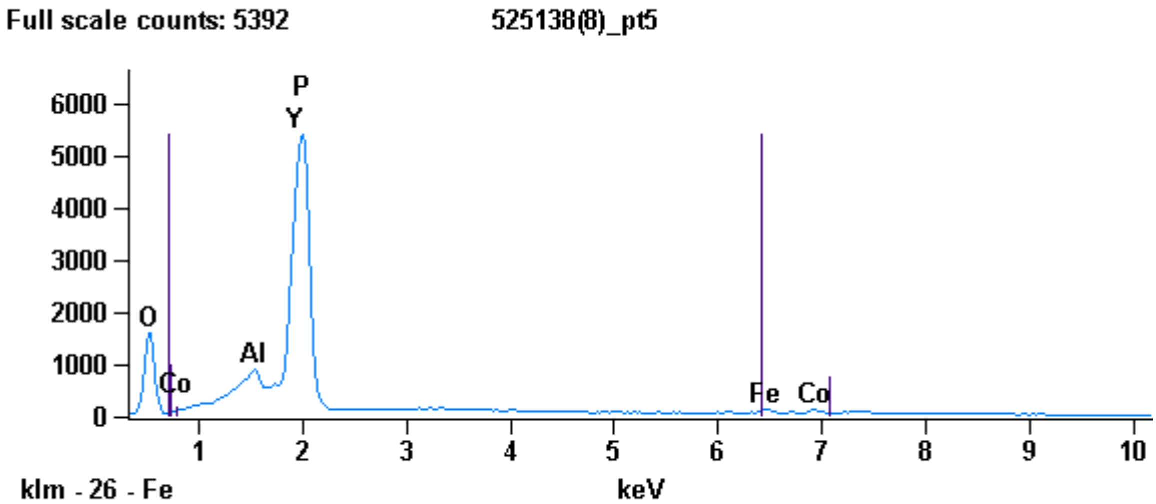
Full scale counts: 5392
525138(8)_pt5
6000
5000
4000
3000
2000
1000
0
P
Y
O
Al
Co
Fe Co
1 2 3 4 5 6 7 8 9 10
klm - 26 - Fe
keV

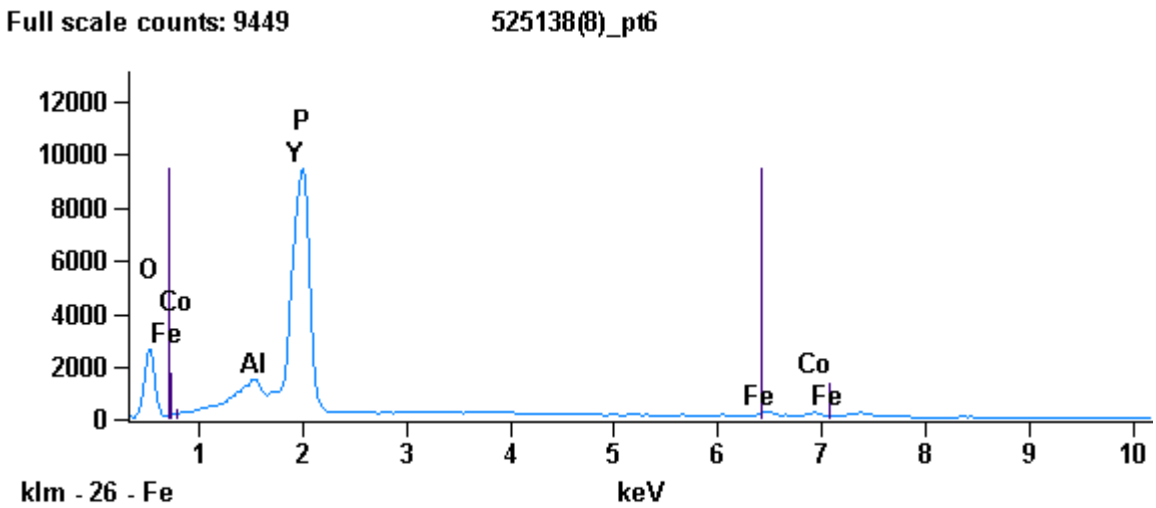
Full scale counts: 9449
525138(8)_pt6
12000
10000
8000
6000
4000
2000
0
P
Y
O
Co
Fe
Al
Fe
Co
Fe
1
2
3
4
5
6
7
8
9
10
klm - 26 - Fe
keV

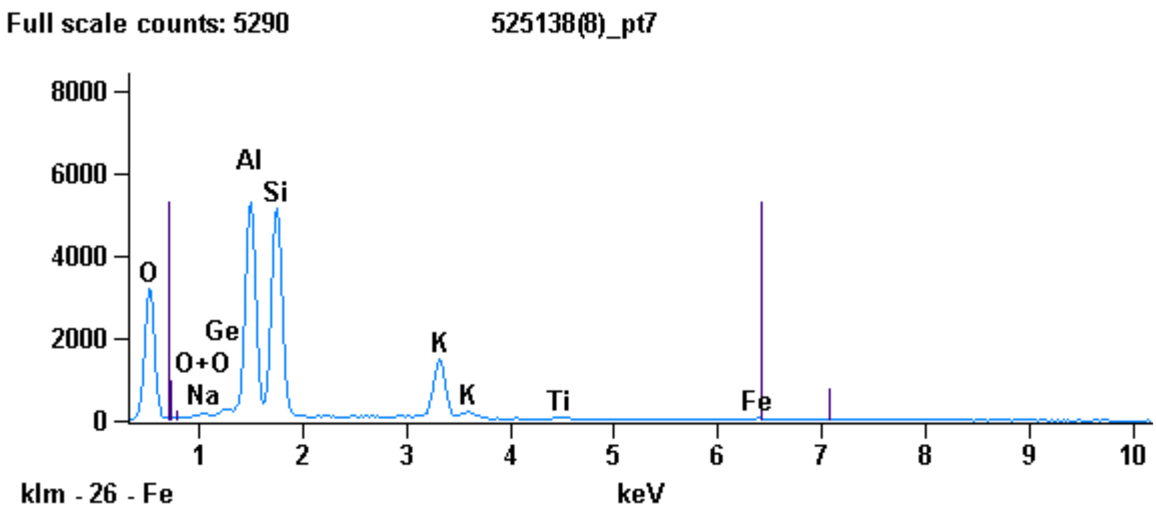
Full scale counts: 5290
525138(8)_pt7
8000
6000
4000
2000
0
Al
Si
O
Ge
O+O
Na
K
K
Ti
Fe
1
2
3
4
5
6
7
8
9
10
klm - 26 - Fe
keV

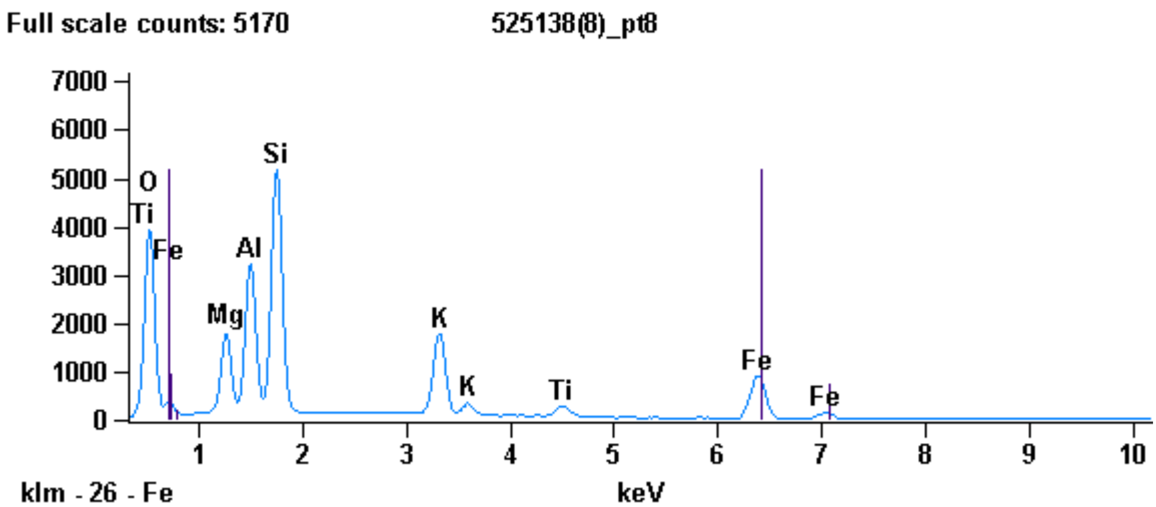
Full scale counts: 5170
525138(8)_pt8
7000
6000
5000
4000
3000
2000
1000
0
Si
O
Ti
Fe
Al
Mg
K
K
Ti
Fe
Fe
1
2
3
4
5
6
7
8
9
10
klm - 26 - Fe
keV

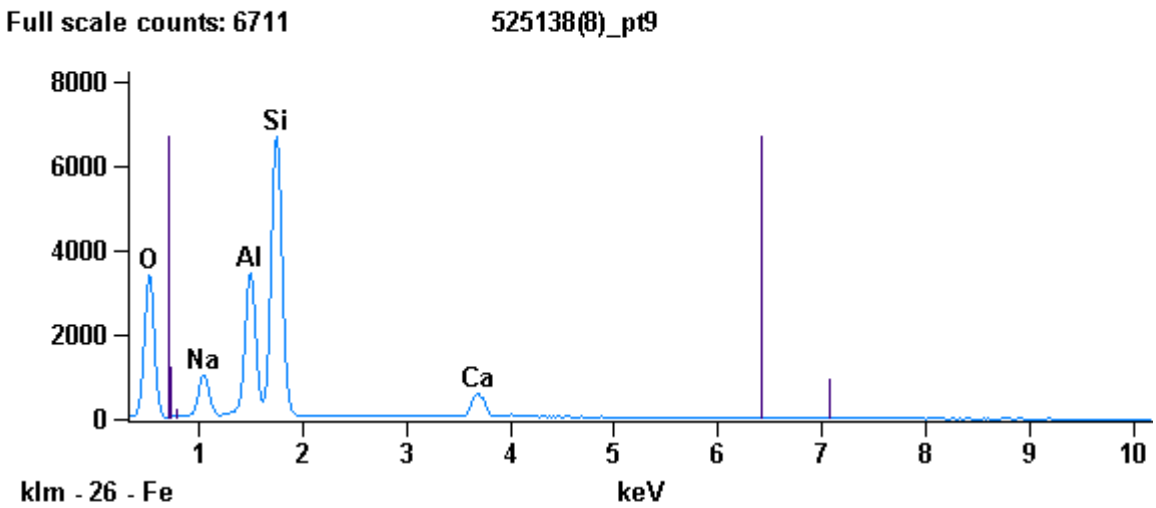

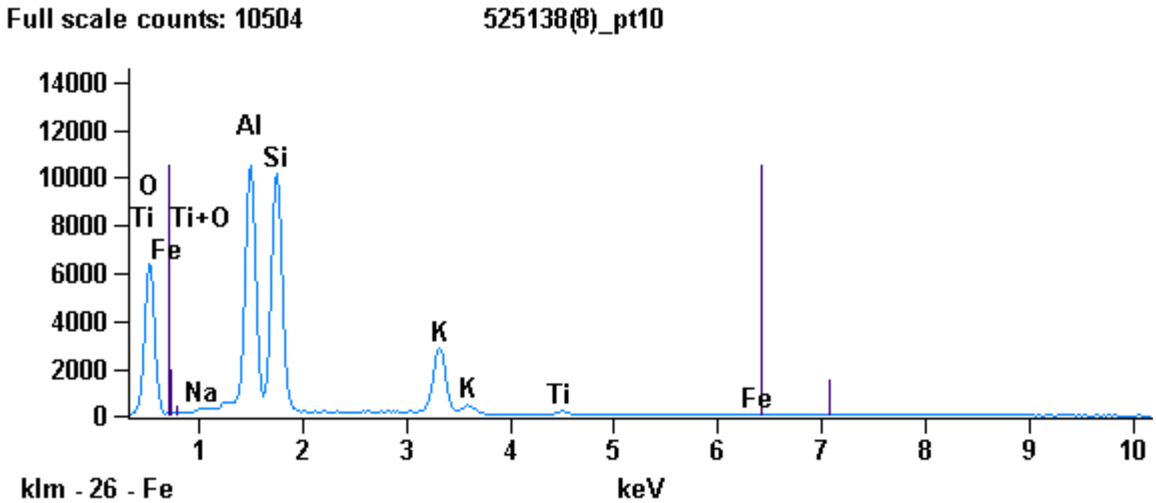

Weight %

	O-K	Na-K	Mg-K	Al-K	Si-K	P-K	K-K	Ca-K	Ti-K	Mn-K	Fe-K	Co-K	Ge-K	Y-L	Zr-L
525138(8)_pt1	41.61S		1.62	10.58	17.20			1.06		6.43	21.51				
525138(8)_pt2	41.70S		2.00	10.79	16.97			1.00		5.60	21.94				
525138(8)_pt3	35.08S			1.86		15.76					1.84	2.71		42.74	
525138(8)_pt4	34.68S				14.93										50.39
525138(8)_pt5	35.65S			2.03		16.50					1.01	2.45		42.37	
525138(8)_pt6	35.70S			2.00		16.49					1.59	2.29		41.93	
525138(8)_pt7	46.44S	0.56		19.10	23.43		9.12		0.47		0.89		0.00		
525138(8)_pt8	42.08S		6.29	10.11	17.66		7.96		1.53		14.37				
525138(8)_pt9	47.90S	6.56		12.83	28.58			4.13							
525138(8)_pt10	46.44S	0.27		19.21	23.38		9.32		0.49		0.90				

Atom %

	O-K	Na-K	Mg-K	Al-K	Si-K	P-K	K-K	Ca-K	Ti-K	Mn-K	Fe-K	Co-K	Ge-K	Y-L	Zr-L
525138(8)_pt1	61.92		1.59	9.33	14.58			0.63		2.79	9.17				
525138(8)_pt2	61.88		1.96	9.49	14.34			0.59		2.42	9.33				
525138(8)_pt3	65.84			2.07		15.28					0.99	1.38		14.44	
525138(8)_pt4	66.67				16.35										16.99
525138(8)_pt5	66.07			2.23		15.79					0.53	1.23		14.13	
525138(8)_pt6	66.08			2.19		15.77					0.84	1.15		13.97	
525138(8)_pt7	61.39	0.51		14.97	17.64		4.93		0.21		0.34		0.00		
525138(8)_pt8	59.98		5.91	8.55	14.34		4.64		0.73		5.87				
525138(8)_pt9	61.41	5.85		9.75	20.87			2.12							
525138(8)_pt10	61.45	0.25		15.08	17.62		5.05		0.22		0.34				

Compound %

		Na2O	MgO	Al2O3	SiO2	P2O5	K2O	CaO	TiO2	MnO	Fe2O3	CoO	GeO2	Y2O3	ZrO2
525138(8)_pt1	0.00		2.69	19.98	36.80			1.48		8.31	30.75				
525138(8)_pt2	0.00		3.32	20.38	36.30			1.39		7.23	31.37				
525138(8)_pt3	0.00			3.52		36.12					2.63	3.44		54.28	
525138(8)_pt4	0.00				31.94										68.06
525138(8)_pt5	0.00			3.84		37.80					1.44	3.12		53.81	
525138(8)_pt6	0.00			3.77		37.79					2.28	2.92		53.24	
525138(8)_pt7	0.00	0.75		36.09	50.12		10.98		0.78		1.28		0.00		
525138(8)_pt8	0.00		10.44	19.11	37.79		9.58		2.54		20.54				
525138(8)_pt9	0.00	8.84		24.24	61.14			5.78							
525138(8)_pt10	0.00	0.36		36.30	50.01		11.23		0.82		1.28				

Minerals, 525138(8)

pt1: Garnet - pyralspite-group
pt2: Garnet - pyralspite-group
pt3: Xenotime
pt4: Zircon
pt5: Xenotime
pt6: Xenotime
pt7: Muscovite
pt8: Biotite
pt9: Alkali feldspar
pt10: Muscovite

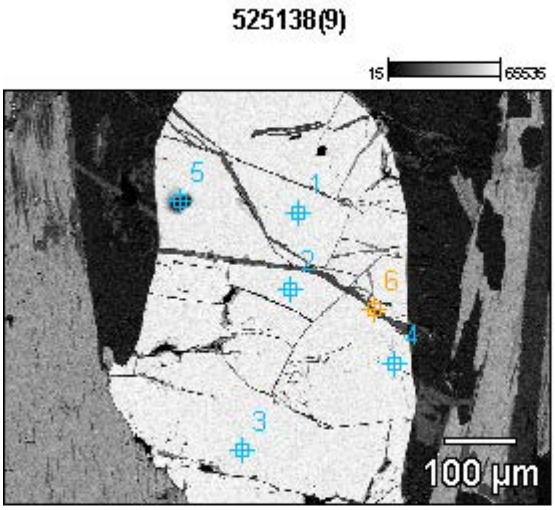

Image name: 525138(9)
Magnification: 160

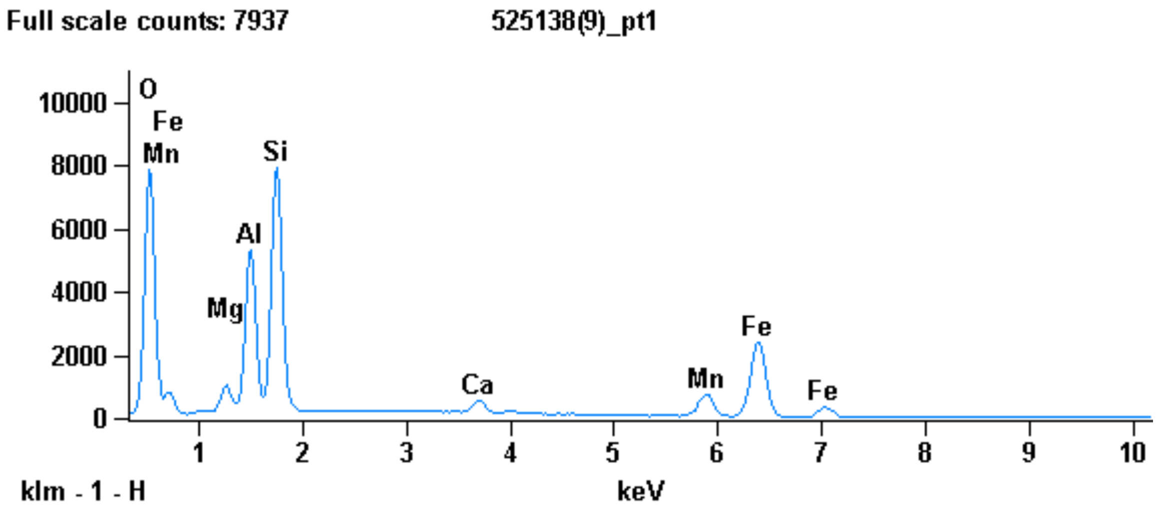

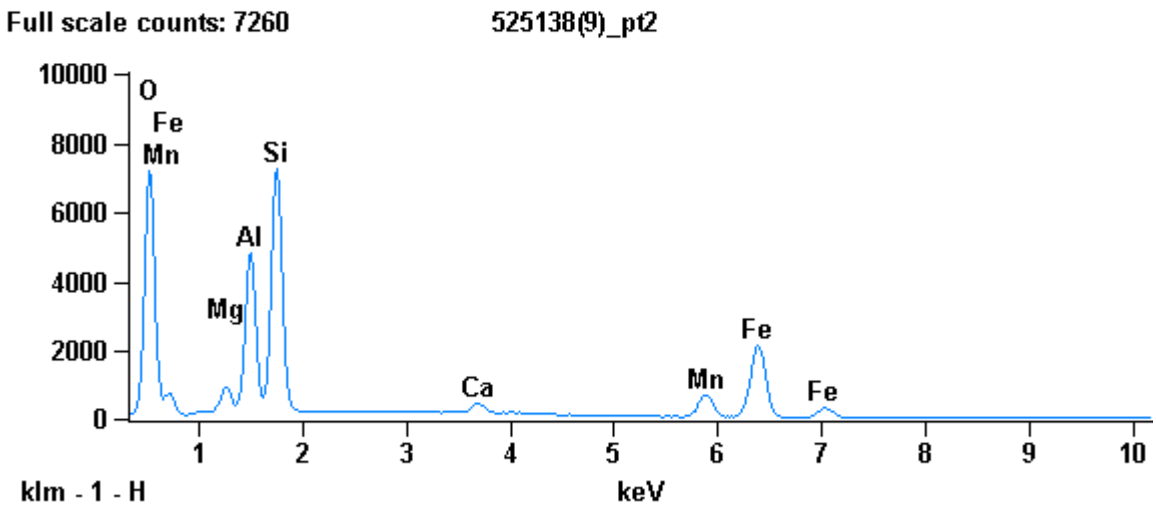

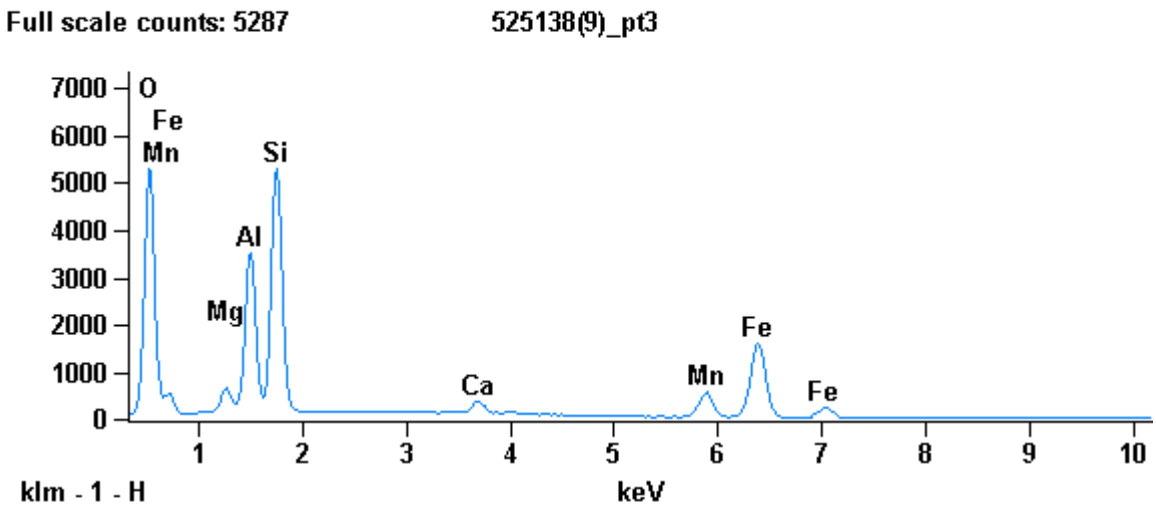
Full scale counts: 5287
525138(9)_pt3
7000
6000
5000
4000
3000
2000
1000
0
O
Fe
Mn
Si
Al
Mg
Ca
Mn
Fe
Fe
1
2
3
4
5
6
7
8
9
10
klm - 1 - H
keV

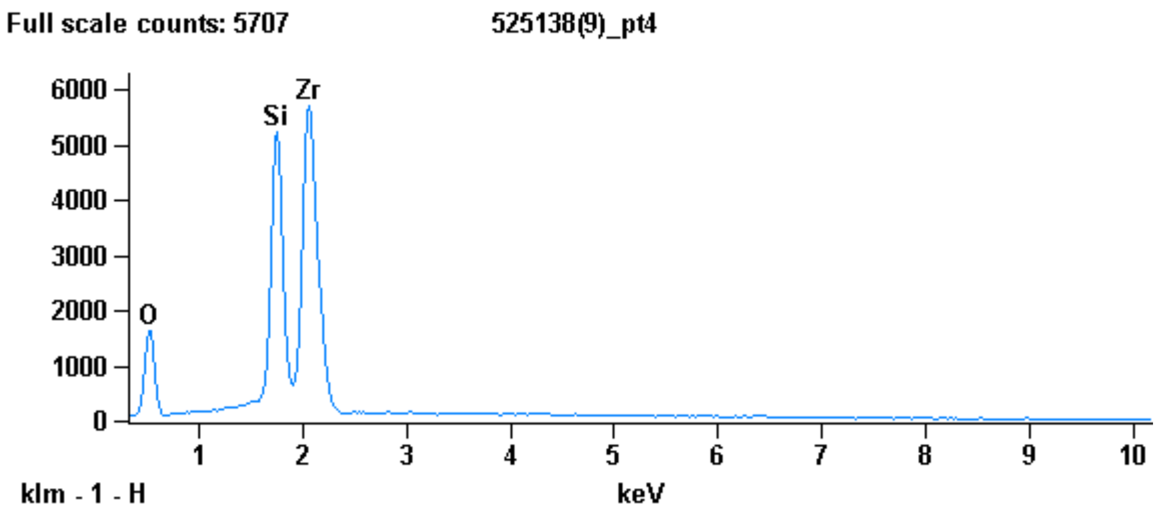
Full scale counts: 5707
525138(9)_pt4
6000
5000
4000
3000
2000
1000
0
Zr
Si
O
1
2
3
4
5
6
7
8
9
10
klm - 1 - H
keV

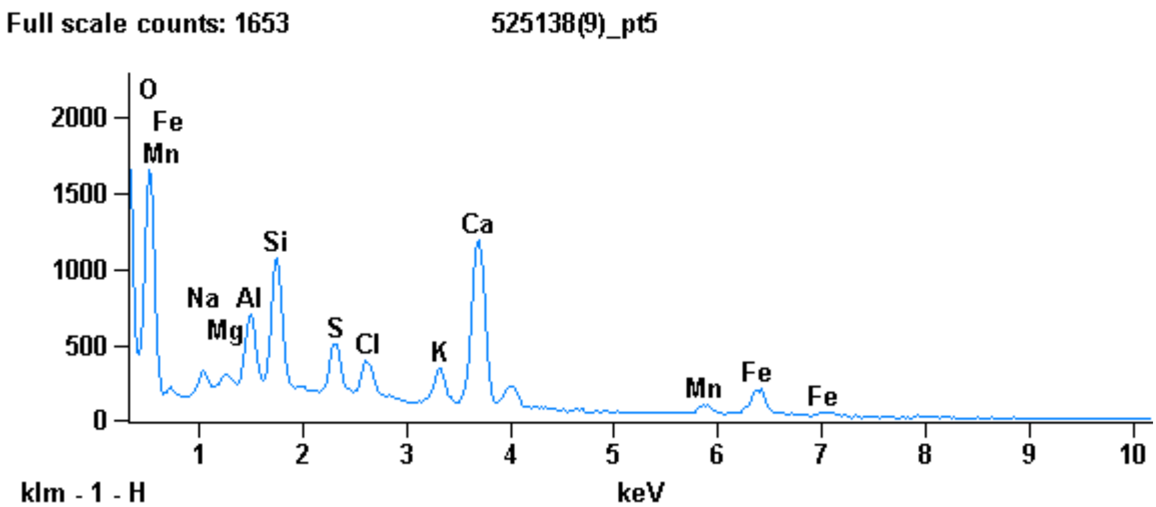
Full scale counts: 1653
525138(9)_pt5
2000
1500
1000
500
0
O
Fe
Mn
Si
Ca
Na
Al
Mg
S
Cl
K
Mn
Fe
Fe
1
2
3
4
5
6
7
8
9
10
klm - 1 - H
keV

Weight %

	O-K	Na-K	Mg-K	Al-K	Si-K	S-K	Cl-K	K-K	Ca-K	Mn-K	Fe-K	Zr-L
525138(9)_pt1	41.65S		1.95	10.89	16.81				1.10	5.62	21.99	
525138(9)_pt2	41.76S		1.96	10.79	17.14				1.05	5.79	21.51	
525138(9)_pt3	41.67S		1.78	10.70	17.03				1.10	5.57	22.15	
525138(9)_pt4	34.65S				14.88							50.47
525138(9)_pt5	37.64S	3.57	1.25	5.44	9.62	4.49	3.53	3.22	19.91	3.03	8.31	
525138(9)_pt6	43.24S	2.09	1.23	11.03	20.38			0.86	1.54	4.05	15.59	

Atom %

	O-K	Na-K	Mg-K	Al-K	Si-K	S-K	Cl-K	K-K	Ca-K	Mn-K	Fe-K	Zr-L
525138(9)_pt1	61.85		1.91	9.59	14.22				0.65	2.43	9.35	
525138(9)_pt2	61.89		1.91	9.48	14.47				0.62	2.50	9.13	
525138(9)_pt3	61.92		1.74	9.43	14.41				0.65	2.41	9.43	
525138(9)_pt4	66.67				16.30							17.03
525138(9)_pt5	57.02	3.76	1.25	4.89	8.30	3.39	2.41	2.00	12.04	1.34	3.60	
525138(9)_pt6	61.54	2.07	1.15	9.30	16.53			0.50	0.88	1.68	6.35	

Compound %

		Na2O	MgO	Al2O3	SiO2	SO3	Cl	K2O	CaO	MnO	Fe2O3	ZrO2
525138(9)_pt1	0.00		3.24	20.57	35.97				1.54	7.25	31.43	
525138(9)_pt2	0.00		3.25	20.38	36.68				1.46	7.48	30.75	
525138(9)_pt3	0.00		2.96	20.22	36.42				1.54	7.19	31.67	
525138(9)_pt4	0.00				31.83							68.17
525138(9)_pt5	0.00	4.81	2.08	10.28	20.57	11.21	3.53	3.88	27.86	3.91	11.87	
525138(9)_pt6	0.00	2.82	2.04	20.83	43.61			1.04	2.16	5.22	22.28	

Minerals, 525138(9)

pt1: Garnet - pyralspite-group
pt2: Garnet - pyralspite-group
pt3: Garnet - pyralspite-group
pt4: Zircon
pt5: Pitt - mixed signal/edge effect
pt6: Full scale count below 3000 - invalid/inconclusive result

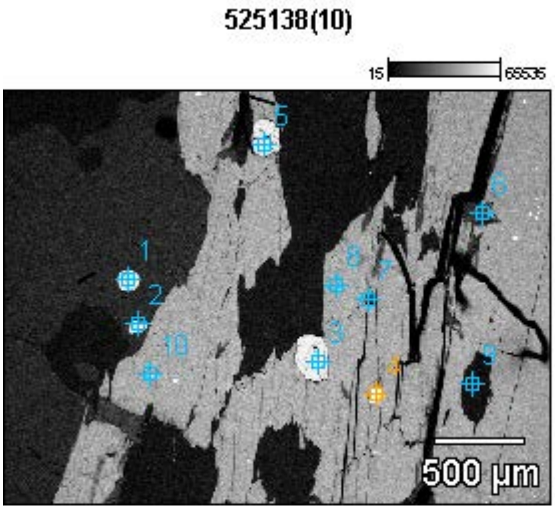

Image name: 525138(10)
Magnification: 40

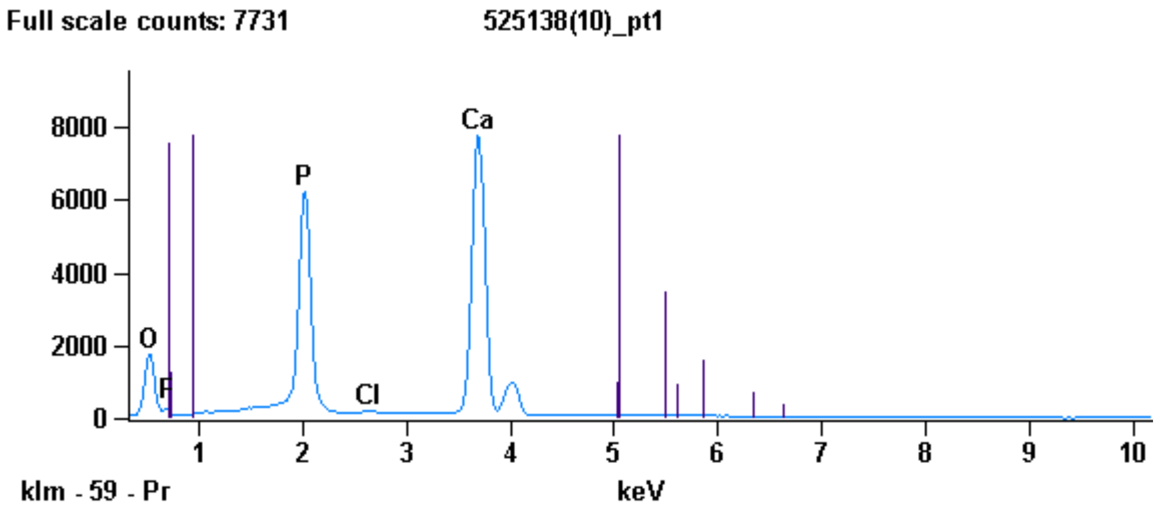

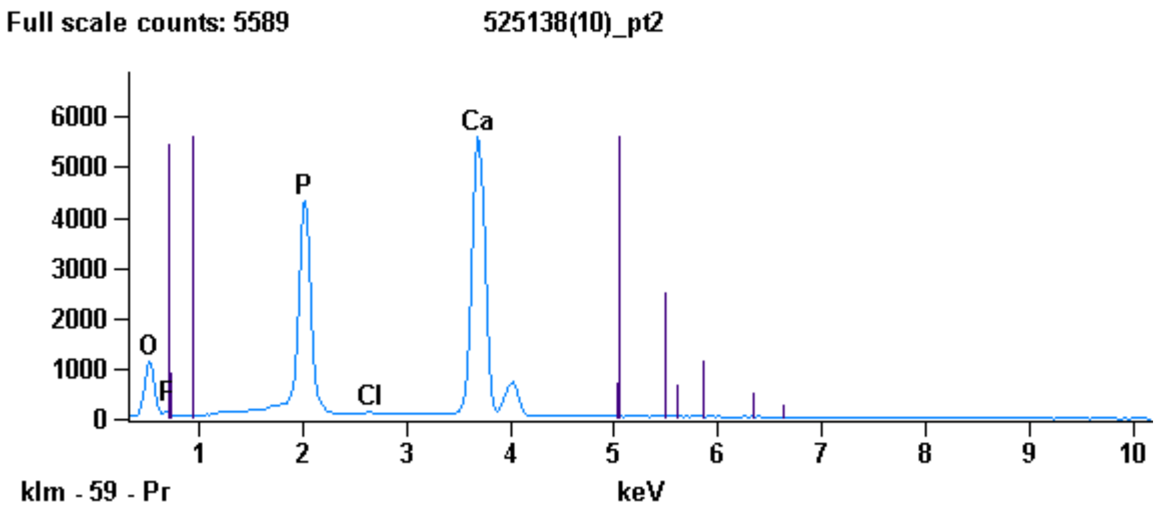

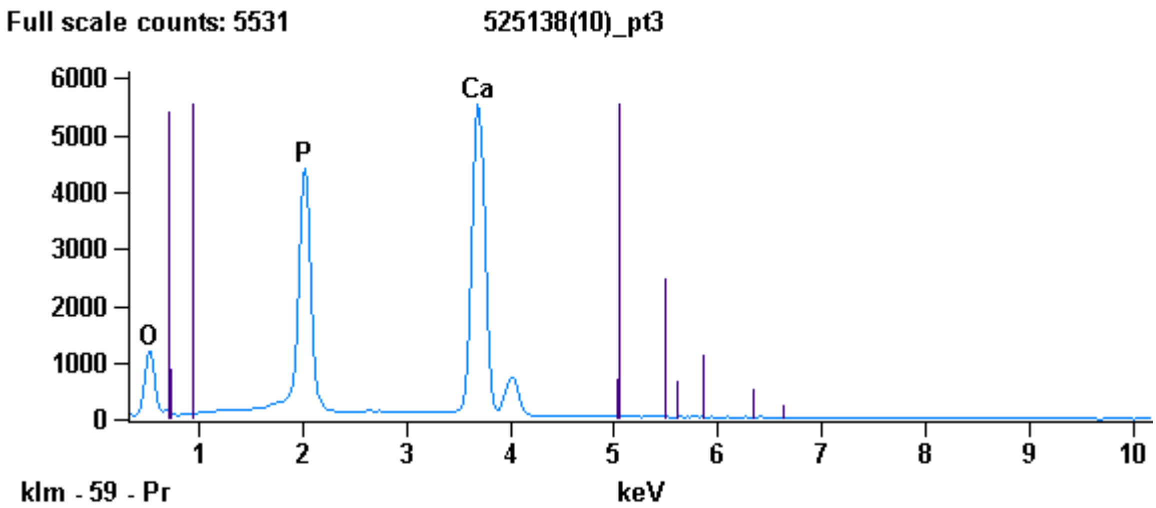
Full scale counts: 5531
525138(10)_pt3
6000
5000
4000
3000
2000
1000
0
O
P
Ca
1
2
3
4
5
6
7
8
9
10
klm - 59 - Pr
keV

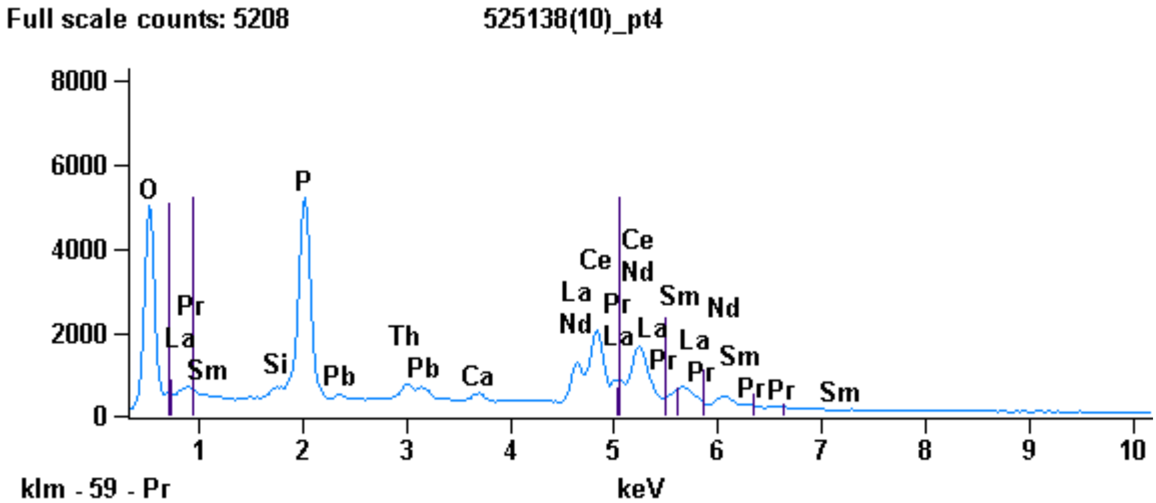
Full scale counts: 5208
525138(10)_pt4
8000
6000
4000
2000
0
O
Pr
La
Sm
Si
P
Pb
Th
Pb
Ca
La
Nd
Ce
Pr
La
Ce
Nd
La
Pr
Sm
Nd
La
Pr
Sm
Pr
Pr
Sm
1
2
3
4
5
6
7
8
9
10
klm - 59 - Pr
keV

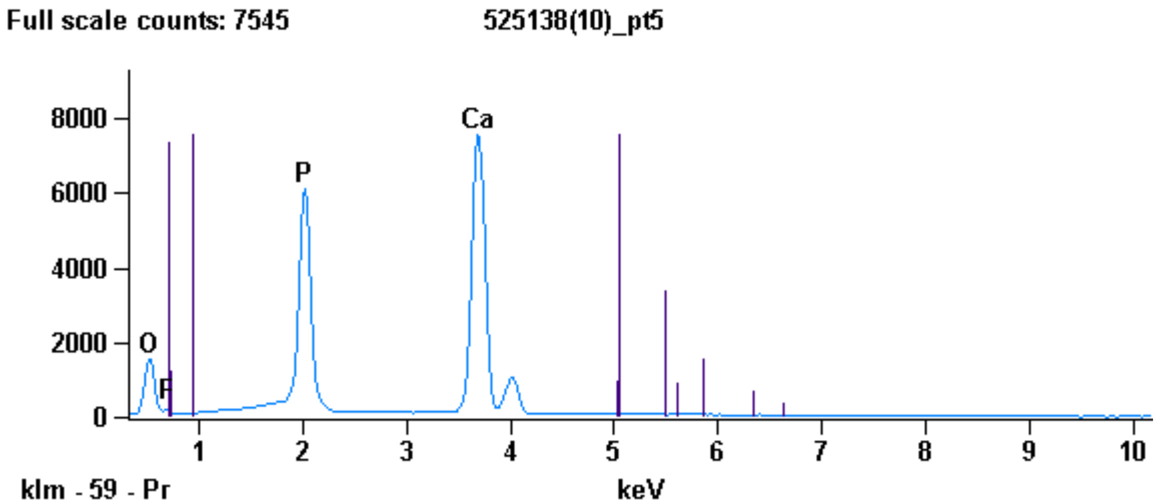
Full scale counts: 7545
525138(10)_pt5
8000
6000
4000
2000
0
O
P
Ca
1
2
3
4
5
6
7
8
9
10
klm - 59 - Pr
keV

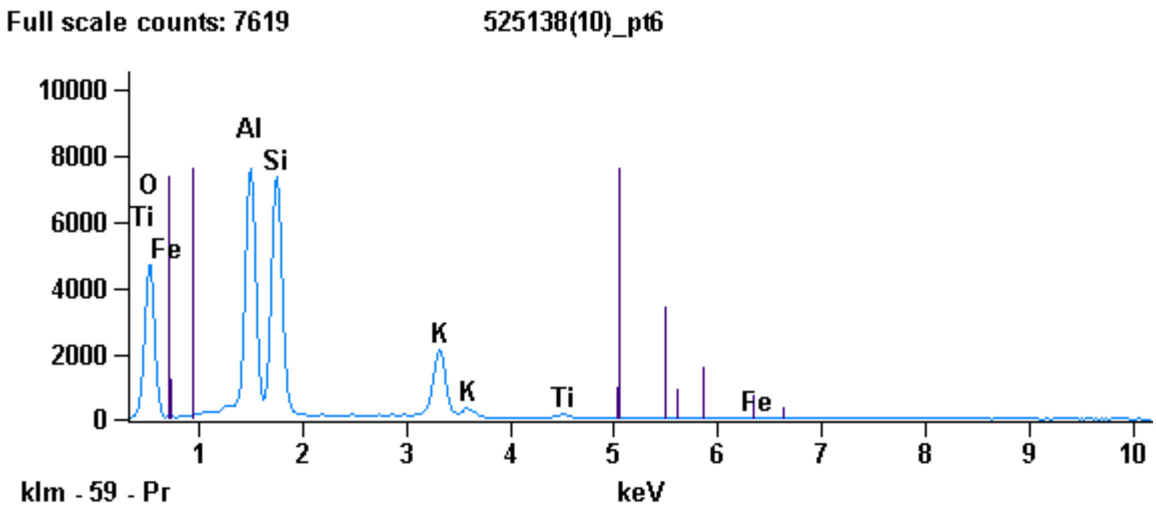
Full scale counts: 7619
525138(10)_pt6
10000
8000
6000
4000
2000
0
Al
Si
O
Ti
Fe
K
K
Ti
Fe
1
2
3
4
5
6
7
8
9
10
klm - 59 - Pr
keV

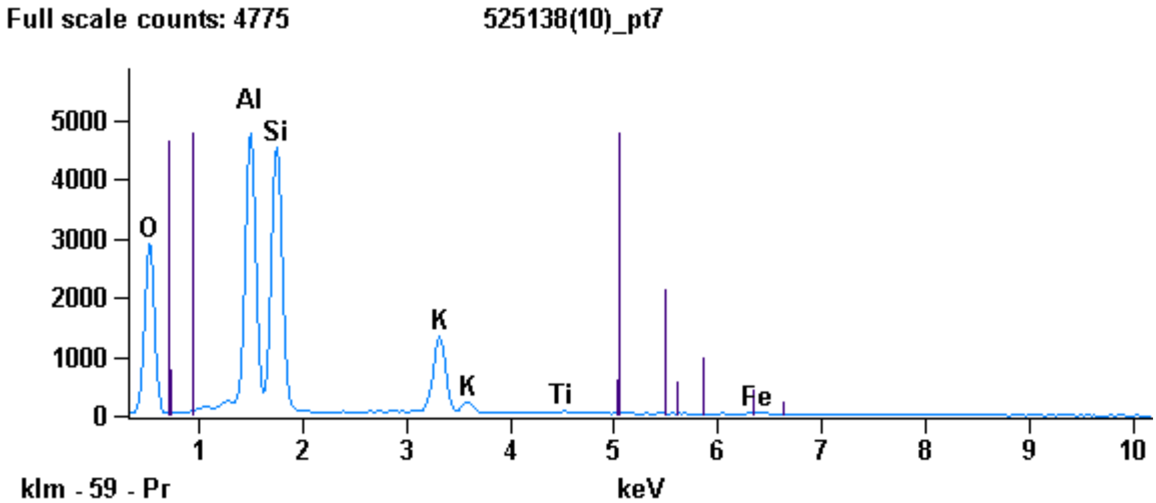
Full scale counts: 4775
525138(10)_pt7
5000
4000
3000
2000
1000
0
Al
Si
O
K
K
Ti
Fe
1
2
3
4
5
6
7
8
9
10
klm - 59 - Pr
keV

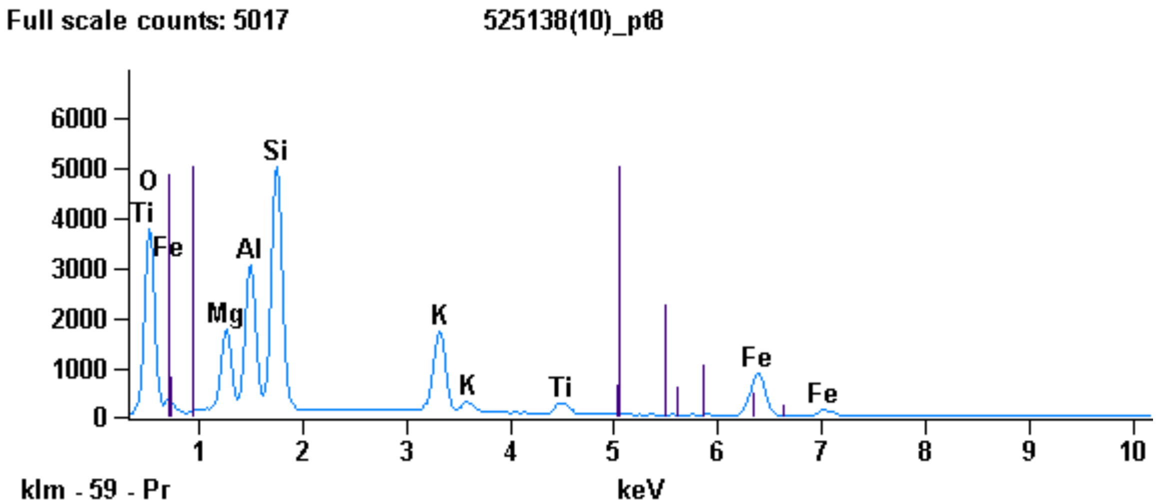
Full scale counts: 5017
525138(10)_pt8
6000
5000
4000
3000
2000
1000
0
Si
O
Ti
Fe
Al
Mg
K
K
Ti
Fe
Fe
1
2
3
4
5
6
7
8
9
10
klm - 59 - Pr
keV

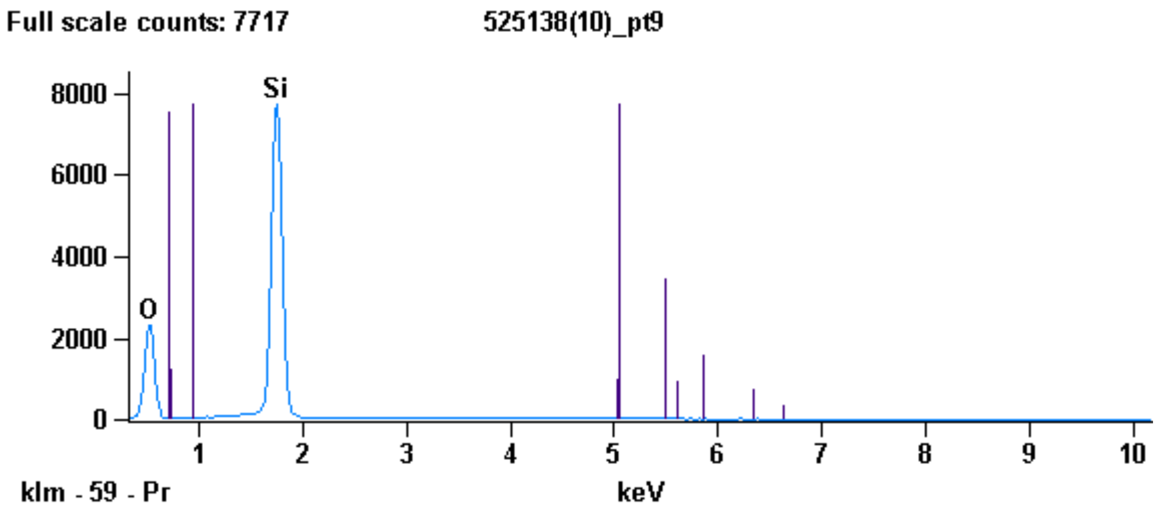

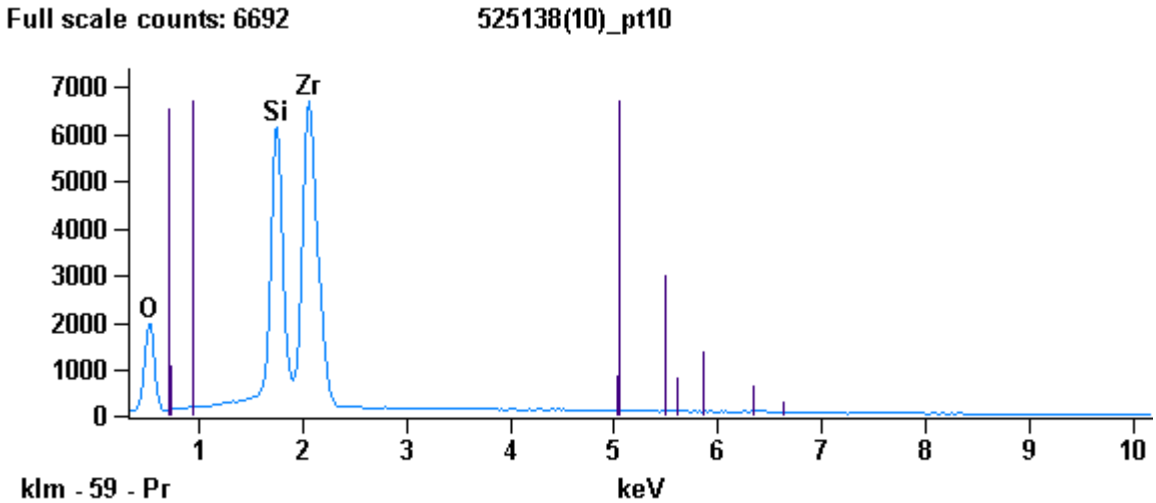

Weight %

	O-K	F-K	Mg-K	Al-K	Si-K	P-K	Cl-K	K-K	Ca-K	Ti-K	Fe-K	Zr-L	La-L	Ce-L	Nd-L	Pb-L	Th-L
525138(10)_pt1	37.94S	5.76				17.45	0.23		38.62								
525138(10)_pt2	38.04S	4.97				17.21	0.17		39.62								
525138(10)_pt3	40.19S					18.29			41.51								
525138(10)_pt4	28.94S				0.20	15.01			0.80				9.36	26.22	7.84	0.00	11.62
525138(10)_pt5	37.85S	5.94				17.27			38.95								
525138(10)_pt6	46.48S			19.25	23.44			9.46		0.54	0.83						
525138(10)_pt7	46.42S			19.21	23.41			9.55		0.42	0.99						
525138(10)_pt8	42.15S		6.54	9.94	17.75			7.86		1.67	14.08						
525138(10)_pt9	53.26S				46.74												
525138(10)_pt10	34.70S				14.95							50.35					

Atom %

	O-K	F-K	Mg-K	Al-K	Si-K	P-K	Cl-K	K-K	Ca-K	Ti-K	Fe-K	Zr-L	La-L	Ce-L	Nd-L	Pb-L	Th-L
525138(10)_pt1	56.36	7.20				13.39	0.16		22.90								
525138(10)_pt2	56.77	6.24				13.27	0.11		23.60								
525138(10)_pt3	60.70					14.27			25.03								
525138(10)_pt4	67.51				0.26	18.09			0.74				2.52	6.98	2.03	0.00	1.87
525138(10)_pt5	56.22	7.43				13.25			23.10								
525138(10)_pt6	61.53			15.11	17.67			5.12		0.24	0.32						
525138(10)_pt7	61.50			15.09	17.67			5.18		0.18	0.38						
525138(10)_pt8	59.98		6.13	8.39	14.39			4.58		0.80	5.74						
525138(10)_pt9	66.67				33.33												
525138(10)_pt10	66.67				16.36							16.97					

Compound %

		F	MgO	Al2O3	SiO2	P2O5	Cl	K2O	CaO	TiO2	Fe2O3	ZrO2	La2O3	Ce2O3	Nd2O3	PbO	ThO2
525138(10)_pt1	0.00	5.76				39.98	0.23		54.03								
525138(10)_pt2	0.00	4.97				39.44	0.17		55.43								
525138(10)_pt3	0.00					41.92			58.08								
525138(10)_pt4	0.00				0.42	34.40			1.12				10.98	30.71	9.15	0.00	13.23
525138(10)_pt5	0.00	5.94				39.57			54.50								
525138(10)_pt6	0.00			36.38	50.14			11.39		0.90	1.19						
525138(10)_pt7	0.00			36.29	50.08			11.51		0.70	1.42						
525138(10)_pt8	0.00		10.85	18.79	37.96			9.47		2.79	20.13						
525138(10)_pt9	0.00				100.00												
525138(10)_pt10	0.00				31.98							68.02					

Minerals, 525138(10)

pt1: Apatite
pt2: Apatite
pt3: Apatite
pt4: Xenotime
pt5: Apatite
pt6: Muscovite
pt7: Muscovite
pt8: Biotite
pt9: Quartz
pt10: Zircon

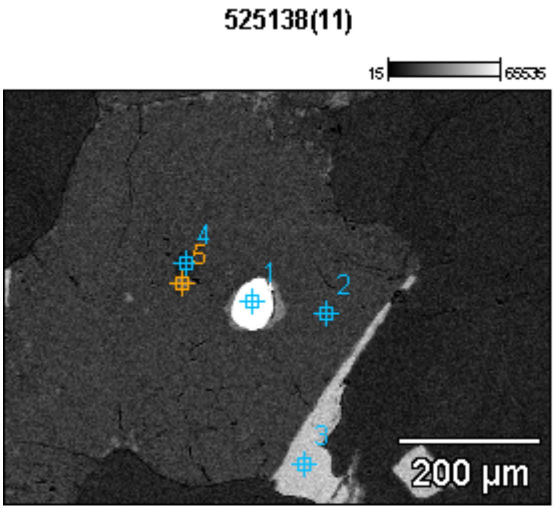

Image name: 525138(11)
Magnification: 159

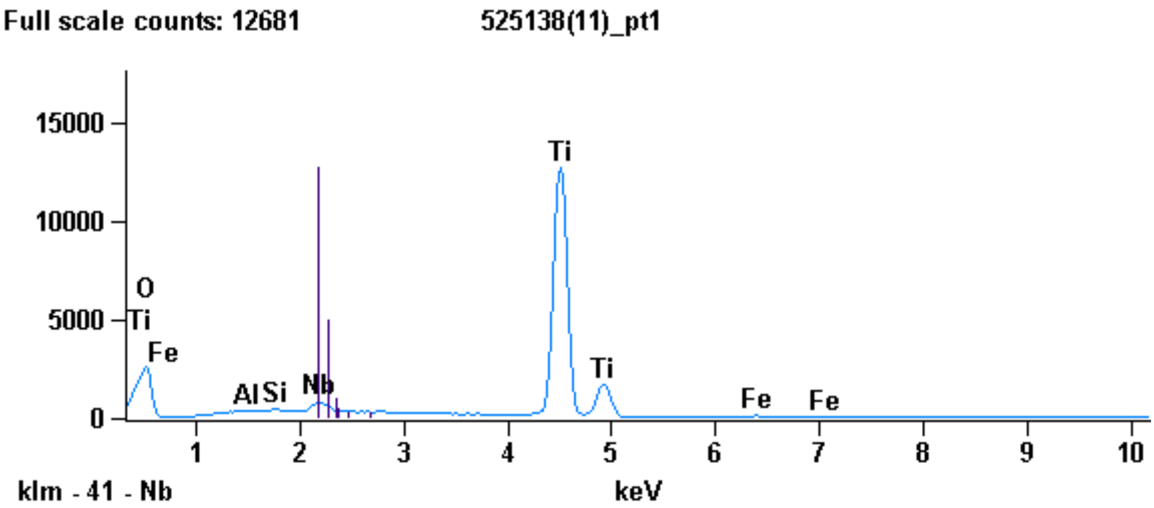

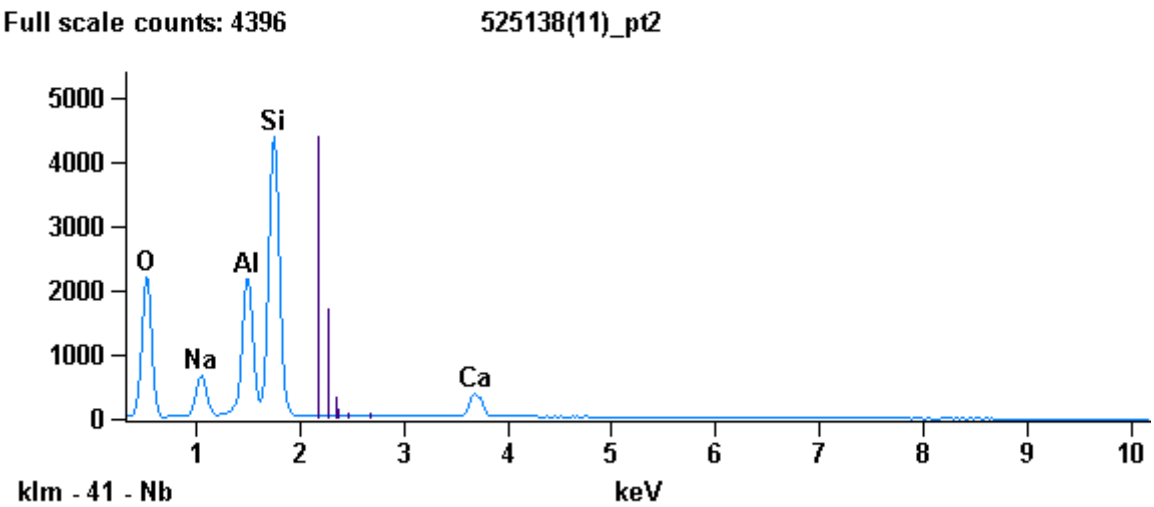

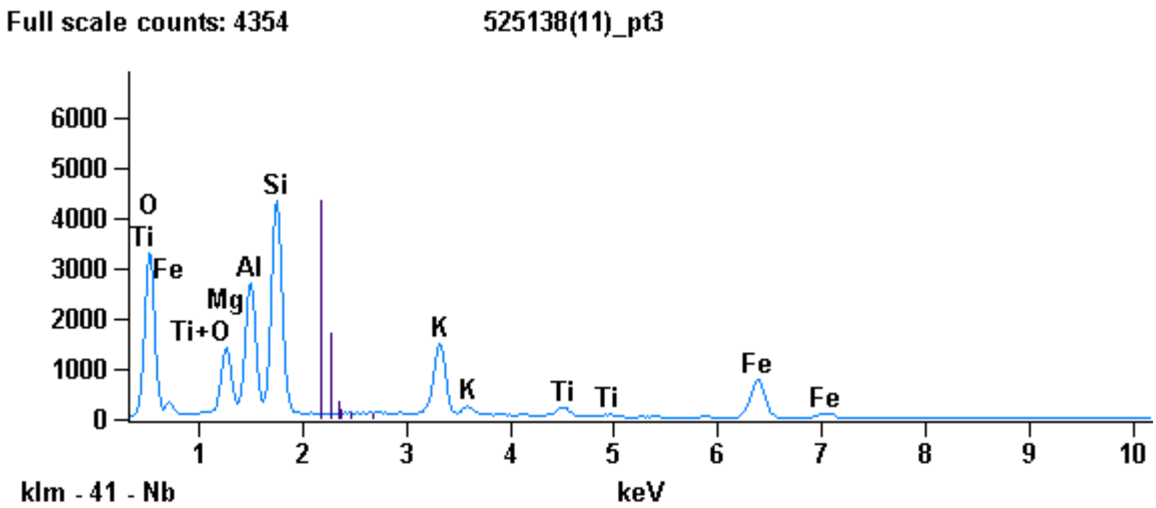
Full scale counts: 4354
525138(11)_pt3
6000
5000
4000
3000
2000
1000
0
O
Ti
Fe
Ti+O
Mg
Al
Si
K
K
Ti
Ti
Fe
Fe
1
2
3
4
5
6
7
8
9
10
klm - 41 - Nb
keV

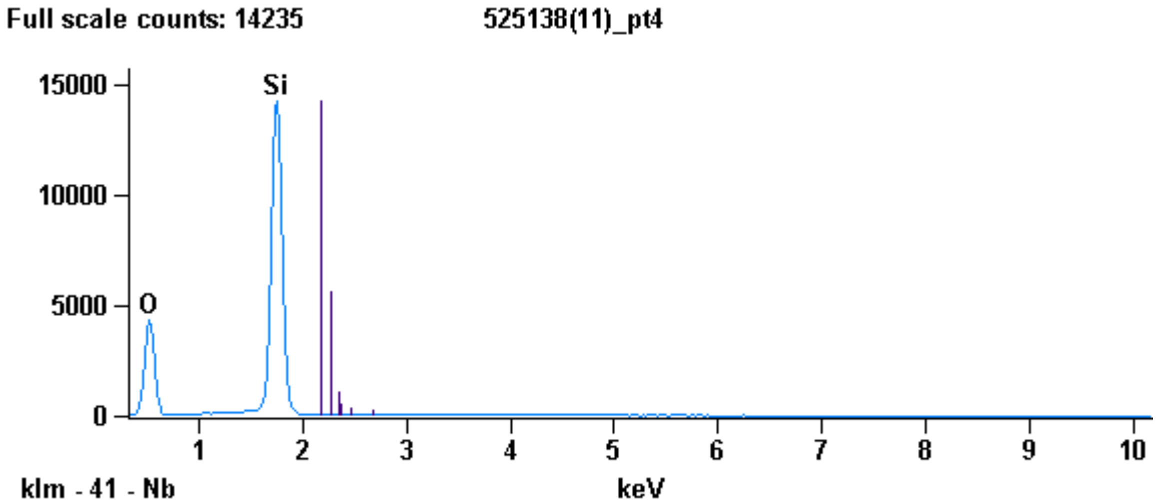
Full scale counts: 14235
525138(11)_pt4
15000
10000
5000
0
O
Si
1
2
3
4
5
6
7
8
9
10
klm - 41 - Nb
keV

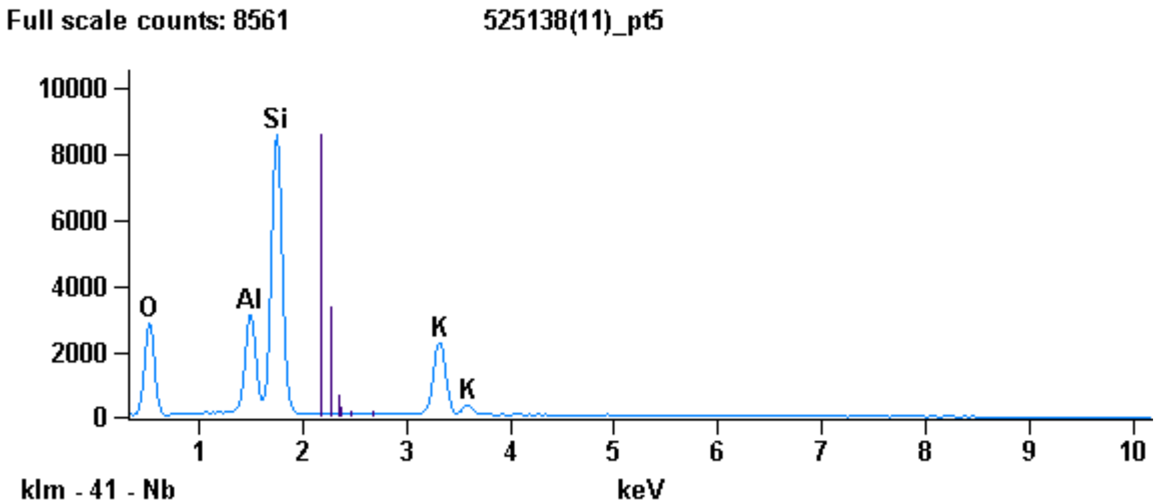
Full scale counts: 8561
525138(11)_pt5
10000
8000
6000
4000
2000
0
O
Al
Si
K
K
1
2
3
4
5
6
7
8
9
10
klm - 41 - Nb
keV

Weight %

	O-K	Na-K	Mg-K	Al-K	Si-K	K-K	Ca-K	Ti-K	Fe-K	Nb-L
525138(11)_pt1	39.71S			0.12	0.29			56.84	0.84	2.19
525138(11)_pt2	47.93S	6.69		12.54	28.83		4.00			
525138(11)_pt3	42.17S		6.20	10.27	17.73	7.94		1.63	14.05	
525138(11)_pt4	53.26S				46.74					
525138(11)_pt5	46.34S			9.70	30.73	13.23				

Atom %

	O-K	Na-K	Mg-K	Al-K	Si-K	K-K	Ca-K	Ti-K	Fe-K	Nb-L
525138(11)_pt1	66.69			0.12	0.28			31.88	0.40	0.63
525138(11)_pt2	61.41	5.97		9.53	21.04		2.04			
525138(11)_pt3	60.02		5.81	8.67	14.38	4.62		0.78	5.73	
525138(11)_pt4	66.67				33.33					
525138(11)_pt5	61.78			7.67	23.34	7.22				

Compound %

		Na2O	MgO	Al2O3	SiO2	K2O	CaO	TiO2	Fe2O3	Nb2O5
525138(11)_pt1	0.00			0.23	0.62			94.81	1.20	3.14
525138(11)_pt2	0.00	9.02		23.70	61.68		5.59			
525138(11)_pt3	0.00		10.28	19.41	37.94	9.56		2.72	20.09	
525138(11)_pt4	0.00				100.00					
525138(11)_pt5	0.00			18.32	65.74	15.94				

Minerals, 525138(11)

pt1: Rutile (inclusion in plagioclase)
pt2: Feldspar - plagioclase
pt3: Biotite
pt4: Quartz
pt5: Alkali feldspar - orthoclase

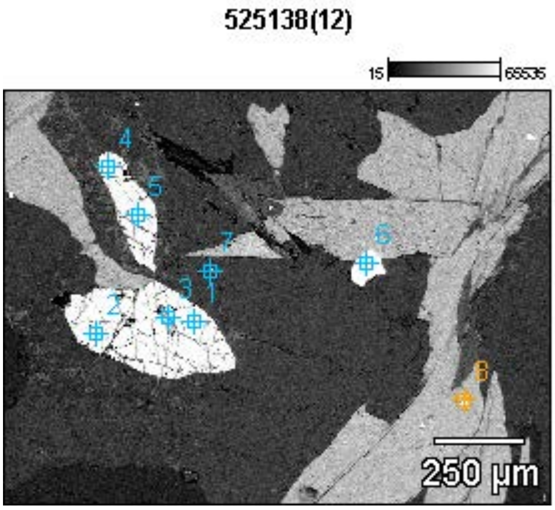

Image name: 525138(12)
Magnification: 79

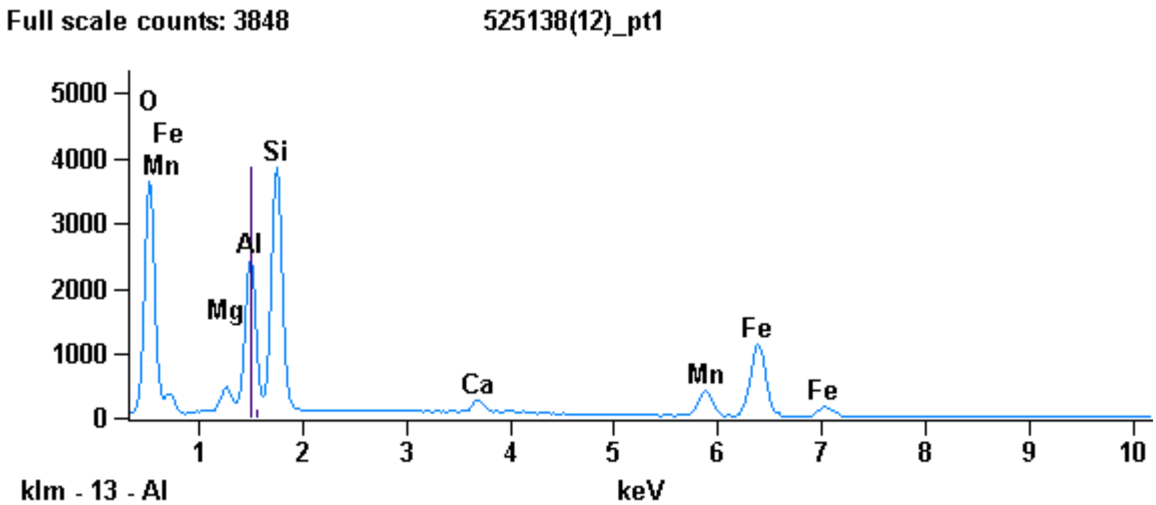

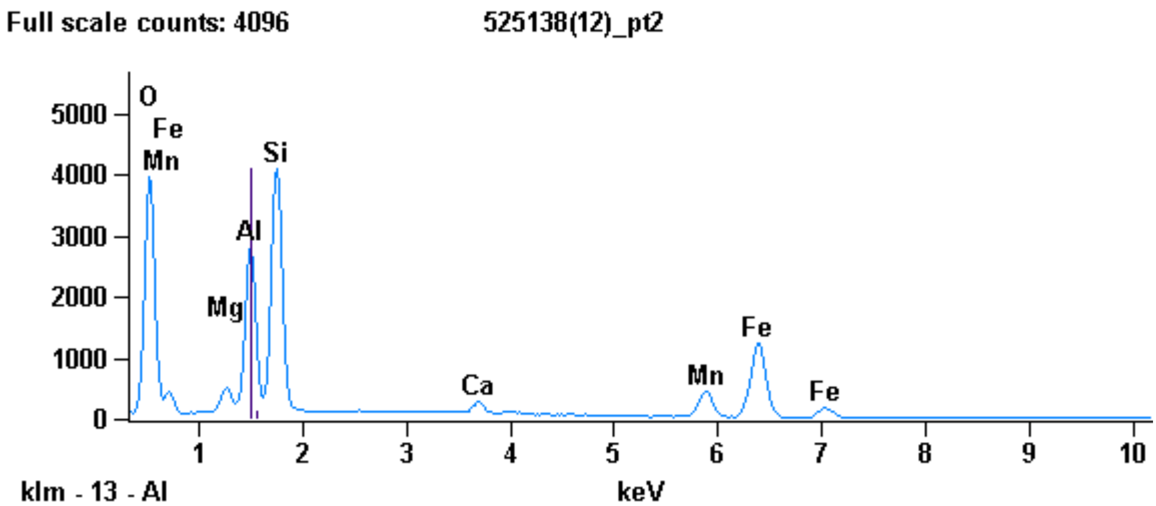

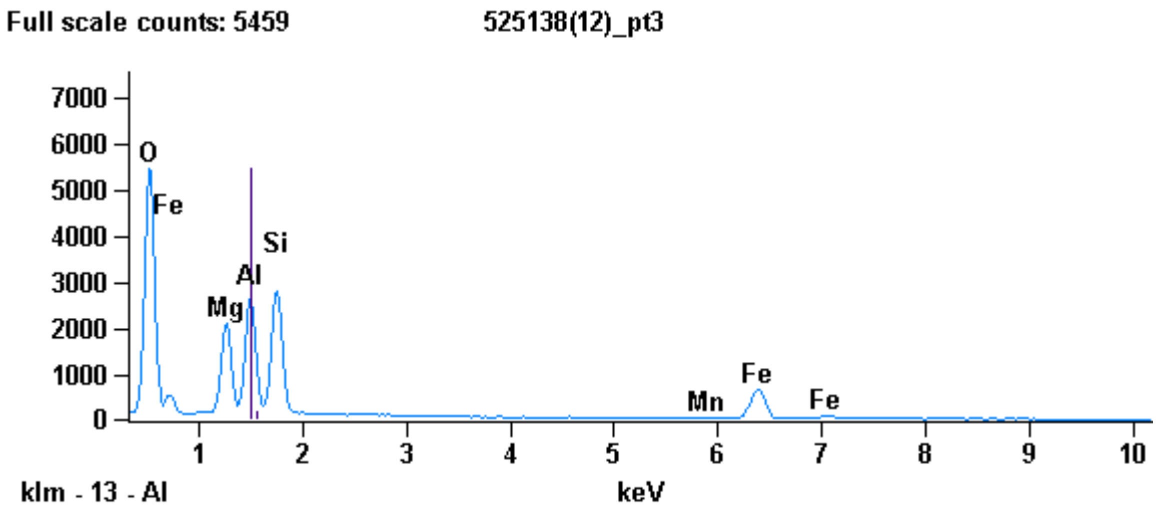
Full scale counts: 5459
525138(12)_pt3
7000
6000
5000
4000
3000
2000
1000
0
O
Fe
Mg
Al
Si
Mn
Fe
Fe
1
2
3
4
5
6
7
8
9
10
klm - 13 - Al
keV

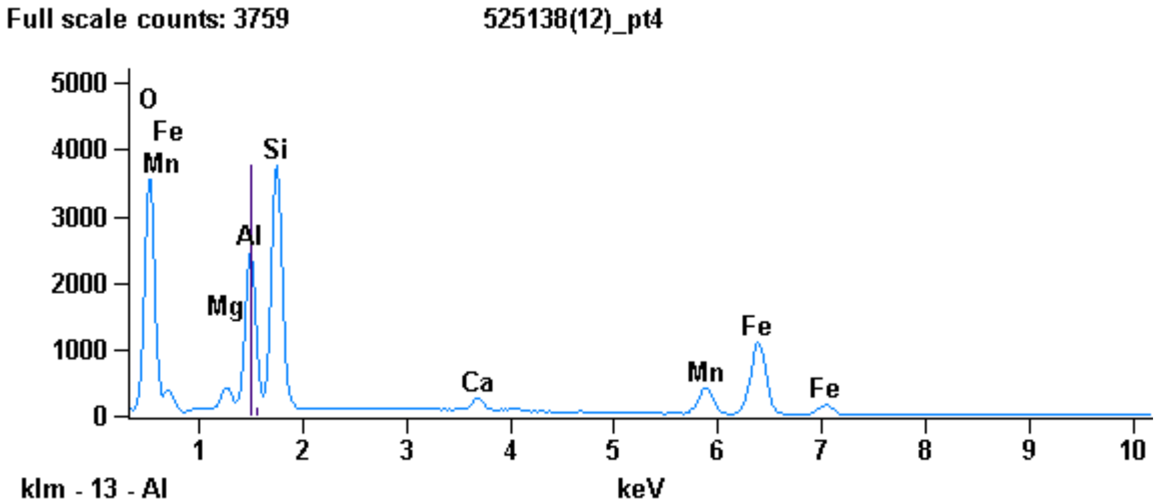
Full scale counts: 3759
525138(12)_pt4
5000
4000
3000
2000
1000
0
O
Fe
Mn
Si
Al
Mg
Ca
Mn
Fe
Fe
1
2
3
4
5
6
7
8
9
10
klm - 13 - Al
keV

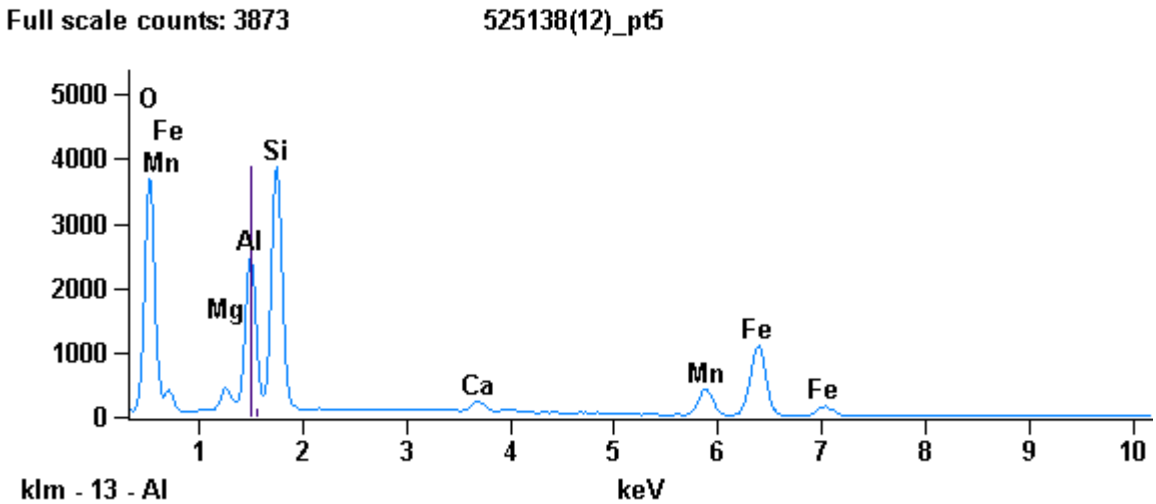
Full scale counts: 3873
525138(12)_pt5
5000
4000
3000
2000
1000
0
O
Fe
Mn
Si
Al
Mg
Ca
Mn
Fe
Fe
1
2
3
4
5
6
7
8
9
10
klm - 13 - Al
keV

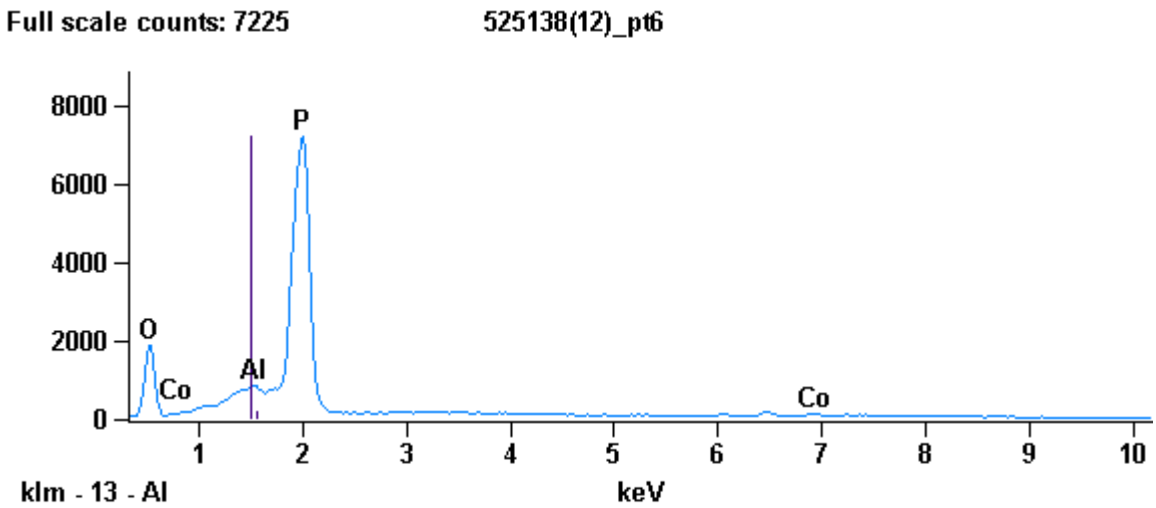
Full scale counts: 7225
525138(12)_pt6
8000
6000
4000
2000
0
O
Co
Al
P
Co
1 2 3 4 5 6 7 8 9 10
klm - 13 - Al
keV

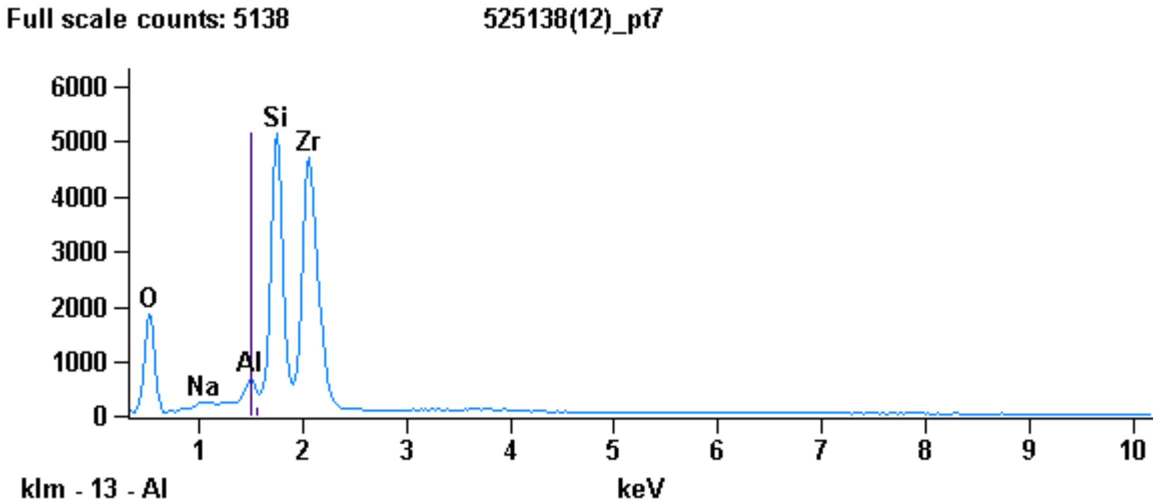
Full scale counts: 5138
525138(12)_pt7
6000
5000
4000
3000
2000
1000
0
O
Na
Al
Si
Zr
1 2 3 4 5 6 7 8 9 10
klm - 13 - Al
keV

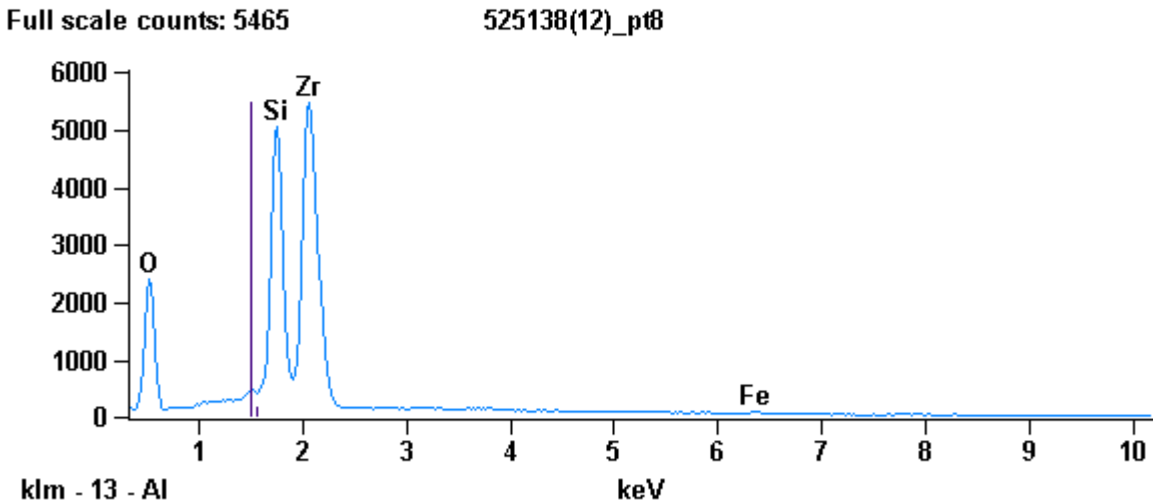
Full scale counts: 5465
525138(12)_pt8
6000
5000
4000
3000
2000
1000
0
O
Si
Zr
Fe
1 2 3 4 5 6 7 8 9 10
klm - 13 - Al
keV

Weight %

	O-K	***Na-K***	***Mg-K***	***Al-K***	***Si-K***	***P-K***	***Ca-K***	***Mn-K***	***Fe-K***	***Co-K***	***Zr-L***
525138(12)_pt1	41,68S		1,82	10,69	17,13		1,13	6,05	21,50		
525138(12)_pt2	41,71S		1,85	10,96	17,07		0,90	6,36	21,16		
525138(12)_pt3	43,95S		11,60	13,47	15,59			0,34	15,05		
525138(12)_pt4	41,47S		1,68	10,70	16,96		1,03	7,13	21,03		
525138(12)_pt5	41,59S		1,69	10,71	17,12		1,03	6,82	21,05		
525138(12)_pt6	55,06S			0,82		41,54				2,58	
525138(12)_pt7	35,80S	0,72		1,06	16,12						46,29
525138(12)_pt8	34,60S				14,75				0,38		50,28

Atomic %*

AT%	O	Na	Mg	Al	Si	P	Ca	Mn	Fe	Co	Zr
525138(12)_pt1	61,88746		1,778612	9,413056	14,48774		0,669801	2,616144	9,147195		
525138(12)_pt2	61,86152		1,805873	9,639822	14,42056		0,532863	2,747064	8,992297		
525138(12)_pt3	60,31767		10,47801	10,96305	12,18709			0,135893	5,918297		
525138(12)_pt4	61,80793		1,64799	9,457405	14,39807		0,61283	3,094789	8,980986		
525138(12)_pt5	61,85854		1,654369	9,446659	14,50383		0,611562	2,954109	8,970929		
525138(12)_pt6	70,85541			0,62579		27,61735			0	0,901447	
525138(12)_pt7	66,01404	0,923989		1,159143	16,93115				0		14,97167
525138(12)_pt8	66,62871				16,17877				0,209673		16,98285

Compound%*

Com%	O	Na2O	MgO	Al2O3	SiO2	P2O5	CaO	MnO	Fe2O3	CoO	ZrO2
525138(12)_pt1			6,688628	15,52811	42,22777		2,984291	12,63092	19,94029		
525138(12)_pt2			6,793514	15,90774	42,04665		2,374993	13,26764	19,60946		
525138(12)_pt3			36,97491	16,9704	33,33269			0,615661	12,10634		
525138(12)_pt4			6,135116	15,44445	41,54459		2,703011	14,79166	19,38117		

525138(12)_pt5			6,182875	15,48704	42,0129		2,707934	14,17431	19,43494		
525138(12)_pt6				2,399752		87,32609			0	10,27416	
525138(12)_pt7		1,744265		1,561016	40,28715				0		56,40757
525138(12)_pt8					37,42833				0,362781		62,20889

***data calculated after Weight%-data, as the software system had a breakdown.**

Minerals, 525138(12)
pt1: Garnet - pyralspite-group
pt2: Garnet - pyralspite-group
pt3: Mixed signal/edge effect
pt4: Garnet, pyralspite-group
pt5: Garnet, pyralspite-group
pt6: Xenotime (P-peak overlap Y-peak - thus Y is not present in EDS spectrum or in calculated data)
pt7: Zircon
pt8: Zircon

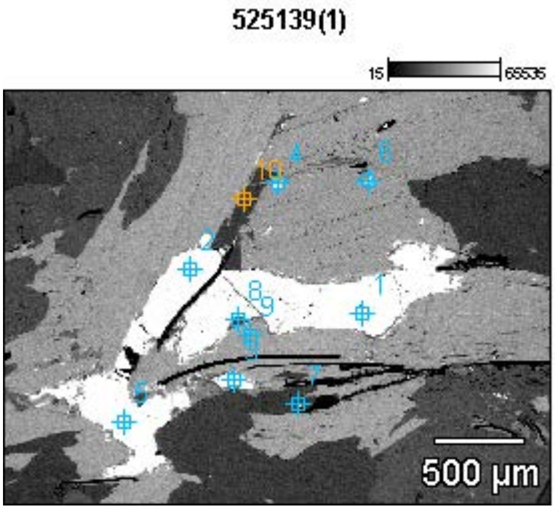

Image name: 525139(1)
Magnification: 40

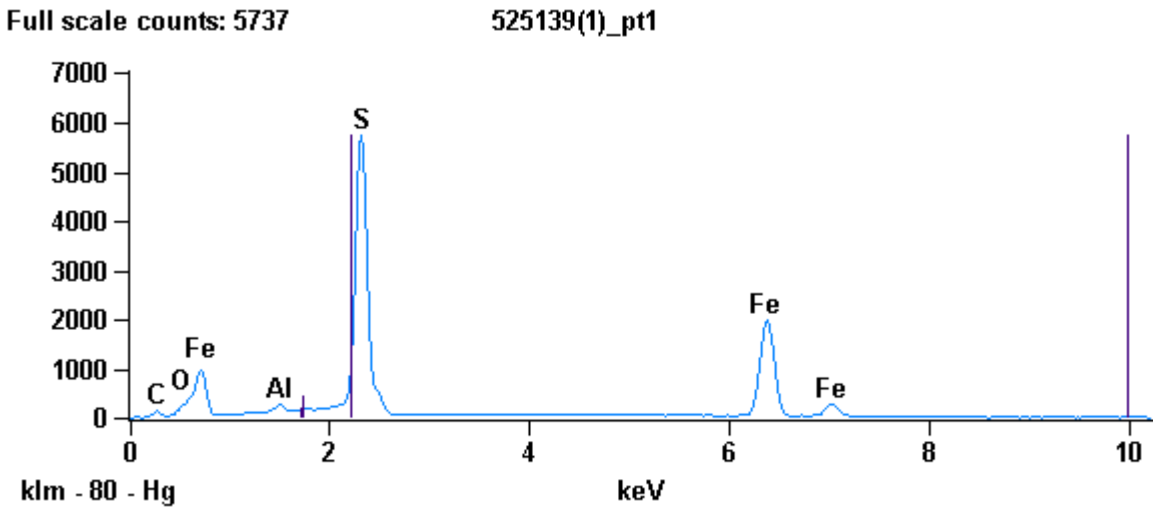

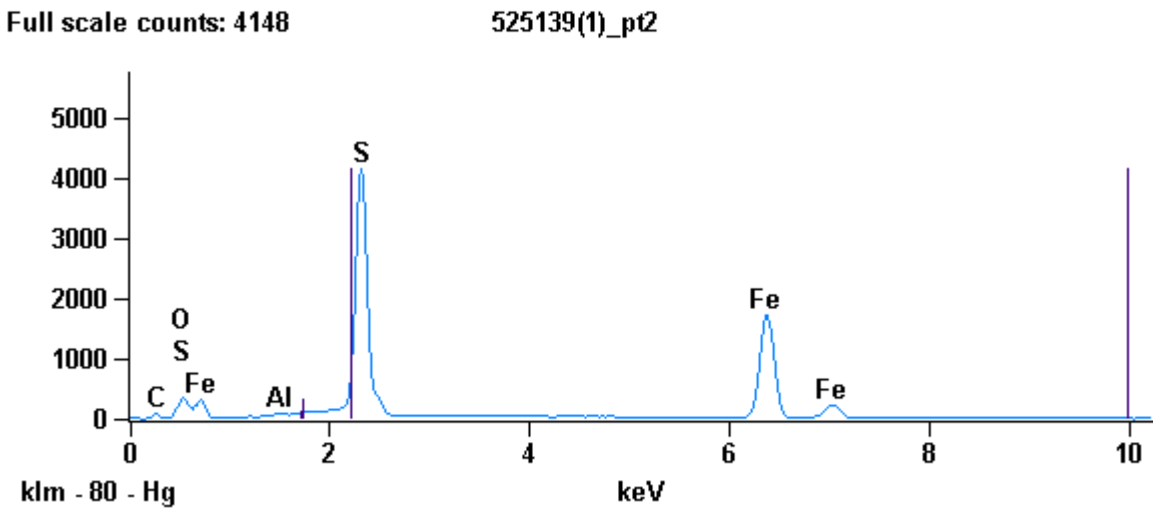

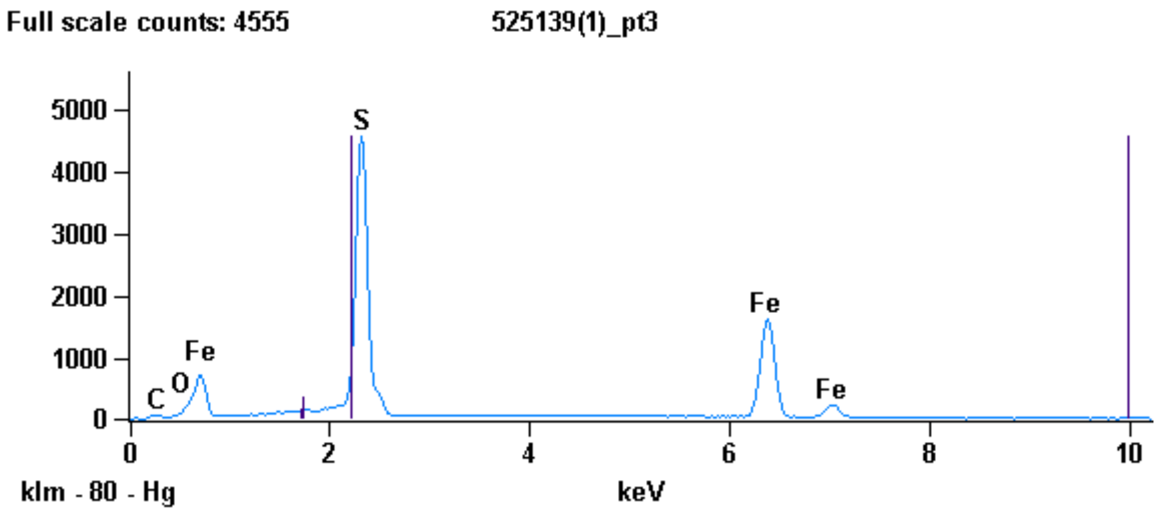
Full scale counts: 4555
525139(1)_pt3
5000
4000
3000
2000
1000
0
S
Fe
Fe
C
O
Fe
0
2
4
6
8
10
klm - 80 - Hg
keV

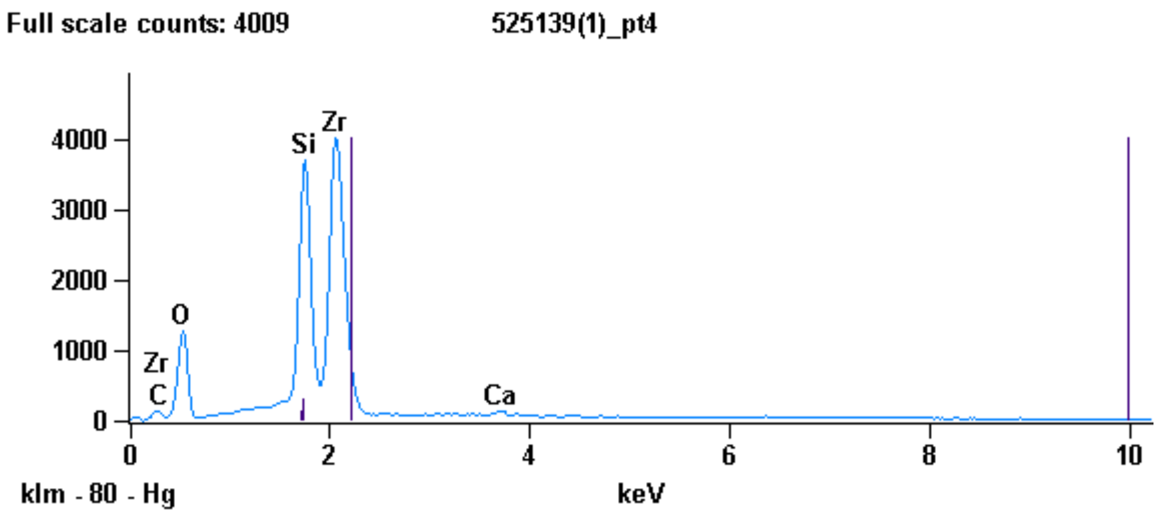
Full scale counts: 4009
525139(1)_pt4
4000
3000
2000
1000
0
Si
Zr
O
Zr
C
Ca
0
2
4
6
8
10
klm - 80 - Hg
keV

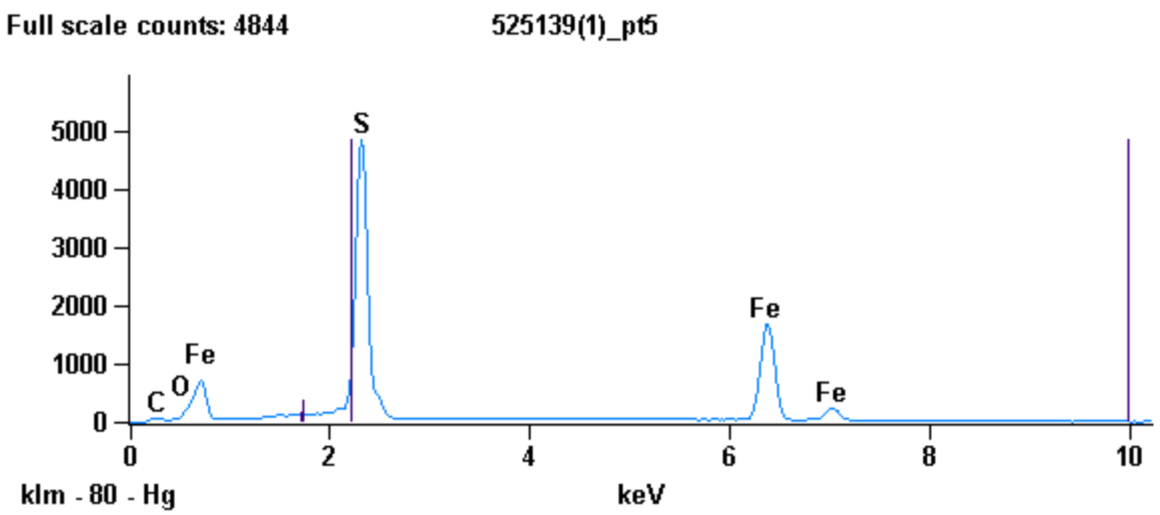
Full scale counts: 4844
525139(1)_pt5
5000
4000
3000
2000
1000
0
S
Fe
Fe
C
O
Fe
0
2
4
6
8
10
klm - 80 - Hg
keV

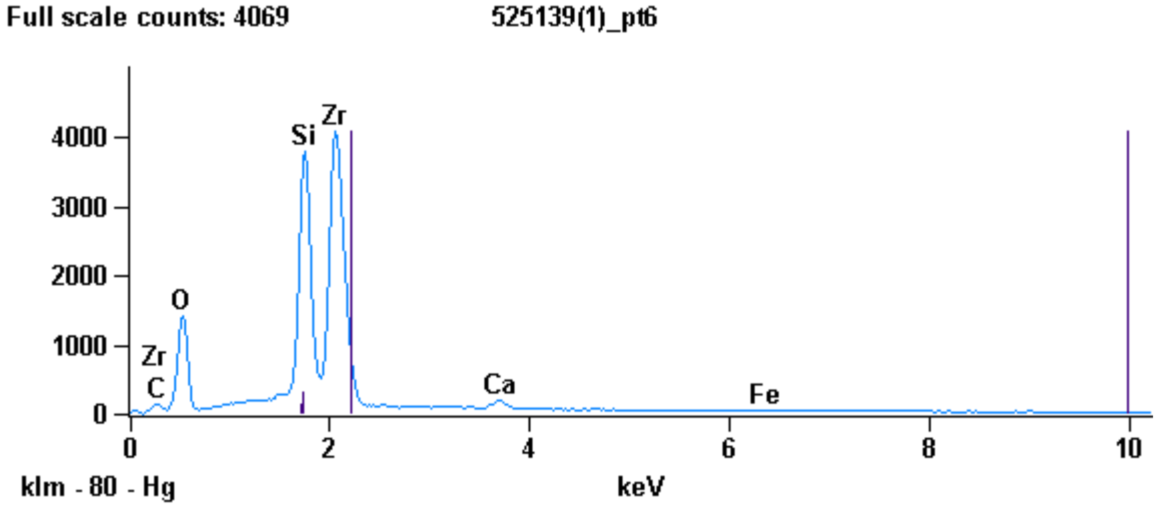
Full scale counts: 4069
525139(1)_pt6
Si
Zr
O
Zr
C
Ca
Fe
klm - 80 - Hg
keV

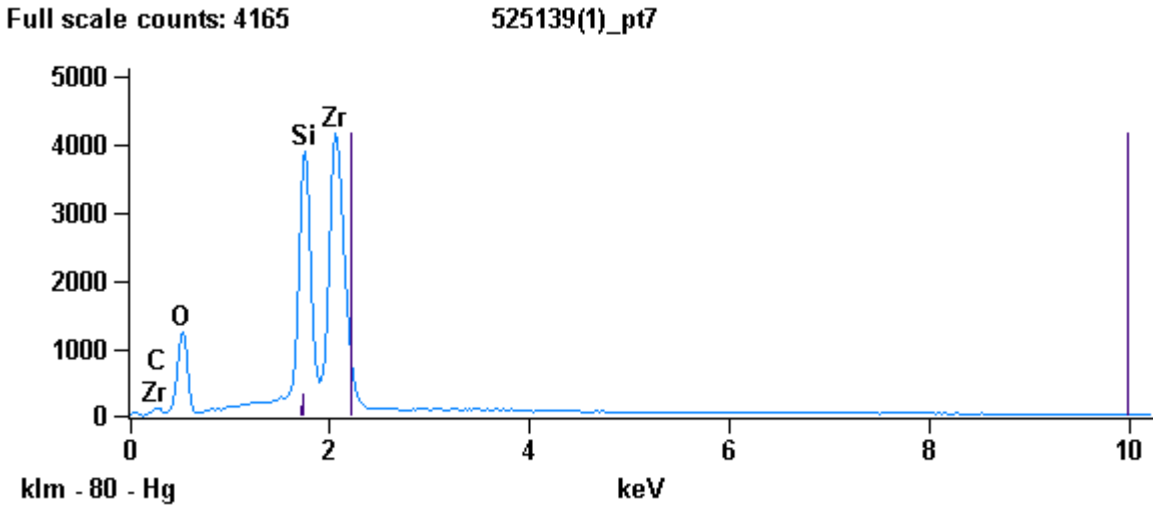
Full scale counts: 4165
525139(1)_pt7
Si
Zr
O
C
Zr
klm - 80 - Hg
keV

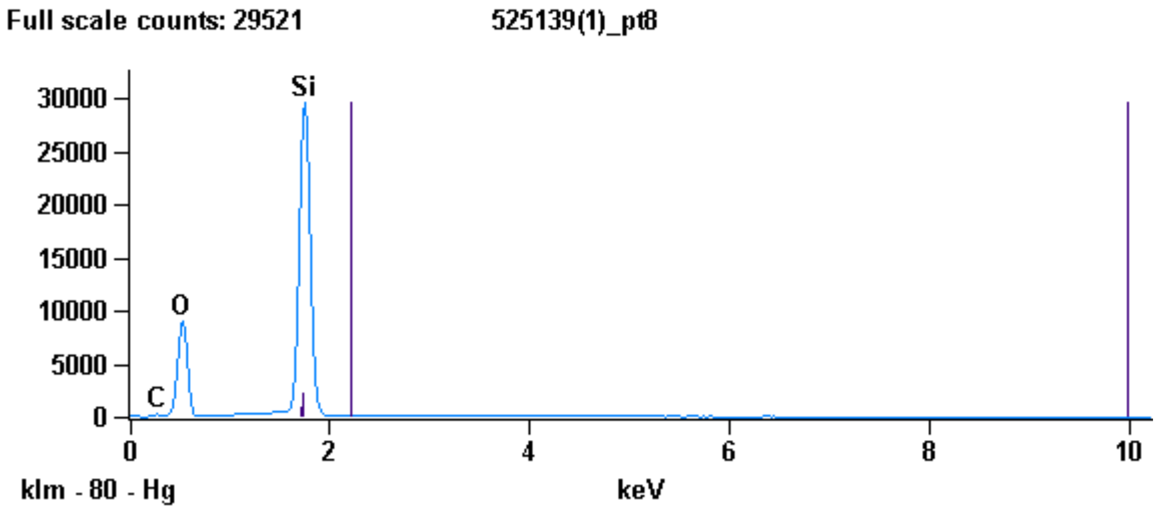
Full scale counts: 29521
525139(1)_pt8
Si
O
C
klm - 80 - Hg
keV

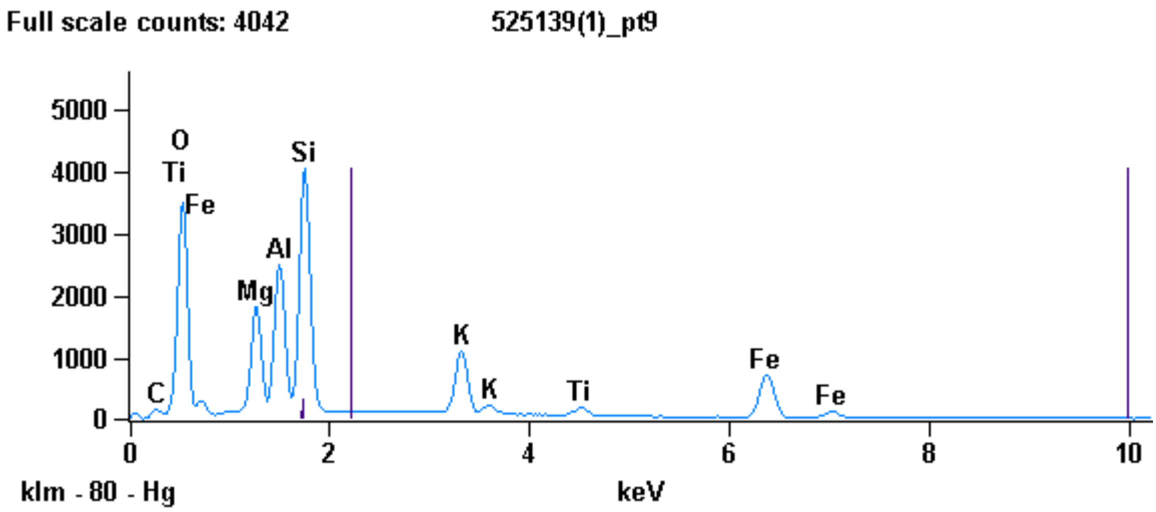

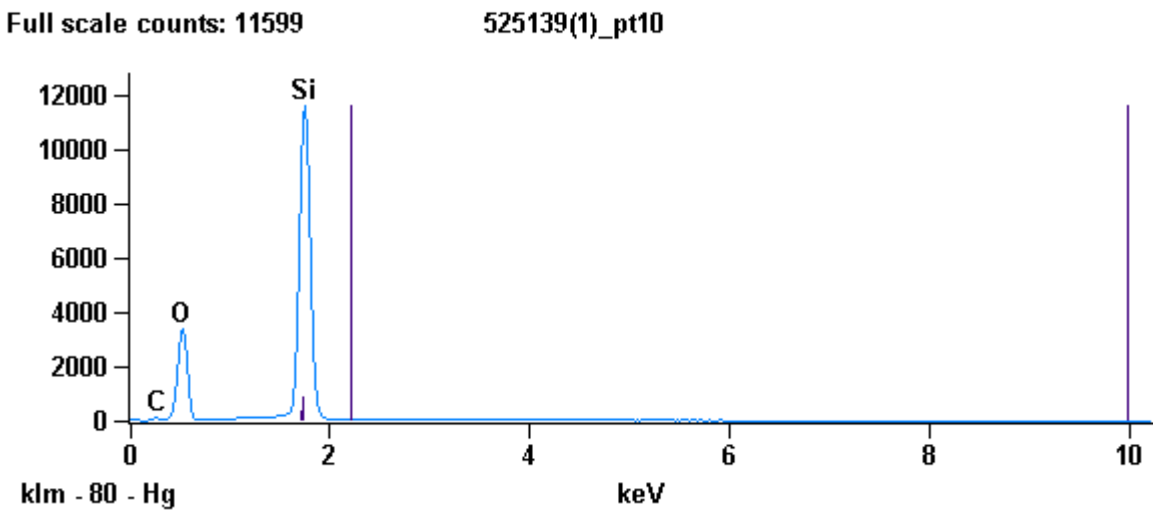

Weight %

	O-K	*Mg-K*	*Al-K*	*Si-K*	*S-K*	*K-K*	*Ca-K*	*Ti-K*	*Fe-K*	*Zr-L*
525139(1)_pt1	46.09S		0.41		21.30				32.21	
525139(1)_pt2	44.75S		0.07		19.65				35.53	
525139(1)_pt3	45.88S				21.20				32.92	
525139(1)_pt4	34.47S			14.54			0.42			50.57
525139(1)_pt5	46.05S				21.42				32.53	
525139(1)_pt6	34.54S			14.57			0.96		0.60	49.33
525139(1)_pt7	34.65S			14.87						50.49
525139(1)_pt8	53.26S			46.74						
525139(1)_pt9	42.59S	8.36	10.35	17.45		6.11		1.01	14.12	
525139(1)_pt10	53.26S			46.74						

Atom %

	O-K	Mg-K	Al-K	Si-K	S-K	K-K	Ca-K	Ti-K	Fe-K	Zr-L
525139(1)_pt1	69.63		0.37		16.06				13.94	
525139(1)_pt2	69.08		0.06		15.14				15.71	
525139(1)_pt3	69.63				16.06				14.31	
525139(1)_pt4	66.56			15.99			0.32			17.13
525139(1)_pt5	69.71				16.18				14.11	
525139(1)_pt6	66.37			15.95			0.73		0.33	16.62
525139(1)_pt7	66.67			16.29						17.04
525139(1)_pt8	66.67			33.33						
525139(1)_pt9	59.94	7.75	8.64	13.99		3.52		0.48	5.69	
525139(1)_pt10	66.67			33.33						

Compound %

		MgO	Al2O3	SiO2	SO3	K2O	CaO	TiO2	Fe2O3	ZrO2
525139(1)_pt1	0.00		0.77		53.18				46.05	
525139(1)_pt2	0.00		0.13		49.07				50.79	
525139(1)_pt3	0.00				52.94				47.06	
525139(1)_pt4	0.00			31.10			0.59			68.31
525139(1)_pt5	0.00				53.49				46.51	
525139(1)_pt6	0.00			31.17			1.34		0.85	66.64
525139(1)_pt7	0.00			31.80						68.20
525139(1)_pt8	0.00			100.00						
525139(1)_pt9	0.00	13.87	19.56	37.34		7.36		1.69	20.19	
525139(1)_pt10	0.00			100.00						

Minerals, 525139(1)
pt1: Pyrrhotite
pt2: Pyrrhotite
pt3: Pyrrhotite
pt4: Zircon
pt5: Pyrrhotite
pt6: Zircon
pt7: Zircon
pt8: Quartz
pt9: Biotite
pt10: Quartz

525139(2)

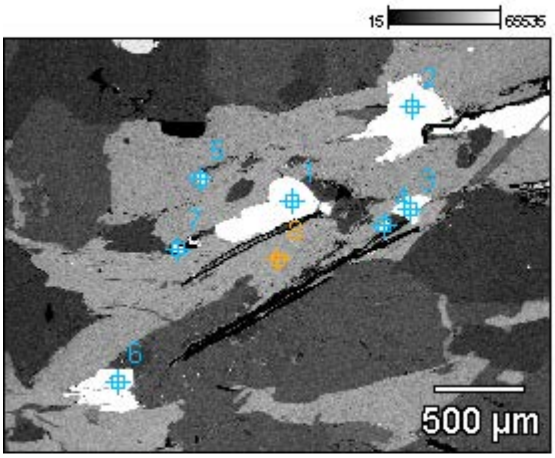

Image name: 525139(2)
Magnification: 40

Full scale counts: 5806 525139(2)_pt1

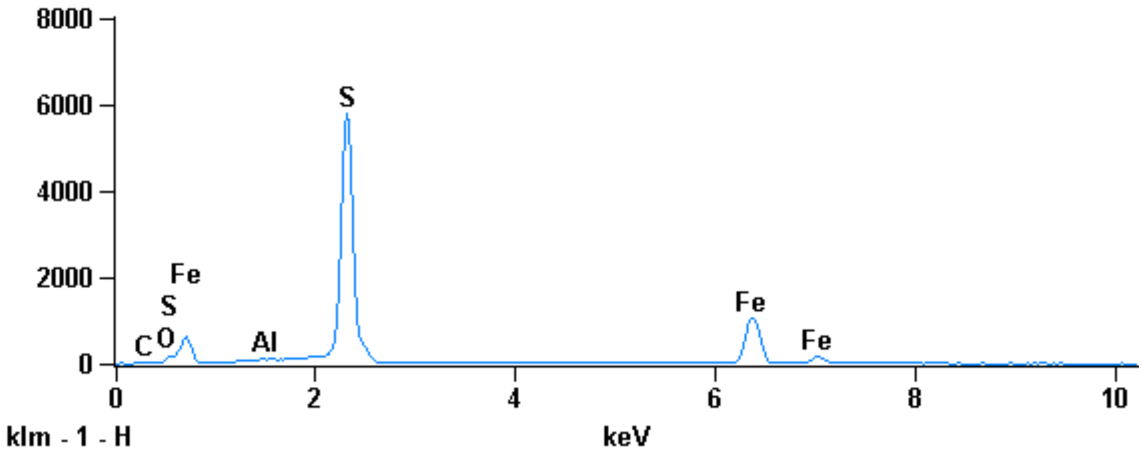

Full scale counts: 5278 525139(2)_pt2

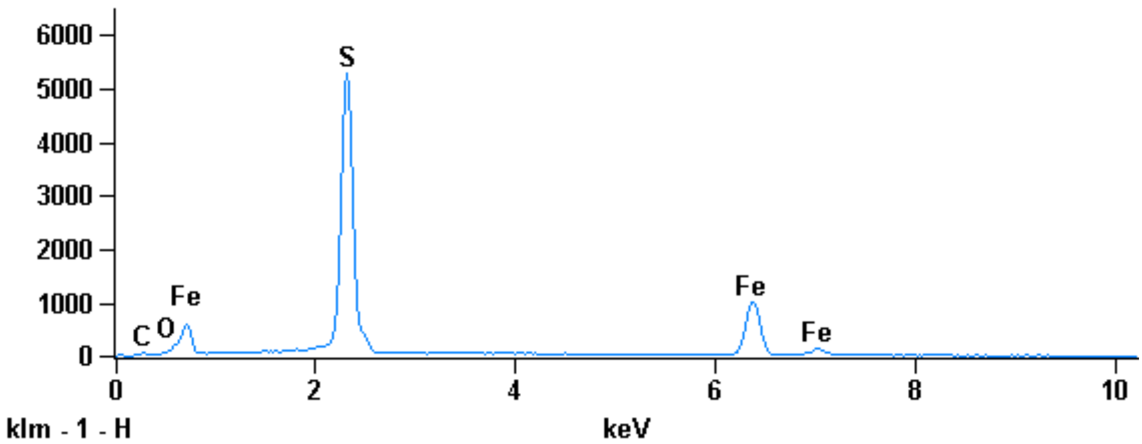

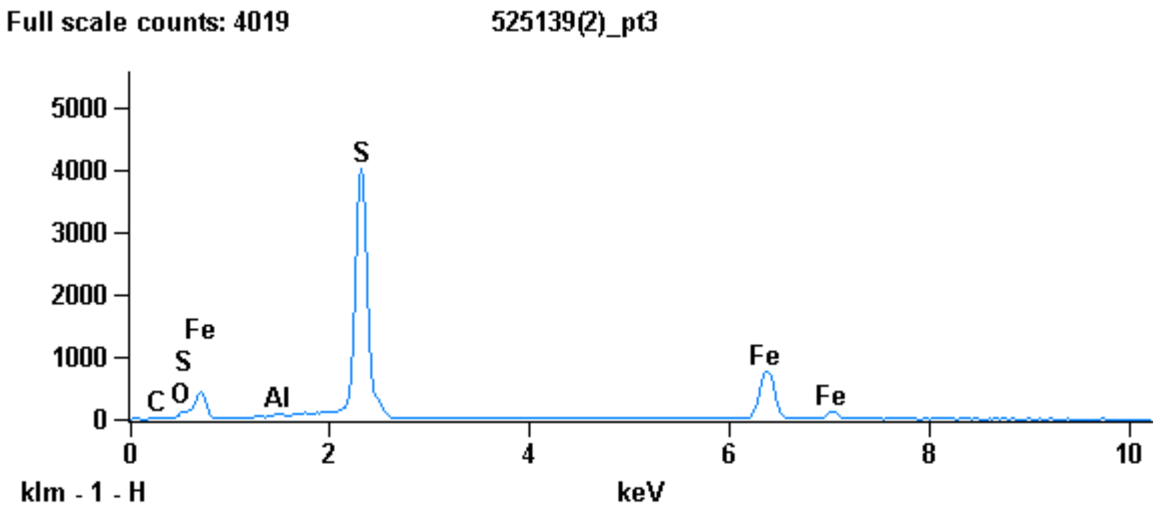
Full scale counts: 4019
525139(2)_pt3
5000
4000
3000
2000
1000
0
S
Fe
S
O
C
Al
Fe
Fe
0
2
4
6
8
10
klm - 1 - H
keV

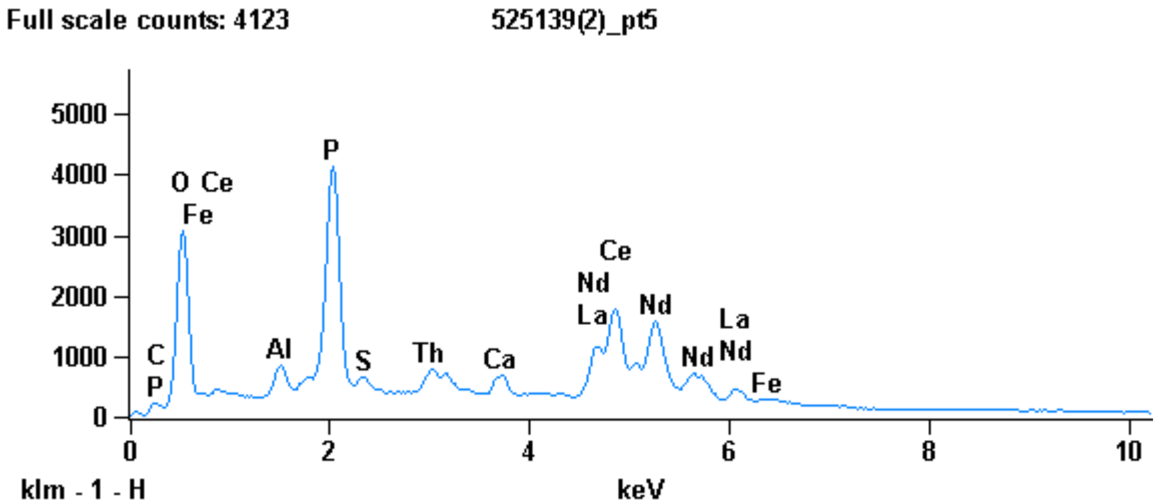
Full scale counts: 4123
525139(2)_pt5
5000
4000
3000
2000
1000
0
P
O Ce
Fe
C
P
Al
S
Th
Ca
Ce
Nd
La
Nd
La
Nd
Nd
Fe
0
2
4
6
8
10
klm - 1 - H
keV

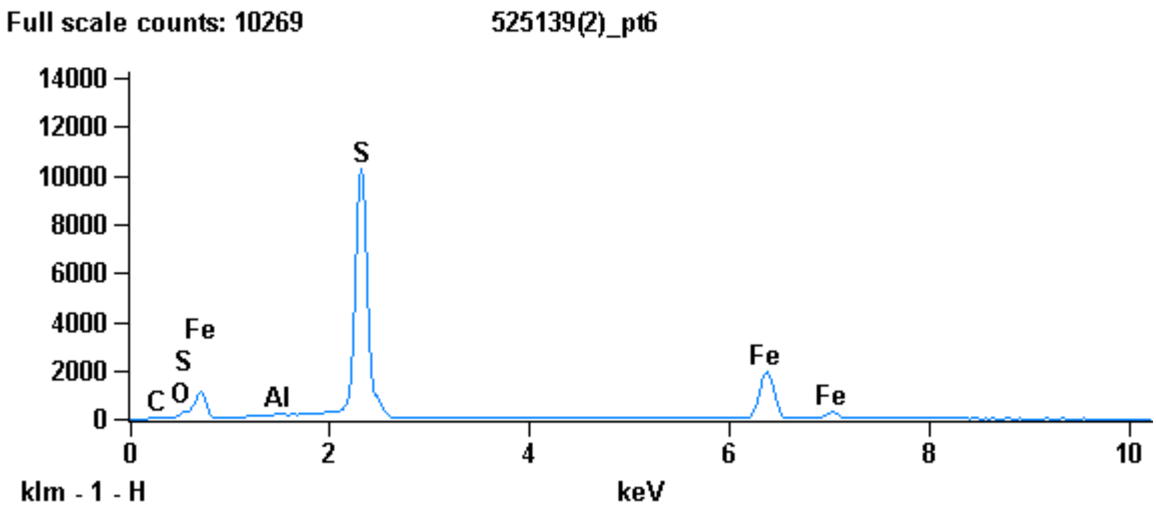
Full scale counts: 10269
525139(2)_pt6
14000
12000
10000
8000
6000
4000
2000
0
S
Fe
S
O
C
Al
Fe
Fe
0
2
4
6
8
10
klm - 1 - H
keV

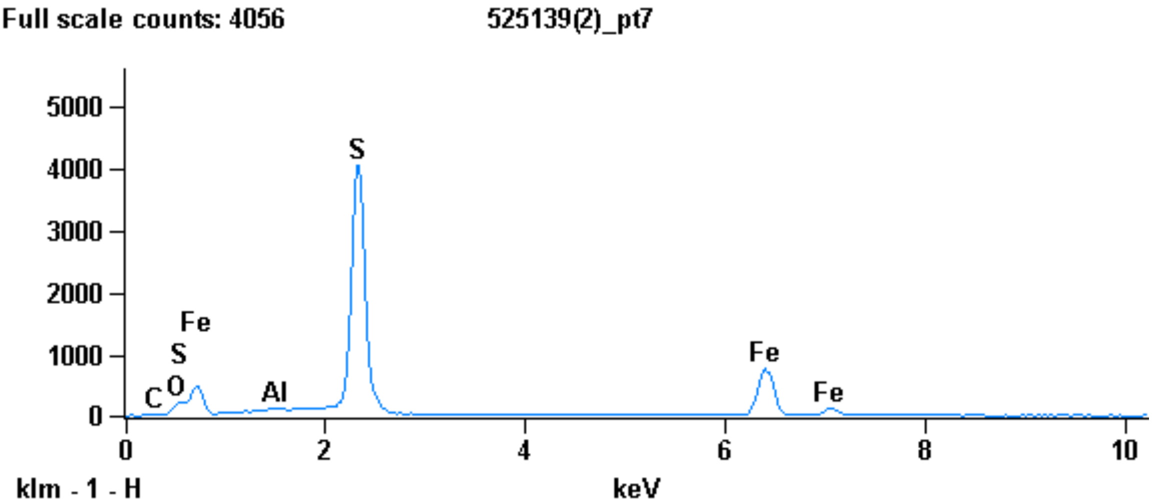

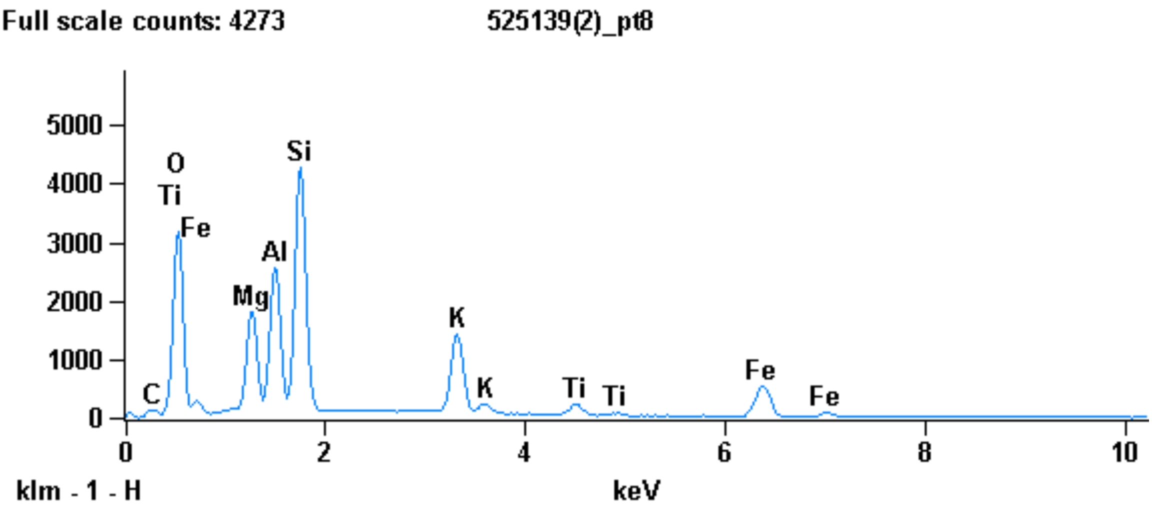

Weight %

	O-K	Mg-K	Al-K	Si-K	P-K	S-K	K-K	Ca-K	Ti-K	Fe-K	La-L	Ce-L	Nd-L	Th-L
525139(2)_pt1	49.98S		0.07			26.66				23.29				
525139(2)_pt2	50.12S					26.88				23.00				
525139(2)_pt3	49.95S		0.11			26.60				23.33				
525139(2)_pt4	49.94S		0.05			26.61				23.40				
525139(2)_pt5	30.62S		2.20		14.32	0.61		1.70		0.74	9.90	24.15	8.95	6.81
525139(2)_pt6	50.04S		0.06			26.74				23.17				
525139(2)_pt7	50.57S		0.26			27.36				21.81				
525139(2)_pt8	42.73S	8.39	10.22	18.29			8.28		1.62	10.47				

Atom %

	O-K	Mg-K	Al-K	Si-K	P-K	S-K	K-K	Ca-K	Ti-K	Fe-K	La-L	Ce-L	Nd-L	Th-L
525139(2)_pt1	71.40		0.06			19.01				9.53				
525139(2)_pt2	71.48					19.13				9.40				
525139(2)_pt3	71.38		0.10			18.97				9.55				
525139(2)_pt4	71.39		0.05			18.98				9.58				
525139(2)_pt5	66.75		2.84		16.12	0.66		1.48		0.46	2.49	6.01	2.16	1.02
525139(2)_pt6	71.43		0.05			19.05				9.47				
525139(2)_pt7	71.60		0.22			19.33				8.85				
525139(2)_pt8	59.63	7.71	8.46	14.54			4.73		0.76	4.18				

Compound %

		MgO	Al2O3	SiO2	P2O5	SO3	K2O	CaO	TiO2	Fe2O3	La2O3	Ce2O3	Nd2O3	ThO2
525139(2)_pt1	0.00		0.13			66.57				33.30				
525139(2)_pt2	0.00					67.11				32.89				
525139(2)_pt3	0.00		0.21			66.43				33.35				
525139(2)_pt4	0.00		0.10			66.44				33.46				
525139(2)_pt5	0.00		4.15		32.81	1.51		2.37		1.06	11.62	28.29	10.44	7.75
525139(2)_pt6	0.00		0.11			66.76				33.12				
525139(2)_pt7	0.00		0.49			68.32				31.19				
525139(2)_pt8	0.00	13.91	19.32	39.13			9.97		2.71	14.97				

Minerals, 525139(2)

pt1: Pyrite
pt2: Pyrite
pt3: Pyrite
pt4: Pyrite
pt5: Monazite
pt6: Pyrite
pt7: Pyrite
pt8: Biotite

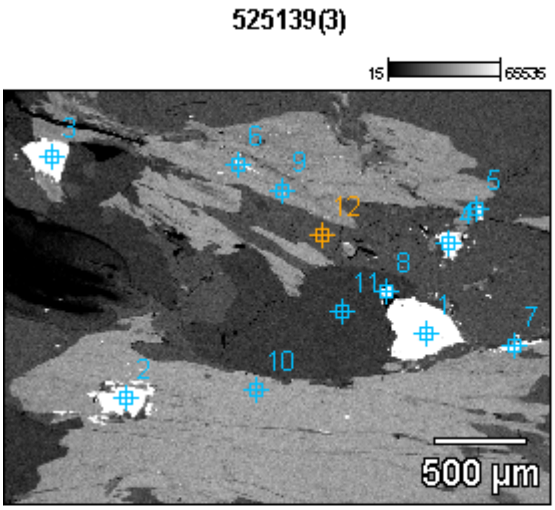

Image name: 525139(3)
Magnification: 41

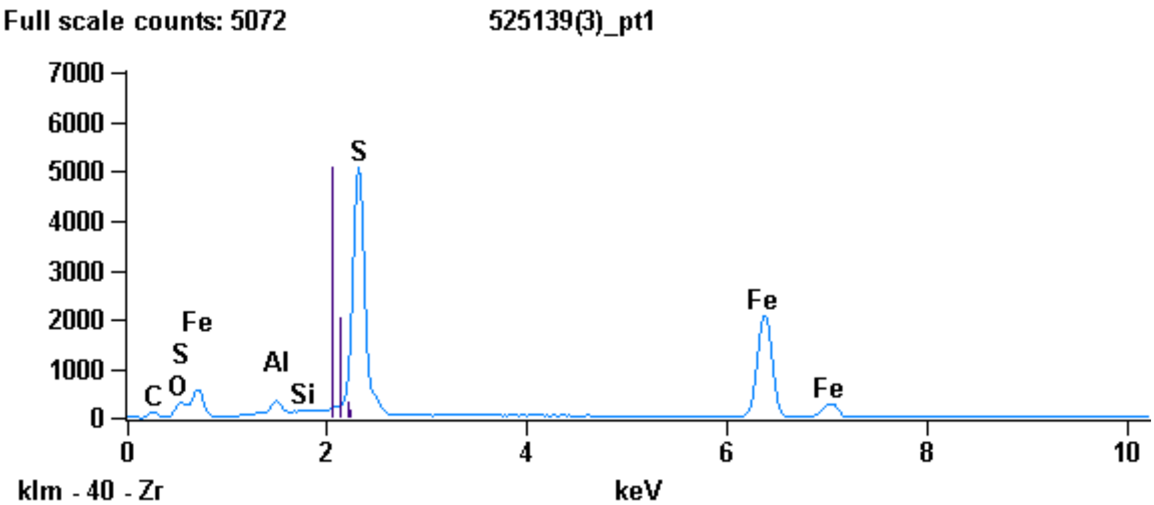

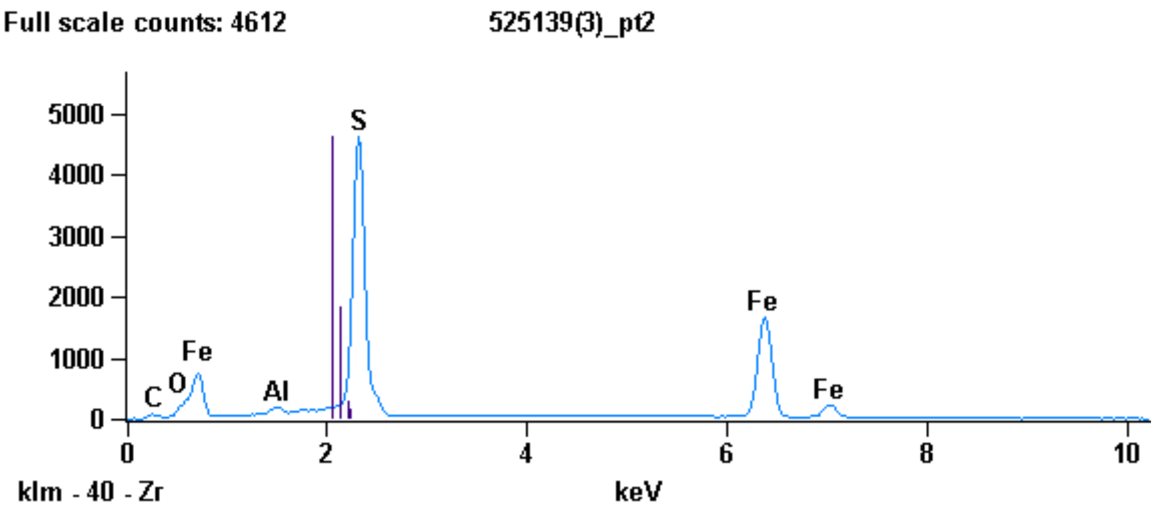

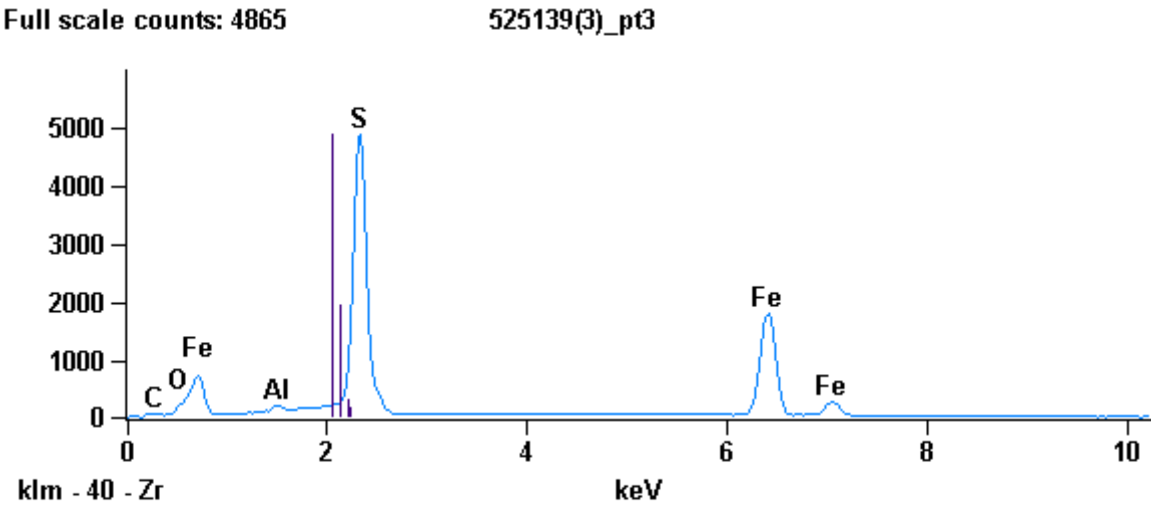
Full scale counts: 4865
525139(3)_pt3
S
Fe
Fe
C
O
Al
Fe
0
1000
2000
3000
4000
5000
0
2
4
6
8
10
klm - 40 - Zr
keV

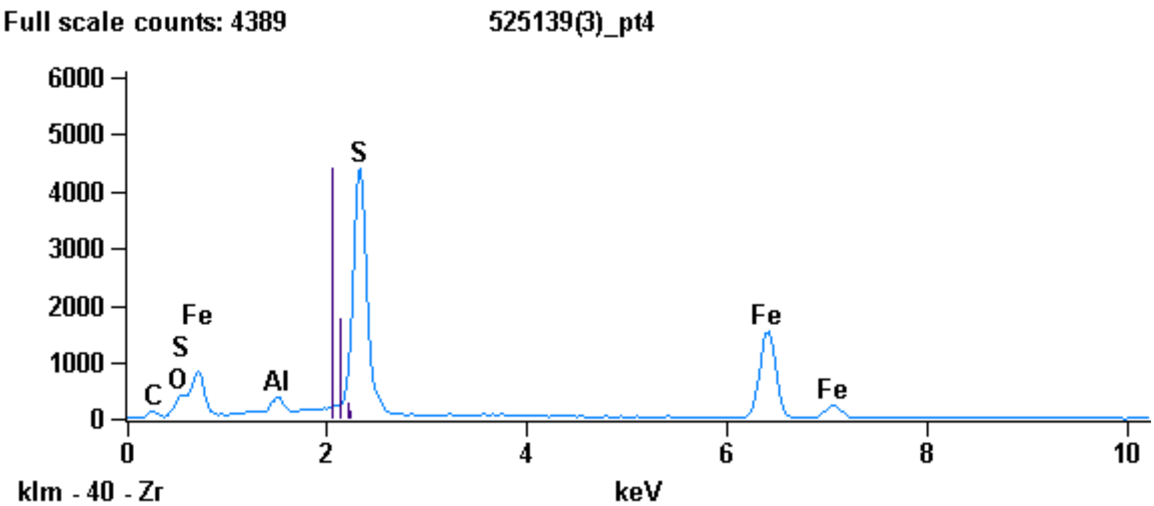
Full scale counts: 4389
525139(3)_pt4
S
Fe
S
C
O
Al
Fe
Fe
0
1000
2000
3000
4000
5000
6000
0
2
4
6
8
10
klm - 40 - Zr
keV

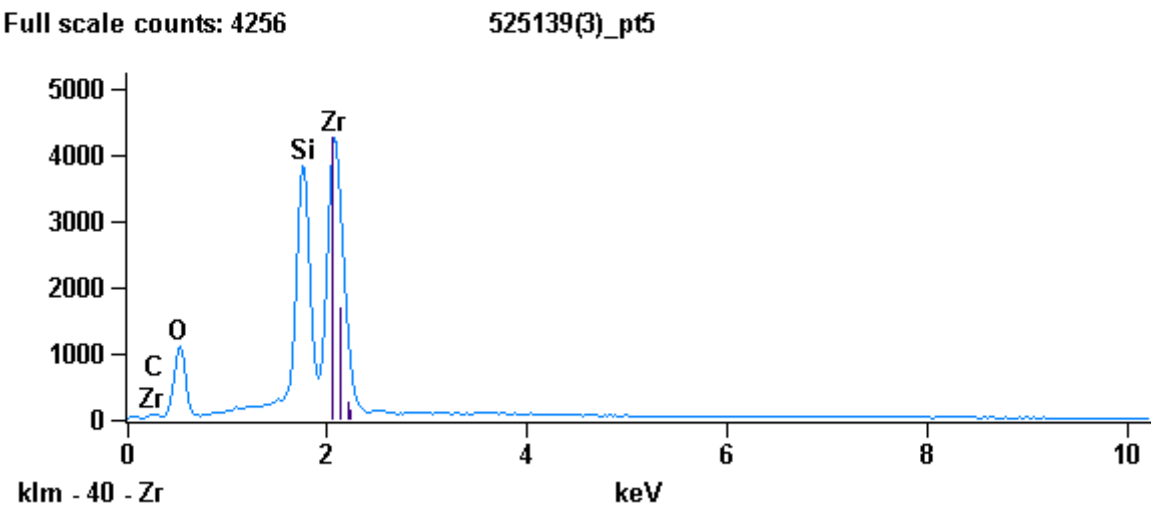
Full scale counts: 4256
525139(3)_pt5
Zr
Si
O
C
Zr
0
1000
2000
3000
4000
5000
0
2
4
6
8
10
klm - 40 - Zr
keV

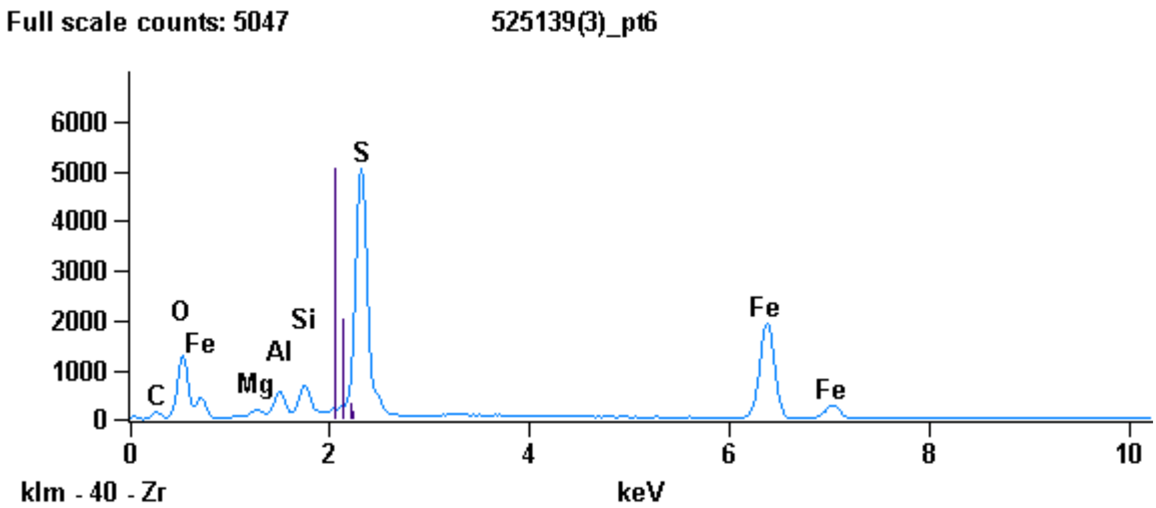
Full scale counts: 5047
525139(3)_pt6
6000
5000
4000
3000
2000
1000
0
S
O
Fe
C
Mg
Al
Si
Fe
Fe
0
2
4
6
8
10
klm - 40 - Zr
keV

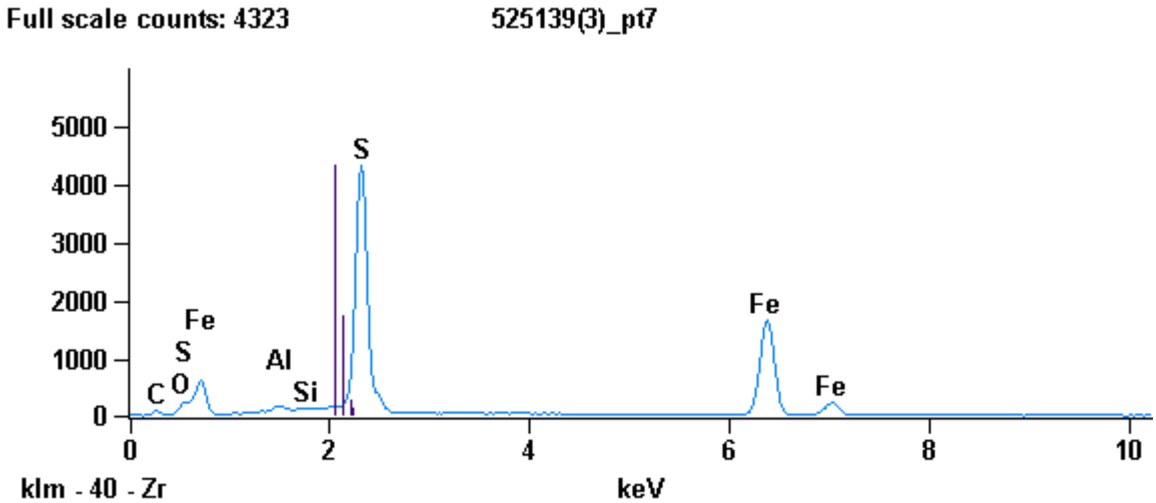
Full scale counts: 4323
525139(3)_pt7
5000
4000
3000
2000
1000
0
S
Fe
S
C
O
Al
Si
Fe
Fe
0
2
4
6
8
10
klm - 40 - Zr
keV

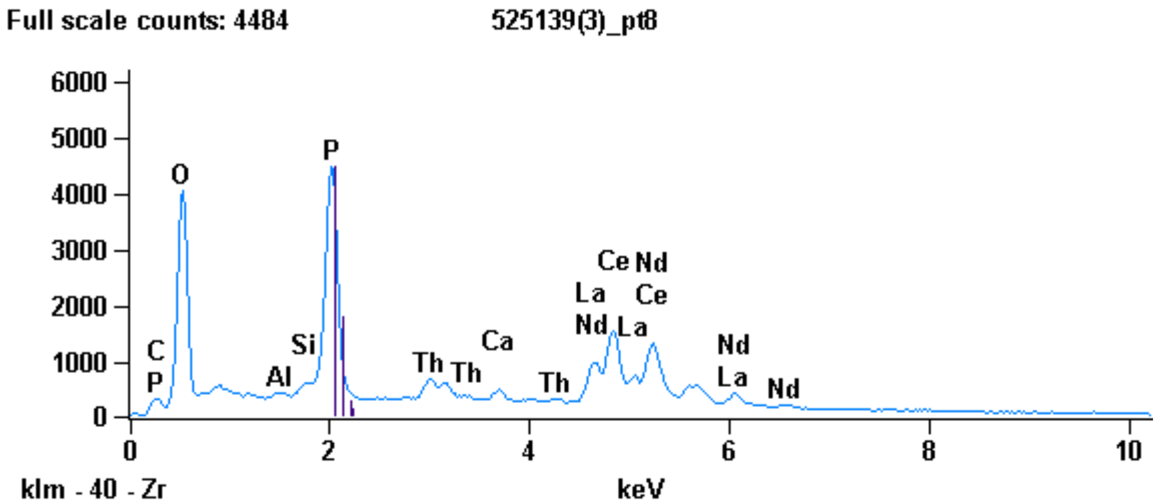
Full scale counts: 4484
525139(3)_pt8
6000
5000
4000
3000
2000
1000
0
P
O
C
P
Al
Si
Th
Th
Ca
Th
Ce Nd
La
Nd
Ce
La
Nd
La
Nd
0
2
4
6
8
10
klm - 40 - Zr
keV

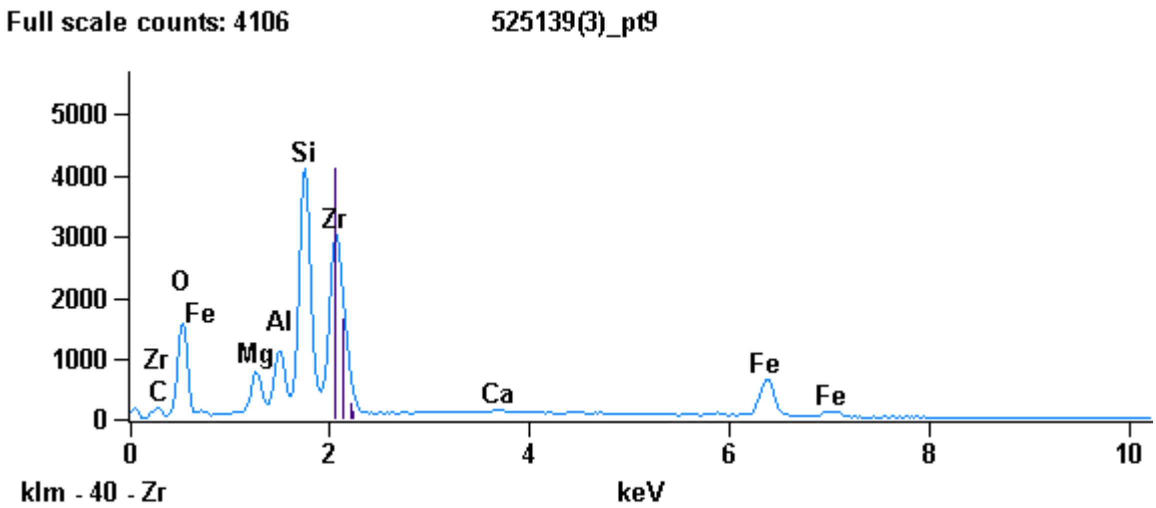
Full scale counts: 4106
525139(3)_pt9
5000
4000
3000
2000
1000
0
Si
Zr
O
Fe
Al
Mg
Zr
C
Ca
Fe
Fe
0
2
4
6
8
10
klm - 40 - Zr
keV

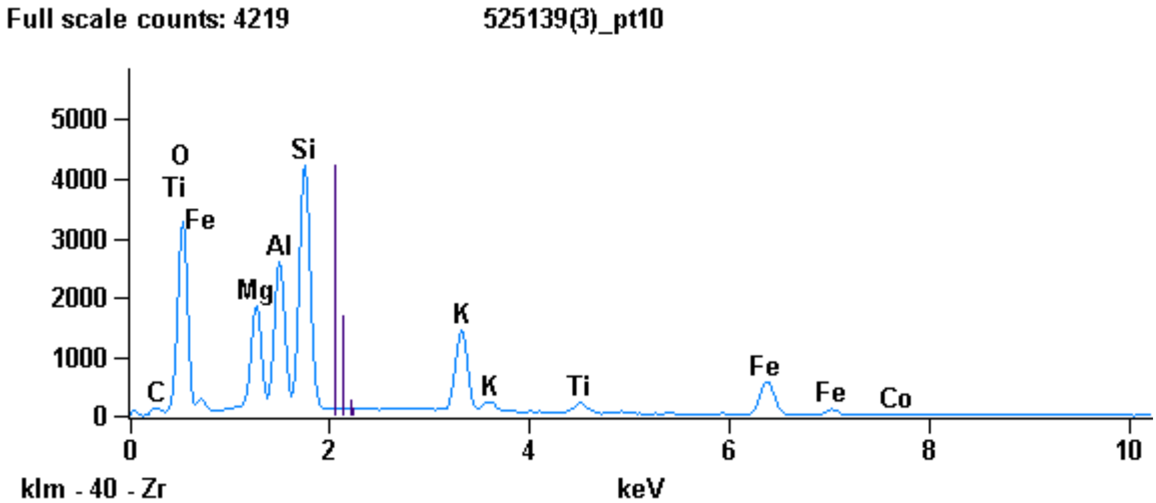
Full scale counts: 4219
525139(3)_pt10
5000
4000
3000
2000
1000
0
O
Ti
Fe
Si
Al
Mg
K
C
K
Ti
Fe
Fe
Co
0
2
4
6
8
10
klm - 40 - Zr
keV

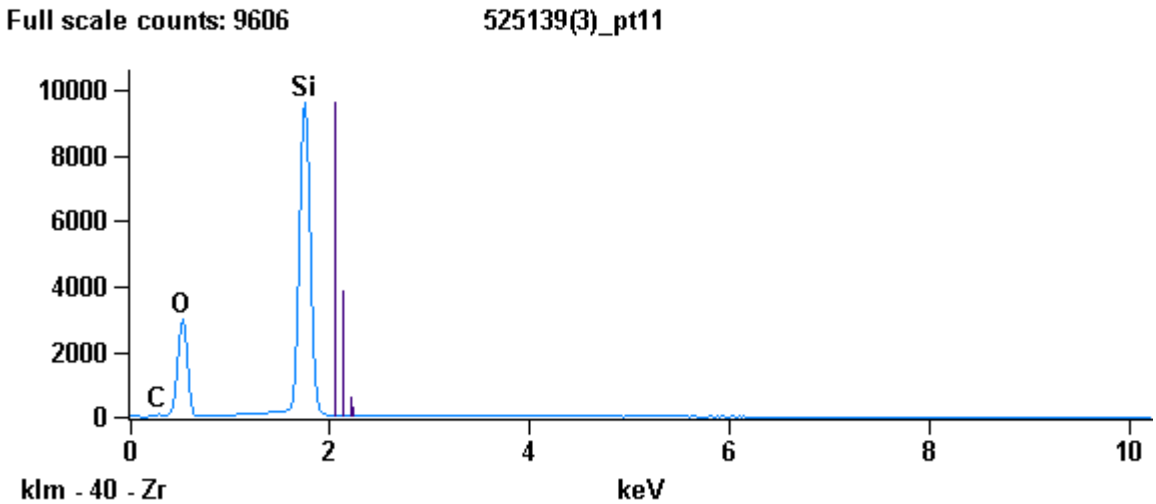
Full scale counts: 9606
525139(3)_pt11
10000
8000
6000
4000
2000
0
Si
O
C
0
2
4
6
8
10
klm - 40 - Zr
keV

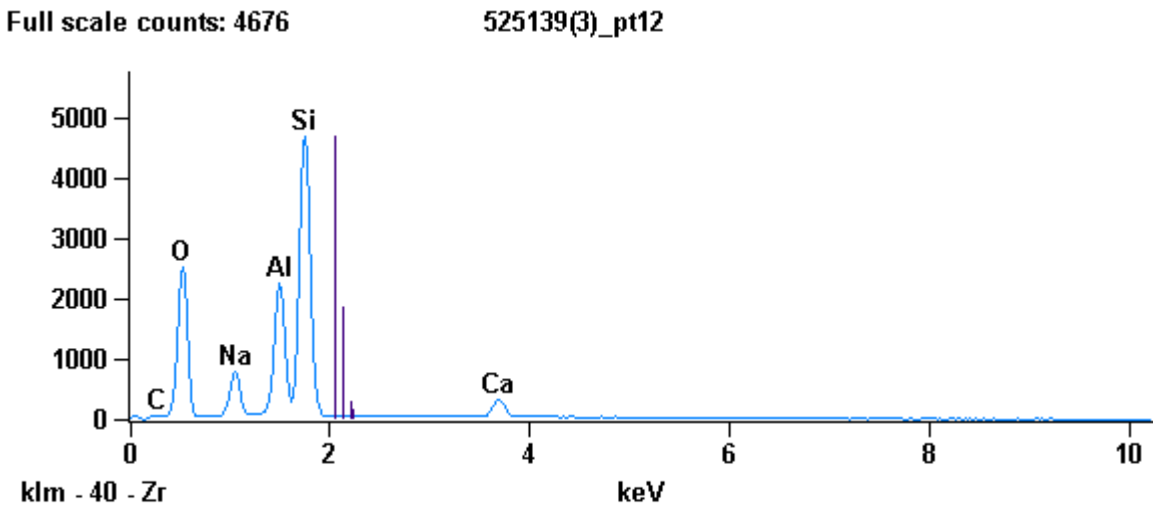

Weight %

	O-K	Na-K	Mg-K	Al-K	Si-K	P-K	S-K	K-K	Ca-K	Ti-K	Fe-K	Co-K	Zr-L	La-L	Ce-L	Nd-L	Th-L
525139(3)_pt1	44.71S			1.04	0.09		19.12				35.04						
525139(3)_pt2	45.83S			0.44			20.94				32.78						
525139(3)_pt3	45.36S			0.32			20.36				33.95						
525139(3)_pt4	46.29S			1.41			21.13				31.17						
525139(3)_pt5	34.81S				15.15								50.04				
525139(3)_pt6	45.78S		0.46	1.76	1.97		18.89				31.12						
525139(3)_pt7	45.49S			0.51	0.07		20.41				33.52						
525139(3)_pt8	31.98S			0.30	0.07	17.84			1.05					10.55	25.41	8.32	4.47
525139(3)_pt9	36.96S		3.19	3.39	14.14				0.38		11.15		30.80				
525139(3)_pt10	42.73S		8.47	10.33	18.11			7.90		1.53	10.88	0.03					
525139(3)_pt11	53.26S				46.74												
525139(3)_pt12	48.14S	7.11		12.15	29.51				3.09								

Atom %

	O-K	Na-K	Mg-K	Al-K	Si-K	P-K	S-K	K-K	Ca-K	Ti-K	Fe-K	Co-K	Zr-L	La-L	Ce-L	Nd-L	Th-L
525139(3)_pt1	68.83			0.95	0.08		14.69				15.45						
525139(3)_pt2	69.51			0.40			15.85				14.24						
525139(3)_pt3	69.32			0.29			15.53				14.86						
525139(3)_pt4	69.50			1.26			15.83				13.41						
525139(3)_pt5	66.67				16.53								16.81				
525139(3)_pt6	68.74		0.46	1.57	1.69		14.16				13.39						
525139(3)_pt7	69.32			0.46	0.06		15.52				14.64						
525139(3)_pt8	67.78			0.38	0.08	19.53			0.89					2.58	6.15	1.96	0.65
525139(3)_pt9	63.87		3.63	3.48	13.91				0.26		5.52		9.33				
525139(3)_pt10	59.66		7.79	8.55	14.41			4.51		0.71	4.35	0.01					
525139(3)_pt11	66.67				33.33												
525139(3)_pt12	61.45	6.31		9.20	21.46				1.58								

Compound %

		Na2O	MgO	Al2O3	SiO2	P2O5	SO3	K2O	CaO	TiO2	Fe2O3	CoO	ZrO2	La2O3	Ce2O3	Nd2O3	ThO2
525139(3)_pt1	0.00			1.96	0.19		47.75				50.10						
525139(3)_pt2	0.00			0.84			52.29				46.87						
525139(3)_pt3	0.00			0.61			50.85				48.53						
525139(3)_pt4	0.00			2.67			52.77				44.56						
525139(3)_pt5	0.00				32.41								67.59				
525139(3)_pt6	0.00		0.77	3.33	4.22		47.18				44.50						
525139(3)_pt7	0.00			0.96	0.15		50.96				47.93						
525139(3)_pt8	0.00			0.58	0.15	40.87			1.47					12.37	29.77	9.71	5.09
525139(3)_pt9	0.00		5.28	6.41	30.24				0.53		15.93		41.60				
525139(3)_pt10	0.00		14.05	19.52	38.75			9.52		2.55	15.56	0.04					
525139(3)_pt11	0.00				100.00												
525139(3)_pt12	0.00	9.58		22.96	63.14				4.33								

Minerals, 525139(3)
pt1: Pyrrhotite
pt2: Pyrrhotite
pt3: Pyrrhotite
pt4: Pyrrhotite
pt5: Zircon
pt6: Pyrrhotite
pt7: Pyrrhotite
pt8: Monazite
pt9: Zircon (+mixed signal/edge effect)
pt10: Biotite
pt11: Quartz
pt12: Feldspar - plagioclase

525139(4)

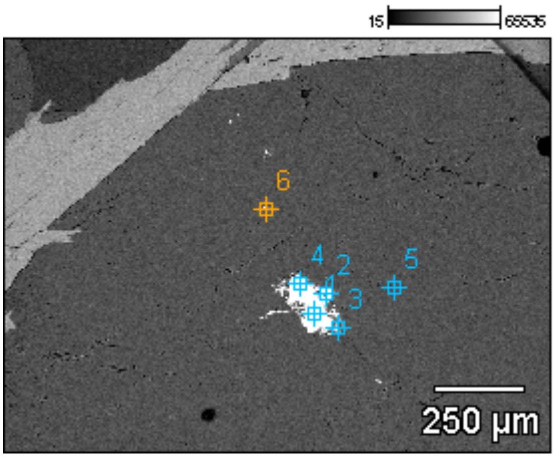

Image name: 525139(4)
Magnification: 80

Full scale counts: 5724 525139(4)_pt1

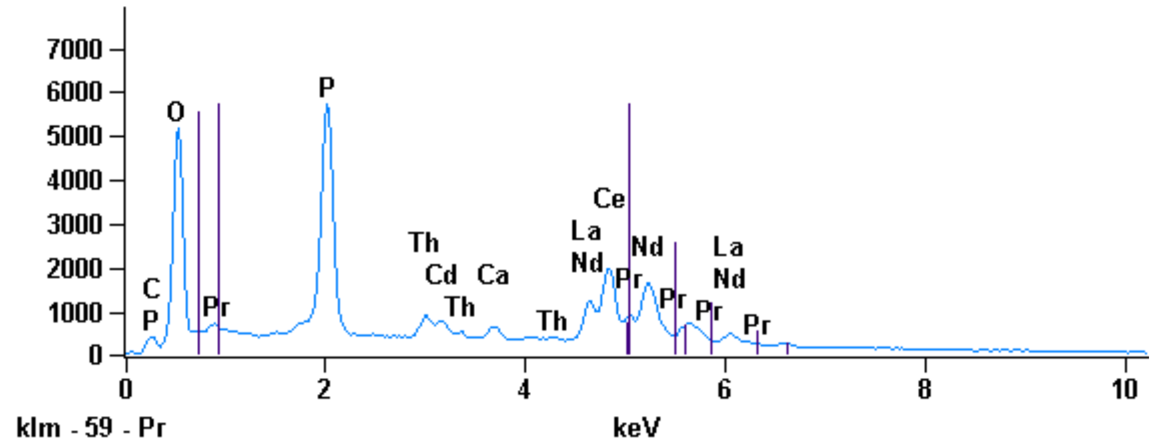

Full scale counts: 11809 525139(4)_pt2

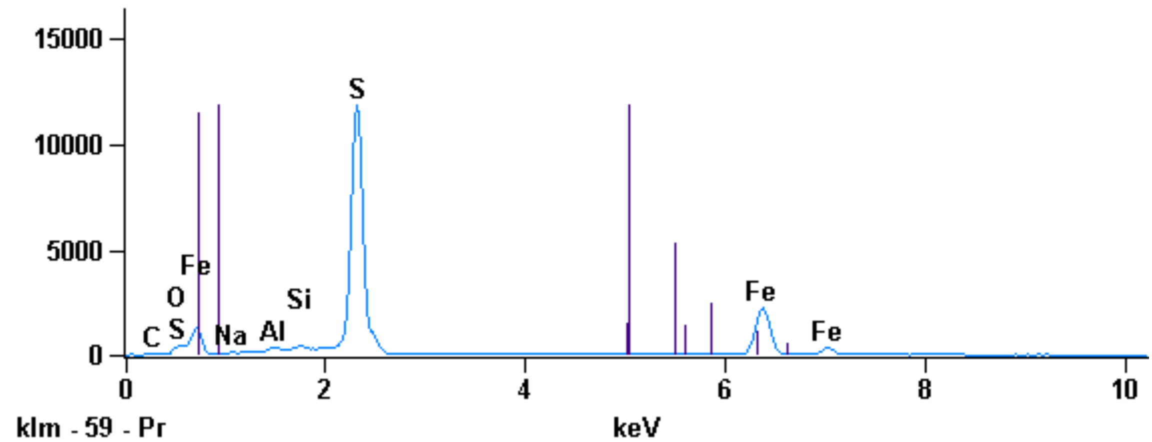

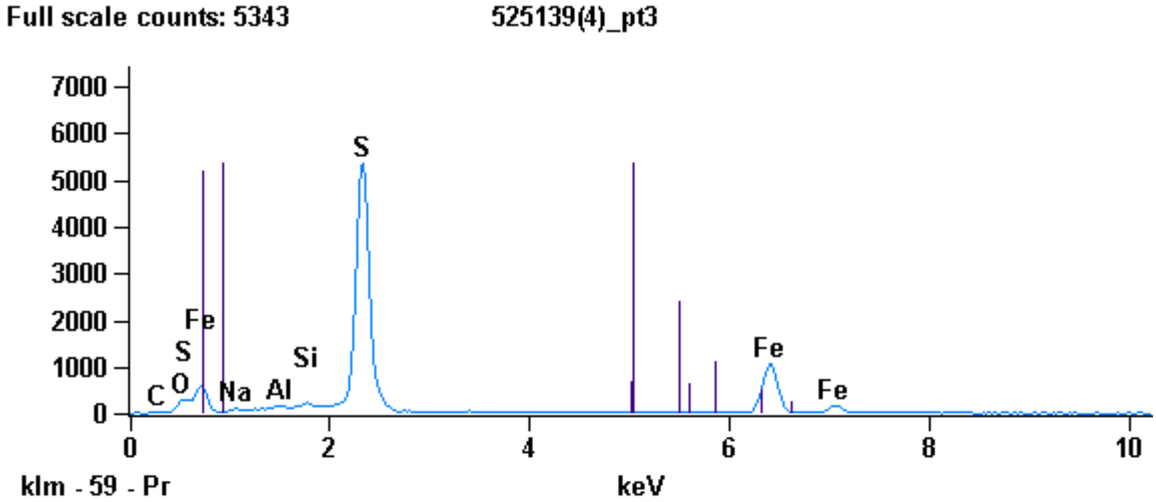
Full scale counts: 5343
525139(4)_pt3
7000
6000
5000
4000
3000
2000
1000
0
C
O
S
Fe
Na
Al
Si
S
Fe
Fe
0
2
4
6
8
10
klm - 59 - Pr
keV

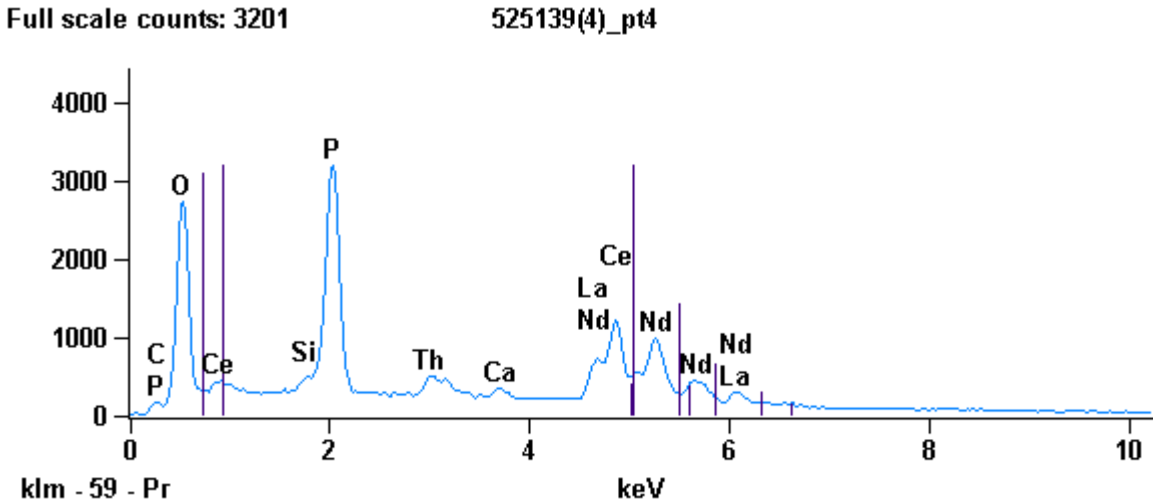
Full scale counts: 3201
525139(4)_pt4
4000
3000
2000
1000
0
P
C
O
Ce
Si
P
Th
Ca
Nd
La
Ce
Nd
Nd
Nd
La
0
2
4
6
8
10
klm - 59 - Pr
keV

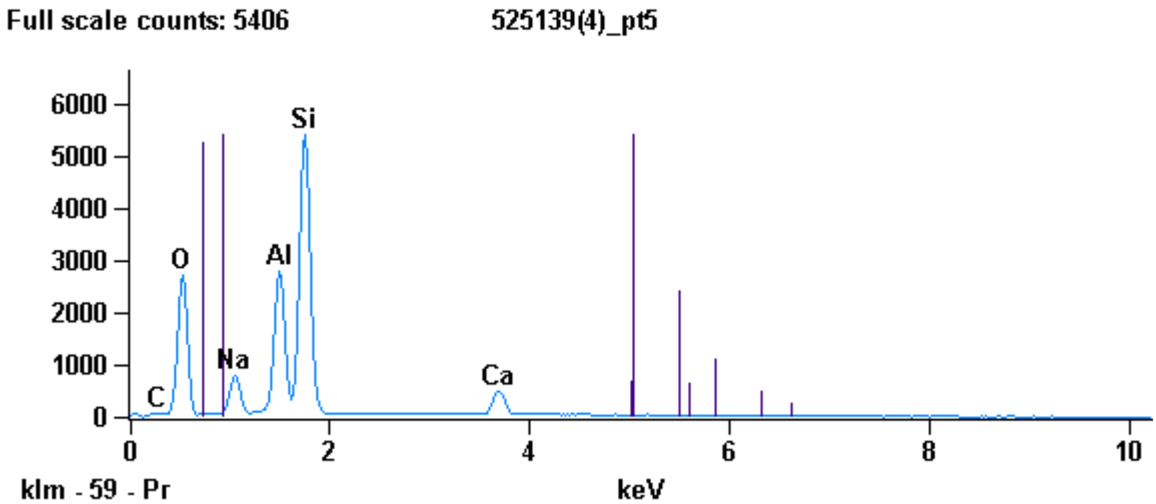
Full scale counts: 5406
525139(4)_pt5
6000
5000
4000
3000
2000
1000
0
C
O
Na
Al
Si
Ca
0
2
4
6
8
10
klm - 59 - Pr
keV

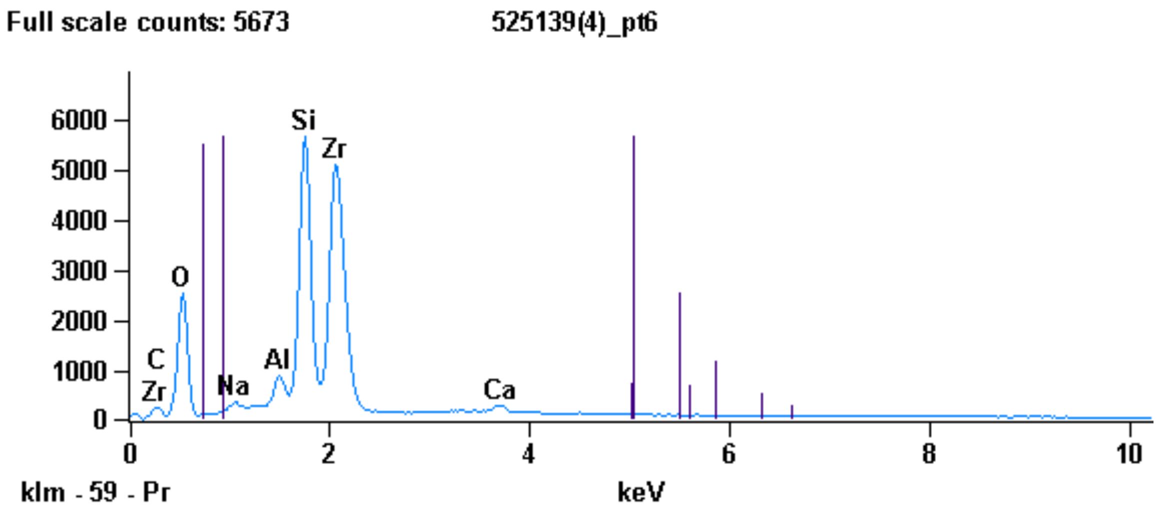

Weight %

	O-K	Na-K	Al-K	Si-K	P-K	S-K	Ca-K	Fe-K	Zr-L	Cd-L	La-L	Ce-L	Nd-L	Th-L
525139(4)_pt1	32.80S				18.77		1.41			0.84	9.47	27.13	9.59	0.00
525139(4)_pt2	50.20S	0.18	0.34	0.53		26.50		22.26						
525139(4)_pt3	50.20S	0.34	0.16	0.42		26.65		22.22						
525139(4)_pt4	28.54S			0.26	14.67		0.93				9.69	20.42	8.16	17.32
525139(4)_pt5	48.01S	6.37	12.80	28.78			4.04							
525139(4)_pt6	35.87S	1.05	1.57	15.86			0.67		44.98					

Atom %

	O-K	Na-K	Al-K	Si-K	P-K	S-K	Ca-K	Fe-K	Zr-L	Cd-L	La-L	Ce-L	Nd-L	Th-L
525139(4)_pt1	67.73				20.02		1.16			0.25	2.25	6.40	2.20	0.00
525139(4)_pt2	71.28	0.17	0.28	0.43		18.78		9.06						
525139(4)_pt3	71.26	0.34	0.14	0.34		18.88		9.04						
525139(4)_pt4	67.65			0.35	17.97		0.88				2.65	5.53	2.15	2.83
525139(4)_pt5	61.52	5.68	9.73	21.01			2.06							
525139(4)_pt6	65.55	1.34	1.70	16.51			0.49		14.41					

Compound %

		Na2O	Al2O3	SiO2	P2O5	SO3	CaO	Fe2O3	ZrO2	CdO	La2O3	Ce2O3	Nd2O3	ThO2
525139(4)_pt1	0.00				43.00		1.97			0.96	11.10	31.78	11.18	0.00
525139(4)_pt2	0.00	0.24	0.64	1.12		66.17		31.83						
525139(4)_pt3	0.00	0.46	0.31	0.90		66.56		31.77						
525139(4)_pt4	0.00			0.56	33.62		1.30				11.37	23.92	9.52	19.71
525139(4)_pt5	0.00	8.59	24.19	61.58			5.65							
525139(4)_pt6	0.00	1.42	2.97	33.93			0.93		60.75					

Minerals, 525139(4)
pt1: Monazite
pt2: Pyrite
pt3: Pyrite
pt4: Monazite
pt5: Feldspar - plagioclase
pt6: Zircon

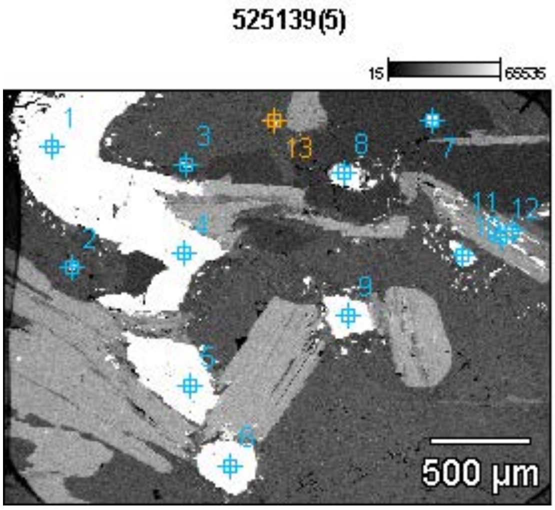

Image name: 525139(5)
Magnification: 44

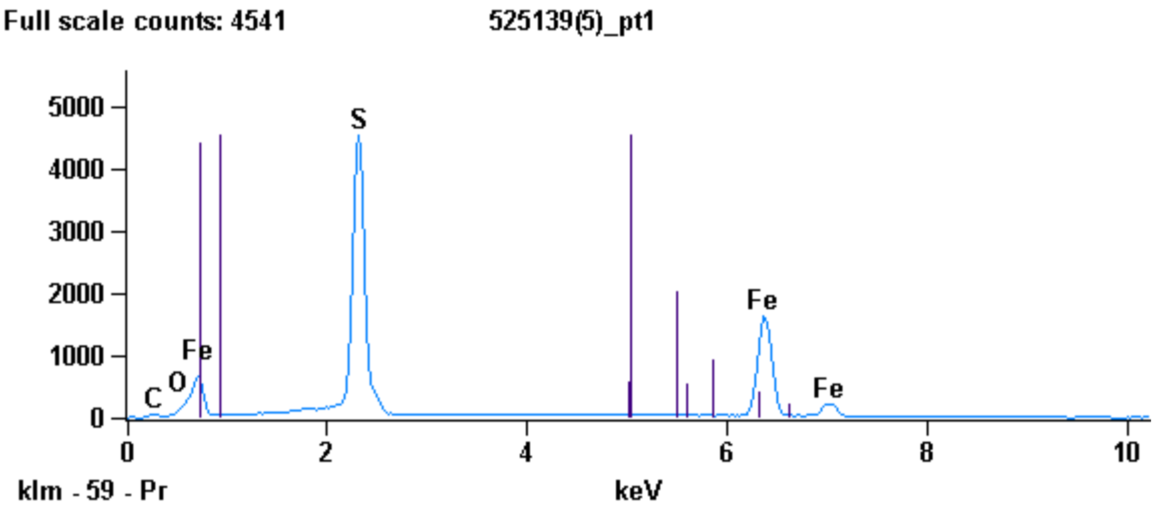

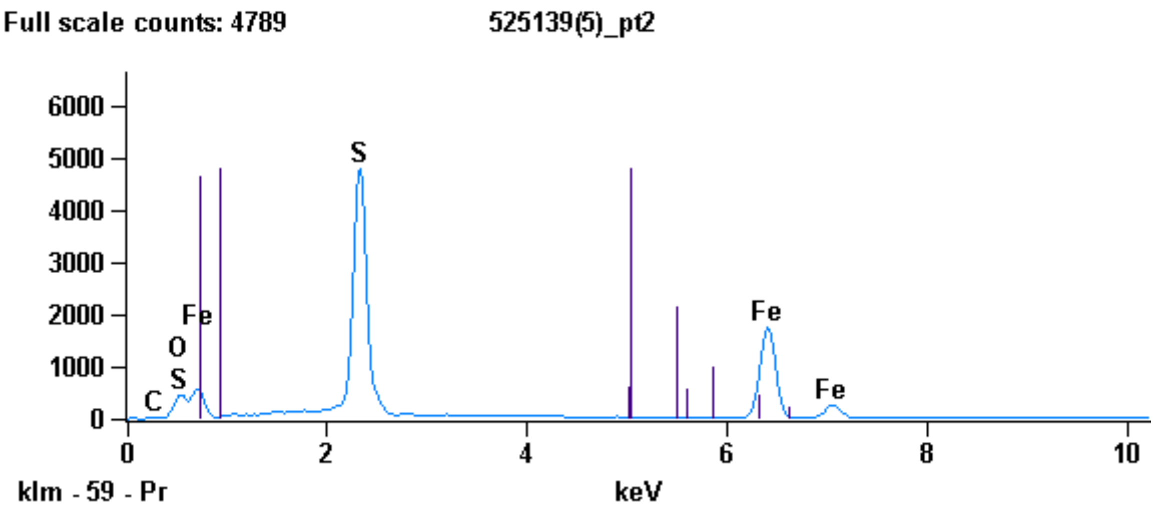

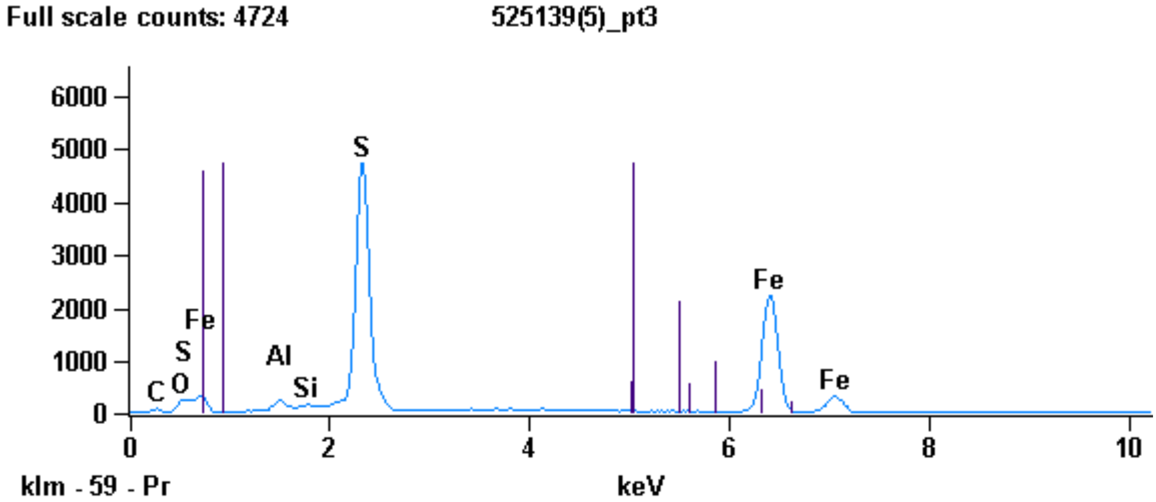
Full scale counts: 4724
525139(5)_pt3
6000
5000
4000
3000
2000
1000
0
C
O
S
Fe
Al
Si
S
Fe
Fe
0
2
4
6
8
10
klm - 59 - Pr
keV

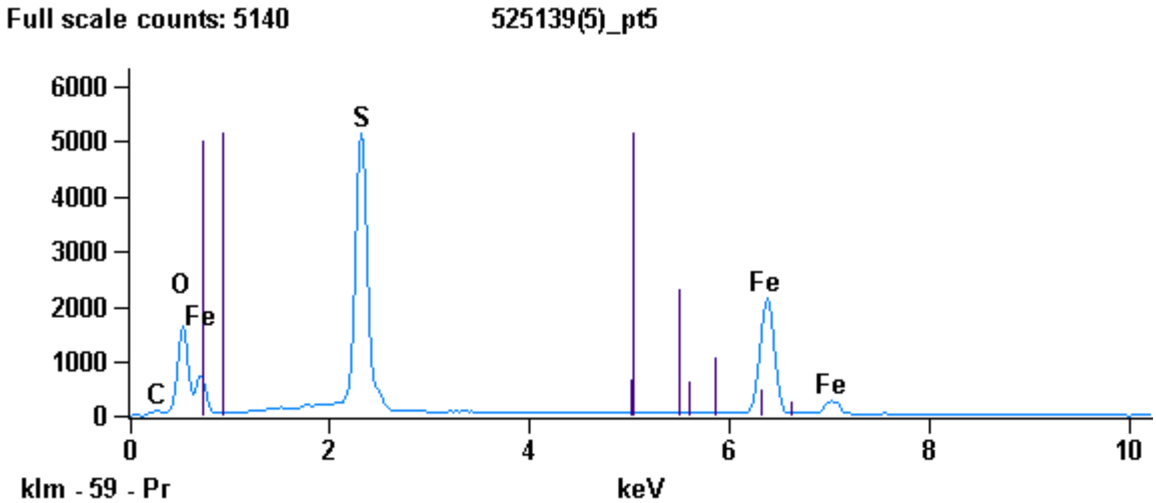
Full scale counts: 5140
525139(5)_pt5
6000
5000
4000
3000
2000
1000
0
C
O
Fe
S
Fe
Fe
0
2
4
6
8
10
klm - 59 - Pr
keV

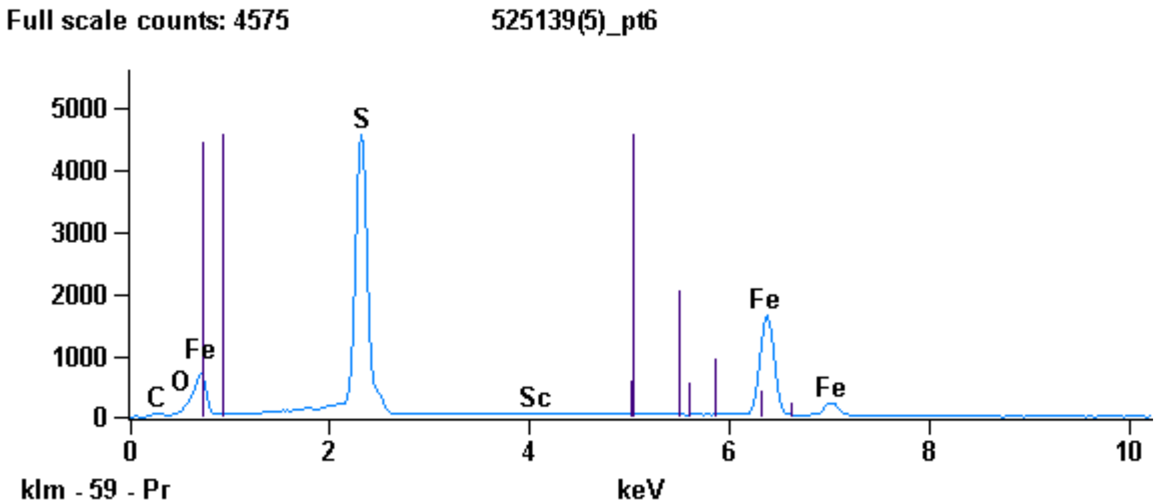
Full scale counts: 4575
525139(5)_pt6
5000
4000
3000
2000
1000
0
C
O
Fe
S
Sc
Fe
Fe
0
2
4
6
8
10
klm - 59 - Pr
keV

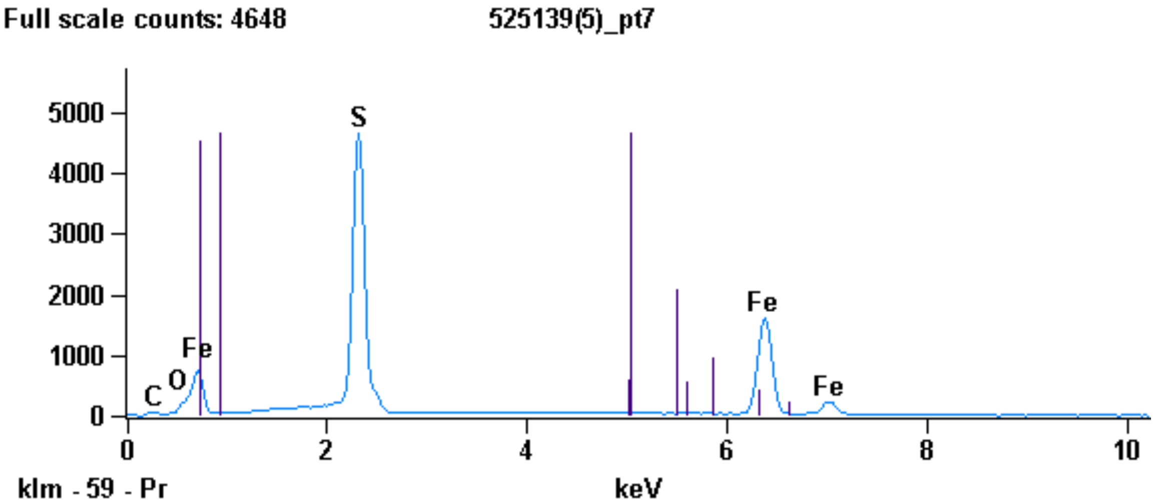
Full scale counts: 4648
525139(5)_pt7
5000
4000
3000
2000
1000
0
S
Fe
Fe
O
C
Fe
0
2
4
6
8
10
klm - 59 - Pr
keV

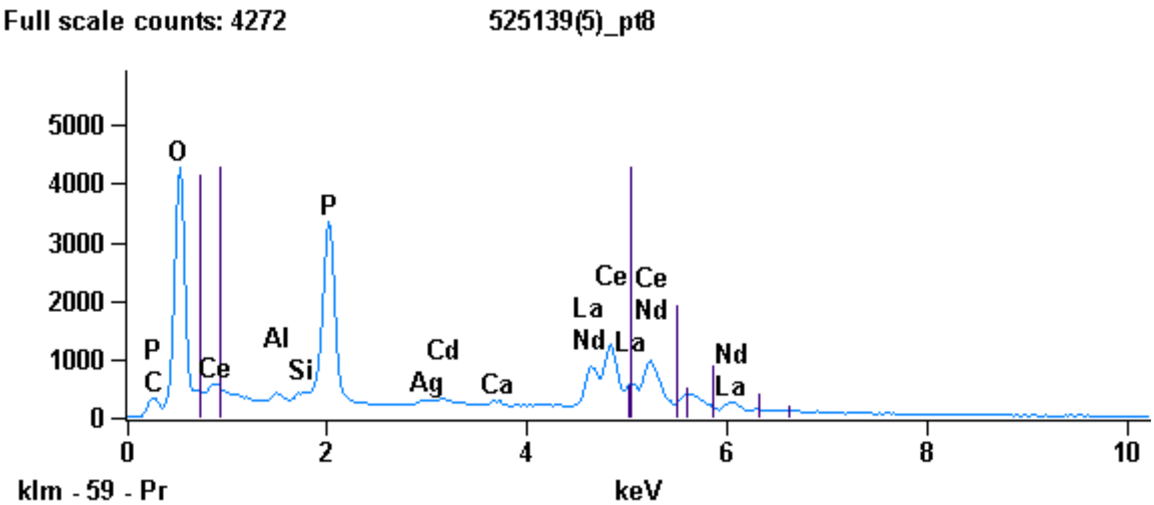
Full scale counts: 4272
525139(5)_pt8
5000
4000
3000
2000
1000
0
O
P
P
C
Ce
Al
Si
Cd
Ag
Ca
Ce
La
Nd
Ce
Nd
La
Nd
La
0
2
4
6
8
10
klm - 59 - Pr
keV

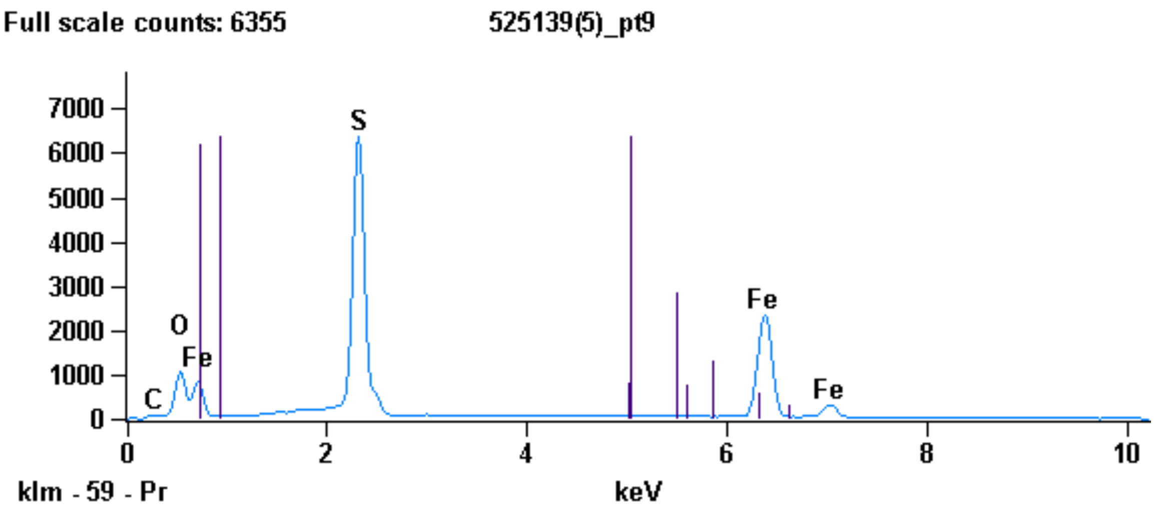
Full scale counts: 6355
525139(5)_pt9
7000
6000
5000
4000
3000
2000
1000
0
S
Fe
O
Fe
C
Fe
0
2
4
6
8
10
klm - 59 - Pr
keV

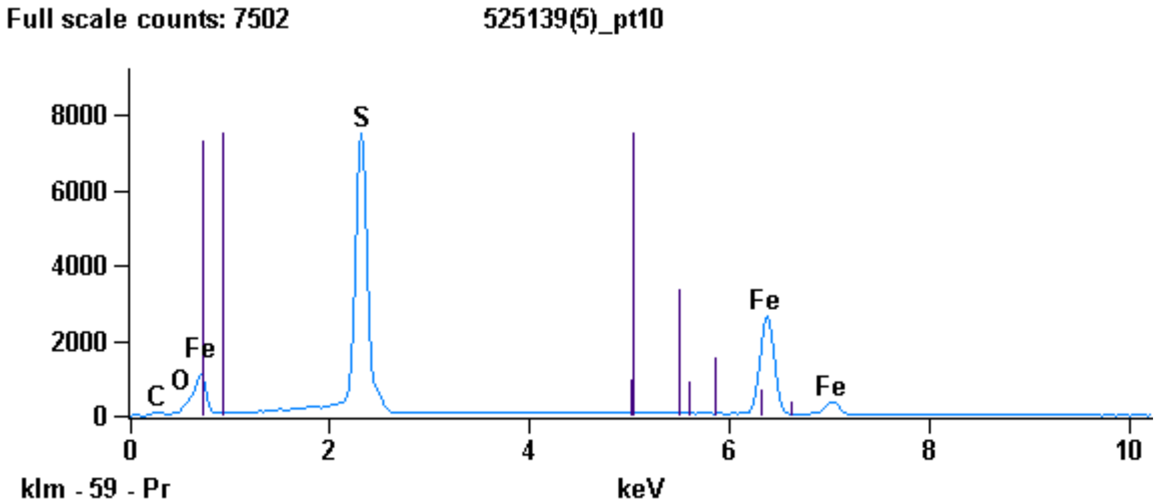
Full scale counts: 7502
525139(5)_pt10
8000
6000
4000
2000
0
S
Fe
Fe
C
O
Fe
0
2
4
6
8
10
klm - 59 - Pr
keV

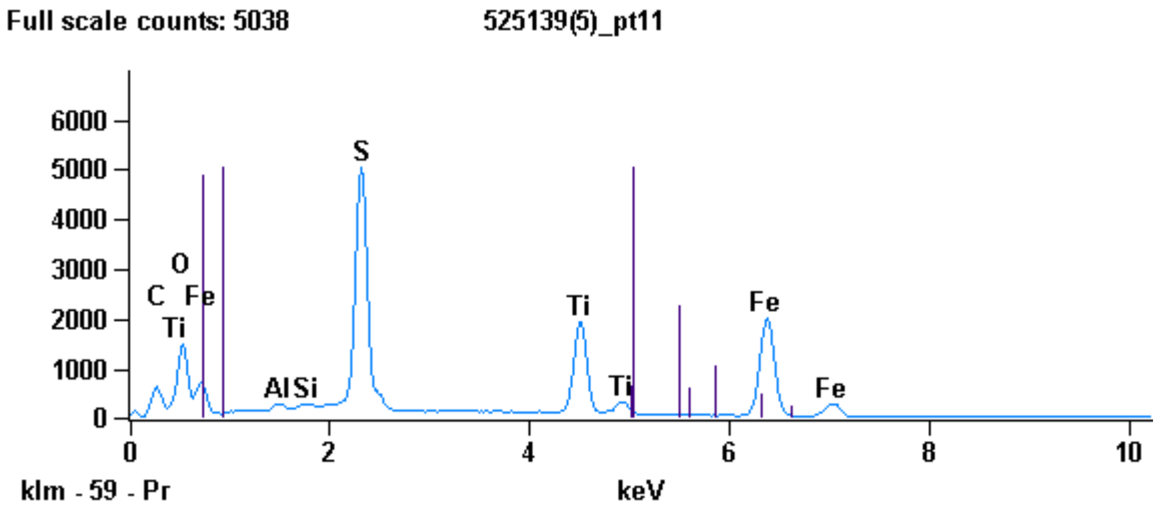
Full scale counts: 5038
525139(5)_pt11
6000
5000
4000
3000
2000
1000
0
S
O
C
Fe
Ti
Ti
Fe
AlSi
Ti
Fe
0
2
4
6
8
10
klm - 59 - Pr
keV

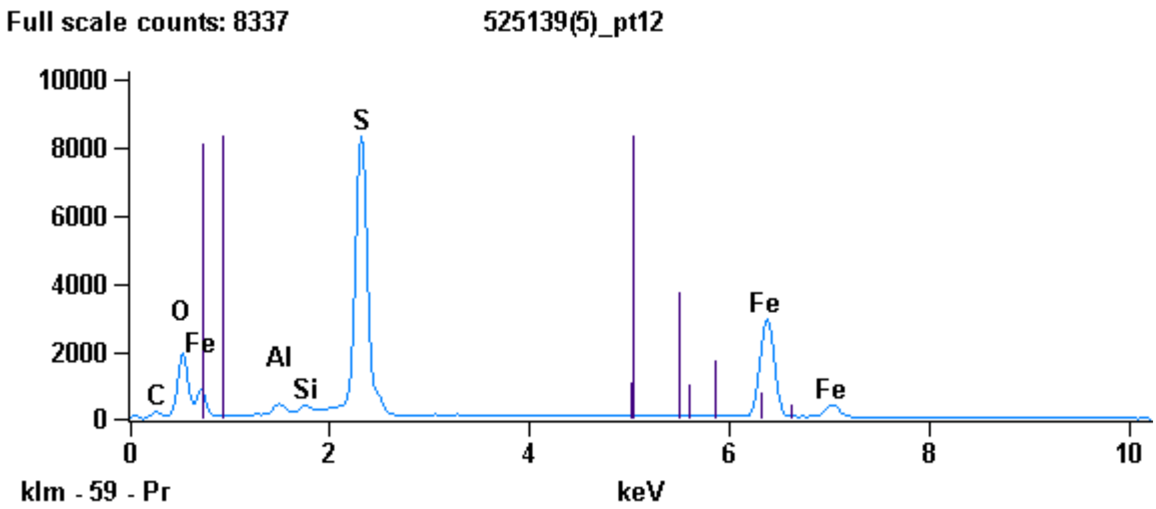
Full scale counts: 8337
525139(5)_pt12
10000
8000
6000
4000
2000
0
S
O
Fe
C
Al
Si
Fe
Fe
0
2
4
6
8
10
klm - 59 - Pr
keV

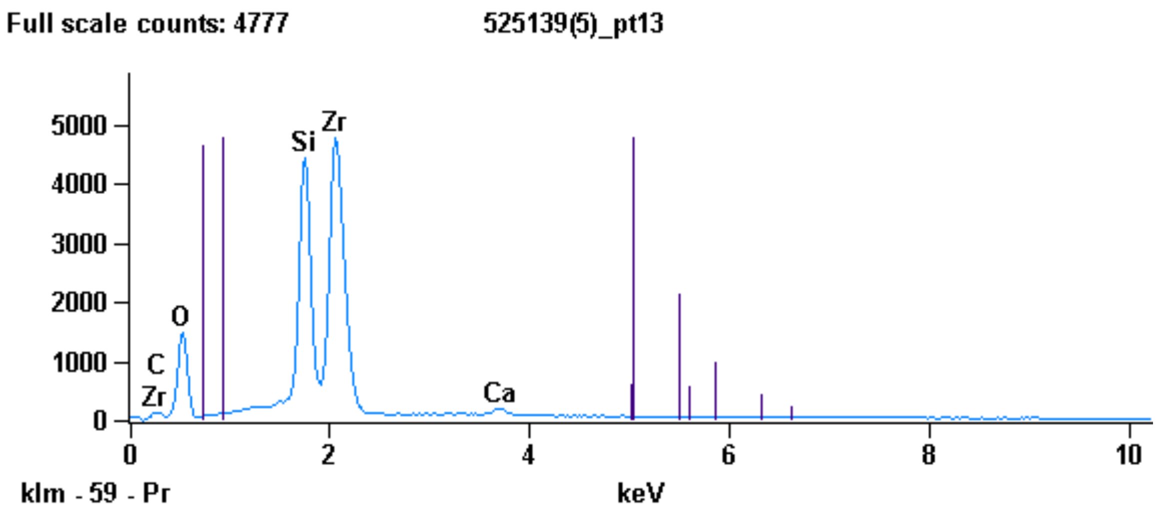
Full scale counts: 4777
525139(5)_pt13
5000
4000
3000
2000
1000
0
Si
Zr
O
C
Zr
Ca
0
2
4
6
8
10
klm - 59 - Pr
keV

Weight %

	O-K	*Al-K*	*Si-K*	*P-K*	*S-K*	*K-K*	*Ca-K*	*Sc-K*	*Ti-K*	*Fe-K*	*Zr-L*	*Ag-L*	*Cd-L*	*La-L*	*Ce-L*	*Nd-L*
525139(5)_pt 1	45.83S				21.13					33.04						
525139(5)_pt 2	46.08S				21.47					32.45						
525139(5)_pt 3	44.36S	0.77	0.19		18.70					35.98						
525139(5)_pt 4	46.36S		0.11		21.78	0.09				31.66						
525139(5)_pt 5	44.78S				19.72					35.49						
525139(5)_pt 6	45.75S				21.01			0.05		33.19						
525139(5)_pt 7	46.18S				21.59					32.23						
525139(5)_pt 8	31.60S	0.68	0.02	17.31			0.55					1.01	0.69	12.98	27.75	7.40
525139(5)_pt 9	45.47S				20.65					33.88						
525139(5)_pt 10	45.93S				21.27					32.80						
525139(5)_pt 11	43.94S	0.30	0.15		15.66				12.13	27.83						
525139(5)_pt 12	46.07S	0.76	0.29		20.92					31.96						
525139(5)_pt 13	34.58S		14.72				0.57				50.13					

Atom %

	O-K	*Al-K*	*Si-K*	*P-K*	*S-K*	*K-K*	*Ca-K*	*Sc-K*	*Ti-K*	*Fe-K*	*Zr-L*	*Ag-L*	*Cd-L*	*La-L*	*Ce-L*	*Nd-L*
525139(5)_pt 1	69.61				16.02					14.37						
525139(5)_pt 2	69.73				16.21					14.07						
525139(5)_pt 3	68.71	0.71	0.17		14.45					15.97						
525139(5)_pt 4	69.82		0.10		16.37	0.05				13.66						
525139(5)_pt 5	69.11				15.19					15.69						
525139(5)_pt 6	69.57				15.95			0.03		14.46						
525139(5)_pt 7	69.77				16.28					13.95						
525139(5)_pt 8	67.36	0.87	0.03	19.05			0.47					0.32	0.21	3.19	6.75	1.75
525139(5)_pt 9	69.44				15.74					14.82						
525139(5)_pt 10	69.66				16.09					14.25						
525139(5)_pt 11	68.61	0.28	0.13		12.20				6.32	12.45						
525139(5)_pt 12	69.50	0.68	0.25		15.75					13.81						
525139(5)_pt 13	66.52		16.13				0.43				16.91					

Compound %

		Al2O3	SiO2	P2O5	SO3	K2O	CaO	Sc2O3	TiO2	Fe2O3	ZrO2	Ag2O	CdO	La2O3	Ce2O3	Nd2O3
525139(5)_pt 1	0.00				52.77					47.23						
525139(5)_pt 2	0.00				53.61					46.39						
525139(5)_pt 3	0.00	1.45	0.41		46.70					51.45						
525139(5)_pt 4	0.00		0.24		54.39	0.10				45.27						
525139(5)_pt 5	0.00				49.25					50.75						
525139(5)_pt 6	0.00				52.47			0.08		47.45						
525139(5)_pt 7	0.00				53.92					46.08						
525139(5)_pt 8	0.00	1.29	0.05	39.65			0.77					1.09	0.79	15.23	32.50	8.63
525139(5)_pt 9	0.00				51.56					48.44						
525139(5)_pt 10	0.00				53.10					46.90						
525139(5)_pt 11	0.00	0.57	0.32		39.10				20.22	39.79						
525139(5)_pt 12	0.00	1.44	0.62		52.24					45.69						
525139(5)_pt 13	0.00		31.49				0.79				67.72					

Minerals, 525139(5)

pt1: Pyrrhotite
pt2: Pyrrhotite
pt3: Pyrrhotite
pt4: Pyrrhotite
pt5: Pyrrhotite
pt6: Pyrrhotite
pt7: Pyrrhotite
pt8: Monazite
pt9: Pyrrhotite
pt10: Pyrrhotite
pt11: Pyrrhotite
pt12: Pyrrhotite
pt13: Zircon

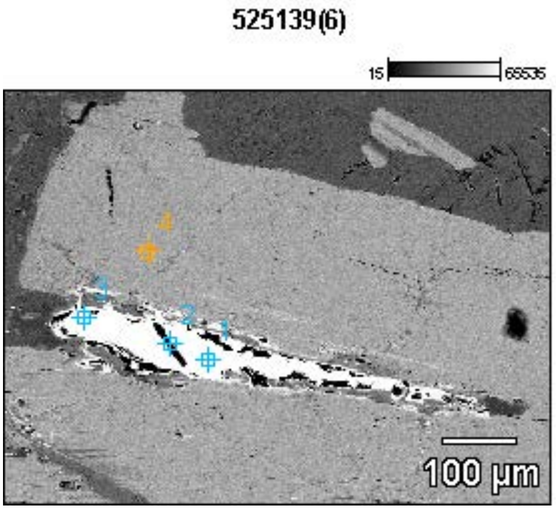

Image Name: 525139(6)

Magnification: 162

Image name: 525139(6)
Magnification: 162

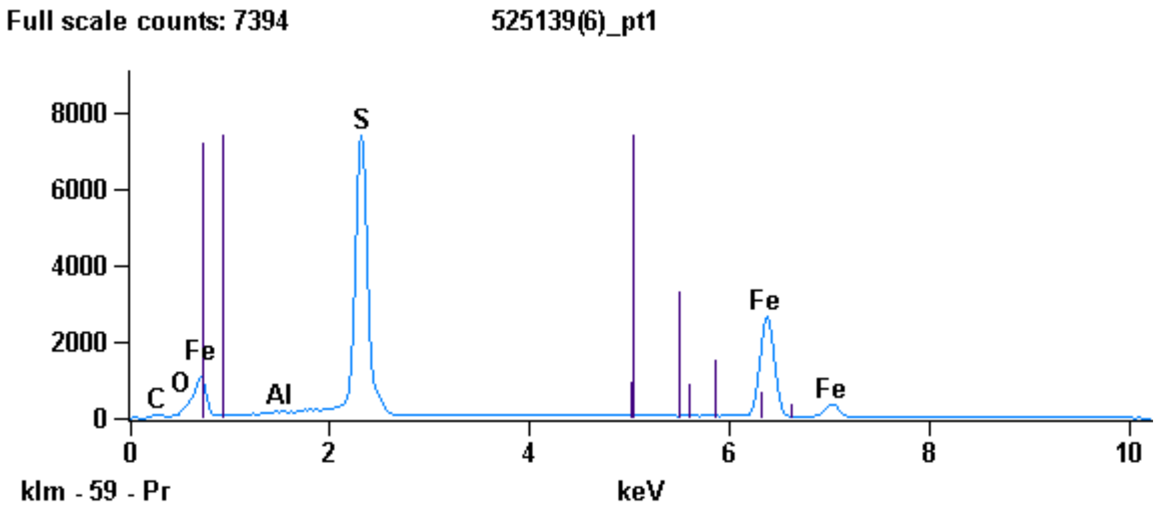

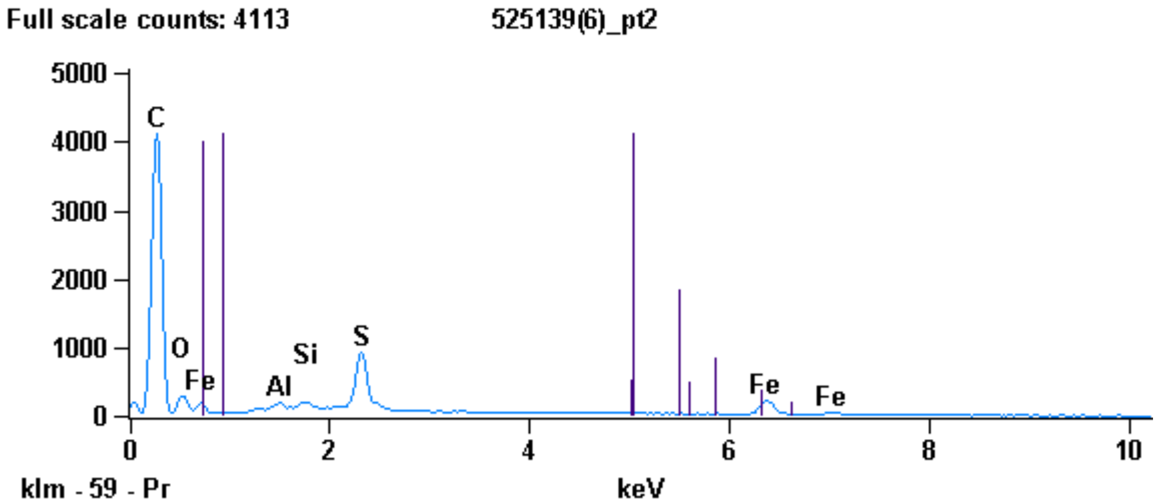

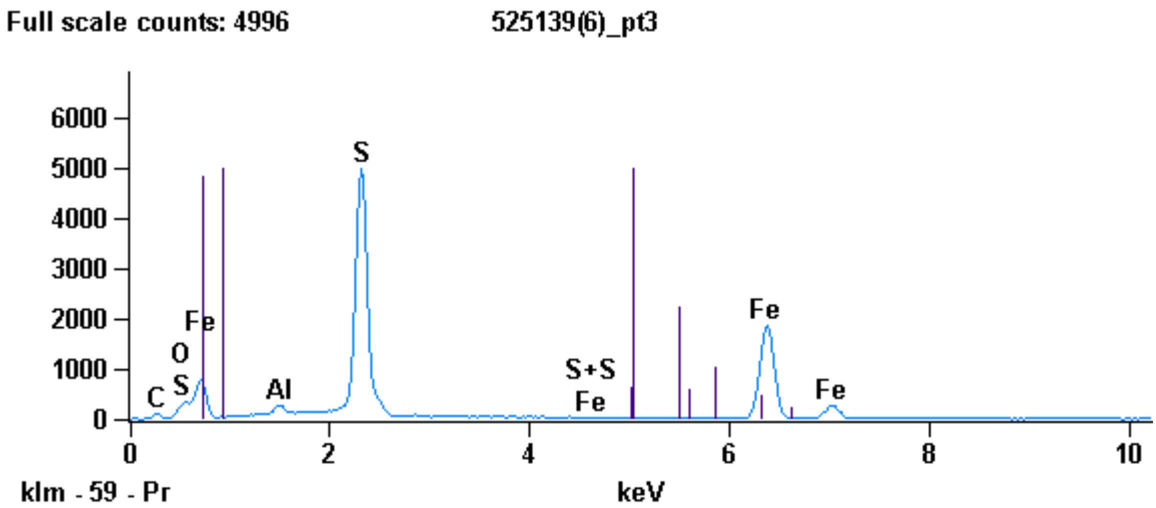
Full scale counts: 4996
525139(6)_pt3
6000
5000
4000
3000
2000
1000
0
C
S
O
Fe
Al
S
S+S
Fe
Fe
Fe
0
2
4
6
8
10
klm - 59 - Pr
keV

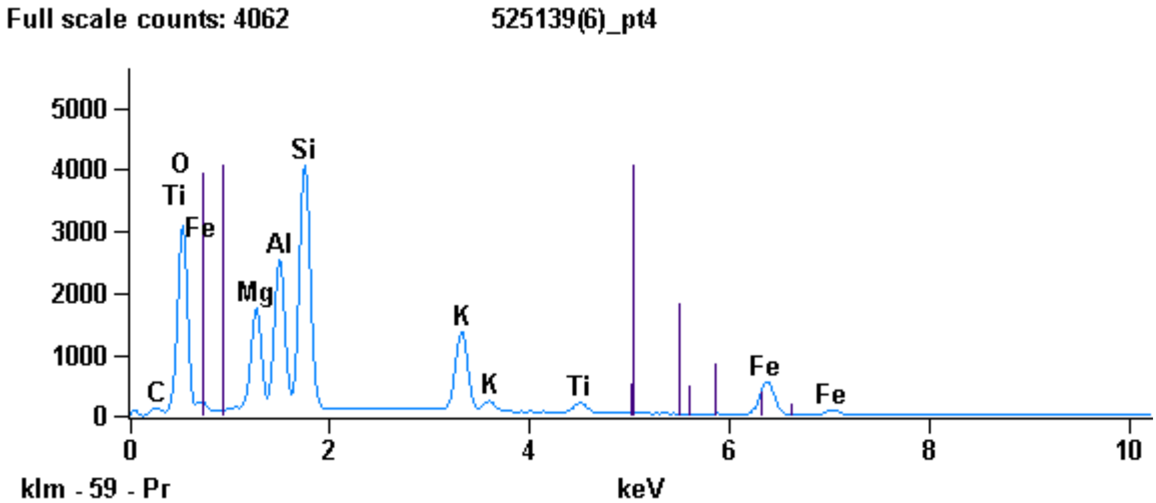
Full scale counts: 4062
525139(6)_pt4
5000
4000
3000
2000
1000
0
C
O
Ti
Fe
Mg
Al
Si
K
K
Ti
Fe
Fe
0
2
4
6
8
10
klm - 59 - Pr
keV

Weight %

	O-K	Mg-K	Al-K	Si-K	S-K	K-K	Ti-K	Fe-K
525139(6)_pt1	45.85S		0.06		21.12			32.96
525139(6)_pt2	48.34S		1.45	2.02	22.52			25.67
525139(6)_pt3	45.41S		0.77		20.23			33.58
525139(6)_pt4	42.71S	8.18	10.32	18.23		8.06	1.46	11.04

Atom %

	O-K	Mg-K	Al-K	Si-K	S-K	K-K	Ti-K	Fe-K
525139(6)_pt1	69.60		0.06		16.00			14.34
525139(6)_pt2	70.11		1.25	1.67	16.30			10.67
525139(6)_pt3	69.24		0.70		15.40			14.67
525139(6)_pt4	59.69	7.52	8.55	14.52		4.61	0.68	4.42

Compound %

		MgO	Al2O3	SiO2	SO3	K2O	TiO2	Fe2O3
525139(6)_pt1	0.00		0.12		52.75			47.13
525139(6)_pt2	0.00		2.74	4.32	56.23			36.71
525139(6)_pt3	0.00		1.46		50.53			48.01
525139(6)_pt4	0.00	13.56	19.49	39.01		9.71	2.44	15.79

Minerals, 525139(6)
pt1: Pyrrhotite
pt2: Pyrrhotite (+mixed signal/edge effect)
pt3: Pyrrhotite
pt4: Biotite

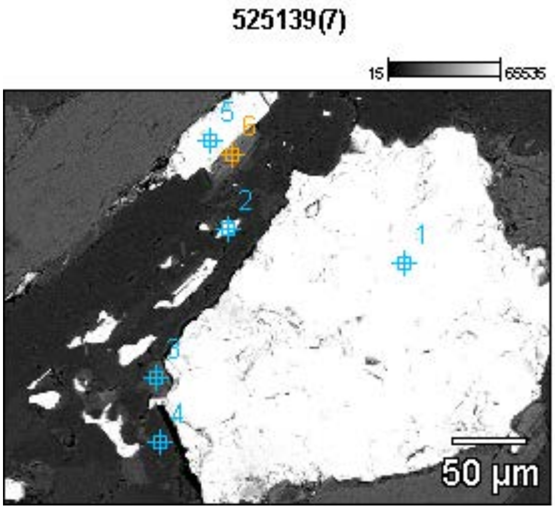

Image name: 525139(7)
Magnification: 325

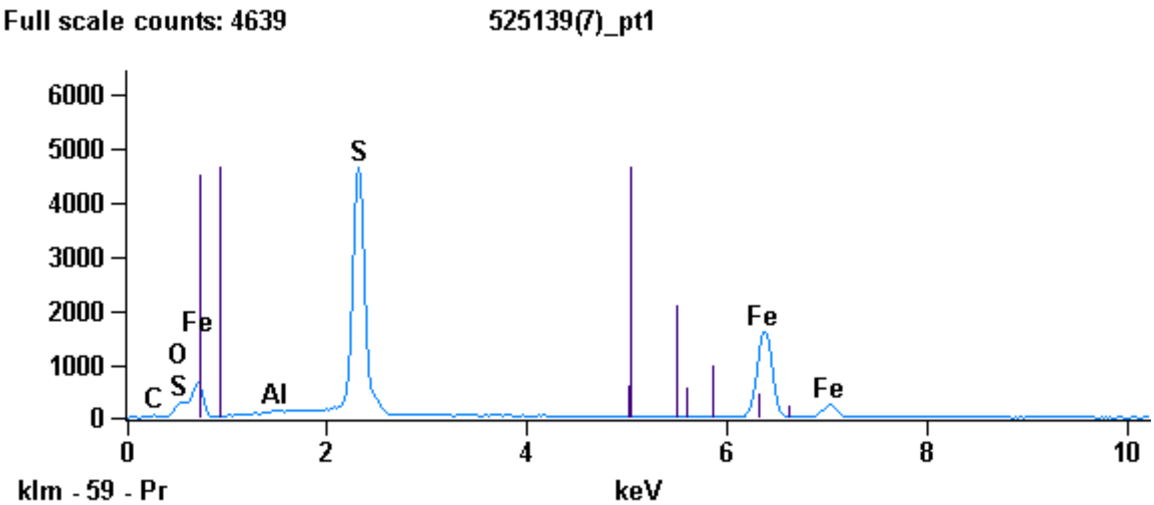

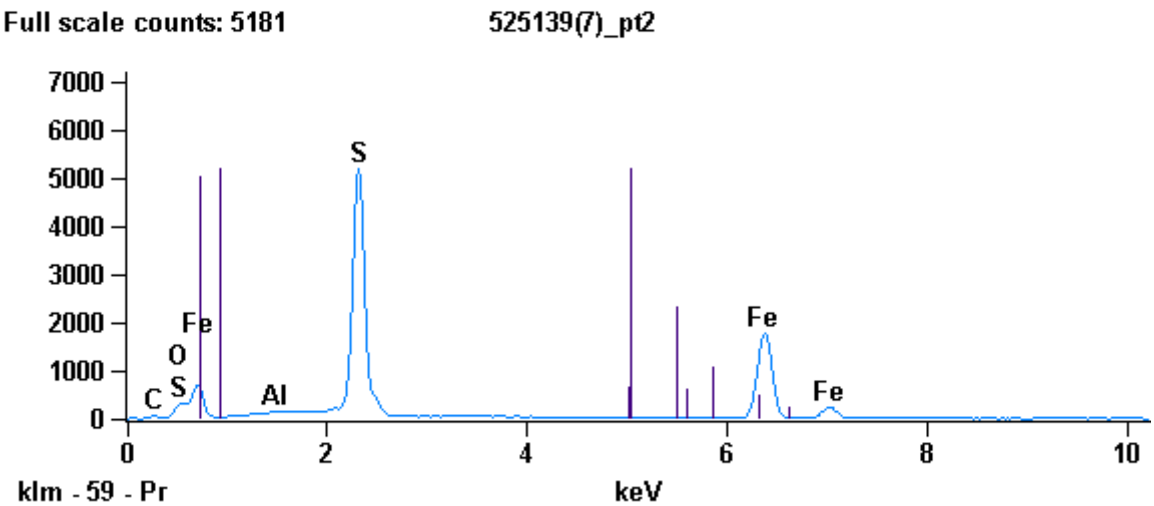

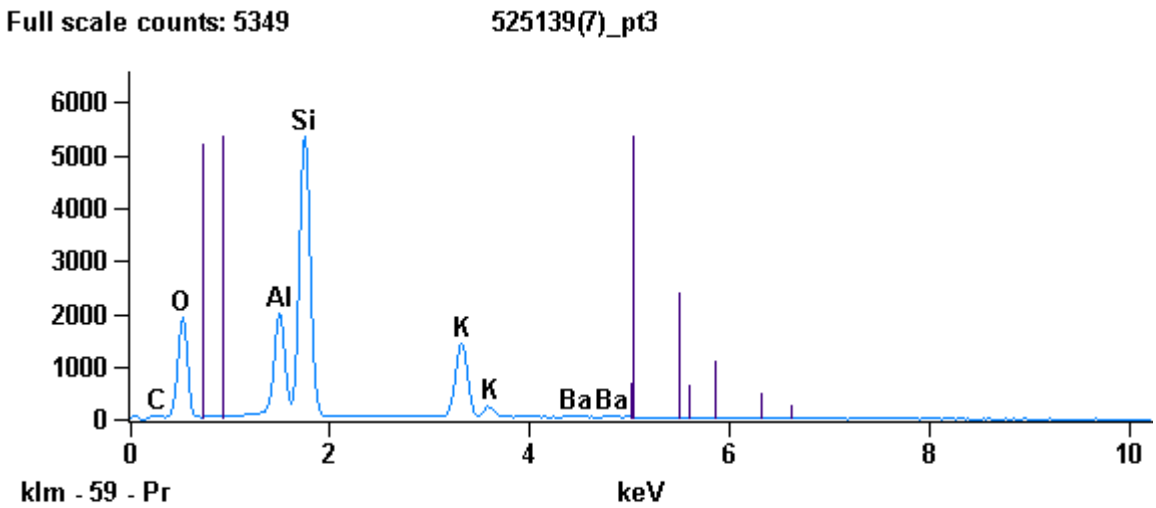
Full scale counts: 5349
525139(7)_pt3
6000
5000
4000
3000
2000
1000
0
Si
O
Al
K
C
K
BaBa
0
2
4
6
8
10
klm - 59 - Pr
keV

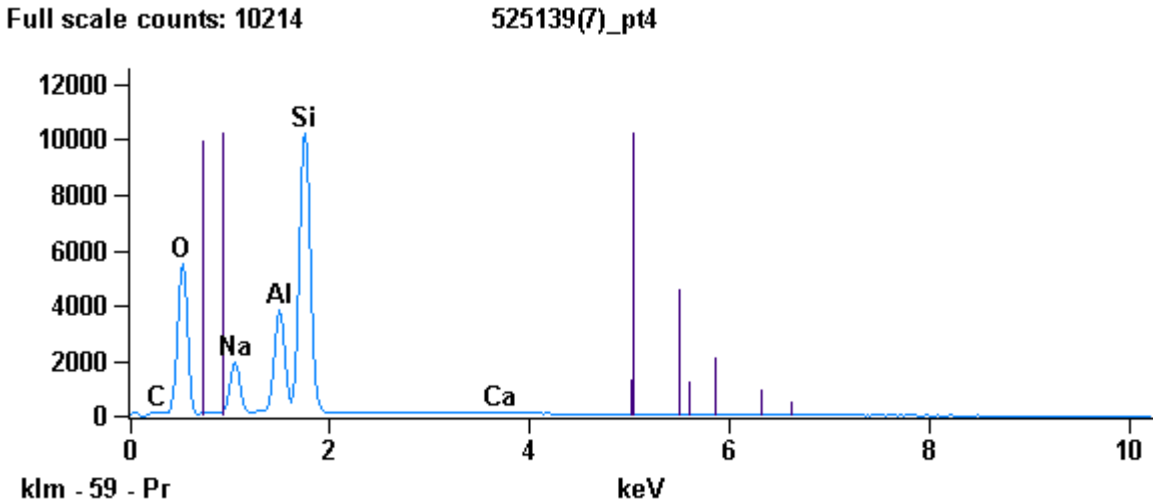
Full scale counts: 10214
525139(7)_pt4
12000
10000
8000
6000
4000
2000
0
Si
O
Al
Na
C
Ca
0
2
4
6
8
10
klm - 59 - Pr
keV

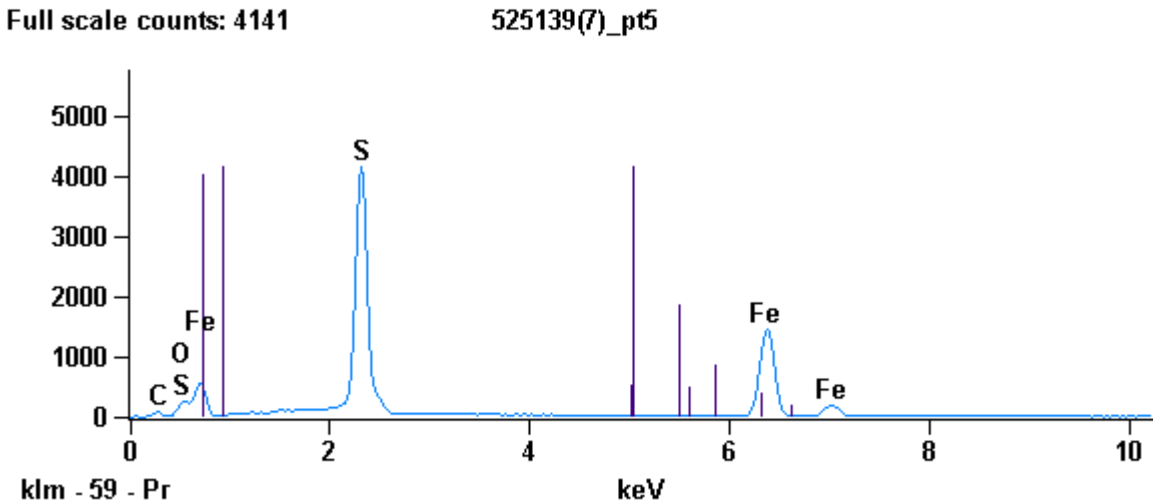
Full scale counts: 4141
525139(7)_pt5
5000
4000
3000
2000
1000
0
S
Fe
Fe
O
C
S
Fe
0
2
4
6
8
10
klm - 59 - Pr
keV

Weight %

	O-K	Na-K	Mg-K	Al-K	Si-K	S-K	K-K	Ca-K	Fe-K	Ba-L
525139(7)_pt1	45.96S			0.08		21.26			32.70	
525139(7)_pt2	46.02S			0.10		21.33			32.55	
525139(7)_pt3	45.69S			9.66	30.09		12.73			1.82
525139(7)_pt4	48.67S	8.81		10.33	31.83			0.36		
525139(7)_pt5	45.81S					21.10			33.09	
525139(7)_pt6	41.35S		0.41	12.71	14.97		1.83		28.72	

Atom %

	O-K	Na-K	Mg-K	Al-K	Si-K	S-K	K-K	Ca-K	Fe-K	Ba-L
525139(7)_pt1	69.65			0.07		16.08			14.20	
525139(7)_pt2	69.67			0.09		16.12			14.12	
525139(7)_pt3	61.76			7.74	23.17		7.04			0.29
525139(7)_pt4	61.45	7.74		7.74	22.89			0.18		
525139(7)_pt5	69.60					16.00			14.40	
525139(7)_pt6	62.03		0.40	11.31	12.79		1.12		12.34	

Compound %

		Na2O	MgO	Al2O3	SiO2	SO3	K2O	CaO	Fe2O3	BaO
525139(7)_pt1	0.00			0.15		53.09			46.75	
525139(7)_pt2	0.00			0.19		53.27			46.54	
525139(7)_pt3	0.00			18.25	64.38		15.34			2.04
525139(7)_pt4	0.00	11.87		19.53	68.09			0.51		
525139(7)_pt5	0.00					52.69			47.31	
525139(7)_pt6	0.00		0.67	24.02	32.03		2.21		41.07	

Minerals, 525139(7)
pt1: Pyrrhotite
pt2: Pyrrhotite
pt3: Alkali feldspar - microcline
pt4: Plagioclase
pt5: Pyrrhotite
pt6: Biotite

Sample	**525137**						
Spot number	91	92	93	94	99	100	101
SiO_2	37.63	37.13	37.35	37.40	37.20	36.36	37.02
TiO_2	2.550	2.560	2.610	2.650	3.010	2.840	2.960
Al_2O_3	19.74	19.44	19.56	19.42	19.23	19.07	19.10
FeO	14.77	14.48	14.84	14.53	14.47	14.88	14.59
MnO	0.23	0.16	0.13	0.20	0.18	0.13	0.20
MgO	12.44	12.41	12.44	12.57	12.62	12.73	12.52
CaO	0.00	0.01	0.01	0.01	0.02	0.00	0.00
Na_2O	0.12	0.12	0.09	0.14	0.09	0.07	0.11
K_2O	10.07	10.31	10.47	10.18	10.31	10.15	10.30
Cr_2O_3	0,065	0,043	0,066	0,008	0,074	0,051	0,051
NiO	0.013	0.000	0.015	0.024	0.019	0.025	0.011
Total	97.631	96.661	97.585	97.128	97.220	96.318	96.863

Reformatted oxide percentages, with H_2O calculated (22 O)							
SiO_2	37.63	37.13	37.35	37.40	37.20	36.36	37.02
TiO_2	2.550	2.560	2.610	2.650	3.010	2.840	2.960
Al_2O_3	19.74	19.44	19.56	19.42	19.23	19.07	19.10
FeO	14.77	14.48	14.84	14.53	14.47	14.88	14.59
MnO	0.23	0.16	0.13	0.20	0.18	0.13	0.20
MgO	12.44	12.41	12.44	12.57	12.62	12.73	12.52
CaO	0.00	0.01	0.01	0.01	0.02	0.00	0.00
Na_2O	0.12	0.12	0.09	0.14	0.09	0.07	0.11
K_2O	10.07	10.31	10.47	10.18	10.31	10.15	10.30
Cr_2O_3	0.065	0.043	0.066	0.008	0.074	0.051	0.051
NiO	0.013	0.000	0.015	0.024	0.019	0.025	0.011
H_2O*	4.14	4.09	4.12	4.11	4.11	4.06	4.09
Total	101.77	100.75	101.71	101.24	101.33	100.38	100.95

Numbers of ions on the basis of 22 (O, OH)							
Tetrahedral (T)							
Si	5.455	5.446	5.435	5.454	5.426	5.372	5.427
^{IV}Al	2.545	2.554	2.565	2.546	2.574	2.628	2.573
Octahedral (M)							
M1-site							
^{VI}Al	0.828	0.806	0.790	0.792	0.732	0.693	0.727
Ti	0.278	0.282	0.286	0.291	0.330	0.316	0.326
Cr	0.007	0.005	0.008	0.001	0.009	0.006	0.006
Sn	0.000	0.000	0.000	0.000	0.000	0.000	0.000
Ga	0.000	0.000	0.000	0.000	0.000	0.000	0.000
M2-site							
Fe^{2+}	1.791	1.776	1.806	1.772	1.765	1.839	1.789
Ni	0.002	0.000	0.002	0.003	0.002	0.003	0.001
Mg	2.688	2.713	2.698	2.733	2.744	2.804	2.736
Mn	0.028	0.020	0.017	0.025	0.022	0.017	0.025
Cu	0.000	0.000	0.000	0.000	0.000	0.000	0.000
Zn	0.000	0.000	0.000	0.000	0.000	0.000	0.000
Interlayer (I)							
Ca	0.000	0.001	0.002	0.001	0.002	0.001	0.000
Na	0.035	0.035	0.024	0.040	0.027	0.021	0.032
K	1.862	1.929	1.943	1.894	1.918	1.913	1.926
Sr	0.005	0.004	0.006	0.001	0.006	0.004	0.004
Ba	0.001	0.000	0.001	0.001	0.001	0.001	0.001
Rb	0.000	0.000	0.000	0.000	0.000	0.000	0.000
Cs	0.000	0.000	0.000	0.000	0.000	0.000	0.000
Hyroxyl (OH)							
OH*	4.000	4.000	4.000	4.000	4.000	4.000	4.000
Total	19.525	19.571	19.582	19.552	19.559	19.616	19.573
End-member parameters							
Annite	40.0	39.6	40.1	39.3	39.1	39.6	39.5
Phlogopite	60.0	60.4	59.9	60.7	60.9	60.4	60.5

50.452598446 35,07746
64.922539509 49,5474

Sample	**525137**					
Spot number	102	111	112	113	114	118
SiO_2	36.65	37.20	37.04	37.14	37.23	37.27
TiO_2	2.850	2.690	2.750	2.780	2.690	2.430
Al_2O_3	19.07	19.47	19.37	19.40	19.42	19.67
FeO	14.71	14.78	15.10	15.11	14.98	14.16
MnO	0.19	0.20	0.16	0.21	0.24	0.24
MgO	12.58	12.75	12.57	12.53	12.76	12.72
CaO	0.01	0.00	0.01	0.01	0.00	0.01
Na_2O	0.12	0.09	0.14	0.13	0.10	0.12
K_2O	10.34	10.13	10.26	10.28	10.40	10.15
Cr_2O_3	0,062	0,042	0,048	0,058	0,044	0,062
NiO	0.000	0.000	0.012	0.000	0.000	0.024
Total	96.578	97.351	97.460	97.643	97.864	96.849

Reformatted oxide percentages, with H_2O calculated (22 O)						
SiO_2	36.65	37.20	37.04	37.14	37.23	37.27
TiO_2	2.850	2.690	2.750	2.780	2.690	2.430
Al_2O_3	19.07	19.47	19.37	19.40	19.42	19.67
FeO	14.71	14.78	15.10	15.11	14.98	14.16
MnO	0.19	0.20	0.16	0.21	0.24	0.24
MgO	12.58	12.75	12.57	12.53	12.76	12.72
CaO	0.01	0.00	0.01	0.01	0.00	0.01
Na_2O	0.12	0.09	0.14	0.13	0.10	0.12
K_2O	10.34	10.13	10.26	10.28	10.40	10.15
Cr_2O_3	0.062	0.042	0.048	0.058	0.044	0.062
NiO	0.000	0.000	0.012	0.000	0.000	0.024
H_2O*	4.07	4.12	4.11	4.12	4.13	4.11
Total	100.65	101.47	101.57	101.76	101.99	100.96

Numbers of ions on the basis of 22 (O, OH)						
Tetrahedral (T)						
Si	5.399	5.419	5.405	5.410	5.410	5.440
^{IV}Al	2.601	2.581	2.595	2.590	2.590	2.560
Octahedral (M)						
M1-site						
^{VI}Al	0.710	0.762	0.737	0.740	0.736	0.825
Ti	0.316	0.295	0.302	0.305	0.294	0.267
Cr	0.007	0.005	0.006	0.007	0.005	0.007
Sn	0.000	0.000	0.000	0.000	0.000	0.000
Ga	0.000	0.000	0.000	0.000	0.000	0.000
M2-site						
Fe^{2+}	1.812	1.801	1.843	1.841	1.820	1.729
Ni	0.000	0.000	0.001	0.000	0.000	0.003
Mg	2.762	2.769	2.734	2.721	2.764	2.768
Mn	0.024	0.025	0.020	0.026	0.030	0.030
Cu	0.000	0.000	0.000	0.000	0.000	0.000
Zn	0.000	0.000	0.000	0.000	0.000	0.000
Interlayer (I)						
Ca	0.001	0.000	0.002	0.001	0.000	0.001
Na	0.033	0.025	0.040	0.035	0.028	0.033
K	1.943	1.882	1.910	1.910	1.928	1.890
Sr	0.005	0.004	0.004	0.005	0.004	0.005
Ba	0.000	0.000	0.001	0.000	0.000	0.001
Rb	0.000	0.000	0.000	0.000	0.000	0.000
Cs	0.000	0.000	0.000	0.000	0.000	0.000
Hyroxyl (OH)						
OH*	4.000	4.000	4.000	4.000	4.000	4.000
Total	19.614	19.566	19.599	19.590	19.608	19.559
End-member parameters						
Annite	39.6	39.4	40.3	40.4	39.7	38.4
Phlogopite	60.4	60.6	59.7	59.6	60.3	61.6

Sample	525137					
Spot number	119	120	121	122	123	124
SiO_2	36.95	37.18	37.03	37.06	37.19	37.23
TiO_2	2.460	2.470	2.610	2.620	2.610	2.540
Al_2O_3	19.60	19.31	19.35	19.23	19.39	19.39
FeO	14.21	14.32	14.48	14.20	14.60	14.51
MnO	0.16	0.20	0.23	0.19	0.19	0.27
MgO	12.62	12.68	12.65	12.59	12.70	12.68
CaO	0.01	0.01	0.01	0.00	0.00	0.01
Na_2O	0.11	0.09	0.12	0.13	0.09	0.13
K_2O	10.23	10.28	10.37	10.18	10.32	10.15
Cr_2O_3	0,072	0,041	0,052	0,059	0,079	0,091
NiO	0.000	0.031	0.000	0.004	0.000	0.023
Total	96.422	96.610	96.894	96.267	97.171	97.013

Reformatted oxide percentages, with H_2O calculated (22 O)						
SiO_2	36.95	37.18	37.03	37.06	37.19	37.23
TiO_2	2.460	2.470	2.610	2.620	2.610	2.540
Al_2O_3	19.60	19.31	19.35	19.23	19.39	19.39
FeO	14.21	14.32	14.48	14.20	14.60	14.51
MnO	0.16	0.20	0.23	0.19	0.19	0.27
MgO	12.62	12.68	12.65	12.59	12.70	12.68
CaO	0.01	0.01	0.01	0.00	0.00	0.01
Na_2O	0.11	0.09	0.12	0.13	0.09	0.13
K_2O	10.23	10.28	10.37	10.18	10.32	10.15
Cr_2O_3	0.072	0.041	0.052	0.059	0.079	0.091
NiO	0.000	0.031	0.000	0.004	0.000	0.023
H_2O*	4.08	4.09	4.09	4.08	4.11	4.11
Total	100.51	100.70	100.99	100.34	101.28	101.12

Numbers of ions on the basis of 22 (O, OH)						
Tetrahedral (T)						
Si	5.425	5.452	5.424	5.450	5.429	5.438
^{IV}Al	2.575	2.548	2.576	2.550	2.571	2.562
Octahedral (M)						
M1-site						
^{VI}Al	0.816	0.790	0.765	0.784	0.766	0.776
Ti	0.272	0.272	0.288	0.290	0.287	0.279
Cr	0.008	0.005	0.006	0.007	0.009	0.011
Sn	0.000	0.000	0.000	0.000	0.000	0.000
Ga	0.000	0.000	0.000	0.000	0.000	0.000
M2-site						
Fe^{2+}	1.745	1.756	1.774	1.746	1.783	1.773
Ni	0.000	0.004	0.000	0.000	0.000	0.003
Mg	2.762	2.772	2.762	2.760	2.764	2.761
Mn	0.020	0.025	0.029	0.024	0.023	0.033
Cu	0.000	0.000	0.000	0.000	0.000	0.000
Zn	0.000	0.000	0.000	0.000	0.000	0.000
Interlayer (I)						
Ca	0.001	0.001	0.001	0.000	0.000	0.001
Na	0.031	0.026	0.033	0.038	0.026	0.035
K	1.916	1.923	1.938	1.910	1.922	1.891
Sr	0.006	0.003	0.004	0.005	0.007	0.008
Ba	0.000	0.002	0.000	0.000	0.000	0.001
Rb	0.000	0.000	0.000	0.000	0.000	0.000
Cs	0.000	0.000	0.000	0.000	0.000	0.000
Hyroxyl (OH)						
OH*	4.000	4.000	4.000	4.000	4.000	4.000
Total	19.577	19.579	19.600	19.564	19.585	19.572
End-member parameters						
Annite	38.7	38.8	39.1	38.8	39.2	39.1
Phlogopite	61.3	61.2	60.9	61.2	60.8	60.9

Sample	525137					
Spot number	128	129	130	131	139	140
SiO_2	37.35	37.22	37.12	36.84	37.15	37.16
TiO_2	2.450	2.300	2.480	2.430	2.610	2.600
Al_2O_3	19.53	19.39	19.60	19.55	19.37	19.49
FeO	14.60	14.44	14.51	14.60	14.97	14.99
MnO	0.28	0.20	0.14	0.13	0.23	0.21
MgO	12.51	12.47	12.52	12.43	12.66	12.75
CaO	0.01	0.00	0.00	0.00	0.02	0.02
Na_2O	0.12	0.16	0.10	0.13	0.14	0.14
K_2O	10.28	10.43	10.48	10.28	10.33	10.25
Cr_2O_3	0,042	0,066	0,036	0,026	0,057	0,022
NiO	0.042	0.003	0.010	0.020	0.013	0.002
Total	97.210	96.679	96.991	96.434	97.552	97.633

Reformatted oxide percentages, with H_2O calculated (22 O)						
SiO_2	37.35	37.22	37.12	36.84	37.15	37.16
TiO_2	2.450	2.300	2.480	2.430	2.610	2.600
Al_2O_3	19.53	19.39	19.60	19.55	19.37	19.49
FeO	14.60	14.44	14.51	14.60	14.97	14.99
MnO	0.28	0.20	0.14	0.13	0.23	0.21
MgO	12.51	12.47	12.52	12.43	12.66	12.75
CaO	0.01	0.00	0.00	0.00	0.02	0.02
Na_2O	0.12	0.16	0.10	0.13	0.14	0.14
K_2O	10.28	10.43	10.48	10.28	10.33	10.25
Cr_2O_3	0.042	0.066	0.036	0.026	0.057	0.022
NiO	0.042	0.003	0.010	0.020	0.013	0.002
H_2O*	4.11	4.09	4.10	4.07	4.11	4.12
Total	101.32	100.77	101.09	100.51	101.67	101.75

Numbers of ions on the basis of 22 (O, OH)						
Tetrahedral (T)						
Si	5.448	5.461	5.430	5.421	5.415	5.409
^{IV}Al	2.552	2.539	2.570	2.579	2.585	2.591
Octahedral (M)						
M1-site						
^{VI}Al	0.806	0.814	0.810	0.812	0.743	0.753
Ti	0.269	0.254	0.273	0.269	0.286	0.285
Cr	0.005	0.008	0.004	0.003	0.007	0.003
Sn	0.000	0.000	0.000	0.000	0.000	0.000
Ga	0.000	0.000	0.000	0.000	0.000	0.000
M2-site						
Fe^{2+}	1.781	1.772	1.775	1.797	1.825	1.825
Ni	0.005	0.000	0.001	0.002	0.002	0.000
Mg	2.720	2.727	2.730	2.727	2.751	2.766
Mn	0.035	0.025	0.017	0.016	0.028	0.026
Cu	0.000	0.000	0.000	0.000	0.000	0.000
Zn	0.000	0.000	0.000	0.000	0.000	0.000
Interlayer (I)						
Ca	0.001	0.000	0.000	0.000	0.003	0.002
Na	0.034	0.044	0.027	0.036	0.041	0.040
K	1.913	1.952	1.955	1.930	1.921	1.903
Sr	0.004	0.006	0.003	0.002	0.005	0.002
Ba	0.002	0.000	0.001	0.001	0.001	0.000
Rb	0.000	0.000	0.000	0.000	0.000	0.000
Cs	0.000	0.000	0.000	0.000	0.000	0.000
Hyroxyl (OH)						
OH*	4.000	4.000	4.000	4.000	4.000	4.000
Total	19.575	19.603	19.597	19.595	19.612	19.605
End-member parameters						
Annite	39.6	39.4	39.4	39.7	39.9	39.7
Phlogopite	60.4	60.6	60.6	60.3	60.1	60.3

Sample	**525137**					
Spot number	141	142	146	147	148	153
SiO_2	37.37	37.45	37.33	37.24	37.73	36.79
TiO_2	2.570	2.500	2.690	2.630	2.560	2.460
Al_2O_3	19.40	19.56	19.52	19.55	19.78	19.22
FeO	14.69	14.71	15.06	14.99	14.94	14.36
MnO	0.24	0.23	0.19	0.18	0.19	0.20
MgO	12.66	12.79	12.48	12.61	12.33	12.82
CaO	0.01	0.01	0.02	0.02	0.02	0.01
Na_2O	0.14	0.11	0.09	0.12	0.12	0.11
K_2O	10.17	10.03	10.12	10.09	10.22	10.11
Cr_2O_3	0,057	0,049	0,064	0,044	0,045	0,050
NiO	0.000	0.000	0.000	0.001	0.059	0.014
Total	97.303	97.445	97.564	97.468	97.993	96.141

Reformatted oxide percentages, with H_2O calculated (22 O)						
SiO_2	37.37	37.45	37.33	37.24	37.73	36.79
TiO_2	2.570	2.500	2.690	2.630	2.560	2.460
Al_2O_3	19.40	19.56	19.52	19.55	19.78	19.22
FeO	14.69	14.71	15.06	14.99	14.94	14.36
MnO	0.24	0.23	0.19	0.18	0.19	0.20
MgO	12.66	12.79	12.48	12.61	12.33	12.82
CaO	0.01	0.01	0.02	0.02	0.02	0.01
Na_2O	0.14	0.11	0.09	0.12	0.12	0.11
K_2O	10.17	10.03	10.12	10.09	10.22	10.11
Cr_2O_3	0.057	0.049	0.064	0.044	0.045	0.050
NiO	0.000	0.000	0.000	0.001	0.059	0.014
H_2O*	4.12	4.13	4.12	4.12	4.15	4.07
Total	101.42	101.57	101.69	101.59	102.14	100.21

Numbers of ions on the basis of 22 (O, OH)						
Tetrahedral (T)						
Si	5.445	5.441	5.430	5.421	5.457	5.424
^{IV}Al	2.555	2.559	2.570	2.579	2.543	2.576
Octahedral (M)						
M1-site						
^{VI}Al	0.776	0.791	0.776	0.775	0.828	0.764
Ti	0.282	0.273	0.294	0.288	0.278	0.273
Cr	0.007	0.006	0.007	0.005	0.005	0.006
Sn	0.000	0.000	0.000	0.000	0.000	0.000
Ga	0.000	0.000	0.000	0.000	0.000	0.000
M2-site						
Fe^{2+}	1.790	1.788	1.832	1.825	1.807	1.771
Ni	0.000	0.000	0.000	0.000	0.007	0.002
Mg	2.750	2.770	2.706	2.736	2.658	2.818
Mn	0.029	0.029	0.023	0.022	0.023	0.025
Cu	0.000	0.000	0.000	0.000	0.000	0.000
Zn	0.000	0.000	0.000	0.000	0.000	0.000
Interlayer (I)						
Ca	0.002	0.002	0.003	0.002	0.003	0.001
Na	0.040	0.032	0.026	0.034	0.034	0.032
K	1.890	1.859	1.878	1.873	1.885	1.901
Sr	0.005	0.004	0.005	0.004	0.004	0.004
Ba	0.000	0.000	0.000	0.000	0.003	0.001
Rb	0.000	0.000	0.000	0.000	0.000	0.000
Cs	0.000	0.000	0.000	0.000	0.000	0.000
Hyroxyl (OH)						
OH*	4.000	4.000	4.000	4.000	4.000	4.000
Total	19.569	19.553	19.551	19.565	19.536	19.597
End-member parameters						
Annite	39.4	39.2	40.4	40.0	40.5	38.6
Phlogopite	60.6	60.8	59.6	60.0	59.5	61.4

Sample	**525137**					
Spot number	154	155	160	161	162	163
SiO_2	36.81	36.46	37.56	37.32	37.41	37.42
TiO_2	2.620	2.490	2.470	2.340	2.270	2.340
Al_2O_3	19.38	19.28	19.36	19.40	19.41	19.46
FeO	14.66	14.28	15.06	14.91	14.53	14.69
MnO	0.23	0.20	0.22	0.19	0.16	0.20
MgO	12.88	12.80	12.37	12.70	12.70	12.72
CaO	0.00	0.00	0.00	0.01	0.02	0.00
Na_2O	0.12	0.11	0.09	0.13	0.12	0.11
K_2O	10.01	9.97	10.22	10.15	10.23	10.16
Cr_2O_3	0,031	0,052	0,036	0,078	0,038	0,061
NiO	0.034	0.000	0.018	0.000	0.000	0.000
Total	96.768	95.634	97.400	97.219	96.883	97.169

Reformatted oxide percentages, with H_2O calculated (22 O)						
SiO_2	36.81	36.46	37.56	37.32	37.41	37.42
TiO_2	2.620	2.490	2.470	2.340	2.270	2.340
Al_2O_3	19.38	19.28	19.36	19.40	19.41	19.46
FeO	14.66	14.28	15.06	14.91	14.53	14.69
MnO	0.23	0.20	0.22	0.19	0.16	0.20
MgO	12.88	12.80	12.37	12.70	12.70	12.72
CaO	0.00	0.00	0.00	0.01	0.02	0.00
Na_2O	0.12	0.11	0.09	0.13	0.12	0.11
K_2O	10.01	9.97	10.22	10.15	10.23	10.16
Cr_2O_3	0.031	0.052	0.036	0.078	0.038	0.061
NiO	0.034	0.000	0.018	0.000	0.000	0.000
H_2O*	4.09	4.05	4.11	4.11	4.10	4.11
Total	100.86	99.68	101.51	101.33	100.98	101.28

Numbers of ions on the basis of 22 (O, OH)						
Tetrahedral (T)						
Si	5.396	5.402	5.473	5.446	5.469	5.456
^{IV}Al	2.604	2.598	2.527	2.554	2.531	2.544
Octahedral (M)						
M1-site						
^{VI}Al	0.745	0.768	0.799	0.783	0.813	0.801
Ti	0.289	0.277	0.271	0.257	0.250	0.257
Cr	0.004	0.006	0.004	0.009	0.004	0.007
Sn	0.000	0.000	0.000	0.000	0.000	0.000
Ga	0.000	0.000	0.000	0.000	0.000	0.000
M2-site						
Fe^{2+}	1.797	1.769	1.835	1.820	1.776	1.791
Ni	0.004	0.000	0.002	0.000	0.000	0.000
Mg	2.815	2.827	2.687	2.763	2.768	2.765
Mn	0.028	0.025	0.027	0.023	0.020	0.025
Cu	0.000	0.000	0.000	0.000	0.000	0.000
Zn	0.000	0.000	0.000	0.000	0.000	0.000
Interlayer (I)						
Ca	0.000	0.000	0.000	0.001	0.002	0.000
Na	0.033	0.030	0.025	0.036	0.035	0.032
K	1.872	1.884	1.900	1.889	1.907	1.890
Sr	0.003	0.004	0.003	0.007	0.003	0.005
Ba	0.002	0.000	0.001	0.000	0.000	0.000
Rb	0.000	0.000	0.000	0.000	0.000	0.000
Cs	0.000	0.000	0.000	0.000	0.000	0.000
Hyroxyl (OH)						
OH*	4.000	4.000	4.000	4.000	4.000	4.000
Total	19.591	19.592	19.554	19.587	19.578	19.572
End-member parameters						
Annite	39.0	38.5	40.6	39.7	39.1	39.3
Phlogopite	61.0	61.5	59.4	60.3	60.9	60.7

Sample	525137					
Spot number	167	168	169	173	174	175
SiO_2	36.98	37.12	37.02	37.13	37.15	37.15
TiO_2	2.490	2.510	2.530	2.760	2.670	2.610
Al_2O_3	19.07	19.15	19.07	19.40	19.54	19.52
FeO	14.48	14.31	14.54	15.06	14.66	14.70
MnO	0.19	0.18	0.17	0.16	0.14	0.22
MgO	12.88	12.86	12.92	12.73	12.71	12.98
CaO	0.01	0.01	0.00	0.01	0.02	0.00
Na_2O	0.10	0.10	0.11	0.10	0.14	0.09
K_2O	10.10	10.17	10.26	10.27	10.00	9.92
Cr_2O_3	0,032	0,039	0,049	0,058	0,039	0,063
NiO	0.000	0.018	0.009	0.000	0.000	0.000
Total	96.332	96.462	96.671	97.676	97.068	97.254

Reformatted oxide percentages, with H_2O calculated (22 O)						
SiO_2	36.98	37.12	37.02	37.13	37.15	37.15
TiO_2	2.490	2.510	2.530	2.760	2.670	2.610
Al_2O_3	19.07	19.15	19.07	19.40	19.54	19.52
FeO	14.48	14.31	14.54	15.06	14.66	14.70
MnO	0.19	0.18	0.17	0.16	0.14	0.22
MgO	12.88	12.86	12.92	12.73	12.71	12.98
CaO	0.01	0.01	0.00	0.01	0.02	0.00
Na_2O	0.10	0.10	0.11	0.10	0.14	0.09
K_2O	10.10	10.17	10.26	10.27	10.00	9.92
Cr_2O_3	0.032	0.039	0.049	0.058	0.039	0.063
NiO	0.000	0.018	0.009	0.000	0.000	0.000
H_2O*	4.07	4.08	4.08	4.12	4.11	4.12
Total	100.41	100.55	100.76	101.80	101.18	101.37

Numbers of ions on the basis of 22 (O, OH)						
Tetrahedral (T)						
Si	5.442	5.450	5.434	5.403	5.420	5.409
^{IV}Al	2.558	2.550	2.566	2.597	2.580	2.591
Octahedral (M)						
M1-site						
^{VI}Al	0.750	0.764	0.734	0.731	0.780	0.759
Ti	0.276	0.277	0.279	0.302	0.293	0.286
Cr	0.004	0.005	0.006	0.007	0.004	0.007
Sn	0.000	0.000	0.000	0.000	0.000	0.000
Ga	0.000	0.000	0.000	0.000	0.000	0.000
M2-site						
Fe^{2+}	1.782	1.757	1.785	1.833	1.789	1.790
Ni	0.000	0.002	0.001	0.000	0.000	0.000
Mg	2.825	2.815	2.827	2.762	2.764	2.817
Mn	0.024	0.022	0.021	0.019	0.017	0.028
Cu	0.000	0.000	0.000	0.000	0.000	0.000
Zn	0.000	0.000	0.000	0.000	0.000	0.000
Interlayer (I)						
Ca	0.002	0.001	0.000	0.002	0.003	0.000
Na	0.027	0.027	0.030	0.029	0.040	0.025
K	1.896	1.905	1.921	1.906	1.861	1.842
Sr	0.003	0.003	0.004	0.005	0.003	0.005
Ba	0.000	0.001	0.001	0.000	0.000	0.000
Rb	0.000	0.000	0.000	0.000	0.000	0.000
Cs	0.000	0.000	0.000	0.000	0.000	0.000
Hyroxyl (OH)						
OH*	4.000	4.000	4.000	4.000	4.000	4.000
Total	19.588	19.580	19.609	19.595	19.555	19.560
End-member parameters						
Annite	38.7	38.4	38.7	39.9	39.3	38.9
Phlogopite	61.3	61.6	61.3	60.1	60.7	61.1

Sample	525137					
Spot number	179	180	181	182	187	188
SiO_2	36.92	36.96	37.20	37.07	37.11	37.20
TiO_2	2.780	2.770	2.740	2.710	2.790	2.840
Al_2O_3	19.54	19.32	19.33	19.53	19.63	19.57
FeO	15.12	15.04	15.19	14.89	15.01	15.09
MnO	0.20	0.18	0.22	0.25	0.22	0.19
MgO	12.58	12.55	12.49	12.63	12.33	12.27
CaO	0.01	0.00	0.01	0.01	0.01	0.01
Na_2O	0.14	0.07	0.12	0.14	0.09	0.12
K_2O	10.27	10.09	10.17	10.21	10.13	10.24
Cr_2O_3	0,049	0,052	0,047	0,067	0,067	0,049
NiO	0.029	0.010	0.000	0.036	0.022	0.000
Total	97.641	97.051	97.515	97.538	97.416	97.574

Reformatted oxide percentages, with H_2O calculated (22 O)						
SiO_2	36.92	36.96	37.20	37.07	37.11	37.20
TiO_2	2.780	2.770	2.740	2.710	2.790	2.840
Al_2O_3	19.54	19.32	19.33	19.53	19.63	19.57
FeO	15.12	15.04	15.19	14.89	15.01	15.09
MnO	0.20	0.18	0.22	0.25	0.22	0.19
MgO	12.58	12.55	12.49	12.63	12.33	12.27
CaO	0.01	0.00	0.01	0.01	0.01	0.01
Na_2O	0.14	0.07	0.12	0.14	0.09	0.12
K_2O	10.27	10.09	10.17	10.21	10.13	10.24
Cr_2O_3	0.049	0.052	0.047	0.067	0.067	0.049
NiO	0.029	0.010	0.000	0.036	0.022	0.000
H_2O*	4.11	4.10	4.11	4.12	4.11	4.12
Total	101.76	101.15	101.63	101.66	101.53	101.69

Numbers of ions on the basis of 22 (O, OH)						
Tetrahedral (T)						
Si	5.381	5.410	5.423	5.399	5.408	5.417
^{IV}Al	2.619	2.590	2.577	2.601	2.592	2.583
Octahedral (M)						
M1-site						
^{VI}Al	0.737	0.743	0.745	0.752	0.781	0.776
Ti	0.305	0.305	0.300	0.297	0.306	0.311
Cr	0.006	0.006	0.005	0.008	0.008	0.006
Sn	0.000	0.000	0.000	0.000	0.000	0.000
Ga	0.000	0.000	0.000	0.000	0.000	0.000
M2-site						
Fe^{2+}	1.843	1.841	1.852	1.814	1.830	1.838
Ni	0.003	0.001	0.000	0.004	0.003	0.000
Mg	2.733	2.738	2.714	2.742	2.679	2.663
Mn	0.025	0.023	0.028	0.030	0.028	0.024
Cu	0.000	0.000	0.000	0.000	0.000	0.000
Zn	0.000	0.000	0.000	0.000	0.000	0.000
Interlayer (I)						
Ca	0.002	0.001	0.001	0.002	0.002	0.001
Na	0.040	0.021	0.033	0.039	0.025	0.033
K	1.909	1.884	1.891	1.897	1.883	1.902
Sr	0.004	0.004	0.004	0.006	0.006	0.004
Ba	0.002	0.001	0.000	0.002	0.001	0.000
Rb	0.000	0.000	0.000	0.000	0.000	0.000
Cs	0.000	0.000	0.000	0.000	0.000	0.000
Hyroxyl (OH)						
OH*	4.000	4.000	4.000	4.000	4.000	4.000
Total	19.608	19.568	19.575	19.592	19.550	19.557
End-member parameters						
Annite	40.3	40.2	40.6	39.8	40.6	40.8
Phlogopite	59.7	59.8	59.4	60.2	59.4	59.2

Sample	525137					
Spot number	192	193	194	195	200	201
SiO_2	37.10	37.28	37.22	37.44	37.40	37.12
TiO_2	2.610	2.590	2.560	2.450	2.550	2.470
Al_2O_3	19.72	19.96	19.72	19.80	19.56	19.38
FeO	14.74	14.56	14.43	14.80	14.46	14.49
MnO	0.19	0.23	0.18	0.20	0.30	0.17
MgO	12.56	12.48	12.66	12.43	12.52	12.66
CaO	0.02	0.05	0.04	0.05	0.02	0.01
Na_2O	0.10	0.13	0.11	0.14	0.10	0.11
K_2O	10.01	10.08	10.28	10.18	10.22	10.28
Cr_2O_3	0,035	0,029	0,071	0,019	0,045	0,068
NiO	0.017	0.009	0.000	0.021	0.038	0.000
Total	97.089	97.392	97.267	97.528	97.214	96.750

Sample	525137	
Spot number	202	203
SiO_2	37.29	37.55
TiO_2	2.650	2.630
Al_2O_3	19.56	19.75
FeO	14.39	14.73
MnO	0.19	0.13
MgO	12.58	12.52
CaO	0.00	0.00
Na_2O	0.11	0.12
K_2O	10.19	10.32
Cr_2O_3	0,050	0,079
NiO	0.016	0.014
Total	97.022	97.839

Reformatted oxide percentages, with H_2O calculated (22 O)						
SiO_2	37.10	37.28	37.22	37.44	37.40	37.12
TiO_2	2.610	2.590	2.560	2.450	2.550	2.470
Al_2O_3	19.72	19.96	19.72	19.80	19.56	19.38
FeO	14.74	14.56	14.43	14.80	14.46	14.49
MnO	0.19	0.23	0.18	0.20	0.30	0.17
MgO	12.56	12.48	12.66	12.43	12.52	12.66
CaO	0.02	0.05	0.04	0.05	0.02	0.01
Na_2O	0.10	0.13	0.11	0.14	0.10	0.11
K_2O	10.01	10.08	10.28	10.18	10.22	10.28
Cr_2O_3	0.035	0.029	0.071	0.019	0.045	0.068
NiO	0.017	0.009	0.000	0.021	0.038	0.000
H_2O*	4.11	4.13	4.12	4.13	4.12	4.09
Total	101.20	101.52	101.38	101.65	101.33	100.84

Reformatted oxide perc., with H_2O calc. (22 O)		
SiO_2	37.29	37.55
TiO_2	2.650	2.630
Al_2O_3	19.56	19.75
FeO	14.39	14.73
MnO	0.19	0.13
MgO	12.58	12.52
CaO	0.00	0.00
Na_2O	0.11	0.12
K_2O	10.19	10.32
Cr_2O_3	0.050	0.079
NiO	0.016	0.014
H_2O*	4.11	4.14
Total	101.13	101.98

Numbers of ions on the basis of 22 (O, OH)						
Tetrahedral (T)						
Si	5.413	5.418	5.420	5.441	5.449	5.439
^{IV}Al	2.587	2.582	2.580	2.559	2.551	2.561
Octahedral (M)						
M1-site						
^{VI}Al	0.805	0.837	0.805	0.832	0.809	0.786
Ti	0.286	0.283	0.280	0.268	0.279	0.272
Cr	0.004	0.003	0.008	0.002	0.005	0.008
Sn	0.000	0.000	0.000	0.000	0.000	0.000
Ga	0.000	0.000	0.000	0.000	0.000	0.000
M2-site						
Fe^{2+}	1.799	1.770	1.757	1.799	1.762	1.776
Ni	0.002	0.001	0.000	0.002	0.004	0.000
Mg	2.732	2.704	2.748	2.693	2.719	2.765
Mn	0.023	0.028	0.022	0.024	0.037	0.021
Cu	0.000	0.000	0.000	0.000	0.000	0.000
Zn	0.000	0.000	0.000	0.000	0.000	0.000
Interlayer (I)						
Ca	0.002	0.008	0.006	0.008	0.003	0.002
Na	0.027	0.035	0.030	0.039	0.028	0.030
K	1.863	1.868	1.909	1.887	1.899	1.921
Sr	0.003	0.002	0.006	0.002	0.004	0.006
Ba	0.001	0.001	0.000	0.001	0.002	0.000
Rb	0.000	0.000	0.000	0.000	0.000	0.000
Cs	0.000	0.000	0.000	0.000	0.000	0.000
Hyroxyl (OH)						
OH*	4.000	4.000	4.000	4.000	4.000	4.000
Total	19.547	19.540	19.573	19.557	19.553	19.587
End-member parameters						
Annite	39.7	39.6	39.0	40.0	39.3	39.1
Phlogopite	60.3	60.4	61.0	60.0	60.7	60.9

Numbers of ions on the basis of 22 (O, OH)		
Tetrahedral (T)		
Si	5.440	5.438
^{IV}Al	2.560	2.562
Octahedral (M)		
M1-site		
^{VI}Al	0.803	0.809
Ti	0.291	0.286
Cr	0.006	0.009
Sn	0.000	0.000
Ga	0.000	0.000
M2-site		
Fe^{2+}	1.756	1.784
Ni	0.002	0.002
Mg	2.736	2.703
Mn	0.023	0.016
Cu	0.000	0.000
Zn	0.000	0.000
Interlayer (I)		
Ca	0.000	0.000
Na	0.031	0.033
K	1.896	1.906
Sr	0.004	0.007
Ba	0.001	0.001
Rb	0.000	0.000
Cs	0.000	0.000
Hyroxyl (OH)		
OH*	4.000	4.000
Total	19.548	19.555
End-member parameters		
Annite	39.1	39.8
Phlogopite	60.9	60.2

Sample	525138					
Spot number	31	32	33	34	35	36
SiO_2	36.25	36.44	36.53	36.54	36.56	35.66
TiO_2	2.590	2.570	2.490	2.580	2.470	2.580
Al_2O_3	19.52	19.51	19.51	19.45	19.30	19.24
FeO	17.66	17.80	17.60	17.73	17.76	17.88
MnO	0.28	0.27	0.24	0.27	0.21	0.26
MgO	10.49	10.51	10.45	10.50	10.37	10.41
CaO	0.03	0.01	0.02	0.03	0.03	0.03
Na_2O	0.22	0.15	0.19	0.13	0.14	0.16
K_2O	9.74	10.16	10.16	10.07	10.10	10.17
Cr_2O_3	0,048	0,023	0,045	0,050	0,015	0,048
NiO	0.000	0.012	0.003	0.027	0.002	0.000
Total	96.817	97.450	97.240	97.373	96.960	96.446

Reformatted oxide percentages, with H_2O calculated (22 O)						
SiO_2	36.25	36.44	36.53	36.54	36.56	35.66
TiO_2	2.590	2.570	2.490	2.580	2.470	2.580
Al_2O_3	19.52	19.51	19.51	19.45	19.30	19.24
FeO	17.66	17.80	17.60	17.73	17.76	17.88
MnO	0.28	0.27	0.24	0.27	0.21	0.26
MgO	10.49	10.51	10.45	10.50	10.37	10.41
CaO	0.03	0.01	0.02	0.03	0.03	0.03
Na_2O	0.22	0.15	0.19	0.13	0.14	0.16
K_2O	9.74	10.16	10.16	10.07	10.10	10.17
Cr_2O_3	0.048	0.023	0.045	0.050	0.015	0.048
NiO	0.000	0.012	0.003	0.027	0.002	0.000
H_2O*	4.04	4.05	4.05	4.05	4.04	4.00
Total	100.85	101.50	101.29	101.43	101.00	100.44

Numbers of ions on the basis of 22 (O, OH)						
Tetrahedral (T)						
Si	5.385	5.391	5.409	5.404	5.431	5.349
^{IV}Al	2.615	2.609	2.591	2.596	2.569	2.651
Octahedral (M)						
M1-site						
^{VI}Al	0.804	0.793	0.815	0.795	0.811	0.750
Ti	0.289	0.286	0.277	0.287	0.276	0.291
Cr	0.006	0.003	0.005	0.006	0.002	0.006
Sn	0.000	0.000	0.000	0.000	0.000	0.000
Ga	0.000	0.000	0.000	0.000	0.000	0.000
M2-site						
Fe^{2+}	2.194	2.202	2.180	2.193	2.207	2.243
Ni	0.000	0.001	0.000	0.003	0.000	0.000
Mg	2.323	2.318	2.307	2.315	2.297	2.328
Mn	0.035	0.033	0.030	0.033	0.027	0.033
Cu	0.000	0.000	0.000	0.000	0.000	0.000
Zn	0.000	0.000	0.000	0.000	0.000	0.000
Interlayer (I)						
Ca	0.004	0.002	0.003	0.005	0.004	0.005
Na	0.062	0.042	0.056	0.037	0.041	0.048
K	1.846	1.917	1.919	1.900	1.914	1.946
Sr	0.004	0.002	0.004	0.004	0.001	0.004
Ba	0.000	0.001	0.000	0.002	0.000	0.000
Rb	0.000	0.000	0.000	0.000	0.000	0.000
Cs	0.000	0.000	0.000	0.000	0.000	0.000
Hyroxyl (OH)						
OH*	4.000	4.000	4.000	4.000	4.000	4.000
Total	19.567	19.601	19.596	19.579	19.579	19.653
End-member parameters						
Annite	48.6	48.7	48.6	48.6	49.0	49.1
Phlogopite	51.4	51.3	51.4	51.4	51.0	50.9

Sample	525138					
Spot number	43	44	45	46	51	52
SiO_2	36.08	35.89	36.00	36.00	36.01	36.02
TiO_2	2.680	2.640	2.660	2.600	2.860	2.820
Al_2O_3	19.60	19.54	19.57	19.71	19.65	19.54
FeO	17.54	17.33	17.50	17.43	17.36	17.44
MnO	0.24	0.28	0.32	0.24	0.27	0.24
MgO	10.46	10.44	10.43	10.51	10.35	10.37
CaO	0.01	0.02	0.00	0.01	0.01	0.01
Na_2O	0.15	0.17	0.17	0.13	0.15	0.16
K_2O	10.12	10.29	10.14	10.03	10.08	10.09
Cr_2O_3	0,053	0,026	0,062	0,032	0,023	0,045
NiO	0.034	0.000	0.000	0.025	0.027	0.012
Total	96.965	96.623	96.850	96.718	96.788	96.742

Reformatted oxide percentages, with H_2O calculated (22 O)						
SiO_2	36.08	35.89	36.00	36.00	36.01	36.02
TiO_2	2.680	2.640	2.660	2.600	2.860	2.820
Al_2O_3	19.60	19.54	19.57	19.71	19.65	19.54
FeO	17.54	17.33	17.50	17.43	17.36	17.44
MnO	0.24	0.28	0.32	0.24	0.27	0.24
MgO	10.46	10.44	10.43	10.51	10.35	10.37
CaO	0.01	0.02	0.00	0.01	0.01	0.01
Na_2O	0.15	0.17	0.17	0.13	0.15	0.16
K_2O	10.12	10.29	10.14	10.03	10.08	10.09
Cr_2O_3	0.053	0.026	0.062	0.032	0.023	0.045
NiO	0.034	0.000	0.000	0.025	0.027	0.012
H_2O*	4.04	4.02	4.03	4.03	4.03	4.03
Total	101.00	100.64	100.88	100.75	100.82	100.77

Numbers of ions on the basis of 22 (O, OH)						
Tetrahedral (T)						
Si	5.361	5.357	5.359	5.358	5.357	5.363
^{IV}Al	2.639	2.643	2.641	2.642	2.643	2.637
Octahedral (M)						
M1-site						
^{VI}Al	0.794	0.795	0.792	0.815	0.802	0.792
Ti	0.299	0.296	0.298	0.291	0.320	0.316
Cr	0.006	0.003	0.007	0.004	0.003	0.005
Sn	0.000	0.000	0.000	0.000	0.000	0.000
Ga	0.000	0.000	0.000	0.000	0.000	0.000
M2-site						
Fe^{2+}	2.180	2.163	2.179	2.169	2.160	2.172
Ni	0.004	0.000	0.000	0.003	0.003	0.001
Mg	2.317	2.323	2.314	2.332	2.295	2.302
Mn	0.030	0.035	0.040	0.030	0.034	0.030
Cu	0.000	0.000	0.000	0.000	0.000	0.000
Zn	0.000	0.000	0.000	0.000	0.000	0.000
Interlayer (I)						
Ca	0.002	0.003	0.000	0.001	0.002	0.002
Na	0.042	0.049	0.049	0.038	0.043	0.045
K	1.918	1.959	1.925	1.904	1.913	1.916
Sr	0.005	0.002	0.005	0.003	0.002	0.004
Ba	0.002	0.000	0.000	0.001	0.002	0.001
Rb	0.000	0.000	0.000	0.000	0.000	0.000
Cs	0.000	0.000	0.000	0.000	0.000	0.000
Hyroxyl (OH)						
OH*	4.000	4.000	4.000	4.000	4.000	4.000
Total	19.600	19.630	19.610	19.592	19.577	19.585
End-member parameters						
Annite	48.5	48.2	48.5	48.2	48.5	48.5
Phlogopite	51.5	51.8	51.5	51.8	51.5	51.5

Sample	**525138**					
Spot number	53	54	59	60	61	62
SiO_2	35.70	35.79	36.89	36.83	36.64	36.78
TiO_2	2.930	2.820	2.600	2.630	2.790	2.490
Al_2O_3	19.43	19.38	19.19	19.38	19.07	19.32
FeO	17.50	17.39	17.15	17.15	17.49	17.47
MnO	0.28	0.25	0.21	0.28	0.24	0.25
MgO	10.33	10.24	10.37	10.31	10.12	10.40
CaO	0.01	0.01	0.02	0.03	0.00	0.01
Na_2O	0.14	0.18	0.14	0.10	0.12	0.12
K_2O	10.27	10.15	10.24	10.05	10.28	10.29
Cr_2O_3	0,055	0,040	0,032	0,047	0,052	0,047
NiO	0.014	0.000	0.000	0.000	0.050	0.000
Total	96.669	96.246	96.835	96.803	96.855	97.170

Reformatted oxide percentages, with H_2O calculated (22 O)						
SiO_2	35.70	35.79	36.89	36.83	36.64	36.78
TiO_2	2.930	2.820	2.600	2.630	2.790	2.490
Al_2O_3	19.43	19.38	19.19	19.38	19.07	19.32
FeO	17.50	17.39	17.15	17.15	17.49	17.47
MnO	0.28	0.25	0.21	0.28	0.24	0.25
MgO	10.33	10.24	10.37	10.31	10.12	10.40
CaO	0.01	0.01	0.02	0.03	0.00	0.01
Na_2O	0.14	0.18	0.14	0.10	0.12	0.12
K_2O	10.27	10.15	10.24	10.05	10.28	10.29
Cr_2O_3	0.055	0.040	0.032	0.047	0.052	0.047
NiO	0.014	0.000	0.000	0.000	0.050	0.000
H_2O*	4.01	4.00	4.04	4.05	4.03	4.05
Total	100.68	100.25	100.88	100.85	100.89	101.22

Numbers of ions on the basis of 22 (O, OH)						
Tetrahedral (T)						
Si	5.334	5.362	5.471	5.458	5.449	5.447
^{IV}Al	2.666	2.638	2.529	2.542	2.551	2.553
Octahedral (M)						
M1-site						
^{VI}Al	0.755	0.785	0.826	0.844	0.792	0.819
Ti	0.329	0.318	0.290	0.293	0.312	0.277
Cr	0.006	0.005	0.004	0.006	0.006	0.006
Sn	0.000	0.000	0.000	0.000	0.000	0.000
Ga	0.000	0.000	0.000	0.000	0.000	0.000
M2-site						
Fe^{2+}	2.187	2.179	2.127	2.126	2.175	2.164
Ni	0.002	0.000	0.000	0.000	0.006	0.000
Mg	2.301	2.287	2.293	2.278	2.243	2.296
Mn	0.036	0.031	0.026	0.035	0.030	0.031
Cu	0.000	0.000	0.000	0.000	0.000	0.000
Zn	0.000	0.000	0.000	0.000	0.000	0.000
Interlayer (I)						
Ca	0.002	0.002	0.002	0.004	0.000	0.001
Na	0.042	0.051	0.040	0.028	0.034	0.034
K	1.957	1.940	1.937	1.900	1.950	1.944
Sr	0.005	0.003	0.003	0.004	0.004	0.004
Ba	0.001	0.000	0.000	0.000	0.003	0.000
Rb	0.000	0.000	0.000	0.000	0.000	0.000
Cs	0.000	0.000	0.000	0.000	0.000	0.000
Hyroxyl (OH)						
OH*	4.000	4.000	4.000	4.000	4.000	4.000
Total	19.622	19.602	19.548	19.517	19.557	19.576
End-member parameters						
Annite	48.7	48.8	48.1	48.3	49.2	48.5
Phlogopite	51.3	51.2	51.9	51.7	50.8	51.5

Sample	**525138**					
Spot number	63	64	65	76	89	90
SiO_2	36.85	36.89	36.75	36.31	36.49	36.57
TiO_2	2.560	2.470	2.430	1.980	2.580	2.550
Al_2O_3	19.21	19.35	19.51	19.58	19.58	19.60
FeO	17.14	17.33	17.36	17.36	18.45	18.15
MnO	0.29	0.26	0.26	0.23	0.21	0.28
MgO	10.38	10.41	10.48	10.46	10.17	10.00
CaO	0.00	0.00	0.02	0.03	0.05	0.05
Na_2O	0.14	0.14	0.15	0.15	0.16	0.15
K_2O	10.54	10.42	10.29	9.92	10.12	9.92
Cr_2O_3	0,034	0,028	0,052	0,043	0,073	0,053
NiO	0.000	0.008	0.000	0.030	0.008	0.000
Total	97.152	97.305	97.303	96.090	97.885	97.314

Reformatted oxide percentages, with H_2O calculated (22 O)						
SiO_2	36.85	36.89	36.75	36.31	36.49	36.57
TiO_2	2.560	2.470	2.430	1.980	2.580	2.550
Al_2O_3	19.21	19.35	19.51	19.58	19.58	19.60
FeO	17.14	17.33	17.36	17.36	18.45	18.15
MnO	0.29	0.26	0.26	0.23	0.21	0.28
MgO	10.38	10.41	10.48	10.46	10.17	10.00
CaO	0.00	0.00	0.02	0.03	0.05	0.05
Na_2O	0.14	0.14	0.15	0.15	0.16	0.15
K_2O	10.54	10.42	10.29	9.92	10.12	9.92
Cr_2O_3	0.034	0.028	0.052	0.043	0.073	0.053
NiO	0.000	0.008	0.000	0.030	0.008	0.000
H_2O*	4.05	4.06	4.06	4.01	4.06	4.05
Total	101.20	101.36	101.36	100.10	101.95	101.36

Numbers of ions on the basis of 22 (O, OH)						
Tetrahedral (T)						
Si	5.459	5.455	5.432	5.429	5.386	5.415
^{IV}Al	2.541	2.545	2.568	2.571	2.614	2.585
Octahedral (M)						
M1-site						
^{VI}Al	0.814	0.828	0.832	0.880	0.793	0.837
Ti	0.285	0.275	0.270	0.223	0.286	0.284
Cr	0.004	0.003	0.006	0.005	0.009	0.006
Sn	0.000	0.000	0.000	0.000	0.000	0.000
Ga	0.000	0.000	0.000	0.000	0.000	0.000
M2-site						
Fe^{2+}	2.124	2.143	2.146	2.171	2.278	2.248
Ni	0.000	0.001	0.000	0.004	0.001	0.000
Mg	2.292	2.295	2.309	2.331	2.238	2.208
Mn	0.037	0.033	0.033	0.030	0.026	0.035
Cu	0.000	0.000	0.000	0.000	0.000	0.000
Zn	0.000	0.000	0.000	0.000	0.000	0.000
Interlayer (I)						
Ca	0.000	0.000	0.002	0.004	0.007	0.007
Na	0.041	0.040	0.044	0.043	0.046	0.042
K	1.992	1.965	1.940	1.892	1.905	1.874
Sr	0.003	0.002	0.004	0.004	0.006	0.005
Ba	0.000	0.000	0.000	0.002	0.000	0.000
Rb	0.000	0.000	0.000	0.000	0.000	0.000
Cs	0.000	0.000	0.000	0.000	0.000	0.000
Hyroxyl (OH)						
OH*	4.000	4.000	4.000	4.000	4.000	4.000
Total	19.593	19.585	19.587	19.588	19.596	19.545
End-member parameters						
Annite	48.1	48.3	48.2	48.2	50.4	50.5
Phlogopite	51.9	51.7	51.8	51.8	49.6	49.5

Sample	**525138**						
Spot number	91	92	93	103	104	105	106
SiO_2	36.74	36.75	36.72	36.61	37.19	36.76	36.57
TiO_2	2.310	2.460	2.520	2.160	2.250	2.210	2.240
Al_2O_3	19.91	19.79	19.61	20.12	20.16	19.79	19.89
FeO	17.54	17.45	17.51	17.13	17.23	17.22	17.41
MnO	0.29	0.22	0.26	0.23	0.21	0.20	0.25
MgO	10.03	10.04	9.94	10.16	10.27	10.18	10.16
CaO	0.04	0.03	0.03	0.05	0.02	0.00	0.07
Na_2O	0.20	0.19	0.20	0.17	0.18	0.14	0.21
K_2O	10.16	10.18	10.32	10.19	10.09	10.11	9.93
Cr_2O_3	0,045	0,063	0,057	0,050	0,022	0,032	0,026
NiO	0.001	0.000	0.024	0.007	0.009	0.013	0.018
Total	97.259	97.176	97.184	96.875	97.627	96.657	96.770

Reformatted oxide percentages, with H_2O calculated (22 O)							
SiO_2	36.74	36.75	36.72	36.61	37.19	36.76	36.57
TiO_2	2.310	2.460	2.520	2.160	2.250	2.210	2.240
Al_2O_3	19.91	19.79	19.61	20.12	20.16	19.79	19.89
FeO	17.54	17.45	17.51	17.13	17.23	17.22	17.41
MnO	0.29	0.22	0.26	0.23	0.21	0.20	0.25
MgO	10.03	10.04	9.94	10.16	10.27	10.18	10.16
CaO	0.04	0.03	0.03	0.05	0.02	0.00	0.07
Na_2O	0.20	0.19	0.20	0.17	0.18	0.14	0.21
K_2O	10.16	10.18	10.32	10.19	10.09	10.11	9.93
Cr_2O_3	0.045	0.063	0.057	0.050	0.022	0.032	0.026
NiO	0.001	0.000	0.024	0.007	0.009	0.013	0.018
H_2O*	4.06	4.05	4.05	4.05	4.09	4.04	4.04
Total	101.32	101.23	101.23	100.92	101.71	100.70	100.81

Numbers of ions on the basis of 22 (O, OH)							
Tetrahedral (T)							
Si	5.432	5.435	5.440	5.423	5.455	5.456	5.426
^{IV}Al	2.568	2.565	2.560	2.577	2.545	2.544	2.574
Octahedral (M)							
M1-site							
^{VI}Al	0.901	0.885	0.864	0.936	0.941	0.917	0.905
Ti	0.257	0.274	0.281	0.241	0.248	0.247	0.250
Cr	0.005	0.007	0.007	0.006	0.003	0.004	0.003
Sn	0.000	0.000	0.000	0.000	0.000	0.000	0.000
Ga	0.000	0.000	0.000	0.000	0.000	0.000	0.000
M2-site							
Fe^{2+}	2.169	2.158	2.169	2.122	2.114	2.137	2.160
Ni	0.000	0.000	0.003	0.001	0.001	0.002	0.002
Mg	2.210	2.213	2.195	2.243	2.246	2.252	2.247
Mn	0.036	0.028	0.033	0.029	0.026	0.026	0.031
Cu	0.000	0.000	0.000	0.000	0.000	0.000	0.000
Zn	0.000	0.000	0.000	0.000	0.000	0.000	0.000
Interlayer (I)							
Ca	0.006	0.005	0.004	0.007	0.003	0.001	0.011
Na	0.056	0.054	0.056	0.049	0.051	0.039	0.061
K	1.916	1.920	1.950	1.925	1.888	1.914	1.879
Sr	0.004	0.005	0.005	0.004	0.002	0.003	0.002
Ba	0.000	0.000	0.001	0.000	0.001	0.001	0.001
Rb	0.000	0.000	0.000	0.000	0.000	0.000	0.000
Cs	0.000	0.000	0.000	0.000	0.000	0.000	0.000
Hyroxyl (OH)							
OH*	4.000	4.000	4.000	4.000	4.000	4.000	4.000
Total	19.560	19.550	19.567	19.564	19.522	19.541	19.553
End-member parameters							
Annite	49.5	49.4	49.7	48.6	48.5	48.7	49.0
Phlogopite	50.5	50.6	50.3	51.4	51.5	51.3	51.0

Sample	**525139**					
Spot number	14	15	16	17	21	22
SiO_2	36.93	36.92	37.09	36.88	37.42	37.38
TiO_2	2.510	2.510	2.510	2.570	2.490	2.510
Al_2O_3	19.26	19.48	19.29	19.33	19.74	19.42
FeO	13.84	13.94	13.87	13.95	13.77	13.58
MnO	0.21	0.28	0.24	0.26	0.26	0.26
MgO	13.09	13.05	13.03	12.99	13.20	13.20
CaO	0.00	0.01	0.00	0.01	0.00	0.00
Na_2O	0.16	0.08	0.15	0.12	0.14	0.17
K_2O	10.13	10.09	10.29	10.02	10.46	10.31
Cr_2O_3	0,032	0,052	0,034	0,022	0,060	0,028
NiO	0.000	0.000	0.030	0.005	0.000	0.005
Total	96.155	96.406	96.531	96.154	97.544	96.857

Reformatted oxide percentages, with H_2O calculated (22 O)						
SiO_2	36.93	36.92	37.09	36.88	37.42	37.38
TiO_2	2.510	2.510	2.510	2.570	2.490	2.510
Al_2O_3	19.26	19.48	19.29	19.33	19.74	19.42
FeO	13.84	13.94	13.87	13.95	13.77	13.58
MnO	0.21	0.28	0.24	0.26	0.26	0.26
MgO	13.09	13.05	13.03	12.99	13.20	13.20
CaO	0.00	0.01	0.00	0.01	0.00	0.00
Na_2O	0.16	0.08	0.15	0.12	0.14	0.17
K_2O	10.13	10.09	10.29	10.02	10.46	10.31
Cr_2O_3	0.032	0.052	0.034	0.022	0.060	0.028
NiO	0.000	0.000	0.030	0.005	0.000	0.005
H_2O*	4.08	4.09	4.09	4.08	4.14	4.11
Total	100.23	100.49	100.62	100.23	101.68	100.97

Numbers of ions on the basis of 22 (O, OH)						
Tetrahedral (T)						
Si	5.430	5.414	5.437	5.423	5.423	5.449
^{IV}Al	2.570	2.586	2.563	2.577	2.577	2.551
Octahedral (M)						
M1-site						
^{VI}Al	0.768	0.782	0.769	0.773	0.794	0.786
Ti	0.278	0.277	0.277	0.284	0.271	0.275
Cr	0.004	0.006	0.004	0.003	0.007	0.003
Sn	0.000	0.000	0.000	0.000	0.000	0.000
Ga	0.000	0.000	0.000	0.000	0.000	0.000
M2-site						
Fe^{2+}	1.702	1.710	1.700	1.716	1.669	1.656
Ni	0.000	0.000	0.004	0.001	0.000	0.001
Mg	2.869	2.853	2.847	2.847	2.851	2.868
Mn	0.026	0.035	0.030	0.032	0.032	0.032
Cu	0.000	0.000	0.000	0.000	0.000	0.000
Zn	0.000	0.000	0.000	0.000	0.000	0.000
Interlayer (I)						
Ca	0.000	0.001	0.000	0.002	0.000	0.000
Na	0.045	0.022	0.042	0.033	0.040	0.047
K	1.900	1.887	1.924	1.879	1.933	1.917
Sr	0.003	0.004	0.003	0.002	0.005	0.002
Ba	0.000	0.000	0.002	0.000	0.000	0.000
Rb	0.000	0.000	0.000	0.000	0.000	0.000
Cs	0.000	0.000	0.000	0.000	0.000	0.000
Hyroxyl (OH)						
OH*	4.000	4.000	4.000	4.000	4.000	4.000
Total	19.594	19.577	19.601	19.572	19.603	19.587
End-member parameters						
Annite	37.2	37.5	37.4	37.6	36.9	36.6
Phlogopite	62.8	62.5	62.6	62.4	63.1	63.4

Sample	525139					
Spot number	23	27	28	29	36	37
SiO_2	37.43	37.56	37.60	37.49	38.13	38.08
TiO_2	2.480	2.730	2.620	2.740	2.640	2.820
Al_2O_3	19.59	19.74	19.76	19.74	19.45	19.56
FeO	13.76	13.93	13.95	13.97	13.29	13.28
MnO	0.25	0.26	0.22	0.18	0.25	0.31
MgO	13.20	12.71	12.99	12.88	13.03	12.87
CaO	0.00	0.03	0.01	0.04	0.01	0.04
Na_2O	0.13	0.16	0.15	0.14	0.13	0.13
K_2O	10.42	10.20	10.23	10.16	10.65	10.33
Cr_2O_3	0,046	0,082	0,068	0,056	0,065	0,073
NiO	0.003	0.000	0.000	0.000	0.000	0.000
Total	97.306	97.403	97.590	97.388	97.646	97.491

Reformatted oxide percentages, with H_2O calculated (22 O)						
SiO_2	37.43	37.56	37.60	37.49	38.13	38.08
TiO_2	2.480	2.730	2.620	2.740	2.640	2.820
Al_2O_3	19.59	19.74	19.76	19.74	19.45	19.56
FeO	13.76	13.93	13.95	13.97	13.29	13.28
MnO	0.25	0.26	0.22	0.18	0.25	0.31
MgO	13.20	12.71	12.99	12.88	13.03	12.87
CaO	0.00	0.03	0.01	0.04	0.01	0.04
Na_2O	0.13	0.16	0.15	0.14	0.13	0.13
K_2O	10.42	10.20	10.23	10.16	10.65	10.33
Cr_2O_3	0.046	0.082	0.068	0.056	0.065	0.073
NiO	0.003	0.000	0.000	0.000	0.000	0.000
H_2O*	4.13	4.14	4.15	4.14	4.15	4.15
Total	101.43	101.54	101.74	101.53	101.80	101.65

Numbers of ions on the basis of 22 (O, OH)						
Tetrahedral (T)						
Si	5.436	5.444	5.439	5.434	5.504	5.496
^{IV}Al	2.564	2.556	2.561	2.566	2.496	2.504
Octahedral (M)						
M1-site						
^{VI}Al	0.790	0.817	0.808	0.806	0.813	0.824
Ti	0.271	0.298	0.285	0.299	0.287	0.306
Cr	0.005	0.009	0.008	0.006	0.007	0.008
Sn	0.000	0.000	0.000	0.000	0.000	0.000
Ga	0.000	0.000	0.000	0.000	0.000	0.000
M2-site						
Fe^{2+}	1.671	1.689	1.688	1.693	1.604	1.603
Ni	0.000	0.000	0.000	0.000	0.000	0.000
Mg	2.858	2.746	2.801	2.783	2.804	2.769
Mn	0.031	0.032	0.027	0.021	0.031	0.038
Cu	0.000	0.000	0.000	0.000	0.000	0.000
Zn	0.000	0.000	0.000	0.000	0.000	0.000
Interlayer (I)						
Ca	0.000	0.004	0.001	0.006	0.001	0.006
Na	0.035	0.046	0.041	0.039	0.036	0.036
K	1.930	1.886	1.888	1.878	1.961	1.902
Sr	0.004	0.007	0.006	0.005	0.005	0.006
Ba	0.000	0.000	0.000	0.000	0.000	0.000
Rb	0.000	0.000	0.000	0.000	0.000	0.000
Cs	0.000	0.000	0.000	0.000	0.000	0.000
Hyroxyl (OH)						
OH*	4.000	4.000	4.000	4.000	4.000	4.000
Total	19.596	19.533	19.552	19.537	19.550	19.498
End-member parameters						
Annite	36.9	38.1	37.6	37.8	36.4	36.7
Phlogopite	63.1	61.9	62.4	62.2	63.6	63.3

Sample	525139					
Spot number	38	43	44	45	53	54
SiO_2	37.85	38.3	37.55	38.13	36.61	36.77
TiO_2	2.840	2.290	2.430	2.170	2.540	2.580
Al_2O_3	19,320	19,710	19,160	19,460	19,460	19,370
FeO	13.29	13.20	13.62	13.20	14.33	14.47
MnO	0.24	0.29	0.19	0.27	0.29	0.21
MgO	12.98	13.10	12.86	12.87	12.96	13.22
CaO	0.01	0.04	0.10	0.09	0.08	0.08
Na_2O	0.14	0.12	0.15	0.15	0.13	0.13
K_2O	10.51	10.25	9.81	9.99	10.17	9.89
Cr_2O_3	0.05	0.06	0.06	0.07	0.07	0.08
NiO	0.000	0.025	0.000	0.000	0.017	0.000
Total	97.234	97.384	95.927	96.396	96.655	96.802

Reformatted oxide percentages, with H_2O calculated (22 O)						
SiO_2	37.85	38.3	37.55	38.13	36.61	36.77
TiO_2	2.840	2.290	2.430	2.170	2.540	2.580
Al_2O_3	19,320	19,710	19,160	19,460	19,460	19,370
FeO	13.29	13.20	13.62	13.20	14.33	14.47
MnO	0.24	0.29	0.19	0.27	0.29	0.21
MgO	12.98	13.10	12.86	12.87	12.96	13.22
CaO	0.01	0.04	0.10	0.09	0.08	0.08
Na_2O	0.14	0.12	0.15	0.15	0.13	0.13
K_2O	10.51	10.25	9.81	9.99	10.17	9.89
Cr_2O_3	0.050	0.058	0.064	0.067	0.066	0.076
NiO	0.000	0.025	0.000	0.000	0.017	0.000
H_2O*	4,136	4,157	4,088	4,119	4,084	4,097
Total	101.37	101.54	100.01	100.51	100.74	100.90

Numbers of ions on the basis of 22 (O, OH)						
Tetrahedral (T)						
Si	5.488	5.524	5.509	5.551	5.375	5.382
^{IV}Al	2.512	2.476	2.491	2.449	2.625	2.618
Octahedral (M)						
M1-site						
^{VI}Al	0.789	0.875	0.822	0.891	0.743	0.723
Ti	0.310	0.248	0.268	0.238	0.280	0.284
Cr	0.006	0.007	0.007	0.008	0.008	0.009
Sn	0.000	0.000	0.000	0.000	0.000	0.000
Ga	0.000	0.000	0.000	0.000	0.000	0.000
M2-site						
Fe^{2+}	1.611	1.592	1.671	1.607	1.760	1.771
Ni	0.000	0.003	0.000	0.000	0.002	0.000
Mg	2.805	2.817	2.812	2.793	2.837	2.884
Mn	0.030	0.036	0.023	0.033	0.036	0.026
Cu	0.000	0.000	0.000	0.000	0.000	0.000
Zn	0.000	0.000	0.000	0.000	0.000	0.000
Interlayer (I)						
Ca	0.002	0.005	0.015	0.014	0.013	0.013
Na	0.039	0.034	0.042	0.043	0.038	0.037
K	1.944	1.886	1.836	1.855	1.905	1.846
Sr	0.004	0.005	0.005	0.006	0.006	0.006
Ba	0.000	0.001	0.000	0.000	0.001	0.000
Rb	0.000	0.000	0.000	0.000	0.000	0.000
Cs	0.000	0.000	0.000	0.000	0.000	0.000
Hyroxyl (OH)						
OH*	4.000	4.000	4.000	4.000	4.000	4.000
Total	19.540	19.509	19.502	19.487	19.627	19.601
End-member parameters						
Annite	36.5	36.1	37.3	36.5	38.3	38.0
Phlogopite	63.5	63.9	62.7	63.5	61.7	62.0

Sample	**525139**					
Spot number	55	63	64	65	69	70
SiO_2	36.61	38.06	37.89	37.79	37.61	37.69
TiO_2	2.530	2.390	2.340	2.320	2.440	2.460
Al_2O_3	19.34	19.54	19.55	19.41	19.15	19.27
FeO	14.40	13.20	13.47	13.32	13.00	13.17
MnO	0.16	0.22	0.28	0.26	0.21	0.26
MgO	13.19	13.47	13.46	13.30	13.16	13.21
CaO	0.06	0.01	0.00	0.04	0.01	0.00
Na_2O	0.15	0.10	0.13	0.11	0.15	0.18
K_2O	10.14	10.44	10.56	10.25	10.47	10.49
Cr_2O_3	0,047	0,019	0,033	0,000	0,034	0,025
NiO	0.000	0.000	0.013	0.010	0.007	0.000
Total	96.626	97.446	97.724	96.809	96.233	96.763

Reformatted oxide percentages, with H_2O calculated (22 O)						
SiO_2	36.61	38.06	37.89	37.79	37.61	37.69
TiO_2	2.530	2.390	2.340	2.320	2.440	2.460
Al_2O_3	19.34	19.54	19.55	19.41	19.15	19.27
FeO	14.40	13.20	13.47	13.32	13.00	13.17
MnO	0.16	0.22	0.28	0.26	0.21	0.26
MgO	13.19	13.47	13.46	13.30	13.16	13.21
CaO	0.06	0.01	0.00	0.04	0.01	0.00
Na_2O	0.15	0.10	0.13	0.11	0.15	0.18
K_2O	10.14	10.44	10.56	10.25	10.47	10.49
Cr_2O_3	0.047	0.019	0.033	0.000	0.034	0.025
NiO	0.000	0.000	0.013	0.010	0.007	0.000
H_2O*	4.08	4.15	4.15	4.12	4.10	4.12
Total	100.71	101.60	101.88	100.93	100.33	100.88

Numbers of ions on the basis of 22 (O, OH)						
Tetrahedral (T)						
Si	5.376	5.496	5.471	5.496	5.505	5.491
^{IV}Al	2.624	2.504	2.529	2.504	2.495	2.509
Octahedral (M)						
M1-site						
^{VI}Al	0.723	0.821	0.798	0.823	0.809	0.801
Ti	0.279	0.260	0.254	0.254	0.269	0.270
Cr	0.005	0.002	0.004	0.000	0.004	0.003
Sn	0.000	0.000	0.000	0.000	0.000	0.000
Ga	0.000	0.000	0.000	0.000	0.000	0.000
M2-site						
Fe^{2+}	1.768	1.594	1.627	1.620	1.591	1.605
Ni	0.000	0.000	0.002	0.001	0.001	0.000
Mg	2.887	2.899	2.897	2.883	2.871	2.869
Mn	0.020	0.027	0.034	0.032	0.026	0.033
Cu	0.000	0.000	0.000	0.000	0.000	0.000
Zn	0.000	0.000	0.000	0.000	0.000	0.000
Interlayer (I)						
Ca	0.010	0.001	0.000	0.006	0.001	0.001
Na	0.042	0.028	0.037	0.031	0.041	0.051
K	1.899	1.923	1.945	1.901	1.955	1.950
Sr	0.004	0.002	0.003	0.000	0.003	0.002
Ba	0.000	0.000	0.001	0.001	0.000	0.000
Rb	0.000	0.000	0.000	0.000	0.000	0.000
Cs	0.000	0.000	0.000	0.000	0.000	0.000
Hyroxyl (OH)						
OH*	4.000	4.000	4.000	4.000	4.000	4.000
Total	19.639	19.557	19.600	19.553	19.571	19.583
End-member parameters						
Annite	38.0	35.5	36.0	36.0	35.7	35.9
Phlogopite	62.0	64.5	64.0	64.0	64.3	64.1

Sample	**525139**					
Spot number	71	76	77	78	79	84
SiO_2	37.58	38.16	37.99	37.97	38.17	37.61
TiO_2	2.390	2.260	2.210	2.190	2.150	2.560
Al_2O_3	19.20	19.67	19.57	19.69	19.55	19.06
FeO	13.40	13.03	13.11	13.16	13.11	13.40
MnO	0.18	0.29	0.28	0.23	0.24	0.24
MgO	13.16	13.53	13.54	13.50	13.42	13.38
CaO	0.00	0.01	0.01	0.01	0.00	0.01
Na_2O	0.14	0.14	0.14	0.18	0.14	0.19
K_2O	10.50	10.58	10.50	10.40	10.40	10.37
Cr_2O_3	0,000	0,040	0,025	0,060	0,058	0,058
NiO	0.009	0.000	0.027	0.007	0.031	0.002
Total	96.559	97.703	97.403	97.400	97.270	96.868

Reformatted oxide percentages, with H_2O calculated (22 O)						
SiO_2	37.58	38.16	37.99	37.97	38.17	37.61
TiO_2	2.390	2.260	2.210	2.190	2.150	2.560
Al_2O_3	19.20	19.67	19.57	19.69	19.55	19.06
FeO	13.40	13.03	13.11	13.16	13.11	13.40
MnO	0.18	0.29	0.28	0.23	0.24	0.24
MgO	13.16	13.53	13.54	13.50	13.42	13.38
CaO	0.00	0.01	0.01	0.01	0.00	0.01
Na_2O	0.14	0.14	0.14	0.18	0.14	0.19
K_2O	10.50	10.58	10.50	10.40	10.40	10.37
Cr_2O_3	0.000	0.040	0.025	0.060	0.058	0.058
NiO	0.009	0.000	0.027	0.007	0.031	0.002
H_2O*	4.10	4.16	4.15	4.15	4.15	4.12
Total	100.66	101.87	101.55	101.55	101.42	100.98

Numbers of ions on the basis of 22 (O, OH)						
Tetrahedral (T)						
Si	5.493	5.495	5.491	5.485	5.517	5.479
^{IV}Al	2.507	2.505	2.509	2.515	2.483	2.521
Octahedral (M)						
M1-site						
^{VI}Al	0.800	0.834	0.825	0.837	0.847	0.751
Ti	0.263	0.245	0.240	0.238	0.234	0.280
Cr	0.000	0.005	0.003	0.007	0.007	0.007
Sn	0.000	0.000	0.000	0.000	0.000	0.000
Ga	0.000	0.000	0.000	0.000	0.000	0.000
M2-site						
Fe^{2+}	1.638	1.569	1.585	1.590	1.585	1.632
Ni	0.001	0.000	0.003	0.001	0.004	0.000
Mg	2.867	2.905	2.917	2.907	2.891	2.905
Mn	0.022	0.035	0.035	0.028	0.030	0.029
Cu	0.000	0.000	0.000	0.000	0.000	0.000
Zn	0.000	0.000	0.000	0.000	0.000	0.000
Interlayer (I)						
Ca	0.000	0.001	0.001	0.002	0.000	0.001
Na	0.040	0.039	0.040	0.050	0.039	0.053
K	1.958	1.943	1.936	1.916	1.917	1.927
Sr	0.000	0.003	0.002	0.005	0.005	0.005
Ba	0.001	0.000	0.002	0.000	0.002	0.000
Rb	0.000	0.000	0.000	0.000	0.000	0.000
Cs	0.000	0.000	0.000	0.000	0.000	0.000
Hyroxyl (OH)						
OH*	4.000	4.000	4.000	4.000	4.000	4.000
Total	19.590	19.579	19.588	19.581	19.559	19.591
End-member parameters						
Annite	36.4	35.1	35.2	35.4	35.4	36.0
Phlogopite	63.6	64.9	64.8	64.6	64.6	64.0

Sample	**525139**		
Spot number	85	86	87
SiO_2	37.41	37.70	37.67
TiO_2	2.500	2.500	2.560
Al_2O_3	19.11	18.93	19.05
FeO	13.46	13.55	13.44
MnO	0.21	0.26	0.17
MgO	13.42	13.36	13.25
CaO	0.00	0.02	0.05
Na_2O	0.18	0.21	0.18
K_2O	10.29	10.26	10.26
Cr_2O_3	0,046	0,060	0,053
NiO	0.052	0.010	0.000
Total	96.680	96.856	96.685

Sample Ujarrasiorit						
Spot number	210	211	212	216	217	218
SiO_2	37.50	37.07	37.26	36.93	37.07	37.00
TiO_2	0.717	0.726	0.781	0.966	0.923	0.991
Al_2O_3	13.89	13.78	13.77	13.67	13.54	13.60
FeO	25.07	25.11	24.81	24.69	24.51	24.42
MnO	0.33	0.30	0.29	0.36	0.33	0.38
MgO	11.08	11.08	11.09	11.07	11.01	10.92
CaO	0.02	0.04	0.05	0.11	0.07	0.10
Na_2O	0.09	0.11	0.11	0.10	0.11	0.08
K_2O	9.65	9.70	9.67	9.35	9.63	9.69
Cr_2O_3	0,063	0,050	0,060	0,054	0,031	0,053
NiO	0.019	0.000	0.000	0.018	0.025	0.000
Total	98.426	97.964	97.886	97.320	97.246	97.237

Reformatted oxide perc., with H_2O calc. (22 O)			
SiO_2	37.41	37.70	37.67
TiO_2	2.500	2.500	2.560
Al_2O_3	19.11	18.93	19.05
FeO	13.46	13.55	13.44
MnO	0.21	0.26	0.17
MgO	13.42	13.36	13.25
CaO	0.00	0.02	0.05
Na_2O	0.18	0.21	0.18
K_2O	10.29	10.26	10.26
Cr_2O_3	0.046	0.060	0.053
NiO	0.052	0.010	0.000
H_2O*	4.11	4.12	4.11
Total	100.79	100.97	100.80

Reformatted oxide percentages, with H_2O calculated (22 O)						
SiO_2	37.50	37.07	37.26	36.93	37.07	37.00
TiO_2	0.717	0.726	0.781	0.966	0.923	0.991
Al_2O_3	13.89	13.78	13.77	13.67	13.54	13.60
FeO	25.07	25.11	24.81	24.69	24.51	24.42
MnO	0.33	0.30	0.29	0.36	0.33	0.38
MgO	11.08	11.08	11.09	11.07	11.01	10.92
CaO	0.02	0.04	0.05	0.11	0.07	0.10
Na_2O	0.09	0.11	0.11	0.10	0.11	0.08
K_2O	9.65	9.70	9.67	9.35	9.63	9.69
Cr_2O_3	0.063	0.050	0.060	0.054	0.031	0.053
NiO	0.019	0.000	0.000	0.018	0.025	0.000
H_2O*	3.95	3.92	3.92	3.90	3.90	3.90
Total	102.37	101.88	101.81	101.22	101.15	101.14

Numbers of ions on the basis of 22 (O, OH)			
Tetrahedral (T)			
Si	5.462	5.493	5.493
^{IV}Al	2.538	2.507	2.507
Octahedral (M)			
M1-site			
^{VI}Al	0.750	0.745	0.767
Ti	0.274	0.274	0.281
Cr	0.005	0.007	0.006
Sn	0.000	0.000	0.000
Ga	0.000	0.000	0.000
M2-site			
Fe^{2+}	1.643	1.651	1.639
Ni	0.006	0.001	0.000
Mg	2.921	2.902	2.880
Mn	0.026	0.032	0.021
Cu	0.000	0.000	0.000
Zn	0.000	0.000	0.000
Interlayer (I)			
Ca	0.000	0.003	0.007
Na	0.051	0.058	0.052
K	1.916	1.907	1.908
Sr	0.004	0.005	0.004
Ba	0.003	0.001	0.000
Rb	0.000	0.000	0.000
Cs	0.000	0.000	0.000
Hyroxyl (OH)			
OH*	4.000	4.000	4.000
Total	19.601	19.586	19.566
End-member parameters			
Annite	36.0	36.3	36.3
Phlogopite	64.0	63.7	63.7

Numbers of ions on the basis of 22 (O, OH)						
Tetrahedral (T)						
Si	5.698	5.672	5.693	5.672	5.701	5.692
^{IV}Al	2.302	2.328	2.307	2.328	2.299	2.308
Octahedral (M)						
M1-site						
^{VI}Al	0.185	0.157	0.172	0.147	0.155	0.157
Ti	0.082	0.084	0.090	0.112	0.107	0.115
Cr	0.008	0.006	0.007	0.007	0.004	0.006
Sn	0.000	0.000	0.000	0.000	0.000	0.000
Ga	0.000	0.000	0.000	0.000	0.000	0.000
M2-site						
Fe^{2+}	3.186	3.213	3.170	3.172	3.152	3.142
Ni	0.002	0.000	0.000	0.002	0.003	0.000
Mg	2.510	2.527	2.526	2.535	2.524	2.504
Mn	0.042	0.039	0.037	0.047	0.043	0.050
Cu	0.000	0.000	0.000	0.000	0.000	0.000
Zn	0.000	0.000	0.000	0.000	0.000	0.000
Interlayer (I)						
Ca	0.003	0.007	0.008	0.018	0.012	0.016
Na	0.027	0.031	0.032	0.030	0.032	0.024
K	1.870	1.893	1.884	1.832	1.889	1.901
Sr	0.006	0.004	0.005	0.005	0.003	0.005
Ba	0.001	0.000	0.000	0.001	0.002	0.000
Rb	0.000	0.000	0.000	0.000	0.000	0.000
Cs	0.000	0.000	0.000	0.000	0.000	0.000
Hyroxyl (OH)						
OH*	4.000	4.000	4.000	4.000	4.000	4.000
Total	19.921	19.961	19.932	19.906	19.924	19.921
End-member parameters						
Annite	55.9	56.0	55.7	55.6	55.5	55.6
Phlogopite	44.1	44.0	44.3	44.4	44.5	44.4

x 55.534632599 70.3741

29.625902739 44.46537

Sample Ujarrasiorit						
Spot number	219	223	224	225	229	230
SiO_2	37.13	37.09	37.00	37.24	37.20	37.24
TiO_2	0.980	0.923	0.954	0.891	1.104	1.125
Al_2O_3	13.50	13.58	13.76	13.85	13.65	13.52
FeO	24.79	25.15	24.93	25.00	24.97	25.02
MnO	0.32	0.34	0.34	0.31	0.30	0.33
MgO	11.03	10.96	10.85	11.08	10.71	10.82
CaO	0.09	0.23	0.22	0.24	0.01	0.01
Na_2O	0.13	0.07	0.08	0.09	0.06	0.08
K_2O	9.64	8.88	8.74	8.76	10.02	9.96
Cr_2O_3	0,044	0,015	0,026	0,038	0,062	0,031
NiO	0.000	0.000	0.017	0.002	0.000	0.000
Total	97.647	97.244	96.922	97.490	98.086	98.143

Reformatted oxide percentages, with H_2O calculated (22 O)						
SiO_2	37.13	37.09	37.00	37.24	37.20	37.24
TiO_2	0.980	0.923	0.954	0.891	1.104	1.125
Al_2O_3	13.50	13.58	13.76	13.85	13.65	13.52
FeO	24.79	25.15	24.93	25.00	24.97	25.02
MnO	0.32	0.34	0.34	0.31	0.30	0.33
MgO	11.03	10.96	10.85	11.08	10.71	10.82
CaO	0.09	0.23	0.22	0.24	0.01	0.01
Na_2O	0.13	0.07	0.08	0.09	0.06	0.08
K_2O	9.64	8.88	8.74	8.76	10.02	9.96
Cr_2O_3	0.044	0.015	0.026	0.038	0.062	0.031
NiO	0.000	0.000	0.017	0.002	0.000	0.000
H_2O*	3.91	3.90	3.90	3.92	3.92	3.92
Total	101.56	101.15	100.82	101.41	102.01	102.07

Numbers of ions on the basis of 22 (O, OH)						
Tetrahedral (T)						
Si	5.693	5.696	5.691	5.690	5.689	5.693
^{IV}Al	2.307	2.304	2.309	2.310	2.311	2.307
Octahedral (M)						
M1-site						
^{VI}Al	0.133	0.155	0.186	0.184	0.149	0.129
Ti	0.113	0.107	0.110	0.102	0.127	0.129
Cr	0.005	0.002	0.003	0.005	0.007	0.004
Sn	0.000	0.000	0.000	0.000	0.000	0.000
Ga	0.000	0.000	0.000	0.000	0.000	0.000
M2-site						
Fe^{2+}	3.179	3.230	3.207	3.195	3.193	3.199
Ni	0.000	0.000	0.002	0.000	0.000	0.000
Mg	2.521	2.509	2.488	2.524	2.441	2.466
Mn	0.041	0.045	0.045	0.040	0.039	0.043
Cu	0.000	0.000	0.000	0.000	0.000	0.000
Zn	0.000	0.000	0.000	0.000	0.000	0.000
Interlayer (I)						
Ca	0.014	0.038	0.037	0.039	0.001	0.002
Na	0.038	0.021	0.024	0.025	0.018	0.023
K	1.885	1.740	1.715	1.707	1.954	1.942
Sr	0.004	0.001	0.002	0.003	0.005	0.003
Ba	0.000	0.000	0.001	0.000	0.000	0.000
Rb	0.000	0.000	0.000	0.000	0.000	0.000
Cs	0.000	0.000	0.000	0.000	0.000	0.000
Hyroxyl (OH)						
OH*	4.000	4.000	4.000	4.000	4.000	4.000
Total	19.933	19.847	19.819	19.824	19.937	19.941
End-member parameters						
Annite	55.8	56.3	56.3	55.9	56.7	56.5
Phlogopite	44.2	43.7	43.7	44.1	43.3	43.5

Sample Ujarrasiorit						
Spot number	231	232	236	237	238	248
SiO_2	37.33	37.50	37.14	37.38	37.36	36.70
TiO_2	1.056	1.143	1.109	1.122	1.143	1.113
Al_2O_3	13.56	13.68	13.55	13.65	13.59	13.33
FeO	25.36	24.88	24.87	24.72	24.65	26.62
MnO	0.33	0.33	0.36	0.35	0.42	0.31
MgO	10.76	10.68	10.79	10.75	10.70	9.53
CaO	0.01	0.00	0.01	0.01	0.02	0.02
Na_2O	0.07	0.06	0.06	0.08	0.07	0.14
K_2O	10.02	9.95	9.81	10.08	9.90	9.48
Cr_2O_3	0,035	0,036	0,039	0,073	0,013	0,042
NiO	0.016	0.017	0.017	0.001	0.000	0.038
Total	98.556	98.272	97.758	98.216	97.858	97.330

Reformatted oxide percentages, with H_2O calculated (22 O)						
SiO_2	37.33	37.50	37.14	37.38	37.36	36.70
TiO_2	1.056	1.143	1.109	1.122	1.143	1.113
Al_2O_3	13.56	13.68	13.55	13.65	13.59	13.33
FeO	25.36	24.88	24.87	24.72	24.65	26.62
MnO	0.33	0.33	0.36	0.35	0.42	0.31
MgO	10.76	10.68	10.79	10.75	10.70	9.53
CaO	0.01	0.00	0.01	0.01	0.02	0.02
Na_2O	0.07	0.06	0.06	0.08	0.07	0.14
K_2O	10.02	9.95	9.81	10.08	9.90	9.48
Cr_2O_3	0.035	0.036	0.039	0.073	0.013	0.042
NiO	0.016	0.017	0.017	0.001	0.000	0.038
H_2O*	3.93	3.94	3.91	3.93	3.92	3.86
Total	102.49	102.21	101.67	102.15	101.78	101.19

Numbers of ions on the basis of 22 (O, OH)						
Tetrahedral (T)						
Si	5.691	5.713	5.693	5.702	5.715	5.698
^{IV}Al	2.309	2.287	2.307	2.298	2.285	2.302
Octahedral (M)						
M1-site						
^{VI}Al	0.128	0.170	0.142	0.156	0.166	0.137
Ti	0.121	0.131	0.128	0.129	0.132	0.130
Cr	0.004	0.004	0.005	0.009	0.002	0.005
Sn	0.000	0.000	0.000	0.000	0.000	0.000
Ga	0.000	0.000	0.000	0.000	0.000	0.000
M2-site						
Fe^{2+}	3.233	3.170	3.188	3.154	3.154	3.456
Ni	0.002	0.002	0.002	0.000	0.000	0.005
Mg	2.445	2.426	2.466	2.444	2.440	2.206
Mn	0.043	0.042	0.046	0.046	0.054	0.041
Cu	0.000	0.000	0.000	0.000	0.000	0.000
Zn	0.000	0.000	0.000	0.000	0.000	0.000
Interlayer (I)						
Ca	0.002	0.000	0.002	0.002	0.003	0.003
Na	0.021	0.018	0.019	0.022	0.020	0.043
K	1.948	1.934	1.918	1.961	1.932	1.877
Sr	0.003	0.003	0.003	0.006	0.001	0.004
Ba	0.001	0.001	0.001	0.000	0.000	0.002
Rb	0.000	0.000	0.000	0.000	0.000	0.000
Cs	0.000	0.000	0.000	0.000	0.000	0.000
Hyroxyl (OH)						
OH*	4.000	4.000	4.000	4.000	4.000	4.000
Total	19.952	19.901	19.921	19.930	19.903	19.910
End-member parameters						
Annite	56.9	56.7	56.4	56.3	56.4	61.0
Phlogopite	43.1	43.3	43.6	43.7	43.6	39.0

Sample Ujarrasiorit				
Spot number	249	250	254	256
SiO_2	36.70	36.55	36.96	36.22
TiO_2	1.104	1.082	0.846	0.930
Al_2O_3	13.31	13.48	14.08	13.69
FeO	26.53	26.57	30.02	29.85
MnO	0.44	0.35	0.28	0.34
MgO	9.47	9.47	7.31	7.05
CaO	0.02	0.01	0.31	0.26
Na_2O	0.08	0.09	0.19	0.18
K_2O	9.56	9.60	8.27	8.53
Cr_2O_3	0,050	0,048	0,014	0,034
NiO	0.000	0.005	0.016	0.000
Total	97.266	97.244	98.292	97.082

Reformatted oxide perc., with H_2O calc. (22 O)				
SiO_2	36.70	36.55	36.96	36.22
TiO_2	1.104	1.082	0.846	0.930
Al_2O_3	13.31	13.48	14.08	13.69
FeO	26.53	26.57	30.02	29.85
MnO	0.44	0.35	0.28	0.34
MgO	9.47	9.47	7.31	7.05
CaO	0.02	0.01	0.31	0.26
Na_2O	0.08	0.09	0.19	0.18
K_2O	9.56	9.60	8.27	8.53
Cr_2O_3	0.050	0.048	0.014	0.034
NiO	0.000	0.005	0.016	0.000
H_2O*	3.86	3.86	3.87	3.81
Total	101.12	101.10	102.17	100.89

Numbers of ions on the basis of 22 (O, OH)				
Tetrahedral (T)				
Si	5.704	5.683	5.720	5.702
^{IV}Al	2.296	2.317	2.280	2.298
Octahedral (M)				
M1-site				
^{VI}Al	0.142	0.153	0.288	0.242
Ti	0.129	0.127	0.098	0.110
Cr	0.006	0.006	0.002	0.004
Sn	0.000	0.000	0.000	0.000
Ga	0.000	0.000	0.000	0.000
M2-site				
Fe^{2+}	3.448	3.455	3.885	3.930
Ni	0.000	0.001	0.002	0.000
Mg	2.194	2.195	1.686	1.654
Mn	0.058	0.045	0.036	0.045
Cu	0.000	0.000	0.000	0.000
Zn	0.000	0.000	0.000	0.000
Interlayer (I)				
Ca	0.004	0.001	0.052	0.044
Na	0.025	0.026	0.056	0.055
K	1.895	1.904	1.632	1.713
Sr	0.005	0.004	0.001	0.003
Ba	0.000	0.000	0.001	0.000
Rb	0.000	0.000	0.000	0.000
Cs	0.000	0.000	0.000	0.000
Hyroxyl (OH)				
OH*	4.000	4.000	4.000	4.000
Total	19.905	19.917	19.741	19.800
End-member parameters				
Annite	61.1	61.2	69.7	70.4
Phlogopite	38.9	38.8	30.3	29.6

Sample	525138					
Spot number	28	29	30	37	38	47
SiO_2	61.960	61.970	61.790	62.350	62.100	59.670
TiO_2	0.012	0.046	0.022	0.000	0.000	0.004
Al_2O_3	24.160	24.230	24.360	24.150	24.060	23.550
FeO	0.012	0.007	0.000	0.000	0.007	0.044
MnO	0.000	0.010	0.010	0.000	0.020	0.037
MgO	0.003	0.000	0.001	0.006	0.000	0.000
CaO	6.120	6.000	6.110	5.880	5.870	5.760
Na_2O	8.770	8.720	8.790	8.770	9.040	8.780
K_2O	0.165	0.153	0.189	0.154	0.146	0.201
Cr_2O_3	0.000	0.012	0.000	0.000	0.000	0.021
NiO	0.036	0.023	0.000	0.000	0.000	0.000
Total	101.238	101.171	101.271	101.310	101.243	98.068
Numbers of ions on the basis of 8 (O)						
Tetrahedral (T)						
Si	2.725	2.726	2.718	2.736	2.731	2.714
Al	1.253	1.256	1.263	1.249	1.247	1.263
Fe	0.000	0.000	0.000	0.000	0.000	0.002
Octahedral (M)						
Ti	0.000	0.002	0.001	0.000	0.000	0.000
Ni	0.001	0.001	0.000	0.000	0.000	0.000
Cr	0.000	0.000	0.000	0.000	0.000	0.001
Mg	0.000	0.000	0.000	0.000	0.000	0.000
Mn	0.000	0.000	0.000	0.000	0.001	0.001
Ca	0.288	0.283	0.288	0.276	0.277	0.281
Na	0.748	0.744	0.750	0.746	0.771	0.774
K	0.009	0.009	0.011	0.009	0.008	0.012
Total	5.026	5.021	5.030	5.017	5.035	5.047
End-member parameters						
Orthoclase	0.9	0.8	1.0	0.8	0.8	1.1
Albite	71.5	71.8	71.5	72.4	73.0	72.6
Anorthite	27.6	27.3	27.5	26.8	26.2	26.3

Sample	525138					
Spot number	48	49	50	55	56	57
SiO_2	62.290	62.040	62.260	62.350	62.380	62.100
TiO_2	0.017	0.018	0.032	0.024	0.000	0.005
Al_2O_3	24.220	24.300	24.190	24.190	24.290	24.110
FeO	0.029	0.036	0.044	0.044	0.000	0.015
MnO	0.000	0.000	0.000	0.024	0.017	0.005
MgO	0.000	0.000	0.000	0.000	0.004	0.000
CaO	5.950	5.860	5.980	6.010	5.980	6.010
Na_2O	8.650	8.710	8.850	8.910	8.700	8.730
K_2O	0.181	0.194	0.219	0.226	0.268	0.227
Cr_2O_3	0.000	0.036	0.000	0.000	0.000	0.010
NiO	0.000	0.000	0.000	0.000	0.003	0.009
Total	101.337	101.194	101.575	101.779	101.642	101.222
Numbers of ions on the basis of 8 (O)						
Tetrahedral (T)						
Si	2.733	2.727	2.729	2.729	2.731	2.731
Al	1.253	1.259	1.250	1.248	1.254	1.250
Fe	0.001	0.001	0.002	0.002	0.000	0.001
Octahedral (M)						
Ti	0.001	0.001	0.001	0.001	0.000	0.000
Ni	0.000	0.000	0.000	0.000	0.000	0.000
Cr	0.000	0.001	0.000	0.000	0.000	0.000
Mg	0.000	0.000	0.000	0.000	0.000	0.000
Mn	0.000	0.000	0.000	0.001	0.001	0.000
Ca	0.280	0.276	0.281	0.282	0.280	0.283
Na	0.736	0.742	0.752	0.756	0.738	0.744
K	0.010	0.011	0.012	0.013	0.015	0.013
Total	5.013	5.019	5.027	5.031	5.019	5.022
End-member parameters						
Orthoclase	1.0	1.1	1.2	1.2	1.4	1.2
Albite	71.7	72.1	72.0	72.0	71.4	71.6
Anorthite	27.3	26.8	26.9	26.8	27.1	27.2

Sample	525138					
Spot number	58	73	74	75	81	82
SiO_2	62.090	62.210	62.220	62.180	62.110	62.630
TiO_2	0.015	0.000	0.000	0.000	0.000	0.010
Al_2O_3	24.160	24.250	23.940	24.340	23.950	23.850
FeO	0.015	0.000	0.000	0.009	0.050	0.055
MnO	0.032	0.000	0.000	0.000	0.010	0.000
MgO	0.003	0.002	0.000	0.000	0.000	0.000
CaO	5.980	6.050	5.930	6.020	5.770	5.780
Na_2O	8.760	8.670	8.810	8.610	8.830	8.750
K_2O	0.208	0.338	0.324	0.313	0.316	0.278
Cr_2O_3	0.006	0.004	0.000	0.000	0.003	0.006
NiO	0.029	0.012	0.008	0.000	0.000	0.000
Total	101.299	101.536	101.231	101.473	101.039	101.358
Numbers of ions on the basis of 8 (O)						
Tetrahedral (T)						
Si	2.729	2.728	2.737	2.727	2.737	2.748
Al	1.252	1.254	1.241	1.259	1.244	1.234
Fe	0.001	0.000	0.000	0.000	0.002	0.002
Octahedral (M)						
Ti	0.000	0.000	0.000	0.000	0.000	0.000
Ni	0.001	0.000	0.000	0.000	0.000	0.000
Cr	0.000	0.000	0.000	0.000	0.000	0.000
Mg	0.000	0.000	0.000	0.000	0.000	0.000
Mn	0.001	0.000	0.000	0.000	0.000	0.000
Ca	0.282	0.284	0.279	0.283	0.272	0.272
Na	0.746	0.737	0.751	0.732	0.754	0.744
K	0.012	0.019	0.018	0.018	0.018	0.016
Total	5.024	5.023	5.027	5.019	5.027	5.015
End-member parameters						
Orthoclase	1.1	1.8	1.7	1.7	1.7	1.5
Albite	71.8	70.9	71.6	70.9	72.2	72.2
Anorthite	27.1	27.3	26.6	27.4	26.1	26.3

Sample	525138					
Spot number	83	84	107	108	109	110
SiO_2	62.530	62.160	62.170	62.300	62.120	61.050
TiO_2	0.000	0.006	0.000	0.007	0.000	0.000
Al_2O_3	24.130	24.050	23.970	23.920	24.010	23.950
FeO	0.014	0.000	0.000	0.000	0.014	0.036
MnO	0.000	0.005	0.010	0.007	0.066	0.000
MgO	0.000	0.000	0.000	0.000	0.000	0.000
CaO	5.790	5.760	5.820	5.850	5.920	5.760
Na_2O	8.590	8.650	8.870	8.790	8.790	8.680
K_2O	0.315	0.301	0.303	0.248	0.242	0.356
Cr_2O_3	0.000	0.002	0.003	0.000	0.009	0.000
NiO	0.012	0.011	0.010	0.012	0.022	0.055
Total	101.381	100.945	101.156	101.133	101.193	99.888
Numbers of ions on the basis of 8 (O)						
Tetrahedral (T)						
Si	2.741	2.738	2.736	2.740	2.733	2.723
Al	1.247	1.249	1.244	1.240	1.245	1.260
Fe	0.001	0.000	0.000	0.000	0.001	0.001
Octahedral (M)						
Ti	0.000	0.000	0.000	0.000	0.000	0.000
Ni	0.000	0.000	0.000	0.000	0.001	0.002
Cr	0.000	0.000	0.000	0.000	0.000	0.000
Mg	0.000	0.000	0.000	0.000	0.000	0.000
Mn	0.000	0.000	0.000	0.000	0.002	0.000
Ca	0.272	0.272	0.274	0.276	0.279	0.275
Na	0.730	0.739	0.757	0.750	0.750	0.751
K	0.018	0.017	0.017	0.014	0.014	0.020
Total	5.009	5.015	5.029	5.021	5.026	5.032
End-member parameters						
Orthoclase	1.7	1.6	1.6	1.3	1.3	1.9
Albite	71.6	71.9	72.2	72.1	71.9	71.8
Anorthite	26.7	26.5	26.2	26.5	26.8	26.3

Sample	525138	
Spot number	111	112
SiO_2	60.760	60.900
TiO_2	0.000	0.013
Al_2O_3	23.750	23.740
FeO	0.024	0.022
MnO	0.000	0.027
MgO	0.002	0.000
CaO	5.740	5.730
Na_2O	8.740	8.840
K_2O	0.391	0.378
Cr_2O_3	0.014	0.000
NiO	0.000	0.000
Total	99.421	99.650
Numbers of ions on the basis of 8 (O)		
Tetrahedral (T)		
Si	2.724	2.725
Al	1.255	1.252
Fe	0.001	0.001
Octahedral (M)		
Ti	0.000	0.000
Ni	0.000	0.000
Cr	0.000	0.000
Mg	0.000	0.000
Mn	0.000	0.001
Ca	0.276	0.275
Na	0.760	0.767
K	0.022	0.022
Total	5.039	5.043
End-member parameters		
Orthoclase	2.1	2.0
Albite	71.8	72.1
Anorthite	26.1	25.8

Sample	525139					
Spot no.	18	19	20	24	25	26
SiO_2	60.080	59.970	59.940	61.690	61.700	61.770
TiO_2	0.000	0.000	0.014	0.020	0.000	0.009
Al_2O_3	25.730	25.700	25.800	24.950	24.840	24.610
FeO	0.028	0.010	0.009	0.009	0.014	0.000
MnO	0.007	0.002	0.000	0.052	0.000	0.005
MgO	0.000	0.000	0.000	0.002	0.000	0.000
CaO	7.890	7.940	7.900	6.600	6.790	6.640
Na_2O	7.650	7.730	7.640	8.350	8.350	8.270
K_2O	0.233	0.249	0.228	0.344	0.327	0.266
Cr_2O_3	0.011	0.000	0.002	0.000	0.000	0.010
NiO	0.054	0.000	0.000	0.000	0.000	0.017
Total	101.683	101.602	101.533	102.017	102.021	101.596
Numbers of ions on the basis of 8 (O)						
Tetrahedral (T)						
Si	2.644	2.642	2.641	2.697	2.698	2.709
Al	1.335	1.335	1.340	1.286	1.281	1.272
Fe	0.001	0.000	0.000	0.000	0.001	0.000
Octahedral (M)						
Ti	0.000	0.000	0.000	0.001	0.000	0.000
Ni	0.002	0.000	0.000	0.000	0.000	0.001
Cr	0.000	0.000	0.000	0.000	0.000	0.000
Mg	0.000	0.000	0.000	0.000	0.000	0.000
Mn	0.000	0.000	0.000	0.002	0.000	0.000
Ca	0.372	0.375	0.373	0.309	0.318	0.312
Na	0.653	0.660	0.653	0.708	0.708	0.703
K	0.013	0.014	0.013	0.019	0.018	0.015
Total	5.021	5.027	5.021	5.023	5.024	5.013
End-member parameters						
Orthoclase	1.3	1.3	1.2	1.9	1.7	1.4
Albite	62.9	62.9	62.9	68.3	67.8	68.3
Anorthite	35.8	35.7	35.9	29.8	30.5	30.3

Sample	525139					
Spot number	30	31	32	33	34	35
SiO_2	61.760	61.950	61.680	61.310	61.320	61.620
TiO_2	0.035	0.014	0.050	0.000	0.000	0.020
Al_2O_3	24.790	24.650	24.750	24.840	24.860	24.700
FeO	0.010	0.021	0.000	0.023	0.027	0.000
MnO	0.017	0.010	0.000	0.017	0.015	0.000
MgO	0.000	0.000	0.008	0.000	0.003	0.000
CaO	6.550	6.390	6.520	6.620	6.750	6.610
Na_2O	8.360	8.410	8.280	8.430	8.300	8.370
K_2O	0.346	0.350	0.364	0.242	0.274	0.289
Cr_2O_3	0.003	0.011	0.001	0.000	0.002	0.013
NiO	0.000	0.000	0.029	0.010	0.023	0.000
Total	101.871	101.806	101.682	101.492	101.573	101.623
Numbers of ions on the basis of 8 (O)						
Tetrahedral (T)						
Si	2.703	2.712	2.704	2.695	2.694	2.703
Al	1.279	1.272	1.279	1.287	1.287	1.278
Fe	0.000	0.001	0.000	0.001	0.001	0.000
Octahedral (M)						
Ti	0.001	0.000	0.002	0.000	0.000	0.001
Ni	0.000	0.000	0.001	0.000	0.001	0.000
Cr	0.000	0.000	0.000	0.000	0.000	0.000
Mg	0.000	0.000	0.001	0.000	0.000	0.000
Mn	0.001	0.000	0.000	0.001	0.001	0.000
Ca	0.307	0.300	0.306	0.312	0.318	0.311
Na	0.709	0.714	0.704	0.718	0.707	0.712
K	0.019	0.020	0.020	0.014	0.015	0.016
Total	5.020	5.018	5.017	5.028	5.024	5.021
End-member parameters						
Orthoclase	1.9	1.9	2.0	1.3	1.5	1.6
Albite	68.5	69.1	68.3	68.8	68.0	68.5
Anorthite	29.7	29.0	29.7	29.9	30.5	29.9

Sample	525139					
Spot number	39	40	41	42	46	47
SiO_2	60.570	60.710	60.860	60.750	61.350	61.440
TiO_2	0.000	0.007	0.000	0.009	0.002	0.020
Al_2O_3	24.330	24.540	24.430	24.310	24.600	24.710
FeO	0.058	0.052	0.066	0.063	0.062	0.041
MnO	0.000	0.020	0.000	0.000	0.012	0.000
MgO	0.000	0.000	0.000	0.000	0.000	0.000
CaO	6.290	6.290	6.130	6.270	6.290	6.350
Na_2O	8.480	8.380	8.640	8.400	8.490	8.570
K_2O	0.168	0.179	0.162	0.167	0.183	0.208
Cr_2O_3	0.001	0.028	0.005	0.002	0.019	0.013
NiO	0.000	0.000	0.000	0.003	0.023	0.000
Total	99.896	100.206	100.293	99.973	101.031	101.352
Numbers of ions on the basis of 8 (O)						
Tetrahedral (T)						
Si	2.703	2.700	2.704	2.707	2.706	2.702
Al	1.280	1.287	1.280	1.277	1.279	1.281
Fe	0.002	0.002	0.002	0.002	0.002	0.002
Octahedral (M)						
Ti	0.000	0.000	0.000	0.000	0.000	0.001
Ni	0.000	0.000	0.000	0.000	0.001	0.000
Cr	0.000	0.001	0.000	0.000	0.001	0.000
Mg	0.000	0.000	0.000	0.000	0.000	0.000
Mn	0.000	0.001	0.000	0.000	0.000	0.000
Ca	0.301	0.300	0.292	0.299	0.297	0.299
Na	0.734	0.723	0.744	0.726	0.726	0.731
K	0.010	0.010	0.009	0.009	0.010	0.012
Total	5.029	5.023	5.032	5.022	5.023	5.028
End-member parameters						
Orthoclase	0.9	1.0	0.9	0.9	1.0	1.1
Albite	70.3	70.0	71.2	70.1	70.2	70.2
Anorthite	28.8	29.0	27.9	28.9	28.8	28.7

Sample	525139					
Spot number	57	58	59	60	61	62
SiO_2	61.390	61.110	61.730	61.740	61.640	61.400
TiO_2	0.047	0.031	0.000	0.013	0.000	0.000
Al_2O_3	24.340	24.510	24.270	24.320	24.370	24.470
FeO	0.064	0.030	0.031	0.022	0.000	0.000
MnO	0.012	0.015	0.012	0.000	0.027	0.000
MgO	0.000	0.002	0.002	0.000	0.000	0.009
CaO	6.360	6.320	6.250	6.170	6.140	6.530
Na_2O	8.310	8.530	8.590	8.600	8.630	8.440
K_2O	0.221	0.211	0.347	0.373	0.361	0.371
Cr_2O_3	0.000	0.000	0.003	0.000	0.004	0.000
NiO	0.004	0.000	0.000	0.023	0.000	0.000
Total	100.748	100.758	101.235	101.261	101.172	101.221
Numbers of ions on the basis of 8 (O)						
Tetrahedral (T)						
Si	2.714	2.704	2.718	2.718	2.716	2.706
Al	1.268	1.278	1.260	1.262	1.266	1.272
Fe	0.002	0.001	0.001	0.001	0.000	0.000
Octahedral (M)						
Ti	0.002	0.001	0.000	0.000	0.000	0.000
Ni	0.000	0.000	0.000	0.001	0.000	0.000
Cr	0.000	0.000	0.000	0.000	0.000	0.000
Mg	0.000	0.000	0.000	0.000	0.000	0.001
Mn	0.000	0.001	0.000	0.000	0.001	0.000
Ca	0.301	0.300	0.295	0.291	0.290	0.308
Na	0.712	0.732	0.733	0.734	0.737	0.721
K	0.012	0.012	0.019	0.021	0.020	0.021
Total	5.013	5.028	5.028	5.028	5.030	5.029
End-member parameters						
Orthoclase	1.2	1.1	1.9	2.0	1.9	2.0
Albite	69.4	70.1	70.0	70.2	70.4	68.7
Anorthite	29.4	28.7	28.1	27.8	27.7	29.4

Sample	525139					
Spot number	48	49	50	51	52	56
SiO_2	61.440	61.670	61.870	61.800	61.530	61.280
TiO_2	0.000	0.035	0.000	0.000	0.005	0.000
Al_2O_3	24.690	24.730	24.600	24.500	24.610	24.560
FeO	0.042	0.057	0.026	0.019	0.035	0.034
MnO	0.000	0.017	0.032	0.052	0.015	0.027
MgO	0.000	0.000	0.000	0.000	0.001	0.000
CaO	6.340	6.320	6.270	6.340	6.290	6.300
Na_2O	8.540	8.570	8.520	8.580	8.840	8.320
K_2O	0.186	0.161	0.190	0.187	0.199	0.242
Cr_2O_3	0.026	0.004	0.007	0.000	0.004	0.009
NiO	0.001	0.013	0.000	0.016	0.005	0.000
Total	101.264	101.577	101.514	101.493	101.535	100.772
Numbers of ions on the basis of 8 (O)						
Tetrahedral (T)						
Si	2.704	2.705	2.714	2.713	2.703	2.708
Al	1.281	1.279	1.272	1.268	1.275	1.280
Fe	0.002	0.002	0.001	0.001	0.001	0.001
Octahedral (M)						
Ti	0.000	0.001	0.000	0.000	0.000	0.000
Ni	0.000	0.000	0.000	0.001	0.000	0.000
Cr	0.001	0.000	0.000	0.000	0.000	0.000
Mg	0.000	0.000	0.000	0.000	0.000	0.000
Mn	0.000	0.001	0.001	0.002	0.001	0.001
Ca	0.299	0.297	0.295	0.298	0.296	0.298
Na	0.729	0.729	0.725	0.730	0.753	0.713
K	0.010	0.009	0.011	0.010	0.011	0.014
Total	5.025	5.023	5.018	5.023	5.041	5.015
End-member parameters						
Orthoclase	1.0	0.9	1.0	1.0	1.1	1.3
Albite	70.2	70.4	70.4	70.3	71.0	69.6
Anorthite	28.8	28.7	28.6	28.7	27.9	29.1

Sample	525139					
Spot number	66	67	68	72	73	74
SiO_2	60.750	60.630	60.450	61.840	61.730	62.030
TiO_2	0.000	0.000	0.000	0.000	0.005	0.021
Al_2O_3	23.890	23.770	23.780	24.670	24.190	24.400
FeO	0.001	0.012	0.024	0.033	0.016	0.007
MnO	0.000	0.007	0.000	0.000	0.000	0.024
MgO	0.004	0.000	0.000	0.002	0.000	0.000
CaO	6.000	5.900	5.870	6.180	6.190	6.180
Na_2O	8.630	8.470	8.600	8.540	8.580	8.590
K_2O	0.366	0.392	0.338	0.321	0.349	0.377
Cr_2O_3	0.000	0.000	0.000	0.000	0.004	0.000
NiO	0.000	0.000	0.000	0.008	0.012	0.000
Total	99.641	99.181	99.062	101.593	101.076	101.629
Numbers of ions on the basis of 8 (O)						
Tetrahedral (T)						
Si	2.718	2.724	2.720	2.712	2.722	2.720
Al	1.260	1.259	1.261	1.275	1.257	1.261
Fe	0.000	0.000	0.001	0.001	0.001	0.000
Octahedral (M)						
Ti	0.000	0.000	0.000	0.000	0.000	0.001
Ni	0.000	0.000	0.000	0.000	0.000	0.000
Cr	0.000	0.000	0.000	0.000	0.000	0.000
Mg	0.000	0.000	0.000	0.000	0.000	0.000
Mn	0.000	0.000	0.000	0.000	0.000	0.001
Ca	0.288	0.284	0.283	0.290	0.292	0.290
Na	0.749	0.738	0.750	0.726	0.733	0.730
K	0.021	0.022	0.019	0.018	0.020	0.021
Total	5.036	5.027	5.034	5.023	5.026	5.025
End-member parameters						
Orthoclase	2.0	2.2	1.8	1.7	1.9	2.0
Albite	70.8	70.7	71.3	70.2	70.2	70.1
Anorthite	27.2	27.2	26.9	28.1	28.0	27.9

Sample	**525137**					
Spot number	107	108	109	110	115	116
SiO_2	59.870	60.210	60.210	59.350	58.600	58.480
TiO_2	0.001	0.000	0.014	0.000	0.000	0.005
Al_2O_3	25.690	25.520	25.470	25.350	25.040	25.130
FeO	0.049	0.019	0.021	0.787	0.005	0.050
MnO	0.056	0.020	0.002	0.000	0.005	0.000
MgO	0.000	0.000	0.000	0.000	0.000	0.000
CaO	7.640	7.620	7.570	7.480	7.540	7.610
Na_2O	7.680	7.660	7.650	7.600	7.640	7.670
K_2O	0.296	0.231	0.302	0.266	0.249	0.261
Cr_2O_3	0.000	0.000	0.014	0.006	0.000	0.001
NiO	0.038	0.000	0.000	0.000	0.000	0.000
Total	101.321	101.279	101.253	100.839	99.079	99.208
Numbers of ions on the basis of 8 (O)						
Tetrahedral (T)						
Si	2.645	2.657	2.658	2.641	2.647	2.640
Al	1.338	1.327	1.325	1.330	1.333	1.337
Fe	0.002	0.001	0.001	0.029	0.000	0.002
Octahedral (M)						
Ti	0.000	0.000	0.000	0.000	0.000	0.000
Ni	0.001	0.000	0.000	0.000	0.000	0.000
Cr	0.000	0.000	0.000	0.000	0.000	0.000
Mg	0.000	0.000	0.000	0.000	0.000	0.000
Mn	0.002	0.001	0.000	0.000	0.000	0.000
Ca	0.362	0.360	0.358	0.357	0.365	0.368
Na	0.658	0.655	0.655	0.656	0.669	0.671
K	0.017	0.013	0.017	0.015	0.014	0.015
Total	5.024	5.014	5.015	5.029	5.028	5.034
End-member parameters						
Orthoclase	1.6	1.3	1.7	1.5	1.4	1.4
Albite	63.5	63.7	63.6	63.8	63.8	63.7
Anorthite	34.9	35.0	34.8	34.7	34.8	34.9

Sample	**525139**				
Spot number	75	80	81	82	83
SiO_2	61.710	59.540	59.500	59.400	59.490
TiO_2	0.000	0.000	0.007	0.021	0.000
Al_2O_3	24.540	23.700	23.920	23.840	23.850
FeO	0.043	0.015	0.023	0.013	0.070
MnO	0.056	0.000	0.000	0.027	0.034
MgO	0.009	0.006	0.000	0.000	0.000
CaO	6.160	5.980	6.010	5.940	6.050
Na_2O	8.590	8.410	8.320	8.580	8.510
K_2O	0.329	0.395	0.400	0.380	0.387
Cr_2O_3	0.003	0.000	0.000	0.000	0.005
NiO	0.000	0.006	0.009	0.000	0.000
Total	101.441	98.052	98.188	98.200	98.397
Numbers of ions on the basis of 8 (O)					
Tetrahedral (T)					
Si	2.712	2.709	2.703	2.701	2.701
Al	1.271	1.271	1.281	1.278	1.276
Fe	0.002	0.001	0.001	0.000	0.003
Octahedral (M)					
Ti	0.000	0.000	0.000	0.001	0.000
Ni	0.000	0.000	0.000	0.000	0.000
Cr	0.000	0.000	0.000	0.000	0.000
Mg	0.001	0.000	0.000	0.000	0.000
Mn	0.002	0.000	0.000	0.001	0.001
Ca	0.290	0.292	0.293	0.289	0.294
Na	0.732	0.742	0.733	0.756	0.749
K	0.018	0.023	0.023	0.022	0.022
Total	5.028	5.038	5.034	5.049	5.047
End-member parameters					
Orthoclase	1.8	2.2	2.2	2.1	2.1
Albite	70.3	70.2	69.9	70.8	70.3
Anorthite	27.9	27.6	27.9	27.1	27.6

Sample	**525137**					
Spot number	117	125	126	127	132	133
SiO_2	58.390	58.620	58.640	58.720	59.700	59.690
TiO_2	0.000	0.000	0.021	0.010	0.003	0.004
Al_2O_3	25.240	25.070	25.160	25.050	25.550	25.650
FeO	0.010	0.017	0.009	0.005	0.017	0.014
MnO	0.024	0.000	0.007	0.000	0.000	0.002
MgO	0.000	0.000	0.000	0.000	0.000	0.004
CaO	7.640	7.570	7.580	7.490	7.580	7.630
Na_2O	7.570	7.630	7.690	7.620	7.860	7.710
K_2O	0.280	0.273	0.248	0.247	0.268	0.282
Cr_2O_3	0.000	0.000	0.000	0.000	0.018	0.016
NiO	0.000	0.000	0.000	0.000	0.000	0.000
Total	99.155	99.180	99.356	99.141	100.997	101.003
Numbers of ions on the basis of 8 (O)						
Tetrahedral (T)						
Si	2.637	2.645	2.642	2.649	2.645	2.644
Al	1.344	1.334	1.336	1.332	1.335	1.339
Fe	0.000	0.001	0.000	0.000	0.001	0.001
Octahedral (M)						
Ti	0.000	0.000	0.001	0.000	0.000	0.000
Ni	0.000	0.000	0.000	0.000	0.000	0.000
Cr	0.000	0.000	0.000	0.000	0.001	0.001
Mg	0.000	0.000	0.000	0.000	0.000	0.000
Mn	0.001	0.000	0.000	0.000	0.000	0.000
Ca	0.370	0.366	0.366	0.362	0.360	0.362
Na	0.663	0.668	0.672	0.667	0.675	0.662
K	0.016	0.016	0.014	0.014	0.015	0.016
Total	5.031	5.029	5.032	5.025	5.032	5.025
End-member parameters						
Orthoclase	1.5	1.5	1.4	1.4	1.4	1.5
Albite	63.2	63.6	63.9	63.9	64.3	63.7
Anorthite	35.3	34.9	34.8	34.7	34.3	34.8

Sample	**525137**					
Spot number	134	135	136	137	138	143
SiO_2	59.860	59.930	60.050	59.850	60.000	60.000
TiO_2	0.000	0.000	0.000	0.024	0.000	0.000
Al_2O_3	25.550	25.420	25.740	25.520	25.450	25.490
FeO	0.027	0.002	0.020	0.012	0.035	0.000
MnO	0.002	0.052	0.039	0.024	0.000	0.049
MgO	0.000	0.000	0.000	0.003	0.003	0.000
CaO	7.640	7.670	7.610	7.580	7.660	7.570
Na_2O	7.670	7.770	7.760	7.840	7.620	7.740
K_2O	0.254	0.232	0.254	0.236	0.228	0.301
Cr_2O_3	0.019	0.000	0.000	0.000	0.000	0.006
NiO	0.007	0.000	0.000	0.000	0.000	0.001
Total	101.029	101.076	101.473	101.089	100.995	101.156
Numbers of ions on the basis of 8 (O)						
Tetrahedral (T)						
Si	2.650	2.652	2.647	2.649	2.655	2.653
Al	1.333	1.326	1.337	1.331	1.328	1.329
Fe	0.001	0.000	0.001	0.000	0.001	0.000
Octahedral (M)						
Ti	0.000	0.000	0.000	0.001	0.000	0.000
Ni	0.000	0.000	0.000	0.000	0.000	0.000
Cr	0.001	0.000	0.000	0.000	0.000	0.000
Mg	0.000	0.000	0.000	0.000	0.000	0.000
Mn	0.000	0.002	0.001	0.001	0.000	0.002
Ca	0.362	0.364	0.359	0.359	0.363	0.359
Na	0.658	0.667	0.663	0.673	0.654	0.664
K	0.014	0.013	0.014	0.013	0.013	0.017
Total	5.020	5.024	5.023	5.028	5.014	5.023
End-member parameters						
Orthoclase	1.4	1.3	1.4	1.3	1.2	1.6
Albite	63.6	63.9	64.0	64.3	63.5	63.9
Anorthite	35.0	34.9	34.7	34.4	35.3	34.5

Sample	525137					
Spot number	157	158	159	164	165	166
SiO_2	59.970	60.310	60.280	59.950	60.250	60.130
TiO_2	0.009	0.003	0.015	0.000	0.018	0.006
Al_2O_3	25.610	25.470	25.490	25.460	25.570	25.670
FeO	0.007	0.000	0.000	0.021	0.006	0.040
MnO	0.042	0.000	0.024	0.005	0.032	0.020
MgO	0.012	0.000	0.000	0.000	0.000	0.006
CaO	7.580	7.570	7.530	7.590	7.530	7.610
Na_2O	7.750	7.860	7.690	7.890	7.710	7.720
K_2O	0.207	0.263	0.247	0.285	0.299	0.269
Cr_2O_3	0.000	0.000	0.000	0.000	0.000	0.006
NiO	0.006	0.006	0.000	0.000	0.025	0.000
Total	101.193	101.482	101.276	101.201	101.439	101.477
Numbers of ions on the basis of 8 (O)						
Tetrahedral (T)						
Si	2.650	2.657	2.659	2.651	2.655	2.650
Al	1.334	1.323	1.326	1.327	1.328	1.334
Fe	0.000	0.000	0.000	0.001	0.000	0.001
Octahedral (M)						
Ti	0.000	0.000	0.000	0.000	0.001	0.000
Ni	0.000	0.000	0.000	0.000	0.001	0.000
Cr	0.000	0.000	0.000	0.000	0.000	0.000
Mg	0.001	0.000	0.000	0.000	0.000	0.000
Mn	0.002	0.000	0.001	0.000	0.001	0.001
Ca	0.359	0.357	0.356	0.360	0.356	0.359
Na	0.664	0.671	0.658	0.677	0.659	0.660
K	0.012	0.015	0.014	0.016	0.017	0.015
Total	5.021	5.024	5.014	5.032	5.018	5.020
End-member parameters						
Orthoclase	1.1	1.4	1.4	1.5	1.6	1.5
Albite	64.2	64.3	64.0	64.3	63.9	63.8
Anorthite	34.7	34.2	34.6	34.2	34.5	34.7

Sample	525137					
Spot number	144	145	149	150	151	156
SiO_2	60.000	59.800	60.200	59.770	59.900	60.080
TiO_2	0.031	0.013	0.000	0.013	0.000	0.019
Al_2O_3	25.400	25.510	25.600	25.360	25.570	25.440
FeO	0.016	0.021	0.064	0.000	0.000	0.007
MnO	0.000	0.000	0.000	0.000	0.044	0.029
MgO	0.000	0.000	0.000	0.000	0.002	0.000
CaO	7.660	7.640	7.740	7.570	7.580	7.560
Na_2O	7.770	7.640	7.790	7.730	7.720	7.890
K_2O	0.298	0.268	0.241	0.256	0.221	0.268
Cr_2O_3	0.000	0.000	0.000	0.018	0.008	0.000
NiO	0.018	0.000	0.000	0.000	0.006	0.000
Total	101.193	100.892	101.635	100.717	101.050	101.294
Numbers of ions on the basis of 8 (O)						
Tetrahedral (T)						
Si	2.653	2.650	2.650	2.654	2.650	2.654
Al	1.324	1.333	1.329	1.327	1.334	1.325
Fe	0.001	0.001	0.002	0.000	0.000	0.000
Octahedral (M)						
Ti	0.001	0.000	0.000	0.000	0.000	0.001
Ni	0.001	0.000	0.000	0.000	0.000	0.000
Cr	0.000	0.000	0.000	0.001	0.000	0.000
Mg	0.000	0.000	0.000	0.000	0.000	0.000
Mn	0.000	0.000	0.000	0.000	0.002	0.001
Ca	0.363	0.363	0.365	0.360	0.359	0.358
Na	0.666	0.657	0.665	0.665	0.662	0.676
K	0.017	0.015	0.014	0.014	0.012	0.015
Total	5.025	5.019	5.025	5.022	5.020	5.029
End-member parameters						
Orthoclase	1.6	1.5	1.3	1.4	1.2	1.4
Albite	63.7	63.5	63.7	64.0	64.0	64.4
Anorthite	34.7	35.1	35.0	34.6	34.8	34.1

Sample	525137					
Spot number	170	171	172	176	177	178
SiO_2	60.060	59.880	60.090	57.770	57.760	57.880
TiO_2	0.000	0.000	0.000	0.008	0.000	0.035
Al_2O_3	25.500	25.360	25.460	25.040	25.070	25.090
FeO	0.000	0.002	0.052	0.034	0.015	0.021
MnO	0.039	0.000	0.012	0.000	0.015	0.010
MgO	0.000	0.000	0.000	0.000	0.002	0.000
CaO	7.600	7.600	7.630	7.640	7.570	7.620
Na_2O	7.800	7.680	7.570	7.670	7.640	7.550
K_2O	0.259	0.272	0.273	0.268	0.259	0.283
Cr_2O_3	0.017	0.000	0.000	0.000	0.000	0.000
NiO	0.000	0.000	0.014	0.006	0.000	0.003
Total	101.275	100.794	101.101	98.436	98.331	98.492
Numbers of ions on the basis of 8 (O)						
Tetrahedral (T)						
Si	2.653	2.656	2.657	2.631	2.632	2.633
Al	1.328	1.326	1.327	1.344	1.347	1.345
Fe	0.000	0.000	0.002	0.001	0.001	0.001
Octahedral (M)						
Ti	0.000	0.000	0.000	0.000	0.000	0.001
Ni	0.000	0.000	0.000	0.000	0.000	0.000
Cr	0.001	0.000	0.000	0.000	0.000	0.000
Mg	0.000	0.000	0.000	0.000	0.000	0.000
Mn	0.001	0.000	0.000	0.000	0.001	0.000
Ca	0.360	0.361	0.361	0.373	0.370	0.371
Na	0.668	0.660	0.649	0.677	0.675	0.666
K	0.015	0.015	0.015	0.016	0.015	0.016
Total	5.025	5.019	5.012	5.043	5.040	5.034
End-member parameters						
Orthoclase	1.4	1.5	1.5	1.5	1.4	1.6
Albite	64.1	63.7	63.3	63.6	63.7	63.2
Anorthite	34.5	34.8	35.2	35.0	34.9	35.2

Sample	525137					
Spot number	183	184	185	189	190	191
SiO_2	58.280	58.740	58.580	60.160	59.880	60.110
TiO_2	0.012	0.000	0.000	0.000	0.000	0.018
Al_2O_3	25.160	24.910	24.750	25.690	25.670	25.690
FeO	0.023	0.055	0.019	0.010	0.000	0.000
MnO	0.000	0.022	0.037	0.010	0.000	0.079
MgO	0.000	0.000	0.003	0.000	0.010	0.000
CaO	7.460	7.320	7.280	7.670	7.750	7.790
Na_2O	7.600	7.840	7.720	7.820	7.890	7.580
K_2O	0.224	0.227	0.188	0.228	0.243	0.265
Cr_2O_3	0.009	0.000	0.011	0.003	0.011	0.004
NiO	0.000	0.000	0.000	0.000	0.000	0.000
Total	98.769	99.114	98.587	101.591	101.453	101.536
Numbers of ions on the basis of 8 (O)						
Tetrahedral (T)						
Si	2.640	2.652	2.657	2.649	2.642	2.648
Al	1.344	1.326	1.323	1.333	1.335	1.334
Fe	0.001	0.002	0.001	0.000	0.000	0.000
Octahedral (M)						
Ti	0.000	0.000	0.000	0.000	0.000	0.001
Ni	0.000	0.000	0.000	0.000	0.000	0.000
Cr	0.000	0.000	0.000	0.000	0.000	0.000
Mg	0.000	0.000	0.000	0.000	0.001	0.000
Mn	0.000	0.001	0.001	0.000	0.000	0.003
Ca	0.362	0.354	0.354	0.362	0.366	0.368
Na	0.668	0.686	0.679	0.668	0.675	0.647
K	0.013	0.013	0.011	0.013	0.014	0.015
Total	5.028	5.035	5.026	5.025	5.034	5.016
End-member parameters						
Orthoclase	1.2	1.2	1.0	1.2	1.3	1.4
Albite	64.0	65.1	65.1	64.1	64.0	62.9
Anorthite	34.7	33.6	33.9	34.7	34.7	35.7

Sample	525137			
Spot number	196	197	198	199
SiO_2	58.970	59.610	59.260	59.310
TiO_2	0.006	0.008	0.000	0.003
Al_2O_3	25.350	25.610	25.700	25.630
FeO	0.014	0.000	0.041	0.022
MnO	0.047	0.024	0.039	0.020
MgO	0.000	0.000	0.000	0.000
CaO	7.680	7.770	7.660	7.760
Na_2O	7.640	7.660	7.600	7.660
K_2O	0.275	0.288	0.263	0.254
Cr_2O_3	0.000	0.001	0.006	0.005
NiO	0.008	0.000	0.000	0.000
Total	99.990	100.972	100.569	100.664
Numbers of ions on the basis of 8 (O)				
Tetrahedral (T)				
Si	2.641	2.642	2.637	2.638
Al	1.338	1.338	1.348	1.344
Fe	0.001	0.000	0.002	0.001
Octahedral (M)				
Ti	0.000	0.000	0.000	0.000
Ni	0.000	0.000	0.000	0.000
Cr	0.000	0.000	0.000	0.000
Mg	0.000	0.000	0.000	0.000
Mn	0.002	0.001	0.001	0.001
Ca	0.369	0.369	0.365	0.370
Na	0.663	0.658	0.656	0.660
K	0.016	0.016	0.015	0.014
Total	5.029	5.026	5.024	5.028
End-member parameters				
Orthoclase	1.5	1.6	1.4	1.4
Albite	63.3	63.1	63.3	63.2
Anorthite	35.2	35.4	35.3	35.4

Sample	525138					
Spot number	24	26	27	40	41	42
SiO_2	38.04	38.02	37.73	37.31	37.15	37.42
TiO_2	0.01	0.00	0.01	0.02	0.00	0.00
Al_2O_3	21.80	21.72	21.89	21.63	21.72	21.64
Cr_2O_3	0.00	0.02	0.03	0.03	0.02	0.00
FeO	29.60	29.72	29.46	29.43	29.17	29.43
MnO	8.02	8.30	8.26	9.09	8.97	8.84
MgO	3.36	3.38	3.37	3.23	3.27	3.27
NiO	0.00	0.00	0.01	0.00	0.01	0.00
CaO	1.66	1.66	1.63	1.60	1.65	1.70
Na_2O	0.00	0.02	0.02	0.01	0.02	0.06
K_2O	0.00	0.00	0.02	0.00	0.01	0.01
Total	102.49	102.84	102.42	102.34	101.99	102.37

Reformatted oxide percentages, with Fe2+/Fe3+ calculated (12 O)						
SiO_2	38.04	38.02	37.73	37.31	37.15	37.42
TiO_2	0.01	0.00	0.01	0.02	0.00	0.00
Al_2O_3	21.80	21.72	21.89	21.63	21.72	21.64
Cr_2O_3	0.00	0.02	0.03	0.03	0.02	0.00
Fe_2O_3	0.00	0.24	0.05	0.53	0.40	0.48
FeO	29.60	29.50	29.42	28.96	28.81	29.00
MnO	8.02	8.30	8.26	9.09	8.97	8.84
MgO	3.36	3.38	3.37	3.23	3.27	3.27
NiO	0.00	0.00	0.01	0.00	0.01	0.00
CaO	1.66	1.66	1.63	1.60	1.65	1.70
Na_2O	0.00	0.02	0.02	0.01	0.02	0.06
K_2O	0.00	0.00	0.02	0.00	0.01	0.01
Total	102.49	102.87	102.42	102.39	102.03	102.42

Numbers of ions on the basis of 12 (O)						
Tetrahedral (T)						
Si	2.984	2.977	2.966	2.946	2.942	2.953
^{IV}Al	0.016	0.023	0.034	0.054	0.058	0.047
8-co-ordinated site (A)						
^{VI}Al	2.000	1.983	1.995	1.962	1.972	1.968
Fe^{3+}	0.000	0.014	0.003	0.031	0.024	0.029
Ti	0.001	0.000	0.000	0.001	0.000	0.000
Cr	0.000	0.001	0.002	0.002	0.001	0.000
Octahedral (B)						
Fe^{2+}	1.942	1.932	1.934	1.912	1.908	1.913
Ni	0.000	0.000	0.001	0.000	0.001	0.000
Mg	0.393	0.395	0.395	0.380	0.386	0.385
Mn	0.533	0.550	0.550	0.608	0.602	0.591
Zn	0.000	0.000	0.000	0.000	0.000	0.000
Ca	0.140	0.139	0.137	0.135	0.140	0.144
Total	8.008	8.014	8.017	8.032	8.033	8.029
End-member parameters						
Almandine	64.3	63.6	63.5	61.9	61.7	62.1
Spessartine	17.9	18.5	18.5	20.6	20.5	20.0
Pyrope	13.2	13.3	13.3	12.9	13.1	13.0
Grossular	4.7	3.9	4.4	2.9	3.5	3.4
Andradite	0.0	0.7	0.1	1.6	1.2	1.5
Uvarovite	0.0	0.1	0.1	0.1	0.1	0.0

Sample	525138					
Spot number	66	67	68	69	85	86
SiO_2	38.39	38.50	38.47	38.41	36.38	36.43
TiO_2	0.07	0.01	0.00	0.01	0.04	0.00
Al_2O_3	21.31	21.10	21.39	21.35	21.74	21.65
Cr_2O_3	0.02	0.00	0.01	0.00	0.00	0.00
FeO	29.51	29.67	29.76	29.75	29.79	29.92
MnO	6.93	6.66	6.63	6.65	9.67	9.29
MgO	4.07	4.08	4.01	4.03	2.95	2.95
NiO	0.00	0.00	0.01	0.01	0.01	0.00
CaO	1.66	1.61	1.64	1.70	1.68	1.66
Na_2O	0.04	0.01	0.02	0.01	0.02	0.06
K_2O	0.00	0.00	0.00	0.00	0.01	0.01
	101.99	101.63	101.95	101.93	102.29	101.98

Reformatted oxide percentages, with Fe2+/Fe3+ calculated (12 O)						
SiO_2	38.39	38.50	38.47	38.41	36.38	36.43
TiO_2	0.07	0.01	0.00	0.01	0.04	0.00
Al_2O_3	21.31	21.10	21.39	21.35	21.74	21.65
Cr_2O_3	0.02	0.00	0.01	0.00	0.00	0.00
Fe_2O_3	0.22	0.26	0.09	0.18	0.93	0.85
FeO	29.31	29.43	29.68	29.58	28.95	29.16
MnO	6.93	6.66	6.63	6.65	9.67	9.29
MgO	4.07	4.08	4.01	4.03	2.95	2.95
NiO	0.00	0.00	0.01	0.01	0.01	0.00
CaO	1.66	1.61	1.64	1.70	1.68	1.66
Na_2O	0.04	0.01	0.02	0.01	0.02	0.06
K_2O	0.00	0.00	0.00	0.00	0.01	0.01
	102.01	101.66	101.96	101.94	102.38	102.06

Numbers of ions on the basis of 12 (O)						
Tetrahedral (T)						
Si	3.010	3.026	3.016	3.012	2.893	2.904
^{IV}Al	0.000	0.000	0.000	0.000	0.107	0.096
8-co-ordinated site (A)						
^{VI}Al	1.970	1.956	1.977	1.974	1.935	1.943
Fe^{3+}	0.013	0.016	0.005	0.011	0.056	0.051
Ti	0.004	0.000	0.000	0.001	0.002	0.000
Cr	0.001	0.000	0.001	0.000	0.000	0.000
Octahedral (B)						
Fe^{2+}	1.922	1.935	1.946	1.940	1.925	1.944
Ni	0.000	0.000	0.001	0.001	0.000	0.000
Mg	0.476	0.478	0.469	0.471	0.350	0.351
Mn	0.460	0.443	0.440	0.442	0.651	0.627
Zn	0.000	0.000	0.000	0.000	0.000	0.000
Ca	0.139	0.136	0.138	0.143	0.143	0.142
Total	7.996	7.990	7.993	7.996	8.063	8.058
End-member parameters						
Almandine	63.9	64.2	64.8	64.5	60.4	61.4
Spessartine	15.5	15.0	14.8	14.8	22.5	21.6
Pyrope	16.0	16.2	15.8	15.8	12.1	12.1
Grossular	4.0	3.8	4.3	4.2	2.1	2.3
Andradite	0.7	0.8	0.3	0.5	2.9	2.6
Uvarovite	0.1	0.0	0.0	0.0	0.0	0.0

Sample	525138					
Spot number	87	88	94	95	96	97
SiO_2	36.42	36.18	37.22	38.47	38.34	38.28
TiO_2	0.00	0.00	0.00	0.00	0.00	0.00
Al_2O_3	21.66	21.76	21.61	21.53	21.60	21.77
Cr_2O_3	0.01	0.01	0.03	0.03	0.02	0.02
FeO	29.89	29.58	30.02	29.54	29.97	29.58
MnO	9.57	9.29	8.53	8.26	8.62	8.58
MgO	2.91	2.98	3.43	3.35	3.29	3.28
NiO	0.00	0.00	0.00	0.01	0.00	0.00
CaO	1.64	1.67	1.66	1.71	1.71	1.68
Na_2O	0.00	0.01	0.03	0.01	0.01	0.00
K_2O	0.01	0.02	0.01	0.01	0.01	0.00
	102.12	101.50	102.53	102.93	103.57	103.19

Reformatted oxide percentages, with Fe2+/Fe3+ calculated (12 O)						
SiO_2	36.42	36.18	37.22	38.47	38.34	38.28
TiO_2	0.00	0.00	0.00	0.00	0.00	0.00
Al_2O_3	21.66	21.76	21.61	21.53	21.60	21.77
Cr_2O_3	0.01	0.01	0.03	0.03	0.02	0.02
Fe_2O_3	0.91	0.71	0.77	0.16	0.47	0.15
FeO	29.07	28.95	29.33	29.40	29.55	29.44
MnO	9.57	9.29	8.53	8.26	8.62	8.58
MgO	2.91	2.98	3.43	3.35	3.29	3.28
NiO	0.00	0.00	0.00	0.01	0.00	0.00
CaO	1.64	1.67	1.66	1.71	1.71	1.68
Na_2O	0.00	0.01	0.03	0.01	0.01	0.00
K_2O	0.01	0.02	0.01	0.01	0.01	0.00
	102.21	101.57	102.61	102.94	103.61	103.21

Numbers of ions on the basis of 12 (O)						
Tetrahedral (T)						
Si	2.900	2.895	2.935	3.005	2.984	2.986
^{IV}Al	0.100	0.105	0.065	0.000	0.016	0.014
8-co-ordinated site (A)						
^{VI}Al	1.938	1.951	1.947	1.983	1.968	1.989
Fe^{3+}	0.055	0.042	0.046	0.009	0.027	0.009
Ti	0.000	0.000	0.000	0.000	0.000	0.000
Cr	0.001	0.001	0.002	0.002	0.001	0.001
Octahedral (B)						
Fe^{2+}	1.936	1.937	1.934	1.920	1.924	1.921
Ni	0.000	0.000	0.000	0.001	0.000	0.000
Mg	0.345	0.355	0.403	0.390	0.382	0.381
Mn	0.645	0.630	0.570	0.546	0.568	0.567
Zn	0.000	0.000	0.000	0.000	0.000	0.000
Ca	0.140	0.143	0.140	0.143	0.143	0.140
Total	8.060	8.060	8.041	7.999	8.013	8.009
End-member parameters						
Almandine	61.0	61.0	62.1	63.9	63.4	63.5
Spessartine	22.3	21.7	19.4	18.3	19.0	19.0
Pyrope	11.9	12.3	13.7	13.0	12.8	12.8
Grossular	2.0	2.7	2.4	4.2	3.4	4.2
Andradite	2.8	2.2	2.3	0.5	1.4	0.4
Uvarovite	0.0	0.0	0.1	0.1	0.0	0.1

Sample	525138			
Spot number	98	99	100	101
SiO_2	38.01	37.87	37.99	38.12
TiO_2	0.00	0.02	0.00	0.00
Al_2O_3	21.80	21.82	21.90	21.91
Cr_2O_3	0.02	0.03	0.03	0.01
FeO	30.11	29.98	30.06	30.19
MnO	7.41	7.26	7.37	7.33
MgO	3.87	3.90	3.91	3.89
NiO	0.01	0.03	0.00	0.01
CaO	1.74	1.74	1.73	1.70
Na_2O	0.003	0.045	0.023	0.042
K_2O	0.01	0.00	0.00	0.00
	102.98	102.70	103.01	103.21

Reformatted oxide percentages, with Fe2+/Fe3+ calculated (12 O)				
SiO_2	38.01	37.87	37.99	38.12
TiO_2	0.00	0.02	0.00	0.00
Al_2O_3	21.80	21.82	21.90	21.91
Cr_2O_3	0.02	0.03	0.03	0.01
Fe_2O_3	0.42	0.34	0.34	0.32
FeO	29.73	29.68	29.75	29.90
MnO	7.41	7.26	7.37	7.33
MgO	3.87	3.90	3.91	3.89
NiO	0.01	0.03	0.00	0.01
CaO	1.74	1.74	1.73	1.70
Na_2O	0.003	0.045	0.023	0.042
K_2O	0.01	0.00	0.00	0.00
	103.02	102.73	103.04	103.24

Numbers of ions on the basis of 12 (O)				
Tetrahedral (T)				
Si	2.965	2.962	2.962	2.966
^{IV}Al	0.035	0.038	0.038	0.034
8-co-ordinated site (A)				
^{VI}Al	1.971	1.975	1.976	1.978
Fe^{3+}	0.025	0.020	0.020	0.019
Ti	0.000	0.001	0.000	0.000
Cr	0.001	0.002	0.002	0.001
Octahedral (B)				
Fe^{2+}	1.940	1.941	1.940	1.946
Ni	0.001	0.002	0.000	0.001
Mg	0.450	0.455	0.454	0.451
Mn	0.490	0.481	0.487	0.483
Zn	0.000	0.000	0.000	0.000
Ca	0.145	0.146	0.145	0.142
Total	8.022	8.022	8.023	8.020
End-member parameters				
Almandine	63.4	63.5	63.3	63.7
Spessartine	16.5	16.2	16.4	16.3
Pyrope	15.2	15.4	15.3	15.2
Grossular	3.6	3.8	3.8	3.8
Andradite	1.2	1.0	1.0	1.0
Uvarovite	0.1	0.1	0.1	0.0

Sample Ujarrasiorit						
Spot number	207	208	209	213	214	215
SiO_2	38.33	38.17	38.49	38.19	38.21	38.35
TiO_2	0.02	0.01	0.00	0.00	0.03	0.00
Al_2O_3	20.76	20.85	20.73	20.73	20.96	20.90
Cr_2O_3	0.07	0.07	0.02	0.08	0.06	0.04
FeO	26.39	26.71	26.41	27.19	27.23	27.24
MnO	9.77	9.94	9.72	10.06	9.69	9.99
MgO	1.67	1.70	1.66	2.02	2.05	2.02
NiO	0.00	0.00	0.00	0.01	0.00	0.00
CaO	5.82	5.80	5.77	4.20	4.33	4.32
Na_2O	0.01	0.00	0.00	0.00	0.02	0.03
K_2O	0.03	0.00	0.00	0.01	0.00	0.00
	102.87	103.25	102.80	102.48	102.57	102.89

Reformatted oxide percentages, with Fe2+/Fe3+ calculated (12 O)						
SiO_2	38.33	38.17	38.49	38.19	38.21	38.35
TiO_2	0.02	0.01	0.00	0.00	0.03	0.00
Al_2O_3	20.76	20.85	20.73	20.73	20.96	20.90
Cr_2O_3	0.07	0.07	0.02	0.08	0.06	0.04
Fe_2O_3	0.92	1.15	0.87	0.81	0.61	0.75
FeO	25.56	25.68	25.63	26.46	26.68	26.57
MnO	9.77	9.94	9.72	10.06	9.69	9.99
MgO	1.67	1.70	1.66	2.02	2.05	2.02
NiO	0.00	0.00	0.00	0.01	0.00	0.00
CaO	5.82	5.80	5.77	4.20	4.33	4.32
Na_2O	0.01	0.00	0.00	0.00	0.02	0.03
K_2O	0.03	0.00	0.00	0.01	0.00	0.00
Total	102.92	103.36	102.88	102.55	102.62	102.93

Numbers of ions on the basis of 12 (O)						
Tetrahedral (T)						
Si	3.008	2.989	3.020	3.011	3.007	3.011
^{IV}Al	0.000	0.011	0.000	0.000	0.000	0.000
8-co-ordinated site (A)						
^{VI}Al	1.925	1.919	1.921	1.930	1.947	1.937
Fe^{3+}	0.054	0.068	0.051	0.048	0.036	0.044
Ti	0.001	0.000	0.000	0.000	0.002	0.000
Cr	0.004	0.004	0.001	0.005	0.004	0.002
Octahedral (B)						
Fe^{2+}	1.678	1.682	1.681	1.745	1.756	1.744
Ni	0.000	0.000	0.000	0.000	0.000	0.000
Mg	0.195	0.198	0.194	0.237	0.240	0.236
Mn	0.650	0.659	0.646	0.672	0.646	0.664
Zn	0.000	0.000	0.000	0.000	0.000	0.000
Ca	0.489	0.487	0.485	0.355	0.365	0.363
Total	8.005	8.018	8.000	8.003	8.003	8.003
End-member parameters						
Almandine	55.1	55.0	55.2	57.4	57.9	57.4
Spessartine	21.9	22.1	21.9	22.6	21.7	22.4
Pyrope	6.6	6.6	6.6	8.0	8.1	8.0
Grossular	13.5	12.7	13.8	9.3	10.3	9.9
Andradite	2.8	3.4	2.6	2.4	1.8	2.2
Uvarovite	0.2	0.2	0.0	0.2	0.2	0.1

Sample Ujarrasiorit						
Spot number	245	246	247	251	252	253
SiO_2	38.13	38.05	38.13	38.17	38.14	38.23
TiO_2	0.03	0.03	0.01	0.04	0.00	0.00
Al_2O_3	21.46	21.47	21.61	21.42	21.24	21.14
Cr_2O_3	0.03	0.01	0.01	0.05	0.05	0.05
FeO	30.74	30.40	30.62	26.14	25.96	25.66
MnO	7.36	7.61	7.30	11.29	11.12	11.05
MgO	2.33	2.38	2.34	1.92	1.94	1.94
NiO	0.02	0.00	0.01	0.00	0.00	0.00
CaO	3.67	3.69	3.72	4.79	4.75	4.88
Na_2O	0.01	0.02	0.03	0.02	0.01	0.00
K_2O	0.01	0.00	0.00	0.01	0.03	0.01
	103.79	103.65	103.78	103.85	103.25	102.96

Reformatted oxide percentages, with Fe2+/Fe3+ calculated (12 O)						
SiO_2	38.13	38.05	38.13	38.17	38.14	38.23
TiO_2	0.03	0.03	0.01	0.04	0.00	0.00
Al_2O_3	21.46	21.47	21.61	21.42	21.24	21.14
Cr_2O_3	0.03	0.01	0.01	0.05	0.05	0.05
Fe_2O_3	0.73	0.76	0.60	0.77	0.71	0.66
FeO	30.08	29.72	30.08	25.45	25.32	25.07
MnO	7.36	7.61	7.30	11.29	11.12	11.05
MgO	2.33	2.38	2.34	1.92	1.94	1.94
NiO	0.02	0.00	0.01	0.00	0.00	0.00
CaO	3.67	3.69	3.72	4.79	4.75	4.88
Na_2O	0.01	0.02	0.03	0.02	0.01	0.00
K_2O	0.01	0.00	0.00	0.01	0.03	0.01
Total	103.85	103.71	103.81	103.90	103.28	103.01

Numbers of ions on the basis of 12 (O)						
Tetrahedral (T)						
Si	2.973	2.969	2.971	2.973	2.986	2.997
^{IV}Al	0.027	0.031	0.029	0.027	0.014	0.003
8-co-ordinated site (A)						
^{VI}Al	1.948	1.948	1.959	1.944	1.949	1.953
Fe^{3+}	0.043	0.044	0.035	0.045	0.042	0.039
Ti	0.002	0.002	0.001	0.003	0.000	0.000
Cr	0.002	0.000	0.000	0.003	0.003	0.003
Octahedral (B)						
Fe^{2+}	1.961	1.940	1.960	1.658	1.658	1.643
Ni	0.002	0.000	0.001	0.000	0.000	0.000
Mg	0.271	0.277	0.272	0.223	0.226	0.227
Mn	0.486	0.503	0.482	0.745	0.737	0.734
Zn	0.000	0.000	0.000	0.000	0.000	0.000
Ca	0.307	0.309	0.311	0.400	0.398	0.410
Total	8.021	8.023	8.021	8.020	8.015	8.009
End-member parameters						
Almandine	64.2	63.3	64.2	54.0	54.4	54.2
Spessartine	16.4	16.9	16.2	25.1	24.7	24.5
Pyrope	9.1	9.3	9.1	7.5	7.6	7.6
Grossular	8.1	8.1	8.6	11.0	11.1	11.6
Andradite	2.2	2.2	1.8	2.3	2.1	1.9
Uvarovite	0.1	0.0	0.0	0.2	0.2	0.1

Geothermobarometry – averages used in models

Plagioclase

Numbers of ions on the basis of 8 (O)

Sample	Ca	Na	K
525137	0.362	0.665	0.015
525138	0.279	0.749	0.014
525139	0.304	0.722	0.016

Garnet

Numbers of ions on the basis of 12 (O)

Sample	Fe	Mn	Mg	Ca
525138	1.957	0.544	0.409	0.141
Uja – high Mn	1.745	0.685	0.220	0.418
Uja – low Mn	1.995	0.491	0.273	0.309
Uja (tot)	1.870	0.588	0.246	0.363

Biotite

Numbers of ions on the basis of 22 (O, OH)

Sample	Fe(tot)	Mg	^{VI}Al	Ti
525137	1.827	2.796	0.791	0.291
525138	2.172	2.282	0.829	0.283
525139	1.650	2.856	0.797	0.271
Uja(tot)	3.287	2.374	0.165	0.114

Numbers of ions on the basis of 11 (O, OH)

Sample	Fe(tot)	Mg	^{VI}Al	Ti
525137	0.913	1.398	0.395	0.145
525138	1.086	1.141	0.415	0.141
525139	0.825	1.428	0.399	0.136
Uja (tot)	1.643	1.187	0.083	0.057

		U (PPM)		**error**	**Th (PPM)**		**error**	**207Pb/235Pb**		**error**	**206Pb/238Pb**		**error**	**207Pb/206Pb**		**error**	**207Pb/206Pb date**			**Signal duration**	**C.Pb**
Sample	**Mineral**	Approx.		2SE	Approx.		2SE	ratio		2SE	ratio		2SE	ratio		2SE	**Corrected ages**			seconds	**correction**
525137	Mnz	4170	±	370	33300	±	2800	5.2300	±	0.2300	0.3490	±	0.0200	0.1122	±	0.003	**1834**	**±**	**25**	24.30	*
525137	Mnz	3740	±	240	36300	±	2600	4.9000	±	0.1900	0.3270	±	0.0120	0.1087	±	0.0021	**1790**	**±**	**29**	24.50	*
525137	Mnz	4005	±	79	34930	±	930	4.8300	±	0.1300	0.3156	±	0.0096	0.1097	±	0.002	**1790**	**±**	**32**	21.30	
525137	Mnz	4500	±	110	43400	±	1300	4.9500	±	0.1100	0.3162	±	0.0073	0.1115	±	0.0025	**1820**	**±**	**40**	17.01	
525137	Mnz	4248	±	75	33290	±	790	4.8700	±	0.1100	0.3187	±	0.0082	0.1102	±	0.0017	**1805**	**±**	**25**	23.03	
525137	Mnz	3400	±	150	36510	±	490	5.0000	±	0.1300	0.3226	±	0.0081	0.1108	±	0.0014	**1808**	**±**	**23**	19.60	
525138	Mnz	4720	±	170	38600	±	1700	5.1600	±	0.1300	0.3245	±	0.0081	0.1139	±	0.003	**1907**	**±**	**43**	24.34	*
525138	Mnz	4080	±	140	38940	±	660	5.1100	±	0.1700	0.3270	±	0.0130	0.112	±	0.0027	**1829**	**±**	**22**	23.91	*
525138	Mnz	4640	±	240	34300	±	1100	5.0800	±	0.1200	0.3289	±	0.0085	0.1122	±	0.0012	**1830**	**±**	**20**	14.85	
525138	Xtm	3320	±	130	865	±	15	4.5900	±	0.1300	0.3130	±	0.0130	0.1059	±	0.0035	**1723**	**±**	**60**	12.79	
525138	Mnz	4560	±	260	40780	±	660	4.7300	±	0.1200	0.3148	±	0.0086	0.1087	±	0.0017	**1772**	**±**	**30**	21.56	
525138	Mnz	5360	±	270	40100	±	1100	4.9750	±	0.0940	0.3169	±	0.0091	0.1139	±	0.0024	**1859**	**±**	**37**	14.47	
525138	Mnz	5120	±	130	41100	±	1200	5.0200	±	0.1200	0.3295	±	0.0066	0.11	±	0.0021	**1795**	**±**	**35**	24.47	
525139	Mnz	7330	±	220	41300	±	2200	5.5200	±	0.3700	0.3290	±	0.0150	0.1203	±	0.0053	**1961**	**±**	**47**	24.51	*
525139	Mnz	2900	±	1200	25000	±	9300	6.2000	±	1.1000	0.4000	±	0.0660	0.1136	±	0.0021	**1862**	**±**	**23**	24.69	*
525139	Mnz	5400	±	1100	17900	±	1100	4.5700	±	0.3900	0.3110	±	0.0240	0.106	±	0.0027	**1752**	**±**	**22**	24.04	*
525139	Mnz	9830	±	170	46100	±	2000	5.1000	±	0.1000	0.3272	±	0.0082	0.1128	±	0.0017	**1843**	**±**	**28**	16.17	
525139	Mnz	5960	±	220	45500	±	1600	4.9540	±	0.0980	0.3230	±	0.0100	0.1109	±	0.0021	**1810**	**±**	**34**	16.17	
525139	Mnz	5090	±	180	42200	±	2100	5.0000	±	0.1200	0.3230	±	0.0110	0.1116	±	0.0023	**1821**	**±**	**38**	14.21	
525139	Mnz	4960	±	260	42800	±	2700	5.1280	±	0.0600	0.3271	±	0.0057	0.1124	±	0.0015	**1835**	**±**	**25**	18.51	
525139	Mnz	6530	±	410	38100	±	1600	4.6800	±	0.1400	0.3020	±	0.0100	0.1109	±	0.0012	**1812**	**±**	**19**	24.47	
525137	Zrn	236	±	21	22	±	2	5.4700	±	0.1900	0.3336	±	0.0096	0.1171	±	0.0013	**1803**	**±**	**23**	24.47	

* Ages corrected for common Pb content by measuring mass 204 procedure

	unit	525133	525134	525137	525138	525139
SiO_2	wt.%	38.17	46.89	62.15	66.54	64.22
TiO_2	wt.%	0.098	0.225	0.665	0.668	0.545
Al_2O_3	wt.%	4.23	14.63	0.665	14.66	16.91
Fe_2O_3	wt.%	17.5	12.44	7.06	5.53	5.68
MnO	wt.%	0.204	0.143	0.051	0.129	0.052
MgO	wt.%	35.28	7.79	2.97	2.57	2.56
CaO	wt.%	1.24	10.78	2.01	1.91	2.4
Na_2O	wt.%	0.23	2.02	1.99	2.74	3.89
K_2O	wt.%	0.04	0.44	4.75	2.75	2.26
P_2O_5	wt.%	0.01	0.02	0.15	0.15	0.12
LOI	wt.%	2.72	3.48		1.12	2.2
Total	wt.%	99.71	98.86	99.59	98.77	100.8
				82.461		

	unit	525133	525134	525135	525137	525138	525139
Cr	ppm	2780	1380		100	84	51
Ni	ppm	1170	130		50	30	30
Co	ppm	150	26		18	13	11
Sc	ppm	20	52.2			16.9	15.3
V	ppm	127	205		124	92	89
Cu	ppm	< 10	100		50	< 10	20
Pb	ppm	< 5	8		29	20	19
Zn	ppm	120	160		130	110	100
Bi	ppm	< 0.1	0.5		0.4	< 0.1	0.2
Sn	ppm	< 1	< 1		3	3	2
In	ppm	< 0.1	< 0.1		< 0.1	< 0.1	< 0.1
Tl	ppm	< 0.05	0.09			0.98	0.9
W	ppm	< 0.5	< 0.5		0.9	1.1	1.3
Mo	ppm	< 2	< 2		< 2	< 2	2
As	ppm	< 5	< 0.5		< 5	< 0.5	< 0.5
Se	ppm		< 3			< 3	< 3
Sb	ppm	< 0.2	< 0.2		< 0.2	< 0.2	< 0.2
Ag	ppm	< 0.5	< 0.5		0.8	0.9	0.8
Au	ppb	< 1	< 2	3		< 2	< 2
Pt	ppb	13.1					
Pd	ppb	49.7					
Ir	ppb		< 5			< 5	< 5
Rb	ppm	< 1	4		168	133	119
Cs	ppm	< 0.1	0.2		8.4	7.1	5
Ba	ppm	< 3	69		953	301	236
Sr	ppm	8	108		220	133	221
Ga	ppm	7	10		20	18	22
Ge	ppm	1.3	1.5		1.6	2	2
Hf	ppm	< 0.1	0.4		4	5.4	4.4
Zr	ppm	2	12		141	201	156
Nb	ppm	< 0.2	0.6		11.4	11	12
Y	ppm	1.6	12.3		24	31	27.1
Th	ppm	< 0.05	0.07		13.8	13.7	15.6
U	ppm	0.02	0.34		3.28	3.05	5.04
La	ppm	0.29	0.57		42.9	42.5	47.1
Ce	ppm	0.65	1.37		86.8	85.4	92
Pr	ppm	0.08	0.21		9.84	9.54	10.2
Nd	ppm	0.43	1.04		38.7	36.7	39.1
Sm	ppm	0.15	0.44		7.33	7.13	7.32
Eu	ppm	0.02	0.185		1.44	1.29	1.3
Gd	ppm	0.23	0.86		5.85	6	5.76
Tb	ppm	0.04	0.22		0.87	0.94	0.86
Dy	ppm	0.3	1.82		4.71	5.53	4.85
Ho	ppm	0.07	0.44		0.89	1.16	0.98
Er	ppm	0.21	1.47		2.42	3.42	2.85
Tm	ppm	0.033	0.251		0.342	0.532	0.441
Yb	ppm	0.22	1.78		2.16	3.76	3
Lu	ppm	0.035	0.292		0.337	0.602	0.489
Ta	ppm	< 0.01	0.03		0.89	0.85	1.17
Be	ppm	< 1	< 1		2	2	3
Br	ppm		< 0.5			< 0.5	< 0.5